Ólafur Arnalds
François Bartoli
Peter Buurman
Hlynur Óskarsson
Georges Stoops
Eduardo García-Rodeja
Editors

Soils of Volcanic Regions in Europe

Springer

Ó. Arnalds, F. Bartoli, P. Buurman, H. Óskarsson,
G. Stoops, E. García-Rodeja
Soils of Volcanic Regions in Europe

Ó. Arnalds, F. Bartoli, P. Buurman,
H. Óskarsson, G. Stoops, E. García-Rodeja
(Eds.)

Soils of Volcanic Regions in Europe

With 169 Figures and a CD-ROM

Springer

EDITORS:

Ó. ARNALDS, H. ÓSKARSSON
AGRICULTURAL UNIVERSITY OF ICELAND,
DEPARTMENT OF ENVIRONMENTAL SCIENCES
KELDNAHOLT
IS-112 REYKJAVÍK, ICELAND
E-mail: oa@lbhi.is; hlynur@lbhi.is

F. BARTOLI
LABORATOIRE SOLS ET ENVIRONNEMENT UMR
1120 ENSAIA-INPL/INRA
BP 172
54505 VANDOEUVRE LES NANCY CEDEX,
FRANCE
E-mail:
Francois.Bartoli@ensaia.inpl-nancy.fr

P. BUURMAN
DEPARTMENT OF ENVIRONMENTAL SCIENCES
LABORATORY OF SOIL SCIENCE AND GEOLOGY,
WAGENINGEN UNIVERSITY
P.O. BOX 37
6700 AA WAGENINGEN,
THE NETHERLANDS
E-mail: peter.buurman@wur.nl

G. STOOPS
LABORATORIUM VOOR MINERALOGIE,
PETROLOGIE EN MICROPEDOLOGIE,
UNIVERSITEIT GENT, KRIJGSLAAN 281
S8 BELGIUM
E-mail: stoops.georges@skynet.be

E. GARCÍA-RODEJA
DEPARTAMENTO DE EDAFOLOXÍA E QUÍMICA
AGRÍCOLA, FACULTADE DE BIOLOXÍA,
UNIVERSIDADE DE SANTIAGO DE
COMPOSTELA, LOPE GÓMEZ DE
MARZOA S/N, CAMPUS SUR
E-15782 SANTIAGO DE
COMPOSTELA, SPAIN
E-mail: edcone@usc.es

ISBN 10 3-540-48710-7 **Springer Berlin Heidelberg New York**
ISBN 13 978-3-540-48710-4 **Springer Berlin Heidelberg New York**

Library of Congress Control Number: 2006936098

Springer is a part of Springer Science+Business Media
springeronline.com

Cover design: E. Kirchner, Heidelberg
Production: A. Oelschläger
Typesetting: Camera-ready by the Editors

Printed on acid-free paper 30/2132/AO 543210

Preface

F. Bartoli, O. Arnalds, P. Buurman, E. Garcia-Rodeja,
J. Hernandez-Moreno, H. Oskarsson, J. Pinheiro, P. Quantin,
G. Stoops, F. Terribile and F. van Oort

Volcanic soils of Europe

Soils of volcanic regions are unique natural resources. When volcanic materials are exposed to weathering, short-range order minerals, such as allophane, imogolite and ferrihydrite are formed, as well as specific types of humic substances. These colloidal materials give the soils distinctive properties, collectively termed andic properties, which separate volcanic soils from other types of soils. These properties include high organic carbon content, variable charge characteristics, high phosphorus retention, low bulk density and great water retention capacity. These kind of soils are named Andosols (FAO-WRB) or Andisols (Soil Taxonomy), a term derived from Japanese, where "an" means black and "do" is soil. Andosols are typically relatively young soils, but when left to prolonged weathering, other soil types can develop, but the evidence of their volcanic origin can be preserved for a long time.

Volcanic soils cover only 1–2% of the world's land surface. They are often among the most fertile soils and therefore are the foundations for some of the most densely populated areas of the world. They often occur in scenic areas and are commonly subjected to extreme pressures from tourism. The unique physical and chemical properties of Andosols make these ecosystems susceptible to disturbance. They have effective pollutant binding properties resulting in possible accumulation of toxic substances. Degradation of volcanic soils also includes salinization by irrigation, reduced ground-water quality and loss of fertility, particularly under humid climates and intense leaching. The low bulk density of Andosols, often low amount of lattice clay minerals, and sometimes the presence of light tephra grains make them both prone to wind erosion and sometimes erosion by water. Their peculiar thixotropic behavior, with unstable solid state which can become liquefied upon disturbance, explains the relatively common occurrence of catastrophic landslides in volcanic areas. Understanding the fundamental properties of soils in volcanic areas is therefore important for

developing policies for the use and protection of these important soil resources.

Volcanic areas occur in many parts of the world, but most studies on soils of volcanic areas have been conducted in Japan, New Zealand and the Americas. Such soils have received less attention in Europe. This book is dedicated to soils of volcanic regions of Europe with a comprehensive coverage of most aspects of such soils in Europe. It is the largest such publication on soils of volcanic regions to date and presents results of research that has international implications.

Geographic differences

The range of environmental conditions shaping the soils discussed in this publication is noteworthy as is evident from the first part of the book. The climate ranges from Mediterranean Italy to the southern Massif Central in France and the continental climate of the Carpathian basin and mountains of Germany, to the warm Atlantic of the Azores, Madeira and Canary Island and sub-arctic Iceland. Rarely has such a wide variety of environmental conditions for soil development been summarized in one publication. The diversity in geology, including the chemistry and morphology of the parent materials is substantial.

The largest European volcanic area is in Iceland, under wet and cold climate. It is characterized by a variety vitric, allophanic and peaty Andosols together with of vitric volcanic soils on barren surfaces or deserts. The Andosols exhibit well expressed andic features often with a peaty texture in wetland soils. Cryoturbation and hydromorphic features are common.

In the Mediterranean countries such as Greece, continental Italy, Sicily and southern France there is a large variety of young volcanic soils, such as vitric and typical Andosols on young pyroclatic materials. More evolved soils, such as Brown soils Alfisols and Vertisols occur on older volcanic materials. Millennia of cultivation and fertilization have deeply modified many of the volcanic ash soils, and caused erosion.

Typical allophanic Andosols are found on young pyroclastic materials in Continental Europe, such as in the Chaine des Puys and the Cantal in France, Eifel and Vogelsberg in Regions in Germany and Carpathian countries (Hungary, Slovakia, Romania). Andosols rich in organo-aluminium complexes appear on older volcanic formations together with other soil types. Under cold and wet climate of some European mountains, soils with

andic properties and rich in organo-aluminium complexes are also observed on old basic, non-volcanic plutonic rocks.

In the Atlantic Canary, Madeira and Azores Islands, there is a large variety of climates, from sub-tropical to temperate temperatures, and from very wet to semi-arid moisture regimes. The volcanic deposits are mostly basaltic of variable age. The results in diversity of volcanic soils depending on the age and climatic conditions: vitric and typical Andosols on young pyroclastic materials, Andosols rich in organo-aluminium complexes or more evolved soils on old volcanic formations. A peculiar type of Andosol, characterized by a extreme water retention capacity is found on the Azores Islands. Paleosols are often well preserved on these Atlantic Islands.

Physical and chemical degradation of volcanic soils is also common in Europe, depending on climate and land use. Landslides regularly occur in European volcanic areas, some catastrophic and causing losses of human lives and property damage. An example is the slide near Napoli, Italy in 1998, which left 161 people dead, and causing huge property damage.

The COST-622 Action joint research approach

This comprehensive publication is the result of European funded scientific collaboration program entitled "COST-622; Soil Resources of European Volcanic Systems". The program was initiated in 1998, leading to a fruitful co-operation among scientists from Belgium, France, Germany, Greece, Hungary, Iceland, Italy, the Netherlands, Portugal, Slovakia, Spain, and the United Kingdom. It included a number of scientific workshops and conferences hosted by the participating countries, often within volcanic areas. The program has already resulted in two special issues of scientific journals (Bartoli et al. 2003, Arnalds and Stahr 2004). This program was completed in 2004.

The objectives of the COST-622 program were to assess the impact of age and nature of volcanic parent materials, climatic parameters and anthropic effects on the formation and properties of the European volcanic soils. This task was undertaken by (i) joint sampling and analysis of number of reference pedons in the countries (2–4 in each country); and (ii) by collaborative research efforts between European institutes working on Andosols.

Descriptions of the selected European volcanic soils were made and both undisturbed and bulk soil samples were obtained. The undisturbed soil samples were used for micromorphological and physical studies. The

bulk soil samples were distributed to the various laboratories of the participating countries for research on mineralogy and weathering, organic and mineral chemistry, physical chemistry and biological studies. We conclude that this multi-disciplinary and multinational approach is quite unique for soil sciences.

The aim of the research included:

- obtaining more detailed information about the nature and distribution of volcanic soils in Europe, which included collaboration with and reference soil collection by ISRIC, the Netherlands
- a genetic study of the reference pedons and the development of soil classification considerations for volcanic soils (WRB)
- to investigate the mineral and organic soil constituents in volcanic soils, weathering, bio-geochemical processes, physical-chemical properties and physical properties of European volcanic soils
- and to adapt methods for three-dimentional studies of macrostructure, particle size, chemical dissolution techniques, and pyrolysis of soil organic materials

Data handling and integration includes multivariate statistical analysis. The results generated in these studies have international relevance for volcanic soils and soil science in general.

Organization of this book

This book is divided into five sections. Section I describes the diversity of European volcanic soil resources and their environments and provides background information for the reference pedons. Section II provides discussion on parent materials and it provides results on mineral composition and genesis of the soils. Results on chemical, biological and physical characteristics are presented in Sections III and IV. The scale of observation ranges from the meter and centimeter scale, for soil descriptions and down to the micrometer scale for characterization of soil constituents, interrelationships and reactivity, soil structure, and soil properties. In Section V, examples of the soil behavior is given with respect to soil properties and land use considerations, together with a synthesis of geographical data. Finally, the content of the accompanying CD is presented.

English is the language of this book. However, the authors come from a variety of language areas, and allowance is be made for letting the original or native tongue and the style of each author to show through as much as possible, as long as the contents are clear and of high quality, and the English is reasonably correct.

Acknowledgements

J. Pinheiro and M. Madeira (Azores, Portugal), J. Dejou and F. van Oort (France), M. Kleber and R. Jahn (Germany), A. Economou and D. Pateras (Greece), G. Füleky and A. Kertesz (Hungary), O. Arnalds and H. Oskarsson (Iceland), L. Lulli and F. Terribile (Italy), J. Balkovic and B. Jurani (Slovakia), M. Tejedor and J. Hernandez-Moreno (Tenerife, Spain) selected the COST 622 reference profiles; T. Jongmans (The Netherlands) and F. van Oort (France) made the soil and site descriptions; O. Spaargaren (The Netherlands) sampled soil monoliths and made classifications. P. Buurman (The Netherlands) oversaw coordination of the data base, staffs of Lisbon (Portugal), Santiago de Compostella (Spain) and Wageningen (The Netherlands) Universities made valuable technical assistance as well as staffs from CNRS Nancy and IRD Bondy (France), CNR Naples (Italy), Halle (Germany), La Laguna (Tenerife, Spain) and Godello (Hungary) Universities. Support and funding from EU COST Actions (1998–2004) are greatly appreciated. Our final thanks and appreciation are due to L. Szendrodi and E. Fulajtar, Scientific Secretaries of COST Actions on Environmental Research, and their staff, for their help and support, to the authors for their cooperation and contribution, to the editors for their scientific editing, to the reviewers for their valuable help and comments, to Margret Jónsdóttir and Tryggvi Gunnarsson (Agricultural University of Iceland) for careful management and final editing, and to Springer Verlag for valuable support, from the beginning of this book project to its end.

References

Bartoli F, Buurman P, Delvaux B, Madeira M (2003). Volcanic Soils: Properties and Processes as Function of Soil Genesis and Land Use. Geoderma, Special Issue Vol 117, Elsevier

Arnalds O, Stahr K (2004). Volcanic Soil Resources: Occurrence, Development and Properties. Catena, Special Issue Vol 56, Elsevier

Contents

I. European Volcanic Soil Resources

Ed.: O. Arnalds

II. Reference Pedons: morphology, mineralogy and classification

Ed.: G. Stoops

III. Reference Pedons: chemical and biological characteristics

Ed.: P. Buurman

IV. Reference Pedons: physical characteristics

Ed.: F. Bartoli

V. Volcanic Soils and Land Use

Ed.: H. Oskarsson

Contributors

P. ADAMO

Department of Soil, Plant and Environmental Science, University of Naples Federico II, Via Università, 100 – 80055 Portici (NA) – Italy
adamo@unina.it

O. ARNALDS

Agricultural University of Iceland, Department of Natural Resources and Environmental Sciences, Keldnaholt, IS-112 Reykjavík, Iceland
ao@lbhi.is

E. AUXTERO

Instituto Superior de Agronomia, Departamento de Ciências do Ambiente, Tapada da Ajuda, 1349-017, Lisboa, Portugal
eauxtero@iol.pt

J. BALKOVIČ

Department of Soil Science, Faculty of Natural Sciences CU, Mlynská dolina, 842 15 Bratislava 4, Slovak Republic
balkovic@vupu.sk

V. BARRÓN

Departamento de Ciencias y Recursos Agrícolas y Forestales, Universidad de Córdoba, Apdo 3048 Córdoba, Spain
vidal@uco.es

F. BARTOLI

Laboratoire Sols et Environnement UMR 1120 ENSAIA - INPL/INRA, BP 172, 54505 Vandoeuvre les Nancy Cedex, France
Francois.Bartoli@ensaia.inpl-nancy.fr

A. BASILE

Istituto per i Sistemi Agricoli e Forestali del Mediterraneo – Consiglio Nazionale delle Ricerche (ISAFOM-CNR), Via Patacca 85, 80056 Ercolano, NA, Italy
a.basile@ispaim.na.cnr.it

G. BURTIN†

Passed away January 2004

P. BUURMAN

Department of Environmental Sciences, Laboratory of Soil Science and Geology, Wageningen University, P.O. Box 37, 6700 AA Wageningen, the Netherlands
peter.buurman@wur.nl

W. CHESWORTH

Land Resource Science Department, Ontario Agricultural College, University of Guelph, Guelph, Ontario, N1G 2W1 Canada
wcheswor@lrs.uoguelph.ca

C. COLOMBO

Dipartimento di Scienze Animali Vegetali e dell'Ambiente, Unversità del Molise, Campobasso, 86100 Italy
colombo@unimol.it

A. COPPOLA

Dipartimento per la gestione del territorio agricolo-forestale (DITEC) – Via dell'Ateneo Lucano, 85100 Potenza, Italy
acoppola@unibas.it

C. DAZZI

Dipartimento di Agronomia Ambientale e Territoriale – Università di Palermo, Italy
dazzi@unipa.it

R. DE MASCELLIS

Istituto per i Sistemi Agricoli e Forestali del Mediterraneo – Consiglio Nazionale delle Ricerche (ISAFOM-CNR), Via Patacca 85, 80056 Ercolano, NA, Italy

P. DE PAEPE

Laboratorium voor Mineralogie, Petrologie en Micropedologie, Universiteit Gent, Belgium
paul.depaepe@ugent.be

A. ECONOMOU

National Agricultural Research Foundation / Forest Research Institute of Athens, Terma Alkmanos, 115 28, Ilissia, Athens, Greece
oika@fria.gr

O. FEHÉR

Szent István University, Department of Soil Science and Agrochemistry Gödöllő, Hungary
olenyka@spike.fa.gau.hu

E.A. FITZPATRICK

Department of Plant and Soil Science, University of Aberdeen, Cruickshank Building, St. Machar Drive, Aberdeen, AB24 3UU, UK
e.a.fitzpatrick@btinternet.com

M. FONSECA

Instituto de Investigação Científica Tropical, Lisboa, Portugal
madfons@isa.utl.pt

A. FRASER

Macaulay Land Use Research Institute, Craigiebuckler, Aberdeen, AB15 8QH, UK

GY. FÜLEKY

Szent István University, Department of Soil Science and Agricultural Chemistry, Gödöllő Pater K u 1., H-2103 Hungary
fuleky.gyorgy@mkk.szie.hu

C. GARCÍA

Departamento de Edafoloxía e Química Agrícola, Facultade de Bioloxía, Universidade de Santiago de Compostela, E-15782 Santiago de Compostela, Spain
edcmgp@usc.es

E. GARCÍA-RODEJA

Departamento de Edafoloxía e Química Agrícola, Facultade de Bioloxía, Universidade de Santiago de Compostela, Lope Gómez de Marzoa s/n, Campus Sur, E-15782 Santiago de Compostela, Spain
edcone@usc.es

M. GÉRARD

Institut de Recherches pour le Développement (IRD), 32. avenue Henri Varagnat, Bondy cedex, France
martine.gerard@bondy.ird.fr

J.M. HERNÁNDEZ-MORENO

Dept. Edafología y Geología, Facultad de Biología, Universidad de La Laguna, Tenerife, Spain
jhmoreno@ull.es

M. IAMARINO

Dipartimento di Scienze del Suolo, della Pianta e dell'Ambiente, Università degli Studi di Napoli "Federico II" – Via Università, 100 – 80055 Portici NA, Italy

R. JAHN

Institut für Bodenkunde und Pflanzenernährung, Martin Luther Universität Halle-Wittenberg, Weidenplan 14, 06108 Halle, Germany
reinhold.jahn@landw.uni-halle.de

S. JAKAB

Sapientia University, Targu Mures, Romania
jakab.bocskai@fx.ro

C.C. JIMÉNEZ

Dept. Edafología y Geología, Facultad de Biología, Universidad de La Laguna, Tenerife, Spain
cacojime@ull.es

B. JURÁNI

Department of Soil Science, Faculty of Natural Sciences, Comenius University in Bratislava, Mlynská dolina, 842 15 Bratislava 4, Slovakia
jurani@nic.fns.uniba.sk

Á. KERTÉSZ

Hungarian Academy of Sciences, Geographical Research Institute, Budaörsi út. 45, 1112 Budapest, Hungary
kertesza@helka.iif.hu

M. KLEBER

Earth Sciences Division, Lawrence Berkeley National Laboratory, One Cyclotron Road, 97420 Berkeley, CA, USA
MKleber@lbl.gov

L.N. KONDA

Institute for Veterinary Medicinal Products, 8 Szallas Street, H-1107 Budapest, Hungary
livia@oai.hu

L. LULLI

Instituto Sperimentale per lo studio e la Difesa del Suolo, Piazza Massimo D´azeglio 30, 50 121 Firenze, Italy
l.lulli@aliceposta.it

B. MADARÁSZ

Hungarian Academy of Sciences, Geographical Research Institute, Budaörsi út. 45, 1112 Budapest, Hungary
madaraszb@sparc.core.hu

M. MADEIRA

Instituto Superior de Agronomia, Departamento de Ciências do Ambiente, Tapada da Ajuda, 1349-017 Lisboa, Portugal
mavmadeira@isa.utl.pt

J. MADRUGA

Universidade dos Açores, Departamento de Ciências Agrárias, Terra Chã, 9700 Angra do Heroísmo, Portugal
madruga@notes.angra.uac.pt

P. MAGLIULO

Istituto per i Sistemi Agricoli e Forestali del Mediterraneo, Consiglio Nazionale delle Ricerche, (CNR-ISAFoM) – Via Patacca, 85 – 80056 Ercolano NA, Italy

A. MARTÍNEZ-CORTIZAS

Departamento de Edafoloxía e Química Agrícola, Facultade de Bioloxía, Universidade de Santiago de Compostela, Facultad de Biología, Campus Sur, E-15782 Santiago de Compostela, Spain
edantxon@usc.es

L. MATOS

Universidade dos Açores, Departamento de Ciências Agrárias, Terra Chã, 9700 Angra do Heroísmo, Portugal

E.L. MEIJER

Laboratory of Soil Science and Geology, Wageningen University, P.O. Box 37, 6700 AA Wageningen, the Netherlands
ed.meijer@bodeco.beng.wau.nl

G. MELE

Istituto per i Sistemi Agricoli e Forestali del Mediterraneo – Consiglio Nazionale delle Ricerche (ISAFOM-CNR), Via Patacca 85, 80056 Ercolano, NA, Italy
g.mele@isafom.cnr.it

P. MICHOPOULOS

N.AG.RE.F. / Forest Research Institute, Terma Alkmanos, Ilissia, 115 28 Athens, Greece
mipa@fria.gr

F. MONTEIRO

Instituto Superior de Agronomia, Departamento de Ciências do Ambiente, Tapada da Ajuda, 1349-017 Lisboa, Portugal
fgmonteiro@isa.utl.pt

K.G.J. NIEROP

IBED-Physical Geography, University of Amsterdam, Nieuwe Achtergracht 166, 1018 WV Amsterdam, the Netherlands
k.g.j.nierop@science.uva.nl

J.C. NÓVOA

Área de Edafoloxía, Depto. Bioloxía Vexetal e Ciencias do Solo, Facultade de Ciencias de Ourense, Universidade de Vigo, As Lagoas s/n, 32004 Ourense, Spain

J.C. NÓVOA-MUÑOZ

Dept. de Edafoloxía e Química Agrícola, Facultade de Bioloxía, Universidade de Santiago de Compostela, Campus Sur s/n 15706, Santiago de Compostela, Galicia, Spain
edjuanca@usc.es

H. OSKARSSON

Agricultural University of Iceland, Department of Natural Resources and Environmental Sciences, Keldnaholt, IS-112 Reykjavík, Iceland
hlynur@lbhi.is

G. PALUMBO

Dipartimento di Scienze Animali Vegetali e dell'Ambiente, Unversità del Molise, Campobasso, Italy

D. PATERAS

National Agricultural Research Foundation / Forest Research Institute of Athens, Terma Alkmanos, 115 28, Ilissia, Athens, Greece
pateras@nagref.gr

S. PEPE

Dipartimento di Scienze del Suolo, della Pianta e dell'Ambiente, Università degli Studi di Napoli "Federico II" – Via Università, 100 – 80055 Portici NA, Italy

J. PINHEIRO

Universidade dos Açores, Departamento de Ciências Agrárias, Terra Chã, 9700 Angra do Heroísmo, Portugal
jpinheiro@angra.uac.pt

X. PONTEVEDRA

Dept. de Edafoloxía e Química Agrícola, Facultade de Bioloxía, Universidade de Santiago de Compostela, Campus Sur s/n 15706, Santiago de Compostela, Galicia, Spain
edpombal@usc.es

P. QUANTIN

5, rue Boileau, F21000 Dijon, France
quantin.paul@wanadoo.fr

C. REGALADO

Instituto Canario de Investigaciones Agrarias (ICIA), Dep. Suelos y Riegos, Apdo 60 La Laguna, 38200 Tenerife, Spain
cregalad@icia.es

M.V. SELLITTO

Dipartimento di Scienze Animali Vegetali e dell'Ambiente, Unversità del Molise, Campobasso, 86100 Italy

V. SIMOES

Universidade dos Açores, Departamento de Ciências Agrárias, Terra Chã, 9700 Angra do Heroísmo, Portugal

A. SKOUTERI

N.AG.RE.F. / Forest Research Institute, Terma Alkmanos, Ilissia, 115 28 Athens, Greece
skmi@fria.gr

O. SPAARGAREN

ISRIC – World Soil Information, World Data Centre for Soils, P.O. Box 353, 6700 AJ Wageningen, the Netherlands
otto.spaargaren@wur.nl

G. STOOPS

Laboratorium voor Mineralogie, Petrologie en Micropedologie, Universiteit Gent, Krijgslaan 281, S8, Belgium
stoops.georges@skynet.be

T. TABOADA

Dept. Edafoloxía e Química Agrícola, Facultade de Bioloxía, Universidade de Santiago de Compostela, 15782 Santiago de Compostela, Spain
edteresa@usc.es

H. TANNEBERG

Institute of Soil Science and Plant Nutrition, University of Halle-Wittenberg, Weidenplan 14, D-06108 Halle (Saale), Germany
Tannebg@mluagis1.landw.uni-halle.de

M. TEJEDOR,

Dept. Edafología y Geología, Facultad de Biología, Universidad de La Laguna, Tenerife, Spain
martesa@ull.es

F. TERRIBILE

Dipartimento di Scienze del Suolo della Pianta e dell'Ambiente, Università di Napoli Federico II, Via Universitá 100, 80055 Portici NA, Italy
terribil@unina.it

J.D.J. VAN DOESBURG

Laboratory of Soil Science and Geology, Department of Environmental Sciences, Wageningen University, P.O. Box 37, 6700 AA Wageningen, the Netherlands
jan.vandoesburg@hetnet.nl

A. VAN DRIESSCHE

Laboratorium voor Mineralogie, Petrologie en Micropedologie, Universiteit Gent, Krijgslaan 281, S8, B-9000 Gent, Belgium

F. VAN OORT

INRA, Unité de Science du Sol, RD-10, 78026 Versailles, France

EV. VAVOULIDOU

National Agricultural Research Foundation / Forest Research Institute of Athens, Terma Alkmanos, 115 28, Ilissia, Athens, Greece
ssia@otenet.gr

S. VINGIANI

Dipartimento di Scienze del Suolo, della Pianta e dell'Ambiente, Università degli Studi di Napoli "Federico II" – Via Università, 100 – 80055 Portici NA, Italy

M. ZAMPELLA

Department of Soil, Plant and Environmental Science, University of Naples Federico II, Via Università, 100 – 80055 Portici (NA) – Italy
mvzampel@unina.it

I. European Volcanic Soil Resources

Ed.: O. Arnalds

Introduction to Section I. European Volcanic Soil Resources

Olafur Arnalds

Introduction

The first section of this book, titled European Volcanic Soil Resources, provides a unique compilation of papers describing soils of volcanic regions in Europe. The widely scattered distribution of volcanic soils in Europe may come as a surprise to many readers, but most of these areas are relatively small, especially in Central Europe. Iceland represents by far the largest volcanic area, of about 100,000 km^2, while the largest area on the continent is in France.

The papers in this section describe soils and environments of volcanic areas of mainland Europe and of the Atlantic islands, including the Azores, Canaries, and Madeira Islands. The papers give vital background information about the volcanic soils of Europe and the environments that have shaped these soils, enhancing the usefulness of the subsequent chapters, which deal with the COST-reference pedons from these countries in greater detail. However, the papers not only describe soils; due to the origin of the volcanic soils, most of the papers have sections describing the volcanism in these areas, enriching the book with geological accounts of recent volcanisms in Europe. Sections on vegetation, climate, and land use are present, but more detailed papers on land use considerations are found in the last section of this book.

Many of the papers have sections explaining the history of the study of volcanic soils in each country, which in some cases are presented in English for the first time. These accounts are extremely valuable for casting light on the progression of the study of volcanic soils in general, in addition to being important for soil science in each of the countries. The literature reviews which the papers provide are also quite important for students and future research of volcanic soils in Europe.

The papers vary considerably in how the subject is treated. Many adhere to classical explanation of soil genesis such as by emphasis on the state factors (soil forming factors). The papers reflect great differences in scholarly approach, general perception about soil formation, and training among

the various European countries. These differences, however, are worth consideration.

The papers

France has the largest area of volcanic soils in continental Europe (about 6000 km^2) – a fact that otherwise might elude many. The French paper is presented by Paul Quantin who gave many European soil scientists graduate training in the field of volcanic soils, including to some of the authors of this book. Quantin's paper adds new information to his previous overview of volcanic soils in France (Quantin 2004), including classification aspects of the French reference pedons.

The paper by Lugiano Lulli is of particular interest for many reasons. It summarizes many important studies of Italian volcanic soils mostly unavailable before to the general reader outside of Italy, and provides additional new information. The same can be stated for the Slovakian paper by Juráni and Balkovic and the Hungarian paper by Füleky et al., which is extended to the Carpathian basin; both are very significant contributions to knowledge of volcanic soils in Europe.

Economou et al. give a short overview of the volcanic soils of Greece, which rarely if at all qualify as Andosols but many are vitric in nature. Andosols are also rare in Germany, but the story of their study has many interesting aspects, both historical and scientific.

A detailed account of soils of the volcanic North-Atlantic islands is provided, in papers by Madeira et al. for the Azores and Madeira Islands by Tejedor et al. for the Canary Islands, and Arnalds and Oskarsson for Iceland.

Notes on soil genesis

The soils described have evolved under a wide range of climatic conditions, ranging from the Mediterranean to sub-Arctic Iceland; the parent materials are often of contrasting chemical and morphological composition, and age is also considerably varied. Some areas are subjected to periodic rejuvenation of volcanic materials on the surface, while other soils have developed in old volcanic parent materials, often reworked by the Quaternary glaciation. Thus, the information portrayed gives rise to possibilities for contrasting environmental conditions of volcanic regions for the better understanding of soil genesis in these areas.

Where soils have had sufficient time or weathering intensity is substantial, the soils are no longer Andosols, as exemplified by many soils discussed in the Italian, Spanish and Portuguese papers. The following discussion in intended to give the less developed volcanic soils more attention, but is by no means intended to be a thorough review of the papers.

Quantin notes that climate, especially udic and perudic moisture regime, are important for the occurrence of Andosols in the volcanic regions of France, but the type of volcanic rock is less important. Rhyolite favors formation of Podzols. Silandosols (allophanic) are found on rather recent pyroclastics while Aluandosols (dominated by metal-humus complexes) have formed on older materials.

Aspect has also important influence on genetic pathways shown in the Canary paper by Tejedor et al., with Andisols reaching further down on the cooler northern slopes.

Kleber and Jahn point out that silandic influences are more dominating in younger soils in Germany and aluandic in older soils. Even so, they conclude that Andosols as such are rare in Germany. Andosols occur in Slovakia, according to Juráni and Balkovic, mostly on andesitic rocks in humid areas at >700–1000 m elevation. It is interesting to note horizons more aluandic in character at higher elevations and silandic in nature at lower because of increase of precipitation with elevation. Andosols are found at intermittent elevations in the volcanic Madeira Islands according to the paper by Madeira et al., often at 400–1200 m elevations. Leptosols are found above the Andosol elevation belt. Andosols are found at all elevations in the Azores where age of the parent materials plays a major role in determining the character of the soils. In the Mediterranean Italy, Andosols occur at higher elevations in relatively humid climates where vitric sources are rejuvenated, according to Lugiano Lulli's thorough review of soil genesis of Italian volcanic systems.

The Icelandic soils have formed in eolian materials consisting mostly of materials and in tephra deposits. Climatic factors and parent materials are not discussed in relation to soil formation in the Icelandic paper. However, it is noted that coarse tehpra layers and silicious tephra layers in profiles are often preserved poorly weathered over many millennia.

The existence of poorly developed Andosols in basaltic vitric materials is both evident in the Canaries (see discussion of Torrents in the Tejedor et al. paper) and in Iceland. However, if the parent materials are more siliceous, the soils do not meet criteria for Andosols, as the soils of Santorini, Greece, which are relatively young in a dry climate. Such poorly developed volcanic soils (qualifying as Andosols or not) are termed Vitrisols by Arnalds and Oskarsson in the Icelandic paper.

Materials on accompanying CD

The attention of the reader should also be drawn to the accompanying CD disk, which has a variety of materials supporting the contents of many of the papers. These include color photographs of soils and landscapes, and tables with a wealth of both descriptive and analytical data for soils of these regions.

Volcanic Soil Resources in France

P. Quantin

Introduction

This paper summarizes informations about volcanic soils observed in the continental country of France and especially for the COST-622 pedons EUR16 and 17, located in the Chaîne des Puys and the Cantal, and on a paleosol (Cut of Puy Courny) near Aurillac, Cantal, in the Massif Central. This paper also provides a background for successive papers that deal with analysis of soils in relation to the COST-622 program and which are discussed in many papers of this book.

The information presented here is partially based on the paper entitled 'Volcanic soils of France' published in Catena (Quantin 2004), which gave an overview on the study of volcanic soils in France which began nearly 40 years before the initiation of the European COST-622 program.

Location and parent materials

Volcanic soils cover about 6000 km^2 in France, or about 1% of the continental area. The largest area is in the Massif Central (>5000 km^2); although isolated small areas of volcanic soils occur also in the Vosges, north-eastern France and the Morvan, mid-eastern France.

Massif Central

In the Massif Central area (Figure 1), volcanism started 65 M y (million years) ago, and was very active from 20 M y to 6000 years BP. We can distinguish the 'old' formations, 20–0.25 M y old, in the regions of Cantal, Cézallier, Mts Dore, Aubrac, Devès, Velay, Vivarais, Coirons and Escandorgue, from the 'recent' formations of the Chaîne des Puys dating from 95,000 to 6000 y BP, where the volcanic shapes of cones, domes and lava flows are still well preserved (de Goër de Herve et al. 1991).

In the Chaîne des Puys (Camus and De Goër de Herve 1995) the surface formations are very recent, from 13,000 to 6000 BP. The composition of

cinders and lava is mostly basaltic or trachyandesitic, but is trachytic on the Puy de Dôme.

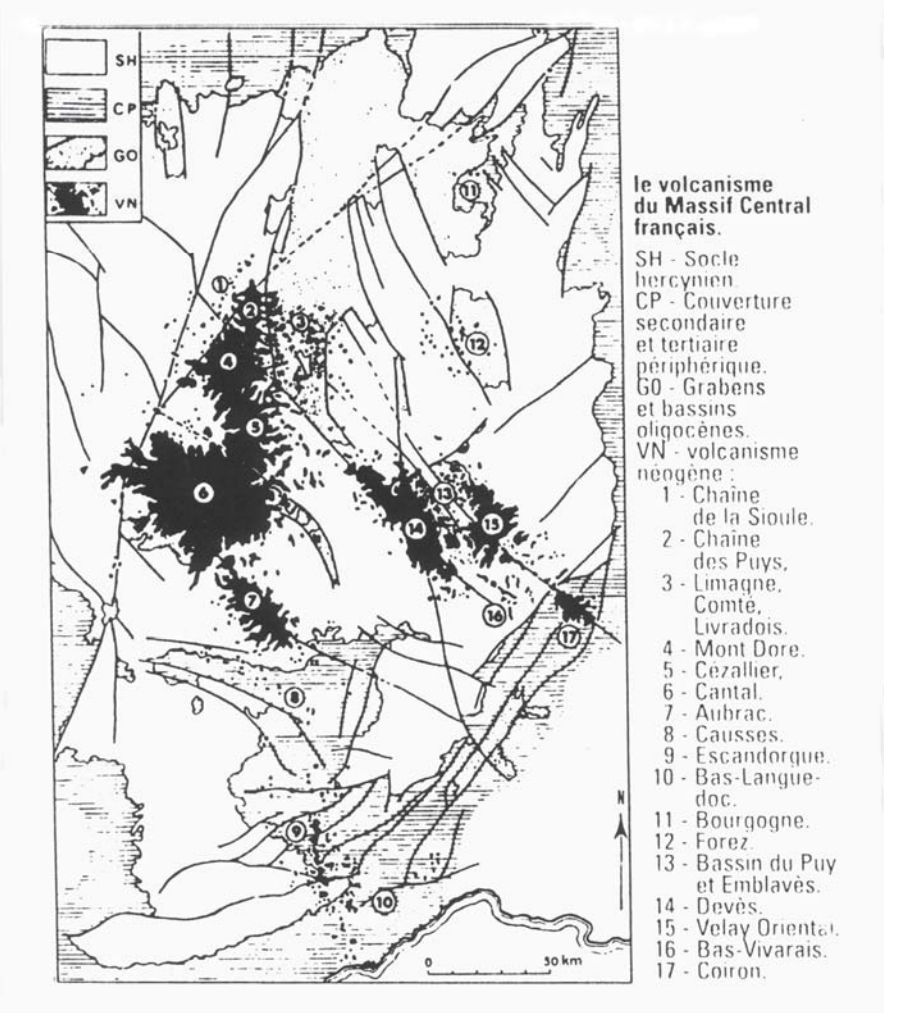

Figure 1. Volcanism of the Massif Central, Central France (De Goër 1995. Adapted from Catena 56(1–3):96, Elsevier, the Netherlands).

The Cantal is a very large stratovolcano (2700 km^2) over a former 'infracantalian' basaltic basement of lava flows, 11 to 7.3 M y old, covering a substratum of granite, metamorphic and sedimentary rocks. The 'cantalian' eruptive formations, 7.3 to 6.4 M y old, consist mostly of pyroclasts of trachyte or latite composition, and of radial lava flows of trachyandesite composition. They end with 'supracantalian' lava flows, 6.4 to 4 M y old,

of trachybasalte or trachyandesite composition (de Goër de Herve 1995, Quantin et al. 2004).

Vosges and Morvan

The Hercynian massif of the Vosges and Morvan areas is mostly composed of sandstones, granite and metamorphic rocks, but some volcanic and volcano-sedimentary rocks crop out over nearly 30% of the area (Aran 1998, Bellier et al. 1989). They are complex and very old volcanic materials, ranging from 400 to 250 M y BP (Devonian, Carboniferous and Permian).

Glacial and periglacial reworking

The old highland surfaces were eroded by glaciers during the Pleistocene (Hétier 1975). After the ice had melted or at the margin of the glaciers, they accumulated glacial and/or periglacial deposits, such as the 'limon à blocs' (loess with blocks of rock), or the 'arène litée' (stratified sand). They overlie weakly weathered and eroded bedrock or a truncated paleosaprolite (C horizon). Therefore, there is often a relationship between the present topsoil and the bedrock as was reported in details by Hétier (1975). These deposits generally appear above 600–700 m elevation in the Morvan and the Massif Central, where andic soils are found.

Soil units and soil classification

French volcanic soils units

In France, before 1995, the 'CPCS Classification des Sols' (1967) was in use for mapping of soil units. That system was improved with increased knowledge, especially for Andosols (Groupe de travail Andosols, CPCS 1972). The volcanic soils of France are related to three soil classes: Andosols, Sols Brunifiés and Sols Podzolisés.

Since 1995, a new 'Référentiel Pédologique' (AFES 1995) is in use. The Andosols are divided into three major groups: Vitrosols, Silandosols (allophanic) and Aluandosols (Al-complexed). The French volcanic soils are related to Andosols, Brunisols and Podzosols. Among them at subgroup level are (French qualifiers): Vitrosols; Silandosols, (eutriques, dystriques or humiques); Aluandosols, (humiques or hapliques); Brunisols,

(mésosaturés (eutriques), oligosaturés (acides), or andiques); and Podzosols (either humiques or hapliques).

French COST-622 reference pedons: EUR16 and 17

Based on earlier studies, two references soil profiles of Andosols were selected in the Massif Central: EUR16, on recent basaltic cinders of the Chaîne des Puys, representative of Silandosols, and EUR17 reference pedon, developed in Miocene basalt lava flow of Cantal, representative of Aluandosols. More details on soil description of these two reference pedons, soil micromorphology, chemical and physical characteristics are reported in the relevant chapters of this book and in its accompanying CD-Rom.

Three systems were used to classify the soils based on diagnostic criteria from the available analytical data: French 'Référentiel Pédologique' (FRP 1995), World Reference Base for Soil Resources (ISSS-ISRIC-FAO 1998, FAO-ISRIC 2001, WRB 2004), and USDA Soil Taxonomy (1994, 2003), termed US-ST 1994 and US-ST 2003 below.

EUR16 COST-622 Reference Pedon

Local data: Puy de la Vache, Chaîne des Puys, downslope of cinder cone dated 7650 BP, altitude 1000 m, udic frigid regime, on basaltic cinders.

Diagnostic criteria: andic throughout 120 cm for all systems; *silandic* for FRP & WRB; *umbric and fulvic* for WRB and US-ST, but either not *pachic* for ST 1994 or *eutric pachic* for ST 2003; *eutric* (from sum of bases > 15 mol kg^{-1}) for FRP, or partially *dystric* for WRB & US-ST (from base saturation <50% or sum of bases >25 cmol kg^{-1}).

FRP (1995): Silandosol eutrique, on recent basaltic cinders.

WRB (2001): Umbri-Silandic Andosol (endoskeletic, endoeutric), (BS >50% down 55 cm), (but near pachic and fulvic). But for WRB 2004, Umbric becomes Pachifulvic.

US-ST (1994): frigid, Typic Fulvudands.

US-ST (2003): Eutric Pachic Fulvudands.

In the French Référentiel Pédologique, Silandosol is at the boundary between eutric for sum of bases >15 cmol kg^{-1} in the top 45 cm, and dystric for base saturation <50% from 10 to 55 cm. The three systems express, although at different levels, some eutric properties of this Andosol, probably related to the young age of basaltic cinders.

EUR17 COST-622 Reference Pedon

L*ocal data*: Buron de Perle, Cantal, on Miocene trachybasalt flow, altitude 1080 m, udic frigid regime, glacial aeolico-colluvial sediment, age of present soil <12,000 BP.

Diagnostic criteria: *andic* throughout the profile for the three systems; *aluandic* to 32 cm for FRP & WRB, then *silandic* down; *alic* to 50 cm for ST; *humique* for FRP; *umbric, fulvic* and *pachic* for WRB & ST (2003) but not *pachic* for ST (1994); *hyperdystrique* (base saturation <10%) for FRP; *dystric, acroxic* for WRB or *acrudoxic* for ST down 50 cm.

FRP (1995): Aluandosol humique hyperdystrique, from glacial sediment on Miocene basalt lava flow.

WRB (2001): Epialuandi-Silandic Andosol (Umbric-near Pachic, Endoacroxic).

WRB (2004): Umbric becomes Pachifulvic.

US-ST (1994): frigid, Alic Fulvudands (near Pachic).

US-ST (2003): frigid Pachic Fulvudands (but also Alic to 50 cm and Acrudoxic down).

The three systems, although at different levels, express the alic properties of this Andosol related to their high content in Al-organic complexes, and to the old age of pre-weathered volcanic parent materials, although the age of present soil is probably less than 12,000 years, due to glacial influences.

Brown soil and red paleosol of the Puy Courny cut

This cut of Puy Courny, located near Aurillac, Cantal, shows a red paleosol over a basalt lava flow, 7.3 M y old, buried by 5 partially altered pyroclasts deposits of quartziferous latite, and the present Brown soil over an upper basalt flow, 6.4 M y old (Quantin et al. 2004). The deep red paleosol, over a green 'alterite' and the lower basalt, is related to Fersialsols, near Ferralsols, while the shallow present soil is classified Brunisol eutrique (Eutric Cambisol). This sequence testifies a great change in climatic conditions and time of weathering. The paleosol signifies a long time under warm, udic regime and a short dry season, such as prevail in many present day tropical soils (Quantin 1992). The Brunisol represents relatively young soils developed under mesic and ustic conditions.

Soil distribution

Publications by Hétier (1975), Moinereau (1977), Lassausse (1991) and Aran (1998), as well as the map explanatory note of Bonfils (1993), can be used to compare climato-topo-sequences of volcanic soils on recent (Holocene) pyroclastic rocks and lavas, with these on Mio-Pliocene and even older volcanic materials (Figure 2).

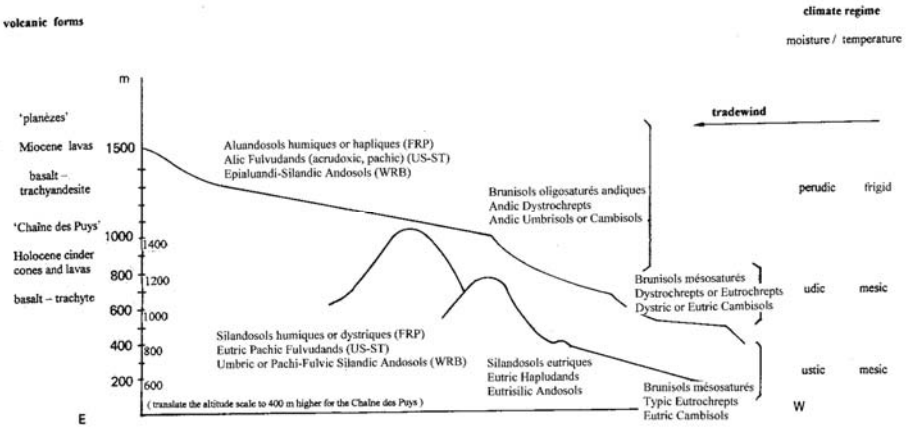

Figure 2. Climato-topo-sequences of Massif Central soils (Quantin 2004. Adapted from Catena 56(1–3):103, Elsevier, the Netherlands).

Recent pyroclastic rocks and lavas in the Chaîne des Puys

Above 800 m elevation, Silandosols predominate on both basaltic and trachytic cinders (Figure 2). Above 1000 m elevation, the Silandosols are dystric and fulvic (umbri-silandic). However on trachytic pumices (at the Puy de Dôme) the pH is lower. Between 800 and 1000 m elevation on recent (6000 BP) basaltic cinders the soil can be eutrisilic. From 400 to 800 m on basalt lava flows, the soils intergrade to Brunisols mésosaturés (Eutric Cambisols).

Miocene lavas in the Cantal and south-eastern Massif Central

Aluandosols (very acid and non-allophanic at least in the topsoil) predominate above 1000 m elevation on basaltic, trachyandesitic, trachytic and even phonolitic lava flows (Figure 2). These soils have fulvic and alic features and are classified as Epialuandi-Silandic Andosols (WRB 2001) or Alic Fulvudands (U.S. Soil Taxonomy 1994). There is a transitional

stage between 800 and 1000 m elevation from Brunisols andiques (Andic Cambisols) to Brunisols oligosaturés (Dystric Cambisols) and sometimes to Brunisols saturés or vertiques (Eutric or Vertic Cambisols) on basaltic lavas and tuffs under the xeric climate of the southern lowlands (Bonfils 1993). On rhyolite, podzolic soils (Haplic Podzols) occur above 800 m elevation and Brunisols oligosaturés at lower elevation (Hétier 1975).

Paleozoic and Permian volcanic materials in the Vosges and Morvan

Aluandosols appear above 700 m elevation only on rocks of rather basic composition (Figure 2). Podzolic soils are found on rhyolitic materials. Transitional andic Brunisols (Andic Cambisols) occur between 700 and 900 m elevation which show some andic features only in the topsoil. The boundary between Aluandosols and andic Brunisols is rather difficult to determine in the field (Aran 1998). However, typical Aluandosols always appear on the wettest and coldest highlands.

Conclusions

In continental France, volcanic soils cover about 6000 km^2, mostly in the Massif Central (>5000 km^2), but also in small area of Vosges and Morvan. Most of these soils are Andosols, although there are also Cambisols (Brunisols) and exceptionally Podzols.

The volcanic soils distribution is fairly well related to the present climato-topo-sequence, as well on recent pyroclasts as on old volcanic or basic metamorphic formations.

The key factor for Andosols occurrence is the climate, and notably udic or perudic moisture regimes. The chemical composition of parent rock has rather weak influences on the soil genesis, except rhyolitic materials, which favour Podzol formation. However, the age of parent rock is important. The Silandosols are related to recent pyroclastics on the Chaîne des Puys. Aluandosols have formed on older compact lavas, but their effective parent material is often a loose pre-weathered volcanic or basic metamorphic material. Their final development occurred during Holocene. The anthropic effects on soil transformation, except erosion or alteration of soil surface properties, are not obvious.

References

AFES (1995). Référentiel Pédologique. INRA Edit pp 332

Aran D (1998). Andosolisation dans les Hautes-Vosges. Conditions de développement et comparaison avec les autres processus de pédogénèse. Thèse Université Nancy I

Bellier G, Leneuf N, Simonot JL, Chrétien J, Meunier D (1989). Journée d'étude dans le Haut-Morvan, 18 octobre 1989, livret-guide AFES section Bourgogne, Dijon

Bonfils P (1993). Lodève. Carte pédologique de France à 1/100 000 °, notice et carte, INRA, Paris

CPCS (1967). Classification des sols. Commission de Pédologie et Cartographie des Sols Lab Géol Pédol, Ecole Nat Sup Agron (Grignon, France) pp 87

CPCS (1972). Groupe de travail Andosols. Proposition de classification des Andosols. Cah ORSTOM, sér Pédologie X 3:303–304

De Goër de Herve A (1995). Les volcans d'Auvergne. Le Cantal. La dépêche scientifique du Parc des Volcans d'Auvergne, N °8 32–35

De Goër de Herve A, Boivin P, Camus G, Gourgaud A, Kieffer G, Mergoil J, Vincent PM (1991). Volcanologie de la Chaîne des Puys. Carte à 1/25 000 ° Volcanologie de la Chaîne des Puys. Publication du Parc Naturel Régional des Volcans d'Auvergne et de l'Université Blaise Pascal, Clermont-Ferrand

FAO-ISRIC et al. (2001). Lecture notes on the Major Soils of the World. World Soil Resources Reports, n ° 94, FAO, Rome, pp 334

Hétier JM (1975). Formation et évolution des andosols en climat tempéré. Thèse, Université Nancy I

ISSS-ISRIC-FAO (1998). World Reference Base for Soil Resources. World Soil Resources Reports, N ° 84, FAO, Rome, pp 88

Lassausse C (1991). Organisation et comportement physico-hydrique comparés de deux sols à structure microagrégée de l'Aubrac (Massif Central, France): sols andiques et sols bruns acides. Thèse Université de Paris 6

Moinereau J (1977). Altération des roches, formation et évolution des sols sur basalte, sous climat tempéré humide (Velay – Vivarais – Coirons). Université des Sciences et Techniques du Languedoc, Montpellier

Quantin P (1992). Les sols de l'Archipel volcanique des Nouvelles-Hébrides (Vanuatu). ORSTOM Paris, Coll. Etudes et Thèses

Quantin P (2004). Volcanic soils of France. Catena 56(1–3):95–109

Quantin P, Dejou J, Tejedor M (2004). Soils and paleosols on volcanic rocks of Cantal (Massif Central, France); example of Puy Courny, Aurillac. Rala Rep no 214. Volcanic Soils Resources in Europe. COST Action 622 final meeting. Abstracts, pp 58–59

USDA Soil Survey Staff (1994). Keys to Soil Taxonomy. 6th edn, 19, Chap 7:89–94

USDA (2003). Keys to Soil Taxonomy. Soil Survey Staff. 9th edn, 2003. USDA-NRCS, Washington, pp 332

WRB (2004). FAO. New recommendations for soil classification. Unpublished

Soils of volcanic regions of Germany

M. Kleber and R. Jahn

Introduction

Quaternary, Tertiary and Palaeozoic eruptions have created a belt of volcanic rocks extending west to east through the center of Germany along a line from Trier to Zittau. Along this line, the majority of volcanic parent materials in Germany occur, covering 7853 km^2 or 2.2% of the national territory (for details see Figure 1 and Table 1 in Kleber et al. 2004).

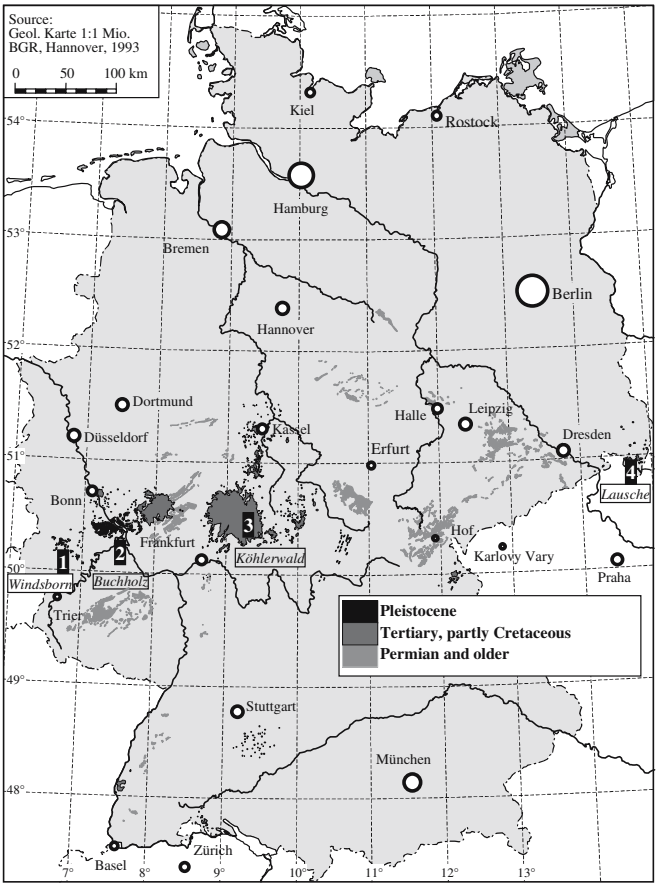

Figure 1. Distribution of volcanic rocks in Germany and location of investigated sites.

Table 1. Important soil parameters based on 1 $m^2 \cdot 1$ m soil (without organic surface layers).

	Rock Fragments	FE_{sil} [1]	Sand	Silt	Clay	OM	$\frac{OM}{Fe_{sil}}$ [2]	$\frac{OM}{Clay}$	Fe_d	$Fe_{o/d}$	$\frac{Fe_d}{Clay}$	Alloph. [3]	$\frac{Alloph.}{Clay}$	$\frac{CaO+MgO+Na_2O+K_2O}{SiO_2}$
	----------		kg m^{-3}			----------			kg m^{-3}			kg m^{-3}		
Windsborn	509	350	119	201	30	16.2	0.05	0.54	7.4	0.51	0.25	28	0.93	0.29
Buchholz	477	729	339	250	140	13.5	0.02	0.10	7.7	0.39	0.05	8	0.06	n.d.
Köhlerwald	107	751	82	517	151	29.9	0.04	0.20	22.7	0.44	0.15	0	0.00	0.08
Lausche	459	312	124	147	40	19.2	0.06	0.48	2.9	0.50	0.07	10	0.25	0.14

1) Silicatic fine earth <2 mm.
2) Organic matter = $C_{org} \cdot 1.724$.
3) Calculated allophane see Table 5.

The sequence of soils presented here follows this line from west to east. Quarternary volcanism, the most important source for easily weatherable, glassy scoria and tephra extends over an area of only 545 km^2 in the Eifel region in the western part of Germany. Here the silandic Andosol '**Windsborn**' (Kleber et al. 2004) has formed in a 30–40,000 year old scoria cone, representing the 'active volcano associated' archetype of volcanic soils.

About 11,000 years ago, a major eruption of alkalic tephra and pumice took place at the Laacher See volcano in the Eastern Eifel Volcano field. The soil '**Buchholz**' is situated about 28 km south of the Laacher See. It has developed from a periglacial mixture of loess and pumice layers, which in turn overlie Devonian schist. This soil has once been famous as the 'locus typicus' of the German Lockerbraunerde (Stöhr 1971).

Basaltic rocks are characteristic of the Vogelsberg, which is situated east of Frankfurt/Main and represents one of the largest volcanic structures (>2000 km^2) in Europe. The Vogelsberg Stratovolcano resulted from Miocene volcanic activity. It reaches an elevation of 774 m above sea level. The basalt is tholeiitic (Schönhals 1986) with a SiO_2 content of 52–55%. The '**Köhlerwald**' soil has developed from periglacial solifluction deposits of basaltic debris with loess admixtures and is the one that inspired Schönhals (1957) to invent the 'Lockerbraunerde' of the German soil taxonomy. It is also the first soil on German territory that has reportedly been connected with andic properties (Meyer and Sakr 1970).

The German/Bohemian mountain range 'Zittauer Gebirge' has been formed by phonolithic Tertiary volcanism that penetrated a Cretaceous sandstone layer, thereby forming several isolated volcanic cones. The summit of the Lausche rises to an elevation of 793 m a.s.l., where a cold

climate regime and intense weathering conditions are encountered. A few meters beneath the summit we found an aluandic, nonallophanic Andosol, the **Lausche** soil (Kleber et al. 2003).

Recognition of soils with andic properties in Germany

German soil scientists, when they first encountered soils with andic properties far away from areas of active volcanism, initially thought they had discovered an entirely new and yet unknown taxonomic soil type. The first to report on this presumably novel soil category was Schönhals (1957). He encountered a soil that had "an intense light brown color and low bulk density extending down the whole soil profile" in the higher reaches of the central German mountain ranges Vogelsberg and Taunus, both of Tertiary age and not related to active volcanism. He further noticed that the prevailing climate should have been favorable for the formation of Spodosols, but that "indications for a vertical translocation of colloidal matter were neither expressed in soil profile morphology nor evident from analytical data".

Schönhals (1957) was most impressed by the extraordinary low bulk density of the newly discovered soil, and his attempt to explain the genesis of the soil focused largely on this particular property. He hypothesized that the accumulation of aeolian sediments (loess) from the last glaciation was the main pedogenetic process, and called the new soil "Lockerbraunerde", which means to indicate that pedogenesis has progressed to a stage where a B-horizon has formed (the Braunerde in the German soil taxonomy or Cambisol of the FAO/WRB system) and is, at the same time, characterized by a low bulk density (indicated by the prefix 'locker').

However, only a couple of years later, while involved in soil mapping activities in the Odenwald region, Bargon (1960) discovered that "Lockerbraunerden" regularly contained fairly high amounts of iron oxides. Bargon (1960) speculated that the high iron oxide contents were inherited from "the lower horizons of a Tertiary, probably lateritic soil". Bargon (1960) synthesized his own observations with the findings of Schönhals (1957) by speculating that the "Lockerbraunerde" of the Vogelsberg region might have resulted from aeolian sediments derived from periglacial solifluction materials especially rich in concretionary iron oxides.

Thus, by the year 1960, soils with an andic character had been recognized on German territory, but were interpreted as some kind of a paleosol, consisting of admixtures of periglacial loess and Tertiary laterites. This understanding was challenged when Stöhr (1963) published the discovery

of "Lockerbraunerden" on volcanic ejecta of Holocene age in the southwestern parts of the mountain range Rheinisches Schiefergebirge. This observation strongly suggested that the accumulation of pedogenic oxides in Lockerbraunerden, as observed by Bargon (1960), was not the result of inheritence from Tertiary laterites, but of a special kind of Holocene pedogenesis.

The first to relate certain special weathering conditions to the genesis of Lockerbraunerden was Brunnacker (1965), who had observed that the occurrence of Lockerbraunerden on the granite rocks of the "Bayerischer Wald" mountains was restricted to an elevation range from 800 to 1150 meters above see level. Brunnacker (1965) further related the "permanently high soil moisture content, which, however, must not result in high levels of percolation" to the intense weathering of iron containing primary minerals. He used this concept to explain the:

1. absence of evidence for the vertical translocation of colloids (= absence of spodic properties)
2. enrichment of iron oxides within the soil
3. low bulk density as a result of the disintegration/dissolution of iron containing primary minerals

At about the same time, the first publication appears that reports on the occurrence of imogolite (Jaritz 1968) in soils developed from tephra and pumice deposited by the eruption of the Laacher See volcano about 11,000 BP. One particular site (soil 'Buchholz', Stöhr 1971) was even advertised as the "locus typicus" of the German Lockerbraunerde. This designation, however, was based mainly on bulk density information and morphological evidence rather than on chemical analyses (neither information on Al_o+½Fe_o nor determination of phosphate retention and glass content).

By now, the German soil science community had become aware of the developments leading to the inclusion of the Andepts and later the Andisol in the US Soil Taxonomy (Soil Survey Staff 1960), and Meyer and Sakr (1970) recognized that the properties of the German Lockerbraunerde were strikingly similar to those lined out for the Andisol of the US Soil Taxonomy (Soil Survey Staff 1967). Meyer and Sakr (1970), who were working at the same Vogelsberg soil consociation as Schönhals (1957), developed the hypothesis that the genesis of the Lockerbraunerde might be a consequence of a "large contribution of easily weatherable magmatites (trachytes, basaltic debris, tephra) to the soil parent material". They further hypothesized that the special physical properties of the Lockerbraunerde were a result of the presence of so-called "structure stabilizers" (in German "Gefüge-Stabilisatoren"). They used this term to include iron oxides, allophane and other "free amorphous aluminium phases", which they believed

to have developed in the course of pedogenesis from the easily weatherable "vulcanitic" constituents of the parent material. Thus, Meyer and Sakr (1970) were first to relate a soil on German territory with the Andisols of the US Soil Taxonomy (Soil Survey Staff 1967).

Prior to the work of Shoji and Ono (1978), both the Andisols of the US Soil Taxonomy (Soil Survey Staff 1975) and the Andosols of the FAO/Unesco system (FAO/Unesco 1974) were considered as having a short-range order type mineralogy with allophane and/or imogolite as the dominating mineral phase (allophane being a metastable aluminosilicate forming tiny spheres with a diameter of approx. 5 nm, while imogolite forms elongated tubes of similar diameter). Therefore, Meyer and Sakr (1970) searched for and eventually diagnosed the presence of allophane in their soils. However, they arrived at this conclusion having used a chemical extraction procedure that is today known to dissolve and extract much more mineral constituents than just the metastable allophane (initial extraction with boiling NaOH, subsequent extraction at 400°C, Hashimoto and Jackson 1960).

The idea that the special properties of the Lockerbraunerde might result from the presence of allophane had to be discarded when Wilke and Becher (1980) succeeded to prove that the soil "Köhlerwald/Hoherodskopf", on whose investigation Meyer and Sakr (1970) had based their conclusions, contained large amounts of amorphous mineral constituents but no allophane. Wilke and Becher (1980) now explained the extraordinary low bulk density of the soil through micromorphological evidence of what they called "humic microaggregates" (in German 'humose Feinstaggregate') but offered no explanation for the formation of such microaggregates.

During the following years, reports on the occurrence of Lockerbraunerden in Germany have accumulated (for list of locations see Kleber et al. 2003), mainly as the result of research concerning periglacial solifluction layers of mixed mineralogy in the higher areas of mountain ranges. Most of these reports are based on soil color, a high organic matter content and often estimated but seldom measured low bulk density. None of the reports on Lockerbraunerden available prior to the year 2001 contained the analytical data necessary to determine whether the respective soils might qualify as either silandic or aluandic andosols with respect to the FAO/WRB soil classification system.

Andic properties

To qualify as Andosols in the WRB (ISSS-ISRIC-FAO 1998), volcanic soils need to contain either large amounts of unweathered volcanic glass (a vitric horizon) or exhibit andic properties. Figure 2 shows the extent, to which the selected German volcanic soils conform to the andic properties as required by the WRB.

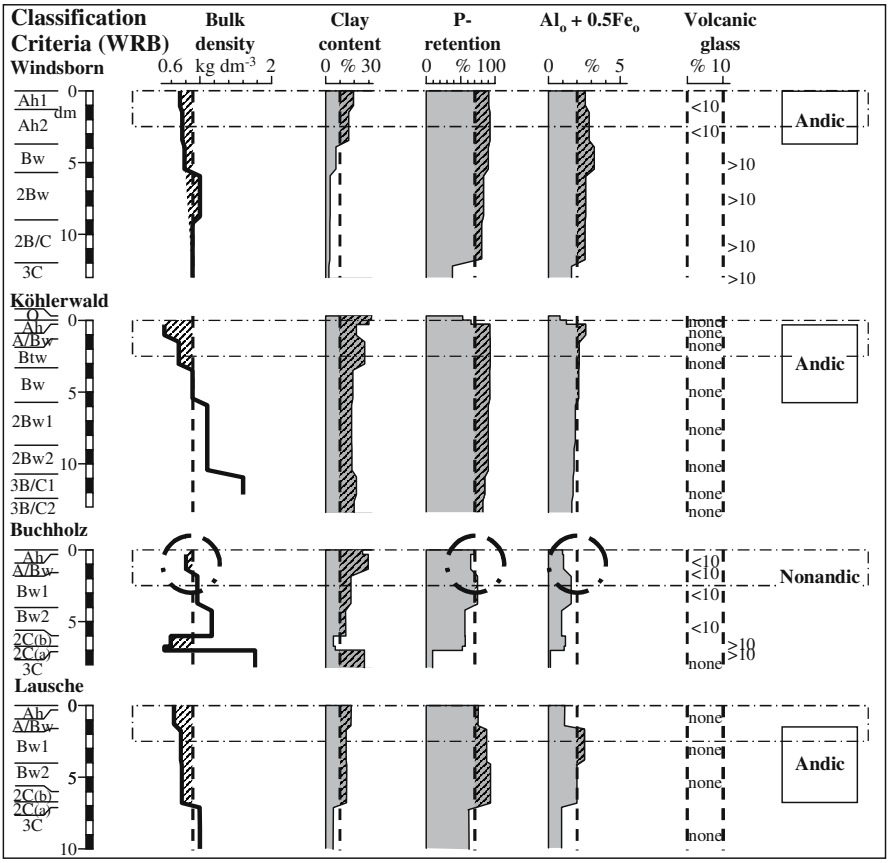

Figure 2. Andic properties of German volcanic soils.

The formation of poorly crystalline minerals is most developed in the silandic Windsborn as indicated by the Al_o+½Fe_o criterion. The former 'locus typicus' of the German Lockerbraunerde, the Buchholz soil, is the one in this selection of four soils that fails to meet the requirements for an andic horizon, although its mineral matrix shows clear indications for the presence of poorly crystalline components (P_{ret} and Al_o+½Fe_o values in the

Bw1 horizon). The soils from the basaltic (Köhlerwald) and phonolithic (Lausche) parent materials easily match the required values and both show a greater vertical extension of andic properties than the silandic Windsborn. This is presumably a consequence of the more intense weathering conditions prevailing at these sites.

Pedogenesis

The formation of both (1) poorly crystalline mineral phases and (2) metal-organic complexes is clearly related to weathering intensity. The rate of weathering (and thus the release rate of elements) is mainly a function of (1) the stability of primary minerals and (2) climate. Volcanic glass (Windsborn, Buchholz) is kinetically much less stable than basaltic (Köhlerwald) and phonolitic (Lausche) rocks. Climatic conditions indicate that weathering intensity increases from Buchholz (mean annual precipitation, MAP= 660 mm; mean annual air temperature, MAT= 7.9°C) to Windsborn (800 mm / 7°C) to Lausche (900 mm / 5.5°C) to the Köhlerwald site (1200 mm / 5.5°). Both rate controlling factors – stability of primary minerals and climate have interacted through time to create an allophane containing (silandic) Andosol at the Windsborn site. Periglacial incorporation of Devonian schist and late glacial additions of loess together with a lack of moisture have restrained the release rates of elements and the precipitation of metastable short range order phases at Buchholz, which otherwise would probably have developed silandic properties as well.

Metal-humus dominated, aluandic soils have developed at the Köhlerwald and the Lausche. A number of indices suggest that soil development at the Köhlerwald site has been in progress for a much greater time interval than at the other three sites. The soil has accumulated the largest amount of clay, the greatest amount of pedogenic iron oxides and shows the lowest rock fragment content (Table 1). It is the most acid of the four profiles and ΔpH values that are only slightly negative corroborate that it is an old and highly weathered soil.

The Lausche soil seems to be much younger than the Köhlerwald and derived from more recent (on a geological time scale) periglacial layers as indicated by the high rock fragment content. It contains much less crystalline iron oxides and, additionally, tubular halloysite (Kleber et al. 2003). Tables 2–5 represent the soil profile data of the four soils selected for this review.

Table 2. Soil texture and bulk density.

Horizon[1)]	Depth cm	Particle size distribution (fine earth; µm) <2 clay	2–6.3	6.3-20	20–63	63–200	200–630	630–2000	Rock fragments Weight %	Bulk density g cm^{-3}
			Silt			Sand				
		%								
Windsborn										
Ah 1	0–13	19	13	15	20	10	13	9	50	0.8
Ah 2	13–37	16	15	17	23	10	11	8	59	0.8
Bw	37–57	7	8	15	38	14	10	8	52	0.8
2Bw	57–90	3	3	8	48	17	11	9	62	1.0
2B/C	90–120	3	3	7	50	19	9	9	64	0.9
3C	>120	2	1	1	4	7	20	65	88	0.9
Buchholz										
Ah	0–3	26	12	7	13	11	21	10	10	0.6[2)]
A/Bw	3–16	30	8	9	11	11	22	9	14	0.81
Bw1	16–40	18	9	9	13	15	25	12	13	0.96
Bw2	40–68	14	7	9	15	17	31	9	9	1.16
2C(a)	68–70	6	3	5	4	3	18	60	28	0.51
2C(b)	68–70	5	4	6	9	9	44	24	87	0.51[2)]
3C	>70	27	15	18	18	7	6	9	74	1.77
Köhlerwald										
O	3–0	32	11	22	27	4	2	1	11	n.d.
Ah	0–3	30	12	24	27	4	2	1	7	0.3[2)]
A/Bw	3–13	22	14	26	29	5	3	1	12	0.5
Btw	13–33	27	15	24	26	4	3	1	11	0.7
Bw	33–57	19	14	27	29	6	4	1	9	0.9
2Bw1	57–87	18	14	28	28	7	4	1	16	1.1
2Bw2	87–107	18	13	26	30	7	4	2	11	1.1
3B/C1	107–124	22	9	18	30	12	7	2	43	1.6
3B/C2	>124	20	9	17	27	13	10	3	54	n.d.
Lausche										
Ah	0–15	18	9	15	24	11	12	11	40	0.62
BA	15–40	13	10	17	21	11	14	15	37	0.71
Bw	40–70	14	9	16	24	10	12	15	46	0.73
Cw	70–100	5	5	10	26	16	19	19	85	1.0[2)]

1) According to FAO 1990.
2) Assumed for calculation of Table 2.

Table 3. Organic matter, exchange properties and plant available nutrients.

Depth cm	C_{org}	N_{org}	C/N	Ca^{2+}	Mg^{2+}	K^+	Na^+	EA	ECEC	PCEC	pH H_2O	pH KCl	ΔpH	pH NaF	FRI	P_{ret}
	g kg^{-1}			cmol$_c$ kg^{-1}										mol g^{-1}	%	
Windsborn																
0–13	71	4.5	16	7.0	1.6	0.4	0.1	0.5	9.6	39	5.6	4.6	–1.0	10.3	3.08	90
13–37	38	2.7	14	1.9	0.7	0.1	0.1	0.7	3.6	29	5.6	4.5	–1.1	10.5	3.16	92
37–57	14	1.1	13	3.1	1.1	0.1	0.1	0.1	4.5	22	6.2	5.5	–0.7	10.5	4.21	90
57–90	11	0.7	16	5.6	1.7	0.2	0.1	0.1	7.6	20	6.6	5.5	–1.1	10.4	3.99	83
90–120	9	0.6	15	6.0	1.6	0.2	0.1	0.1	8.0	22	6.7	5.7	–0.9	10.4	3.42	80
>120	5	0.2	29	2.6	0.5	0.3	0.0	0.7	4.1	n.b.	6.4	5.8	–0.6	7.7	2.52	38
Buchholz																
0–3	96	5.5	17	1.2	0.5	0.5	0.2	8.2	10.6	n.b.	4.4	3.6	–0.8	8.5	0.91	69
3–16	18	1.5	12	0.2	0.1	0.3	0.2	5.5	6.1	n.b.	4.4	3.8	–0.6	9.7	1.36	64
16–40	10	1.1	9	0.1	0.0	0.2	0.1	3.8	4.3	n.b.	4.4	4.0	–0.4	10.1	2.15	74
40–68	8	0.9	9	0.5	0.2	0.6	0.4	3.5	5.2	n.b.	4.6	3.8	–0.8	9.6	1.90	56
68–70	4	0.5	8	1.3	0.1	1.7	0.5	2.1	5.7	n.b.	5.1	3.8	–1.3	10.0	3.21	52
68–70	4	0.7	6	0.7	0.1	1.2	0.4	3.9	6.2	n.b.	n.d.	4.0	n.d	10.3	3.00	57
>70	2	n.d.	n.b.	5.1	4.3	0.3	0.2	0.7	10.6	n.b.	5.8	3.6	–2.2	7.6	0.26	9
Köhlerwald																
3–0	230	9.6	24	10.0	4.4	0.3	0.0	10.3	25.0	n.b.	4.3	3.3	–1.0	6.8	0.18	53
0–3	162	6.1	27	4.1	3.1	0.1	0.0	15.0	22.4	47	4.3	3.2	–1.1	7.4	0.32	65
3–13	78	3.2	24	0.2	0.4	0.0	0.0	10.8	11.4	30	4.6	3.9	–0.7	11.1	1.50	92
13–33	33	1.6	21	0.1	0.1	0.0	0.0	7.1	7.4	n.b.	4.6	4.1	–0.5	11.1	1.42	93
33–57	16	1.1	14	0.0	0.1	0.0	0.0	6.0	6.2	19	4.5	4.1	–0.4	11.1	1.55	92
57–87	13	1.2	11	0.0	0.2	0.0	0.0	5.8	6.0	17	4.3	4.2	–0.1	11.2	1.52	90
87–107	15	1.4	10	0.1	0.1	0.1	0.0	5.9	6.1	n.b.	4.5	4.1	–0.3	11.2	1.91	90
107–124	3	0.3	10	0.1	0.3	0.1	0.0	10.1	10.7	24	4.5	3.9	–0.6	10.7	1.46	85
>124	3	0.3	12	1.2	1.8	0.1	0.0	8.2	11.3	25	5.1	4.0	–1.1	10.4	1.55	82
Lausche																
0–15	59	4.4	13	1.4	0.1	0.5	0.1	n.b.	n.b.	59	4.5	3.7	–0.8	10.5	0.85	76
15–40	38	2.3	16	1.0	0.0	0.4	0.1	n.b.	n.b.	55	4.9	4.1	–0.8	11.3	2.94	88
40–70	28	2.0	14	1.7	0.1	0.2	0.1	n.b.	n.b.	52	5.2	4.1	–1.1	11.2	2.77	93
70–100	8	0.5	14	3.8	0.3	0.2	0.2	n.b.	n.b.	30	5.4	4.1	–1.3	10.7	1.06	62

EA = Exchangeable acidity.
ECEC = Effective cation exchange capacity (NH_4Cl; Schlichting et al. 1995[5.4.3.5]).
PCEC = Potential cation exchange capacity (NH_4Ac/NaAc; ISRIC 1992).
FRI = Fluoride reactivity index (Perrott et al. 1976).
P_{ret} = Phosphate retention (Blakemore et al. 1987).

Table 4. Chemical characterisation.

Depth cm	Element fractions[1]							Total contents[2]									
	Si_o	Fe_o	Al_o	Fe_d	Al_d	Fe_p	Al_p	Al_2O_3	SiO_2	Fe_2O_3	MnO	CaO	MgO	Na_2O	K_2O	P_2O_5	ZrO_2	TiO_2
	g kg^{-1}																	
Windsborn																		
0–13	7.6	11.4	20.2	22.2	16.2	3.6	7.9	187	407	137	2.7	69	36	6	16	9.7	0.79	29
13–37	8.4	12.5	22.0	24.6	20.1	2.5	5.9	190	431	133	2.4	66	47	7	17	9.1	0.76	29
37–57	13.3	12.2	25.4	22.2	21.0	0.5	2.2	196	465	127	2.2	70	37	6	16	9.9	1.23	29
57–90	13.3	8.0	21.7	16.5	13.6	0.1	1.3	177	512	103	1.7	72	47	7	15	9.9	1.04	24
90–120	13.2	8.0	21.3	16.7	13.6	0.1	1.4	174	505	105	1.8	75	48	7	15	10.1	1.00	25
>120	10.1	5.2	13.2	8.9	5.9	0.1	0.6	141	428	147	2.3	110	75	17	21	9.1	0.53	30
Buchholz																		
0–3	2.2	5.1	7.3	12.2	6.4	5.8	13.5											
3–16	2.8	4.9	8.2	11.5	4.4	4.0	11.3											
16–40	6.8	5.1	13.1	10.7	4.2	1.6	5.7											
40–68	3.3	4.3	6.9	9.8	3.0	2.4	8.0											
68–70	5.6	1.6	10.8	3.6	1.2	0.3	1.4											
68–70	5.4	1.9	11.1	4.9	1.7	0.3	1.7											
>70	0.4	1.4	0.7	10.1	0.8	1.9	3.6											
Köhlerwald																		
3–0	0.6	8.3	3.8	16.4	4.1	11.3	5.3	99	378	74	0.6	9	6	4	11	4.1	0.77	18
0–3	1.7	14.4	5.1	23.5	5.1	17.2	10.2	111	398	94	0.8	8	8	3	11	3.7	0.86	21
3–13	2.8	17.6	17.1	33.6	16.0	22.7	30.8	162	380	99	1.0	4	8	3	11	2.9	0.99	19
13–33	3.9	14.5	14.1	33.2	12.4	16.4	24.9	177	459	97	1.3	4	10	4	14	3.1	1.14	19
33–57	6.1	13.3	14.1	27.6	9.4	8.8	13.1	186	500	98	1.8	4	12	4	17	3.6	1.23	19
57–87	4.9	11.5	13.1	27.6	9.7	6.8	9.7	186	487	95	2.0	4	12	4	20	4.7	1.20	19
87–107	4.2	11.1	12.4	29.5	10.2	7.3	10.0	188	493	102	2.3	5	13	4	20	5.0	1.26	20
107–124	6.0	16.5	8.9	56.4	8.0	3.3	7.1	209	425	179	3.2	5	15	2	13	6.3	1.18	34
>124	5.2	15.1	8.5	71.8	9.0	3.9	7.2	205	391	218	2.1	3	12	0	10	7.1	1.06	33
Lausche																		
0–15	1.3	5.4	9.0	11.1	8.3	5.2	8.8	173	432	73	1.9	11	12	11	30	5.9	1.41	16
15–40	8.4	4.5	22.5	7.8	11.5	3.3	10.9	216	437	59	1.4	10	11	9	32	6	1.80	12
40–70	5.2	4.5	17.3	9.5	9.9	4.7	12.0	215	428	77	2.2	11	11	9	30	6	1.73	16
70–100	2.2	1.9	8.0	5.7	3.1	1.4	3.3	191	529	75	1.6	17	14	12	37	3.1	2.47	18

1) Blakemore et al. 1987.
2) X-Ray fluorescence.

Table 5. Short range order components.

Depth cm	Fe_o-Fe_p	Fe_d-Fe_o	Al_o-Al_p	Al_o+½Fe_o	Fe_o/Fe_d	Al_p/Al_o	$(Al_o$-$Al_p)/Si_o$	Calculated Allophane	Calculated Ferrihydrite
	g kg^{-1}								
Windsborn									
0–13	8	11	12	26	0.51	0.4	1.6	50	19
13–37	10	12	16	28	0.51	0.3	1.9	62	21
37–57	12	10	23	32	0.55	0.1	1.7	92	21
57–90	8	9	20	26	0.49	0.1	1.5	85	14
90–120	8	9	20	25	0.48	0.1	1.5	84	14
>120	5	4	13	16	0.59	0.0	1.3	59	9
Buchholz									
0–3	neg	7	neg	10	0.42	1.9	neg		9
3–16	1	7	neg	11	0.43	1.4	neg		8
16–40	3	6	7	16	0.47	0.4	1.1	38	9
40–68	2	6	neg	9	0.43	1.2	neg		7
68–70	1	2	9	12	0.46	0.1	1.7	38	3
68–70	2	3	9	12	0.38	0.2	1.7	37	3
>70	neg	9	neg	1	0.13	5.3	neg		2
Köhlerwald									
3–0	neg	8	neg	8	0.51	1.4	neg		14
0–3	neg	9	neg	12	0.61	2.0	neg		25
3–13	neg	16	neg	26	0.53	1.8	neg		30
13–33	neg	19	neg	21	0.44	1.8	neg		25
33–57	5	14	1	21	0.48	0.9	0.2		23
57–87	5	16	3	19	0.42	0.7	0.7		20
87–107	4	18	2	18	0.38	0.8	0.6		19
107–124	13	40	2	17	0.29	0.8	0.3		28
>124	11	57	1	16	0.21	0.8	0.3		26
Lausche									
0–15	0	6	0	12	0.49	0.98	0.1		9
15–40	1	3	12	25	0.58	0.48	1.4	51	8
40–70	neg	5	5	20	0.47	0.69	1.0	29	8
70–100	1	4	5	9	0.33	0.41	2.1	18	3

Allophane = $100/[-5.1 \cdot (Al_o\text{-}Al_p)/Si_o)+23.5] \cdot Si_o$.
Ferrihydrite = $(Fe_o) \cdot 1.72$.
neg = Calculation leads to negative value.

Conclusion

There are limited occurrences of vitric (at the Windsborn site, data not shown), silandic and aluandic Andosols in Germany. Also, the rare soil type of an andic Luvisol can be found in the Vogelsberg – region near Frankfurt. We observe that, in Germany, this and other soils containing poorly crystalline aluminosilicate phases (as reflected by their Al_o and Si_o contents) have been regularly mistaken for Cambisols of low bulk density. We propose that appropriate measures should be taken to protect and conserve these soils, because they are valuable as archives of natural history and provide opportunities to study unique soil processes.

References

(References for materials on appendix are included here)

Bargon E (1960). Über die Entwicklung von Lockerbraunerden aus Solifluktionsmaterial im vorderen Odenwald. Z Pflanzenernähr Bodenk 90:229–243

Blakemore LC, Searle PL, Daly BK (1987). Methods for Chemical Analysis of Soils. Scientific Report No. 80. New Zealand Soil Bureau, Lower Hutt, New Zealand

Brunnacker K (1965). Die Lockerbraunerde im Bayerischen Wald. Geol Bl NO-Bayern 15:65–76

DBG (1998). Systematik der Böden und der bodenbildenden Substrate Deutschlands. Mittteilgn Dtsch Bodenk Gesellsch 86:1–180

FAO (1990). Guidelines for soil description. 3rd edn (rev.). Soil Resources, Management and Conservation Service, Land and Water Development Division. FAO, Rome, pp 70

FAO-Unesco (1974). FAO/Unesco Soil map of the world 1:5.000.000, Vol. 1, Legend. Unesco, Paris

Hashimoto J, Jackson ML (1960). Rapid dissolution of allophane and kaolinite – halloysite after dehydration. In: 7th Conf Clays and Clay Minerals, Pergamon Press, New York, NY, p 102–113

ISRIC (1992). Procedures for Soil Analysis. Wageningen

Jaritz G (1968). Ein Vorkommen von Imogolit in Bimsböden Westdeutschlands. Z Pflanzenern Düngung Bodenkd 117:65–77

Kleber M, Mikutta C, Jahn R (2004). Andosols in Germany – pedogenesis and properties. Catena 56:67–83

Kleber M, Zikeli S, Kastler M, Jahn R (2003). An Andosol from Eastern Saxony, Germany. J Plant Nutr Soil Sci 166:33–542

Meyer B, Sakr R (1970). Mineralverwitterung und -umwandlung in typischen sauren Lockerbraunerden in einigen Mittelgebirgen Hessens. Göttinger Bodenkundl Ber 14:49–105

Perrott KW, Smith BFI. Inkson RHE (1976). The reaction of fluoride with soils and soil minerals. J Soil Sci 27:58–67
Schlichting E, Blume HP, Stahr K (1995). Bodenkundliches Praktikum. Blackwell Scientific, pp 295
Schönhals E (1957). Spätglaziale äolische Ablagerungen in einigen Mittelgebirgen Hessens. Eiszeitalter Gegenwart 8:5–17
Schönhals E (1986). The landscape of Middle Hesse (Vogelsberg and Wetterau). Mittteilgn Dtsch Bodenk Gesellsch 46:181–224
Schönhals E (1973). Exkursionsführer zur Jahrestagung 1973 in Giessen. Exkursion C/E. Mittteilgn Dtsch Bodenk Gesellsch 17:182–225
Shoji S, Ono T (1978). Physical and chemical properties and clay mineralogy of Andosols from Kitakama, Japan. Soil Science 126:297–312
Soil Survey Staff (1975). Soil Taxonomy: A basic system of soil classification for making and interpreting soil surveys. Agric Handb 436. US Gov Print Office. Washington DC
Soil Survey Staff (1967). Soil Conservation Service, US-Dept. of Agriculture: Supplement to Soil Classification System. 7th Approximation, 2nd printing, US Gov Print Office, Washington DC
Soil Survey Staff (1960). Soil Classification: A comprehensive system – 7th approximation. US Gov Print Office, Washington DC
Stöhr W (1963). Der Bims (Trachyttuff): seine Verlagerung, Verlehmung und Bodenbildung (Lockerbraunerden) im südwestlichen Rheinischen Schiefergebirge. Notizbl Hess L.-Amt Bodenforsch 91:318–337
Stöhr W (1967). Exkursion A/E. Mittteilgn Dtsch Bodenk Gesellsch 6:45–115
Stöhr W (1971). Böden aus Pyroklastika und ihren Mischsedimenten im Verbreitungsgebiet des Laacher Trachyt – Tuffs. Mitteilgn Dtsch Bodenk Gesellsch 13:393–410
Wilke B-M, Becher HH (1980). Über die “Lockerheit” von Braunerden aus Granitzersatz im Bayerischen Wald. Z Pflanzenernähr Bodenk 143:546–552
WRB (1998). ISSS-ISRIC-FAO: World Reference Base for Soil Resources. Rome

Appendix on CD-Rom

Soil morphology / soil profile descriptions

Volcanic soil resources of Greece

A. Economou, D. Pateras and Ev. Vavoulidou

Extent, age and climate

Volcanic soils in Greece are found on some of the Aegean Sea islands (e.g. Santorini, Milos, Nisiros, Patmos, Lesvos, Limnos, Kos, Aegina), on Methana Peninsula in northeast Peloponnesus and on some localities in northern Greece (central and east Macedonia and Thrace). They cover an area of about 2698 km^2 or about 2.1% of the total area of Greece.

Extensive volcanic activity took place during the Tertiary and Pleistocene, until recently in the broader Aegean Sea. The volcanism was manifested in several areas and it is believed to relate to the convergence of the Eurasian and African tectonic plates (Katsikatsos 1992). The Hellenic volcanic arc is one of the dominant tectonic features of the southern Aegean. The long duration of the volcanic activity in the Aegean region (53 M y – present) produced a great quantity and variety of calc-alkaline volcanic rocks ranging in composition from basaltic and andesites to rhyolites. The age of the south Aegean volcanos is Pliocene-Quaternary (4–0 M y). North of them, in the central and north Aegean, are found other calc-alkaline volcanic rocks, which, from their age, are divided into three groups: one of the upper Miocene (13–7 M y) in the central Aegean, the second of the lower Miocene (23–14 M y) in the central and north Aegean, and the third one of the Eocene – Oligocene (53–26 M y) in the central and east Macedonia and Thrace.

The great majority of the volcanic rocks mentioned above are acid to intermediate in composition, consisting mainly of rhyolites, rhyo-dacites, dacites, andesites, trachy-andesites and trachytes. Basic volcanic rocks, consisting of basalt and basaltic andesites, cover various isolated areas in the Aegean islands (IGME 2001).

The south Aegean Sea islands is characterized as xero-thermo-Mediterranean climate with >150 biologically dry days (BDS) (Mavrommatis 1980). The climate of the east and central Aegean Sea islands is intense-thermo-Mediterranean to weak-thermo-Mediterranean, with 100–150 BDS, while the climate of north Aegean islands is considered as weak-thermo-Mediterranean. The climate of the north Greece is quite variable, ranging from weak-thermo-Mediterranean (100–125 BDS) to weak-mid-

Mediterranean (40–75 BDS) and sub-Mediterranean (<40 BDS) up to axeric temperate (BDS=0) as one moves from the coast and the plains to the north and the uplands.

In general terms, the climate of the Aegean islands is characterized by mild winders and relatively cool summers, because of the presence of the north trade-winds, that start blowing at the beginning of May, with low intensity, whilst from early June until the middle of September these winds are both frequent and intense. The average mean temperature ranges from 16.8°C, in the north Aegean, to 18.5°C, in the central, and 19.5°C, in the south Aegean. The annual precipitation for most of the islands is very low, ranging between 400–630 mm, being the driest region of Greece (Tsagari 2004).

Natural vegetation and land use

The natural vegetation of the south Aegean volcanic islands consists of sparse, low, shrubby plants (frygana and broadleaved evergreens) and grasses. However, the island of Aegina and the peninsula of Methana carry also a few Aleppo pine stands.

The same can be said for the remainder of the Aegean volcanic islands (east, central and north Aegean islands) except for Lesvos, where Calabrian pine stands are found, and Chios with just a few trees of the same species.

Almost all lands on the islands have shrubby vegetation and grasses which are used by the local inhabitants for grazing animals (sheep and goats).

The natural vegetation of the volcanic soils in north Greece includes beech, deciduous oaks, fir, black pine, mixed forest of chestnut trees with oaks and other broadleaved evergreens. This is because of the more favourable climatic conditions of these areas and lower human pressure. The land use of the majority of these lands is forestry, particularly for timber production.

Soil development and classification

In Greece, particularly in the Aegean Sea region, millennia of cultivation and other human interference (wood cutting, clearing, cultivation, wild fires, grazing, wars, ancient civilization) have modified the environment

substantially, including the volcanic soils. Consequently, the soils have suffered by severe wind and water erosion for quite a long time.

Soil development is slow under the dry and warm climate condition of the Mediterranean region, and the lack of continuous natural vegetation also has a slowing effect of soil formation. However, most of the described volcanic soil parent materials are very old (>7 and up to 53 million years old), and climatic conditions were quite variable during this long time. Velitzelos (1998) quotes, for the climate of the island of Lesvos and its paleo-flora: "The paleo-flora was developed at the cainophytic age, 20–25 million years ago, under tropic to sub-tropic climate with seasonal variation".

Soil profiles, mainly undisturbed, derived from volcanic rocks on several Aegean islands and described by the land resource survey of Greece (Nakos 1983) and other sources (Cost Action 622), were classified as shown in Table 1.

Table 1. Soil profiles on volcanic materials. Derived from the land resource survey of Greece (Nakos 1983) and other sources (Cost Action 622).

Profile No. / Year	Region / island	Soil Unit (FAO-Unesco 1974)	Soil parent Material	Land cover
1832/93	Limnos	Eutric Regosol	Trachy-andesites and Andesites	Herb vegetation (grasses)
1880/93	Lesvos	Humic Acrisol	Volcanic Tuffs	Closed forest of Calabrian pine
1881/93	Lesvos	Chromic Luvisol	Vitro-phyric lava, rhyolitic	Closed forest of Calabrian pine
1882/93	Lesvos	Eutric Regosol	Rhyo-dacitic, latitic lava	Closed forest of Calabrian pine
1889/93	Lesvos	Luvic Phaeozem	Acidic igneous	Closed forest of Calabrian pine
1/2003	Methana	Dystric Regosol	Pyroclastic lava andesites–SiO_2 56–63%	Open Aleppo pine forest
2/2002	Santorini	Eutric Regosol	Upper pumice series	Herbaceous natural vegetation
3/2002	Santorini	Eutric Regosol	Upper pumice series	Frygana and herbs
4/2002	Santorini	Eutric Regosol	Black scoriae of upper volcanic series (andesitic)	Frygana and herbs

The soils derived from recent volcanic material (Santorini, Methana) are light textured, neutral to alkaline in reaction, low in CEC, usually low in available P (Olsen) content, and low to very low in organic carbon content.

Methana profile does not contain $CaCO_3$, while the Santorini profiles tend to be characterized as calcareous ($CaCO_3$ content between 0.95% to 3.0% in the different profiles examined). All these profiles are classified according to FAO-Unesco 1974 as Regosols (Dystric and Eutric), while none of the profiles examined in the frame of the land resource survey of Greece (2363 profiles) was classified as Andosol.

Conclusions

A variety of soils occur on volcanic parent materials in Greece, spanning diverse soil groups. Some of the parent materials are quite old (>7 M y), too old for maintaining Andosol characteristics, and none of 2363 profiles of the national database classifies as Andosols. Young volcanism is found on Santorini where relatively poorly developed vitric soils predominate.

References

IGME (Institute of Geology and Mineral Exploitation) (2001). Geologic Map of Greece, scale 1:500,000

Katsikatsos G (1992). Geology of Greece. Athens, pp 451

Mavrommatis G (1980). The Bio-climate of Greece: Relation between climate and natural vegetation, bio-climatic maps. Forest Science, V.1 (Suppliment). Edition of the Forest Research Institute of Athens, Greece, pp 63

Nakos G (1983). The land resource survey of Greece. Journal of Environmental Management 17:153-169

Tsagari K (2004). Research scientist, Forest Research Institute of Athens. Personal communication

Velitzelos Ev (1998). The petrified forest of Lesvos. A rare geologic monument of the nature. 1st scientific symbosium for the Petrified Forest of Lesvos, held in Mytilini and Sigri, Lesvos, Greece, April 26–27, Proceedings in Greek, pp 35–42

Hungary and the Carpathian Basin

Gy. Füleky, S. Jakab, O. Fehér, B.Madarász and Á. Kertész

Introduction

Soils that have developed on volcanic parent material occur in the Hungarian National Genetic Classification system among the Lithomorphic (Fekete Nyirok) or Brown Forest soils (for example Acidic, Non-podzolised, Brown Forest Soils) on acidic volcanic hydroandesite (Stefanovits 1956). The re-evaluation of pedological data of Hungary based on the concept of diagnostic criterias is under way for the Revised National Genetic Classification System (Michéli 2002). In Romania diagnostic concept has been introduced since the 1980's (Conea et al. 1980). Andosols were included into the later edition of Romanian Soil Classification system (Florea and Munteanu 2000).

The aim of this paper is to present a study on soils developed on volcanic material in Hungary and in the Eastern Carpathian Mountains in Romania and to correlate present climatic, geographic conditions with existence or absence of certain diagnostic properties. In the selected Miocene and Pliocene volcanic areas of the Carpatho-Pannonian regions 13 representative soil profiles were sampled and analysed as a part of international co-operation described in the introduction of this book. The research included morphological descriptions, classification (WRB, Soil Taxonomy), and both physical and chemical analysis.

Nature of volcanism of the Carpatho-Pannonian territories

Volcanism played a significant role in the neogene history of the Carpathian Basin. In the early to middle Miocene, large strato-volcanoes dominated the landscape covering almost the entire basin interior by their products. Today the volcanic activity is restricted to smaller areas. The main reasons for the decreasing extent and number of volcanic regions are: (1) several volcanic centres have disappeared below the late Miocene sedimentary sequence of the Great Hungarian Plain; (2) primary volcanic forms are old, therefore they are largely eroded; (3) loess and other sediments were deposited on hillslopes during the Pleistocene, when perigla-

cial conditions prevailed in the area (Szakács and Karátson 1999). On the basis of spatial distribution (1), age (2), petrological-geochemical character (3) and type of volcanic activity (4) scientist divide the Neogene to Pleistocene volcanism into two: **calc-alkaline** (within it: silicic and intermediate volcanism) and **alkali basalt volcanism** (Szakács and Karátson 1999, Fehér 2005). The two main types of volcanisms occurred separately in space and time in the Carpathian Basin. Origin of the volcanism related to plate tectonics (Gyarmati 1977, Jaskó 1986, Varga et al. 1975).

Age of eruptions and morphology of volcanic edifices

The calc-alkaline volcanism occurred during the early and middle Miocene (approx. from 22 to 10 M y) of the so called Inner Carpathians. The volcanic activity started with *silicic volcanism*, which produced huge amounts of pumiceous pyroclastic flow deposits (ignimbrites). Ideal examples of such territories could be found in the Mátraalja and Bükkalja (Hungary) (Figure 1).

In the middle Miocene magma composition of the intermediate phase is *andesite-dacite dominated*. During this Badenian period (17–14 M y), large strato-volcanoes developed in the northern part of the country as part of the Inner Carpathian Volcanic Chain. The strato-volcanoes are built up from pumice-and-ash and block-and-ash flow deposits Sub-volcanic forms, like dykes and laccolites can also be formed. The pyroclastic and lava material ranges from rhyolitic to basaltic. However, the main phase of the volcanism has an andesitic-dacitic composition. The strato-volcanoes belong to the current North Hungarian Mountains (NHM). The volcanic parts of the NHM from west to east are as follows: Visegrád-Börzsöny, Western-Cserhát, Mátra, Bükkalja and Eperjes-Tokaj Mountains. The average height varies between 400–700 m a.s.l. The highest is the Mátra, with the highest peak of Hungary (1015 m).

According to Szakács and Karátson (1999) magmatic activity shows eastward migration of this is why volcanoes are becoming younger towards the East. Along the internal side of the Carpathian-loop magmatism reached the Eastern Carpathians 9 million years ago and terminated in the south in the Late Pleistocene (Karátson 1999). As a result the Călimani-Gurghiu-Harghita (CGH hereafter) volcanic chain was formed, which is situated on the territory of Romania. CGH is 160 km long and nearly 60 km wide. The maximum altitude is of 2102 m in Călimani Mts., 1780 m in Gurghiu Mts. and 1801 in Harghita Mts. The K-Ar ages suggest that volcanic activity started roughly at the same time in the Călimani and Gurghiu, but lasted 1.5 M y longer along the later segment. The youngest

volcano of all the Carpathian and Eastern Europe is Ciomadul (2.8–0.2 M y) in the southernmost part of the Harghita Mts. (Pécskay et al. 1995). The region is still showing post-volcanic activity (fumarola, solfatara). The most common rock-type in the whole CGH volcanic chain is pyroxene andesite. Here and there, some basalts, basaltic andesites and dacites occur. All these rocks are typically porphyritic. Plagioclase, magnetite and ilmenite are ubiquitous in all rock-types. Clino- and ortopyroxene are common in basalts, andesites and some dacites (Radulescu et al. 1964). They could be the main sources of allophane during the soil forming processes.

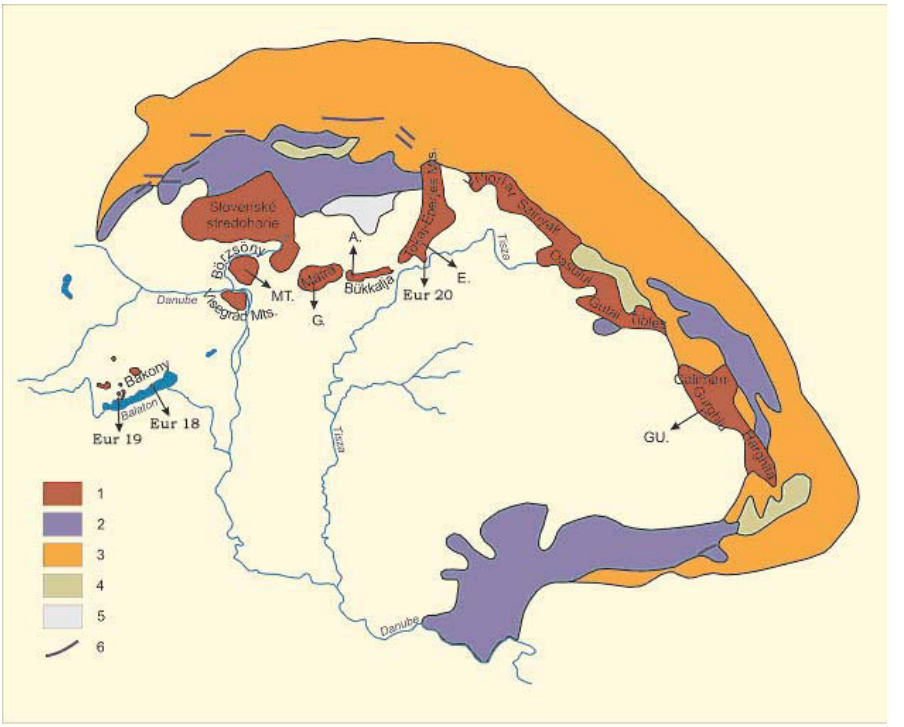

Figure 1. Volcanic chain of Carpathians and fields of the alkaline basalt volcanism within the Carpathian Basin with the study sites. Map legend is 1: Neogene volcanic belt; 2: Crystalline belt; 3: Paleogene flysch belt; 4: Inner-Carpathian basins; 5: Mezozoic limestone and dolomite plateaus; 6: Pieniny klippen belt. Letters indicate study sites; MT.: Magas-Tax; G: Galyatető; A: Andornaktálya; E: Tolcsva; GU: Gurghiu; and EUR18. EUR19. EUR20 represent COST-622 soil sampling sites.

The *alkaline basalt magmatism began in* the Pliocene-Pleistocene some 7 M y ago and ended only about 500,000 years ago. During this phase, alkaline basalts were produced, but in lesser amounts than during the Mio-

cene calc-alkaline volcanism. The eruptive centers are concentrated in several volcanic fields dispersed within the Carpathian Basin. There are three alkaline basalt volcanic areas in Hungary. Two of these are in Transdanubia on the Little Hungarian Plain and in Balaton Uplands-Bakony Mountains. The Nógrád-Gömör area is in the northern part of the country and it continues into Slovakia. Three types of the alkaline basalt volcanism can be distinguished. The first group is represented by maars and tuff rings, resulting from phreato-magmatic eruptions. The second group is a mixed type: the tuff rings are filled by basaltic lava, and sometimes with scoria cones. The volcanic centers of the above groups are individual volcanic cones of moderate size, and they are more or less eroded. The third group is of basaltic lava flows, forming larger lava plateaus. They are situated mainly in the higher regions of the Bakony and of the NHM. Average height of the smaller volcanic cones is 300–400 m a.s.l. The higher basalt plateaus can reach the up to 600 m a.s.l.

Study sites for pedological investigations were chosen from the territory of Balaton Uplands, NHM and CGH.

Present-day climatic conditions

In general climatic conditions controlled by the elevation differences and geographic location of the chosen site. On the territory of Balaton Uplands, the climate is mild, with a mean annual temperature of 10–10.5°C and a mean annual precipitation of 600–700 mm. The average number of days with snow cover is 35–50. The average thickness of the snow cover is 25–30 cm. The territory of NHM belongs to the humid continental climate zone. The mean annual temperature there is around 9.3°C, somewhat lower than for the countryside below, with still lower values of 6–7°C in the higher regions. The mean annual precipitation varies between 600 and 900 mm, with a late-spring-early summer maximum in May and June. The second half of the summer is dryer and sunny. During wintertime, there are 40–60 days with snow cover in the lower areas, and 80–100 days in the higher parts on average. The average thickness of the snow cover is 25–60 cm.

Present day climate of the CGH characterized by three factors: continental influences, significant vertical elevation differences, and the north-south orientation of the mountain ranges. The average annual precipitation varies between 800–1200 mm, mean annual number of days with snow cover may reach 200, the mean annual number of frost days may exceed

160–180, and the mean annual temperature is around 3.5°C. Elevation differences may cause significant changes within short distances.

Soil temperature regime (TR) at the depth of 50 cm for the study sites was estimated from the 30 years measured average air temperature data by adding 2.5ºC to mean annual and reducing amplitude by a factor 0.66 (Wernstedt 1981, 1983, Fehér 2005). Based on this soil temperature regime in the study sites is mesic. Soil moisture regime (MR) varies: for Balaton Uplands it is dominantly ustic, however it shows elements of xeric moisture regime, which is related to the Mediterranean climatic influences – these are pronounced mainly on the southern slopes. In the NHM and CGH, soil moisture regime primarily controlled by the altitude, exposure and dissection of the surface (Table 1).

Table 1. Soil temperature regime (TR) and soil moisture regime (MR) for the study sites.

Carpatho-Pannonian				Soil Climate	
Macroregion	Mesoregion	Microregion	Location	TR	MR
Transdanubian Mts.	Bakony region	Balaton Uplands	Badacsony	Mesic	Ustic
			Tihany	Mesic	Xeric/Ustic
Northwest-Carpathians	NHM	Börzsöny Mts.	Magas-Tax	Mesic	Udic
		Mátra Mts.	Galyatető	Mesic	Udic
		Bükkalja foothills	Andornaktálya	Mesic	Ustic
		Tokaj-Slanec Volcanic Range	Tokaj	Mesic	Ustic
		Tokajhegyalja Foothills	Tolcsva	Mesic	Ustic
East Carpathians	CGH Volcanic Range	Gurghiu Mountains	Mezőhavas (Seaca Tatarca)	Mesic (Frigid)	Udic

Natural vegetation and land-use

Transdanubian Mts. belong to the Transdanubian floristic region (*Bakonyikum*) of the Pannonicum flora province. Characteristic forest associations are the hornbeam grove-sessile oak forests (*Querco petraeae-Carpinetum pannonicum*), the austrian-sessile oak forests (*Quercetum Petraeae-cerris pannonicum*) and the calciphobic oak forests (*Luzulo-Quercetum*) (Kőrössy 1980).

Major part of the NHM belongs to the Northern Hungarian floristic region (*Matricum*) of the Pannonian flora province (*Pannonicum*). In the North, smaller areas form part of the North Carpathian flora province. Above 800 m a.s.l. mountain beech forest vegetation (*Aconito-Fagetum*) is

typical. The lower areas are covered by submontane beech forests, calciphobic beech forests (*Luzulo-Fagetum*), hornbeam grove-sessile oak forests (*Querco-Petraeae-Carpinetum*), and austrian-sessile oak forests (*Querco-Petraeae-Cerris*). The typical vegetation of the northern slopes is the calciphobic oak forest (*Genisto tinctoriae-Quercetum petaeae*) (Kőrössy 1980).

More than 70% of the CGH volcanic range is covered by forest, the reminder of the area is extensive pasture lands. The vegetation cover at 600–950 m elevation is mainly beech forest (*Symphito cordati-Fagetum* and *Fagetum nudum*). After a transitional beech-spruce stripe, the spruce forest *(Picetum myrtilletosum* and/or *Luzulo sylvaticae-Picetum)* stretch up to 1600–1650 m height above sea level. Above this level the Dwarf mountain pine *(Pinetum mugi-carpaticum)* becomes dominant, coupled with small shrub of *Vaccinium myrtillus, V. uliginosum* and a grass association of *Festuceto-Nardetum strictae montanum* (Höhn 1998).

Majority of the studied sites from the Balaton Uplands (Badacsony, Tihany) and NHM (Andornaktálya, Tolcsva, Tokaj) have been cultivated intensively since the Middle Ages (Bodnár 1987, Nagymarossy 2004). In case of the Transdanubian territories (Badacsony and Tihany) – continuous wine production dates back to the Romans (Palágyi 1996, Lichtneckert 1990).

At higher altitudes of the NHM (Galyatető and Magas-Tax) and in CGH human disturbance is minimal; in some patches might be interrupted by charcoal-burning places and restricted to woodlands and extensive pasture lands.

Selection of the soil profiles and methods

While choosing study sites, an attempt was made to allocate them in areas of limited human disturbance, using historical maps. Thirteen representative soil profiles according to the nature of origin of volcanic parent material have been selected from the Balaton Uplands and NHM: 2 profiles from the silicic volcanic areas on ignimbrites (Andornaktálya and Tolcsva), 9 from the andesite-dacitic intermediate volcanism area (Tokaj, Magas-Tax, Galyatető; 6-profiled toposequence from the CHG) and 2 from alkaline basalt volcanism area (Badacsony and Tihany). Site and soil profile descriptions are included in the annex. Profile descriptions were made according to FAO (1990) guidelines.

All laboratory analyses were done on air-dried <2 mm soil samples in duplicates. Soil pH was determined in 1 M KCl and H_2O at a soil-solution

ratio of 1:2.5 (Buzás et al. 1993), pH_{NaF} according to Blakemore et al. (1987). Organic carbon (C_{org}) was determined by Tyurin-method; available phosphorous (P) by Olsen-method. Phosphate retention (P_{ret}%) was determined according to Blakemore et al. (1987) in a potassium di-hydrogen phosphate solution at pH 4.6 buffered by sodium acetate. Cation Exchange Capacity (CEC) and exchangeable bases was extracted with the ammonium acetate at pH 7 Blakemore et al. (1987). Pedogenic Fe_d and Al_d compounds were extracted with dithionite-citrate-bicarbonate solution according to Mehra and Jackson method, amorphous Al_o, Fe_o, Si_o compounds with acid ammonium oxalate solution and organically bounded Fe_p, Al_p compounds in pyrophosphate solution as described in (Blakemore et al. 1987). For particle size analysis the air dried bulk samples were treated with H_2O_2 and HCl. Coarse fractions were separated by wet sieving (50 μm); silt and clay fractions were determined by the pipette method (Buzás et al. 1993). Bulk density (BD) was determined on undisturbed ring samples in three replicates according to Buzás et al. (1993).

Results and discussion

Field morphology

Morphological properties of soil profiles from the **silicic volcanic areas** (Andornaktálya, Tolcsva) showed undisturbed profile development since the boundary between the solum and the parent rock were continuous and weathering frontline in the rhyolitic tuff/ignimbrites were well visible. Soil profile development exceeded 40–50 cm depth, but the effective rooting depth is great, or more then 1 m. Soil profile horizonation is characterised by dark coloured organic rich A horizon of mainly granular structure, rich in angular very fine rhyolitic gravel.

In case of the soil profiles on **intermediate volcanism products** from the NHM striking feature in the field was the accumulation of fresh, non-weathered, 10–18 cm angular andesite boulders at the depth of 30–40 cm in case of Magas-Tax and Galyatető and at the depth of 45–60 cm in Tokaj. Above this horizon, eolian silty deposits were recognised. At depth, strongly weathered andesite (especially in Galyatető) was described. In case with Mezőhavas (CGH) toposequence beside strongly weathered pyroxene-andesite rock fragments-strong thixotropy, very dark soil colours was experienced in the field. Humus type of all of the soil profiles from the intermediate volcanism area is acid mull type. Soil structure can be characterised by a very well developed fine granular porous structure with many

eye-visible macro-pores. All of the profiles described as biologically very active, rich in fine and medium roots. Evidences of faunal activity (crotovinas of worms) were well visible in the field.

There was a sharp boundary between the solum and the underlying substrate in the soils of the alkaline basaltic area. There was a humus rich (mull type) mineral horizon with a wavy boundary grading to a basaltic, angular gravel rich but still dark coloured horizon. Field texture seemed to be more clay rich, than it was determined in the texture analysis. Structure was more coarse granular in these soils than in soils of the other volcanic areas. In the case of Badacsony profile, bleached quartz grains were recognised in the topsoil. The sharp boundaries between the solum and substrate below are possibly related to erosion of these territories in the past.

Chemical and physical properties

The basic chemical and physical properties of the soils are presented in Table 2. All of the profiles tend to show strong accumulation of humus in the A1 horizons and showing decrease in carbon from A1 to AC or Bw horizons. Organic matter accumulation is pronounced (up to 16%) in the Badacsony profile, where even at the depth of 50 cm, organic matter content values are >4%. High phosphor content is also striking in the Badacsony profiles. One hundred years old land-use maps show that the limit of vineyards was much higher than nowadays, suggesting that such high organic matter content and high phosphorous content could mainly be related to the human influence with continuous manuring of territories under viticulture.

In case with CGH and Galyatető from the NHM the clay content indicates an advanced stage of weathering, which seems to be characteristic for soil profiles above the altitude of 925 m a.s.l. In our opinion it is due to the Pleistocene periglacial climatic conditions, which could have caused the pre-weathering of the parent materials (Table 2–3). In case with the toposequence from the CGH the thixotropy experienced in the field, high content of organic carbon (C_{org}), the very low bulk density (BD), high phosphate retention (P_{ret}) and pH_{NaF} are parameters all to fulfil the WRB (1998) criteria of andic diagnostic horizon. Striking is that in case with CGH soils lying below the 1000–950 m altitude do not show andic properties. Nevertheless, the extremely acid to acid reaction of the soils developed on volcanic parent material does not allow for the formation of allophane, but favours the accumulation of aluminium-humus complexes. Low $(Al_o\text{-}Al_p)/Si_o$ ratio (not shown in table) in the surface and or subsurface ho-

rizons in soils of the CGH volcanic chain place the soils as the non-allophanic, aluandic soil type.

Table 2. Some selected properties of Hungarian volcanic soil profiles.

Soil profile	Horizon	Depth cm	d_b g cm^{-3}	Clay %	P_{ret} %	P mg kg^{-1}	Al_o+½Fe_o %	pH_{H2O}	C_{org}%
EUR18 Tihany	Ah1	0–15	0.88	36	30	47.6	0.59	6.67	4.64
	Ah2	15–35	0.87	32	36	2.7	0.65	7.41	1.74
	AC	35–70	0.90	14	34	na	0.67	7.75	1.56
EUR19 Badacsony	Ah1	0–7	0.87	20	23	109.8	0.61	5.57	9.46
	Ah2	7–25	0.92	17	29	103.9	0.70	5.20	5.78
	A+R	25–50	0.98	3.3	28	na	0.80	5.61	2.79
EUR20 Tokaj	Ah1	0–12	0.72	25	21	12.7	0.33	5.14	4.54
	Ah2	12–45	0.74	27	26	10.7	0.35	5.34	3.85
	AW+R	45–60	1.2	28	15	16.7	0.26	5.80	1.35
Tolcsva	Ah	0–12	1.0	14	12	75.86	0.11	6.49	2.6
	AC1	15–25	1.0	24	23	24.64	0.10	6.20	0.56
	AC2	25–55	nd	9.5	12	20.17	0.09	6.37	0.37
Magas Tax	Ah	5–20	1.0	21	23	2.76	0.44	5.43	1.22
	B1	20–40	1.0	11	30	1.68	0.44	5.78	0.31
	B2	40–80	1.3	7.4	38	0	0.54	5.74	0.22
Galyatető	0	0–10	nd	23	61	nd	0.82	4.11	4.71
	Ah1	10–20	0.66	5.2	39	10.62	0.78	5.04	3.99
	Ah2	20–33	0.77	5.0	38	4.33	0.76	5.17	1.74
	B1	33–44	nd	2.8	47	2.76	0.71	5.21	0.95
	B2	44–58	nd	5.8	40	0	0.73	5.11	0.72
	Bw1	58–70	0.9	13	30	1.3	0.60	5.15	0.40
	Bw2	>70	nd	12	30	0	0.47	5.20	0.24
Andornaktálya	Ah	0–25	1.1	18	17	2.76	0.17	6.29	1.09
	AC	25–40	0.88	2.4	12	1.68	0.08	6.56	0.30
	C	>44	nd	0.1	12	0	0.04	6.65	0.12

Classification and pedogenesis

Considering the values defining the andic soil properties – investigated sites can be grouped into two main groups:

1. Volcanic non-andic soils described and studied from the Balaton Uplands and NHM
2. Andosols from the CGH

Table 3. Some selected properties of the Gurghiu soil profiles.

Profile	Horizon	Depth cm	d_b g cm^{-3}	pH_{H2O}	C_{org} %	Clay %	Bases cmol kg^{-1}	CEC cmol kg^{-1}	Base saturation, %	P_{ret} %	pH_{NaF}	Si_o %	Al_o %	Al_p %	Fe_o %	Fe_p %	Al_o+½Fe_o %
N1	Ah	5–17	0.51	4.0	13.0	43.9	2.40	47.0	5.1	82	8.9	0.07	1.00	1.18	2.00	1.84	2.00
1775m	ABw	17–21	0.55	4.3	10.1	33.6	1.36	51.8	2.6	94	10.1	0.13	1.96	2.35	3.76	3.80	3.84
	Bw	21–35	0.62	4.3	6.8	29.1	1.35	46.4	2.9	94	9.7	0.15	1.71	2.05	4.68	5.05	4.05
N2	Ah	7–20	0.35	3.7	12.7	34.5	2.24	58.7	3.8	80	8.6	0.06	0.84	0.98	1.69	1.73	1.68
1475m	ABw	20–28	0.47	4.3	7.0	14.8	2.03	47.7	4.3	90	12.0	0.74	4.91	4.30	1.02	0.91	5.42
	Bw1	28–38	0.88	4.5	3.3	6.9	1.97	30.7	6.4	85	11.4	0.75	3.39	1.68	0.46	0.36	3.62
	Bw2	40–60	0.79	4.8	2.3	7.2	2.20	27.3	8.1	81	11.4	0.94	3.41	1.10	0.56	0.33	3.39
N3	Ah1	3–13	0.35	3.6	10.7	34.4	3.24	49.9	6.5	82	8.6	0.08	1.17	1.35	1.16	1.08	1.75
1350m	Ah2	13–25	0.5	4.2	7.4	20.3	1.13	26.1	4.3	90	10.4	0.32	2.57	2.67	1.18	1.18	3.16
	ABw	25–35	0.89	4.3	3.2	3.6	1.06	21.0	5.1	90	10.4	0.54	2.70	1.40	1.07	0.89	3.23
	Bw	40–60	0.67	4.4	1.6	3.1	0.58	18.3	3.2	88	10.0	0.68	2.68	0.09	1.01	0.68	3.18
N10	Ah	4–14	0.35	3.2	17.2	37.2	3.11	59.8	5.2	71	8.2	0.06	0.60	0.83	2.03	1.31	1.27
1250m	ABw	14–21	0.5	4.0	8.6	30.4	0.37	46.8	0.8	94	10.8	0.19	2.57	3.29	1.17	2.05	3.58
	Bw	30–50	0.65	4.1	2.8	2.4	0.53	21.6	4.0	85	10.2	0.43	2.06	1.18	nd	0.91	2.65
N5	Ah	5–20	0.31	3.8	22.8	36.7	5.28	67.2	7.8	83	9.2	0.18	1.84	1.89	0.12	1.18	1.90
1050m	ABw	20–25	0.4	4.6	9.8	4.2	2.99	30.6	9.8	95	11.3	1.21	5.17	2.26	1.15	0.93	5.74
	Bw	25–45	0.67	4.7	3.8	1.1	2.15	20.6	10.4	90	10.2	0.07	2.77	1.26	1.13	0.86	3.33
N6	Am	5–25	1.02	5.3	1.9	15.0	12.57	18.5	68.0	38	8.8	0.15	0.45	0.26	0.69	0.21	0.80
900m	AB	30–40	1.16	5.7	1.5	10.6	12.42	16.2	76.6	33	8.4	0.15	0.42	0.20	0.69	0.18	0.77
	Bw	45–65	1.31	6.0	0.9	9.1	12.30	15.6	78.8	28	8.2	0.16	0.36	0.20	0.69	0.15	0.71

Profiles developed under ustic with elements of xeric moisture regime

In Andornaktálya, a shallow dark epipedon is at the limit to fulfil criteria for mollic surface horizon and the underlying horizon fulfils criteria of a cambic subsurface horizon based on structure development. There are incipient vertic features (slickensides) on peds surfaces near the bottom, but not sufficiently to be classified as a vertic horizon. Lithic contact near the 50 cm depth does not disturb root penetration into the soft substrate. For the Andornaktálya profile, climatic conditions are characterised by moist and cool winters, while summers and autumns are warm and dry, providing particularly favourable conditions for wine-growth. Leaching is effective in winter and spring time, when there is limited evapo-transpiration. Such conditions favour development of endoleptic Phaeozems (WRB 1998), or Lithic Xerochrepts, rather than Lithic Haploxerolls according to the US ST (1999).

The surface horizon of the Tolcsva profile fulfils only the ctriteria for an ochric horizon, since it is shallow. The structural development in the subsurface horizon is sufficient to be diagnosed as cambic. The lithic contact located below 50 cm depth at the Tolcsva profile, which can be explained by the more northerly and more exposed territory location than the pedon discussed before, with more intensive leaching and weathering of the sub-

strate during winter time. Soil genesis leads to formation of endoleptic eutric Cambisols (WRB 1998) or Typic Xerochrepts (US ST 1999).

Ustic soil moisture of the Tihany peninsula has also elements of xeric, so the soil evolution results similar soil properties as under the Andornaktálya conditions. Formation of thick, organic mollic horizon without other diagnostic horizon classified as haplic Phaeozem (WRB 1998) or Typic Haploxerolls (US ST 1999).

In Badacsony temperature differences between summer and winter are not variable, moisture supply is balanced. Leaching – in the periods without vegetation (early spring and late autumn) – is therefore more advanced. Loess contamination of the surface horizons have high amount of quartz, which leads to the formation of umbric horizons on the surface, with an acid soil reaction. Since there are no other diagnostic horizons, the profiles were classified as humic Umbrisols (WRB 1998) or Dystric Xerochrepts (US ST 1999).

In Tokaj profile, a sufficient input of airborne dust was observable in the surface horizon, which probably contains low amount of weatherable minerals. Vegetation cover and land use accelerates humus accumulation. This is resulting dark coloured umbric horizon. The profile was classified as humic Umbrisols (WRB 1998) or Dystric Xerochrepts (US ST 1999).

Profile development under Udic moisture regimes

Mountain areas of the NHM receive generous moisture supply throughout the year with continuous leaching. Mean annual temperatures are below 8 degrees so there is enhanced accumulation of organic matter due to cool climate. Under such conditions surface horizons are diagnosed as Umbric and the profile at Magas-Tax in Börzsöny Mountains keys out as skeletic Umbrisol.

The Galyatető profile in the Mátra Mountains is located at the elevation 925 m, which favours snow accumulation for about 90 days. The fast melting of snow in the spring period enhances leaching and chemical weathering of the fine silty material, which was described in the surface horizons. This is resulting in weakly develop Andic (Aluandic) features and Umbric horizon at the surface. Classification of profiles resulted in humic Umbrisol which is intergrading to humic andic Umbrisol (WRB) or Dystric Ustochrepts (US ST 1999).

In CGH the distribution of the main soil types is mostly correlated to altitude, topography and parent material. Most soils that have developed on the pyroxene andesitic lava flows in Transylvanian Neogene volcanic

chain have andic features which could be observed from the top downwards to the lower boundary of the lava flows (950–1000 m a.s.l.). The limit between the lava flows and the volcano-sedimentary formations represents an abrupt transition towards Cambisol and/or Luvisol. The clay content indicates an advanced stage of weathering in all studied profiles, independently of altitude between the highest point and 950–1000 m a.s.l., due to the Pleistocene periglacial climatic conditions, which could have caused pre-weathering of the parent materials (Table 2).

The thixotropy experienced in the field, the dark colour, a high content of organic carbon (C_{org}), the very low bulk density (BD), high phosphate retention (P_{ret}) and pH_{NaF} are parameters that fulfil the WRB criteria of Andosol. Soils lying below 1000–950 m altitude have no andic properties.

The extremely acid to acid reaction of the soils developed on volcanic parent material does not allow for the formation of allophane, but favours the accumulation of aluminium-humus complexes. Low $(Al_o\text{-}Al_p)/Si_o$ ratio (not shown in table) in the surface and/or subsurface horizons in soils of the CGH volcanic chain place the soils as the non-allophanic, aluandic soil type. This is a normal situation in the mesic-udic climate of the East Carpathians. Moreover the Al_p, Fe_p and $Al_o+½Fe_o$ values for the profile, sometimes indicate a translocation of organically complexed aluminium and iron. These, coupled with low pH values in the surface soil, could be sign of a spodification process. Vasu (1986) underlined the necessity to mention the effects of the two processes at the level of subtype and proposed the classification as Criptospodic Andosol.

Conclusions

The Carpathian Basin, with diverse volcanic parent materials, age of rocks, type of vegetation and climatic conditions, is an excellent field within a small region to study the main influences of soil development on volcanic material. At ustic/xeric moisture regime, independently from the type of the rock (ignimbrite, andesite, basalt) Phaeozems and Cambisols develop. At ustic and udic moisture regimes, both on pyroxene andesite and basalt, Umbrisols develop. Under udic moisture regime, above 1000 m elevation, on pyroxene andesite in Romania and Slovakia, Andosols can develop. In a topo-sequence on pyroxene andesite, under udic moisture regime, between 700–1000 m, Cambisols or Luvisols dominate, but Andosols, sometimes with spodic features from 1000 to 1800 m elevation.

Acknowledgements

We are grateful for the financial support of the Sapientia University (Tirgu Mures, Romania). We thank O. Arnalds for his great help in reviewing this manuscript. The authors also gratefully acknowledge the help of P. Buurman and P. Quantin given in the soil profile descriptions and classification according to the international standards at the first stages of this project.

References

Blakemore LC et al. (1987). Methods for chemical analysis of soils. NZ Soil Bureau Scientific Report 80, pp 103

Bodnár L (1987). Az egri és mátraaljai történelmi borvidék (The historical wine-region of Eger and Mátraalja Foothills. In Hungarian). Eger

Buzás I et al. (1988). Talaj- és agrokémiai vizsgálati módszerkönyv 2 (Soil- and agrochemical methods manual. Part 2.) Budapest. Mezőgazdasági Kiadó

Buzás I et al. (1993). Talaj- és agrokémiai vizsgálati módszerkönyv 1 (Soil- and agrochemical methods manual. Part 1.) Budapest. INDA 4231 Kiadó

Conea A, Florea N, Puiu Şt (coord.) (1980). Sistemul Român de Clasificare a Solurilor (Romanian System of Soil Classification). ICPA, Bucharest

FAO (1990). Guidelines for soil description. 3rd (rev.) edn. FAO-ISRIC

Fehér O (2005). Morphological and chemical characterization of soils developed on andesitic rocks in South-Eastern Carpathians. MSc thesis, Ghent University-ITC, Belgium

Florea N, Munteanu I (2000). Sistemul Român de Taxonomie a Solurilor (Romanian System of Soil Taxonomy). Univ "Al. I. Cuza" Iasi

Gyarmati P (1977). A Tokaji-hegység intermedier vulkanizmusa (The intermedier volcanism of the Tokaj Mountains). Földt Int Évk LVIII:1–195

Höhn M (1998). A Kelemen-havasok növényzetéről (The vegetation of the Calimani Mountains. In Hungarian). Mentor Kiadó, Marosvásárhely

Jaskó S (1986). A Mátra. a Bükk és a Tokaji-hegység neotektonikája (The neotectonics of the Mátra. Bükk and Tokaj Mountains). Földtani Közlöny. Bull of the Hungarian Geol Soc 116:147–160

K. Palágyi S (1996). Római kor (the Roman-Age. In Hungarian). A Veszprém Megyei Levéltár kiadványai 11. Veszprém, 1996

Kőrössy L (1980). Neogén ősföldrajzi vizsgálatok a Kárpát-medencében (Neogene paleogeographic investigations in the Carpathian-basin). Földt Közl 110:473–484

Lichtneckert A (1990). A Balatonfüred-Csopaki borvidék története (The history of Balatonfüred-Csopak wine-region. In Hungarian). Veszprém

Michéli E (2002). Új. diagnosztikai szemlélet a talajosztályozásban (New, diagnostic concept in soil classification). DSc tesises

Munteanu I, Florea N (2001). Present-day status of Soil Classification in Romania. In: Micheli E et al. (eds) Soil Classification 2001. European Soil Bureau. Research Report 7:55–62

Nagymarosy A (2004). A termõhely vonzásában. In: Rohály G (ed.) Terra Benedicta. Akó Kiadó, Budapest, pp 10–23

Pécskay Z, Edelstein O, Seghedi I, Szakács A, Kovacs M, Crihan M, Bernad A (1995). K-Ar datings of Neogene-Quaternary calc-alkaline volcanic rocks in Romania. Acta Vulcanologica 7(2):15–28

Radulescu D, Vasilescu A, Peltz S (1964). Contribuţii la cunoaşterea structurii geologice a munţilor Gurghiu (In Romania). An Com Geol XXXIII:87–151

Stefanovits P (1956). Magyarország talajai (Soil cover of Hungary. In Hungarian). Akadémiai Kiadó, Budapest, p 252

Szakács S. Karátson D (1999). The Inner Carpathian calc-alkaline volcanism. In: Karátson D (ed.) Pannon Encyclopaedia. The land that is Hungary. Kertek 2000 Publishing House; Budapest, 1999. CD-rom. ISBN 963 8602937

US ST (1999). Soil Taxonomy. A Basic System of Soil Classification for Making and Interpretations Soil Surveys. 2nd edn. USDA-NRCS, Washington DC

Varga Gy, Csillagné TE, Félegyházi Zs (1975). A Mátra hegység földtana (The geology of Mátra Mountains). Földt Int Évk LVII /1:1–575

Vasu A (1986). Contribuţii la clasificarea solurilor spodice şi a solurilor andice. An ICPA XLVII:179–187

Wernstedt FL (1981). World Climatic Data. Romania. Dossier nr 101. 88 stations. (Not published document). Kept at the Department of Geology and Soil Science at University of Ghent

Wernstedt FL (1983). World Climatic Data. Romania. Dossier nr 101. 88 stations. (Not published document). Kept at the Department of Geology and Soil Science at University of Ghent

WRB (1998). World Reference Base for Soil Resources. FAO, ISRIC and ISSS, Rome

Icelandic volcanic soil resources

O. Arnalds and H. Oskarsson

Introduction

Iceland is an active volcanic island with frequent volcanic eruptions that produce tephra. The soil environment of most Icelandic soils is therefore dominated by volcanic ash. Andosols and Vitrisols are dominant soil types. Work in relation to the European COST-622 Action (see preface) has added valuable information about Icelandic soils and a new classification scheme was developed for Icelandic soils (Arnalds 2004). The purpose of this paper is to give a short overview of volcanic soil resources in Iceland, which also serves as background information in relation to data from the Icelandic COST-622 pedons. Some of the information presented here was discussed previously (Arnalds 2004, Oskarsson et al. 2004) in the special issue of Catena (no 56) which presented research related to the COST-622 Action.

Physiography and volcanism

Iceland is a volcanic island of about 100,000 km^2 on the Mid-Atlantic Ridge. Volcanic eruptions occur on average every 4–5 years, and produce both solid lavas and tephra. Oldest rocks found on land are about 16 M y old, but much of the surface is of Quaternary age (<3 M y).

The climate is oceanic and moist with mild winters but cool summers. The soils experience many freeze-thaw cycles yearly, often over a 9 month period, causing intense cryoturbation that influences Icelandic soils.

The volcanism is confined to volcanic zones that run from the southwest and southern parts of Iceland through the center to the northeast (Figure 1). Valleys carved out by the Quaternary glaciers with steep slopes dissect the Tertiary basalt stack that lies outside of the current active volcanic zone. Glaciers occupy about 10,000 km^2, capping some of the active volcanoes. Volcanic eruptions under glaciers cause catastrophic floods, which create large unstable sandy areas. Desert areas are widespread, formed both by natural events such as floods and tephra depositions, but also due to desertification processes (see Arnalds 2000, Arnalds et al. 2001ab). The surface

of these areas (Figure 2) is often very unstable with intense wind erosion, causing eolian redistribution of volcanic materials over great distances (>200 km).

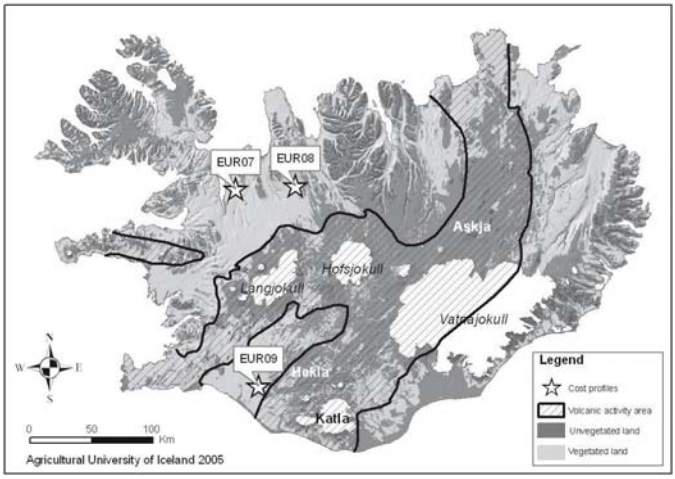

Figure 1. The location of the volcanic zone in Iceland. Sampling sites of the COST-622 pedons are shown, the main glaciers (white), the location of some important volcanoes (Askja, Hekla and Katla) mentioned in the text, as well as the extent of desert areas (dark areas).

Figure 2. Desert landscape in Iceland, barren surface covered by Vitrisols (Cambic Vitrisols). Rocks on the surface are frost heaved.

Since the Quaternary glaciation, the surface of Iceland has been mantled by eolian and tephra materials in which Icelandic soils have developed. Lavas from Holocene also cover substantial areas, but again, often mantled with a varying degree of eolian materials. This eolian input is a major factor controlling the nature of Icelandic soils. Deposition rates range between <0.1 mm to >1 mm y^{-1}, with the mantle commonly being 0.5–1.5 m thick, depending on the distance from active eolian surfaces and volcanoes (Ar-

nalds et al. 1995). The eolian deposition features are well preserved in the profiles (see Stoops et al. this book).

The volcanism produces mostly basaltic to andesitic volcanic materials, while large rhyolitic eruptions are less frequent but often leave distinct markers in the soils. The basaltic nature of the volcanic glass leads to more rapid weathering than in volcanic areas where parent materials are more siliceous. Pedogenic products include allophane, imogolite and ferrihydrite, but layer silicates are nearly absent.

Additional factor that has a dominant influence on the soil environment is the drainage of the soils. The bedrock is quite permeable on the active volcanic belt, and the water table is therefore most often well below the active soil surface, except the terrain is relatively level. The areas outside the active volcanic belt are dominated by Tertiary basaltic lava stacks with relatively slow water permeability compared to the volcanic areas, and water is therefore more often in or near the surface. Organic matter content is controlled by these two factors, eolian input and drainage, with histic soils found far from the eolian surfaces on poorly drained terrain.

A distinctive feature of Icelandic soil environments is the existence of widespread desert areas with poorly developed vitric soils, namely Vitrisols.

Soil types

Two main groups of soils are distinguished within the island, soils of andic and/or histic nature formed under vegetation cover and vitric soils of deserts. Other groups exist, such as Cryosols in the highlands and calcareous soils near sandy beaches in some areas, and also Regosols and Leptosols of rocky terrain, but the nature of these soil types has not been examined in Iceland. The dominant influence of eolian and tephra input on one hand, and drainage on the other are used for separating the more common soils into classes. This relationship is shown in Figure 3. The soil types (from left to right) are Histosols (>20% C), Histic Andosols (12–20% C), Gleyic Andosols (<12% C, poorly drained), and Brown Andosols (<12% C, freely drained). The trend towards wetter conditions and decreased eolian input (towards left and bottom) marks increased organic content with Histosols (>20% C) in the lower left corner. Allophane content also decreases gradually towards the lower left corner. Andosols have in general tendency to accumulate organic matter (see Dahlgren et al. 2004) and here the 20% C is used as a cutoff criteria as is done for the histic/andic boundary in the WRB (FAO 1998). Soil reaction (pH) generally decreases from about 6 to

the right on the diagram to about 4 in the Histosols. Moving up the diagram, vitric materials start to become more dominant. Weathering of volcanic glass releases sufficiently basic cations to maintain the pH of the soil, which rises with vitric material content (to about 7.5 in Vitrisols in desert areas). Allophane content is highest in soils that form under dry conditions with relatively low eolian input (lower right on the diagram). Intermittent stages exhibit both allophane and organic matter influences. The Histic Andosols are peculiar in that they have morphologically all the characteristics of Histosols (see Stoops et al. this book), often with poorly decomposed litter, but andic influences (as expressed by the $Al_o+½Fe_o>2\%$ criteria) are pronounced. An example of vegetated surface with Gleyic and Brown Andosols are shown in Figure 4.

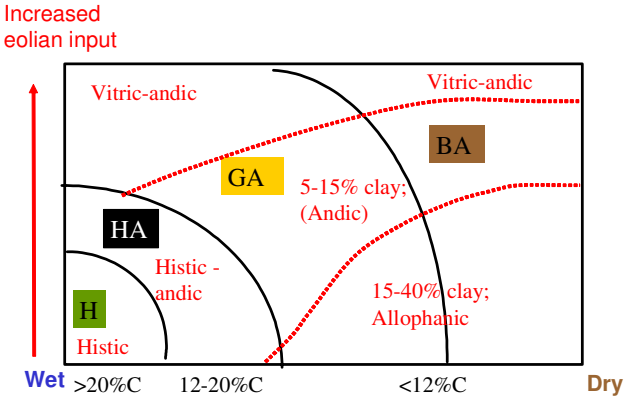

Figure 3. The classification of Andosols and Histosols under vegetation cover in Iceland. Rate of eolian input (y-axis) and drainage (x-axis). The brake line between Gleyic (GA) and Histic Andosols (HA) is 12% C. Brown Andosols also contain <12% C on average in surface horizons. Soils are vitric if eolian input is rapid, but allophanic when dry and eolian input is low with intermittent stages between (andic). The soils tend to become histic and alu-andic when wet far from eolian sources (lower left).

Figure 4. Vegetated landscape covered with Brown and Gleyic Andosols. Note the hummocky relief.

The Agricultural University of Iceland has compiled a soil map in the scale of 1:250,000 (see www.lbhi.is/desert). The aerial extent of major soil types is presented in Table 1.

Table 1. Distribution of soil types in Iceland.

Soil type	Symbol	Extent km^2	Extent %
Brown Andosol	BA	13,360	14.8
Gleyic Andosol	GA	2,390	2.6
Complex	BA-WA	28,080	31.1
Histic Andosol	HA	4,920	5.5
Histosol	H	1,090	1.2
Leptosols	L	7,310	8.1
Cambic Vitrisols	CV	17,640	19.5
Arenic Vitrisols	AV	4,550	5.0
Complex	CV-AV	6,000	6.6
Complex	AV-L	4,790	5.3
Cryosol *complex*	C-GA	140	0.2
Total		90,270	99.9

Table 1 reveals that Brown Andosols (BA; 13,360 km^2 + part of the 28,080 km^2 BA/GA complex) are the most common soils, together with the Cambic Vitrisols (17,640 + part of the MV/SV complex). Gleyic Andosols are also common, consisting of the 2390 km^2 plus approximately half of the 28,080 km^2 area where they occur with Brown Andosols (BA/GA complex). Vitrisols (Cambic, Arenic,) and Leptosols of desert areas total an 40,290 km^2 area according to our soil map.

Cryosols cover only 140 km^2 according to the map, but we have unpublished information that shows that they are more common in the highlands than this number indicates. Many Icelandic Cryosols are peculiar in that they combine organic and vitric characteristics, and most meet criterion for Andosols.

The Icelandic COST-622 reference pedons

The Icelandic COST-622 reference pedons were sampled in September 1999. They give a good representation of Icelandic Andosols, as Histic Andosol (EUR07), Brown Andosol (EUR08) and Gleyic Andosol (EUR09). Vitrisols were not included with the reference profiles, but Arnalds and Kimble (2001) gave a representation of several such pedons.

EUR07-IS

The first reference pedon (EUR07) is located in NW Iceland from a lowland position. It represents poorly drained soils, bordering Histosols with

>16% C in surface horizons, which is common in areas relatively far from eolian sources. It represents Histic Andosol according to the Icelandic classification. The intense cryoturbation has formed hummocks on the surface, which are very common in Iceland. They are termed 'thufur' in Icelandic. The cryoturbation features are also well expressed within the profile and also in thin sections (Stoops this book).

Allophane and ferrihydrite dominate the clay mineralogy of the pedon. As stated earlier, lattice clays, such as smectite, are in very low concentration in Icelandic soils that form in eolian-andic materials. However, lattice phyllosilicates such as smectite have been identified in profiles where Tertiary materials (e.g., paleosols) have been transported from Tertiary hill slopes into profiles (M. Kleber and O. Arnalds unpublished materials). Traces of smectite are also found in this pedon.

EUR08

The second Icelandic reference pedon is located in the North Icelandic highlands at about 400 m elevation. It is a typical Brown Andosol under relatively well drained heath land and low annual precipitation (about 400 mm). The surface is hummocky and both the soil and surface characteristics are influenced by the 7–9 month long frost activity in the soil. Allophane and ferrihydrite dominate the mineralogy, but the soil is more vitric than EUR07, as its location is not far from unstable desert areas. This soil is quite characteristic of relatively poorly developed Andosols, showing clear andic soil properties.

EUR09

The third Icelandic reference pedon was sampled in the peaty lowlands of South Iceland. Extensive peatlands (>10,000 km^2) have been drained in the region for agricultural purposes. The pedon is located near active volcanoes and eolian sources. It's surface has therefore accumulated enough vitric materials and at such rapid rate, that andic properties override the organic properties in that OC is <20%, but the soil is, however, quite organic in nature.

Conclusions

Iceland has the largest area of Andosols and Vitrisols in Europe. The COST reference pedons give a good representation of the Icelandic An-

dosols. Their characteristics are strongly influenced by a relatively steady rate of additions of tephra and eolian materials of vitric nature, which are well reflected by their micromorphology (Stoops et al. this book). The soils differ from most of the other European Andosols discussed in this book because of near absence of layer silicates. Their young weathering state is interesting, as basaltic tephra in a humid environment weathers quite rapidly, and in that they compare with more silicious soils in dry climates. This, of course, can be in part attributed to the cold climate of Iceland, but not entirely. Weathering rates are rapid (Gislason et al. 1996), but one has also to consider the steady eolian and tephra additions to the top of the profiles, maintaining young age of the most active weathering environment in surface horizons. In places of relatively low tephra and eolian inputs, organic, and alu-andic soil forming processes become dominant. The peculiar mixture of organic materials, often poorly decomposed, and andic materials sets Icelandic soils apart from the other European soils.

There also seems to be more abundance of wetland Andosols in Iceland than in most other areas. The Gleyic Andosols of areas with relatively rapid eolian deposition of vitric materials (and tephra deposition events) are of particular interest (example EUR09), with relatively high pH (>6) and both allophanic mineralogy and organic matter dominating the colloidal behavior, while alu-andic influences are not as pronounced as in places far from eolian sources.

The Vitrisols were not sampled. Many of the Vitrisols are Andosols according to WRB and Andisols according to Soil Taxonomy. These soils are rather unique on world scale, being poorly weathered basaltic glass, often with clear andic soil properties (>90% vitric and 1–2% $(Al+½Fe)_o$), forming extensive black desert areas (see Arnalds and Kimble 2001, Arnalds et al. 2001a).

References

Arnalds O (2000). The Icelandic “rofabard” soil erosion features. Earth Surface Processes and Landforms 25:17–28

Arnalds O (2004). Volcanic Soils of Iceland. Catena 56:3–20

Arnalds O, Kimble J (2001). Andisols of deserts in Iceland. Soil Sci Soc Am J 65:1778–1786

Arnalds O, Gisladóttir F, Sigurjónsson H (2001a). Sandy Deserts of Iceland. An overview. J Arid Environ 47:359–371

Arnalds O, Thorarinsdottir EF, Metusalemsson S, Jonsson A, Grearsson E, Arnason A (2001b). Soil Erosion in Iceland. Soil Conservation Service and Agri-

cultural Research Institute, Reykjavik, 155 p. Original edition in Icelandic, 1997

Arnalds O, Hallmark CT, Wilding LP (1995). Andisols from four different regions of Iceland. Soil Sci Soc Am J 59:161–169

Dahlgren RA, Saigusa M, Ugolini FC (2004). The nature, properties and management of volcanic soils. Adv Agr 82:113–182

FAO (1998). World Reference Base for Soil Resources. World Soil Resources Report 84. FAO, Rome

Gislason SR, Arnorsson S, Armansson H (1996). Chemical weathering of basalt in Southwest Iceland: Effects of runoff, age of rocks and vegetative/glacial cover. Am J Sci 296:837–907

Oskarsson H, Arnalds A, Gudmundsson J, Gudbergsson G (2004). Organic carbon in Icelandic Andosols: geographical variation and impact of erosion. Catena 56:225–238

Italian volcanic soils

L. Lulli[1]

Introduction

Volcanic soils are extensive in Italy's central-southern area. Most volcanic rocks belong to the co-magmatic Roman-Campano province as expression of a perpotassic volcanism which started about one million years ago in connection with the last phases of Apennine's orogenesis, when the rapid collapse of the Tirrenic area occurred, generating a series of Horst and Graben. Rocks deriving from these magmas are relatively saturated with silica and contain potassium and sodium-rich minerals. Most older effusions are trachitic, but more recent tend to be basic.

This review relies on various publications by a number of scientists on Italian volcanic soils. The nature of these publications is quite variable, which makes the attempt of to produce a coherent review difficult**.** I first try to set forth the progression of research made on different volcanic systems, followed by analysis of soil genesis. Finally I synthesize soil evolution conditions in various Italian volcanic systems which are not active any more.

Criteria used in studying Italian volcanic soils

Soils derived from volcanic rocks were first studied in a systematic way in Italy by Mancini (1950) on Amiata's volcano, in an effort to establish a relationship between soil nature and climate variations due to altitude. Lulli later studied volcanic soils of the Sabatini mountains north of Rome, further analyzing the soils Amiata (Lulli 1971a) had studied, on an isolated trachitic volcano which erupted 0.4 ky ago. He also studied the Vulture (Lulli et al. 1978), another isolated volcano in Southern Italy, relatively unaffected by pyroclastic materials from other volcanic centres. This was the first time in Italy when soils that develop in pyroclastic flows were analyzed. Most of these studies focused on soil-climate relationships. Lulli et al. (1988) published a study of the Roccamonfina complex north of

[1] With **contributions** of Carmelo Dazzi and Fabio Terribile.

Napoli which was followed by a complete study of Vico, the last volcano that was active in the Latium region. The basic idea was that in determining pedogenesis processes the type of emissions were of greater importance than the magma chemistry itself. This fact had been observed by Lulli in several excursions he made in the alkali-potassic region and on volcanic deposits of **Etna**. In summary, the major hypothesis was that soils that develop in volcanic materials differ according to their deposition modalities.

The results indicate that, if a volcanic rock is continuous and firm enough, soils always have a certain content in clay, thus developing horizons with clay leaching as a main feature. On the other hand, if the original materials are finely divided, the organic matter increases, while the percentage of clay content decreases with no evidence of clay movement.We also attained one more important observation: if those finely divided materials present a continuos vegetation cover, andic features are accentuated, and in presence of a mesophile vegetation, typical Andosols are usually found.

Paul Quantin's experience was crucial in studying the soils of Vico volcanic apparatus, wich can be regarded as a model of pedological evolutions in the Mediterranean area, thanks to the multiplicity of situations and detailed studies carried out. Some subsequent studies by Di Gennaro and Terribile (1999) regarding the Vesuvian environments, and some more studies, in the framework of an European program in relation to soil survey activities in other sites in Campania and Sicily have substantiated the early hypothesis about the effect of readily available vitreous materials in soil forming processes.

Studied environments

Sabatini mounts

The first systematic study on volcanic soils is a work by Lulli (1971b) on Sabatini Mountains in Latium.

Most of the statements later made about other Italian locations (Amiata, Vico, Cimino, Flegrei area, Vesuvium, Etna, Pantelleria) which we are going to summarize in this work, can already be found in this study. The Sabatini area extends around the large caldera of Bracciano Lake, North of Rome. Its activity began more than 0.6 M y ago, contemporaneously with the other alkaline-potassic volcanic centres of Lazio. A notable paroxysmal eruptive phase of Sacrofano occurred about 0.4 M y ago, when large

volumes of pyroclastics were erupted from the central eruptive vent and other smaller ones; this activity furthermore produced lava flows.

Altitudes here rarely exceed 500 m a.s.l. In this area Lulli carried out the first mapping of volcanic soils in Italy. The work clearly showed that if pedoclimate accentuates summer drought, a strong parent material control exists on soil evolution. Therefore, even at relatively low altitudes (and under vegetation cover), soils can be observed with strong andic features on finely subdivided deposits, while a clear profile argillification with evidences of iron release on some lahars or ignimbrites, or pyroclastic flows, can be observed as the parent material becomes compact.

The most important observation was the brown soils genesis on explosion tuffs, the latest forms of emission in the Sabatini area, presenting large amounts of carbonate inclusions (Photo 1).

Soils that form on such deposits lack andic characteristics, but evolve in the direction allowed by climate on **non-volcanic** materials. The presence of calcium and magnesium in the exchange complex is strong and saturation is high. The soils have a cambic horizon and a mollic epipedon. They are classified as Eutric Cambisols or Mollisols. The calcareous nature of sediments is confirmed by the presence at the valley's bottom of Stracciacappa and Baccano lakes, reclaimed in Roman ages, with soils presenting vertic features. These soils well-match those encountered in Vulture (profile 4, Tables 3 and 4 in the Appendix) and those of Albani mountains south of Rome around the Castel Gandolfo Lake.

The mount Amiata

Monte Amiata is a late Quaternary complex (until ca180 ky ago) mainly formed of ignimbrite sheets and trachytic lava domes and flows, with very subordinate mafic lava flows from late in the activity.

We started studying the Amiata, an isolated old volcano, very homogenous from petrographic point of view. On Mt. Amiata, Lulli (1971a) verified that the sequence studied by Mancini could be substantially held for true for all expositions, with soils changing from browns to podzols according to altitude.

Mt. Amiata is one of the first trachitic emissions of Pleistocenic volcanism in Italy. It rises between 800 to 1740 m a.s.l. in an udic moisture regime. Here, all soils have andic features, which had already been recognized in 1970 (Lulli 1971a). A climato-sequence has been recognized. The soil under chestnut (*Castanea sativa*) cover, at an altitude of 950 m, shows andic features, a bulk density >1g cm^{-3} in subsurface horizons. The soil shows well developed andic forms with some brunification elements. Soil

at higher altitudes, under beech (*Fagus sylvatica*), represents a transition to spodic soils, although it had then been classified as an Andept (now Andisol, US Soil Taxonomy). These Podzols are always found under beach stands, at 1400 m a.s.l., and are a good example of podzolization processes of soils on volcanic materials in colder moist climate.

The Roccamonfina complex

Within a broader work on morphology and soils on Tyrrhenian coastal area of central Italy, Remmelzwall (1978) studied the environment of Roccamonfina's volcano, formed from 800 to 400 ky ago.

In this work, it was evident that all soils evolving on level surfaces of pyroclastic flow in a xeric moisture regime present clay leaching, as Lulli had pointed out on Sabatini mountains and on Vulture.

As Remmelzvarl wrote: "The field observations show that large differences exist in the degree of alteration of the pyroclastic rocks. The soil profiles selected are characterized by a relatively advanced stage of weathering. They have an argillic horizon and have relatively low CEC values (generally 10–25 meq/l00g clay). "The absence of altitude in profile descriptions limits the considerations to the mere geomorphological and lithological evidences; nevertheless, the classification of leached soils in xeric regimes supports results from the other volcanic complexes. Soils developing on compact tephra (as some pyroclastic flows) present kandite genesis and migration (mixture of kaolinite, metahalloysite and amorphous materials) and, in addition, genesis of illite, due to additions of silica inn deeper parts of older profiles (Table 1).

Table 1. Mineralogical composition of clay fraction (<2 μm) D.R.X. of Vico's Chromic Luvisol (Lulli et al. 1990).

		Other prime minerals		Secondary minerals				
Horizons	Feldspars F	Q	Ma	mH	H	I_o	I-Sm	Go(He)
E	tr.	++	tr.	++	tr.	+	+	tr.
Bt_{g1}	tr.	++	tr.	+++	tr.	+	+	tr.
BC_{tg}	tr.	tr.	tr.	+++	tr.	tr.	tr.	-
BC_{t1}	tr.	-	tr.	+++	-	tr.	tr.	-

F= feldspars, Q= quarz, Ma= magnetite H= halloysite, mH= metahalloysite, I_o= illite, I-Sm= illite-smectite, Go(He)= goethite (hematite).
++++ = very abundant, +++ = abundant, ++ = medium, + = poor, tr.= traces ε= minimal traces.

Furthermore, they present quartz and an increased presence of silica on most superficial strata, interpreted as products of alteration. Beyond a certain altitude limit (600 m), soils show the presence of amorphous materials of neogenesis and tend to form cambic horizons and a mollic epipedon.

According to Lulli et al. (1978, 1983a,b) probable criptopodzolic forms are recognized inside the caldera at an altitude of about 865 m, while it is certain that andic developments are present on tufaceous materials. However, scoria cones surrounding the volcanic apparatus located in a clearly Mediterranean environment (like xeric and ustic regimes) support soils with translocation of a kaolinitic clay (metahalloysite), featuring high permeability of parent material in presence of dry-season climate (Photo 2).

The mount Vulture

Lulli et al. (1978) on Vulture volcano shows the climatic sequence Haplohumods, Fulvudands and Hapludepts. The sequence is illustrated in Figure 1. The soils here have formed in identical or very similar tuffs. Moreover, the soils have developed without additions of more pyroclastic sediments or consistent removal of materials by erosion. The soils occur at different elevations which in turn are responsible for the different climates. The Haplohumods (Andic? Podzols WRB) occur at the highest elevations with the heaviest rainfall and the lowest temperature. The Fulvudands (Dystric Andosols) occur at intermediate elevations with inter-mediate rainfall and temp-erature. The Hap-ludepts (Andic Cam-bisols, WRB) occur at the lowest el-evations within the study area and have the lowest rainfall and highest temp-erature. All of the soils have udic moisture regimes, but the Inceptisols may border to an ustic regime.

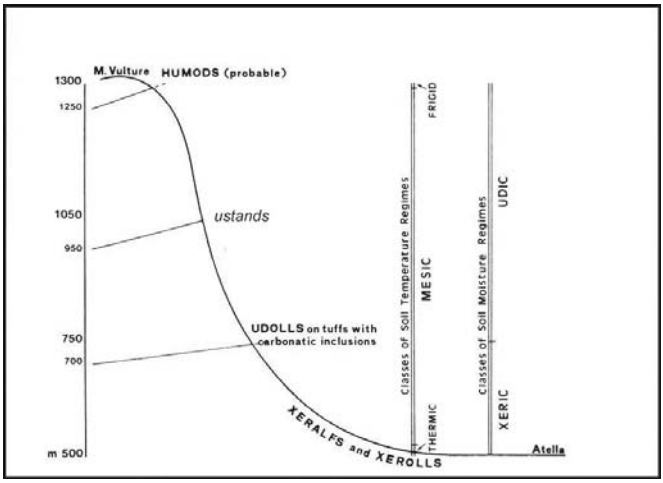

Figure 1. Soils climo-sequence on slopes of Vulture apparatus.

Several features of the Haplohumod profile indicate dominant processes of genesis of the soils. A large amount of organic matter has accumulated, resulting in both high CEC and extractable acidity. In turn, the acidity can contribute to weathering and leaching. Evidence of translocation of materials is provided by the presence of the spodic horizon, lacking in the other three profiles. These features are attributed to the combination of high rainfall and relatively low temperatures.

The Fulvudands lie above an elevation of 1000 m with rainfall ranging from 1051 to 1322 mm and with mean annual temperatures between 10.4 and 8.0°C (Photo 3). Under those climatic conditions, we believe that the soils remain moist throughout the year. Further, we postulate that this moisture regime does not permit the transformation of amorphous materials into better-organized clays than imogolite. This hypothesis is consistent with observations of Hetiér (1975) on soils formed from volcanic rocks in the Massif Central of France. Hetier found that the organic matter in Andosols was made insoluble and immobile by combination with amorphous aluminium. Evolution of the Andosols on the slopes of Mt. Vulture seems to be similar to conditions of the Massif Central. The distribution of Haplumdepts and Haplohumods on Mt. Vulture indicates that the former can be developed and persist in places at higher elevations and possibly at lower sites under strongly acidifying vegetation. In either of those situations, it seems that Fulvudands will be converted to Humods.

The Haplumdepts occur below elevations of 1000 m with mean annual precipitation ranging from 835 to 1050 mm and with mean temperatures between 12.8 and 10.4°C. Short periods of drought occur in summers. We postulate that the temporary drying of the soil permits polymerization of amorphous materials and their transformation into better organized clays. Such changes might also be promoted by the longer moisture recharge periods at lower elevations. Further indications are provided by the color and the extractable iron in the B2 horizon of the Hapludept profile. The chroma is higher and slightly more iron is extractable with dithionite from that B2 horizon than from the B horizons of the Fulvudand profile. Both of these characteristics could be expected from better organized clays.

Strictly speaking, the Hapludoll profile (profile 4, Tables 3 and 4 in the Appendix) is not part of the climosequence. The Hapludolls occur in the same climatic belt as the Hapludepts but have been derived from tuffs rich in carbonate xenoliths. These carbonates are believed to be responsible for differences in pathways of genesis of the Hapludolls and Hapludepts. Duchaufour (1977) states that the process of brownification is linked to the presence of calcium in parent materials. The carbonates in the tuffs from which the Hapludolls were formed are believed responsible for the higher

levels of exchangeable calcium and higher base saturation of all horizons of the soil, as compared to the other three profiles. The Hapludoll profile is also richer in clay than any of the others, which could be due to greater initial amounts in the parent materials, or because of formation of clay in the soil, or both. Formation of additional clay in the soil as it was being developed cannot be demonstrated with the data available but does seem possible. Not much further down the slopes of Mt. Vulture, we have observed Xeralfs and Argixerolls with distinct argillic horizons and those soils seem to have undergone both clay formation and translocation.

The Vico volcanic system

In contrast with most of the other volcanoes in the Lazio region, Vico has a fairly simple structure, constituted by a central strato-volcano truncated by a caldera. Most types of rocks of Latium-Campania region magmas, as well as the most diffused mechanisms of tephra deposition are present.

The Vico volcano consists of a main structure of tephritic-fonolitic lavas with leucite. It also includes a summit caldera with a trachitic central cone and important pyroclastic deposits that have peneplaned a large area in the surroundings. The final phase of volcanism at Vico was strongly influenced by the presence of a lake in the newly formed caldera, and thus was violently hydromagmatic. Only in its very final stage the character of the eruptions became magmatic again, building the cone of Monte Venere within the caldera. The activity of this fourth period lasted from 140 to about 90 ky ago.

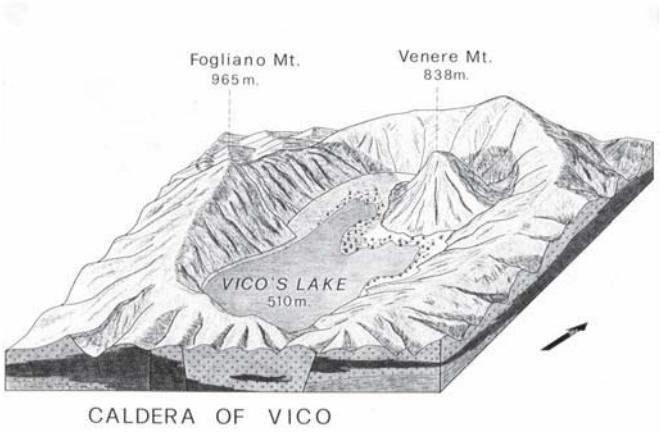

Figure 2. Block diagram of Vico's caldera with a pyroclastic cone (Mt. Venere).

The volcanic materials are alkali-potassic in composition and representative of most Italian volcanic emissions. The volcano's location, rising

from 100 m above the Tevere river basis up to 965 m of the Mt. Fogliano's summit, makes volcanic features and climatic conditions quite variable. Like Vulture, the Vico is not influenced by materials from other volcanic centres; which is important for formulating hypotheses for soil-climate or soil-lithotype relationships. The statements that follow have been excerpted from the conclusions of a work by Lulli et al. (1978), but soils classification terms have been updated.

The soils of Vico show how, in a Mediterranean country, a moderate relief (965 m) can produce an important differentiation in climate as well as in soils properties, according to the altitude and to the slope orientation. The studied sequence shows clearly a gradient: (a) from the Andosols, very deep, dark, humiferous, porous and fluffy materials; (b) to Vitrandic Cambisols marked by an intense clay formation (mainly halloysite) in free drainage conditions, but with only slight remaining andic properties and with very little clay translocations (profile 7 – Tables 5 and 6 in the Appendix; (Photo 4); (c) further down the slope are Dystric Cambisols with little evidences of andic characteristics in the top and little evidences of clay translocation in the lower part of the profile (Photo 5). At the bottom very clayey Chromic Luvisols (*Ultic Xeralfs or Palexeralfs*) are found, compact with bad drainage, argillans and ferri-argillans through the major part of the profile (profile 9 – Tables 5 and 6 in the Appendix; Photo 6).

Near the summit of the Caldera, the Al-chelatation process is predominating in the Andosols over the formation of allophane and other clay minerals. These Andosols (*Fulvudands ST*) (Photo 3) are akin to Haplohumods (ST) although there is no clear evidence of Al-chelates translocation through the soil profile (profile 5, Tables 5 and 6 in the Appendix; Photo 7).

The effects of the climate variation are reinforced by two other local factors. On the upper part of the soil climosequence, a very porous, freely drained, and more recent pyroclastic material favours the genesis of Andosols. Whereas, downward to the middle and lower part of the soil climosequence, where the pyroclastic parent materials become more and more cemented, indurated and older, the formation of clay minerals and then their translocation are favoured.

The Albani complex and Ernici mounts

In spite of frequent seismic activity, the "Colli Albani" is considered an extinct volcano, in the sense that no future eruptions are expected, even though historical documents indicate eruptive activity as recently as 114

BC. Sevink et al. (1984) studied the relationship between soils and surfaces in the Southern part of Latium. This study, following Remmelzwall's (1978) studies on Roccamonfina, includes part of the Ernici mountains. On tuffs of the Albani mountains, which are often inter-stratified with buried soils, leached soils (Luvisols) are encountered, associated with soils at early evolution phases (Regosols) on erosion surfaces. Andosols with mollic character on loose materials of flat or slightly tilted surfaces can also be encountered. Soils with leaching and clay formation (Luvisols) also predominate on the Ernici mountains. Sometimes, Luvisols with mollic characteristics can be encountered. Regosols prevail on lapilli tuffs. All such features mostly depend on a xeric pedoclimate. An unpublished thesis by Biondi demonstrates how, on Latium's volcanos above 500 m, Andosols can form on hydromagmatic emissions, with well developed cambic horizons.

Somma Vesuvio complex

On the huge ignimbritic and pyroclastic past depositions of the Ischia's complex and Flegrei activity that covered large areas including the Apennine reliefs and Sorrentine Peninsula, Vesuvio eruptions mainly emitted pyroclastics and basic lava flows. On recent depositions of pyroclastic materials, soils have vitric features, except on the northern slopes of Mt. Somma, Mt. Faito, which are covered by a continuous forest vegetation and the soils there have marked andic features. A separate case seems to be the Flegrei area, where a large amount of finely divided materials and very deep soils allow for the presence of a vegetation more hygrophilous than we can expect: there are Chestnut woods, and even a Beech woods around the little lake of Astroni caldera, practically at sea level.

The relatively high rainfall of the area and recent depositions give the soils marked andic properties. However, on ignimbritic Flegree depositions, which are a few thousand years old (near Caserta), the author has noted the presence of Luvisols, perhaps favoured by level surfaces.

The Sorrentine Peninsula and the calcareous Lattani mountains are almost completely covered by pyroclastic falls and have soils with marked andic features, as most of the Apennine reliefs closest to the Vesuvio area. All these soils are vitric. Conversely, on the island of Ischia, soils tend to be Andic Cambisols, for the old age of the complex and the intense man activity in a climate with a marked dry season.

A brief note on the soils legend of Somma-Vesuvio complex (Di Gennaro and Terribile 1999): "soils of the Somma-Vesuvio volcano, developing on ash, lapilli and scoria falls, pyroclastic flows and lava of

historic age. This group includes: (i) soils with weak to moderate profile differentiation, and andic properties ranging from weakly to moderately expressed, related to the activities of primary volcanic glass; (ii) calcareous soils developing on pyroclastic deposits containing calcium carbonate; (iii) weakly developed soils on lapilli and ash from the 1944 eruption".

It is interesting to note that all soils that have developed on old deposits present vitrandic or andic features if cultivated, mollic features if containing carbonates, and are Regosol if found on the most recent deposits of the main cone. In summary, within active volcanic areas both deposition modalities and pedoclimatic conditions are of great importance in directing pedogenesis, but also time.

The Etna's region

On Etna mount, studies have been carried out to define the relationships between soil nature and vegetation typology. In addition, an investigation of some soils has been presented by Dazzi (2000) for the COST-622 Action. It is only possible to draft a brief report on evolution trends of the soils in the region.

Due to the southern location of the Etna massif, climatic and vegetation belts are shifted higher in elevation compared to the northern regions of Italy. The volcanism is partly explosive magmatism and pyroclastic falls between lavas can be encountered.

Both the note prepared for the COST action by Dazzi (2000) and the study by Lo Papa et al. (2003) on the relationship between soil and vegetation cover point out that all the soils are vitric. In fact, according to Lo Papa et al., Typic Vitrixerands can be encountered under ilex, Typic Udivitrands under oak and Vitric Hapludands under beech forest. All soils presented by Dazzi were Vitrands (Photo 8). The recent age of depositions explain the vitric nature of the soils.

Certini et al. (2001) made a study on the relationship between features of 30 years old soils under broom and pine covers. Since the soils are so young, the vegetation gains importance; but it still remains difficult for a pedo-geographer to draw some considerations about the actual evolution of soils, which are Regosols.

General remarks

By observing the main genesis factors of volcanic areas in Italy it can be concluded that Mediterranean climate does not favour the conservation of

primary glasses or the genesis of allophane and that almost no finely subdivided deposits can be encountered which have not undergone some prepedogenesis or diagenesis. Neither climate, nor the age of volcanism favour the genesis of andic properties. Soils forming on volcanic depositions of any kind can be andic, but this is almost never sufficient in order to produce "proper" Andosols.

In case of pyroclastic flows, the marked andic features don't appear, even if these are in moist environments, showing a clear effect of effusion modalities. On the other hand, some lavas, like the leucititic one, can present andic properties. Much depends by the speed of parent material alteration. A prolonged evolution depresses andic features. This phenomenon is explained by lability of volcanic glass and of short range clays, in addition to the continuous climatic changes that rocks and soils are submitted to in temperate belts.

Finally, some soils at high locations show clear andic features. Considering that weatherable rocks and sufficient and continuous soil moisture must coexist, such soils must not experience dryness or water stagnations in order to preserve their andic properties. This condition is rare, almost all soils present clay neogenesis and we can therefore include them in the great family of brown soils, which normally evolve in Italian environments. In the Mediterranean climate, well developed soils show important clay formation and movement. They are very similar to all other advanced soils, differing only in their higher fertility.

Climate effect

The length of summer dryness has influence on the genesis of crystallized clay, while high rainfall, combined with the persistence of moistness and favourable drainage conditions, favour the formation of allophane. Between these two extremes are soils showing both features, resulting from the presence of amorphous materials and crystallized clays, generally halloysite.

In a pedologic sense, when passing from udic to xeric environments, the soil's degree of browniness increases, from Andosols to Cambisols domain. Under a thermic regime, clay formation is dominant leading to a Luvisols domain.

For the peninsular volcanic areas the borderline between Andosols/Cambisols vs Luvisols is at about 600/800 m, as on the Vulture and Vico mountains, and at about 1200 m a.s.l. at Etna.

In areas near the xeric and udic boundaries, with a mesic temperature regime, the soil nature is markedly affected by vegetation type.

In forest environments near lake Vico at about 520 m a.s.l., soils featuring amorphous materials are observed that fit into the requirements of Andosols but under cultivation such materials are not found. On lacustrine terraces inside the caldera there is a change from Andosols (Photo 9) under forest to Vitric Cambisols (Photo 4) depending on the persistence of a continuous forest cover.

As we have observed on all the volcanic systems rising to about thousand meters, the temperature regime tends to become frigid, and podzolitation becomes evident in addition to andic features (Photo 7).

Excluding the low-altitude beech forests of Vico, Bracciano, and Vulture, which most favour the preservation of andic characters, in all remaining cases the existence of beech wood is suggestive of the presence of podzolitation phenomena in andic soils.

Organic matter that forms at low temperatures, induce migration processes of chelate iron and aluminium towards the organic fraction at depths.

The A horizon is always deep and well mixed with the mineral fraction (it tends to a no-acid Mull), an E horizon is seldom present, the B horizon presents the features of a structured cambic horizon. But at the contact with the C horizon, some different forms of iron accumulation appear.

It is concluded that with decreasing altitude, the climate factor clearly affects a sequence from podzolic soil to typical andic forms, then changing to soils with a clear genesis of cristallized clay, most often halloysite.

The threshold between soils featuring amorphous materials, the Andosols, and those with crystallized clays is at the passage from the udic to the ustic regimes. With sufficient time and a level topography, the xeric regime, in addition to the genesis of crystallized clay, tends to favour clay migration.

Rock effect

If the climate has a primary function in directing the soil evolution, another important factor is the parent material, and it has a great influence on genetic processes of volcanic soils.

Two of the rock features are of special importance: the amount of readily available amorphous material and the permeability. We consider of secondary importance the chemical and mineralogical composition of rocks. In order to obtain short range clays, excluding podzolization processes, the presence of vitreous materials and a constantly moist climate is needed. Only in such conditions do the typical Andosols characters remain in the soil.

In some cases, short range clay mineral formation is affected by the drying up of the profile which causes an irreversible water loss from amorphous materials. In these cases the parent material must have sufficient amounts of vitreous materials readily available.

When there is dryness in the profile in some periods of the year, the necessary condition for Andosol genesis is the capacity of the volcanic tephra to release materials for the formation of amorphous materials at a sufficient speed to encounter their continuous transformation into crystallized clays. Clay genesis in scoria under moist and fresh climates is a good example, when, in some periods of the year, the rapid drainage produces soil dryness. Typical examples are scoria cones soils in Roccamonfina and those of pyroclastic flows in Vico.

Some types of volcanic rocks can also inhibit the availability of glass for weathering. Examples are lavas or consolidated tuffs. In such cases, the limited availability of vitreous materials determines the soil features and well crystallized clays without any andic features are formed. All these affirmations refer to Italian environments and should not be subject to a greater degree of generalization, but they are likely to apply to other Mediterranean countries.

Pyroclastics flows, although in environments that otherwise favor the genesis of short range order clays, always promote the formation of well crystallized clays, such as halloysite.

Lorenzoni and Quantin (1988) demonstrated that pumices of Vico's pyroclastic flows directly produce meta-halloysite. This process is easily verifiable in the field, provided that we can find some pumices in the flow completely transformed into halloysite (Photo 10).

A study by Lorenzoni et al. (1995) has pointed out two important elements, which are: the genesis of soils with poor andic features on latitic rocks and the genesis of typical Andosols on leucititic lavas. On Mount Cimino, the oldest extinct volcano of Latium region, Vitric Luvisols develops (Vitrandic Hapludalfs S.T.) with crystalline clays: kaolinite, illite and hydroxy-interlayered vermiculite (profile 12, Tables 7 and 8 in the Appendix). The soil remains leached at relatively high altitudes (880 m a.s.l.).

At the same altitude, on Fogliano leucititic lavas there is well developed Dystric Andosol due to the very rapid alteration of leucite that would induce aluminium release and the genesis of short range order products like allophane and imogolite (Quantin and Lorenzoni 1992, Lorenzoni et al. 1995) (profile 10, Tables 7 and 8 in the Appendix; Photo 11). That is a clear rock effect, in contrast with the common trend we can find on most tephra of the alkali-potassic emissions in Italy.

Morphology effects

The form of the surfaces, their slope and exposition interference with climate and the Andosols, according their exposition, are placed at different altitudes. A strong slope generally prevents the genesis of Andosols. But in absence of excessive perturbations, for their high permeability soils on slopes are deep.

A morphology effect can be found on soils evolving on flat surfaces of fluid flows or on terraced surfaces, submitted to falls of tephra or to volcanoclastic flows. In these cases found hydrous levels with clay genesis can be found. And, if flat surfaces are at higher altitudes in permanently moist climates, some spodic characteristics can develop with a clear dif ferentiation of horizons, like an E horizon (Table 2).

Table 2. Vulture – Chemical characterization of B-horizons in relation to spodic horizon requirements by US Soil Survey Staff (1975) (Lulli and Bidini 1980).

Horizon	$Fe\%_{dit}$	$Fe\%_{pir}$	$Al\%_{dit}$	$Al\%_{pir}$	Clay%	$\frac{(Fe+Al)_{pir}}{Clay}$	$\frac{(Fe+.Al)_{pir}}{(Fe+Al)_{dit}}$	Combined index
Andic Haplohumod at 1300 m a.s.l.								
B_{21}	0.73	0.28	0.50	0.60	3.90	>0.2	>0.5	>65
B_{22}	0.72	0.29	0.80	0.76	5.40	>0.2	>0.5	
Typic Fulvudand at 1150 m a.s.l.								
B_2	0.48	0.05	0.28	0.20	3.00	<0.2	<0.5	>65

Explanation of extraction symbols: dit=dithonate, pir=pyrophosphate.

Another effect is the accumulation of soil materials at the slope basis or along small rivers. Soils there accumulate and store a lot of organic materials, a dark color, and their depth can reach 2–3 m (Photo 12).

Time effect

Quarzolatites extrusions of Cimino do not have soils with marked andic or vitric features at high elevations. On domes and on layers of pyroclastic flows, at altitudes starting at 800–1000 m, in Fagetum and Castanetum domains, soils do not present sufficient primary and secondary vitreous materials to include them in the Andosols order. Soils are clayey in all parts, and in some cases are hydrous at depth, even when they are on steep slopes. This is attributed to the age, but Monte Cimino is the oldest of the studied volcanoes (1.350 to 800 ky).

Man effect

Profile thinning, modification of some soil features and depression of andic features result because of the action of man. Indirect impacts include modification of the natural vegetation.

On almost all pyroclastic flows of the Latium and Campania regions, we can observe that most soils are thin, although clayey, because they have undergone intense soil erosion. In presence of deep surface incisions (barrancos), bared morphological plateaux are observed. These are probably caused by a prolonged man action and less water penetration into the soil, resulting in pronounced sheet erosion. This is a hypothesis explaining the scanty presence of soils on uplands of volcanic origin.

Vegetation effect

The soils are influenced by the presence or absence of a continuous vegetation cover. An increased ground exposure to sun rays coincides with stronger soil dryness. The greater quantity of energy absorbed by the soil, causes reduction in organic matter, favouring crystallized clay genesis over development of andic properties.

A cusp-model, according to the catastrophes theory of Thom (1980), in which the control factors are soil temperature and length of dryness, could well represent this phenomenon. The hysteresis for a comeback of glass materials into the soil would be represented by the lack of a continuous vegetation cover. A similar bio-sequence was encountered in Vico's caldera. On leucititic lavas under beech forest Andosols were present, while nearby ploughed soils had lost all diagnostic features of andic soils.

Conclusions

In this excursus on volcanic soils of Italy, we have tried to review the relationship between soil features and both the genesis factors and the dominant processes. Italian soils on volcanic materials, which have had sufficient time to develop, such as soils resting on extinct or dormant volcanic areas, are conditioned by the environment and by the availability of vitreous materials. Soils with available vitreous material result in andic features, while slow evolution enhances the genesis of well crystallized clays. There are, therefore, some podzolic soils, where climate is moist and cool, and Andosols in the whole belt of moist and temperate soil regimes. The extension of dry season, that also exists to a lesser degree in 'udic' belts,

favours the genesis of well organized clays, but clay translocation becomes dominant in Mediterranean environments.

From a lithological point of view, confined environments, such as in pyroclastic flows, tend to produce metahalloysite, as showed first by Violante and Wilson (1983) and then by Quantin and Lorenzoni (1992), while the open pedo-environments tend to result in andic features deriving from the rapid weathering of glasses.

References

Certini G, Fernadez Sanjurjo MJ, Corti G, Ugolini FC (2001). The contrasting effect of broom and pine on pedogenic processes in volcanic soils (Mt. Etna, Italy)

Dazzi C (2000). Field excursion, guidebook. COST Action 622. Soil resources of European volcanci system. Meeting in Palmermo, Italy 27 September – 1 october 2000

Di Gennaro A, Terribile F (1999). I suoli della provincia di Napoli, carta e legenda. Camera di Commercio, Ge Pro Ter, Napoli, pp 63

Duchaufour P (1977). Pedology: pedogenesis and classification. Allen and Unwin, London

Hetier JM (1975). Formation et Evolution des Andosols en Climat tempéré. Thèse Doct, Univ Nancy I, pp 258

Lo Papa G, Palermo V, Parisi S, Laudacina VA, Tusa D, Scalenghe R (2003). Caratteristiche di una sequenza di suoli forestali nel versante Nord-occidentale dell'Etna. Boll Soc It Scienza Suolo 52(1–2):513–522

Lorenzoni P, Mirabella A, Bidini D, Lulli L (1995). Soil genesis on trachytic and leucititic lavas of Cimini volcanic complex (Latium, Italy). Geoderma 68:79–99

Lulli L (1971a). Prime considerazioni sui rapporti tra clima e suoli dell'Amiata. Ann Ist Studi Difesa Suolo, Firenze 1:239–255

Lulli L (1971b). I suoli delle vulcaniti che circondano il Lago di Bracciano (Roma). Ann Ist Studi Difesa Suolo, Firenze 2:23–130

Lulli L, Bidini D (1980). A climosequence of soils from tuffs on slopes of an extinct volcano in southern Italy. Geoderma 24:129–142

Lulli L, Bidini D, Arretini A (1978). Guida escursione dibattito sui suoli dei vulcani Roccamonfina e Vulture. Soc Ita Scienza Suolo, 27–30 Settembre, pp 95

Lulli L, Bidini D, Quantin P (1988). A climo and litho soil-sequence on the Vico volcano (Italy). Cahier ORSTOM, ser. Pedologie, vol XXIV, 1:49–60

Lulli L, Bidini D, Dabin B, Quantin P (1983a). Etude de deux sols andiques derive de roches volcaniques d'Italie du Sud (Monts Roccamonfina et Vulture) a caractere cryptopodzolique. 1. Environnement, morphologie et caracteres des costituents mineraux. Cah Pedol vol XX, 1:27–43

Lulli L, Bidini D, Dabin B, Quantin P (1983b). Etude de deux sols andiques derive de roches volcaniques d'Italie du Sud (Monts Roccamonfina et Vulture) a caractere cryptopodzolique. 2. Formes de la matiere organique et du phosphore; interpretation generale. Cah Pedol vol XX, 1:45–61

Lulli L, Bidini D, Lorenzoni P, Quantin P, Raglione M (1990). I suoli caposaldo dell'apparato vulcanico di Vico. Ist Sper Studio Difesa Suolo, Firenze, pp 158

Mancini F (1950). I terreni del monte Amiata. L'Italia forestale e montana, anno V, fasc 4

Quantin P, Lorenzoni P (1992). Weathering of leucite to clay minerals in tephrites of the Vico volcano. Miner Petrogr Acta 35(A):289–296

Quantin P, Gautheyrou J, Lorenzoni P (1988). Halloysite formation through in-situ weathering of volcanic glass from thrachytic pumice, vico´s Volcano, Italy. Clay Minerals 23:423–437

Remmelzwall A (1978). Soil Genesis and quaternary landscape development in the Tyrrhenian costal area of south-central Italy. Publication Fysical Geography Bodemk Lab University of Amsterdam 28

Sevink J, Remmelzwall A, Spaargaren OC (1984). The soils of southern Lazio and adjacent Campania. Publ Fys Geogr Bodemk. Lab University of Amsterdam 38

Thom R (1980). Modèles mathematiques de la morfogénès. Christian Bourgois, Paris

US Soil Survey Staff (1975). Soil Taxonomy. A basic system of soil classification for making and interpreting soil survey. Agriculture Handbook no 246, p 754

Violante P, Wilson MJ (1983). Mineralogy of some Italian Andosols with special reference to the origin of the clay fraction. Geoderma 29:157–174

Appendix materials on CD-Rom

Italian volcanic soils – photos
Tables 3–8 Italian Volcanic Soils

Soils of volcanic systems in Portugal

M. Madeira, J. Pinheiro, J. Madruga and F. Monteiro

Introduction

The volcanic areas of Portugal are located, almost exclusively, in the Azores and Madeira Archipelagos. Small areas occur around Lisbon (basalts and tuffs). The characteristics and age of volcanic systems of those archipelagos as well as the respective environmental conditions are quite variable (Ricardo et al. 1977, Pinheiro 1990, Ricardo et al. 1992, Franco 1994, Madeira 1998). Due to the volcanic origin and climate conditions of these Archipelagos, a high proportion of their soils meet the criteria of the Andisols order (SSS 2003) and the Andosols major group of the WRB (Driessen et al. 2001). However, their characteristics vary considerably with the age, the nature of the parent material, and with climatic conditions (Pinheiro 1990, Pinheiro et al. 2001, Madeira et al. 2002). Additionally, soils other than Andisols also occur in both Archipelagos (Madeira 1980, Pinheiro 1990, Ricardo et al. 1992, Franco 1994, Madeira et al. 1994). Soils of the Archipelagos have been mapped and studied in detail, and their characteristics and classification have been discussed in several papers (Ricardo et al. 1977, Madeira 1980, Pinheiro 1990, Ricardo et al. 1992, Franco 1994, Madeira et al. 1994, Pinheiro et al. 2001, Madeira et al. 2002). The present paper gives a synthesis of the environmental conditions of those Archipelagos and of the characteristics, distribution and classification of the soils based on the publications cited above.

Environmental conditions

Location

The Madeira Archipelago is located in the Atlantic Ocean between 32°38' and 33°07' N and 16°11' and 17°16' W. It includes the Madeira (728 km^2) and Porto Santo (42.3 km^2) Islands, and the Selvagens and Desertas Islands which are not inhabited. The Azores Archipelago is located at the Mid Atlantic Rift between 36°55'43" and 39°43'23" N and 24°46'15" and 31°16'34" W. This Archipelago has a total area of 2326 km^2 and comprises

nine islands (Figure 1). S. Miguel is the largest (759 km^2) and Corvo is the smallest (17 km^2). The other islands are: Santa Maria (97 km^2), Terceira (402 km^2), S. Jorge (246 km^2) Pico (448 km^2), Faial (174 km^2), Graciosa (61 km^2) and Flores (142 km^2).

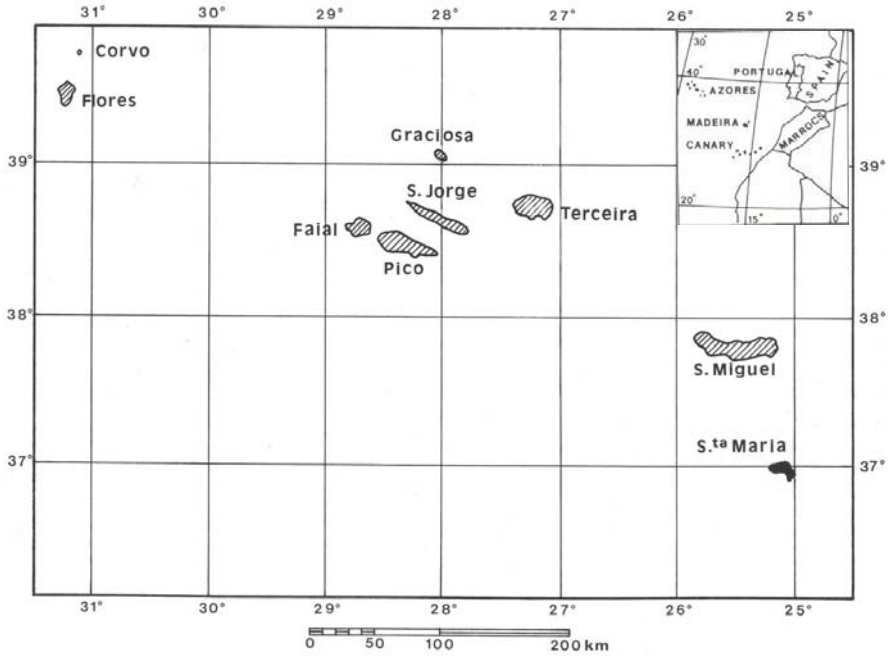

Figure 1. The Azores Archipelago. COST profiles EUR05 and EUR06 are located, respectively, on Faial and Pico Islands.

Geology and morphology

Both Madeira and Porto Santo Islands are dated from the Miocene (Ferreira 1985). The oldest rocks present in Madeira Island are 5.2 M y old. Madeira Island is mostly made of basaltic rocks (basalts, basanite, hawaiite, mugearite) and pyroclastic materials (volcanic scorias, cinders, ashes and tuffs) of basaltic composition (Zbyszewski et al. 1975). Porto Santo is older than Madeira Island and the first volcanic activity there is estimated to have occurred 13.5 M y ago (Ferreira 1985). It has a more complex geology comprising basalts, andesites, trachytes, rhyolites, pyroclastic materials (tuffs and scorias) of variable composition and sedimentary material (calcareous sandstone and dunes).

The Azores Archipelago is located on the Azores platform which is in the confluence of the American, Eurasian and African plates (Madeira

1998), and is younger than the Madeira Archipelago. Only Santa Maria Island is dated from Miocene (8–6 M y). The other islands are dated from Pliocene and Pleistocene. S. Miguel, Graciosa, Flores and Terceira Islands show a maximum age, 2–4 M y old. Faial and S. Jorge Islands are younger (0.73 and 0.55 M y), and for the Pico Island a dating of only 37,000 y was found (Madeira 1998). Rock composition varies from one island to another. Some islands are mostly formed by basaltic rocks (basalts, mugearite, hawaiite) and pyroclastic materials of basaltic composition (Pico, S. Jorge, and Santa Maria Islands) or by trachytes and pyroclastic material (cinders, ashes, pumices, tuffs) of trachyte composition (S. Miguel, Terceira, Graciosa, Faial, Flores, and Corvo Islands) (J.E: Madeira personal communication). In most of the islands historical lava flow fields ("mistérios") and volcanic cinder cones are frequent. At least 30 eruptions (on land or at sea) have occurred since 1439 to the present (Madeira 1998).

The maximum altitude of the Azores Archipelago is about 2351 m a.s.l. (Pico Island). Maximum altitude of the smaller islands (Santa Maria, Graciosa and Corvo) is lower (402–718 m). That maximum in the other islands is 914 m (Flores), 1043 m (Faial), 1021 m (Terceira), 1053 m (S. Jorge) and 1103 m (S. Miguel). Each island has landscapes that are dependent on the volcanic system, tectonics and age. Nevertheless, in all the islands mountainous areas with steep slopes coexist with undulating or flat areas both at low and high altitude.

Altitude of the Madeira Island reaches a maximum of about 1860 m in the central part, which is characterized by rugged mountain massifs with steep slopes and high plateaus. The landscape outside the central region has both steep slopes as well as gentle ones, and is deeply incised by V-shaped valleys (Madeira et al. 1994). Porto Santo Island shows lower altitude (maximum 517 m), and the relief is much less abrupt than in Madeira Island, with significant flat areas (Franco 1994).

Climate

The climate of the Madeira and Azores Archipelagos is predominantly temperate with oceanic characteristics and strongly influenced by elevation. The mean annual air temperature (MAT) in the former varies from about 19°C to about 9°C, on the plateaus and mountain tops. At sea level, maximum (22.6°C) and minimum (15.4°C) monthly mean temperatures occur in August and February, respectively. The MAT in the Azores Archipelago decreases from about 17.0°C to about 11ºC at 1000 m a.s.l. At sea level, maximum (21.0°C) and minimum (14°C) mean monthly temperature also occur in August and February.

Mean annual precipitation (MAP) in the Madeira Island increases from 500 mm (southern aspect) to about 3000 mm in the uplands, whereas in the neighboring Porto Santo Island the MAP is much lower varying between 300 and 400 mm. In the Azores Archipelago the MAP increases from 750 mm (in the west part of Santa Maria Island) to more than 3000 mm in areas of high elevation. Precipitation occurs mostly from October to May.

The climate of both archipelagos is strongly influenced by the occurrence of cloudy, and misty conditions. The soil temperature regime in the Madeira Archipelago is thermic below altitudes of about 450–750 m, but mesic at higher altitudes. The soil profiles of the southern aspect of Madeira Island are characterized by xeric soil moisture regime, below altitudes of 400 m. Other areas are characterized by an udic (or even perudic at high altitude) soil moisture regime, except in some areas near the northern coast line which have an ustic regime (Franco 1990). Soil profiles of Porto Santo show a xeric or xeric/aridic soil moisture regime (Franco 1990).

In the Azores Archipelago the soil temperature regime is mostly mesic, being thermic at altitudes below 200–400 m according to the aspect. The soil moisture regime is mostly udic (or perudic at high altitude), except in areas of low altitude where it can be ustic or even xeric (e. g. west part of the Santa Maria Island).

Vegetation cover

The native vegetation of Azores Islands was a dense and evergreen formation dominated by *Myrica faya*, *Laurus azorica*, *Ilex perado* subsp. *azorica*, *Juniferus brevifolia*, *Erica scoparia* subsp. *azorica*, *Myrsine africana*, *Calluna vulgaris*, *Vaccinium cylindraceum* and *Sphagnum* spp. In Madeira Island species like *Ocotea foetens*, *Clethra arborea*, *Prunus lusitanica*, *Erica arborea*, and *Vaccinium padifolium* were also common. In the Porto Santo Island, due to the climate dryness, the native vegetation was dominated by *Dracaena drago*, *Juniperus phoenicia*, *Erica scoparia* spp. *platycodon*, *Olea europaea* spp. *maderensis* and *Sideroxylon marmulano* var. *marmulllano*. This type of vegetation covered the islands when they were discovered, in the beginning of the fifteenth century. Nowadays, it is confined to the mountainous and lava field areas, and is more extensive in the northern than in the southern aspect. In other areas native vegetation have been replaced by agricultural crops, pastures, and *Criptomeria*, *Eucalyptus* and *Pinus* forests.

Soil distribution and classification

Madeira Archipelago

Soils of Madeira Island were mapped at a 1:50,000 scale, and their characteristics, distribution and classification were reported by Ricardo et al. (1992) and by Madeira et al. (1994). Those of Porto Santo Island were mapped at a 1:25,000 scale, and their respective characteristics and classification were reported by Franco (1994).

Soils of the Porto Santo Island reflect the nature of the parent material and the dry climate. They occur in a thermic soil temperature regime and a xeric/aridic soil moisture regime and do not show andic soil properties. Judging from the soil map of Porto Santo Island (Franco 1994), the main soil types in the island are: Petro- and Haplocalcids, Calcixerepts, Calcipsamments, Calcixererts, Calcixerolls, Palexeralfs and Haploxeralfs (Soil Taxonomy classification). The dominant major soil groups *sensu* WRB (Driessen et al. 2001) are Calcisols and to a lesser extent Regosols, Arenosols, Leptosols, Vertisols, Cambisols, Kastanozems, Phaeozems and Luvisols. Soils other than Calcisols mostly show calcaric or calcic character (Franco 1994). There is not a clear pattern of soil-unit distribution according to elevation, because 75% of the island has an altitude below 150 m. However, Calcisols are more common at lower altitude than the other soil types. There are areas of rock outcrops and soils that are strongly affected by erosion and soil degradation (Franco 1994).

Soil distribution in Madeira Island shows a clear relationship with altitude (Figure 2) and climate conditions (mostly precipitation). Vertisols (Haploxererts) occur below 200 m altitude, whereas Mollisols (Haplustolls and Haploxerolls) and Inceptisols (Haplustepts, Eutrudepts and Dystrudepts) are found up to 400 and 700 m, respectively. The Andisols (SSS 2003) or Andosols (Driessen et al. 2001) have developed on both basaltic rock and pyroclastic materials (of basaltic composition), usually under laurel rainforest and eucalyptus and pine forests and occupy about 50–60% of the total area of the island, mostly under mesic soil temperature regime and udic soil moisture regime (cloud zone). This soil sequence following the WRB system is as follows: Vertisols, Phaeozems, Cambisols and Andosols.

Andisols occur from 700 to 1000 m, in areas with southern aspect, and from 400 to 1200 m in those with northern aspect (Figure 2). These soils, formerly considered as Dystrandepts, were mapped according to their color: dark brown, yellowish brown, reddish brown and red (Madeira et al. 1994). Dark brown Andisols were found only on basaltic rocks while red

Andisols were found to develop from both basaltic rocks and deeply weathered pyroclastic materials.

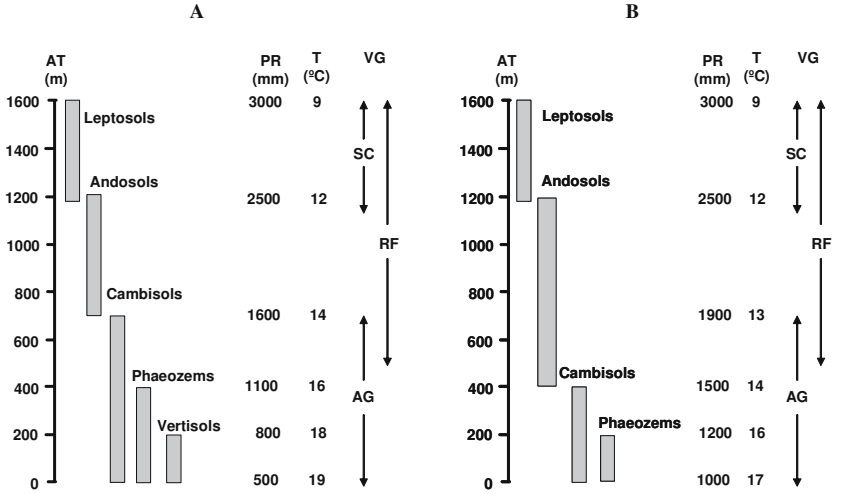

Figure 2. Soil type distribution in the southern (A) and northern (B) aspects of the Madeira Island, according to altitude (AL), precipitation (PR), temperature (T) and vegetation cover (VG). AG: agricultural zone; RF: temperate laurel rainforest and eucalyptus and pine forests, SC: scrub grassland formation.

Due to their dark color, brown Andisols and brown reddish Andisols are Fulvudands and are likely to key out as Pachic Fulvudands (Madeira et al. 1994). The Andisols with red color were classified as Hapludands which might be either Typic or Alic. In the WRB (Driessen et al. 2001) classification scheme, Andosols of Madeira Island are mostly Silandic Andosols, Aluandic Andosols and Fulvic Andosols.

The Andisols occupy about 50% of Madeira Island, and show several particularities. Firstly, they have a high clay content (<2 μm). Secondly, they show a quite high organic C content not only in their epipedon but also at lower depth (Madeira et al. 1994, Ricardo et al. 2004), showing an organic status similar to those of either Melanudands or Fulvudands, and containing up to 50 kg C m^{-2} within the soil profile (100 cm depth). Thirdly, the dark Andosols show an increase of allophane content with depth while the red ones contain either very little or no allophane. Finally, they have an high total iron content and low oxalate Fe content when compared with dithionite Fe content, with hematite (both pedogenic and lithogenic) as the predominant iron oxide; the nature and origin of hematite has not been clearly identified (Furtado et al. 1990, Madeira et al. 1994).

A gradual variation of andic characteristics occurs from brown or reddish brown Andisols to the red ones: (a) increase of the chroma of B horizon, bulk density values, clay content and day minerals, hematite content and KCl-extractable Al values, and (b) decrease of oxalate extractable Si and Al, and total reserve in bases (Ricardo et al. 1992, Madeira et al. 1994).

Andisols from Madeira (especially those with red color) have a limited oxalate-soluble fraction. These soils also show all the characteristics of non-allophanic Andisols, having reactive materials composed mainly of Al-humus complexes and crystalline clay minerals belonging to both the 1:1 types (mostly halloysite-7A°) and the 2:1 types (Al-vermiculite). There is no evidence that the development of non-allophanic character has been accompanied by a particular accumulation of organic matter. Instead, this characteristic seems to result from a process of desilication and leaching of bases affecting preferentially soil top horizons (Madeira et al. 1994).

Archipelago of the Azores

The systematic study of soils from the Azores began during the seventies with the characterization, classification and mapping (Ricardo et al. 1978/79) of soils from S. Miguel (Ricardo et al. 1977), Santa Maria (Madeira 1980) and Graciosa Islands (Medina and Grilo 1981). These studies were followed by the characterization, classification and distribution of soils from Terceira Island (Pinheiro 1990) and by the characterization and genesis of placic horizons in soils from Terceira, Pico and S. Jorge Islands (Madruga 1995). More recently, a systematic survey was carried out in the other islands of the archipelago, and results for Faial Island (Madeira et al. 2002) and Pico Island (Pinheiro et al. 2001).

Santa Maria Island

In Santa Maria Island soils other than Andisols are predominant (Madeira 1980). This is attributed to the age of the island, which is the oldest of the Archipelago (Madeira 1998), and to the low mean annual precipitation (750–1000 mm) in most of the areas of the island. However, a sequence of soils can be defined according to altitude, i.e. with increasing mean annual rainfall. It is common to find in succession Vertisols (Lithic, Sodic, and Typic Haploxererts), Mollisols (Lithic Haplustolls), Inceptisols (Dystric- and Typic Haplustepts), Alfisols (Paleustalfs and Haplustalfs) and Andisols (Madeira 1980 unpublished data). According to the WRB system

(Driessen et al. 2001) the sequence comprises: Vertisols, Phaeozems, Cambisols, Nitisols and Andosols.

Entisols (or Leptosols sensu WRB), associated to rock outcrops occur in large areas of the island, especially at altitude below 250 m, where the soil moisture regime is ustic or even xeric, and which have been affected by water and wind erosion, following inadequate agriculture practices and overgrazing (Madeira 1980). Such soils also occur in steep areas or mountainous areas, at altitude above 400 m.

Andisols only occur in small areas at altitude higher than 350 m (udic soil moisture regime), under forest cover or old pastures. Andisols from Santa Maria Island have a limited oxalate-soluble fraction and negligible contents of allophane, but have the andic characteristics of non-allophanic Andisols. They have low pH and very high contents of extractable Al (2.8–11.4 $cmol_c\ kg^{-1}$) and, therefore, can be classified as Alic Hapludands. They are characterized by a crystalline clay fraction containing clay minerals of the 1:1 type (kaolinite), and show similarity to non-allophanic Andisols from Madeira Island, with reactive materials composed mainly of Al- and Fe-humus complexes. As they have no allophane along the soil profile and show low values of total reserve in bases (36–55 $cmol_c\ kg^{-1}$), these Andisols are strongly weathered soils and represent an advanced evolution stage as compared to Alic Hapludands from Madeira Island.

Other Islands

Available data allow the establishment of the main trends of soil type distribution within the landscape in the Azores Archipelago. Most of the soils other than of Santa Maria Island meet the criteria of the Andisols Order (SSS 2003), Udands being the prevailing Suborder. According to the WRB system (Driessen et al. 2001) Andosols is the major soil group.

Soils other than Andisols (mostly Inceptisols) are only found in areas at low altitudes and close to the coast line (subgroups Typic and Andic Haplustepts), where the soil moisture regime is ustic (Figure 3). Independent of the climate conditions and altitude, Entisols (Leptosols in the WRB system) associated with rock outcrops, occur both on steep slopes and in mountainous areas and lava flow fields (Ricardo et al. 1977, Pinheiro 1990).

Ustands (Typic- and Lithic Haplustands) occur in some areas at low altitude close to the coast line, where the soil moisture regime is ustic.

Distribution of soil groups and subgroups, and characteristics of Udands in the Azores are dependent on the age and nature of parent material and on altitude, i.e. precipitation and soil moisture regime (Pinheiro 1990, Madeira

et al. 2002). At low altitude (especially in older geological areas), marked by thermic soil temperature regime and udic soil moisture regime, Andisols correspond to Hapludands (subgroups Eutric or Typic). Hapludands tend to show Acrudoxic character with increasing altitude above 200 m elevation (Figure 3), due to higher rainfall and organic matter accumulation. The subsurface horizons of these soils usually show low capacity to retain cations. Conversely, they show a high capacity to retain anions, contributing to soil fertility through the accumulation of anions in soil layers and to reduction in leaching of mobile anions (Madeira et al. 2003, Auxtero et al. 2004).

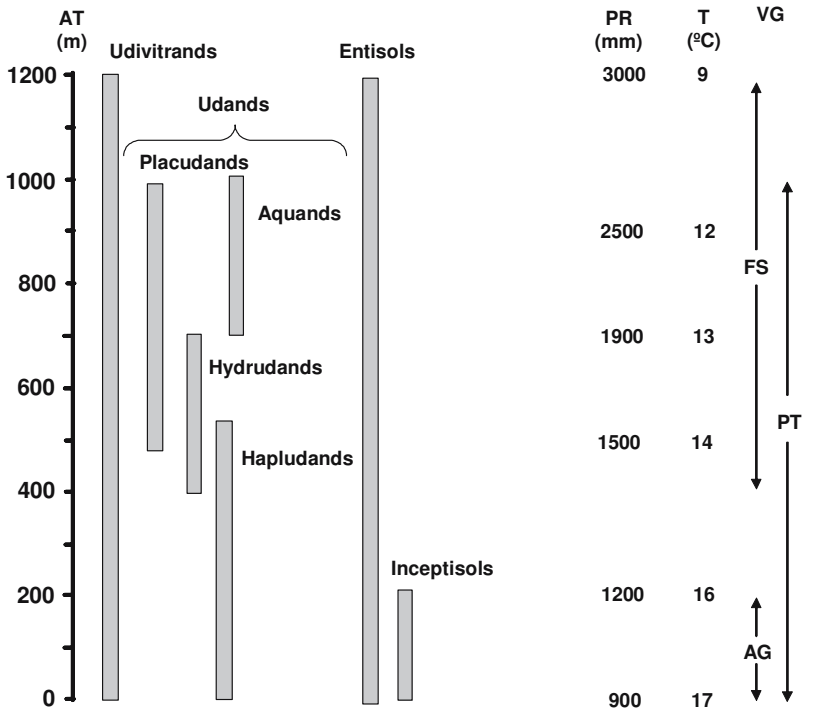

Figure 3. Distribution of soil types in the Azores Islands other than Santa Maria according to the altitude (AL), precipitation (PR), temperature (T) and vegetation cover (VG). AG: agriculture crops; PT: pastures; FS: forest plantations and shrubland.

Above 400–500 m, mostly in the areas where native vegetation still present and where low temperature and permanently wet conditions prevail, segregation and accumulation of iron in thin iron pans occurs (placic horizon), Placudands being the predominant soils (Ricardo et al. 1977, Pin-

heiro 1990, Madruga 1995). The formation of the placic horizons is mainly attributable to reduction processes, favored either by organic rich or by slowly permeable stratified horizons, followed by re-oxidation of iron in the drier soil horizon below (Pinheiro et al. 2004).

In all the islands of the Archipelago the Udivitrands (Lithic and Typic), developed on pyroclastic materials of both basaltic and trachytic composition, can be found at any altitude.

Hydrudands have developed only on pyroclastic materials of basaltic composition, in Pico Island (the youngest of the Archipelago) and, to a lesser extent, on S. Jorge Island, in areas at altitude from 350–800 m, under udic soil moisture regime and mesic soil temperature regime and various types of vegetation cover. The area occupied by Hydrudands is estimated to be about 5500 ha. They show very low bulk density (0.20–0.45 g cm^{-3}), high water retention at 1500 kPa (between 150 and 437%) for the Bw horizon, quite high organic carbon content (>8.3%), high contents of Al extractable by oxalate, and extremely high phosphate adsorption capacity, can reach 52 g P kg^{-1} (E. Auxtero personal communication). Variable contents of allophanic materials can be present in the clay fraction of these soils, showing either allophanic or non-allophanic character. As allophane contents decrease with rainfall and organic matter, the non-allophanic character tends to be more accentuated in the surface horizons. Because Hydrudands from the Azores show very low amounts of extractable bases and extractable Al they classify mostly as Acrudoxic Hydrudands.

Hydrudands show an irreversible hardening after drying (Madeira et al. 1996, Pinheiro et al. 1998). Nevertheless, the change of vegetation cover (natural vegetation by forest or pasture, or forest by pasture) did apparently not cause changes in their characteristics. This should be assigned to specificities of the permanently wet conditions where they occur.

Soils and land use

Madeira Archipelago

In Madeira Island, agricultural land occupies most areas below 400–600 m altitude, respectively in the northern and southern aspects. The land has been turned mostly into bench terraces adapted for irrigation, which involved considerable earthmoving. It was suggested that besides the major effect of climatic factors, anthropic influence would also be responsible for the present day distribution of Andisols in Madeira Island (Madeira et al.

1994), through deforestation, earthmoving and decrease of soil organic matter content.

At elevation higher than 1000–1200 m, native vegetation was strongly degraded due to wildfires and overgrazing, being now mostly represented by *Pteridium aquilinum* (L.) Kuhn, and soils have been subjected to degradation through water erosion (Ricardo et al. 1992).

In the Porto Santo Island, given its climate dryness, soils are strongly degraded due to water erosion (rill, gully and stream erosion) and wind erosion as a result of inadequate agriculture practices for cereals crops and overgrazing. Efforts should be developed to control erosion and to rehabilitate vast areas of the island (Franco 1994).

Azores Archipelago

The andic properties of non-allophanic Andisols from Santa Maria Island are mainly due to Al- and Fe-humus complexes. Therefore they might disappear as a consequence of anthropic perturbation affecting their carbon stocks, as observed in areas where forest cover was replaced by pastures, and Inceptisols became the predominant soils. Nevertheless, several observations suggested the recover of andic properties through accumulation of organic matter in old pastures (M. Madeira unpublished). As mentioned about Porto Santo Island, soils of the driest parts of the Santa Maria Island are degraded due to water and wind erosion, this degradation being noticed since the 16th century (Madeira 1980).

Agricultural crops in the Azores are nowadays confined to areas below 200 m altitude. Pasture for cattle grazing is the main land use system in the archipelago, occupying presently about 95% of the agricultural area, after significant expansion over the last few decades. Large fertilizer applications on pastures have brought serious euthrofication problems to the nearby water bodies, especially in the S. Miguel Island. Mechanical practices used for new pastures in steep and wet areas (mostly in pyroclastic friable material) have increased the risk of water erosion (gully erosion) and land slides. Additionally, grazing and overgrazing in pastures of such areas have also favored soil compaction (especially where Hydrudands occur), leading to an accentuated soil microrelief which hinders cattle mobility.

Acknowledgements

The authors express their appreciation to Prof. Edgar de Sousa for comments on the paper and improvement of English style, and to Prof. José Madeira for information on geologic details of the Madeira and Azores Archipelagos. To Paulo Marques acknowledge technical assistance for the manuscript preparation.

References

Auxtero E, Madeira M, Sousa E (2004). Variable charge characteristics of selected Andisols from the Azores, Portugal. Catena 56:111–125

Driessen P, Deckers J, Spaargaren O, Nachtergaele F (eds) (2001). Lecture Notes on the Major Soils of the World. World Soils Resources Reports 94. FAO, Rome

Ferreira MP (1985). Evolução geocronológica e paleomagnética das ilhas do Arquipélago da Madeira. Uma síntese. Museu do Laboratório de Mineralogia e Geologia da Universidade de Coimbra 99:213–218

Franco EPC (1990). Contribuição para o Estudo do Pedoclima no Arquipélago da Madeira. Secretaria Regional de Economia da Madeira & IICT, Lisboa, pp 44

Franco EPC (1994). Carta dos Solos da Ilha de Porto Santo. Instituto de Investigação Científica Tropical, Lisboa, pp 186 + 2 maps

Furtado AFS, Madeira M, Jeanroy E (1990). Mineralogy of soils from Madeira Island (Portugal). Solubility of the iron oxides. Sciences Geologique Bulletin 43:139–149

Madeira JEO (1998). Estudos de Neotectónica nas Ilhas do Faial, Pico e S. Jorge: Uma Contribuição para o Conhecimento Geodinâmico da Junção Tripla dos Açores. Dissertação de Doutoramento. Faculdade de Ciências da Universidade de Lisboa, Lisboa

Madeira M (1980). Esboço Pedológico da Ilha da Santa Maria (Açores). Instituto Nacional de Investigação Científica, Lisboa

Madeira M, Auxtero E, Sousa E (2003). Cation and anion exchange properties of Andisols from the Azores, Portugal, as determined by the compulsive exchange and the ammonium acetate methods. Geoderma 117:225–241

Madeira M, Furtado AFS, Jeanroy E, Herbillon AJ (1994). Andisols of Madeira Island (Portugal). Characteristics and classification. Geoderma 62:363–383

Madeira M, Pinheiro J, Monteiro F, Fonseca M, Medina J (2002). Características físicas, químicas e mineralógicas dos solos da Ilha do Faial (Arquipélago dos Açores). Revista de Ciências Agrárias 25(3–4):53–66

Madeira M, Pinheiro J, Medina J (1996). Características físico-químicas e mineralógicas de Andossolos do Arquipélago dos Açores (Portugal) que endurecem irreversivelmente por secagem. XIII Congresso Latino Americano

de Ciência do Solo, Águas de Lindóia, SP (Brasil). Comissão 02, n2.14. Edição em CD-ROM

Madruga JS (1995). Características e Génese do Horizonte Plácico em Solos Vulcânicos do Arquipélago dos Açores. Tese de Doutoramento. Universidade dos Açores, Angra do Heroísmo

Medina JMB, Grilo JT (1981). Esboço Pedológico da Ilha Graciosa (Açores). Instituto Nacional de Investigação Científica & Universidade dos Açores, Lisboa

Pinheiro J (1990). Estudo dos Principais Tipos de Solos da Ilha Terceira (Açores). Universidade dos Açores, Angra do Heroísmo

Pinheiro J, Madeira M, Monteiro F, Medina J (2001). Características e classificação dos Andossolos da Ilha do Pico (Arquipélago dos Açores). Revista de Ciências Agrárias 24(3–4):48–60

Pinheiro J, Madeira M, Medina J, Sampaio J, Madruga J (1998). Andisols of the Azores Archipelago (Portugal). Characteristics and classification. XVI World Congress of Soil Science. Symposium 15

Pinheiro J, Rodriguez A, Salguero MT (2004). Genesis of placic horizon in Andisols from Terceira Island (Azores-Portugal). Catena 56:85–94

Ricardo RP, Câmara EMS, Ferreira MAM (1992). Carta dos Solos da Ilha da Madeira (Escala 1:50,000). IICT, UTL, CPUTL & Direcção Regional de Agricultura da Madeira, Lisboa, pp 162 + 2 maps

Ricardo RP, Madeira M, Medina JMB (1978/79). Enquadramento taxonómico dos principais tipos de solos que se admite ocorrerem no Arquipélago dos Açores. Anais do Instituto Superior de Agronomia 38:167–180

Ricardo RP, Madeira M, Medina JMB, Marques MM, Furtado AFS (1977). Esboço pedológico da ilha de S.Miguel (Açores). Anais do Instituto Superior de Agronomia 37:275–385

Ricardo RP, Madeira M, Raposo J (2004). Quantidade e distribuição de carbono orgânico dos solos da ilha da Madeira. Revista de Ciências Agrárias 27(1):24–37

Soil Survey Staff (SSS) (2003). Keys to Soil Taxonomy (9th edn). United States Department of Agriculture, National Resources Conservation Service. Washington

Zbyszewski G, Veiga Ferreira O, Medeiros AC, Aires-Barros L, Silva LC, Munhá J, Barriga F (1975). Carta Geológica de Portugal 1:50,000). Notícia explicativa das folhas A e B da Ilha da Madeira. Serviços Geológicos de Portugal, Lisboa

Soil of volcanic regions in Slovakia

B. Juráni and J. Balkovič

Introduction

Mountains of volcanic origin are rather wide-spread in Slovakia, covering about 10% of the territory. Regions of volcanic origin occur primarily as volcanic mountains, which are mainly built by lava flows and pyroclastic materials, but also as volcanic intrusions in rocks of different origin, mainly as lava residues. Slovakian volcanic mountains can be divided into 4 main volcanic regions (Figure 1):

1. *Middle-Slovakian volcanic region***:** stratovolcanoes of Štiavnické vrchy Mountains and Kremnické vrchy Mountains, stratovolcanic complexes of Javorie Mountains and Poľana Mountains and finally volcanic complexes of Krupinská planina Mountains, Pohronský Inovec Mountains, Vtáčnik Mountains and Ostrôžky Mountains.
2. *South-Slovakian volcanic region*: Cerová vrchovina Mountains and Burda Mountains, which genetically represent the part of Börzsöny Mountains in Hungary.
3. *East-Slovakian volcanic region*: Slánske vrchy Mountains, Vihorlat Mountains and Zemplínske vrchy Mountains.
4. *Volcanic intrusions* in the Slovenské rudohorie Mountains (especially Veporské vrchy Mountains and Čierna hora Mountains).

The aerial extent of each of the volcanic regions is summarised by Table 1. There are also some small intrusions of volcanic material in the Slovenské rudohorie Mountains, the Čierna hora Mountains, and in the Veporské vrchy Mountains.

Volcanic rocks and pyroclastic material create the substrate for various soils including soils with andic properties. Most of the volcanic regions are under forest. Only the lowest mountains, such as Cerová vrchovina, Ostôžky, Krup-

Table 1. The area of volcanic regions in Slovakia.

Volcanic region	Area, km^2	%
Krupinská planina Mts.	868.6	1.8
Štiavnické vrchy Mts.	843.8	1.7
Slánske vrchy Mts.	530.0	1.1
Cerová vrchovina Mts.	496.7	1.0
Kremnické vrchy Mts.	485.2	1.0
Vihorlat Mts.	371.6	0.8
Vtáčnik Mts.	364.1	0.7
Ostrôžky Mts.	269.0	0.5
Javorie Mts.	223.7	0.5
Poľana Mts.	184.0	0.4
Pohronský Inovec Mts.	136.9	0.3
Zemplínske vrchy Mts.	99.9	0.2
Burda Mts.	24.8	0.1

inská planina and Zemplínske vrchy Mountains are mostly used for agriculture.

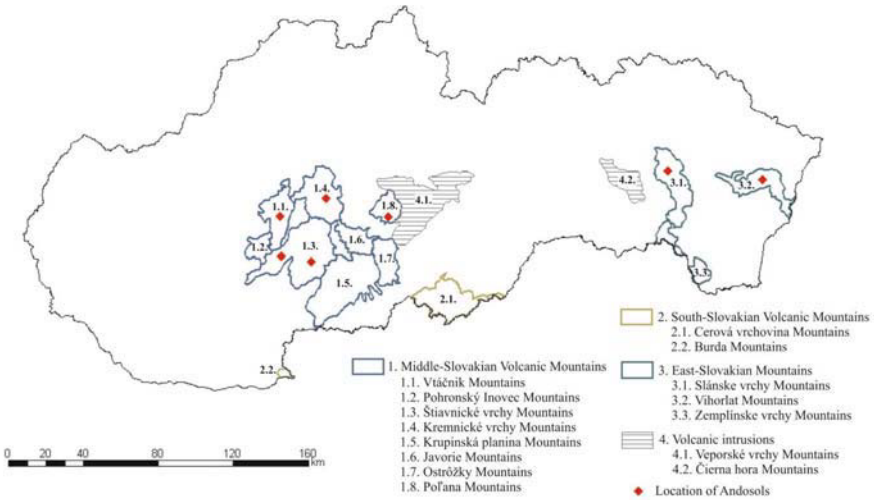

Figure 1. Slovakian volcanic regions and location of Andosols.

Geology and geomorphology

Volcanic mountains in Slovakia occur at the south margin of the Central Carpathians. Most of them have origin in Neogene volcanic activity – the final stage of development of the Carpathian geosynclines, when volcanic activity occurred in terrestrial as well as subaqual conditions.

The genesis of volcanoes occurred in several geological stages. Dominant volcanic activity is dated to Badenian and Sarmatian stages (16.4–11.5 M y) and it is mostly andesite in nature. Badenian formations (16.4–13 M y) can be found in the Middle-Slovakian volcanic region, where they are especially represented by pyroxene- and amphibole-pyroxene andesites. From regional point of view Badenian formations are (i) pyroclastic volcano in the Krupínska planina Mts., (ii) effusive infillings of tectonic depression in the Javorie Mts., (iii) basal floor of the Poľana and Štiavnica stratovolcanos and volcanoes of the Kremnické vrchy Mts., and (iv) relicts of volcanoes in the Slovenské rudohorie Mts.

Geomorphologic structure is closely related to geological composition and intensity of erosion and denudation processes, as is common for old stratovolcanoes. Badenian formations particularly create relicts of pyroclastic cones with breccias of pyroclastic streams and autochthonic brec-

cias and agglomerates in the Krupinská planina Mts. In the Javorie Mts. it forms effusive complex of basaltic and pyroxene andesites accompanied by hyaloclastic breccias, and also the accumulations of hyaloclastic breccias and epiclastic breccias on its slopes. We can find Badenian chloritised lava streams of amphibole-pyroxene andesites and epiclastic volcanic breccias in the Poľana Mts. as well as intrusions of andesite porphyry in relicts of volcanic structures. Thick lava flows of pyroxene- and amphibole-pyroxene andesites or breccias of pyroclastic flows of amphibole-pyroxene andesites are found on slopes of the Štiavnické vrchy Mts. As for the Kremnické vrchy Mts., these Badenian rocks constitute especially lava flows of pyroxene andesites and breccias, intrusions of andesite porphyry and rough epiclastic volcanic breccias. Small relicts can be found also in the Veporské vrchy Mts., where they build mostly rough epiclastic volcanic breccias with small amount of conglomerates. East-Slovakian volcanic region was also affected by Badenian stage of volcanism and both rhyolites and rhyolite-dacites occur there.

Younger parts of volcanic regions are dated to the Sarmatian (13–11.5 M y) and Pannonian stage (11.5–7.1 M y). Apart from pyroxene- and amphibole-pyroxene andesites, basaltic andesites and biotitic-amphibole-pyroxene andesites occur also. Sarmatian layers affect all Slovakian volcanic mountains except the Krupínska planina, Cerová vrchovina and Slovenské rudohorie Mts. They create (i) upper floor of the Javorie, Poľana and Štiavnica stratovolcanoes, (ii) individual stratovolcanoes of Vtáčnik and Kremnické vrchy Mts., (iii) stratovolcanoes of Slánske vrchy, Zemplínske vrchy and Vihorlat Mts.

Sarmatian formations are typical stratovolcano bodies. They occur in form of extrusive piles or short and thick lava flows built up by andesites with features of auto-metamorphic changes and extrusive breccias, also in form of lava flows and effusive complexes of andesites creating the facings of stratovolcanoes and infillings in valleys. Sarmatian and Pannonian effusive cones of inclined lava streams with andesites and breccias occur together with stratovolcano cones of lava streams altering with pyroclastic breccias, agglomerates and tuffs. Re-transported tuffs and pumice tuffs of biotitic-amphibole-pyroxene andesites or infillings of epiclastic volcanic sandstones and fine breccias are common. Accumulations of epiclastic volcanic breccias at the foot of volcanic cones and accumulations of epiclastics in fluvial and sea environment (mixed facies of breccias and conglomerates) occur also in volcanic regions of Slovakia.

Pannonian geological and geomorphological structures are mainly created by basaltic andesites, locally by alkaline basalts and pyroxene andesites. They can be found in the Štiavnické vrchy, Vtáčnik, Kremnické vrchy and Zemplínske vrchy Mts.

The latest stage of volcanism occurred during Pleistocene and it was accompanied by alkaline basaltic lava effusions (Štiavnické vrchy Mts.). The latest volcanism (Late Miocene, Pliocene and Pleistocene) can be found especially in the Cerová vrchovina Mts. and locally also in the Štiavnické vrchy Mountains. This generation of volcanic products consists mostly of nepheline basalts and alkaline olivine basalts. The Pliocene and Pleistocene basaltic formation in the Cerová vrchovina Mountains is 5.4–1.1 M y old and it forms a 10–50 m thick lava stacks with some breccias, maars with pyroclastic infillings and remnants of volcanic cones built by agglomerates with volcanic bombs. Pannonian and Pontian basalts are 8.0–6.6 M y old in these mountains.

Slovakian Neogene volcanic regions have never been directly affected by glaciers.

Sequences of volcanic rocks related to the genesis of main Slovakian volcanic regions are visually described in Figure 2, which is derived from Biely (1996). Most of information on geology and geomorphology was also adopted from this literary source.

Climatic conditions

Due to high diversity in elevation, the climatic conditions in Slovakian volcanic regions are diverse. We used the approach of Konček (1980) to describe the climatic conditions (Table 2). It is evident that moderately cold and very moist regime (G) occurs only in upper parts of higher mountains, which are areas where Andosols can be found. The coldest conditions with mean July temperature between 10–12°C are on the summit of the Poľana stratovolcano.

Vegetation

Volcanic regions of Slovakia have been affected by human activities for a long time and several types of land use and vegetation cover are found. We focus our description on forest vegetation using information from Michalko et al. (1986). Slovakian volcanic areas can be aggregated into three general groups according to their forest cover: low (Burda, Zemplínske vrchy, Čierna hora, Cerová vchovina and Krupínska planina), moderately high (Vihorlat, Slánske vrchy, Ostrôžky, Javorie, Štiavnické vrchy, Pohronský Inovec and Vtáčnik) and high (Poľana, Veporské vrchy and Kremnické vrchy).

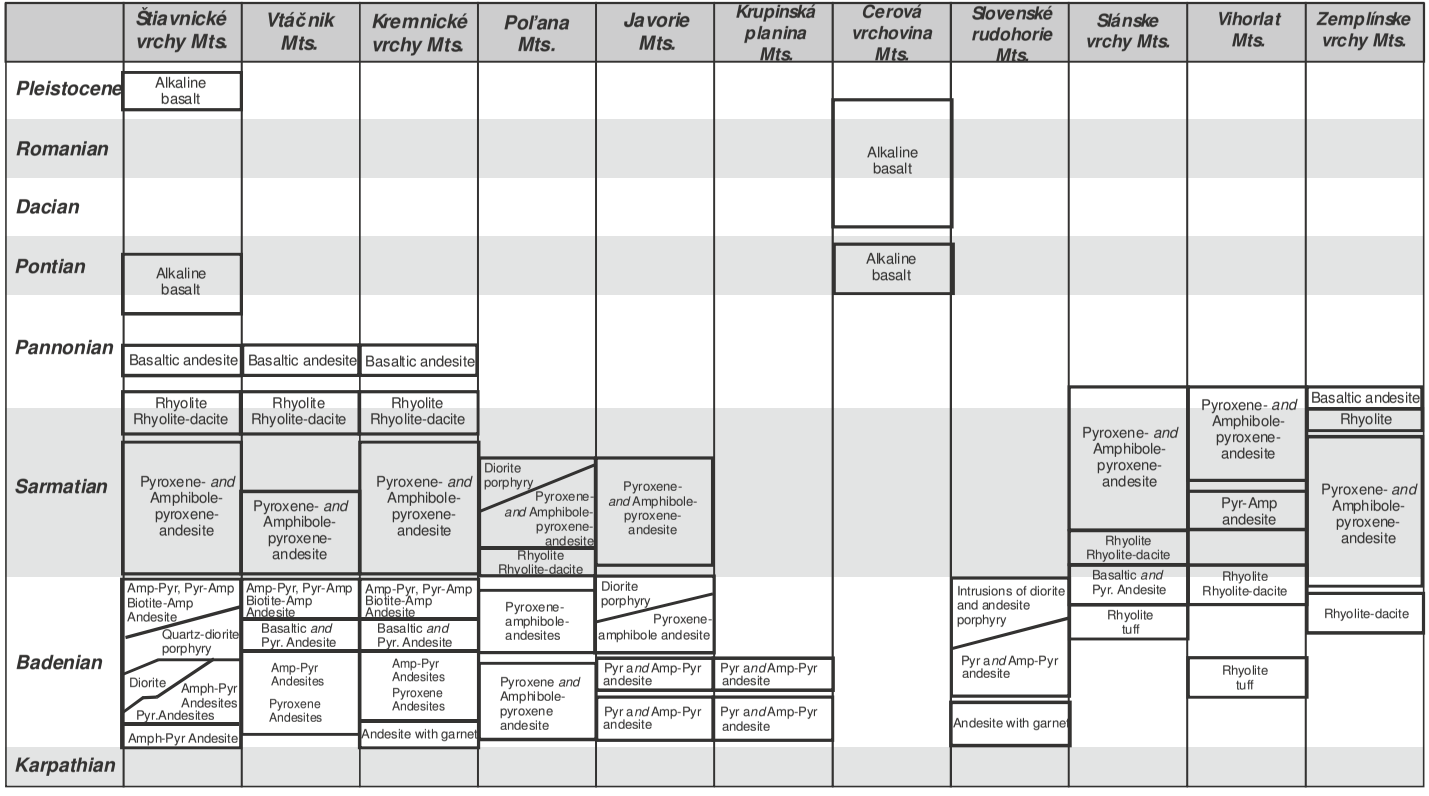

Figure 2. Sequence of volcanic rocks in Neogene volcanic mountains of Slovakia (adapted from Biely 1996).

Thermophilous oak forests with *Quercus cerris* are common in low mountains of Cerová vrchovina, Burda and Krupinská planina, and at the foot of moderately high mountains (Pohronský Inovec, Štiavnické vrchy, Ostrôžky). Stands of the association *Quercetum petraeae-cerris* colonise relatively heavy and acid soils, which are dry in summer and moist in spring. *Quercus cerris* is accompanied by *Q. daleschampii, Q. petraea, Q. robur, Acer campestre* and other trees of oak forests in the tree storey. Herbaceous plants include *Carex montana, Potentilla alba, Poa angustifolia, Pulmonaria mollis, Serratula tinctoria* or *Melica picta*. Extreme reefs and south oriented slopes in low mountains (Cerová vrchovina and Zemplínske vrchy) provide place for submediterranean oak forests, namely the alliance *Quercion pubescenti-petraeae*, with herb layer extremely rich in species. We can find here *Buglosoides purpureo-caerulea, Euphorbia polychroma, Pyrethrum corymbosum, Viola hirta, Inula hirta* and many others. Locally some extrazonal acidophilous oak forests of the alliance *Genisto germanicae-Quercion daleschampii* occur on reefs with shallow and acid soils up to 700 m alti-

Table 2. Climatic characteristics of volcanic regions in Slovakia.

Volcanic region	Designation of climatic region	Remark
Burda Mts.	A	Whole territory
Zemplínske vrchy Mts.	B	Lower part
	C	Higher part
Cerová vrchovina Mts.	B	Bottom part
	D	Medium part
	E	Upper part
Pohronský Inovec Mts.	C	Lower part
	E	Higher part
Štiavnické vrchy Mts.	E	Bottom part
	F	Medium part
	G	Upper part
Krupinská planina Mts.	E	Higher part
	D	Lower part
Ostrôžky Mts.	F	Higher part
	E	Medium part
	D	Bottom part
Javorie Mts.	F	Lower part
	G	Higher part
Slánske vrchy Mts.	G	Higher part
	E	Lower part
Vihorlat Mts.	E	Bottom part
	F	Medium part
	G	Upper part
	H	Northern slopes
Vtáčnik Mts.	E	Bottom part
	F	Medium part
	G	Upper part
Poľana Mts.	G	Dominantly
	I	Upper part
Čierna hora Mts.	E	
Veporské vrchy	G	

A Warm, dry region with mild winter and longer sunshine, mean January temperature over –3°C, sunshine during growing season is >1500 hrs.
B Warm, moderately dry region with cold winter, mean January temperature between –3 and –5°C.
C Warm, moderately moist region with mild winter, mean January temperature > –3°C.
D Warm, moderately moist region with cold winter, mean January temperature between –3 and –5°C.
E Moderately warm, moderately moist region, mountainous, elevation >500 m a.s.l.
F Moderately warm, moist region, mountainous, elevation >500 m a.s.l.
G Moderately cold region, mean July temperature 12–16°C.
H Moderately warm, very moist, mountainous, elevation >500 m a.s.l.
I Cold, mountainous region with mean July temperature 10–12°C.

tudes and they can be found in Slánske vrchy, Čierna hora, Štiavnické vrchy, Vtáčnik or Kremnické vrchy Mountains.

Colline and submontane parts of all volcanic mountains in Slovakia are covered by oak-hornbeam forests. We have to differ between Pannonian oak-hornbeam woods existing in the warmest regions (Burda, Zemplínske vrchy) and the Carpathian ones. Carpathian oak-hornbeam forest (suballiance *Carici pilosae-Carpinenion betuli*) is the vegetation unit spreading to all volcanic regions except of Burda Mts. Tree storey is mostly built up by *Carpinus betulus, Fagus sylvatica, Quercus petraea, Tilia cordata* and *Cerasus avium*, whereas herbs such as *Carex pilosa, Euphorbia amygdaloides, Dentaria bulbifera, Poa nemoralis, Galium schultesii, Dactylis polygama, Stellaria holostea* and many others are common in the undergrowth. Colline and submontane forests have in places been replaced by pastures and meadows and especially grassy vegetation of *Anthoxantho-Agrostietum* or meadows from the alliance *Arrhenatherion elatioris*.

Submontane beech forests create the upper vegetation boundary in low mountains of Zemplínske vrchy, Čierna hora, Cerová vrchovina and Krupínska planina, whereas in moderately high mountains the climax vegetation is formed by montane beech forests of the suballiance *Eu-Fagenion*. Beech forests have their optimum between 500 and 900 m above see level and herbs like *Galium odoratum, Galeobdolon luteum, Oxalis acetosella, Rubus hitrus, Sanicula europaea* etc. are typical for the undergrowth. Such mesophilous beech forests can be edaphically changed to acidophilous and oligotrophic vegetation of the alliance *Luzulo-Fagenion* with typical indicators of acid soils (e.g. *Luzula luzuloides, Avenella flexuosa, Calamagrostis arundinacea, Vaccinium myrtillus, Calluna vulgaris*). Extrazonal acidophilous beech forests can climb up to altitudes of 1300 m in Slovakia.

High mountains of Poľana, Veporské vrchy and Kremnické vrchy are forested by fir-spruce and spruce phytocoenoses on their top. Coniferous forests of *Vaccinio-Abietion* and *Eu-Vaccinio-Piceenion* have *Picea abies, Abies alba, Larix decidua* and sometimes also *Acer pseudoplatanus* in the tree storey. Fir-spruce forests create continual chain at the bottom of climax spruce forests from 700 to 1400 m above see level. We can find typical representatives of montane coniferous forests there, such as *Valeriana tripteris, Cirsium erisithales, Maianthemum bifolium, Gymnocarpium dryopteris, Homogine alpine, Polygonatum verticillatum, Prenanthes purpurea* etc. Spruce forest with *Vaccinium myrtillus* has its optimum between altitudes of 1250 and 1450 m.

Volcanic mountains, especially old lava flows and cones, are frequently capped by scree material. Due to permanent small movements of stones, it is very specific substrate for vegetation to which extrazonal lime-maple

type of forest is related. Forests of *Tilio-Acerion* and montane stands of *Aceri-Fagenion* are typical for prevailing of so-called 'noble trees', such as *Acer pseudoplatanus, A. platanoides, Tilia cordata, T. platyphyllos, Fraxinus excelsior* and *Ulmus glabra*. Nitrophilous character of the undergrowth is indicated by *Lunaria rediviva, Mercurialis perennis, Rumex obtusifolius, Urtica dioica* and many others.

Submontane and montane floodplain forests of *Alnion glutinoso-incanae* are also important as they border creeks and rivers in all volcanic mountains and represent the most diversified and species-rich vegetation units.

Soils and land use

The volcanic area of Slovakia can be divided into 4 groups when evaluating their soil cover. This division follows general conditions, which determine genesis of soil bodies; geology, relief and climate. Human activities have to be taken into account, especially where they have been very intensive and long lasting. Main reference soil groups classified by WRB 1998 in terms of soil mapping units are published in Table 1.8.5 (see Appendix). The information is adopted from the soil map of Slovakia in the scale of 1:1,000,000 (Čurlík and Šefčík 1999) hence it is appropriately generalised.

1. *High volcanic mountains*, with annual precipitations 800–1000 mm and rather low mean annual temperature. Soil cover consists mainly of Eutric and Dystric Cambisols. Andosols are usually situated in the highest parts, over 700–800 m elevation.
   (1.1) *Vtáčnik Mountains:* Fulvic Andosols occur on the main ridge of mountains. High summits (e.g. Vtáčnik summit with 1346 m a.s.l.) are covered by Skeleti-Dystric Leptosols. Slopes are mostly covered by Dystric and Eutric Cambisols, with local occurrence of Leptosols. Fluvisols and Stagnic Luvisols occur at low elevation and alluvium areas.
   (1.2) *Štiavnické vrchy Mountains:* The highest summit (Sitno, 1009 m a.s.l.) is covered by a small area of Melanic and Fulvic Andosols. Andosols can also be found on the Počúvadlo ridge with elevation 700 m a.s.l. Prevailing part of slopes is covered by Eutric, Andic and Dystric Cambisols locally accompanied by Leptosols. Luvisols cover southern foots of slopes and Fluvisols are situated along streams in valleys.
   (1.3) *Kremnické vrchy Mountains:* Relatively large region of Fulvic Andosols occurs on the top of the mountains as well as on upper parts of eastern and north-eastern slopes. They are situated on very steep slopes, however, without any serious signs of water erosion. The main part of

the mountains is covered by Andic, Dystric and partly Eutric Cambisols, often with an admixture of Leptosols. As usually, some Fluvisols follow streams in valleys. A small region of Rendzic Leptosols occurs in a small limestone area.

(1.4) *Poľana Mountains:* Summits and upper parts of southern slopes are covered by Fulvic Andosols and, moreover, this is the place where Andosols reach the highest elevations within the Slovak Republic (1400 m elevation). As it is typical for all high volcanic mountains, the main part is covered by Dystric and Andic Cambisols, and Eutric Cambisols, which are accompanied by Leptosols. Stagnic Luvisols occur in small area at the foot of mountains. Little area of Rendzic Leptosols can be found in the north of the mountains.

(1.5) *Javorie Mountains:* Eutric and Dystric Cambisols as well as Stagnic Luvisols are the main soil types. Gleyic Fluvisols occur in valleys.

(1.6) *Slánske vrchy Mountains:* West and south-west slopes of the highest summit Šimonka (1092 m a.s.l.) located in the north of the main ridge are capped by Fulvic Andosols. The remainder of the area is mostly covered by Dystric and Eutric Cambisols. At the foot of the mountains, some Stagnic Luvisols and Stagnic Cambisols can be found.

(1.7) *Vihorlat Mountains:* Upper parts of south and south-eastern slopes of the main ridge between Vihorlat (1075 m a.s.l.) and Sninský kameň (1006 m a.s.l.) are the places where Fulvic Andosols occur. The main part of Vihorlat massif is covered by Eutric and Dystric Cambisols, Andic Cambisols locally. Some Fluvisols occur along streams and some Rendzic Leptosols are present.

(1.8) *Veporské vrchy Mountains*: Volcanic material intrusion is the substrate for Dystric Cambisols and Leptosols with small spot of Fulvic Andosols in these mountains.

2. *Volcanic mountains built mainly by soft products of volcanism* such as volcanic ash and pyroclastic material, where flat mountain ridges are covered by eolian and solifluction loams.

   (2.1) *Krupinská planina mountains:* Flat mountain ridges are covered by Stagni-Albic Luvisols and Planosols developed from eolian and solifluction loams. Steep slopes inclining down to valleys have rather shallow soils, mainly Eutric Cambisols. Some Fluvisols occur at the bottom of valleys.

3. *Lower volcanic mountains* where dominantly Cambisols occur. This category includes Ostrôžky and Čierna hora Mountains with Eutric and Dystric Cambisols.

4. *Low volcanic mountains* situated in warmer and drier regions.

   (4.1) *Pohronský Inovec Mountains:* Mainly Eutric and partly Dystric Cambisols cover the massif body. Some Fluvisols are situated in valleys

of Pohronský Inovec Mts. Southern slopes are often covered by Cambisols, which are influenced by wine growing (Ari-Anthropic Regosols).
(4.2) *Cerová vrchovina Mountains:* Dystri-Chromic Cambisols (Rothlehm, Brownlehm) and Albic Luvisols occur on the highest parts of flat plateau. Steep slopes are covered by Skeletic Leptosols and Skeletic Cambisols whereas mostly Haplic Luvisols occur at the foot of slopes. Southern expositions are used for vineyards where Ari-Anthropic Regosols can be found.
(4.3) *Zemplínske vrchy Mountains:* Eutric and Dystric Cambisols occupy prevailing part of the mountains. Ari-Anthropic Regosols are common for slopes.

Soils of volcanic mountains are used mainly as forest land (66% of volcanic mountain area) and to a smaller extent as agricultural land, i.e. arable land, vineyards, meadow and pastures (34% of volcanic mountain area). The distribution of land cover in terms of above mentioned categories is shown by Table 3 for individual volcanic regions.

Table 3. Main land cover types in volcanic regions of Slovakia.

Volcanic region	Agricultural land in %	Remark	Forest land in %	Remark
Vtáčnik Mts.	18	Meadows, pastures	82	Deciduous forest
Štiavnické vrchy Mts.	25	Mainly meadows, pastures, arable land	75	Deciduous forest
Kremnické vrchy Mts.	26	Meadows, pastures	74	Deciduous and coniferous forest
Poľana Mts.	24	Meadows, pastures	76	Deciduous and coniferous forest
Javorie Mts.	31	Meadows, pastures	69	Deciduous forest
Slánske vrchy Mts.	21	Meadows, pastures	79	Deciduous forest
Vihorlat Mts.	9	Meadows, pastures	91	Deciduous forest
Krupinská planina Mts.	60	Arable land, meadows, pastures, water erosion	40	Deciduous forest
Ostrôžky Mts.	61	Meadows, pastures, arable land, water erosion	39	Deciduous forest
Veporské vrchy Mts.	–	–	100	Deciduous and coniferous forest
Čierna hora Mts.	–	–	100	Deciduous forest
Pohronský Inovec Mts.	16	Meadows, pastures	84	Deciduous forest
Cerová vrchovina Mts.	58	Arable land, vineyards, pastures	42	Deciduous forest
Zemplínske vrchy Mts.	63	Vineyards, arable land	37	Deciduous forest
Burda Mts.	35	Vineyards, arable land	65	Deciduous forest

Andosols

Some of the soils that have been developed in volcanic mountains of Slovakia have andic soil properties. They are called 'Andozem' by the national classification system of soils (MSCS by Collective 2000) in the case they fulfil specific classification criteria. The criteria for andic properties used by MSCS are derived from WRB (FAO-ISRIC-ISSS 1998) and USDA (Soil Survey Staff 1998), but they are not the same. Horizons have andic properties if:

a) $Al_o + ½Fe_o \geq 2\%$ *or* phosphorus retention >85%
b) Bulk density ≤ 0.90 g cm^{-3}
c) Exchange alkalinity $pH_{NaF} \geq 9.4$

Additional andic features relevant for the classification are:

d) Allophane increase with depth
e) Thixotropy

The criteria mentioned above are a bit weaker compared to those used by WRB and therefore Slovakian Andozem is not fully compatible with Andosol. Soils which are now classified as Andosols have been described only since 70's of the 20th century by Slovakian soil scientists (namely by professor Rudolf Šály). The fact that they have limited extent and were overridden by older field surveys is the main reason why we have only general information on their spatial distribution. Recent estimations refer that volcanic soils with andic properties (Andosols, Andic Cambisols and Andic Leptosols) cover approx. 70,000 ha of forest and 2,500 ha of agricultural land in Slovakia (Juráni 2002).

It is evident that regional and vertical distribution of andic soils in Slovakia follows some general rules. First of all they have developed only from andesite rocks of Neogene age (pyroxene-amphibole andesites, pyroxene andesites, biotitic-pyroxene-amphibole andesites, their breccias and agglomerates) in mountains of Slovakian volcanic regions. Besides geological phenomenon, Andosol genesis is crucially affected by climatic conditions, especially by high humidity, and therefore these soils occur mostly at altitudes above 700–1000 m in Slovakian mountains. In these areas, annual precipitation exceeds 1000 mm and average temperature is about –5°C in January and 15°C in July. The dependence on altitude is also the reason why Andosols have developed on elevated geomorphologic forms, such as lava flows, volcanic cones etc. and, moreover, only in relatively higher mountains (Štiavnické vrchy Mts., Kremnické vrchy Mts., Vihorlat Mts., Poľana Mts., Vtáčnik Mts. and Slánske vrchy Mts.).

Some general catena of distribution and stratification of alu-andic and sil-andic properties as the function of increasing altitude and its related

factors is schematised in Figure 3 (the case study in the Kremnické vrchy Mts.). This general catena starts at Eutric Cambisols, where no andic properties occur, through Andic Cambisols, Dystri-Silic Andosols, Dystri-Pachic Andosols to Dystri-Fulvic Andosols with highly developed alu-andic properties in the topsoil. Increasing humidity enhances andic genesis by supporting the development of poorly-ordered hydrated minerals of aluminium and iron. However, it is evident that high content of organic carbon and extremely acid soil reaction inhibits formation of poorly-ordered minerals in the topsoil horizon due to binding the aluminium by organic carbon in Slovakian Andosols (Balkovič and Bartošová 2003). That is why alu-andic horizons are getting thicker with increasing humidity and decreasing soil reaction, generally with the altitude. Sil-andic properties dominate in Dystri-Silic Andosols occurring generally in the middle of the catena. With increasing altitude sil-andic, properties are shifted deeper to Bw-horizons in well developed Andosols (e.g. Dystri-Fulvic Andosols).

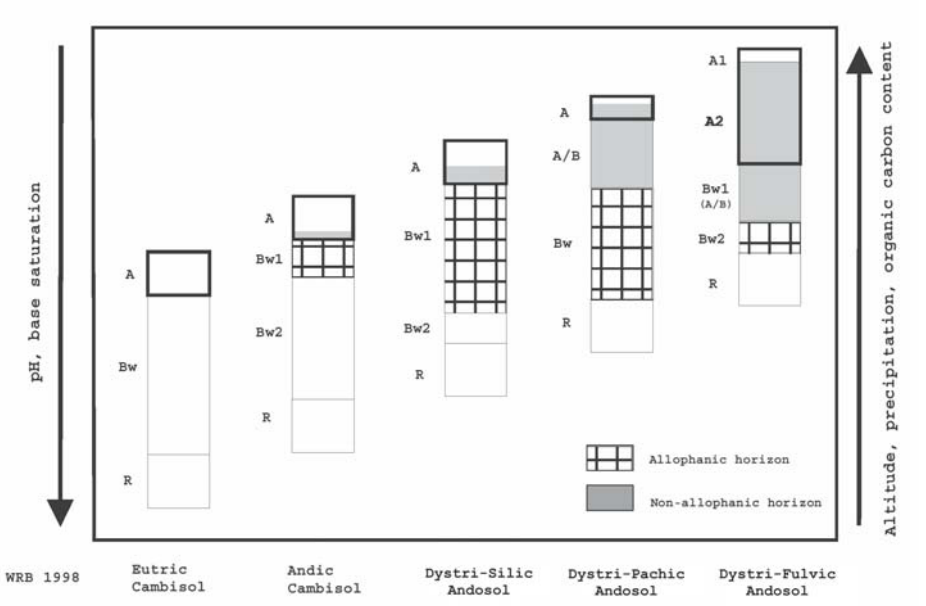

Figure 3. Simplified catena of andic soils in the Kremnické vrchy Mountains.

Multivariate analysis of analytical properties of andic soils is another approach to extract general ideas about andic soil genesis and profile stratification rules in Slovakian mountains. We used analytical data from 12 profiles of andic soils gathered by the Department of Soil Sciences,

Comenius University in Bratislava. This database stores 30 analytical properties analysed in a total of 30 andic as well as non-andic horizons. The results of Partial Principal Component Analysis (PPCA) is summarised in Figure 4. Using multivariate statistics three main pedogenic processes can be identified and expressed by the set of analyses in andic soils (notations are given under Figure 4):

F1 – accumulation of organic matter $\sum (C_{org}, Al_{ex}/CEC, TA, HA, FA)$

F2 – andic soil genesis $\sum (Fe_o, Fe_p, Al_o, Al_p, Si_o, P_{ret}, pH_{NaF})$

F2 – sil-andic: $\sum (Al_o\text{-}Al_p, Fe_o\text{-}Fe_p, Si_o)$

F2 – alu-andi: Al_p/Al_o

F3 – cambic soil genesis $\sum (Fe_o\text{-}Al_o, \Delta pH, pH_{CaCl2})$

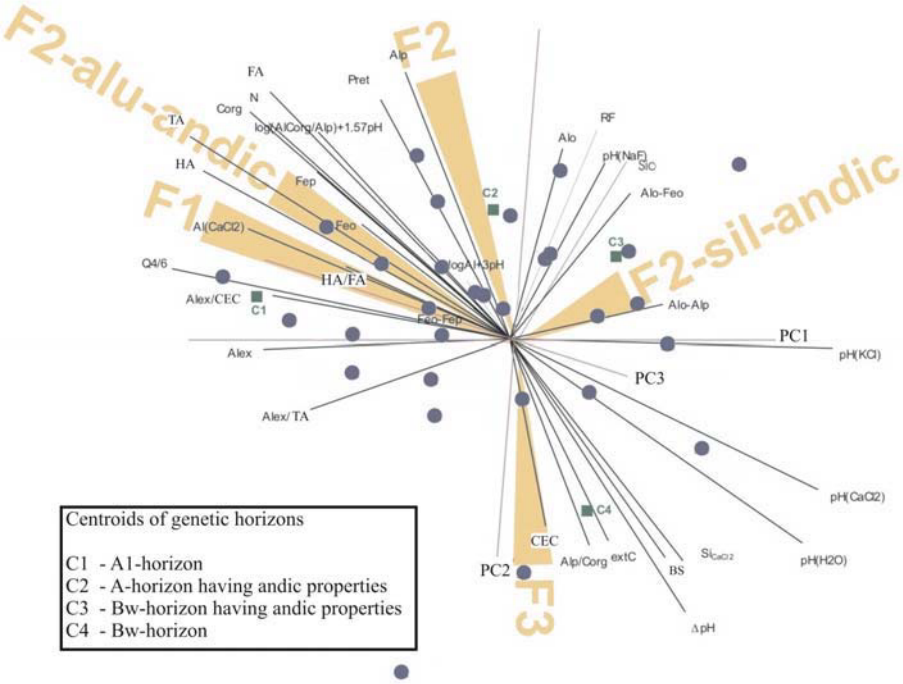

Notes: CEC (cation exchange capacity), Alex (aluminium extractable by 1N KCl), TA (total acidity), Q4/6 (optical density coefficient measured at 400 and 600 nm), oxalate aluminium, iron and silica (Al_o, Fe_o, Si_o), pyrophosphate aluminium and iron (Al_p, Fe_p), HA (humic acids), FA (fulvic acids), $Al(CaCl_2)$ (Al^{3+} extractable by 0.01 M $CaCl_2$ after an hour shaking), C_{org} (total organic carbon), N (total nitrogen), Pret (phosphorus retention), RF (coefficient of HA given by Kumada et al. 1967), pH NaF (exchangeable alkalinity in 1N NaF), $pH(H_20)$, pH(KCl) (soil acidity measured in water and 1N KCl), Si_{CaCl2} (silica extractable by 0.01 M $CaCl_2$ after an hour shaking), BS (base saturation), extC (percentage of extractable carbon by an alkaline extractant $Na_4P_2O_7$+NaOH), $\Delta pH=pH(H_2O)–pH(KCl)$, PC 1–4 (principal component axes). Dots represent soil samples and squares centroids.

Figure 4. PPCA analysis of analytical data of Slovakian Andosols (3D-view).

An ideal or central profile of Slovakian Andosols, which is formed by the above mentioned pedogenic processes, has four genetic horizons signed as C1–C4. Horizon C1 denotes shallow topsoil layer (Ah1-horizon) extremely rich in organic carbon, which is highly saturated by exchangeable aluminium and it does not have andic properties. Horizon C2 identifies alu-andic A(h)-horizon, where organically bounded aluminium is the reactive Al-phase. Sil-andic Bw-horizon (C3 centroid) is usually located somewhere in the subsoil. Mainly mineral reactive aluminium (Al_o-Al_p) and reactive silica (Si_o) determine andic properties. It is quite typical that reactive aluminium highly dominates over reactive iron in andic horizons of Slovakian Andosols. The basal layer (C4) is formed by cambic Bw-horizon without andic properties. It is characterised by high CEC, ΔpH and prevailing of reactive iron over aluminium (Fe_o-Al_o>0).

Four profiles of Andosols have been chosen for the COST 622 Action aiming to gather all essential variability in genetic as well as regional scale. They are classified by WRB 2001 (FAO UN 2001) as Silandi-Vitric Andosol (SK-1), Umbri-Vitric Andosol (Pachic and Skeletic) (SK-2), Molli-Vitric Andosol (SK-3) and Umbri-Vitric Andosol (SK-4). Category 'Vitric', which is based on low content of clay material, probably results from biased analytical values due to insufficient dispersion of soil samples. Textural composition is highly dependent on the parent material and the degree of its weathering, however, clay values published in Table 4 are underestimated in andic horizons. In general, Slovakian Andosols are relatively acid and dystric with base saturation under or only slightly above 50%. This is especially true for those Andosols which have well developed alu-andic properties. Most of them are rich in organic carbon with relatively high degree of humification where melanic index (MI) indicates fulvic type of humus. Reactive aluminium plays the leading role in andic properties and it sometimes exceeds 3% in well developed sil-andic horizons. The highest allophane content estimated by Al_o, Al_p and Si_o analytical values (according to Mizota and Van Reeuwijk 1989) over 10%, was observed in sil-andic Bw-horizon of SK-4. In generally, reactive iron does not occur in high contents and is <1% in studied COST profiles.

It is evident that oxalate aluminium and silica are closely related in the studied soils whereas oxalate iron is standing a bit apart. Reactive iron is not an important diagnostic property for andic soils in Slovakia. Organically bound iron (Fe_p) is dependant on soil acidity and organic carbon, however, pH and C_{org} do not affect the content of reactive mineral iron (Fe_o-Fe_p). Poorly ordered mineral iron is the stable phase of reactive iron except for humus rich topsoil horizons. The amount of ferrihydrites is neither related to alu-andic nor sil-andic properties and the highest values are estimated at around 2.7–3.4% (Pachi-Dystric Andosol in the Kremnické vrchy Mts.).

Table 4. Basic soil properties relevant for describing andic soils.

Profile	Horizon	Depth cm	TA	EB	CEC	BS	Clay	Silt	Sand	pH H_2O	pH KCl	Δ pH	pH $CaCl_2$
			cmol kg^{-1}			%							
SK-1	A	5–10	15.4	4.8	20.2	24.0	6.9	26.8	66.3	4.8	3.9	0.9	4.2
	Bw1	40–50	13.8	4.0	17.8	22.0	16.1	31.2	52.7	5.0	4.1	0.9	4.4
	Bw2	75–85	12.2	17.2	29.4	59.0	14.4	45.1	40.5	5.3	3.8	1.5	4.3
SK-2	A	5–10	18.6	4.8	23.4	21.0	8.7	32.8	58.5	3.9	3.4	0.5	3.5
	A/B	30–50	16.8	2.8	19.6	14.0	4.5	38.6	56.9	4.6	4.1	0.6	4.0
	Bw	70–80	14.2	2.0	16.2	12.0	2.2	11.2	86.6	4.8	4.3	0.5	4.4
SK-3	Ah1	0–10	11.4	30.4	41.8	73.0	11.0	41.6	47.4	5.2	4.5	0.7	4.9
	Ah2	15–25	11.0	15.2	26.2	58.0	10.0	47.9	42.1	5.1	4.1	1.0	4.6
	Bw	60–75	9.6	10.8	20.4	53.0	16.2	47.3	36.5	5.2	4.0	1.1	4.6
SK-4	Ah1	0–5	19.0	2.0	21.0	9.5	10.0	20.9	69.1	3.5	3.1	0.6	3.2
	Ah2	10–20	17.8	1.2	19.0	6.3	9.0	20.5	70.5	4.3	3.8	0.5	3.9
	A/B	30–40	15.6	2.4	18.0	13.3	2.3	18.8	78.9	4.7	4.2	0.5	4.2
	Bw	55–65	14.8	6.8	21.6	31.5	nd	20	80	4.8	4.5	0.3	4.5
	B/C	85–90	10.6	6.4	17.0	37.6	1.0	21.6	77.4	4.9	4.6	0.2	4.7

Profile	Horizon	Si_o	Fe_o	Al_o	Fe_p	Al_p	Al_p/Al_o	Fe_p/Fe_o	$(Al_o-A_p)/Si_o$	Al_o-Al_p	Fe_o-Fe_p	Al_o-Fe_o	Allophane	Ferrihydrite
		%										%		
SK-1	A	0.35	0.32	1.56	0.54	1.24	0.79	1.67	0.93	0.33	–0.22	1.24	1.9	0.6
	Bw1	0.96	0.62	3.28	0.02	0.91	0.28	0.03	2.47	2.37	0.60	2.66	8.8	1.1
	Bw2	0.10	0.41	0.78	0.02	0.27	0.34	0.05	5.24	0.51	0.39	0.37	-	0.7
SK-2	A	0.04	0.98	0.68	0.58	0.67	0.98	0.59	0.29	0.01	0.40	–0.29	0.2	1.7
	A/B	0.25	0.85	1.92	0.52	1.96	1.02	0.61	< 0	–0.04	0.33	1.07	1.0	1.5
	Bw	0.57	0.56	2.07	0.03	0.85	0.41	0.05	2.15	1.22	0.53	1.51	4.5	1.0
SK-3	Ah1	0.10	0.59	0.59	0.14	0.54	0.91	0.24	0.54	0.06	0.45	0.00	0.5	1.0
	Ah2	0.05	0.58	0.61	0.14	0.58	0.96	0.24	0.51	0.03	0.44	0.02	0.2	1.0
	Bw	0.06	0.58	0.69	0.12	0.51	0.74	0.21	2.95	0.18	0.46	0.11	0.7	1.0
SK-4	Ah1	0.03	0.54	0.39	0.30	0.20	0.51	0.56	6.33	0.19	0.24	–0.15	-	0.9
	Ah2	0.22	0.38	1.23	0.05	1.04	0.85	0.13	0.86	0.19	0.33	0.85	1.2	0.7
	A/B	0.44	0.31	1.94	0.09	1.37	0.71	0.29	1.30	0.57	0.22	1.63	2.6	0.5
	Bw	1.18	0.21	3.18	0.04	0.44	0.14	0.19	2.32	2.74	0.17	2.97	10.2	0.4
	B/C	0.86	0.05	1.51	0.03	0.45	0.30	0.60	1.23	1.06	0.02	1.46	5.0	0.1

Profile	Horizon	$Al_o+½Fe_o$ %	pH NaF	C_{org} %	MI	P_{ret} %	BD g cm^{-3}	HA %	FA %	HA/FA	N_{tot} %	Colour wet
SK-1	A	1.7	10.3	10.2	2.2	98.2	0.66	1.31	2.45	0.53	0.82	10YR2/1
	Bw1	3.6	11.1	2.1	2.4	99.7	0.80	0.16	0.79	0.20	0.16	7.5YR4/4
	Bw2	1.0	9.5	0.4	2.2	76.3	1.21	0.05	0.21	0.24	0.03	7.5YR4/5
SK-2	A	1.2	7.9	10.8	2.0	85.5	0.69	2.09	2.74	0.76	0.98	10YR2/1
	A/B	2.3	10.9	5.9	2.1	98.5	0.83	1.01	3.03	0.33	0.43	5YR 2.5/3
	Bw	2.4	10.9	1.9	2.3	97.3	0.86	0.22	1.41	0.15	0.18	10YR4/4
SK-3	Ah1	0.9	9.0	7.2	1.8	65.4	0.72	1.84	2.02	0.91	0.79	10YR2/1
	Ah2	0.9	9.0	4.7	1.7	68.5	0.78	1.25	1.37	0.91	0.39	10YR3/2
	Bw	1.0	9.4	2.6	1.6	70.0	0.92	0.58	0.79	0.73	0.19	10YR4.5/3
SK-4	Ah1	0.7	7.7	15.9	2.4	61.2	0.73	nd	nd	nd	1.03	10YR2/1
	Ah2	1.4	10.8	12.0	1.9	98.4	0.65	nd	nd	nd	0.94	10YR2/2
	A/B	2.1	11.6	8.4	2.4	98.1	nd	nd	nd	nd	0.59	10YR3/2
	Bw	3.3	11.7	6.0	2.2	99.3	nd	nd	nd	nd	0.32	10YR3/3
	B/C	1.5	11.3	0.9	2.0	96.6	nd	nd	nd	nd	0.10	10YR4/4

Notes: Total acidity (*TA*), extractable bases (*EB*), cation exchange capacity (*CEC*), base saturation (*BS*), oxalate silica, aluminium and iron (Si_o,Al_o,Fe_o), pyrophosphate aluminium and iron (Al_p, Fe_p), allophane (*Allophane* = $100/[(-5.1(Al_o-Al_p)/Si_o)+23.5]Si_o$), ferrihydrite (*Ferihydrite* = 1.72 Fe_o), total organic carbon (C_{org}), exchangeable alkalinity in 1N NaF (*pH NaF*), pH in 0.01 M $CaCl_2$ (*pH* $CaCl_2$), melanic index (*MI*), phosphorus retention (P_{ret}), bulk density at field moisture (*BD*), humic acids (*HA*), fulvic acids (*FA*), total nitrogen (N_{tot}), *nd* – not determined.

Oxalate and pyrophosphate extractions are used to approximate the character of reactive Al and Si material (Figure 5). The ratio $(Al_o\text{-}Al_p)/Si_o$ less then 1 indicates high amount of opaline silica in alu-andic conditions where Al is predominantly bounded in Al-humus complexes and silica acid precipitates as SiO_2 minerals. Well developed sil-andic horizons, where Al_p/Al_o is less then 0.4 show the ratio $(Al_o\text{-}Al_p)/Si_o$ within the range 1–2.5 for which probably allophane and imogolite minerals with gibbsite-like mineral admixture are responsible. Parfitt and Childs (1983) expect gibbsite formation in places with high silica acid leaching (e.g. in pores). Bw-horizons without andic properties have the ratio $(Al_o\text{-}Al_p)/Si_o>2.5$, which can be assigned especially to gibbsite-like minerals.

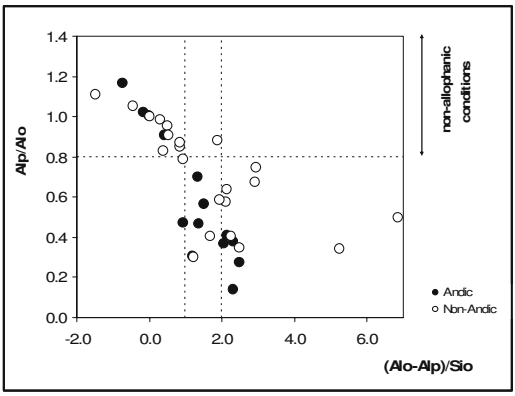

Figure 5. Diagram of Al_p/Al_o plotted against mineral Al/Si ratio.

When we summarise data gathered from Slovakian Andosols, we conclude that these soils fulfil criteria for andic properties required by WRB and they can be compared with other European Andosols (Figure 6). They have typical mountain character accompanied by acid, dystric and skeletic

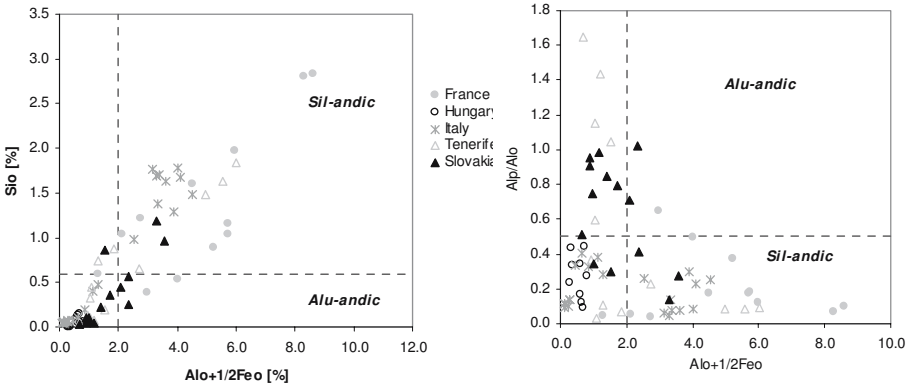

Figure 6. Slovakian analytical data in classification frame of some European volcanic soils.

soil conditions. Andosols represent an unique soil body in Slovakia, which is the part of national heritage and, moreover, they add to the wide ranging family of European volcanic soils.

References

Balkovič J, Bartošová M (2003). Active aluminium, iron and silica in volcanic soils of Slovakia. Phytopedon (Bratislava), vol 2 1:42–50

Biely A (ed) (1996). Annotations to geological map of Slovakia (1:500,000). Ministry of Environment, Geological Service of Slovak republic, Bratislava

Collective (2000). Morphogenetic soil classification system of Slovakia. VÚPOP, Bratislava

Čurlík J, Šefčík P (1999). Geochemical atlas of the Slovak republic, Part V: Soils. Ministry of the Environment of the Slovak republic, Bratislava

FAO-ISRIC-ISSS (1998). World Reference Base for Soil Resources. World Soil Resources Report 84. FAO, Rome

FAO UN (2001). Lecture Notes on the Major Soils of the World. World Soil Resources Report 94, Rome

Juráni B (2002). Volcanic soils in Slovakia. COST Action 622 Soil Resources of European Volcanic Systems, Report, Manderscheid, Germany, p 19

Konček M (1980). Climatic regions. In: Collective: Atlas SSR. SAV, Bratislava

Kumada K, Sato O, Ohta S (1967). Humus composition of mountain soils in Central Japan with special reference to the distribution of P type humic acids. Soil Sci Plant Nutr vol 13(5):151–158

Michalko J (ed) (1986). Geobotanical Map of CSSR. Veda, Bratislava

Mizota C, Van Reeuwijk LP (1989). Clay mineralogy and chemistry of soils formed under volcanic material in diverse climatic regions. Soil Monogr. 2, ISRIC, Wageningen

Parfitt RL, Childs RW (1983). Comments on clay mineralogy of two Northland soils New Zealand. Soil Sci Plant Nutr 29:555–559

Soil Survey Staff (1998). Keys to Soil Taxonomy. 8th edn. USDA/NRCS, Washington D.C.

Appendix materials on CD-Rom

Picture 1.8.1 Sitno summit (Štiavnické vrchy Mts.)

Picture 1.8.2.1 ‘Stonefall’ of basalt in the Cerová vrchovina Mts.

Picture 1.8.2.2 Basaltic lava stream with different types of desegregation (Cerová vrchovina Mts.)

Picture 1.8.2.3 Detailed view on andesite lava flow (Kremnické vrchy Mts.)

Picture 1.8.4.1 Oak forest with *Poa nemoralis* (Štiavnické vrchy Mts.)

Picture 1.8.4.2 Oak-hornbeam forest with *Carex pilosa* (Štiavnické vrchy Mts.)

Soils of volcanic systems in Spain

M. Tejedor, J.M. Hernández-Moreno and C.C. Jiménez

Introduction

The Canary Islands are the most important volcanic zone anywhere in Spain, considering both extension and age of the eruptive events. On mainland Spain, the most important volcanic areas are found in Campo de Calatrava (Ciudad Real, Central Spain), Cabo de Gata (Almería, Southeast) and Olot (Girona, Northeast). In former two, which are older, soils do not present andic characteristics (Vizcayno Muñoz et al. 1979ab, Simón 2005). In Olot, Andisols developed on basaltic scoria and lapilli under perudic climatic conditions have been described (Bech 1976ab).

Andisols on non-volcanic materials have also been described in Galicia, on easily weatherable parent rocks such as gabbros, amphibolites and fine grained schist rich in biotite (García Rodeja et al. 1987). The soils are well drained and formed under a udic moisture and mesic temperature regime. They are non-allophanic Andisols in which the colloidal fraction is dominated by Al-humus complexes. Of a similar nature are the Andisols described in Navarre on phyllites under perudic conditions (Iñiguez and Barragán 1974).

Given the already mentioned greater significance of the soils of the Canary Islands, the variety of soil forming factors, the importance and peculiarity of land use in recent volcanic landscapes and the extensive research performed in the soils of the archipelago from different Soil Science disciplines, this chapter will focus mainly in canarian soils, with brief description of the others-limited by the scarcity of the research.

We will describe the environmental conditions in the Canaries, the soil types and their distribution, with special attention to Andisols, and will situate in this context the Canarian reference profiles used in the COST-622 European project.

Volcanic soils of mainland Spain

Andosols have been described in Garrotxa (Girona, Catalonia) by Bech et al. (1976ab). The area in question measures 150 km^2 and the volcanic parts

occupy 30 km^2, and are mainly Holocene. The deposits are alkaline basalt and basanite lavas as well as pyroclastic deposits and tephra. The climate is Mediterranean, humid mountainous, locally perudic. The land use is mainly forestry and agriculture. A more recent study by Palou and Boixadera (1999) conducted a comprehensive survey of the soils of the region, describing the following: Andosols (silic, mollic, thaptic, eutric), Phaeozems (pachic, thapthic) and Cambisols (eutric).

Soils derived from old volcanic materials have been studied in Ciudad Real (Central Spain) by Vizcayno Muñoz et al. (1979ab). The region is 6000 km^2 in size and lava flows and pyroclastic deposits of basaltic composition dominate, with an age between the Pliocene and Lower Quaternary. Together with the climatic features (Mesomediterranean, dry), this circumstance accounts for the absence of allophane. The main clay mineral component was found to be montmorillonite, although illite and halloysite were also identified. The latter mentioned authors also reported high content of amorphous silica.

Soils derived from old volcanic materials in Cabo de Gata have been studied by Simón (2005). The region is about 190 km^2. The volcanism was generated in two successive steps, from 14 M y to 7.5 M y. The volcanic emissions varied from massive lava flows to different types of pyrocalstic products, mainly of andesitic-dacitic composition. The age of the rocks together with the arid Mediterranean climate explain the absence of andic soil properties. Leptosols, Regosols, Cambisols and Calcisols have been described in the area (Simón 2005). It is worthy to note that the main Spanish bentonite deposits of hydroternal origin are located in Cabo de Gata (Push 2001).

Soils of the Canary Islands

Environmental Conditions

Location

The archipelago of the Canary Islands lies in the Atlantic Ocean, opposite the Sahara Desert and near the Tropic of Cancer. It is located between 27º37’ and 29º25’ northern latitude, and 13º20’ and 18º10’ western longitude (Figure 1). It has seven islands: Tenerife (2034 km^2), La Palma (708 km^2), La Gomera (369 km^2) and El Hierro (269 km^2) – all part of the province of Santa Cruz de Tenerife- and the eastern islands of Gran Canaria (1560 km^2), Fuerteventura (1660 km^2) and Lanzarote (846 km^2), which

make up the province of Las Palmas de Gran Canaria. One of the most eastern islands, Fuerteventura, is a mere 115 km off the west coast of Africa. There are also three very small islands (27–4.7 km^2) and three islets (<4 km^2).

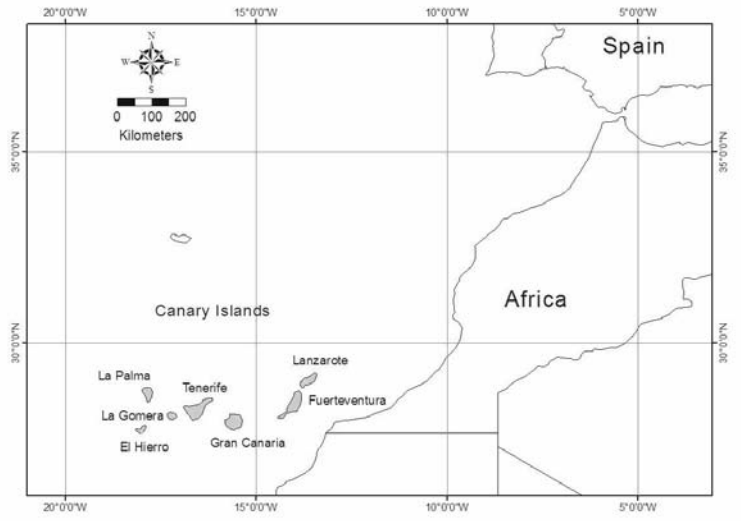

Figure 1. Location of the Canary Islands.

Geology and Relief

The Canary Islands are of volcanic origin, with materials grouped into basal complex and volcanic series. The basal complex, dating back to the Oligocene-Miocene, is formed by plutonic, hypabissal and submarine volcanic rocks, which emerge on the surface in some parts of Fuerteventura, La Gomera and La Palma only. Among the volcanic series the following formations are distinguished, depending on age (Carracedo 1980):

a) 20 M y to 5.1 M y: First volcanic cycle (Miocene) (Tenerife 7 M y, Gran Canaria 14 M y and La Gomera, Fuerteventura and Lanzarote up to 20 M y). There are no materials of this age on the islands of La Palma or El Hierro.
b) 5.1 M y to a few thousand years. Second volcanic cycle (Pliocene-Quaternary), ranging from a few thousand years to 5.1 M y (non-existent in La Gomera).
c) A few thousand years until present: Recent volcanic activity (again none identified for La Gomera), and recent eruptions with historic dates (La Palma, Tenerife and Lanzarote).

Canarian volcanism is entirely alkaline and all the terms of this series are seen in the archipelago: basalts (predominant), trachybasalts, trachytes and phonolites. Salic materials are represented extensively in Tenerife and Gran Canaria only (over 20% of the land area).

Three groups of islands can be differentiated according to height: the more mountainous islands – Tenerife (3718 m at the peak of the Teide volcano, the highest point in Spain), La Palma (2426 m) and Gran Canaria (1950 m); islands of medium-height – La Gomera (1487 m) and El Hierro (1501 m), and the low islands (Lanzarote, 670 m and Fuerteventura, 807 m).

The relief of the islands is generally abrupt, due to the central parts being occupied by the mountains and the resulting steep slopes. Flat plains predominate in Lanzarote and Fuerteventura only.

Factors of Climate variability

Viewed generally, the climate of the Canaries can be defined as subtropical and maritime. However a series of clearly differentiated microclimates exists. Among the factors influencing differentiation are the cool and moist north-easterly trade winds, the Canaries' cold marine current, a thermal inversion area located at about 1500 m altitude and the orography of the islands.

Due to the height and orientation of the mountain systems on the higher islands, the orography throws up two contrasting situations: one characteristic for the north and north-east, where the trade winds help maintain a humid climate, and the other prevailing on the southern and western sides, which are protected from these winds and where the climate is therefore more arid. The altitudinal sequence of the soil temperature regimes is hyperthermic, isothermic/thermic, isomesic, mesic and frigid at the north side and hyperthermic and thermic at the south side (Tejedor et al. 2003b, Rodríguez Paz 2005). The soil moisture regimes on the north side are aridic/ustic, ustic, udic and xeric, and aridic and xeric on the south side (Monteverde 2005).

The absence of orographic systems on Lanzarote and Fuerteventura means that trade winds do not discharge their moisture due to the insufficient elevation for adiabatic condensation. The climate here is very dry and similar to the southern sides of the mountainous islands. The soil moisture regime is aridic (Tejedor et al. 2002b) and the temperature regime is hyperthermic (Díaz 2004).

Vegetation and Land Use

On the higher islands, in addition to the climatic variation, the vegetation is also highly varied. On both the north and south sides there is a first coastal level of halophyte vegetation formed by the association *Frankenio-Astydamion*. The next level corresponds to a *Kleinio-Euphorbion* with *Launaea arborescens, Rumex lunaria* and *Opuntia* in degraded areas. An upper fringe is covered by a transition thermophilic vegetation. Green forest is found only on the northern side, between 600 and 1200 m a.s.l., where the trade winds discharge their moisture. The forest is 'laurisilva' and is home to more than 15 tree and other different species. On the edges of the green forest is the "*Fayal-Brezal*". Higher up on both sides one finds the Association Cisto-Pinion. At heights above 2000 m a.s.l. one finds *Spartocytisus supranubius* and *Adenocarpus viscosus*. This vegetation floor is found on Tenerife and La Palma only. The *Viola cheiranthifolia* is the most striking and emblematic species of Mt. Teide.

Scattered shrubland predominates on the arid islands of Lanzarote and Fuerteventura. Only in very localised areas is denser grass (*Stipa capensis*) found.

Export farming is common below 300 m a.s.l., with bananas and tomatoes as main crops, followed by flowers, plants and some fruit trees. Crops grown for domestic consumption and local markets include potatoes, grapes, fruit trees (particularly citrus fruits).

A broad range of farming practices for soil and water conservation can be seen in the Canary Islands, particularly in the most arid parts; these will be described in a later chapter. Some are based on the use of pyroclastic materials, tephras and pumice, as mulch (Tejedor et al. 2002a, 2003a), while others involve runoff water harvesting (Jiménez et al. 2002, 2004), terraces, transportation of soil (Armas-Espinel et al. 2003), etc.

Soils

Soils of the mountainous islands

As the highest of the islands, Tenerife can be considered a useful reference for the distribution of soils in this group. There is a marked difference in soil types between the north and south of the island, and altitudinal climate variations are closely related to the differences seen in the soils. On the northern side two climosequences have been defined depending on the age of materials (Figure 2). On old basaltic lava flows Vertisols, Alfisols, Ultisols and Inceptisols corresponding to aridic/ustic, ustic, udic and xeric

moisture regime are found. On recent pyroclastic materials, at these same climatic levels, Inceptisols, allophanic Andisols and vitric Andisols are present.

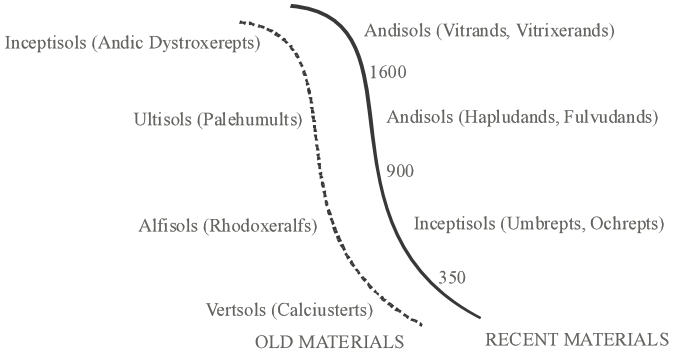

Figure 2. Soil climosequence northern slope (Tenerife Is.).

The study of these two climosequences, formed over similar materials and of very different ages, allows us to conclude that a good correlation exists between soils formed on recent materials and the current climatic conditions. Less clear is the relation with the soils on older materials given that the deep and intense weathering would point to wetter conditions than those currently found. Nevertheless, at each climate level a certain degree of continuity is seen between the secondary materials in the young soils and those present in the older soils, pointing to similar weathering processes. This circumstance leads us to think that the formation of the old soils is also still active, although slower than in previous climatic periods with more rainfall.

From the lithological point of view, the southern side, with fewer altitudinal climatic variations, is characterized by an abundance of acid materials on the surface which cover basaltic formations. The soil climosequence is (Figure 3) Aridisols, Vertisols and Inceptisols. The latter acquire andic properties above 2000 m a.s.l.

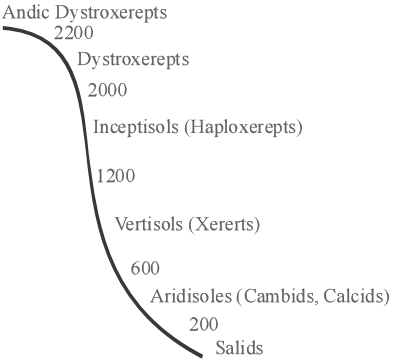

Figure 3. Soil climosequence southern slope (Tenerife Is.).

Andisols are found on recent pyroclasts. The following chronosequence can be defined for the zones with a udic moisture regime: vitric Andisols, allophanic Andisols and non-allophanic Andisols. The absence of allophanic soils in mountainous areas of tertiary zones of the islands have led to the hypothesis of a soil chronosequence for the zones with a udic moisture regime, with other soil forming factors remaining equal. Acidification together with the transformation of allophane and imogolite to crystalline phyllosilicates and gibbsite would lead to the predominance of Al (Fe) humus complexes, therefore, to the organomineral end member of the chronosequence (Mizota and van Reeuvijk 1989, Wada 1989).

The presence of vitric Andisols is not restricted to the humid parts and indeed they have been described at most climate levels, always in association with very young materials. Representative of these soils is reference pedon EUR11, which has a xeric soil moisture regime. These soils have formed on ash and basaltic lapilli, which in many cases cover lava flows. The profile development is limited and the soils have an abundance of coarse elements, organic matter-rich surface horizon, dark colour, high base saturation, coarse texture and good drainage. Mineralogy is dominated by volcanic glass, although in some horizons Al_o+½Fe_o may be greater than 2% and phosphate retention approaches 70%.

Allophanic Andisols (Hapludands) are confined to the northern side, coinciding with the trade wind condensation level. These soils have also formed on pyroclastic materials. They are frequently seen on well-preserved volcanic cones, as is the case of reference pedon EUR10. The profiles tend to be complex, formed by various superimposed soils of the same or different type. Given the good permeability of the surface soil, the buried soils must be assumed to be influenced by leachates originating from the topsoil. The upper soils have a low base saturation, high organic carbon content (1% even at 2 m), high exchange capacity, pH of around 6.0 with minimum (and sometimes no) differences between the values obtained in H_2O and in KCl, no exchangeable aluminium, low bulk density, and high moisture retention. The mineralogy is dominated by allophane, imogolite, gibbsite, some volcanic glass and traces of phyllosilicates. Aluminium oxalate reaches 8% and phosphate retention is more than 99.5%. These Andisols frequently buries older soil layers in which allophane has disappeared and clay minerals predominate, mainly halloysite.

The non-allophanic Andisols (Fulvudands) are found only in udic regime conditions on pyroclastic materials, although these are older than the previous ones. Characteristic of this type is reference pedon EUR12, which has been a reference not only for the COST-622 project but was also used previously when the ICOMAND (International Committee on the Classification of Andisols) group was conducting its work. These soils formed on

basaltic and/or phonolitic pyroclasts 8000–9000 years in age and overlie multiple layers of well developed older soils. In consequence, their profiles are complex.

The non-allophanic Andisols have very high organic matter content, a low degree of saturation, high exchangeable aluminium, low pH, a ΔpH [pH(KCl)–pH(H_2O)] of more than 1, low bulk density, poor dispersion and, in all cases, more fine fraction than the previous Andisols. Halloysite predominates, with traces of illite and vermiculite. The chemical activity of the soils is conditioned not by the allophane but by the aluminium-humus complexes (the content of aluminium extracted with pyrophosphate is greater than with oxalate acid). In some areas, mainly influenced by phonolitic ash, the presence in thin section of grains which are difficult to identify can be misinterpreted as volcanic glass. These are highly weathered grains corresponding to oxides, isotrope gibbsite nodules and glomerular ferruginous structures (Departamento de Edafología 1984).

The developmental sequence of the Andisols under a udic moisture regime would be as follows: a first phase of soils characterised by the presence of volcanic glass and very short-ordered alteration products, rich in silica (siliceous allophane), vitric Andisols. The humid conditions lead to a rapid release of Si and Al, thereby oversaturating the soil solution with these elements and enabling metastable minerals like allophane to form, which may further crystallize to layer silicates over time This phase would correspond to the allophanic Andisol phase. Wada (1989) believes the crystallization of layer silicates to occur after approximately 9000 years in temperate climate zones, an age largely coinciding with that of the third soil (non-allophanic Andisols) of this Andisol sequence, in which crystallised minerals predominate over short-range ordered minerals. However, the nature of the organomineral complexes confers andic properties on these soils.

The chronological sequence formed by profiles EUR10, 11 and 12 clearly shows the progress of desilication with concomitant evolution of the zero point of charge and surface charge characteristics (González-Batista et al. 1982).

The description given above of soils on Tenerife holds true generally for the other mountainous islands, although differences are found depending on orientation, height and the age of the materials. In the particular case of Andisols, the island of La Gomera, despite not having undergone rejuvenation during the Quaternary period, shows additions of Quaternary pyroclastic materials from eruptions on Tenerife. In the more humid parts of the island weathering of these fine materials can be observed in the advanced phase of development of non-allophanic Andisols. Conversely, in the island of El Hierro the dominant Andisols are vitric and – to a lesser

extent – allophanic, while non-allophanic Andisols are not found. La Palma, the most humid of the islands, has a very recent south side (the last volcanic eruption occurred in 1971) and an older northern side, and also with widespread Quaternary volcanic activity. Vitric Andisols predominate in the south and are virtually the only soils found (along with Entisols), while allophanic Andisols predominate in the north and include the soils with the highest water retention capacity among all Canarian Andisols, bordering on Hydrudands and presenting some characteristics of the latter, such as formation of aggregates, shrinking, etc. On Gran Canaria, which has undergone less extensive rejuvenation and is affected by intense erosion processes, vitric and allophanic Andisols are found, although they are less common.

Soils of the low islands

Despite the present-day bioclimatic uniformity of the islands of Lanzarote and Fuerteventura, a wide range of soils can be found here, due mainly to the different ages of the materials and the climatic variations during the Quatenary period. Table 1 shows the soils described. More detailed information can be found in Fernández Caldas et al. 1987, Tejedor et al. 1989, Torres 1995, Díaz 2004.

With annual rainfall of less than 150 mm, the soil moisture regime is aridic and thus the soil Order best represented and with greatest differentiation of horizons is the Aridisol Order. The Andisols and Entisols found are associated with recent volcanic materials. The later also found on organic marine sands deposits and recent sedimentary formations (Table 1). Aridisols and Vertisols are located on old materials. The Vertisols and many of the Aridisols (e.g. those with an argillic horizon) formed un-

Table 1. Soils of the Lanzarote and Fuerteventura.

Soil Taxonomy (Soil Survey Staff 1999)		
Order	Suborder	Great Group
Andisol	Torrands	*Vitritorrands*
Vertisol	Torrerts	*Calcitorrerts*
Aridisol	Salids	*Aquisalids*
		Haplosalids
	Gypsids	*Haplogypsids*
	Argids	*Petroargids*
		Natrargids
		Paleargids
		Calciargids
		Haplargids
	Calcids	*Petrocalcids*
		Haplocalcids
	Cambids	*Haplocambids*
Entisol	Psamments	*Torripsamments*
	Fluvents	*Torrifluvents*
	Orthents	*Torriorthents*

der different environmental conditions to those currently seen (more rainfall). Due to the modifications made in the 2nd version of the Soil Taxonomy (Soil Survey Staff 1999) with respect to the salic horizon, the suborder Salids, hitherto confined to very specific parts affected by saline phreatic waters, has acquired great importance.

The presence of the Andisols Order is limited to the Vitritorrands great group. Indeed, it was the existence of these soils in the Canaries that led the ICOMAND group to propose the suborder Torrands. The soils formed on recent basaltic pyroclastic materials, located on or very near volcanic cones. The profile development is very weak and there is an abundance of coarse elements (pyroclasts). The exchange complex is saturated in bases, some carbonatation is present (1–3%) and salinity increases with depth. Phosphate retention varies between 25–30% in the upper horizons and is lower further down. The Al_o+½Fe_o percentages are between 1.5–0.4%. The mineralogy of these soils is dominated by volcanic glass, with traces of kaolinite and illite. The amorphous gels present are silicic, and diatoms have also been observed.

Given the extremely arid conditions on these two islands, the evolution of the soils will be very different to that undergone by the vitric Andisols on the mountainous islands. In time the amorphous gels will crystallise to clay minerals, as is being seen already, and they will lose their andic properties, shifting to the Aridisol Order.

Acknowledgements

Most of the studies of the soils of the Canary Islands has been conducted by members of the Department of Soil Science and Geology at the University of La Laguna. Among external researchers, Dr Paul Quantin deserves special mention for helping us understand their distribution and characteristics.

References

Armas-Espinel S, Hernández Moreno JM, Muñoz-Carpena R, Regalado CM (2003). Physical properties of “sorriba” cultivated volcanic soils from Tenerife in relation to andic diagnostic parameters. Geoderma 117(3–4):297–311

Bech J, Segalen P, Quantin P (1976a). Etude des Andosols d’Olot (Gerona, Espagne). 1er partie: Ecologie, Morphologie, caractéristiques physiques et chimiques. Cah ORSTOM, ser Pédol XIV 1:73–87

Bech J, Quantin P, Segalen P (1976b). Etude des Andosols d'Olot. 2ème partie: Caracteristiques mineralogiques. Conclusion Cah. ORSTOM ser Pédol XIV 2:95–111

Carracedo JC (1980). Geología. Atlas básico de Canarias. Editorial Interinsular Canaria, S.A., pp 18–27

Departamento de Edafología (1984). Guía de Campo. Congreso Internacional de Suelos Volcánicos. Universidad de La Laguna, pp 282

Díaz F (2004). Sistemas agrícolas tradicionales de las zonas áridas de las islas Canarias. Tesis Doctoral, Universidad de La Laguna, Tenerife, Spain, pp 417

Fernández Caldas E, Tejedor M, Jiménez CC (1987). Soil types in the arid zones of the Canary Islands. Catena 14:317–324

García Rodeja E, Silva BM, Macias F (1987). Andosols developed from non-volcanic materials in Galicia, N.W. Spain. J Soil Sci 38:573–591

Gonzalez Batista A, Hernandez Moreno JM, Fernandez Caldas E, Herbillon A (1982). Influence of Silica content on the surface charge characteristics of allophanic clays. Clays and Clay Minerals 30(2):103–110

Iñiguez J, Barragán E (1974). Andosuelos desarrollados sobre filitas en Ulzama (Navarra). Anal Edaf y Agrob XXXIII nº 11–12:1055–1069

Jiménez CC, Tejedor M, Díaz F (2002). Runoff harvesting systems in the Canaries. In: TRMP paper nº 40 "Water harvesting in Mediterranean zones. An impact assessment and economic evaluation" 2:41–48

Jiménez CC, Tejedor M, Díaz F (2004). The impact of water harvesting on soil properties in the island of Fuerteventura. Soil Use and Management 20:89–91

Mizota C, van Reeuvijk LP (1989). Clay mineralogy and chemistry of soils formed in volcanic material in diverse climatic regions. Soil Monograf 2, ISRIC, Wageningen, The Netherlands, pp 186

Monteverde C (2005). Contribución al conocimiento de los regímenes hídricos de la isla de Tenerife. Tesis Doctoral (in preparation), Universidad de La Laguna, Tenerife, Spain

Palou O, Boixadera J (1999). Mapa de sòls 1:25,000 del Parc Natural de la Zona Volcánica de la Garrotxa. Departament d'Agricultura, Ramaderia i Pesca; Departament de Medi Ambient (Generalitat de Catalunya). Laboratori Polivalent de la Garrotxa

Push R (2001). The Buffer and Backfill Handbook. Part 2: Materials and techniques. Geodevelopment AB. Technical Report TR-02–12. Svensk Kärnbränslehantering ABSE-102 40 Stockholm, Sweden

Rodríguez Paz M (2005). Contribución al conocimiento de los regímenes de temperatura de la isla de Tenerife. Tesis Doctoral, Universidad de La Laguna, Tenerife, Spain

Simón M (2005). Almería. Factores formadores y suelos. Dpto de Edafología y Química Agrícola, Universidad de Almería, pp 71

Soil Survey Staff (1999). Soil Taxonomy: A basic system of soil classification for making and interpreting soil surveys. 2nd edn. U.S. Department of Agriculture Soil Conservation Service Agricultural Handbook, Nº 436, U.S. Government Printing Office, Washington, DC

Tejedor M, de la Cruz M, Jiménez CC, Fernández Caldas E (1989). Capacidad de utilización agronómica de los suelos de la isla de Fuerteventura. Simposio Internacional de la Explotación Caprina en zonas áridas. Serv Public Cabildo Insular de Fuerteventura, pp 360–368

Tejedor M, Jiménez CC, Díaz F (2002a). Traditional agricultural practices in the Canaries as soil and water conservation techniques. In: TRMP paper nº 40 "Water harvesting in Mediterranean zones. An impact assessment and economic evaluation" 1:3–11

Tejedor M, Jiménez CC, Díaz F (2002b). Soil moisture regime changes in tephra-mulched soils: implications for Soil Taxonomy. Soil Sci Soc Am J 66(1):202–206

Tejedor M, Jiménez CC, Díaz F (2003a). Volcanic materials as mulches for water conservation. Geoderma 117(3–4):283–295

Tejedor M, Jiménez CC, Rodríguez Paz M, Hernández Moreno JM (2003b). Soil temperature regime in the island of Tenerife. Altitudinal sequence. ASA-CSSA-SSSA Annual Meetings, Denver

Torres JM (1995). El suelo como recurso natural: procesos de degradación y su incidencia en la desertificación de la isla de Fuerteventura. Tesis Doctoral, Universidad de La Laguna, Tenerife, Spain, pp 560

Vizcayno Muñoz C, García Vicente J, García González MT (1979a). Suelos volcánicos españoles V. Campo de Calatrava (Ciudad Real). Características morfológicas y químicas. Anal Edaf y Agrob XXXVIII:413–429

Vizcayno Muñoz C, García González MT, García Vicente J, (1979b). Suelos volcánicos españoles VI. Campo de Calatrava (Ciudad Real). Mineralogía de la fracción arcilla. Anal Edaf y Agrob XXXVIII:431–445

Wada K (1989). Allophane and Imogolite. In: Dixon JB and Weed SB (eds) Minerals in Soil Environment. 2nd edn. Soil Science Society of America, Madison, WI, pp 1051–1087

II. Reference Pedons: morphology, mineralogy and classification

Ed.: G. Stoops

Intergration and overview

G. Stoops

Introduction

The papers and related annexes presented in Section II deal mainly with the morphology of the profiles, the micromorphology of the horizons and their mineralogical composition. Based on this, and on some chemical and physical data presented in the next sections, the reference profiles were classified. One series of profiles, namely those of Italy, was treated more in detail, and used for genetic interpretations (Colombo et al. this book). Other regional pedogenic studies will be published later elsewhere.

The aim of this paper is to present a first correlation between the results described in the different papers of this section, as a base for a more global interpretation.

Layering, discontinuities

When examining the field descriptions of the reference profiles, the lithological discontinuities and buried horizons are conspicuous, as compared with soils developed from other regoliths. This is due to the stratified parent material and is especially visible in young, less developed soils.

Most, but not all discontinuities observed in the field could be corroborated by laboratory analyses. On the other hand, seemingly homogeneous layers in the field turned out to be stratified or microstratified when subject to mineralogical (Monteiro et al. and Stoops and Van Driessche this book), microscopic (Stoops and Gérard, Stoops et al. this book), physical and chemical analyses (Buurman et al. 2004, Meijer et al. this book). In some cases however this is a question of scale of observation.

Thin section studies reveal millimetre-sized microstratifications in Icelandic soils, pointing to the practical absence of pedoturbation (bioturbation, cryoturbation) and a repeated deposition of thin tephra layers, probably partially due to an aeolian redistribution, of volcanic ash (Stoops et al. submitted). These conditions were seemingly not present in most of the other studied profiles where mostly thicker uniform layers were observed.

A practical problem is caused by the actual nature of pyroclastic deposits: during a single eruption a gradual variation in particle size and composition of the deposit is a common phenomenon, whereas subsequent or different eruptions can deposit similar materials. Thus further research on the concept of lithological discontinuities in volcanic ash deposits, and its practical consequences, is necessary.

Moreover, it is important to consider the question whether sophisticated laboratory analyses (mineralogy, chemistry) should prevail over the field observations (profile description) when naming horizons. This is taken into account when using the RPS (FitzPatrick this book) in which all, and not only selected data are used.

Micromorphology and mineralogy

When considering the results of micromorphological and mineralogical analyses, it is evident that the profiles of Iceland are the least developed. As mentioned above, their fine stratification and the horizontal arrangement of plant remains in the organic (micro)layers points to the absence of pedoturbation, and a gradual construction of the regolith mainly by airborn materials and vegetation phases. No features related to soil formation were observed, except for a granular microstructure, which in some cases can be attributed to enchytraeid activity but in other probably related to the allophane-humic acid complexes produced by weathering. Even some Bw horizons seem to be rather the result of a mechanical accumulation of a more evolved and more clayey material than an in situ developed genetic horizon. The cryic conditions are well reflected by the specific lenticular microstructure and isoband fabric (Stoops et al. submitted).

From a mineralogical point of view, the dominance of fresh glass and pyroclasts in the sand fraction supports the idea of minimally developed soils. This is confirmed by the fact that only primary minerals are found (Monteiro et al., Meijer et al. this book) in the scarce clay fraction that is essentially composed of short-range order constituents. In some classifications applied (Quantin and Spaargaren, FitzPatrick this book) the vitric character of these soils is clearly expressed.

Also the soils of Santorini are very weakly developed, as can be deduced already from their classification as Regosols (WRB) or Entisols (ST). According to micromorphology their coarse constituents, mainly pumice and other pyroclasts, are practically not weathered. Soil formation is expressed only by the arrangement of the fine material, present as coatings around coarser particles, or as interstitial aggregates. The few minera-

logical data available point to the presence of secondary minerals, namely a 1.4 nm phyllosilicate, partly vermiculite and kaolinite. The former may be related to the weathering of deuteric chlorite observed in thin sections. The occurrence of air-born clay particles is not excluded, and could explain the presence of kaolinite and mica in the clay fraction. Decreasing mica content with depth supports this possibility. Large amounts of volcanic glass in the clay fraction (Monteiro et al. this book) corroborate the young stage of weathering.

The Italian profiles were sampled on two rather different parent materials, fact that is reflected in the mineralogical composition. The weathering of Gauro profiles (EUR1 and EUR2) in an ustic pedoclimate appears to depend primarily on time and secondly on the kind of pyroclastic material. In particular in deep and porous soils formed from younger volcanic ash, one of the most important pedogenic process is the formation of low amounts of short-range aluminosilicates with the development of non-allophanic soils. On the contrary the Vico profiles (EUR3 and EUR4) have formed in an udic pedoclimate on trachytic leucititic lava and on consolidated tuffs that are older, less porous, and less permeable than the ash and play an important role in the formation of allophanic soils with increasing amount of short-range-order aluminosilicate minerals. They meet the requirements for Andosols (Colombo et al. this book).

Mineralogical information on the profiles sampled in France is very restricted, and no complete profiles could be studied in thin sections. Pedon EUR17 is moderately weathered and the speckled b-fabric (isotropic matrix sensu FitzPatrick) and anisotropic clay coatings are in agreement with the presence of considerable amounts of (primary or secondary) phyllosilicates in the crystalline clay fraction. Several micromorphological features point to transport (aeolian, colluvial, periglacial) of the material, lithological discontinuities becoming evident. Both profiles are classified as Andosols in the three classification systems applied. The clay minerals are probably inherited from a former pedogenesis, before the last glacial remodelling of the soil surface (Quantin this book).

The reference profiles sampled on Tenerife are medium weathered soils, keying out in the three classification systems applied as Andosols or equivalents. The sand fraction clearly shows the presence of lithological discontinuities. It is dominated either by rock fragments or by orange coloured glass particles, according to thin section studies of similar soils considered as allophane alteromorphs (Gérard et al. submitted). Meijer et al. (this book) observed in the clay fraction of all profiles kandites, primary minerals and gibbsite. In EUR12, kaolinite is the dominant clay mineral (Monteiro et al. this book). These kandites are responsible for the weakly

developed speckled b-fabric observed in thin sections. Gibbsite is found in some of the thin sections.

The dominance of primary minerals in the clay fraction of EUR11, pointing to a lower degree of weathering, (Monteiro et al. this book) seems not in agreement with the degree of weathering of the glass, but is in agreement with the less evolved microstructure of this profile. Moreover, the thin section studies suggest a stronger weathering of the coarse material in EUR10 and EUR12 than in EUR11. The subangular blocky microstructure in the solum of EUR10 and 12 points to a more developed soil than the granular microstructure observed in EUR11.

The profiles of the Azores, are probably the most developed of the reference profiles (Gérard et al. submitted). In the classification systems applied they key out as Andosols or equivalents.

They show a (sub)angular blocky microstructure throughout the profile, whereas this is restricted to the Bw horizons in the other studied soils. The coarse material, as seen in thin sections, consists of weathered rock fragments and fresh mineral grains (feldspar, augite, biotite). In grain mounts practically only rock fragments are observed, which in EUR6 have probably a tachylitic composition, and therefore appear as opaques. The crystalline clay fraction in EUR5 (Monteiro et al., this book) is dominated by secondary phyllosilicate minerals of the vermiculite type. This may be related to the presence of biotite, as observed in thin sections (Stoops et al. this book). The considerable amount of kandites is in accordance with the observation of anisotropic clay coatings. The clay fraction of EUR6 shows a dominance of magnetite, that is probably related to the presence of the opaques in the sand fraction, and maybe responsible for the higher value of Fe_o compared to Fe_d (Meijer et al. this book). The high values for Al_o in EUR6 are in agreement with the gibbsite observed in thin sections.

The Hungarian and Slovakian soils on volcanic material take a specific place among the European volcanic soil reference profiles. The mineralogical composition of their clay fraction is strongly influenced by a large admixture of loess, clearly reflected by the large amounts of mica's and illite observed in the clay fraction. Neither mineralogical data of the sand fraction, nor micromorphological data are available.

General conclusions

In general, there is a relatively good relationship between the different mineralogical and micromorphological routine analyses reported in Section II of this book. Their complementary information leads to a better understanding of the genesis and evolution of the soil material. The optical

study (grain mounts, micromorphology) is often necessary to understand the origin of the crystalline part of the clay fraction (e.g. presence of primary biotite, of deuteric chlorite).

The detailed mineralogical and micromorphological interpretation of the reference profiles is hindered by the fact that for many profiles data are missing. For economic reasons researchers were often obliged to make a selection of samples to be analysed. As this choice was not coordinated, it resulted in different horizons of a same profile being studied by different researchers, making comparison difficult, especially in view of the heterogeneity of the profiles.

It is evident that the mineralogical and micromorphological characteristics mentioned in this section cannot be generalised for all soils on volcanic ash in Europe, as sampling was seriously biased in favour of young soils and soils with andic properties. For instance Vertisols, saline soils, arid soils and Luvisols, described in literature (e.g. on the Canaries) are missing in this COST-622 project.

It is also important to realise that small differences in methodology (e.g. clay extraction procedure) or instrumentation can strongly influence analytical results, as seen when comparing the mineralogical data of the clay fraction by different authors (Colombo et al., Meijer et al., Monteiro et al. this book). Especially the detection limits seem rather variable.

Acknowledgements

The author wants to thank following colleagues for their constructive comments: O. Arnalds O, P. Buurman, C. Colombo, E.A. FitzPatrick, and P. Quantin.

References

Buurman P, Garcia Rodeja E, Martinez Cortizas A, van Doesburg JDJ (2004). Stratification of parent material in European volcanic and related soils studied by laser-diffraction grain sizing and chemical analysis. Catena 56:127–144

Colombo C, Sellitto VM, Palumbo G, Terribile F, Stoops G (2006). Characteristics and genesis of volcanic ash soils in Southern Central Italy: Phlegreaen Fields (Campania) and Vico Lake (Latium) (this book)

FitzPatrick EA (2006). Classification of the soils according to 'Horizon Identification – the Reference Point System' (this book)

Gérard M, Caquineau S, Pinheiro J, Stoops G. Weathering and allophane neoformation in soils on volcanic ash from the Azores (submitted to European Journal of Soil Science)
Meijer EI, Buurman P, Fraser A, Garcia Rodeja E (2006). Extractability and FTIR-characteristics of poorly-ordered minerals in a collection of volcanic ash soils (this book)
Monteiro F, Kleber M, Fonseca M, Madeira M, Jahn R (2006). Crystalline clay constituents of soils from European Volcanic systems (this book)
Quantin P (2006). Volcanic soils of France (this book)
Quantin P, Spaargaren O (2006). Classification of the Reference Pedons. WRB and ST (this book)
Stoops G, FitzPatrick EA, Gérard M (2006). Micromorphological description of thin sections of volcanic ash soils of COST-622 reference profiles (this book)
Stoops G, Gérard M (2006). Micromorphology (this book)
Stoops G, Gérard M, Arnalds O. A Micromorphological Study of Andosol Genesis in Iceland (submitted to Geoderma)
Stoops G, Van Driessche A (2006). Mineralogy of the sand fraction. Results and problems (this book)

A classification of tephra in volcanic soils. A tool for soil scientists

P. De Paepe and G. Stoops

Introduction

Fieldwork and microscopic studies in the frame of the COST-action 622 have shown that there is a great need for a uniform and simple system for the description and classification of pyroclastic debris and rocks in soils and soil thin sections. Although geologists and petrographers dispose today of an internationally accepted and widely used comprehensive system for classification and naming textural characteristics of igneous and pyroclastic rocks (Schmid 1981, Fisher and Schmincke 1984a, MacKenzie et al. 1987, Le Maitre et al. 2002), many soil scientists continue to use local and/or obsolete terms. The aim of the present paper is to propose a selection of terms for a more uniform and standardized description of pyroclastic materials in soil profiles, to be used both in the field and in thin sections. Taking into account that some physical and granulometric properties of pyroclastic materials may influence soil properties, the following properties are of major importance: (1) particle size, (2) vesicularity, (3) crystallinity and texture, and (4) chemical composition. A selection of terms in relation to these parameters will be discussed below.

Particle size

Tephra is a collective term used by petrographers to designate unconsolidated accumulations of solid fragmented matter or ejecta produced by explosive volcanic activity. Individual pyroclastic fragments – also termed **pyroclasts** – can be named and described according to a wide range of criteria, although the most fundamental basis for description in outcrops and under the microscope is **grain size**. Hence, the widely used granulometric classification and nomenclature of pyroclasts and well-sorted pyroclastic deposits elaborated under the authority of a subcommission of the International Union of Geological Sciences (IUGS) (Schmid 1981) should be applied by preference (Table 1). It must be kept in mind that the use of the nomenclature for incoherent and coherent pyroclastic deposits given in

Table 1 (columns 3 and 4) implies that the investigated material contains more than 75 percent by volume of pyroclasts. A different classification should be applied to describe pyroclastic ejecta mingled with abundant non volcanic debris of sedimentary origin such as gravel, sand, silt, clay and peat (tuffite, pyroclastic breccia, tuffaceous sandstone or mudstone, etc.). A discussion of the latter terminology is beyond the scope of this work, and for details the reader is referred to Schmid (1981) and Le Maitre et al. (2002).

Table 1. Classification and nomenclature of pyroclasts and well-sorted pyroclastic deposits based on clast size (after Schmid 1981).

Boundary in mm	Pyroclast	Pyroclastic deposit	
		Mainly unconsolidated: tephra	Mainly consolidated: pyroclastic rock
64	Bomb, block (Photo 5)	Agglomerate bed of blocks or bomb, block tephra	Agglomerate pyroclastic breccia (Photo 6)
	Lapillus	Layer, bed of lapilli or lapilli tephra (Photo 7)	Lapilli tuff
2	Coarse ash grain	Coarse ash	Coarse (ash) tuff
1/16	Fine ash grain (dust grain)	Fine ash (dust)	Fine (ash) tuff (dust tuff)

Vesicularity

Vesicles or cavities of any shape and variable size formed by expansion of gases dissolved in the molten rock material. The resulting texture is called **vesicular**. The abundance of the cavities controls the bulk density and alteration rate of volcanic glasses and crystalline rocks. Vesicles are preferred places for crystallisation of zeolites, carbonates and deuteric alteration products such as chlorites (Micrographs 63 and 64). **Pumice** is light coloured and extremely vesicular silicic glass with low density, which resembles foam (Photos 1 and 2, Micrographs 37, 65, 67, and 77). The density of **pumiceous** fragments is so low that the material will float on water. Vesicular basaltic ejecta (also called **scoriae** as they look like clinker) are

black or iridescent when fresh (Micrographs 47, 69, 70, 78 and 79). Their colour becomes drab to deep reddish brown with increasing degree of oxidation, rendering them nearly opaque in thin sections in transmitted light (Micrograph 59 and 82). Oxidized **scoriaceous** rock fragments are obviously more resistant to weathering than non-oxidized volcanic rock types.

Crystallinity and texture

The term **crystallinity** expresses the degree to which a pyroclast (or rock fragment) is composed of crystalline material in relation to the glass phase. The crystallinity reflects the cooling history and viscosity of the parent magma. Rapid cooling precludes organisation of the constituent atoms into a crystalline structure, and promotes glass formation.

Vitric particles are almost completely glassy and therefore optically isotropic. **Holocrystalline** fragments consists wholly of mineral grains (crystals) (Micrographs 33 and 34). In pyroclasts composed of a mixture of glass and crystals, the texture is said to be **hypocrystalline** (or **merocrystalline**) (Micrographs 30, 31, 74, 75). The IUGS Subcommission on the Systematics of Igneous Rocks recommends the prefixes shown in Table 2 for use with igneous rocks containing glass. To describe rocks with more than 80 percent glass special names have been introduced in literature. **Obsidian** is dense and typically black or dark-coloured in hand specimens, has a very siliceous composition and displays a smooth conchoidal fracture (Photo 3). It contains less than about 1 percent of water. **Pitchstone** is characterized by a dull, resinous luster, a more variable chemical composition and much higher water contents (up to 10 percent) than obsidian. **Sideromelane** and **tachylyte** form by definition from basaltic magmas. The former is transparent in thin slivers (Micrograph 39), while the latter is opaque, even in thin section (Micrographs 55 and 76).

Table 2. Prefixes for use with rocks containing glass (after Le Maitre et al. 2002).

% glass	Prefix
0–20	Glass-bearing
20–50	Glass-rich
50–80	Glassy

Pyroclasts may be made up of individual crystals, glass or rock debris, or of some combination of these components. To describe ashes or tuffs composed mainly or exclusively of crystals, the petrographer uses the adjective ‘crystal’ (**crystal ashes, crystal tuffs**). Ashes and tuffs consisting chiefly of glassy particles would be termed ‘vitric’ (**vitric ashes**, **vitric tuffs**) (Micrographs 39 and 79), whereas those made up predominantly of rock fragments are said to be ‘lithic’ (**lithic ashes**, **lithic tuffs**).

Pyroclasts consisting exclusively of crystals too small to be discernible with the naked eye, or using a hand lens are said to be **aphanitic**-textured, whereas the term **porphyritic** refers to rock fragments or ejecta carrying relatively large, usually well-shaped crystals (**phenocrysts**) set in a fine-grained or glassy groundmass (Photo 4, Micrographs 63 and 64). When there is a sub-parallel arrangement of tabular crystals (especially microlites of feldspars), suggestive of flow, the texture is spoken of as **trachytic**.

Composition

Primary mineral content, vesicularity and physical properties of glassy materials are most useful criteria to determine the approximate chemical composition of the source magma of tephra deposits. A correct naming of volcanic fragments using mineral content (or mode) requires holocrystallinity and an appropriate grain size of the constituent mineral grains. If these conditions are fulfilled, the relative proportions of five mineral groups (labelled Q, A, P, F, and M) are calculated and subsequently plotted on the QAPF modal classification diagram utilized by the IUGS Subcommission on the Systematics of Igneous Rocks (Le Maitre, 2002). The mineral groups defined by the IUGS Subcommission are as follows: Q = quartz, tridymite, cristobalite; A = all kinds of alkali feldspars, and albitic plagioclase (An_0 to An_5); P = plagioclase (An_5 to An_{100}) and scapolite; F = feldspathoids or foids, and M = mafic and related minerals. The diagram facilitates the assignation of a general root name to the rock (fragment) under investigation and to estimate roughly its chemical composition.

If a modal analysis cannot be performed, because of the presence of glass, or because of the tephra is too fine-grained, it is recommendable to use the physical properties of the glass to assess the chemical composition of individual particles. The occurrence of glass is not always restricted to the groundmass of the ejecta as also crystals of any kind and size may be charged with blebs of glass (Micrographs 63 and 64). Unlike minerals, which have a specific chemical composition, natural glasses are chemically as varied as igneous rocks. Observations with regard to colour in thin section and refractive index (or relief) are therefore important. Unaltered basaltic glass (sideromelane) is usually pale green to dark brown under the microscope in transmitted light, relatively poor in vesicles, and characterized by a low positive relief (Micrographs 39 and 79). The refractive indices of sideromelane range up to 1.60. On the other hand, glasses with high silica content tend to be colourless in plane-polarized light, highly vesiculated, and usually have a refractive index (n) substantially lower than 1.54.

Refractive indices between 1.46 and 1.50 are typical for volcanic glasses with a rhyolitic, dacitic, or related chemical composition.

Volcanic glasses are inherently unstable and therefore tend to crystallise or devitrify. They decompose more readily than mineral phases they are associated with. **Palagonite** is known to be the primary alteration product of sideromelane. Nowadays it is generally accepted that palagonitization may result from interaction at ambient temperature of sideromelane with aqueous solutions. The role of percolating ground water e.g. can hardly be overestimated. This explains why in regions with an appropriate climatological environment, palagonite is a common component of volcanic soils developed on lava flows and tephra of basaltic composition. Because of its striking yellow, orange or reddish brown colour, identification of palagonite in outcrops and under the microscope is anything but difficult. The refractive indices of most palagonite are less than 1.54 and diminish with increasing content of water.

Based on optical and structural properties, two main palagonite varieties are recognized: gel-palagonite, and fibro-palagonite. **Gel-palagonite** is isotropic and usually crystal-free and concentrically banded (Micrographs 53, 80, 81 and 82). In a later evolutionary stage of alteration, it is converted partially or entirely into **fibro-palagonite**. The latter is typically anisotropic, slightly to strongly birefringent, and either fibrous or granular in structure. Interference colours of fibro-palagonite bear witness of the presence of crystallising secondary minerals, including different kinds of clays (mainly smectites), zeolites, carbonate minerals, opal and oxides (Micrographs 83 and 84). During the palagonitisation process some chemical elements are leached out, while others show relative gains. Some mobilized elements may precipitate in a later phase in vesicles and pore spaces and contribute to the lithification of the deposits. Enrichment and depletion are reflected by either a decrease, or an increase of the refractive index of the alteration material. Unfortunately, many aspects of the reaction mechanism of palagonitisation remain unresolved or controversial. For full details on palagonite and palagonite formation, we refer to Fisher and Schmincke (1984b) and an excellent review article by Stroncik and Schmincke (2002).

Pyroclastic ejecta derived from intermediate and silicic magmas are much more widespread than their basaltic equivalents. Among the former, many consist chiefly of glass. In an advanced stage of alteration and regardless the geological environment, the glass particles included in intermediate and silicic pyroclasts and tephra are mostly transformed into clay minerals. Opalisation is restricted to very specific settings. Vitric ashes and tuffs of high silica content, which are almost completely converted into smectite-dominated expanding clays, are called **bentonites**. Most bentonite

deposits occur in shallow marine sediments, but bentonite formation may also take place in terrestrial conditions. In a few cases only, siliceous ashes and tuffs are extensively silicified owing to deposition of quartz, chalcedony and opal. These silica minerals result from the leaching out of silica during the devitrification of the glass.

References

Fisher RV, Schmincke H-U (1984a). Pyroclastic rocks. Springer-Verlag, Berlin Heidelberg New York

Fisher RV, Schmincke H-U (1984b). Alteration of volcanic glass. In: Fisher RV, Schmincke H-U (eds) Pyroclastic rocks. Springer-Verlag, Berlin Heidelberg New York 312–345

Le Maitre RW (ed), Streckeisen A, Zanettin B, Le Bas MJ, Bonin B, Bateman P, Bellieni G, Dudek A, Efremova S, Keller J, Lameyre J, Sabine PA, Schmid R, Sorensen H, Woolley AR (2002). Igneous rocks. A classification and glossary of terms. Recommendations of the International Union of Geological Sciences Subcommission on the Systematics of Igneous Rocks. Cambridge University Press, Cambridge

MacKenzie, WS, Donaldson CH, Guilford C (1987). Atlas of igneous rocks and their textures. Longman, Harlow, UK

Schmid R (1981). Descriptive nomenclature and classification of pyroclastic deposits and fragments: Recommendations of the IUGS Subcommission on the Systematics of Igneous Rocks. Geology 9:41–43

Stroncik NA, Schmincke H-U (2002). Palagonite – a review. International Journal of Earth Sciences (Geologische Rundschau) 91:680–697

Appendix materials on CD-Rom

Captions of Micrographs

Micromorphological Description of Reference Profiles of COST 622

Micrograph 30. Hypocrystalline pyroclast. EUR7, 4Bw. PPL

Micrograph 31. Idem as Micrograph 30, but XPL

Micrograph 33. Holocrystalline pyroclast. EUR7, 4Bw. PPL

Micrograph 34. Idem as Micrograph 33, but XPL

Micrograph 37. Subangular pumice fragments with thin coating of organic rich fine material. EUR8 Ah2. PPL

Micrograph 39. Loose packing of fresh vitric ash and aggregates rich in organic matte. EUR8, 2Bw2. PPL

Micrograph 47. Loose packing of highly vesicular scoria (S) and organ residue (OR). EUR9, 4H. PPL

Micrograph 53. Orange, isotropic weathering alteromorph of vesicular siderome-lane. EUR10, Bwb1. PPL
Micrograph 55. Granular microstructure with sideromelane pyroclasts (S), dark, practically opaque hypocrystalline pyroclasts with feldspar microliths (HP) and decomposing organ residues (O). EUR11, Ah. PPL
Micrograph 63. Detail of dark coloured pyroclast with phenocryst of feldspar (F) and deuteric chlorite coating (Cl) on wall of vesicle. EUR13, Ah. PPL
Micrograph 64. Same as Micrographgraph 63, but XPL. EUR13, Ah. XPL
Micrograph 65. Pyroclast with coating and internal hypocoating (hc) of fine mate-rial (left) and feldspar crystal with inclusions of basaltic glass (right). EUR13, Ah. PPL
Micrograph 67. Vesicular pyroclasts surrounded by coating of fine material. EUR14, A. PPL
Micrograph 69. Hypocrystalline pyroclasts and granular microstructure. EUR15, Ah1. PPL
Micrograph 70. Same as Micrographgraph 69, but XPL
Micrograph 74. Hypocrystalline pyroclast. EUR17, Bw. PPL
Micrograph 75. Same as Micrograph 74, but XPL
Micrograph 76. Tachylyte fragments EUR11, 2BC
Micrograph 77. Pumice fragment EUR14
Micrograph 78. Vesicular basaltic glass. EUR11, C
Micrograph 79. Vesicular basaltic glass EUR-
Micrograph 80. Sideromelane with rim of gel palagonite. Galapagos
Micrograph 81. Sideromelane with capping of gel palagonite. Galapagos
Micrograph 82. Sideromelane with rim of gel palagonite. Galapagos
Micrograph 83. Sideromelane with centre of fibous palagonite and calcite. Galapagos
Micrograph 84. Same as 83, but XPL

Captions of Photographs

Micromorphological Description of Reference Profiles of COST 622

Photo 1: pumice block
Photo 2: idem, detail
Photo 3: fragment of obsidian
Photo 4: porphyritic texture
Photo 5: spindel shaped bomb
Photo 6: pumice breccia
Photo 7: lapilli tephra

Soil descriptions

M. Gerard and O. Spaargaren

Description and sampling of the reference pedons was done by Working Group 5 of the COST-622 Action: Soil Resources of European Volcanic Systems. The group members (Basile A, Bartoli F, Gérard M, Jongmans T, van Oort F, Quantin P, Spaargaren O, Terribile F) carried out representative sampling of the selected soil profiles, with a common sampling strategy and standardized sampling procedure. WG5 was mainly composed of participants of Working Group 1 (for aspects of soil genesis and classification) and Working Group 2 (for specific needs of soil samples and conditioning). The sampling programme was decided upon during the second meeting of the management committee in Iceland (July 1998) and updated regularly. Delegates of the local management committees were responsible for the selection of the reference soils, in agreement with the WG5. The sampling programme has been carried out in close collaboration with the local COST 622 members in each country.

The reference soils, part of a well-known chrono-climo sequence, had to fit in the framework of the Andosol/Andisol concept. Descriptions of the reference soils are carried out following the FAO *Guidelines for Soil Description* (FAO-ISRIC 1990). Undisturbed soil samples were taken for micromorphological and physical analysis. Bulk soil samples were sent to the Department of Soil Science and Geology of the Wageningen University (The Netherlands) from where homogenized sub-samples were distributed to the European laboratories on request (Buurman et al. this book).

Twenty four reference soils are described: and sampled (Appendix on CD rom): EUR01 to EUR04 in Italy, EUR05 and EUR06 in Portugal (Azores), EUR07 to EUR09 in Iceland, EUR10 to EUR12 in Spain (Tenerife), EUR13 to EUR15 in Greece (Santorini), EUR16 and EUR17 in France, EUR18 to EUR20 in Hungary, and SK1 to SK4 in Slovakia. The soil descriptions are also available at www.lbhi.is/andosol.

References

Buurman P, Bartoli F, Basile A, Füleky G, Garcia Rodeja E, Hernandez Moreno J, Madeira M (2006). The physico-chemical data base (this book)

FAO-ISRIC (1990). Guidelines for Soil Description. 3rd edn (Rev.). Soil Resources, Management and Conservation Service, Land and Water Development Division. FAO, Rome

Appendix materials on CD-Rom

Soil descriptions for COST-622 reference pedons

Micromorphology

G. Stoops and M. Gérard

Introduction

Relative few studies dealing with micromorphology of soils on volcanic ash in Europe have been published. On Tenerife (Canary Islands) innovative systematic studies have been done in the seventies by a group of Spanish pedologists. Also the micromorphology of some soils in the Eifel has been investigated by several authors, but because of the important admixture of loess these profiles are less characteristic for volcanic materials. Few micromorphological studies of volcanic ash soils from France, Greece, Iceland or Italy were published in international journals, but without doubt more information must exist in reports and thesis manuscripts, not available to outsiders. Soils on volcanic materials in the eastern part of Europe (e.g. Hungary, Romania, Slovakia) were not studied micromorphologically before the COST-622 action.

The COST 622 project gave the opportunity to study and compare volcanic ash soils from different countries formed under a range of climatic, lithologic and geological conditions. This resulted in a better insight in the evolution of the fabric of these soils, and its relation with soil genesis, classification and soil characteristics.

Micromorphological concepts and terminology used in this paper are those proposed by Stoops (2003).

Results and interpretation

Complete standard descriptions made by Stoops et al. (this book) and data sheets are presented in the Appendix.

Discussion per profile

***EUR1**. (Ap, Bw1, BC)*

Microstructure changes from granular (in fact open enaulic) in Ap to angular blocky (Micrograph 2) (weakly separated granular intrapedal) and to

vughy in BC. In the air dried sample the intrapedal granular microstructure is better expressed in the Bw1 horizon than in the samples with acetone replacement. Channels and excrements point to a considerable biological activity throughout the profile.

The mineralogical composition of the parent material seems homogeneous, with a dominance of large fresh pumice fragments (Micrograph 1 and 3) and angular grains of feldspar and augite. Lithological discontinuities are therefore not probable. The larger pyroclasts are surrounded by a coating of fine material comparable to the micromass, which forms also an internal hypocoating in porous pumice fragments (Micrograph 1).

A relative high content of micromass is present, always with an undifferentiated b-fabric, pointing to the presence of amorphous clay.

***EUR2**. (Ah, Bw, BC2, C1)*

The microstructure changes from granular (in fact open enaulic) in the Ah (Micrograph 4) to subangular blocky (with weakly separated granular intrapedal microstructure) mixed with granular (Micrographs 6 and 7) in the middle of the profile to become again granular in the C.

The parent material, containing pyroclasts and pumice, seems not completely homogeneous; below the Bw more volcanic glass is found. Internal hypocoatings of fine material are present in the pumice fragments. The C1 consists of a partly stratified material, containing denser layers (old surface crusts?) (Micrograph 8).

Fine material is relatively abundant, and the micromass is weakly speckled to undifferentiated, pointing to the presence of some phyllosilicate clays. A high biological activity is observed throughout the profile (Micrograph 5). Fungal hyphae in the upper horizons suggest a rather acid environment.

The sharp boundary in the C1 between the tephra and the argillic horizon with strongly developed coatings of illuviated 2/1 clay (high interference colours) (Micrograph 9 and 10) points to a buried truncated palaeosol.

***EUR3**. (Ah1, AB, Bw1, 2Bw2)*

The microstructure is bimodal granular (enaulic) throughout the profile, except in the Bw1 where it becomes subangular blocky, with a moderately separated granular intrapedal microstructure.

The parent material changes gradually with depth: more porous pyroclasts (Micrograph 13) are found in the deeper part; also the oxibiotite content increases with depth. Coatings of fine material cover the larger pyroclasts. In the Bw1 the coarse material is partially weathered and has a

coating of lighter coloured fine material, similar to the micromass of the deeper horizon, e.g. the 2Bw2. The b-fabric remains undifferentiated throughout the profile, due to the amorphous fine material.

Fungal hyphae are seen in upper horizons only (Micrograph 12).

***EUR4**. (Ah1, Bw2, C)*

The microstructure is granular (enaulic) (Micrograph 14) throughout the profile.

The coarse material consists essentially of denser, darker pyroclasts, vitric material being rare. They are surrounded by a coating of micromass (Micrograph 15). The top layer contains material similar to the C (pyroclasts with weathered leucite) (Micrographs 16–19); this material is absent in the Bw2. Therefore the following sequence of events could be proposed, based on micromorphological evidence only: C-material in leucite bearing andesitic rock covered by a different volcanic deposit (Bw horizon), which in turn is covered by a material, similar to the C, probably eroded from a Bw or C-horizon of a higher located profile. This is supported by the fact that, in the Ah1, the micromass around the free coarse grains is lighter in colour, whereas it is dark brown in the granules, and by the presence of organic pigment in the Bw2. The b-fabric of the micromass is always undifferentiated.

Fungal hyphae occur in the upper horizons.

***EUR5**. (Ah1, 2Ahb, 2Bwb/2C, 2C, 3C, 4BC)*

The microstructure is subangular blocky throughout the profile, with about 10% of granular zones (Micrograph 21), especially in the infillings in the upper horizon.

The coarse material has a variable composition throughout the profile, comprising pumice, microlithic pyroclasts, feldspars, biotite and quartz (Micrograph 20). Several different layers seem therefore to be present (lithological discontinuities), confirming the field description. The micromass has an undifferentiated b-fabric throughout the profile pointing to a dominance of short-range order clay.

Coatings and infillings of isotropic and weakly anisotropic reddish clay indicate a mobility of allophanes and crystalline clays with weak low interference colours (halloysite and/or kaolinite). Iron hydroxide hypocoatings and diffuse nodules are related to some hydromorphic conditions.

The C3 horizon represents a layer of hydrothermalised ashes. The alternation of materials with different degrees of weathering clearly points to a polygenetic profile.

***EUR6**. (Ah, AB, 2AB, 2Bwb2, 2Bwb3, 3C)*

Not accommodating angular and subangular blocky microstructures dominate (Micrograph 24), except in the top 4 cm where a granular microstructure is found.

The coarse material consists mainly of mineral fragments (pyroxenes, feldspars) and some partly weathered vesicular lapilli. The degree of weathering of the scoria and the subangular blocky microstructure suggest a more advanced pedogenesis. The orange alteromorphs strongly resemble palagonite. Infillings of orange amorphous clay however point to a mobility of the latter. The presence in the 3C of gibbsite coatings on weathered pyroclasts indicates a locally strong weathering and leaching.

The b-fabric of the micromass is undifferentiated throughout indicating a dominance of short-range order clays.

Roots and hyphae are common in the A horizons.

***EUR7**. (O1,O2,Ah,AC,2CB, 3BC, 3CB, 4Bw, 4B/Cg) (Air-dried)*

The fine granular microstructure (Micrograph 26) in the top 5 cm changes to flat angular blocky peds with subhorizontal orientation and a moderately to weakly separated intrapedal granular microstructure. The incipient platy and lenticular microstructure in the middle of the profile, corresponding to an isoband fabric (Dumanski and St. Arnaud 1966) can be related to freeze-thaw processes (Micrographs 27 and 32).

The top 3 cm is purely organic; below 3 cm grains of augite and volcanic glass, phytoliths and diatoms appear, sometimes showing a banded distribution.

The mineral particles and pyroclasts show no direct evidence of weathering. Tissue fragments and amorphous organic material are dominant in the Ah and very frequent in the 2CB, where they have a horizontal orientation (Micrograph 28). With depth the decomposition of the organic matter increases, as shown by a decrease of interference colours. An alternation of organic and mineral material is observed in the 3CB horizon.

The micromass (mainly organic) has an undifferentiated b-fabric.

The linear and banded distribution of the coarser grains and the subhorizontal orientation of the tissue fragments can be explained by a sedimentary or colluvial origin of the material; the composition of the micromass and the numerous organic remains resembles a peat like environment**.** This hypothesis is further supported by the presence of diatoms and rare sponge spicules, and the occurrence of dark reddish hypocoatings on channels in the 2CB and 3BC (Micrograph 29), which indicate hydromorphic conditions.

The 3BC horizon is dominated by soil aggregates or nodules of different colour and limpidity suggesting a soil sediment, formed by colluvial or aeolian (saltation) transport.

***EUR8**. (Ah1, Ah2, Bw1, 2Bw2, 3Bw3/4C, 4C) (Air-dried)*

Depending upon the c/f ratio a granular (enaulic) (Micrograph 35) or locally a single grain microstructure (monic) (Micrograph 36) occurs in the profile, except in the 2Bw2 where a more massive microstructure is observed. The fine platy microstructure in the Ah1 horizon (isoband fabric) points to freeze-thawing processes.

The composition of the coarse material is variable, even within a single thin section, pointing to lithological discontinuities and microstratification. Main constituents are pumice, feldspathic pyroclasts, green-beige volcanic glass, augite and feldspar crystals. The material is essentially unweathered. In one sub-layer the greenish glass shows internal hypocoatings of orange isotropic appearance, considered as palagonite (Micrograph 41). The pumice fragments show internal hypocoating and coatings of fine material (Micrographs 37 and 40). The organic material contains many organ and tissue residues without interference colours, indicating a higher degree of decomposition than in the EUR7 in this better drained profile. Part of the 2Bw2 horizon has characteristics similar to the 3BC horizon of profile EUR7.

The preservation of the microstratification is only possible if pedoturbation, especially bioturbation, is strongly restricted.

***EUR9**. (Ah, 3H, 3C, 4H) (acetone replacement)*

The microstructure is clearly function of the c/f ratio and the amount of organic material. The mineral layers often show a single grain (coarse monic) microstructure, whereas the organic ones are more massive or vughy. The fine platy microstructure in the 3H horizon is most probably related to freeze-drying processes. The coarse material has a variable composition and is generally dominated by fresh glass, scoria and volcanic minerals. The alternation of the organic and mineral layers (Micrographs 45 and 46), sometimes at a millimetre scale, even as the horizontal orientation of larger organ residues (Micrograph 42), points to a gradual deposition of materials in subsequent periods, not affected later by pedoturbation, especially bioturbation. The peaty aspect of some organic layers and the presence of diatoms indicate an at least temporarily subaquatic environment. The organ and tissue residues show stronger interference colours in the top of the profile (Micrographs 43 and 44) than in the deeper parts, due to a gradual decomposition. Pedogenesis is limited to absent. Cappings of

fine material on organ residues (Micrograph 48) can be related to freeze-thaw processes.

***EUR 10**. (Ah, Bw, Bwb1, Bwb2, 2Bwb3)*

The microstructure is granular (enaulic) (Micrograph 50) and crumb in the Ah, but becomes angular blocky (Micrographs 51) from the Bw on, preserving however a weakly separated intrapedal granular microstructure. In the top layer a strong biological activity can be deduced from the high concentration of excrements.

The coarse material is strongly weathered (pyroclasts, augite grains), especially the presence of isotropic orange alteromorphs after glass is remarkable. The micromass, dark brown in the Ah, greyish orange in the Bw, has always an undifferentiated b-fabric, pointing to a dominance of short-range order clays. The low c/f ratio indicates a relative high degree of weathering.

The presence of rare gibbsite coatings in pyroclasts in the Bw illustrates the strong degree of weathering in this pedon.

***EUR11**. (Ah, C, 2Bwb, 2BCb)*

Throughout the profile a granular (Micrograph 55) microstructure is observed, corresponding to an enaulic c/f related distribution pattern, combined with a chitonic one in the subsurface horizons, caused by the presence of coatings of fine material surrounding the coarse fragments. The coarse material consists of vesicular vitric ash and lapilli and fragments of trachytic rocks, up to 5 mm. The vitric material clearly shows an incipient weathering to yellowish alteromorphs.

The micromass has an undifferentiated b-fabric, pointing to a dominance of short-range order clay minerals. The presence of larger charcoal fragments (Micrograph 58) in the 2Bwb suggests that this horizon corresponds to a former surface or colluvial material.

The Ah horizon is rich in large organ residues, some containing whewellite or calcite crystals and fungal hyphae (Micrographs 56 and 57).

***EUR12**. (Ah1, Ah2, Ah2/Bw, Bw, 2Ahb)*

The microstructure is dominantly granular (Micrograph 60) in the A horizons, and subangular blocky in the deeper parts. The upper part is clearly strongly influenced by biological activity. The Ah1 has a high content of organic matter and excrements. The coarse material is poorly presented, and consists mainly of orange weathering products of vitric materials (Micrograph 61). Colourless isotropic alteromorphs after feldspar are visible

in pyroclasts. The micromass has an undifferentiated b-fabric, related to the dominance of short-range order clay, except in the Ah2.

From the point of view of micromorphology there are no indications for a lithological break between the Bw and the 2Ahb horizon. The latter also bears no indications for a former A horizon, except probably a slightly darker colour of the fine material.

EUR13*. (AC)*

This is clearly a weakly developed soil material consisting of a loose packing of larger pyroclastic particles (Micrograph 62), ranging from holohyaline pumice to dense hypocrystalline fragments. The material shows few evidences of weathering, but some indications of earlier alteration (chlorite) (Micrographs 63 and 64). The parent material is rather heterogeneous, what could point to a reworked sediment (colluvium). Pumice fragments show internal hypocoatings and coatings (Micrograph 65) of micromass with undifferentiated b-fabric.

EUR14*. (A)*

This horizon resembles a sediment composed of practically unweathered pumice fragments (Micrograph 66) with some feldspar and pyroxene grains, in a mass of fine glass fragments and limpid isotropic clay. Soil formation is restricted to the formation of coatings and internal hypocoatings of fine material on the pumice (Micrograph 67). Organic material is limited, and fungal hyphae rare.

EUR15*. (Ah1)*

Loose packing (Micrograph 68) of irregular pyroclasts, including pumice and scoria, different from EUR13 and EUR14, because of a less acid character, and showing a first stage of weathering. Rare pyroclasts show the typical colour of palagonite. Soil formation is restricted to a grouping of the fine material as small aggregates and as coatings around the larger fabric units.

EUR16*. (Ah1, 2Bw)*

A granular (enaulic) (Micrographs 71 and 72) to crumb microstructure in top horizon is strongly expressed, whereas the 2Bw is rather a packing of large pyroclasts. The composition of the coarse material of the Ah and the 2Bw horizons is different, the former consisting of pyroxene fragments and irregular volcanic rock fragments, the latter consisting mainly of scoria, partially transformed to a yellowish or reddish limpid isotropic mate-

rial. This suggests a lithological discontinuity. The coarse material in the 2Bw shows a higher degree of weathering. The b-fabric is undifferentiated.

***EUR17**. (Ah1, 2Bw)*

Accommodating angular blocky microstructure in the Ah1 evolving to a more spongy, less pedal microstructure with depth points to more advanced stage of soil development. The difference in coarse material between the Ah and the 2Bw indicates a lithological discontinuity. The upper layer is less weathered. Weathering of the pyroclasts has moderately progressed, especially in the deeper parts where anisotropic clay coatings are formed. The micromass has an undifferentiated b-fabric in the Ah, becoming weakly speckled in the 2Bw, most probably due to the presence of phyllosilicates.

The presence of micromass coatings with a lighter colour and high limpidity around pyroclasts in the Ah1 probably points to a transported material derived from a deeper part of a truncated profile.

General discussion

The studied profiles can be classified in three groups. The least developed profiles are found on Iceland and Santorini, more developed profiles occur in the Massif Central (France), and southern and central Italy, whereas the most developed ones were sampled on Tenerife and the Azores.

Extraordinary environmental factors determine soil formation in Iceland: a cryic/frigid climate, an active volcanism and a continuous aeolian deposition of volcanic products either directly from volcanic activities, or as a product of intense wind erosion. The alternation of organic and mineral layers, the latter often presenting a millimetre-sized microstratification of different mineral parageneses, reflects the gradual building up of the profiles (EUR 7–9) by aeolian material. Also the horizontal arrangement of larger organ residues (probably leafs) points to a gradual sequential accumulation at the surface. The fact that microstratification and horizontal arrangements are preserved throughout the profile indicate moreover a very low pedoturbation, especially bioturbation as a result of the cold climate. The latter, in combination with the young age of the deposits, explains also the quasi absence of weathering features. Cryic conditions are reflected furthermore in the local occurrence of lenticular or platy microstructures corresponding to the isoband fabric of Dumanski and St. Arnaud (1966) caused by repeated freezing and thawing. Accumulations of reddish coloured, structurally well preserved organic matter and diatoms skeletons in-

dicate conditions favourable for peat formation. The Bw horizons contain dominantly aggregates or nodules with different colours and limpidity and have a higher micromass content. It is suggested therefore that they are rather of sedimentary origin (soil sediment of colluvial or saltation origin) than of pedogenic origin. A more detailed analysis of the micromorphology of the Iceland profiles is prepared by Stoops et al. (submitted).

The Santorini profiles (EUR13 – EUR15) (only Ah horizons sampled) are merely coarse volcanic deposits of different composition, some pumice rich, other dominantly composed of pyroclasts, with only a low degree of weathering. Feldspars and pyroxenes are general angular and fresh. Organic material is limited. The only indication of pedogenesis is the formation of coatings of fine material around coarser pyroclasts. In the case of pumice fragments also internal hypocoatings occur. The micromass always displays an undifferentiated b-fabric.

The Italian profiles (EUR1–4) are all characterised by a bimodal granular microstructure in the topsoil, grading with depth to a blocky one with a weakly separated granular intrapedal microstructure. Especially in the Vico pedons (EUR3 and EUR4) the coarse material shows marks of weathering. Compared to the profiles of Iceland and Santorini the amount of micromass has considerably increased, but the b-fabric remains undifferentiated. Rock fragments, especially pumice fragments, show a micromass coating. Infillings and excrements point to a high biological activity. Some horizons seem to be composed of soil sediments (colluvial transport). In the lower part of profile EUR2 truncated, more evolved palaeosols, with anisotropic clay coatings, appear pointing to polygenetic soils. A more detailed discussion of the Italian profiles is given by Colombo et al. (in this book).

The French profiles (EUR16 and EUR17) (only thin sections of Ah and Bw horizons available) have a granular microstructure, sometimes weakly separated forming angular blocky peds in the Bw horizon. The coarse material is a mixture of mainly microlithic pyroclasts, pyroxenes and feldspars, with a dominance of pumice in the Bw of EUR16. Rock fragments are surrounded by a coating of micromass with undifferentiated b-fabric, sometimes with a lighter colour than the rest of the micromass in the same horizon, pointing to a transported material, either from the lower part of a truncated profile higher on the slope, or from a deeper horizon of the same profile by biological activity.

Two profiles were sampled on the Azores, one on Faial (EUR5) and one on Pico (EUR6). Angular blocky microstructures prevail, except in the Ah were granular microstructures occur. Microlithic pyroclasts and vesicular vitric lapilli dominate the coarse material, although fresh pumice is found in the top of EUR5. Most of the vitric vesicular lapilli show a pellicular

weathering to an orange isotropic material composed of Si, Al and some Fe (Gérard et al., submitted). Coatings of a similar material are observed in the profiles. The often dominant micromass has an undifferentiated b-fabric, pointing to the dominance of short-range order clays. Hypocoatings and nodules of iron hydroxides are caused by slightly hydromorphic conditions. Isotropic allophane coatings and anisotropic clay coatings are indications of a more advanced stage of weathering and soil formation.

The profiles of Tenerife (EUR10 – EUR12) are clearly more developed. The microstructure grades from granular in the surface horizons to angular blocky in the solum, except when layers of loosely packed lapilli are intercalated. The glass is commonly weathered to orange isotropic alteromorphs as described in the Azores profiles. In general, rock fragments and minerals show a considerable degree of weathering. The micromass, sometimes dominant, still has an undifferentiated b-fabric, which however locally becomes weakly stipple speckled, pointing to the presence of phyllosilicates.

Comparing the different profiles on volcanic ash studied, following general sequence of features, developed during pedogenesis can be recognized:

In the initial stage a simple packing of pyroclasts and mineral grains (single grain microstructure, coarse monic c/f related distribution pattern) is recognised (e.g. some layers in the Iceland profiles). In a first stage of pedogenesis coatings of micromass form on pyroclasts (e.g. Santorini, Gauro). If pumice is present, internal hypocoatings of micromass appear (e.g. Santorini, Iceland EUR8). From the moment sufficient micromass is available, a granular microstructure gradually develops. One observes thus a gradual transition from coarse monic to close enaulic and open enaulic c/f related distribution patterns to a granular microstructure, combined with a chitonic c/f related distribution pattern for the larger pyroclasts. In some cases a clearly bimodal granular microstructure is observed in the Ah (examples in EUR1 , EUR3 and EUR4). The origin of the granular microstructure is not clear, but most probably other than biological factors, e.g. the type of clay, contribute, as this microstructure is found until the C horizon, and in soils with presumably a very low biological activity. A granular microstructure is characteristic for most Andosols described in literature.

In the more developed profiles (Azores, Tenerife) and in the Bw horizons an angular or subangular blocky microstructure develops, initially with preservation of an intrapedal granular microstructure which is better preserved in air-dried than in acetone replaced samples.

Data on density of a number of horizons by Bartoli (see database in this book) were related to microstructure and c/f ratios (see micromorphologi-

cal description of this sections) by the senior author. As at that moment the thin sections were no longer in his possession, no corrections could be made. It should be kept in mind indeed that in a single thin section several c/f ratio's and several types of microstructure may be present, and that samples taken for bulk density do not always exactly match those taken for micromorphology. Nevertheless some interesting indications for trends are found. The highest density is found in single grain microstructures, followed by granular, and the least dense samples have a blocky microstructure. A study of the relationship between the estimated $c/f_{10\mu m}$ ratio's and bulk density show that the highest bulk densities (1.03) are found in materials with a strong dominance of coarse material ($c/f_{10\mu m}$ ratio of about 16/1), whereas the lowest bulk densities are found in samples where the micromass is dominant ($c/f_{10\mu m}$ ratio > 1/16). A more systematic study of such relationships could be useful for pedimetrics.

A remarkable high amount of phytoliths is found in all profiles, especially in the surface horizons. Depending upon drainage conditions, redoxomorphic features are superposed to the above-described fabric. Only in the most developed profiles, considered as paleosols, where weathering of the pyroclasts is well advanced, traces of clay illuviated are noticed.

A specific feature noticed in the Azores and Canary profiles is the weathering of basaltic or andesitic vitric constituents to alteromorphs of isotropic, limpid yellowish red material, optically similar to palagonite. According to more advanced research (Gérard et al., submitted) this material strongly influences the results of oxalate extractions. Comparison of our descriptions with chemical information from the database in this book confirms this observation. More research needs to be done however on the nature of this constituent and its dynamic behaviour during chemical extractions.

In several soils horizons composed of aggregates and nodules of different composition (as seen by differences in colour and limpidity) are noticed. They can be considered as soil sediment. In some of the least developed soils (Iceland) they form the Bw horizons, suggesting that the Bw characteristics are here more related to the origin of the parent material than to the pedogenic processes.

References

Colombo C, Sellitto VM, Palumbo G, Terribile F, Stoops G (2006). Characteristics and genesis of volcanic soils from South Central Italy: Mt. Gauro (Phlegrean Fields, Campania) and Vico lake (Latium). In: Arnalds O, Bartoli F,

Buurman P, Garcia-Rodeja E, Oskarsson H., Stoops G (eds) Soils of Volcanic Regions of Europe. Springer Verlag

Dumanski J, St Arnaud RJ (1966). A micropedological study of eluvial soil horizons. Canadian Journal of Soil Science 46:287–292

Gérard M, Caquineau S, Pinheiro J, Stoops G. Weathering and allophane neoformation in soils on volcanic ash from the Azores (submitted to European Journal of Soil Science)

Stoops G (2003). Guidelines for the analysis and description of soil and regolith thin sections. Soil Science Society of America Madison, WI, p 184

Stoops G, FitzPatrick EA, Gérard M (2006). Micromorphological description of thin sections of volcanic ash soils of COST-622 reference profiles. In: Arnalds O, Bartoli F, Buurman P, Garcia-Rodeja E, Oskarsson H, Stoops G (eds) Soils of Volcanic Regions of Europe. Springer Verlag

Stoops G, Gérard M, Arnalds O. A micromorphological study of Andosol genesis in Iceland (submitted to Geoderma)

Mineralogy of the sand fraction – results and problems

G. Stoops and A. Van Driessche

Introduction

The sand fractions of 36 horizons, representing 10 soil profiles, were studied by optical methods. Preliminary results were reported by Stoops and Van Driessche (2002).

The first aim of the study was to provide mineralogical data to help explaining results of chemical studies, and to help classifying the pedons. A second objective was to evaluate critically, in the case of volcanic ash soils, the advantages and disadvantages of the optical methods of grain studies compared with other methodologies, such as thin section studies (soil micromorphology) and X-ray diffraction studies.

Material and methods

All analyses were performed on the <2 mm fraction of the soil. After separation of the sand from the silt and clay fraction by wet sieving, the former was subdivided into 3 grain size fractions (2000–500 µm, 500–250 µm and 250–50 µm) by dry sieving. The fractions 500–250 µm and 250–50 µm were thereafter treated with H_2O_2 for removal of organic material and with dithionite-sodium citrate for removal of free iron (Jackson 1965). Grain mounts were prepared for study with a polarising microscope in transmitted light and subsequent line counting of 100 grains was done by the junior author.

Results of the 500–250 µm and the 250–50 µm fractions (respectively the medium and the fine sand fraction) are presented, whenever possible as 100% transparent grains, whereas the opaque grains are presented as an extra value (so called Edelman (1931) method). Where opaque grains are dominant, results are expressed on 100% of total grains (transparent plus opaques).

On a limited number of samples additional techniques were applied for identification, such as selective staining of feldspars (Bailey and Stevens 1960, Houghton 1980), X-ray diffraction of some fractions and microprobe analysis on a few grains.

Results and discussion

Results

Results for pedons 1–12 are presented in Table 1.

Table 1. Mineralogical analysis of cost 622 reference profiles.

Medium sand fraction (500 and 250 µm):

Sample	N°	F	A	H	B	Oth	R	G	Op
EUR1									
Bw1	1999/42	31	9				33	27	22
Bw2	1999/43	31	10				33	26	7
BC	1999/44	29	8				35	28	7
C	1999/45	26	3				27	44	9
EUR2									
O	1999/46	44	14		2		25	15	23
BC1	1999/49	33	3				33	31	28
BC2	1999/50	22	2		1		43	32	8
C1	1999/51	23					57	20	8
EUR3									
AB	1999/55		14		5	3	78		5
2Bw1	1999/56	1	23		2	2	72		5
2Bw2	1999/57	3	18		5	3	71		6
EUR4									
O	1999/58	15	5			9	64	7	20
Bw1	1999/62	38	2			3	57		11
Bw2	1999/63	27	5		1	1	64	2	11
EUR5									
2Bwb	1999/447	6				4	90		5
2Bwb/2C	1999/448	9	1		1		89		2
2C	1999/449	8	3	3	3	4	79		4
EUR6									
2AB	1999/452							1	**99***
2Bwb	1999/453	1							**99***
2Bw2	1999/454	3	2			2			**93***
2Bw3	1999/455	3	1	1	1	3			**91***
EUR7									
O	1999/1044	1				1	43	55	7
3BC	1999/1048					2		98	5
3CB	1999/1049	5				5	67	23	19
4Bw	1999/1050		1				2	97	3
4B/Cg	1999/1051	3				6	91		4

Continued on next page

Sample	N°	F	A	H	B	Oth	R	G	Op
EUR8									
Bw1	1999/1054						7	93	5
2 Bw2	1999/1055						3	97	4
3Bw3/4C	1999/1056	2				1	82	15	31
4C	1999/1057	1				1	91	7	13
EUR9									
3C	1999/1060	2					14	84	2
4H	1999/1061	1						99	4
EUR10									
Bw	2001/02	9	4	1		12	5		**69***
2Bw1	2001/04	11			4	9	5	14**	**57***
Bwb2	2001/05		11	1		7	47	34**	14
EUR11									
C	2001/07						19	81**	11
2Bwb	2001/08	3					97		4
2BCb	2001/09	3			1	1	23	72**	3
EUR12									
Bw	2001/13	14						86**	27
2AhB	2001/14	5						95**	45

F=feldspars, A=augite, H=hornblende, B=biotite, Oth=others, R=rock fragments, G=glass, Op=opaque.
*** (bold)**: 100 transparent **and** opaque grains.
**: Orange brown isotropic grains, similar to palagonite.

Fine sand fraction (250 and 50 µm):

Sample	N°	F	A	H	B	Oth	R	G	Op
EUR1									
Bw1	1999/42	15	3				15	67	
Bw2	1999/43	10	4		3		25	58	
BC	1999/44	9	5	1			8	77	
C	1999/45	9	1	2			8	80	
EUR2									
O	1999/46	8	2	1			24	65	2
BC1	1999/49	12			1		32	55	
BC2	1999/50	6					26	68	
C1	1999/51	13					37	50	
EUR3									
AB	1999/55	8	3		5		84		
2Bw1	1999/56	4	8		1		87		1
2Bw2	1999/57	4	7		1		88		1

Continued on next page

Sample	N°	F	A	H	B	Oth	R	G	Op
EUR4									
O	1999/58	26	3				71		
Bw1	1999/62	29	10		3		48	10	
Bw2	1999/63	41	1				55	3	
EUR5									
2Bwb	1999/447	2	2				96		
2Bwb/2C	1999/448	8	4				85	3	
2C	1999/449	18	2	5			74	1	3
EUR6									
2AB	1999/452							1	**99***
2Bwb	1999/453	1	2						**97***
2Bw2	1999/454	9							**91***
2Bw3	1999/455	6	1			3			**90***
EUR7									
O	1999/1044	2					20	78	14
3BC	1999/1048							100	7
3CB	1999/1049	5				5	67	23	19
4Bw	1999/1050	3					4	93	3
4B/Cg	1999/1051	22					74	4	3
EUR8									
Bw1	1999/1054	1					12	87	4
2 Bw2	1999/1055	3					7	90	3
3Bw3/4C	1999/1056						80	20	15
4C	1999/1057	3	1				89	7	16
EUR9									
3C	1999/1060	2					4	94	2
4H	1999/1061	2					1	97	3
EUR10									
Bw	2001/02	6	3			3		8**	**80***
2Bw1	2001/04	10	2			2	45	37**	**4***
Bwb2	2001/05	1	3			4	3	87**	
EUR11									
C	2001/07	3					25	72**	12
2Bwb	2001/08						21	79**	1
2BCb	2001/09	3					24	73**	1
EUR12									
Bw	2001/13						34	66**	40
2AhB	2001/14	4						96**	35

F=feldspars, A=augite, H=hornblende, B=biotite, Oth=others, R=rock fragments, G=glass, Op=opaque.

*** (bold)**: 100 transparent **and** opaque grains.

**: Orange brown isotropic grains, similar to palagonite.

Discussion of the individual pedons

Following mineral groups were considered: feldspars, comprising plagioclases, K-feldspars, and exceptionally including leucite, augite, hornblende, biotite and others. "Rock fragments" (mainly holo- or hypocrystalline pyroclasts) comprise grains composed of more than one mineral, or a mineral and matrix, mainly glass. As "glass" we considered all isotropic particles without crystals, except sometimes small amounts of microlites. Results of micromorphological studies however later demonstrated that in some cases (e.g. the Tenerife pedons) these anisotropic bodies are weathering products rather than glass. They are indicated in the tables by the symbol (**). The group "opaques" comprises essentially ores such as magnetite and ilmenite, but can also contain very dark basaltic glass (tachylyte).

EUR1

The medium sand fraction points to a rather homogeneous material with equal amounts of glass, rock fragments and feldspars. Only the C horizon contains considerably more glass, confirming the lithological break described in the profile. The fine fraction, dominated by glass, shows a difference between the Bw2 and the lower horizons, which contain considerably more glass and fewer pyroclasts, supporting the lithological discontinuity proposed by Buurman et al. (2004).

In the Bw1 the glass is colourless, has a fibrous aspect and contains crystallites; rock fragments are nearly opaque with a halo of low interference colours. In the Bw2 and the C horizons the glass is colourless to reddish brown and vesicular; opaque grains are sometimes idiomorphic ore minerals, others probably very dark pyroclasts (tachylytes).

Thin section analysis (Stoops et al. this book) point to a dominance of pumice fragments and less other pyroclasts. The glass, which is dominant in the fine fraction, can therefore be considered as a mechanical disintegration product of the pumice, which is supported by the fibrous aspect mentioned above.

Compared to the XRD data (Colombo et al. this book) a similar general trend is observed. Biotite was observed in XRD, but not in grain mounts, which may be due to its occurrence inside rock fragments.

EUR2

In the top soil, the medium sand fraction contains higher amounts of feldspar and augite than the rest of the profile, supporting the lithological discontinuity suggested by Buurman et al. (2004). Throughout the profile the fine fraction is dominated by glass, followed by rock fragments, with con-

siderably smaller amounts of feldspars. A discontinuity between BC1 and BC2 could exist, based on the different contents of opaque grains. The glass in the medium sand fraction often has a fibrous aspect and also contains microlites.

The rock fragments in the O horizon are fibrous, and augite is sometimes idiomorphic. In the BC1 the rock fragments are colourless with opaque parts and phenocrysts; the augite is brownish and the opaque grains are rounded. Glass in fine fraction is fibrous, colourless to pinkish, sometimes fibrous.

The micromorphological analysis (Stoops et al. this book) indicates the presence of both pumice and other pyroclasts, with minor amounts of glass, feldspar and augite. Rare biotite grains are encountered, supporting the grain counts. XRD (Colombo et al. this book) confirms the optical determinations.

EUR3

The medium sand fraction is strongly dominated by pyroclasts (>70%), whereas weakly pleochroic augite is the second most important component and glass is absent. Also the fine fraction is strongly dominated by pyroclasts (>80%), without glass. The relative high amount (up to 5%) of brownish yellow to reddish brown idiomorphic oxybiotite is noteworthy. No indications for a lithological discontinuity are found which would support the field data and the analysis of Buurman et al. (2004). The feldspars are partly weathered.

Micromorphological data (Stoops et al. this book) confirm the data of grain mounts: the coarse material is dominated by coarse pyroclasts, up to 10 mm in diameter, and oxybiotite is present.

The plagioclases and leucite detected by XRD (Colombo et al. this book) are part of the rock fragments.

EUR4

Both the medium and the fine sand fractions are dominated by rock fragments (up to 71%), followed by feldspars. The feldspar group (5–38%) contains considerable amounts of leucite. The three horizons studied show small quantitative differences, especially between the O and the Bw1 horizon.

Micromorphology (Stoops et al. this book) shows a dominance of large (up to 5 mm) dark, dense pyroclasts with feldspar microliths and feldspar and augite phenocrysts even as isolated grains of augite and few glass. Few leucite fragments are observed throughout the profile, but alteromorphs af-

ter leucite are common in the C horizon. The absence of biotite is confirmed by XRD (Colombo et al. this book).

EUR5

The medium sand fraction is dominated (80%) by dark rock fragments, pointing to a basaltic or andesitic composition, followed by feldspar (<10%), and only few opaque grains. The fine fraction has a similar composition. There are no clear indications for a lithological discontinuity, in the sequence of horizons studied, except for the 2C1 containing small amounts of hornblende, not observed in the horizons above, supporting the conclusions of Buurman et al. (2004).

These data are confirmed by micromorphological analyses (Stoops et al. this book). The coarse fraction of the soil mainly consists of pyroclasts, pumice being restricted to the Ah horizon (not studied in grain mounts). In addition grains of feldspars, augite and in the deepest layer hornblende are recognised. The presence of the hornblende points to a different paragenesis.

EUR6

Both the medium and the fine sand fractions contain essentially (>90%) opaques, some of which may be very dark basaltic glass fragments (tachylyte), rather than ore minerals (no diffraction pattern with XRD).

Therefore the mineralogical data do not correspond to the findings of the micromorphological analysis, (Stoops et al. this book) which mention large amounts of pyroclasts, even as feldspar, pyroxenes and olivine in the coarse and medium sand. The micromorphological descriptions also mention the presence of orange brown weathered lapilli which may be partly destroyed during the removal of free iron (Gérard et al. submitted).

EUR7

Both the medium and the fine sand fractions are dominated by glass (up to 100%), followed by rock fragments, except in 4B/Cg where the latter are dominant (91%). Small amounts of feldspars occur in the solum, with a higher amount in the 4B/Cg. The glass is colourless and fibrous (derived from pumice) in the 3BC, 3CB and 4Bw, whereas it is mainly brown and vesicular in the O horizon. Each layer appears to have a different lithology, pointing to strong stratification.

The micromorphological analysis of this profile (Stoops et al. this book) points indeed to a stratification, with fluctuating amounts of pyroclasts, pumice, colourless and greenish brown glass. Additional minerals are feld-

spar and augite. In the 3BC horizon, millimetre thin layers of different composition are observed. The study of bulk samples, homogenising several centimetres, as used here and by Buurman et al. (2004), therefore does not reflect reality.

EUR8

Both the medium and the fine sand fractions are dominated by glass in the Bw1 and 2Bw2 (up to 97%), not allowing recognising the lithological discontinuity observed in the field. In the lower part of the profile rock fragments (up to 91%) are dominant, clearly pointing to a discontinuity between 2Bw2 and 3Bw3/4C, confirmed also by a much higher amount of opaques, in agreement with the field observations of a tephra covering a glacial till. In the Bw1 four types of glass are distinguished: vesicular brownish scoria; colourless glass with opaque particles, dark brown aggregates, and colourless fibrous glass (derived from pumice). In the 3Bw3/4C the glass has a weathered aspect and often a dark brown colour.

Micromorphological description (Stoops et al. this book) also reveal a stratification in this profile. The most common coarse components are colourless pumice and glass, green volcanic glass, pyroclasts and grains of feldspar and augite. In the 3Bw3/4C a pellicular weathering of the greenish beige glass to palagonite is recognised. The changes in mineralogical composition observed in grain mount often reflects more the abundance of a mineral in a given size fraction, than a global mineralogical change.

EUR9

Both medium and fine sand fractions are dominated (up to 99%) by volcanic glass, which ranges from colourless greyish to dark brown, with or without opaque grains, and sometimes with a vesicular fabric.

Thin section studies (Stoops et al. this book) reveal a fine stratification, e.g. of millimetric layers of greyish and of greenish glass, and presence of pyroclasts and rare grains of feldspar and augite. This microstratification is lost when bulk samples are used for grain analysis, as stated also by Buurman et al. (2004).

EUR10

The mineralogical composition points to a stratification in the profile. Opaque grains are dominant (80%) in the fine sand fraction of the Bw, but are negligible in the 2Bw1, whereas rock fragments are especially important in the Bwb2, confirming the field data and the results of Buurman et al. (2004). The opaques in the Bw are probably partly weathered glass with

coatings. The glass in the fine fraction of Bw3b consists of small isotropic orange-brown grains.

In the micromorphological analysis (Stoops et al. this book) no glass was detected. The isotropic orange-brown grains are weathering products of basaltic glass and scoria.

EUR11

The fine sand fraction of the profile is remarkably homogeneous throughout. The medium sand fraction, however, reveals some discontinuities. It is dominated by rock fragments (97%) in the 2Bwb, whereas the 2BCb and the C are dominated by glass (>70%) below (see 3.3). The glass in the 2BCb is weathered; in the fine fraction it is brown (orange in thin sections), sometimes containing microlites and phenocrysts; in the Bw it is colourless or brownish, weathered, with microlites.

The micromorphological description (Stoops et al. this book) confirms the mineralogical data, except for the glass content of the fine fraction.

EUR12

Both the medium and the fine sand fractions are dominated by brown purple glass, especially in the fine fraction (up to 95%). Also the amount of rounded opaques is considerably high. The higher amount of augite in the medium sand fraction of the Bw , compared to the 2Ahb, and the high content of rock fragments in the fine sand fraction of the Bw could indicate either a higher degree of weathering of the lower part of the profile, or a lithological discontinuity, as described in the field.

Micromorphological analysis (Stoops et al. this book) show that the brown isotropic particles identified as glass in the grain mounts are in fact weathering products, resembling a palagonite like substance.

General discussion of results

As shown in the data and in the foregoing discussion, mineralogical compositions of medium and fine sand fractions of a same sample may be different. As a general trend one observes that the amount of glass is higher in the fine sand (50–250 µm) fraction.

As rock fragments in this study are mainly at least partially vitreous pyroclasts, and as glass shards are often fragments of pyroclasts (sometimes even produced during sample preparation), a sum of “rock fragments” and “glass” may be meaningful with regard to the determination of vitric characteristics (Wallace et al. 1985). For both the fine and the medium sand

this sum appears to be more homogeneous throughout the profiles. By summin g rock fragments and glass differences between the medium and the fine sand fraction becomes less significant, with the exception of Pedons EUR 1–3 where the feldspar content is considerably higher in the medium sand fraction. In the other profiles however, the quantity of feldspars is higher in the fine than in the medium sand fraction.

Discussion on methodology

Limitations of optical studies on grain mounts

Grain mounts have been used essentially for the study of so called heavy minerals. These diagnostic minerals, with a specific density of over 2.9 g cm^2 are rather easily identified by their shape, colour, relief and other simple optical characteristics. This is not the case for the light minerals, such as feldspars, which need complicated optical identification, often failing because of initial weathering. In most cases the nature of compound grains, such as rock fragments can not be exactly determined by their optical properties because of overlapping of grains or grains and matrix material, in the relatively thick (>50 µm) grains. Opaques are not necessary all ore grains. X-ray diffraction studies of a few samples (e.g. EUR6) revealed no diffraction pattern, pointing to glass. Indeed, even in thin sections (<30 µm) some basaltic glasses (tachylytes) may seem opaque (see also micrographs n° 55, 59, 72 and 76 on CD-ROM "Micromorphological Description of Reference Profiles of COST 622" Stoops et al. in this book).

A solution for this problem may be the preparation of thin sections of the sand fraction, as recommended for instance by Wallace et al. (1985). A drawback is the cost of the thin section preparation. This technique also allows an easier identification of feldspars based on their twinning pattern. Staining methods for feldspar (e.g. Baily and Stevens 1960, Houghton 1980) were not effective on volcanic feldspars and interfered with other components.

An advantage of optical counting is the fact that grain shapes and colours are easily recognised. Different shapes and colours for a same mineral may point to different origins (e.g. compare fresh euhedral pyroclastic augite grains with rounded ones from sedimentary origin, or green-brown augite with the purple ones from basaltic rocks). This is especially important for volcanic glass (e.g. EUR8).

Grain mount studies compared with micromorphology

Micromorphology has several advantages over grain mount studies to investigate the mineralogy of volcanic ash soils. In the first place thin sections allow the study in transmitted light of coarser grains than grain mounts do. This means that the coarse sand fraction (2000–500 µm) and even gravel sized components can be studied. In thin sections of undisturbed material grains are not mechanically fragmented during preparation, yielding a more precise insight in the mineralogy of different size fractions.

Mineral identification is easier in thin section, and petrographic identification of rock fragments is possible. Additional information is obtained on degree of weathering or pseudomorphosis. A good example is found in the Tenerife soils, where limpid isotropic orange particles were interpreted as volcanic glass in grain mounts, whereas in thin sections the same material was clearly identified as a weathering product.

The disadvantage of thin section studies remains the seemingly high cost of the section preparation and a more difficult quantification. In reality, however, thin sections are not more expensive than most other sophisticated mineralogical analyses. An advantage of using thin sections of undisturbed soils is that mineralogical information on paragenesis in microstratified materials is not lost, as is the case in bulk samples, which may lead to geologically incorrect conclusions (e.g. EUR 7–9).

Information on the shape of the grains is preserved in thin sections, and at least euhedral and anhedral shapes can be distinguished, and for the latter the degree of rounding can be determined. Also the study of inclusion, e.g. basaltic glass in feldspars (see micrographs n° 63 and 64 on CD-ROM "Micromorphological Description of Reference Profiles of COST 622" Stoops et al. in this book) may give additional information about the paragenesis.

Grain mount studies compared with X-ray diffraction (XRD)

XRD is a quicker technique for semi-quantitative mineralogy of a sand fraction than the optical identification and counting of grains. Minerals, not detected in grain mounts, or only in small quantities, can appear in XRD spectra, as rock fragments (pyroclasts) are broken and their enclosed grains released.

Glass gives only a broad bulge in the XRD-spectra and therefore cannot be quantified, which is the most important drawback of this method for volcanic ash soils. Another disadvantage of XRD is that minerals that constitute less than 5% of the bulk may not be detected in XRD and that no information on shape or mineral variety is given. E.g. in the Italian profiles

biotite is detected by XRD, but only the optical methods (grain mounts and micromorphology) allowed to identify it as oxybiotite.

Conclusions

Quantitative mineralogical analysis of the sand fraction of volcanic ash soils by counting in grain mounts, studied in transmitted polarised light, yields useful information for soil description, classification and interpretation of chemical data. It allows the identification of part of the lithological discontinuities observed in the field, although not all. This can be explained mainly by the fact that many discontinuities are recognised in the field based on differences in grain size distribution. This information completely disappears in the mineralogical study of the sand fraction. This is also the reason why there is no complete match with the discontinuities proposed by Buurman et al. (2004). Microscale discontinuities (microstratification) detected by micromorphology cannot be detected in the sand fraction, unless a sampling on centimetre or millimetre scale is done. As grain mounts are limited to restricted size fractions (smaller than coarse sand size) a lot of information, visible in soil thin sections, is lost.

In grain mounts correct identification of the grains is not always easy or possible, especially in the case of pyroclasts and weathered glass fragments. Data therefore should be handled with care when used for classification or interpretation. Counting on thin sections made of the sand fraction would overcome this problem, but grain counts remain unrepresentative for the bulk, as only smaller size fractions of the sand are studied. A quantitative mineralogical/petrographic analysis of undisturbed soil thin sections would be more reliable, but also more time consuming.

X-ray diffraction can yield valuable quantitative information on the crystalline minerals of the sand fraction, but none on the vitric components. Moreover it is not possible to deduce by XRD which minerals are present as individual grains, and which are part of rock fragments. Different mineral varieties cannot be detected.

References

Bailey EH, Stevens RE (1960). Selective staining of K-Feldspars and Plagioclases on rock slabs and thin sections. Am Mineralogist 45:1020–1025

Buurman P, Garcia Rodeja E, Martinez Cortizas A, van Doesburg JDJ (2004). Stratification of parent material in European volcanic and related soils studied by laser-diffraction grain sizing and chemical analysis. Catena 56:127–144

Colombo C, Palumbo G, Sellitto VM, Terribile F, Gérard M, Stoops G (2006). Characteristics and genesis of volcanic ash soils in Southern Central Italy: Phlegreaen Fields (Campania) and Vico Lake (Latium). In: Arnalds O, Bartoli F, Buurman P, Garcia-Rodeja E, Oskarsson H, Stoops G (eds) Soils of Volcanic Regions of Europe. Springer Verlag

Edelman CH (1931). Mineralogische Untersuchungen von Sedimentgesteine. Fortschr der Mineral 15:289–

Gérard M, Caquineau S, Pinheiro J, Stoops G. Weathering and allophane neoformation in soils on volcanic ash from the Azores (submitted to European Journal of Soil Science)

Houghton HF (1980). Refined technique for staining plagioclase and alkali feldspars in thin section. Journal of Sedimentary Petrology 50:629–631

Jackson ML (1965). Free oxides, hydroxides, and amorphous alumino-silicates. In: Black CA. (ed) Methods of Soil Analysis. Part. 1 Agronomy 9:578–603

Stoops G, FitzPatrick EA, Gérard M (2006). Micromorphological description of thin sections of volcanic ash soils of COST-622 reference profiles. In: Arnalds O, Bartoli F, Buurman P, Garcia-Rodeja E, Oskarsson H, Stoops G (eds) Soils of Volcanic Regions of Europe. Springer Verlag

Stoops G, Van Driessche A (2002). Mineralogical composition of the sand fraction of some European volcanic ash soils. Preliminary data. Mainzer naturwiss. Archiv 40:31–32

Wallace RC, Stewart RB, Neall VE (1985). Volcanic glass field laboratory test and procedure to prepare thin sections of the sand fraction of soils. Department of Soil Science, Masseay University, Palmerton North, New Zealand, p 7

Micrographs referred to are situated on CD-ROM:

Micromorphological Description of Reference Profiles of COST 622

Extractability and FTIR-characteristics of poorly-ordered minerals in a collection of volcanic ash soils

E.L. Meijer, P. Buurman, A. Fraser and E. García Rodeja

Introduction

Poorly-ordered minerals in volcanic soils predominantly consist of secondary alumino-silicates, aluminium oxyhydroxides, and iron oxyhydroxides. These substances have structures that range from amorphous to crystalline. For alumino-silicates the corresponding minerals are allophane, proto-imogolite, imogolite, halloysite, and kaolinite (the most crystalline species). For aluminium oxyhydroxides the structural range includes amorphous aluminium hydroxide and gibbsite, and for iron-oxyhydroxides the range includes amorphous ferric hydroxide, ferrihydrite, and goethite, but the water-free crystalline iron-oxide minerals hematite and magnetite are also encountered. The name allophane was first introduced by Strohmeyer and Hausmann in 1816. Parfitt and Furkert (1980) stated that there are at least two different types. Since Fe can be built-in in both artificial (Violante et al. 1998), and natural (Farmer 1997) alumino silicates, both the Al/Si and the Fe/Al ratio influence the final product. As a result, the thermal dehydration of allophane depends on Al/Si ratio (Henmi 1980**,** Violante et al. 1998) but iron-content also plays a role (McKenzie and Cardile 1988).

Fe-hydroxide gels form ferrihydrite, a widely spread Fe-oxyhydroxide (Jambor and Dutrizac 1998). Fe-oxyhydroxides may contain silica (Murad and Schwertmann 1988).

All these products, synthesized or natural, have been studied with a wide variety of techniques: Mössbauer spectroscopy (Takeda et al. 1979**,** Murad and Schwertmann 1988), micromorphology and submicroscopy (Farmer et al. 1985**,** Kawano et al. 1997), IR-spectroscopy (Farmer et al. 1979), ESCA and solid-state NMR (Childs et al. 1990**,** He et al. 1995), ESR (Shimizu et al. 1988), and laser-diffraction grain-sizer (Buurman et al. 1997).

Structural differences between allophane and halloysite and between allophane and imogolite have been studied by De Roy et al. (1980) and Denaix (1993), respectively. Like allophane, imogolite has been studied

also by various techniques (Violante and Tait 1979, Shimizu et al. 1988, McKenzie et al. 1989). Intimate associations between allophane and imogolite have been reported by He and Horikawa (1998, 2000). These two substances are commonly organized into aggregates that are difficult to disperse. Also iron oxyhydrates play a role in aggregation.

The chemical formula of allophane is generally reported as:

$Al_2O_3.SiO2.nH_2O$ or $(Al_2O_3)(SiO_2)_{1.3–2}(H_2O)_{2.5–3}$ or $(Al_2O_3)(SiO_2)_{1–2}$-$(H_2O)_{2.5–4}$. The latter formula is based on data collected by Mizota and van Reeuwijk (1989). The crystalline associates halloysite and kaolinite have a general formula of $(Al_2O_3)(SiO_2)_2(H_2O)_2$. So, allophane has a higher structural water content (21.7% to 24.5%) than halloysite/kaolinite (13.9%). According to Mizota and van Reeuwijk (1989) ferrihydrite contains 15.8% structural water. Therefore, a mixture of allophane with halloysite/kaolinite and/or ferrihydrite has a *lower* structural water content than pure allophane, whereas a mixture with gibbsite or amorphous aluminium hydroxide (structural water content of $Al(OH)_3$ is 34.6%) has a *higher* structural water content.

Extraction of amorphous silicates and iron compounds

For the quantification of amorphous aluminium silicates and poorly crystalline iron oxyhydrates, a single extraction by a Na-oxalate/oxalic acid mixture is commonly used. Solid:solution ratios in such extractions are usually 1:50–1:100 (McKeague and Day 1966, Blakemore 1987, USDA 1996). It is common knowledge that, in case of high contents of poorly crystalline compounds, a single extraction may not extract all amorphous matter. Therefore, Thorlacius (2002) suggested a ratio of 1:200.

In the scope of the behaviour of the amorphous fraction of European and Costa Rican volcanic soils upon extraction with acid oxalate, we found that most samples gave decreasing yields with each consecutive extraction while some samples gave almost steady yields. Al/Si ratios in the extracted material varied widely. In oxalate extraction of iron compounds, the second extraction was frequently more effective than the first and the amount extracted by consecutive oxalate extractions sometimes exceeded that of a single dithionite extraction. We decided to investigate whether there is a relation between extraction behaviour and organization of the ‘amorphous’ fraction. We determined the extraction behaviour upon 5–7 consecutive extractions. For characterization of crystalline and amorphous phases we used X-ray diffraction and Fourier Transform Infra-red Spectroscopy (FTIR). We chose a number of samples from COST soils and from Costa

Rica. The present collection of samples of volcanic soils from various countries contains different assemblages of all mentioned minerals.

Materials and methods

The extraction behaviour and FTIR spectra of 34 volcanic soil samples from different locations in Europe and from the Turrialba volcano in Costa Rica, have been measured. The samples were from various horizons of 17 different profiles (Table 1). The European (COST) samples belong to the set of samples described by Buurman et al. (2004) and the Costa Rican samples to the set of samples described by Meijer and Buurman (2003). The concise sample data in the first three columns of Table 1 are from these two publications, but former profile codes Nxx have been replaced by EURxx.

Chemical methods are detailed in Buurman et al. (1996). The samples were analyzed for carbon (%C), pyrophosphate-extractable Al_p and Fe_p, dithionite-extractable Fe_d, and acid-oxalate extractable Al_o, Si_o, and Fe_o. The oxalate extractions were done using two different procedures: (1) a *single* extraction using a standard procedure with a 1:50 soil:solution ratio, and (2) five to seven *sequential* extractions using a 1:40 sample:extractant ratio. In case of Italian, Azores, and Costa Rican samples, the single and sequential extractions were carried out on field-moist fine-earth (<2 mm) samples, while air-dried fine-earth (<2 mm) samples were used for all other samples and measurements. Elements Al, Si, and Fe, in the extracts were analyzed by AAS; all results are reported with respect to 105ºC-dried material.

X-ray diffraction data were obtained after removal of organic matter by peroxide oxidation, on clay fractions oriented on porous ceramic tiles, upon saturation with Mg, Mg-glycerol, and K.

FTIR spectra were measured for H_2O_2-pretreated fine earth (<2 mm) or clay-sized (<2 µm) fraction if the latter was available. The spectra were recorded for 105ºC-dried material diluted 1:100 in a KBr matrix (compressed disc) using a single-beam Nicolet Magna-IR 550 Spectrofotometer in the wave-number range 4000 to 400 cm^{-1}. Additionally, all spectra in the 650–100 cm^{-1} range were recorded for similar samples diluted 1:100 in a CsBr matrix using a Perkin-Elmer PE2000 FTIR apparatus. For most samples, FTIR spectra have also been recorded of the residue remaining after sequential extraction.

Table 1. Sample data and analytical data.

Location and sample data					Single pyrophosph. extraction[1)]		Single standard oxalate extraction			Cumulative sequential oxalate extraction			Single dithionite extraction
Profile (altitude)	Sample number	Horizon	Depth cm	C %	Al_p %	Fe_p %	Al_o %	Si_o %	Fe_o %	Al_o %	Si_o %	Fe_o %	Fe_d %
Italy													
EUR03 (700 m)	54	Ah2	22–48	4.2	0.4	0.1	3.1	1.4	0.6	3.6	1.6	1.5	1.4
	57	Bw2	98–125	0.7	0.2	0.0	3.1	1.7	0.4	3.6	1.9	1.6	0.7
EUR04 (722 m)	60	Ah2	8–25	11.2	1.0	0.2	4.2	1.5	0.7	3.8	1.6	1.5	1.0
	61	Ah3	25–43	8.2	0.8	0.2	3.7	1.7	0.7	4.5	2.1	1.7	1.3
Azores													
EUR05 (510 m)	446	2Ah	30–45	8.0	1.8	2.9	4.3	1.0	1.8	1.9	0.7	3.0	5.3
					1.4	*1.1*							
	447	2Bw	45–65	3.4	1.4	1.1	6.0	1.7	1.2	3.5	1.2	2.9	3.0
						0.7							
EUR06 (400 m)	450	Ah	0–35/40	19.1	3.5	3.7	5.3	0.7	2.6	5.9	1.3	7.0	6.4
						2.6							
	451	AB	35/40–45	13.0	2.6	3.3	6.3	1.3	2.9	7.0	1.8	8.1	7.6
						2.9							
	452	2AB	45–65	11.0	2.9	4.2	6.1	1.9	4.2	8.9	2.3	9.7	10.1
	453	2Bw1	65–95	9.3	2.5	2.8	10.1	2.8	3.3	10.9	3.2	9.8	10.0
	454	2Bw2	95–125	5.8	1.2	0.6	9.1	2.0	2.9	10.5	3.5	8.3	8.3
	455	2Bw3	125–140	4.5	0.9	0.2	9.5	3.4	3.0	11.0	4.3	9.2	8.7
Iceland													
EUR07 (40 m)	1046	Ah2	17–35/50	13.0	0.8	1.2	2.1	0.9	6.1	2.1	1.4	9.5	11.5
	1049	Bw2	73–82	11.9	1.1	0.6	2.6	1.0	1.1	2.7	1.8	1.8	1.3
	1050	Bw3	82–95	8.5	1.1	0.8	5.2	2.2	0.8	4.9	2.7	1.9	1.7
EUR08 (400 m)	1054	Bw1	19/24–23/31	4.2	0.3	0.3	2.7	1.5	1.6	2.9	2.6	4.5	4.5
	1056	3BwC	34/39–57	2.8	0.2	0.2	3.0	2.0	1.9	2.9	3.2	5.6	5.1

Tenerife													
EUR10 (1130 m)	2	Bw1	45–90	4.2	0.5	0.1	5.1	1.8	1.9	8.5	4.5	5.6	6.9
	4	2Bw3b	115–220	2.0	0.3	0.1	3.6	1.6	4.0	7.0	4.2	12.5	13.1
	5	2Bw4	>220	0.6	0.2	0.4	0.5	0.1	1.0	1.5	0.6	4.0	0.3
EUR11 (1675 m)	7	C1	10–18	0.8	0.1	0.1	0.9	0.7	0.9	3.4	5.3	4.2	0.8
	8	2Bw	18–35	1.9	0.1	0.1	1.4	0.9	0.8	3.1	2.1	2.5	1.6
EUR12(1000 m)	12	Ah2	17–75	8.9	1.3	1.1	1.2	0.2	0.7	2.5	0.5	3.1	4.7
					1.2	*0.7*							
	14	2Ahb	90/120–100/130	3.1	0.6	1.7	0.4	0.1	0.6	1.0	0.2	3.2	5.1
					0.4	*0.6*							
Costa Rica													
T1 (800 m)	3CR	AB	27–60	8.1	1.3	0.9	8.1	2.5	4.0	10.2	2.9	6.5	1.6
	5CR	Bw2	93–120/150	4.3	0.4	0.2	6.2	2.1	4.7	8.0	2.4	7.5	2.9
T2 (930 m)	11CR	2Bw2	72–92	7.9	0.6	0.0	9.8	3.8	2.4	20.0	7.2	6.6	1.4
T3 (660 m)	14CR	AB	18–45	5.8	0.6	0.1	8.6	3.3	2.7	10.4	3.3	4.6	1.4
T4 (1220 m)	21CR	3Bw	108–130	4.0	0.5	0.1	9.8	4.6	4.0	14.4	5.8	6.6	1.2
T6 (2030 m)	31CR	6Ah	69–80	2.8	0.5	0.7	2.0	0.8	0.6	1.5	0.5	3.8	1.1
						0.6							
T8 (1570 m)	106CR	3Bw1	30–49	4.4	0.4	0.2	4.6	1.5	2.4	7.5	2.9	4.4	n.d.[2)]
T9 (1060 m)	154CR	2Bw1	78–130	6.1	0.5	0.0	11.3	4.7	3.2	14.8	5.3	6.2	1.2
	155CR	2Bw2	>130	4.4	0.4	0.0	11.9	5.2	3.0	14.8	5.6	6.3	1.4
T10 (240 m)	187CR	Bw2	100–155	0.7	0.2	0.0	5.8	3.9	1.2	5.2	4.2	3.4	1.4

1) If necessary to avoid negative or anomalous values in the calculations, corrections for Al,Fe-pyrophosphate have been limited to the values shown in italics on the next line (see text).

2) n.d. = not determined.

For most of the minerals mentioned in the Introduction, FTIR spectra from our library are given in Figure A (on CD). Three of these are reproduced in Figure 1. The relevant features in the spectrum to be used in the comparison of samples are: (1) the relative intensity of the OH band around 3500 cm^{-1} which is indicative for structural water and therefore generally decreases upon removal of amorphous fraction, (2) the presence or absence of sharp peaks in the range 3450 to 3700 cm^{-1} which are characteristic for crystalline minerals such as gibbsite and kaolinite/halloysite, (3) the relative intensity of the bands related to polymerized silica (at >1000 cm^{-1}) or monomeric silica (at <1000 cm^{-1}), 4) the intensity of the (difficult to unravel) Al,Fe band(s) in the range 400 to 800 cm^{-1}, and 5) the typical adsorption band of imogolite at 350 cm^{-1}.

Results and discussion

Extraction behaviour

The results of the pyrophosphate, acid oxalate, and dithionite extractions are listed in Table 1. The results of the consecutive extractions are given in Table A (on CD). The curves of consecutive oxalate extractions are reproduced in the following figures on CD: Figure B-E: Italy; Figures F-I: Azores; Figures J-M: Iceland; Figures N-Q: Tenerife, Figures R-U: Costa Rica. The different types of curves are illustrated in Figure 2A for Si, Figure 2B for Al, and Figure 2C for Fe. For iron, Fe_d values are added as final data-points to the sequential extraction curves in Figure 2C for comparison with the results of the dithionite extraction. The reproducibility of sequential extraction data which has been tested for samples 57, 446, 453, and 1050, is found to be satisfactory (parallel curves and a relative difference typically smaller than 10%). The final cumulative levels of Al_o, Si_o, and Fe_o that were reached (or extrapolated if only five instead of seven extractions had been done) in the sequential extractions have been listed in Table 1. Values calculated from the extraction data in Table 1 are listed in Table 2. The third and fourth column of Table 2 show that corrected Al_o/Si_o ratios, that is $(Al_o\text{-}Al_p)/Si_o$, are generally lower in the sequential extraction than in the single extraction, except for seven Costa Rican samples. The exceptions seem to be restricted to samples that have much lower Fe_d than Fe_o(single) or Fe_o(sequential). But, as Tenerife sample 7 shows, this is not a general rule. Similarity of properties of adjacent horizons are indicated by braces in the first column of Table 2. There are three pairs of samples (Costa Rica 3/5, 154/155, and Iceland 1054/1056) that have more or less the same values for all quantitative properties.

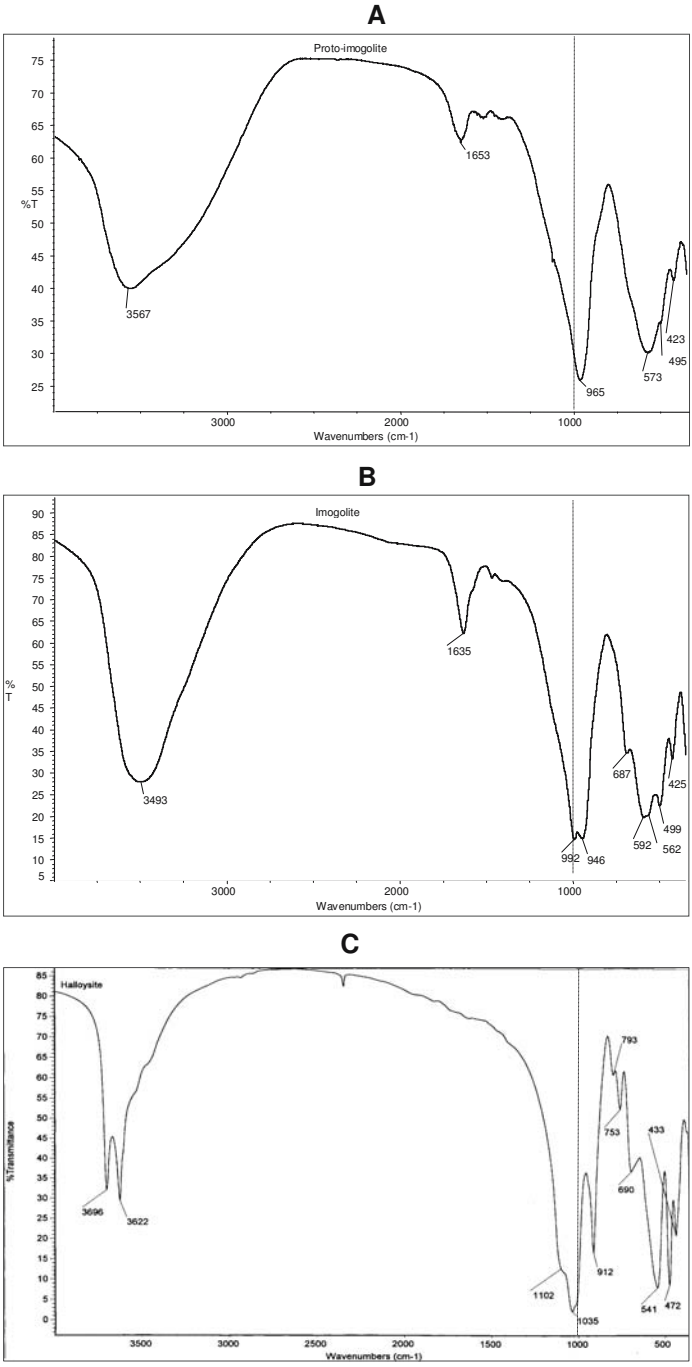

Figure 1. Library FTIR spectra of some relevant minerals. A: Proto-imogolite; B: imogolite; C: halloysite.

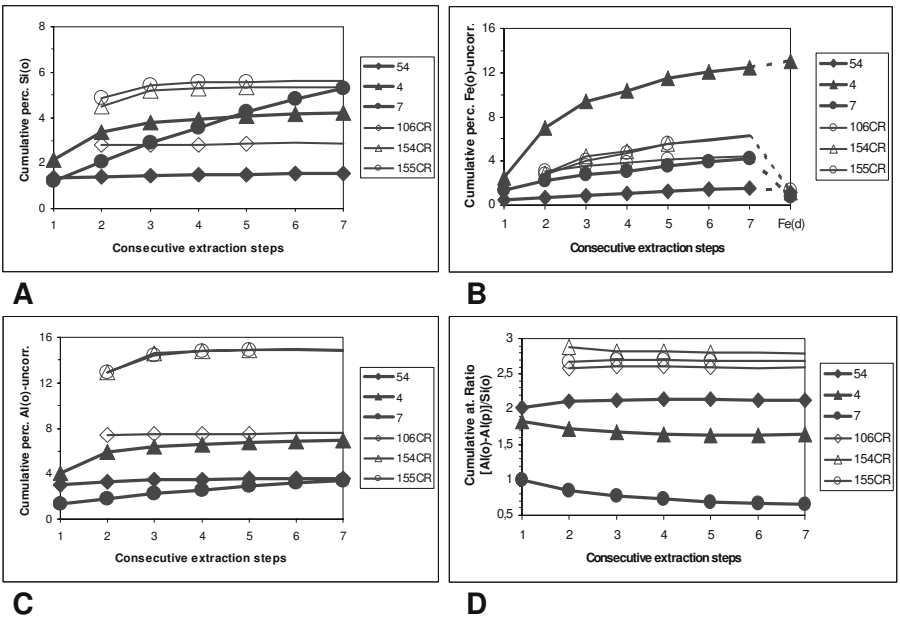

Figure 2. Sequential extraction plots of two samples, Tenerife EUR10–4 and Costa Rica T–11. A: cumulative Si_o; B: cumulative Al_o; C: cumulative Fe_o compared with Fe_d; D: cumulative atomic ratio $(Al_o\text{-}Al_p)/Si_o$.

Al and Si extractions

In extractions of Al and Si, most samples show an asymptotic behaviour, as would be expected when (1) contents of extractable matter are very high, or (2) subsequent extractions remove increasingly inaccessible material. Exceptions are the Tenerife samples 2 and 4, where the yield of second extraction equals or exceeds that of the first, and Tenerife 7, where both Al and Si yield about equal amounts in each subsequent extraction (linear curve). About half of the Costa Rican samples have such linear extraction curves for Si, Al, and Fe, with zero or small slope for Al and Si, and higher slopes for Fe (except CR 31). In some cases the Si yield is very low whereas Al and Fe yields are significant (CR 3, 5, 14 with corrected Al/Si ratios about 3.2 and amounts of extractable oxides about 31%, see Table 2). The Costa Rican samples that show asymptotic extraction curves for Al, Si, and Fe (CR 11, 21, 154, 155), have all corrected Al/Si ratios between 2.5 and 2.8, and amounts of extractable oxides from 47% to 62% (Table 2). Sample CR 106 also has an Al/Si ratio in this range, but its pos-

sible asymptotic character may have been obscured because we combined the first and second extractions, so that we do not have separate information on the first one.

Table 2. Calculated extraction properties of samples.

Sample number	Fe_p/Al_p	Al_o/Si_o corr. for Al_p [1]		(mineral oxides)$_o$ corr. for Al_p,Fe_p [2]	Fe_d-Fe_o(cum)	(Fe_d-Fe_o)/Δ(ox)	Type [3] of track in Fig.3
	Pyroph. extr.	Standard single extr.	*Cumulative sequential extr.*	Cumulative sequential extr.	Dith. minus cumul. seq. extraction	Ratio of increments	
	ratio	at. ratio	at. ratio	%	%	ratio	
Italy							
54	0.2	2.0	2.1	11	-0.1	-0.04	B
57	0.1	1.8	1.8	13	-0.9	-0.27	B
60	0.2	2.2	1.9	10	-0.4	-0.79	B
61	0.2	1.8	1.8	14	-0.4	-0.11	B
Azores							
446	1.6	*3.1*	*0.8*	3	+2.3	-0.65	B
447	0.8	2.8	1.7	9	+0.1	-0.04	B
450	1.1	2.7	2.0	14	-0.6	-0.07	-
451	1.3	3.1	2.6	20	-0.5	-0.06	B
452	1.4	1.8	2.7	24	+0.4	+0.03	B
453	1.1	2.8	2.7	33	+0.2	+0.02	B
454	0.5	4.2	2.7	36	+0.1	0.00	B
455	0.2	2.6	2.3	41	-0.5	-0.04	B
Iceland							
1046	1.4	1.5	0.9	17	+2.0	+0.33	B
1049	0.5	1.6	1.0	9	-0.5	-0.18	C
1050	0.7	2.0	1.5	15	-0.2	-0.11	B
1054	1.0	1.6	1.1	17	0.0	0.00	B
1056	1.0	1.4	0.9	20	-0.4	-0.06	B
Tenerife							
2	0.1	2.6	1.9	33	+1.2	+0.07	B
4	0.3	2.1	1.6	39	+0.6	+0.03	B
5	2.5	2.3	2.4	9	-3.7	-0.51	B
7	0.8	1.1	0.6	24	-3.4	-0.18	D
8	0.5	1.6	1.4	14	-0.9	-0.11	B
12	0.9	*0.0*	*2.5*	7	+1.5	+0.23	B
14	2.8	*0.0*	*3.9*	5	+1.9	+0.36	A
Costa Rica							
3CR	0.2	2.8	3.3	31	-4.9	-0.60	B
5CR	0.7	2.9	3.2	30	-4.6	-0.63	B
11CR	0.5	2.5	2.8	62	-5.2	-0.16	A
14CR	0.0	2.5	3.1	32	-3.2	-0.58	B
21CR	0.2	2.1	2.5	48	-5.3	-0.35	B
31CR	1.4	2.0	2.2	8	-2.7	-0.97	-
106CR	0.5	2.9	2.6	26	n.d.	n.d.	B
154CR	0.0	2.4	2.8	47	-5.0	-0.41	B
155CR	0.0	2.3	2.7	48	-4.9	-0.44	B
187CR	0.0	1.5	1.2	23	-2.0	-1.21	C

[1] Figures in *italics* are zero or adapted values because $Al_p > Al_o$.

[2] (Mineral oxides)$_o$ is the percentage oxalate-extractable $Al_2O_3+SiO_2+Fe_2O_3$ calculated from Al_o, Si_o, and Fe_o data.

[3] Legend: (A): from Al_o-corner; (B): towards Fe_o-corner; (C): from Si_o-corner; (D): towards Si_o-corner; (-): constant composition.

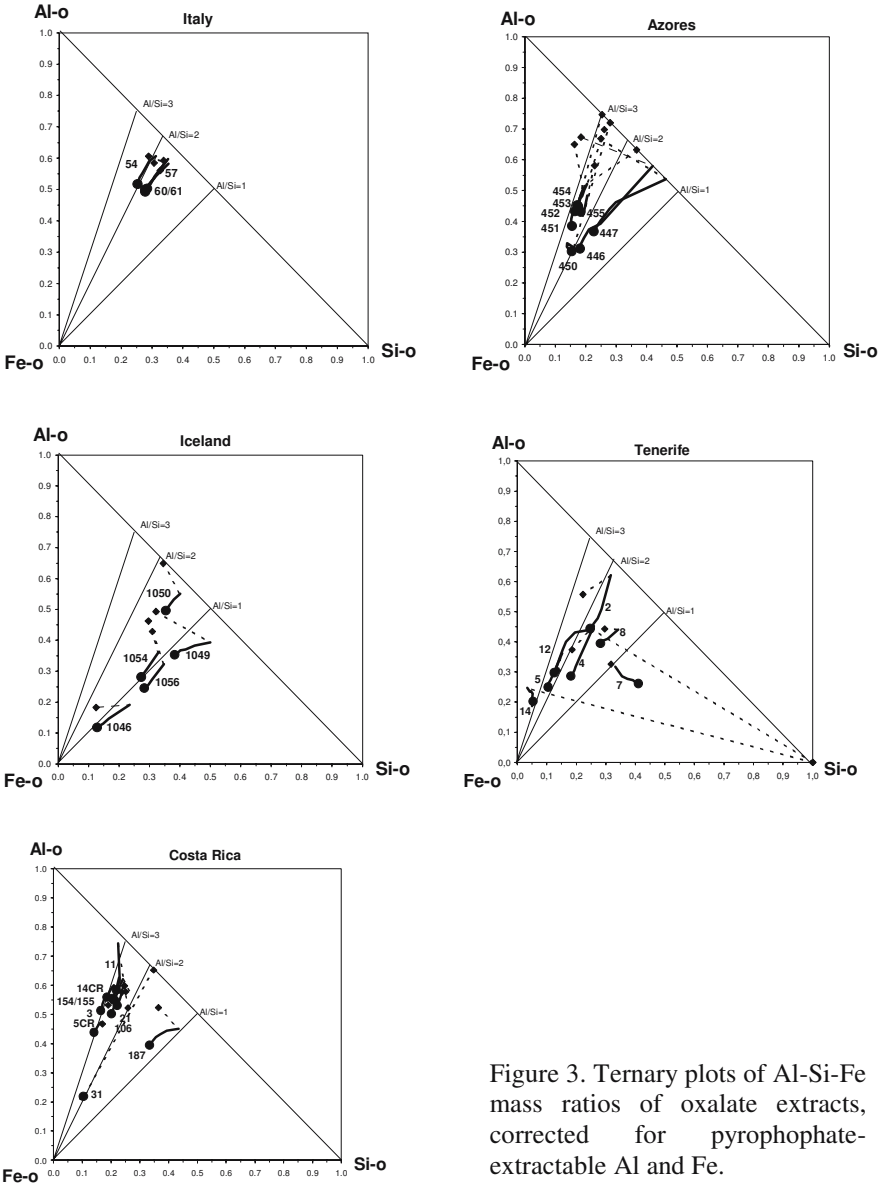

Figure 3. Ternary plots of Al-Si-Fe mass ratios of oxalate extracts, corrected for pyrophophate-extractable Al and Fe.

During subsequent extractions, the Al/Si ratios of the extracted matter remain virtually constant (Table A and figures on CD), indicating that there is no change in the extracted material. Between samples, however, (corrected) ratios vary considerably (Table 2). This is visualized in Figure 3 in which corrected *mass ratios* of Si_o, Al_o, and Fe_o have been plotted.

The corrections consist of subtracting Al_p from Al_o, respectively Fe_p from Fe_o. Values of the final cumulative extractions are represented by full circles in Figure 3, and the results of the standard single extractions are added as full diamonds. Dashed lines connect the standard single extraction and the first value in the sequential extraction experiment. The differences between the two are systematic (see for example the similar Iceland EUR08 samples 1054 and 1056) because the two experiments were carried out in different laboratories and notwithstanding careful homogenisation, subsamples may still show some differences. The homogeneous Italian profiles EUR03 and EUR04 (see the next section on FTIR characteristics) do not show these differences.

In the sequential extractions, the tracks of Al/Si ratios of individual samples follow generally lines of constant Al/Si (labeled values are atomic ratios) and point generally into the direction of the iron corner. This general behaviour is classified as group B in the last column of Table 2.

Per location the observed extraction characteristics are as follows:

- In the Italian samples, from EUR03 and EUR04, the ratios are 1.8–2.1. The extraction curves are quite similar (all four samples have relatively little Fe_o).
- All Azores samples have in common that Fe_o is of the same order as Al_o. The amounts of extractable oxides in EUR06 increase steadily from 14% in the top layer to 41% in the bottom layer. The Al/Si ratios in this profile are between 2.0 and 2.7, and between 2.6 and 2.7 when top- and bottom layer are disregarded. This coincides with the range 2.5 to 2.8 for the Costa Rica samples 11, 21, 154, 155 that are also rich in extractable material. In EUR05, the ratio for sample 447 is 1.7. In sample 446, with 8% carbon (±16% OM) versus 3% extractable oxides, it becomes evident that pyrophosphate figures may be too high, because correction corrected values for Al_o and Fe_o values would be near zero or negative. Therefore reduced corrections have been estimated in the calculations and graphs.
- In the Iceland samples, corrected ratios are between 0.9 and 1.1, except for sample 1050 having a ratio of 1.5. The Si and Al extraction curves of samples 1046 and 1049 (EUR07), have a strong similarity in curvature, but the Fe_o level of 1046 is both absolutely and relatively higher than that of 1049 (corrected Fe_o is exceeded only by Tenerife sample 4). This is not explained by a difference in %C (13% versus 12%), but the dominance of Fe in the oxalate extract is also seen in the pyrophosphate extract (mass ratio Fe_p/Al_p=1.4).
- The sample pair 1054 and 1056, from EUR08, has an identical Al extraction curve and similar curvature of Si and Fe extraction curves.

- In Tenerife, samples 2 and 4 both have a sharp increase in extracted Si, Al, and Fe, from the first to the second extraction. But the Fe extraction curve of sample 4 continues to extremely high levels (12.5% after seven extractions) approaching the 13.1% Fe_d. The Tenerife sample with lowest extractable Si and Al and highest carbon content (12) gives a ratio of 2.5 with reduced Al_p correction. The other samples have ratios between 1.4 and 2.4, with the exception of a lowest value 0.6 for sample 7 and a highest value 3.9 for sample 14. Sample 7 is characterized by linear extraction behaviour with a constant release of much Si_o, which suggests dissolution of weathered silica skeletons. Sample 14 has also linear extraction behaviour, but the very small amounts of Si_o cause a larger error in the calculated Al/Si ratio.
- With two exceptions, the Costa Rican samples have ratios between 2.5 and 3.3. Samples 31 and 187 have ratios of 1.2 and 2.2, respectively.

Figure 4 gives an overview of the similarities and dissimilarities of the samples with respect to the amounts of extractable material, as mass of oxides (SiO_2+Al_2O_3+Fe_2O_3) that are calculated from the corrected amounts of (Al_o-Al_p), (Fe_o-Fe_p), and Si_o. Full diamonds give values for the single extraction, whereas full circles represent the final cumulative value of the sequential extraction. Both values have been corrected for the same amount of pyrophosphate-extractable material (based on the assumption that oxalate extracts also the Al and Fe that is bound to organic matter, and that pyrophosphate specifically extracts this organically-bound Al and Fe). In some cases Fe_p>Fe_o and/or Al_p>Al_o. This is a well-known phenomenon in pyrophosphate extracts (Jeanroy and Guillet, 1981; McKeague and Schuppli, 1982), due to the dispersive action of pyrophosphate, which especially affects ferrihydrite particles. If Fe_p>Fe_o, we have assumed that there is zero inorganic Fe-containing phase extracted. A similar assumption holds true if Al_p>Al_o, but we found this exclusively in samples 12 and 14 of EUR12 that had very low amounts of extractable phases so that the discrepancy can be attributed to analytical error.

We define the amount Δ(ox) as the difference between the total amount of (inorganic) oxides (SiO_2+Al_2O_3+Fe_2O_3) extracted in the sequential extraction and in the standard single extraction (Table 2). Δ(ox) values are shown as bars in the upper part of Figure 4. In the Azores profile EUR05, Δ(ox) is slightly negative, but this is probably due to experimental uncertainty. To avoid that differences between samples in Figure 4 are merely the effect of dilution by organic matter, the values have all been calculated in gram per 100 gram *of inorganic material* (using the approximation %OM=2*%C). The bars in the lower part of Figure 4 show the amount of organically bound Al plus Fe (expressed as Al_2O_3+Fe_2O_3) for which the

points in the upper part have been corrected. For comparison, the amounts of organic carbon are also plotted in the lower part in Figure 4.

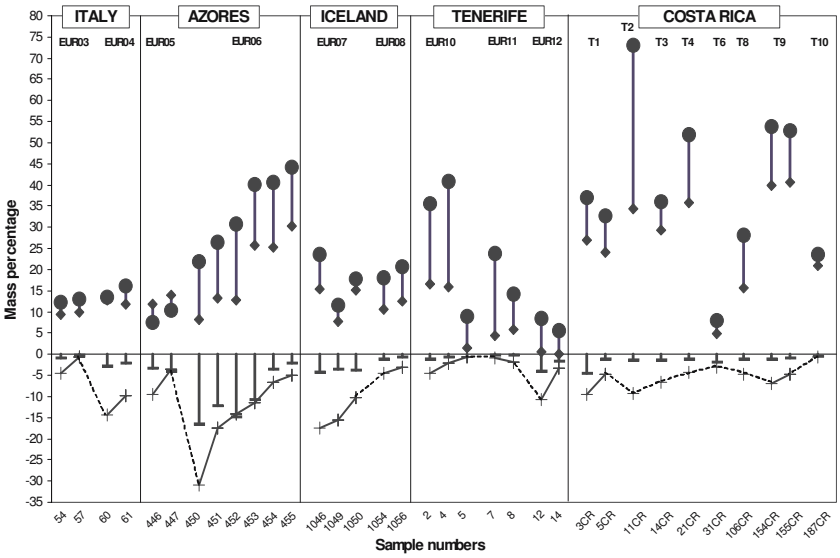

Figure 4. Amounts of oxalate-extractable oxides (SiO_2+Al_2O_3+Fe_2O_3) in standard extraction procedure (♦) and final cumulative values in sequential extraction procedure (•). Both amounts have been corrected for Al,Fe extractable by pyrophosphate. The size of this correction is plotted along the negative Y-axis (▫), together with a line plot of %C of the samples for comparison (+). All data in this figure are in grams per 100 g of 105ºC-dried OM-free material.

The corrected total amounts of inorganic oxides (SiO_2+Al_2O_3+Fe_2O_3) extracted in the sequential extraction are listed in the fifth column of Table 2 (here as mass percentage of dry sample).

Allophane and imogolite should have Al/Si ratios between 1 and 2. Samples with Al/Si ratios above 2 tend to contain gibbsite (Table 3) and it is likely that oxalate extracts some gibbsite. Only sample Tenerife 7 has a ratio of 0.6, and it is unlikely that this can be ascribed to allophane. This sample is also unusual because the extracts smelled of hydrogen sulfide. It is not unlikely that sulphuric acid in the sample caused strong weathering of plagioclase and that the elevated extraction of silica, its linear behaviour (Figure 2) and deviating track in Figure 3 (classified as D in Table 2), should be ascribed to this phase. An Al/Si ratio in the extract of 0.6 would then be logical.

Table 3. XRD-identified crystalline minerals in the unextracted and/or extracted samples.

Sample number	XRD-identified crystalline minerals[1)]										
	Kao/ Hall	2:1	Sm	Chl	Mic	Verm	Q/ Crist	Plag	Gibbs	Pyrox	Hem
Italy											
54	x	x				x	x	x		x	x
57	x	x				x	x	x		x	x
60	x	x				x	x	x		x	x
61	x	x				x	x	x		x	x
Azores											
446	x			x			x	x	x		
447	x			x			x	x	x		
450	not analyzed										
451	not analyzed										
452	not analyzed										
453	not analyzed										
454	not analyzed										
455	not analyzed										
Iceland											
1046	x						x	x		x	
1049	x						x	x		x	
1050							x	x		x	
1054							x	x		x	
1056							x	x		x	
Tenerife											
2							x	x	x		
4	x						x		x		
5	x						x	x			
7	x						x	x	x	x	x
8	x						x	x	x	x	x
12	x			x	x		x	x	x		x
14	x			x	x		x	x	x		x
Costa Rica											
3CR	x	x					x		x	x	x
5CR	x	x					x		x	x	x
11CR	x	x					x		x	x	x
14CR	x	x					x		x		
21CR							x	x	x		
31CR	x		x				x	x	x		
106CR							x	x	x		
154CR							x	x	x		
155CR							x	x	x		
187CR	x						x	x	x	x	x

[1)] Kao: kaolinite, Hall: halloysite, 2:1: generalized 2:1 layer silicate; Sm: smectite, Chl: chlorite, Mic: mica, Verm: vermiculite, Q: quartz, Crist: cristobalite, Plag: plagioclase, Gibbs: gibbsite, Pyrox: pyroxene, Hem: hematite.

Extraction of Fe

In the consecutive extraction of Fe we have various types of behaviour:

1. Normal asymptotic behaviour.
2. An almost linear behaviour with substantial slope.
3. A much higher yield in the second extraction, followed by asymptotic behaviour.

In addition, there is a difference with respect to relative yields of sequential oxalate and single dithionite extractions. The reducing action of the dithionite-citrate reagent in addition to its complexing properties is supposed to extract iron more effectively from poorly-ordered ironoxides than the acid oxalate reagent does. In most of the samples, the sequential extractions show an asymptotic behaviour towards the Fe_d values. Especially in the samples of EUR06 (Azores) and in sample Tenerife 4, the second extraction is far more effective than the first. An increase in yield in the second extraction with respect to the first suggests that part of the Fe-compounds was protected by allophane, after the removal of which it becomes more accessible. In samples 1046 (Iceland) and especially 446 (Azores) the cumulative oxalate values fall far short of the Fe_d values, while in all Italian samples and in Tenerife 5 and 7, the cumulative oxalate values exceed Fe_d. The Costa Rican samples all had cumulative Fe_o values exceeding Fe_d by far, while the extraction curve was either linear or asymptotic. Unlike allophane, Fe compounds frequently occur as separate concretions and consecutive extractions would be expected to gradually peel off such concretions. This would explain the asymptotic behaviour towards the Fe_d content, as e.g. in sample Tenerife 4 and most samples from Azores EUR06. When the cumulative oxalate extraction exceeds the dithionite extraction, there are two possibilities. First, a single dithionite extraction may not be effective if the iron compounds are fairly crystalline, present in large units (concretions), or protected by allophane coatings. Table 3 indicates that many samples contain crystalline hematite. Also magnetite is a likely source, but although its presence was readily demonstrated in most residues, XRD confirmed the presence of magnetite in samples Azores 446 and Tenerife 2 alone. The problem may be that amounts smaller than about 5% will not be detected by this method.

An interesting discussion about the development of surface charge with age and the role of mineral-organic interactions including poorly crystalline (PC) phases on surface properties and on DRIFT-spectra of surface and subsurface volcanic soils, has been published recently by Chorover et al. (2004). Their conclusions that organic matter functional groups are saturated with metal hydroxides and that organic matter is not present as coatings on amorphous material, is consistent with our observations.

In this discussion, the sequential extraction curves are considered as "quasi-kinetic curves". Table 4 summarizes the kinetics of the extractions in a qualitative and quantitative way. The shape of each curve is classified using four codes, whereas for each element the yields obtained in the 6^{th} plus 7^{th} extraction are expressed as fraction of the total cumulative yield in the sequential extraction. In most samples, these fractions are equally small for Si and Al (corresponding with the normal asymptotic curve en-

coded as “a1”), and higher for Fe (with its frequent linear behaviour encoded as “a3” or “b”). Brackets in Table 4 indicate similarities in the same way as in Tables 2 and 3. Only samples Costa Rica 154/155 have equal properties and characteristics in all tables. They can be regarded as duplicates illustrating the reproducibility of the results.

Table 4. Form parameters of standardized sequential extraction curves.

Sample number	Kinetics of sequential extraction					
	Curve type[1)]			Yield fraction of 6th+7th extraction		
	Fe_o	Si_o	Al_o	Fe_o	Si_o	Al_o
Italy						
54	a3	a1	a1	0.16	0.03	0.02
57	a3	a1	a1	0.16	0.02	0.02
60	a2	a1	a1	0.05	0.03	0.02
61	a2	a1	a1	0.06	0.03	0.02
Azores						
446	a2	a3	a3	0.08	0.07	0.02
447	a3	a3	a3	0.18	0.03	0.02
450	a1	b	a1	0.02	0.12	0.01
451	a1	b	a1	0.03	0.06	0.00
455	a2	a1	1	0.06	0.00	0.00
452	a2	a1	a1	0.09	0.00	0.00
453	b	a1	a1	0.14	0.00	0.00
454	b	a1	a1	0.09	0.01	0.01
Iceland						
1046	a2	a1	a3	0.08	0.03	0.02
1049	b	b	b	0.14	0.12	0.08
1050	b	a1	a1	0.06	0.02	0.01
1054	a2	a1	a1	0.04	0.03	0.01
1056	a2	a1	a1	0.07	0.02	0.01
Tenerife						
2	a3	a1	a1	0.14	0.02	0.02
4	a3	a1	a1	0.08	0.03	0.03
5	a3	b	a3	0.16	0.16	0.13
7	a3	b	a3	0.16	0.19	0.15
8	a2	a1	a1	0.07	0.04	0.03
12	b	b	a2	0.23	0.09	0.04
14	b	b	a3	0.25	0.28	0.12
Costa Rica						
3CR	b	a1	a1	0.12	0.02	0.01
14CR	b	a1	a1	0.14	0.02	0.02
5CR	b	a1	a3	0.11	0.02	0.04
11CR	a3	a1	a1	0.22	0.00	0.00
106CR	b	a1	a1	0.07	0.01	0.01
21CR	b	a1	a1	0.08	0.00	0.00
154CR	a3	a1	a1	0.10	0.00	0.00
155CR	a3	a1	a1	0.11	0.00	0.00
187CR	b	b	a3	0.28	0.06	0.05
31CR	a1	b	b	0.02	0.10	0.03

1) Legend for the type of extraction curve;
a1: asymptotic level reached, a2: asymptotic level not reached, a3: from curved to linear, b: continuously linear.

FTIR characteristics

The FTIR spectra in the range 4000 to 400 $cm^{-1}$of KBr pellets of samples that had been pretreated with H_2O_2, and of residues after sequential oxalate extraction, are given in Figures AA to AM (on CD). The FTIR spectra of CsBr pellets in the range 650 to 100 cm^{-1} of these same materials are given in Figures BA to BP (on CD). The Y-scales (percentage transmission) of all spectra have been shifted and rescaled to enable comparison between samples and with the spectral characteristics mentioned in the Materials and methods section. Most spectra contain, in the range 1300 cm^{-1} to 1800 cm^{-1}, adsorption bands that are ascribed to varieties of an ammonium-dioxalato-aluminate complex formed upon oxalate extraction (Farmer and Mitchell, 1963). Peaks reported by these authors (3144, 1722, 1697, 1402, 820 cm^{-1}) are found in all available FTIR spectra of residues, but some of these peaks, especially 820 cm^{-1}, are also found in many of the FTIR spectra of unextracted material. In the latter case, we think that it is a typical artifact in these volcanic soils due to oxidation of organic matter by H_2O_2. In the following discussion, we will not consider these artefacts.

We used the following adsorption bands for comparing the samples: OH band around 3500 cm^{-1}, crystalline range 3450 to 3700 cm^{-1}, CH_3-peaks 2924 and 2854 cm^{-1}, polymeric silica >1000 cm^{-1}, monomeric silica <1000 cm^{-1}, Al,Fe bands in the range 400 to 800 cm^{-1}, and imogolite (OH) band at 350 cm^{-1}.

- The similarity exhibited by the extraction curves and mineralogy of Italian samples from EUR03 and EUR04, is also manifest in the FTIR spectra. As expected, removal of OM (11%C in sample 60) by H_2O_2, and of the structural-water containing amorphous phase by oxalate extractions, caused better visibility in the residue of the crystalline peaks. The effect of extraction of 10 to 14 % dry oxides on the intensity of the silica band is minimal, but the band shifts somewhat from polymeric to monomeric silica and its shape changes. The 350 cm^{-1} band, however, virtually disappears upon extraction.
- The scaled spectra of the two samples from EUR05 (Azores) are similar to those of the Italian samples, although Fe_o levels with respect to Si_o and Al_o are higher in the Azores samples. The relative intensity of the OH band before extraction is somewhat less than in the Italian samples.

  The samples from EUR06 (Azores), with higher Al/Si ratios (2.0 to 2.7) than the Italian samples, have more variation in the silica band before extraction, and a greater relative intensity of the OH band. The silica bands separate the samples into two groups: >1000 cm^{-1} for samples 450 and 454, and <1000 cm^{-1} for samples 451, 452, 453, and 455. This grouping does not coincide with that based on the intensity of the 350

cm^{-1} band, which is strong in samples 453, 454, and 455. Residues and XRD scans were not available for EUR06, so that a differential spectrum of the amorphous phase could not be obtained.

- In the Iceland samples, which have the lowest Al/Si ratios (0.9 to 1.5), the spectra for samples 1046 and 1049 (from EUR07) have a silica band >1000 cm^{-1} of a particular shape that differs from the silica bands of sample 1050 (also from EUR07) and samples 1054 and 1056 (from EUR08) which extend to <1000 cm^{-1}. Further, samples 1046 and 1049 show the most pronounced CH_2 and CH_3 peaks of all samples in this study. This points to incomplete removal of organic matter by the H_2O_2 pre-treatment. This may explain that sample 1046, which has a very high Fe_o level, has an *absence* of the 350 cm^{-1} band in the unextracted sample and *presence* of this band in the residue after extraction (OH bending vibration in organic matter). The residue of 1046 has an intense OH band, probably also due to unextracted OM in this Ah horizon. The spectra of samples 1054 and 1056 are very similar.
- The Tenerife samples 4 and 5 from EUR10 and samples 12 and 14 from EUR12 have in common that the 4000 to 400 cm^{-1} and the 650 to 100 cm^{-1} spectra show many well-defined adsorption bands and are the same before and after extraction. This would imply the presence of primary (and secondary) crystalline minerals and little extractable amorphous phase. This is consistent with the presence, both before and after extraction, of OH bands on which crystalline peaks of kaolinite/halloysite and gibbsite are superimposed. The fact that sample 4 has 39% extractable oxides would contradict this, but it is possible that the consecutive acid-oxalate extractions congruently dissolved pre-weathered primary material (Fe_o less promptly than Si_o and Al_o as the extraction curves show), instead of secondary (amorphous) minerals. There is no other spectral evidence for such a special situation than an exceptionally low transmission in the 900 to 500 cm^{-1} range and a peak at 370 cm^{-1} that occurs also in some Costa Rica samples.
- The lower Al/Si ratios (2.2 and 1.2) of the Costa Rica samples 31 and 187 (other Costa Rica samples have ratios 2.5 to 3.3) are reflected in the spectra by OH bands with superimposed bands of crystalline kaolinite/halloysite and gibbsite, both before and after extraction. Their silica bands show little change upon extraction. As discussed for the Tenerife samples this implies crystalline minerals and little amorphous minerals. For sample 187CR (23% extractable oxides) the spectral change upon extraction is stronger than for 31CR (8% extractable oxides). Yet, the changes are too small to speak of a similar inconsistency as found in the

case of the Tenerife sample 4. For 31CR there is a peak at 360 cm^{-1}, and for 187CR at 350 cm^{-1}, both before *and* after extraction.

The samples 3CR, 5 CR, and 14 CR, that have similar extraction behaviour, also show crystalline features in the spectra, but in contrast to the preceding samples, they show clear and similar changes in the shape of the silica band upon removal of about 31% extractable oxides. Because the amount of extracted material is large, the crystalline peaks are virtually suppressed in the difference spectrum (Figure 5) and the absorption pattern of the extracted amorphous phase is revealed. The difference spectrum is of the protoimogolite type with a silica peak at 961–964 cm^{-1}. In the spectrum of the unextracted sample this peak is only seen as a shoulder. The double silica peak seen in the residues after extraction is of the halloysite type (1102 and 1035 cm^{-1}). Instead of a peak at 350 cm^{-1} that disappears upon extraction, this series shows a peak at 370 cm^{-1}, before *and* after extraction.

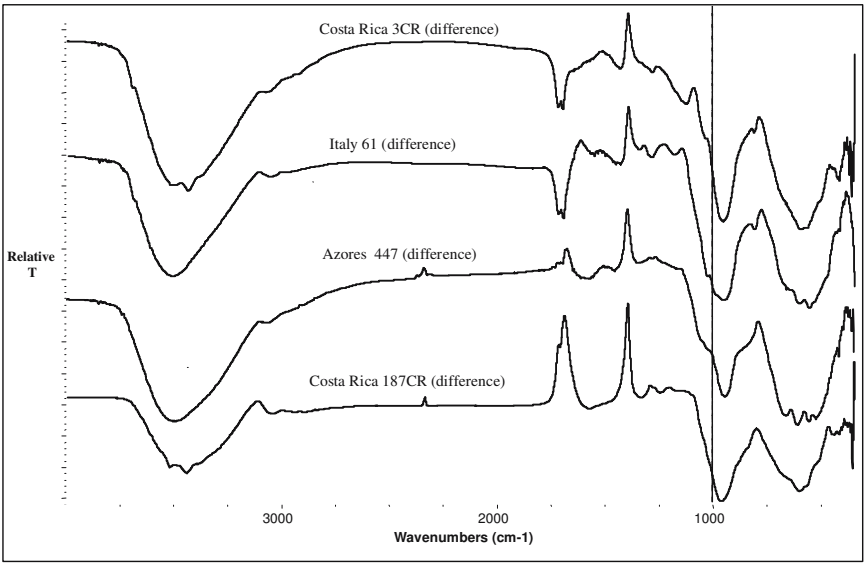

Figure 5. Difference FTIR spectra of four samples.

In samples 11CR and 154CR, the silica band of proto-imogolite at <1000 cm^{-1} is clearly developed and crystalline peaks are not visible in the original sample (the only residue available is of 11CR which shows OH-peaks of gibbsite and kaolinite/halloysite, and the double silica peak of halloysite). Although less pronounced, this development of the proto-imogolite peak is also observed in 21CR and 106CR. Samples 11CR,

21CR, 106CR, and 154CR have a common band at 350 cm^{-1} that disappears upon extraction.

The characteristics of the FTIR spectra have been summarized semi-quantitatively in Table 5. The second and third columns of Table 5 refer to the presence and intensity of bands caused by the crystalline minerals gibbsite (3527 and 3458 cm^{-1}) and kaolinite/halloysite (3696 and 3622 cm^{-1}) before and after the sequential oxalate extraction. The fourth column indicates the presence and intensity of the silica-peak at 965 cm^{-1} of proto-imogolite in the unextracted material (Figure 1A). The fifth column indicates the importance of the same peak in the spectrum of the extracted material. This information is obtained by scaling the spectrum of the residue (if available) and subtracting it from the spectrum of unextracted material. It is clear that a reliable differential spectrum, as shown in Figure 5, can only be obtained if there is a high amount of extractable oxides (see Table 2). The sixth and seventh column refer to the oxalate-related artifacts. The last four columns of Table 5 give details of the absorption bands at 350 and 370 cm^{-1}.

Samples that have been dried insufficiently show a peak of adsorbed water at about 1635 or 1653 cm^{-1} and Ah-horizons frequently show organic matter (CH_2-CH_3) peaks at 2924 and 2854 cm^{-1} due to incomplete organic matter removal, but these characteristics have not been listed.

Proto-imogolite is the allophane-type having Al/Si=2 that has an FTIR spectrum similar to that of imogolite (Figure A on CD). The typical difference between proto-imogolite and imogolite is that in imogolite, the 965 cm^{-1} silica peak is split into a doublet 992–946 cm^{-1} and there is a slight tendency of splitting of the 573 cm^{-1} alumina band into 592–562 cm^{-1}. In earlier publications, an adsorption band at 350 cm^{-1} was used to indicate the presence of imogolite. In our FTIR spectra there is no correlation between the presence (or disappearance upon extraction) of a silica signal at about 965 cm^{-1} and the occurrence of a 350 cm^{-1} signal, as Table 5 shows. The samples 11CR, 21CR, 154CR, and 155CR having the highest levels of extractable oxides (47% to 62%) clearly show both signals, but in none of the Tables 1 to 5 they show unique characteristics. The presence of crystalline peaks of kaolinite/halloysite and gibbsite seems to have some relation with the 370 cm^{-1} peak. In samples 3CR, 5CR, 14CR, and 187CR (with extractable oxide levels of 23% to 32%), these crystalline minerals mask the 965 cm^{-1} band so that it becomes visible in the differential spectrum only. Figure 5 contains some examples of difference spectra that clearly show the 965 cm^{-1} peak of the extractable phase, which is not observed in the original spectrum. It is seen that the crystalline peaks in the spectra of 3CR and 187CR (see second and third column of Table 5) almost com-

pletely vanish in the difference spectrum. But obscuration of the 965 cm^{-1} peak was also found in samples 61 (Italy) and 447 (Azores) that do not show crystalline peaks.

Table 5. FTIR characteristics and form parameters of samples.

Sample number	FTIR-spectrum[1] 4000-400 cm^{-1}						FTIR-spectrum[1] 650-100 cm^{-1}			
	Crystalline peaks[2]		Monom. silica peak 965 cm^{-1}		Peaks of artifacts		Peak 350 cm^{-1}		Peak 370 cm^{-1}	
	Before extr.	After extr.	Before extr.	In differ. spectrum	820 cm^{-1} before extr.	Al-precip. after seq. extraction	Before extr.	After extr.	Before extr.	After extr.
Italy										
54	-	-	-	-	-	+	++	-	-	-
57	-	-	-	-	-	+	+++	-	-	-
60	+	+	-	-	-	++	+++	+	-	-
61	+	+	-	++	+	++	+++	-	-	-
Azores										
446	-	-	-	-	+	++	+	-	-	-
447	-	-	-	++	-	++	++	-	-	-
450	-	n.d.	-	n.d.	++	n.d.	-	n.d.	-	n.d.
451	-	n.d.	++++	n.d.	++	n.d.	+	n.d.	-	n.d.
455	-	n.d.	++++	n.d.	++	n.d.	++	n.d.	-	n.d.
452	-	n.d.	++++	n.d.	++	n.d.	-	n.d.	-	n.d.
453	-	n.d.	++++	n.d.	++	n.d.	++	n.d.	-	n.d.
454	-	n.d.	-	n.d.	-	n.d.	+	n.d.	-	n.d.
Iceland										
1046	-	-	-	-	+	+++	-	++	-	-
1049	-	-	-	-	-	++++	++	-	-	-
1050	-	-	+	+++	-	+++	n.d.	-	-	-
1054	-	-	+	++	-	++	++	-	-	-
1056	-	-	+	++	-	+	+	-	-	-
Tenerife										
2	n.d.	+++	n.d.	n.d.	n.d.	+++	+	-	-	+
4	+++	+++	-	+	-	+	-	-	+++	+++
5	+++	+++	-	-	-	++	+++	+++	-	-
7	+	-	-	-	+	+	+	-	-	-
8	-	-	-	-	-	+	++	-	-	-
12	+++	+++	-	-	+	+++	+++	++	+	++
14	+++	+++	-	-	+	+++	+++	++	-	+
Costa Rica										
3CR	+++	+++	-	+++	+	+++	+	-	+	+++
14CR	+++	+++	-	+++	+	+++	+	-	+++	+++
5CR	+++	+++	-	+++	+	+++	-	-	+++	+++
106CR	-	n.d.	+++	n.d.	-	n.d.	++	-	-	-
11CR	-	+++	+++	+++	+	+++	+++	+	-	++
21CR	-	n.d.	++++	n.d.	-	n.d.	+++	-	-	-
154CR	-	n.d.	++++	n.d.	-	n.d.	++++	-	-	-
155CR	n.d.	n.d.	n.d.	n.d.	n.d.	n.d.	++++	n.d.	-	n.d.
187CR	++	+++	-	+++	++	+++	++	++	+	+
31CR	++	++	-	-	+++	+	-	-	++	++

1) Legend for the FRIR spectrum: n.d. Spectrum not determined; - Peak(s) not or hardly visible; + Peak(s) visible; ++ Peak(s) clearly visible; +++ Substantial peak(s); ++++ Important peak(s).
2) Peaks of gibbsite and kaolinite/halloysite in the range 3450 to 3700 cm^{-1}.

Conclusions

The study of 34 volcanic soil samples from various locations in Europe and from Costa Rica by consecutive acid-oxalate extractions, FTIR, and XRD showed a great variation, for example in amounts of extractable oxides (of elements Si, Al, and Fe), in the shapes of "quasi-kinetic" extraction curves of Si, Al, and Fe, in pyrophosphate-extractable elements Al and Fe per unit of organic carbon, in FTIR spectra (especially silica bands at >1000 cm^{-1} or <1000 cm^{-1}), in the difference between acid-oxalate extractable Fe_o and dithionite extractable Fe_d, and in the corrected ratios between Si_o, Al_o, and Fe_o.

Expected general relations between these properties and characteristics that could help in resolving different types of amorphous phases were not found. This is not due to experimental uncertainty because we found many similarities and trends between samples from the same profile.

Conclusions that can be drawn from the results, are:

1. The ternary plot of the tracks of cumulative Si_o,Al_o,Fe_o-ratios upon sequential extraction (Figure 3) shows that in most samples Fe_o is less promptly extracted than Si_o and Al_o. Therefore the track will continue into the direction of the Fe-corner since the ratio Al_o/Si_o is rather constant.
2. Shifts of the tracks in the ternary plot as a result of Al_p,Fe_p-corrections do not improve the tracks but, on the contrary, may induce anomalies. This makes the assumption that pyrophosphate only extracts organically-bound Al and Fe doubtful for these volcanic soil samples.
3. The majority of samples has a FTIR spectrum showing the 965 cm^{-1} peak of proto-imogolite. In 7 of the 34 samples this peak is masked and is only visible in the difference spectrum that is constructed by subtracting the FTIR spectrum of the residue obtained after extraction from the FTIR spectrum before extraction.
4. All FTIR spectra of residues show peaks of artificial Al-oxalate or Ca-oxalate complexes.
5. The 350 cm^{-1} imogolite band is present in more samples than the 965 cm^{-1} band of proto-imogolite. Three samples (belonging to the group that show crystalline minerals) have a 370 cm^{-1} band instead of the 350 cm^{-1} band.

Acknowledgements

Initial FTIR spectra for reconnaissance were obtained by the second author in the laboratory of Prof. Dr. A. Piccolo of the University Federico II in Naples, Italy. Spectra on CsBr pellets were measured in the Vening Meinesz laboratory of the Utrecht University by courtesy of Prof. Dr. A. Maas. We thank these colleagues for their kind cooperation.

Mrs. N. Nakken of the Laboratory of Soil Science and Geology, Wageningen University, The Netherlands, is thanked for performing the sequential extraction experiments.

References

Blakemore LC, Searle PL, Daly BK (1987). Methods for chemical analysis of soils. N.Z. Soil Bureau Scientific Report 80. Lower Hutt

Buurman P, van Lagen B, Velthorst EJ (1996). Manual for soil and water analysis. Backhuys Publishers, Leiden, 1–314

Buurman P, de Boer K, Pape Th (1997). Laser diffraction grain-size characteristics of Andisols in perhumid Costa Rica: the aggregate size of allophane. Geoderma 78:71–91

Buurman P, García Rodeja E, Martínez Cortizas A,van Doesburg JDJ (2004). Stratification of parent material in European volcanic and related soils studied by laser-diffraction grain-sizing and chemical analysis. Catena 56:127–144

Childs CW, Parfitt RL, Newman RH (1990). Structural studies of silica springs allophane. Clay Minerals 25:329–341

Chorover J, Amistadi MK, Chadwick OA (2004). Surface charge evolution of mineral-organic complexes during pedogenesis in Hawaiian basalt. Geochimica et Cosmochimica Acta 68:4859–4876

Denaix L (1993). Synthèse et propriétés d'aluminosilicates non lamellaires: l'imogolite et les allophanes. Dissertation, University PARIS VI

De Roy G, Verhaert I, Vansant EF (1980). Allophane and halloysite minerals. Structural considerations. Travaux Chimiques de Pays-Bas 100:102–106

Farmer VC (1997). Conversion of ferruginous allophanes to ferruginous beidellites at 95ºC under alkaline conditions with alternating oxidation and reduction. Clays and Clay Minerals 45:591–597

Farmer VC, Mitchell BD (1963). Occurrence of oxalates in soil clays following hydrogen peroxide treatment. Soil Science 96:221–229

Farmer VC, Fraser AR, Tait JM (1979). Characterization of the chemical structures of natural and synthetic aluminosilicate gels and soils by infrared spectroscopy. Geochimica et Cosmochimica Acta 43:1417–1420

Farmer VC, McHardy WJ, Robertson L, Walker A, Wilson MJ (1985). Micromorphology and sub-microscopy of allophane and imogolite in a podzol Bs

horizon: evidence for translocation and origin. Journal of Soil Science 36:87–95

He H, Barr TL, Klinowski J (1995). ESCA and solid-state NMR studies of allophane. Clay Minerals 30:201–209

He M, Horikawa Y (1998). Effect of particle size of halloysite on the deflocculation of mutual flocs of allophane and halloysite at pH 6.5 in dilute xanthan polysaccharide solutions. Soil Science and Plant Nutrition 44:551–558

He M, Horikawa Y (2000). Partial deflocculation of mutual flocs of allophane and halloysite by xanthan and chitosan and relevance to particle arrangement in the flocs. Soil Science and Plant Nutrition 46:81–87

Henmi T (1980). Effect of SiO_2/Al_2O_3 ratio on the thermal reactions of allophane. Clays and Clay Minerals 28:92–96

Jambor JL, Dutrizac JE (1998). Occurrence and constitution of natural and synthetic ferrihydrite, a widespread iron oxyhydroxide. Chemical Review 98:2549–2585

Jeanroy E, Guillet B (1981). The occurrence of suspended ferruginous particles in pyrophosphate extracts of some soil horizons. Geoderma 26:95–105

Kawano M, Tomita K, Shinohara Y (1997). Analytical electron microscopic study of the noncrystalline products formed at early weathering stages of volcanic glass. Clays and Clay Minerals 45:440–447

McKeague JA, Day JH (1966). Dithionite- and oxalate-extractable Fe and Al as acids in differentiating various classes of soils. Canadian Journal of Soil Science 46:13–22

MacKenzie KJD, Cardile CM (1988). The structure and thermal reactions of natural iron-containing allophanes studied by 57-Fe Mössbauer spectroscopy. Thermochimica Acta 130:259–267

McKeague JA, Schuppli PA (1982). Changes in concentration of iron and aluminium in pyrophosphate extracts of soil and composition of sediment resulting from ultracentrifugation in relation to spodic horizon characteristics. Soil Science 134:265–270

McKenzie KJD, Bowden ME, Brown IWM, Meinhold RH (1989). Structure and thermal transformations of imogolite studied by ^{29}Si and ^{27}Al high-resolution solid-state nuclear magnetic resonance. Clays and Clay Minerals 37:317–324

Meijer EL, Buurman P (2003). Chemical trends in a perhumid soil catena on the Turrialba volcano (Costa Rica). Geoderma 117:185–201

Mizota C, van Reeuwijk LP (1989). Clay mineralogy and chemistry of soils formed in volcanic material in diverse climatic regions. Soil Monograph 2, International Soil Reference and Information Center, Wageningen, The Netherlands, p 186

Murad E, Schwertmann U (1988). The characterization of poorly crystalline Si-containing natural iron oxides by Mössbauer spectroscopy. Hyperfine Interactions 41:835–838

Parfitt RL, Furkert RJ (1980). Identification and structure of two types of allophane from volcanic ash soils and tephra. Clays and Clay Minerals 28:328–344

Shimizu H, Watanabe T, Henmi T, Masuda A, Saito H (1988). Studies on allophane and imogolite by high-resolution solid-state ^{29}Si- and ^{27}Al-NMR and ESR. Geochemical Journal 22:23–31

Strohmeyer F, Hausmann JFL (1816). Göttingische Gelehrte Anzeigen 2 (126):1249–1253

Takeda M, Matuso M, Tominaga T (1979). Fe-57 Mössbauer study on the structure of an amorphous mineral: synthetic allophane. Radiochemistry and Radioanalytical Letters 41:1–10

Thorlacius A (2001). Robustness of the acid ammonium oxalate extraction for soils with very high levels of extractable aluminium and iron. International Workshop Volcanic Soils: Properties, Processes and Land Use. Ponta Delgada, Azores, Portugal. Abstracts, p 51

USDA (1996). Soil Survey Laboratory Methods Manual. Soil Survey Investigations report No. 42, United States Department of Agriculture, Washington, p 693

Violante P, Tait JM (1979). Identification of imogolite in some volcanic soils from Italy. Clay Minerals 14:155–158

Violante A, Colombo C, Cinquegrani G, Adamo P, Violante P (1998). Nature of mixed iron and aluminium gels as affected by Fe/Al molar ratio, pH and citrate. Clay Minerals 33:511–519

Appendix materials on CD-Rom

Table A. Results of consecutive extractions of samples by acid oxalate (perc. of extracted element uncorrected for Fe(p) or Al(p) and recalculated to g/100g 105C-dried sample) and results of dithionite-extracted Fe

Figure A. FTIR spectra of reference minerals

Figure B. EUR03 and 04 – sequential Si extractions

Figure C. EUR03 and 04 – sequential Al extractions

Figure D. EUR03 and 04 – sequential Fe extractions

Figure E. EUR03 and 04 – cumulative $(Al_o\text{-}Al_p)/Si_o$ ratios

Figure F. EUR05 and 06 – sequential Si extractions

Figure G. EUR05 and 06 – sequential Al extractions

Figure H. EUR05 and 06 – sequential Fe extractions

Figure I. EUR05 and 06 – cumulative $(Al_o\text{-}Al_p)/Si_o$ ratios

Figure J. EUR07 and 08 – sequential Si extractions

Figure K. EUR07 and 08 – sequential Al extractions

Figure L. EUR07 and 08 – sequential Fe extractions

Figure M. EUR07 and 08 – cumulative $(Al_o\text{-}Al_p)/Si_o$ ratios

Figure N. EUR10–12 – sequential Si extractions

Figure O. EUR10–12 – sequential Al extractions

Figure P. EUR10–12 – sequential Fe extractions

Figure Q. EUR10–12 – cumulative $(Al_o\text{-}Al_p)/Si_o$ ratios

Figure R. Costa Rica – sequential Si extractions

Figure S. Costa Rica – sequential Al extractions
Figure T. Costa Rica – sequential Fe extractions
Figure U. Costa Rica – cumulative $(Al_o\text{-}Al_p)/Si_o$ ratios

Crystalline clay constituents of soils from European volcanic systems

F. Monteiro, M. Kleber, M. Fonseca, M. Madeira and R. Jahn

Introduction

Soils developed from young volcanic ash are often characterized by the preferential formation of non-crystalline constituents (short-range order minerals) and by the accumulation of organic matter. These non-crystalline materials, together with Al- and Fe-humus complexes, frequently represent a significant part of their colloidal fraction (Shoji and Ono 1978), and determine to a great extent the unique physical and chemical properties and behaviour of *Andosols* (FAO 2001). Moreover, depending on climate, vegetation cover characteristics, nature of parent material and time of exposure to weathering, a more or less important assemblage of crystalline phases is usually present. The heterogeneity of this mineralogical assemblage is quite large, comprising both 1:1 (hydrated and non-hydrated) and 2:1 layer silicates, as well as Fe- and Al-oxyhydroxides and primary minerals. Though varying in amounts, these materials can play an important role in soil functioning and are also of great importance in understanding soil genesis.

Methods

The crystalline constituents of the clay fraction (<2 μm) of selected soil samples (of the COST 622 reference soils) were assessed by means of X-Ray Diffraction (XRD) on oriented aggregates. Thirty-five samples of 13 pedons selected from representative volcanic areas of Italy, Portugal (Azores), Iceland, Spain (Tenerife), Greece, France and Hungary were used.

Sample preparation included oxidation of organic matter by hydrogen peroxide, removal of short-range order components by acid oxalate extraction (Blakemore et al. 1987), and treatment with dithionite-citrate-bicarbonate – DCB (Mehra and Jackson 1960) when necessary. Samples were Mg and K saturated with $MgCl_2$ and KCl, washed free of chlorides and then scanned, after air drying, ethylene glycol solvation and heating to

550ºC (sometimes also to 100ºC). XRD scans were performed using Cu-kα radiation (40KV, 30 mA) and 0,04 º2θ step size, 5 or 6 seconds scanning time/step.

For phase identification, overlapping peaks were separated by modelling the non smoothed diffraction line using a Pearson VII profile shape function included in the public domain software package MacDiff v. 4.2.5 (Petschick 2001). Mineral identification was performed by comparing measured *d* values with those tabulated in JCPDS files (JCPDS-ICDD 1996), following usual procedures as those indicated by Moore and Reynolds (1997), Barnhisel and Bertsch (1989) and Sawhney (1989). Quartz was used as an internal standard for angle correction.

Results

A detailed description of the mineralogical composition of the treated clay fraction (<2 μm) of selected horizons from the above mentioned pedons is presented in this section, and summarized in Table 1. Only a few illustrative XRD diagrams are shown in this paper, the remaining being included in the CD accompanying this book.

Italy

Pedon EUR01; Humi-Tephric Regosol (Eutric)

Main layer silicate minerals present in this pedon are an illite type mineral and kaolinite. These phases occur in very small amounts in both Ap and Bw2 horizons, diffraction lines being more perfect in the latter. Vermiculite and hematite appear almost in negligible amounts. Traces of halloysite are also present, especially in the Bw2 horizon (see Figure A in the CD).

Primary minerals account for an important part of the <2 μm separates: K-feldspars (sanidine), leucite, analcime and quartz; some XRD lines also suggest the presence of phillipsite.

Pedon EUR04; Melani-Silandic Andosol (Dystric)

The main secondary phyllosilicates are kaolinite and an illite type mineral, both much better expressed in the 2Bw1 than in the Ah2 horizon (Figure 1 and Figure B, in the CD).

Table 1. Crystalline constituents in the clay fraction of COST 622 pedons.

Pedon	Horizon	Relative importance			
		Main	Medium	Minor	Negligible
EUR01	Ap	Fd, Q	M, K, An	-	V, Hm, L, Ph
	Bw2	Fd, Q	M, K, An	-	V, Hm, L, Ph, Ha
EUR04	Ah2	K	Q, Fd	M, V, Hm, An	Ha
	2Bw1	M, K	Q, Fd	Cl, Hm, An	Ha, mHa
EUR05	Ah	V-Al	K,Fd	Q	Hm, M
	2Ahb	V-Al	K,Q, Fd	Hm	M
	2Bwb	V-Al	K	Cl, Cl/V, Hm, Q, Fd	M
EUR06	Ah	Mgt, Q	K	V, Fd, Hm	M, Go
	AB1	Mgt, K	V, Hm	Q, Fd	M, Go
	2Bw1	Mgt	Hm	K, V, Q, Fd	M, Go
EUR07	AC	-	-	-	Fd,
	3CB	-	-	-	Fd, V
	4Bw	-	-	-	Fd, V, Q
EUR08	Ah2	-	-	Q	Fd, V
	Bw1	-	-	Q	Fd, V
	2Bw2	-	-	-	Fd, V
	3Bw3/4C	-	-	-	Fd, V
EUR11	C	Q, Fd	-	K	M, V
	2Bwb	Q, Fd	-	K	V
EUR12	Ah2	K	Q, Fd	-	V/M, M
	Bw	K	Fd	M, V, Q	-
EUR14	Ah	V, K	M	Cl, S, Q	-
	2AC	V	K	M, Q, S, Cl	-
EUR17	Ah2	V	-	K, S, Q, Fd	M,
	Bw1	V	S, K	Q, Fd	Hm, Go
	2Bw2	Sm	V, K	Q, Fd, Hm	M,Go
EUR18	Ah1	M (70–80%)	S (~20%)	K, Q (<5%)	Cl, Fd
	Ah2	M (70–80%)	S (~20%)	K (<5%)	Cl, Fd
	AC	M (80–90%)	S (~10%)	Q (<5%)	K, Fd
EUR19	Ah1	M (70–80%)	Cl, K (5–10%)	Q, Fd (~5%)	S
	Ah2	M (70–80%)	Cl, K (5–10%)	Q, Fd (~5%)	S
	AR	M (70–80%)	K (5–10%)	Cl, S, Q, Fd (~5%)	-
EUR20	Ah1	M (>90%)	-	K (~5%)	Q, Fd
	Ah2	M (~90%)	-	K, Q (~5%)	Fd
	Bw/R	M (~90%)	-	K, Q (~5%)	S, V-Al, Fd

An: analcime; Cl: chlorite; Cl/V: interstratified chlorite/vermiculite; Fd: feldspars; Go: goethite; Ha: halloysite; Hm: hematite; K: kaolinite; L: leucite; M: mica/illite; Mgt: magnetite; mHa: metahalloysite; Ph: phillipsite; Q: quartz; S: smectite; V: vermiculite V-Al: hydroxy-Al interlayered vermiculite; V/M: interstratified vermiculite/mica.

Non-expandable 1.4 nm minerals appear in both horizons in minor amounts, and halloysite seems also to be present either in a hydrated form (1.04 nm), or as meta-halloysite (0.75 nm), especially in the 2Bw1 horizon. The 1.4 nm phases are likely to be vermiculite in the upper horizon, but in the 2Bw1 their diffraction patterns resemble those of chlorite, as the 1.4 nm reflection line persists after heating to 550ºC (Figure 1).

Hematite is also present in the clay fraction of those horizons. It should have, at least in part, a lithogenic origin, as it was not destroyed by the DCB treatment.

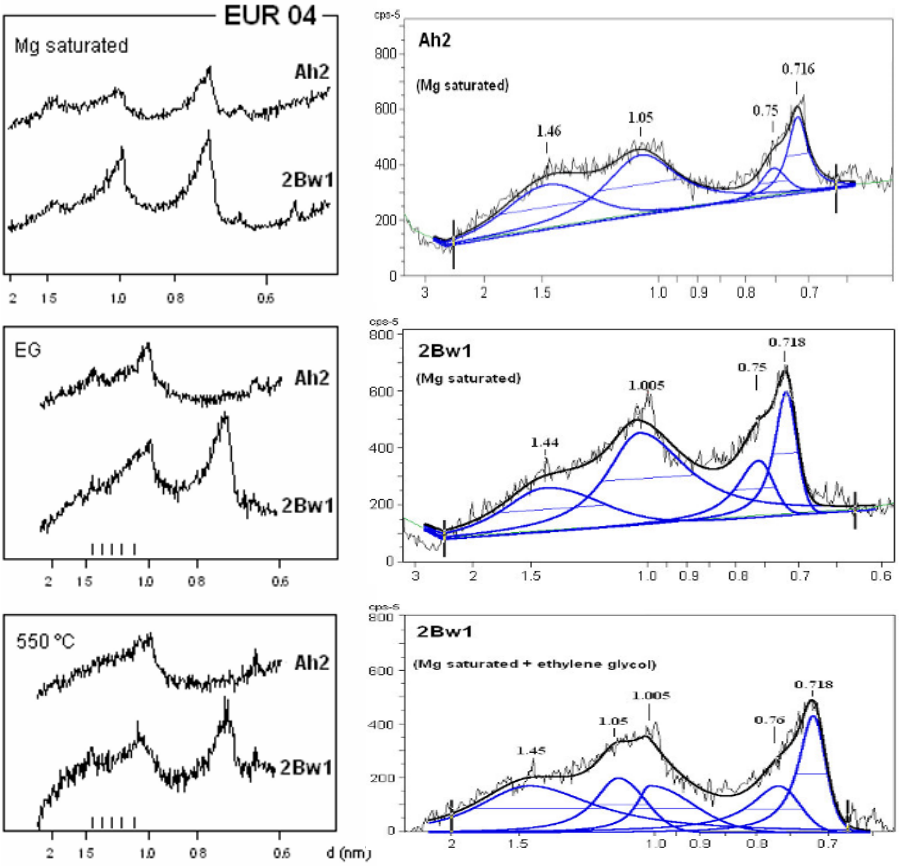

Figure 1. XRD patterns of Mg saturated, ethylene glycol-solvated (EG), and 550ºC heated clay (<2 µm) from pedon EUR04 (on the left, top to bottom); on the right part, by the same order, fitted profiles of Mg saturated Ah2 and 2Bw1, clay and of 2Bw1 glycollated clay.

Primary minerals, namely quartz, sanidine, and analcime, also occur in the clay fraction of this pedon, but in lower amounts than in EUR01. Hence, higher K contents of the exchange complex of the latter (see Madeira et al. this book) should be related with the presence of these K-bearing minerals.

Azores

Pedon EUR05; Acroxi-Silandic Andosol (Hyperdystric)

Non-expandable 1.4 nm minerals and kaolinite dominate the secondary crystalline fraction in all the studied horizons (Ah, 2Ahb and 2Bwb) of this pedon. They appear in very small amounts that increase from top to bottom. Traces of a 1.0 nm mineral (Figure 2 and Figure C, in the CD) are observed.

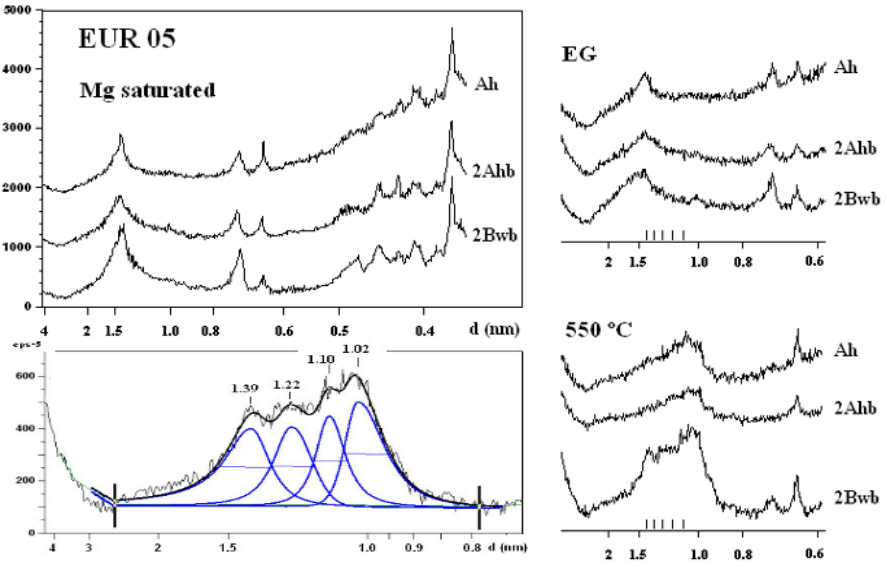

Figure 2. XRD patterns of Mg saturated, ethylene glycol-solvated (EG), and 550ºC heated clay from pedon EUR05; fitted scan corresponds to 2Bwb 550ºC heated clay.

The 1.4 nm minerals shows some differences between the three horizons: in the Ah and 2Ahb, the 550ºC collapsed lines show some opening towards the lower diffraction angles, suggesting some hydroxy-Al interlayering of a vermiculitic phase. In the 2Bwb horizon part of such 1.4 nm

minerals exhibit limited expandability (expandable vermiculite), but some chlorite and irregular interstratified chlorite/vermiculite phases are likely to occur too, given that the 0.7 nm reflection line persists after heating to 550ºC, although evidencing a clear attenuation (Figure 2).

Presence of hematite was observed, especially in the deeper horizon. As its reflection lines, yet less intense, remained visible after DCB treatment, it is most probably of lithogenic origin,

Quartz and a Ca-plagioclase were also identified in the clay separates of all the studied horizons.

Pedon EUR06; Hydri-Silandic Andosol (Umbric and Acroxic)

Clay minerals (a vermiculite-like phase and kaolinite) occur in very low amounts in this pedon. They show a slight increase from the Ah horizon to the AB1, decreasing again towards 2Bw1 horizon. Traces of a 1.0 nm mineral are also observed.

Iron oxides (mainly hematite) appear in quite important proportions throughout the profile, especially in the deeper horizons, in which they markedly mask phyllosilicate XRD peaks (see Figure D, in the CD). Hematite diffraction lines can be seen even after DCB treatment, namely in 2Bw1 horizon, but to a lesser extent also in the AB1, suggesting a lithogenic origin. Magnetite occurs in large proportion in the clay fraction of the 2Bw1 horizon.

All the samples contain quartz and Ca-plagioclases.

From the huge bulges observed in the range 0.6–0.3 nm in the diffractograms, it can be inferred that amorphous material (probably volcanic glass), constitutes a significant proportion of the clay fraction, its amounts decreasing from top to bottom (see CD, Figure D).

Iceland

Pedons EUR07 and EUR08; Orthidystri-Vitric Andosol and Dystri-Vitric Andosol

Practically no reflections of phyllosilicate minerals are visible in XRD diagrams of the <2 μm fraction of the profiles from Iceland. Only traces of a 1.4 nm phase were detected in the 4Bw3 horizon of Pedon EUR07, and in the Ah2 horizon from EUR08.

Samples from both pedons show broad bulges in the range 0.65–0.35 nm, suggesting the presence of significant amounts of glass.

Tenerife

Pedons EUR11 and EUR12; Skeleti-Vitric Andosol (Orthieutric) and Umbri-Vitric Andosol (Pachic and Hyperdystric)

The main crystalline phases present in the very limited clay fraction of Pedon EUR11 are primary minerals (quartz and a Ca-plagioclase). Kaolinite occurs in very low amounts, that are slightly higher in the topsoil. Traces of a 1.4 nm mineral (probably vermiculite) and of a mica-like mineral were also found in this pedon.

The clay fraction of Pedon EUR12 is dominated by kaolinite, that is accompanied by a mica-like mineral, a non-expandable 1.4 nm phase, a 1.4/1.0 nm mixed-layer mineral, quartz and plagioclases. The above mentioned layer silicates occur in higher amounts in the Bw than in Ah horizons (Figure 3 and Figure E, in the CD).

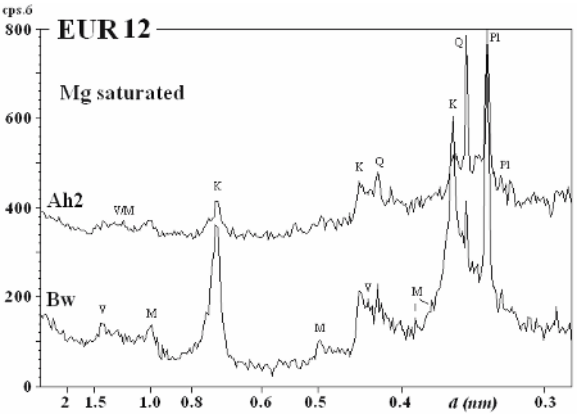

Figure 3. General diffraction patterns of Mg saturated, air dried clay from Ah2 and Bw horizons of pedon EUR12.
V: vermiculite;
V/M: vermiculite/mica interlayer;
M: mica; K: kaolinite;
Q: quartz; Pl: plagioclases.

Greece

Pedon EUR14; Skeleti-Tephric Regosol (Hyposodic)

A complex mixture of expandable and non-expandable 1.4 minerals prevails in the top horizon (Ah), and is accompanied by important amounts of kaolinite, a trioctahedral mica, and by irregularly interstratified 1.4/1.0 phases. Diffraction patterns for 1.4 nm minerals, similar to those observed in the Ah horizon were also found in 2AC horizon, though this one is slightly richer in expandable minerals. Conversely, kaolinite appeared in the 2AC layer in much lower amount. An important decrease in the amount of the 1.0 nm mineral was also found in this layer, pointing to its allochthonous origin (Figure 4).

Expandable 1.4 nm minerals seems to be mainly of a vermiculitic type, as their expansion following ethylene glycol solvation is limited to about 1.54–1.6 nm, only a minor part shifting to the higher *d* values typical of smectitic phases. After heating to 550ºC a set of ill defined peaks are formed at *d* values around 1.4, 1.2 and 1.1 nm , besides a strong 1.0 nm line (Figure 4). As the exchange complex of these hypereutric soil is saturated with basic cations (see Madeira et al. in this book), no hydroxyl-Al interlayering of such minerals is to be hypothesized; therefore, non-expandable, non collapsible phases should be chlorite, that should also participate in the above mentioned mixed-layer minerals.

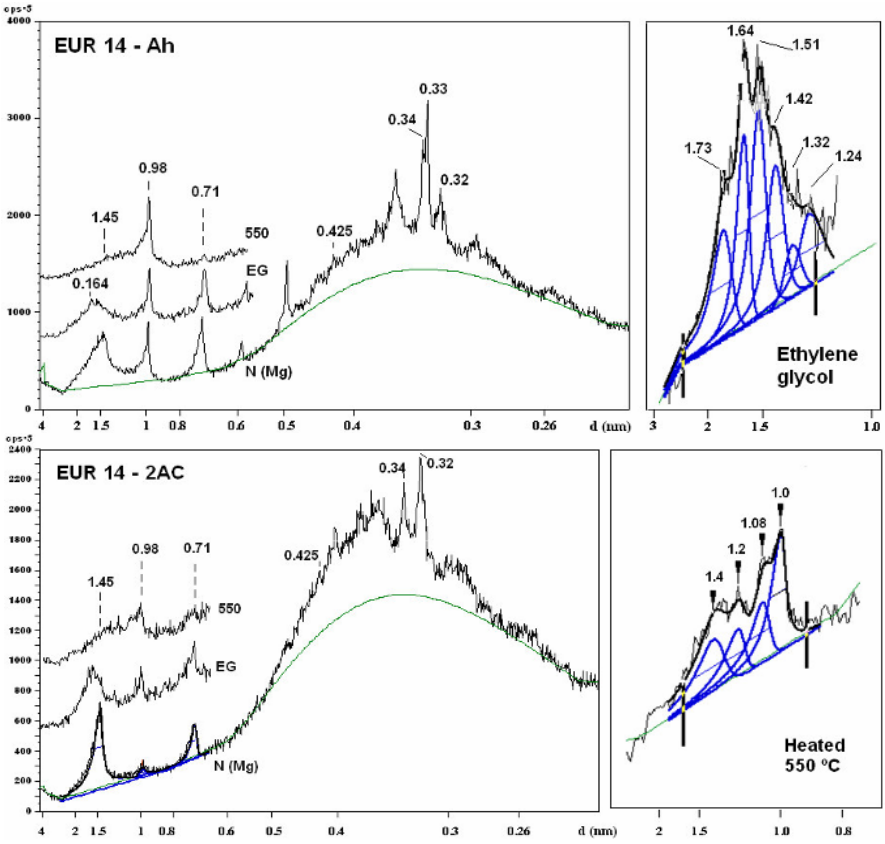

Figure 4. XRD lines of Mg saturated [N(Mg)], ethylene glycol-solvated (EG) and 550ºC heated (550) clay from Ah and 2AC horizons of pedon EUR14; fitted profiles correspond to ethylene glycol-solvated clay from Ah horizon, and to 550ºC heated clay from AC layer.

Broad bulges in the range 0.5–0.23 nm persisting even after DCB cleaning of samples, are clearly visible in the diagrams (Figure 4), pointing to the occurrence of important amounts of amorphous material, likely volcanic glass, in the clay fraction of this pedon.

Quartz appears in the clay fraction of both horizons, but its reflections are to some extent more pronounced in the surface one. Given the nature of the parent material and the weak development of this pedon, an allochthonous (wind blown) origin for this mineral should be considered.

France

Pedon EUR17; Epialuandi-Silandic Andosol (Umbric and Pachic)

The mineralogical composition of the clay fraction of Ah2, Bw1 and 2Bw2 horizons is quite uniform, as shown in XRD diagrams (see Figure 5, and Figure F in the CD).

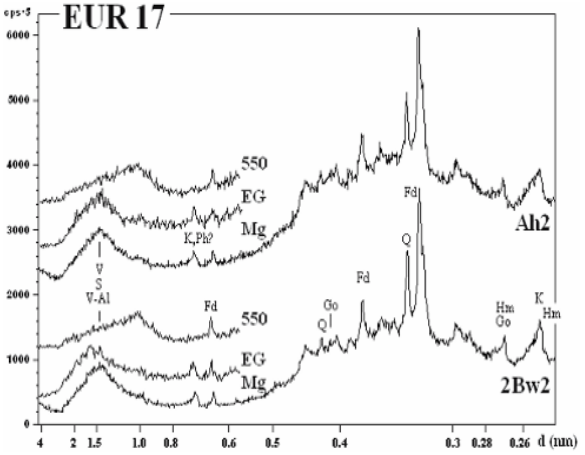

Figure 5. General diffraction patterns of Mg saturated (air dried), glycollated (EG), and heated to 550ºC clay (550) from Ah2 and 2Bw2 horizons of pedon EUR17.
V: vermiculite; S: smectite; V-Al: hydroxy-Al interlayered vermiculite (or smectite); Ph: phillipsite; K: kaolinite; Fd: feldspars; Q: quartz; Hm: hematite; Go: goethite.

A complex mixture of expandable and non-expandable 1.4 nm minerals predominates in all of them. Among such minerals there is a vermiculite-like phase, which is more abundant in the Ah2 than in deeper horizons; conversely, expandable minerals apparently dominate in the 2Bw2 horizon. These minerals seem to be hydroxy-interlayered in variable degree, as indicated by the persistence of a set of reflections between 1.4 (secondary chlorite) and 1.0 nm (smectite or vermiculite) after heating to 550ºC. Kaolinite was also found, but in lower amounts than 1.4 nm phases, as well as a micaceous mineral, whose diffraction lines are just discernible (Figure 5).

Traces of goethite were detected in this pedon, namely in the B horizons, where also traces of hematite occur (Figure 5).

The clay fraction of all the horizons contains a Ca plagioclase, quartz being present only in the Ah2 and 2Bw2 horizons.

Hungary

Phyllosilicate signals in the XRD diagrams from the Hungarian samples are much better expressed than in the other pedons partly because of the higher clay content. A semi-quantitative estimate of phyllosilicate proportions was therefore possible for several samples.

A significant addition of loess-derived mica to all the mentioned pedons may be inferred, as this mineral is by far the main constituent of the clay fraction. Diffraction lines of this mineral are generally sharper in the topsoil horizons than in deeper ones, where some broadening is apparent. Besides these 1.0 nm minerals, which represent some 70–80% in Pedons EUR18 and EUR19, and over 90% in EUR20, other mineral species were found.

Small amounts (<5%) of quartz and feldspars were found in the clay separates of all the pedons, the higher quantities occurring in EUR19 samples.

Pedon EUR18; Molli-Vitric Andosol (Pachic)

Smectite content is especially significant in this pedon, and it represents almost 20% in Ah1 and Ah2 horizons, and about 10% in the AC layer. Kaolinite, as well as chlorite are always below 5%.

Pedon EUR19; Endolepti-Anthric Umbrisol (Episkeletic)

Chlorite appears in amounts ranging from 5 to 10%, and slightly higher in Ah horizons than in AR layer. These amounts should reflect either differences in parent material or in pedogenesis. Kaolinite varies from 5 to 10%, its contents being quite uniform along the profile. Smectite accounts for some 5% in the AR layer, its proportion markedly decreasing in the Ah1 and Ah2 horizons.

Pedon EUR20; Silti-Endoleptic Phaeozem

Clay neoformation seems to be not a particular issue for Pedon EUR20, as micaceous minerals are in excess of 90% of the clay mineral assemblage,

whereas kaolinite accounts for about 5% (Figure 6 and Figure G, in the CD).

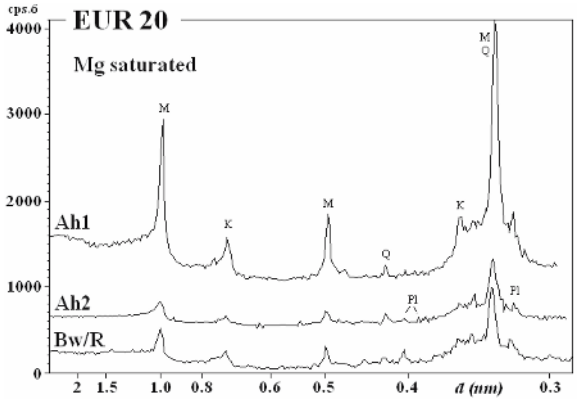

Figure 6. General diffraction patterns of Mg saturated, air dried clay from Ah2 and Bw horizons of pedon EUR20.
M: mica;
K: kaolinite;
Q: quartz;
Pl: plagioclases.

Discussion and conclusions

Soils from European volcanic systems largely differ in terms of mineralogical composition and abundance of crystalline secondary constituents in their treated clay fraction. According to the proportion of phyllosilicate minerals in that fraction, such soils can be grouped as follows:

1. EUR07, EUR08 (Iceland): crystalline secondary silicates are absent or occur in trace amounts;
2. EUR06 (Azores), and EUR11 (Canary Islands): layer silicates are weakly represented in the clay fraction, and their XRD lines are often broad and of weak intensity, pointing to an imperfect crystallinity of such constituents;
3. EUR04 (Italy), EUR05 (Azores), and EUR17 (France): layer silicates are moderately represented in the clay fraction;
4. EUR01 (Italy), EUR12 (Canary Islands), EUR14 (Greece), and EUR18, EUR19 and EUR20 (Hungary): clay minerals dominate, and poorly ordered minerals are almost absent in the clay fraction, as oxalate extracted Si and Al are very low (*physico-chemical data table*, this book).

These differences are mainly related to age and nature of the parent material and to climatic conditions, which strongly influence weathering, organic matter accumulation and horizon differentiation.

Pedons from areas with xeric/aridic soil moisture regimes are among the least developed ones, most of them being non-Andosols. The clay fraction of these pedons is always dominated by phyllosilicates, but their clay contents tend to be low, as weathering and clay formation are slowed by low moisture availability. Such is the case of EUR01 (central Italy) and EUR14 (Greece/Santorini). Also dominated by phyllosilicates are the pedons EUR18, EUR19 and EUR20 (Hungary). However, as they are clearly dominated by loessic materials, they show high clay contents and silt contents up to 68% (see the *physico-chemical data table* in this book).

An early weathering stage also characterises pedons from areas with a cryic soil temperature regime. This is the case of those from Iceland (*Vitric Andosols*), whose colloidal fraction is almost entirely composed of organic materials and allophane (see the *physico-chemical data table* in this book), phyllosilicates occurring only in trace amounts.

More developed pedons, fitting *Andosol* classification criteria, occur in udic areas of the Azores Archipelago (EUR05, EUR06) and Canary Islands (EUR12), those from northern Italy (EUR04) and French Massif Central (EUR17) showing intermediate stages of differentiation. Colloid contents of these pedons are medium to high, but secondary crystalline minerals are a small part of the colloidal fraction of almost all of them. It is known that in sub-acid to neutral conditions and in the absence of a marked influence of complexing organic compounds, short-range order constituents (allophane, imogolite) form preferentially over crystalline products (Ugolini and Dahlgren 1991), to which they tend to transform as weathering progresses. Conversely, in acidic pedo-environments, where strong accumulations of organic products compete for Al impeding allophane formation, occurrence of 2:1 layer silicate clays (often hydroxy-Al interlayered) tend to be common (Shoji and Ono 1978, Shoji et al. 1985).

Owing to the great variability of their forming factors (and possibly to the small number of analysed samples), studied pedons only reflect to some extent those trends. Nonetheless, it should be mentioned that 1) with the exception of Pedon EUR12, all of them have low (sometimes negligible) contents of layer silicate clays, whose amounts generally increase towards subsoil horizons, and 2) 2:1 hydroxy-Al interlayered minerals were also found to occur mainly in the most acidic, low allophanic, topsoil horizons (e. g., EUR05, EUR17). Pedon EUR12, from Canary Islands, constitutes a clear exception to this picture, as well for its huge amounts of clay, as for the dominance of kaolinite and high amounts of Fe_d throughout the profile. In addition to this features, short-range order minerals are also absent in this pedon (see the *physico-chemical data table*, in this book). This can point to a stage of evolution in which poorly ordered minerals have already undergone evolution to crystalline phases. Desiccation or seasonal

variations in soil solution Si concentrations have also been referred to promote such a transformation in climates with a pronounced dry season (Takahashi et al. 1993).

No definite distribution patterns of the different crystalline secondary products prevailing in the clay fraction of studied pedons can be clearly established. Both in *Andosol* and in non-*Andosol* groups, besides climate, parent material and organic matter differences, local specific factors should interfere in such a distribution. That can be the case in areas with recent or on-going volcanic activity, where periodic addition of fresh volcanic materials can cause some profile rejuvenation. Addition of wind blown clay- or silt-sized minerals as for instance reported for the Canary Islands (Jahn et al. 1992, Mizota and Matsuhisa 1995) and for the Aegean region (Nihlén and Olsson 1995) are equally current events in most of the studied areas. Both cases are prone to induce the occurrence of mineral phases otherwise not expected under the prevailing environmental conditions.

References

Barnhisel RI, Bertsch PM (1989). Chlorites and hydroxy-interlayered vermiculite and smectite. In: Dixon JB, Weed SB (eds) Minerals in Soil Environments, 2nd edn. Soil Science Society of America Book Series no 1. Soil Science Society of America, Madison. Wisconsin, pp 730–788

Blakemore LC, Searle PL, Daly BK (1987). Methods for chemical analysis of soils. New Zealand Soil Bureau. Scientific Report no 80. New Zealand Society of Soil Science, Lower Hutt, New Zealand

FAO (2001). Lecture notes on the major soils of the world. Driessen P, Deckers J, Spaargaren O, Nachtergaele F (eds). Rome

Jahn R, Zarei M, Stahr K (1992). Development of andic soil properties and of clay minerals in the semiarid climate of Lanzarote (Spain). Mineralogica et Petrographica Acta 35-A S: 193–201, Bologna

JCPDS-ICDD (1996). PDF-2 Data Base (Sets 1-46). JCPDS – International Centre for Diffraction Data, USA

Madeira M, Auxtero E, Monteiro F, Garcia-Rodeja E, Nóvoa-Muñoz JC (2006). Exchange complex properties of soils from a range of European volcanic areas. In: Arnalds O, Bartoli F, Buurman P, Garcia-Rodeja E, Oskarsson H, Stoops G (eds) Soils of Volcanic Regions of Europe. Springer Verlag (this book)

Mehra OP, Jackson ML (1960). Iron removal from soils and clays by a dithionite-citrate system buffered with sodium bicarbonate. Clays and Clay Minerals 7:377–327

Mizota C, Matsuhisa Y (1995). Isotopic evidence for the eolian origin of quartz and mica in soils developed on volcanic materials in the Canary Archipelago. Geoderma 66:313–320

Moore DM, Reynolds RC (1997). X-Ray diffraction and the identification and analysis of clay minerals, 2nd edn. Oxford University Press, Oxford and New York

Nihlén T, Olsson S (1995). Influence of eolian dust on soil formation in the Aegean region. Z Geomorph N F 39:341–361

Petschick R (2001). MacDiff v 4.2.5 (Free X-ray powder diffractometry analysis tool, <http://www.geol.uni-erlangen.de/macsoftware/macdiff/macdiff.html>)

Sawhney BL (1989). Interstratification in layer silicates. In: Dixon JB, Weed SB (eds) Minerals in Soil Environments, 2nd edn. Soil Science Society of America Book Series no 1. Soil Science Society of America. Madison, Wisconsin, pp 789–828

Shoji S, Ono T (1978). Physical and chemical properties and classification of Andosols from Kitakami, Japan. Soil Science 126:297–312

Shoji S, Hakamada ST, Saigusa M, Yamada I (1985). Properties of non-allophanic Andosols from Japan. Soil Science 140:264–277

Takahashi T, Dahlgren R, van Susteren P (1993). Clay mineralogy and chemistry of soils formed in volcanic materials in the xeric moisture regime of northern California. Geoderma 59:131–150

Ugolini FC, Dahlgren RA (1991). Weathering environments and occurrence of imogolite/allophone in selected Andisols and Spodosols. Soil Science Society of America Journal 55:1166–1171

Appendix materials on CD-Rom

Figure A. XRD clay patterns of Ap and Bw2 horizons from pedon EUR01: Mg: Mg saturated, air dried; EG: solvated with ethylene glycol; 550–550ºC heated. M: mica; Ph: phillipsite; K: kaolinite; An: analcime; L: leucite; Sd: sanidine; Q: quartz; Hm: hematite.

Figure B. XRD clay patterns of Ah2 and 2Bw1 horizons from pedon EUR04, air dried after Mg saturation, ethylene glycol-solvated (EG), and heated to 550ºC. V: vermiculite; M: mica; K: kaolinite; Sd: sanidine; An: analcime; Q: quartz; Hm: hematite.

Figure C. XRD patterns of the clay fraction of Ah, 2Ahb and 2Bwb horizons from pedon EUR05; air dried after Mg saturation, ethylene glycol-solvated (EG), and heated to 550ºC.
V: vermiculite; V-Al: hydroxy-Al interlayered vermiculite; Cl/V: interstratified chlorite/vermiculite; K: kaolinite; Pl: plagioclases; Q: quartz; Hm: hematite.

Figure D. Pedon EUR06: XR difraction patterns of air dried, Mg saturated clay separates from Ah, AB1 and 2Bw1 horizons, after acid oxalate treatment (ox), dithionite-citrate-bicarbonate extraction (dcb) and ethylene glycol solvation after dcb treatment (EG).
V: vermiculite; K: kaolinite; Pl: plagioclases; Q: quartz; Mgt: magnetite; Hm: hematite; Go: goethite.

Figure E. XRD patterns of the clay fraction of Ah2 and Bw horizons from pedon EUR12, air dried after Mg saturation, ethylene glycol-solvated (EG), and heated to 550ºC.
V: vermiculite; V/M: interstratified vermiculite/mica; M: mica; K: kaolinite; Pl: plagioclases; Q: quartz.

Figure F. General diffraction patterns of Mg saturated clay from Ah2, Bw1 and 2Bw2 horizons of pedon EUR17. On the right of the figure more relevant aspects of ethylene glycol-solvated (EG) and 550ºC heated clay from the same horizons are shown.
V: vermiculite; S: smectite; V-Al: hydroxy-Al interlayered vermiculite (or smectite); Ph: phillipsite; K: kaolinite; Fd: feldspars; Q: quartz; Hm: hematite; Go: goethite.

Figure G. Pedon EUR20: XR difraction patterns of air dried, Mg saturated clay separates from Ah1, Ah2, and Bw/R horizons, air dried after Mg saturation, ethylene glycol-solvated (EG), and heated to 550ºC.
M: mica; K: kaolinite; Pl: plagioclases; Q: quartz.

Characteristics and genesis of volcanic soils from South Central Italy: Mt. Gauro (Phlegraean Fields, Campania) and Vico lake (Latium)

C. Colombo, M.V. Sellitto, G. Palumbo, F. Terribile and G. Stoops

Introduction

South Central Italy (Latium and Campania regions) is an interesting geographic area to study soil development in volcanic materials because of: (a) the presence of volcanoes active during late Pleistocene and Holocene; (b) the occurrence of several pyroclastic deposits of known ages, and c) the Mediterranean climate (mesic and ustic/xeric pedoclimate). This district, often called "Campano-Laziale", is geographically divided into the Roman and Campanian petrographic provinces (Figure 1), and is characterized by extensive volcanic deposits with a wide variety in composition of lava and volcanic tephra ranging from alkali-trachytic to latitic (Scandone et al. 1991, Di Vito et al. 1999, De Vivo et al. 2001). Many of the volcanoes in Central Italy are stratovolcanoes formed by alkali-potassic magmatic lava, characteristic of the Campano-Roman petrographic Province. The activity dates back 1300 ka (Sollevanti 1983, Bidini et al. 1984, Barbieri et al. 1988). Two areas have been investigated: an old volcano, the Vico Caldera in the Latium district and a young volcano in the Phlegraean Fields, Campania. Eruptions have been characterized by a variety of explosive event sequences and magnitudes in the past 1500–2000 ka. The Vico volcano consists of lavas of various composition, including leucitites, leucite–tephrites or leucite–phonolites in the first cycle and trachy-andesitic or latitic products in the second cycle (Lulli and Bidini 1978, Lulli et al. 1988, Scandone et al. 1991). The actual body of the Vico volcano is a lake of 7–8 km in diameter that occupies an area of 150 km^2 but the surroundings covered by Vico's pyroclastics are much larger. The Monte Gauro volcano is formed during the last period of activity (10 ka) of the Phlegraean Fields and is therefore considered as very young. The purpose of this study is to investigate the genesis and the properties of four pedons, formed in different tephra-derived materials inside the main caldera of Gauro and Vico volcanoes, to investigate the influence of the parent material and time on pedogenic processes under a Mediterranean climate.

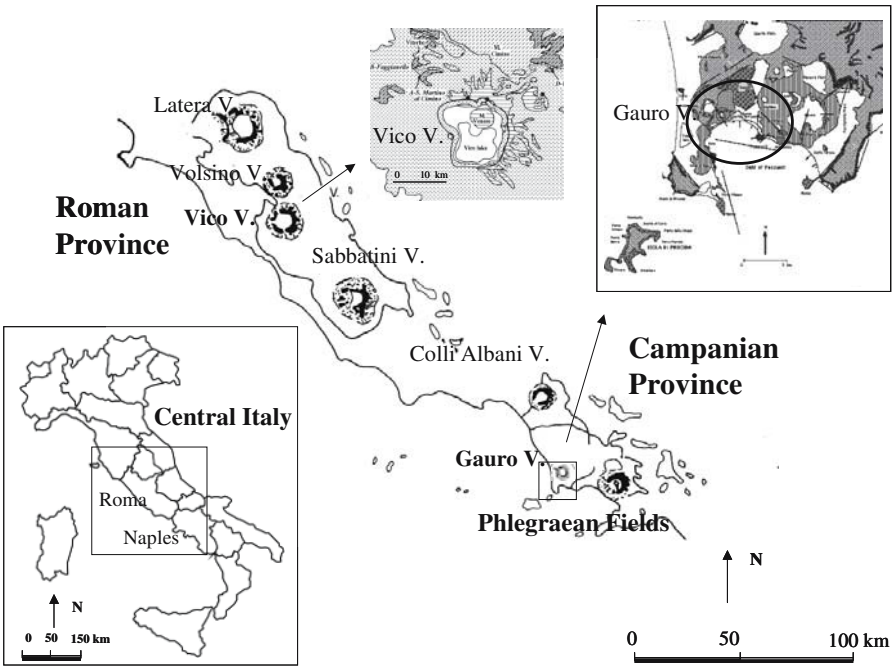

Figure 1. Location of the study area in Central Italy with Roman (Vico volcano) and Campanian (the Phlegraean Fields, Gauro volcano) petrographic districts.

Description of the study area

Profiles EUR01-02 (Gauro volcano)

The Monte Gauro volcano lies in the Phlegraean Fields district in the centre of Campania (north of Naples), between latitude: 40°51'36" N and longitude: 14°06'26.40" E (EUR01) and latitude: 40°52'4" N longitude: 14°06'38,40" E (EUR02). The Phlegraean Fields were formed by about 30 different volcanic events, beginning approximately 30 ka ago (Rosi and Sbrana, 1987; Scandone et al, 1991). The Phlegraean Fields caldera has a very complex volcanic and deformational evolution and consists of heterogeneous pyroclastic rocks. It is formed by two major collapses related to the Campanian Ignimbrite (Di Vito et al. 1999, De Vivo et al. 2001). The intense urbanization and the potential volcanic activity mark this environment as a high volcanic risk area. Monte Gauro is a well-preserved volcano with elliptical structure having axes of about 2 by 1 km (Figure 1). The volcano has a maximum elevation of 253 m a.s.l and was formed by a

series of rapidly succeeding eruptions during the last period of activity (10 ka). The eruptions were mostly phreatomagmatic, with subordinate magmatic explosions, and produced large amounts of pyroclastic falls and surges. The surge beds are generally confined to depressions. Lava domes were emplaced during single effusive eruptions and during the final phases of explosive eruptions. The texture of the pyroclastic deposits varies according to the distance from the vent. The unconsolidated upper part, called "pozzolana" consists of glass shards with an alkali-trachytic composition with a slightly trachytic to latitic trend towards the top. The zeolitisation of this glass by fluids linked to the eruptive mechanism gave rise to a large deposit of yellow tuff with phillipsite, subordinate chabazite and, in some cases, analcime minerals (de Gennaro et al. 2000). At present, Monte Gauro volcano is a green area used for recreation with a park and chestnut forest (private owner). The dominant natural vegetation in the study area is chestnut (Castanea sativa, P. Mill.) forest, but in the past the flat and gently sloping areas inside the caldera were used for agriculture. Pedon EUR01, is located on a flat terrace cultivated as apple and peach orchard on the slope of Mt Gauro; Pedon EUR02 is located in a chestnut copse, cut 10 years ago and exhibiting some relict signs of soil erosion in the surface horizon, induced by the drag of wood. Overall these sites are strongly affected by human disturbance.

Profile EUR03-04 (Vico volcano)

The Vico volcano lies in Northern Latium (northwest of Rome), between latitude 42°10' and 42°31'N and longitude 11°55' and 12°28'E (Figure 1). The Vico volcano stands out from a large ignimbrite plateau formed about 1300 ka ago, typical of the Quaternary south central Italian volcanism (Bidini et al. 1984, Quantin and Lorenzoni 1992, Lorenzoni et al. 1995). The Vico volcano is a stratified volcano with a terminal caldera, now filled by a lake, which received flows of pyroclastic magma, ignimbrite and tuff. Its activity started 419 ka ago and ended 95 ka ago with three intense volcanic phases. The first period of activity began with several Plinian-type eruptions, with different eruptive styles, which discharged tephra and minor pyroclastic flows. Around 400 ka, Plinian eruptions persisted but were accompanied by lava flows. These pyroclastic and effusive products are spread out in the northeastern sector and to a lesser extent in the western area. During the second period, several eruptions occurred from the main crater, which built up and subsequently destroyed the edifice. Post-caldera effusive and explosive activity during the third period came from different

intra- and peri-caldera vents as well as from caldera fractures. The rocks of this volcanic area are composed of lavas of various compositions including phonolitic tephrites, tephritic phonolites and slightly undersaturated trachytes. Phreatomagmatic activity after collapse of the caldera led to the accumulation of pyroclastic deposits and potassium-rich lava with leucite-bearing rocks. During the last two periods, the eruptions were fed mainly by evolved, mildly to strongly silica undersaturated potassium-rich magmas of the Roman Magmatic Province (Bidini et al. 1984, Barbieri et al. 1988, Barbieri et al. 1994).

The permanent vegetation changes toward higher altitudes from oak forest (*Quercus pubescens*), to chestnut forest (*Castanea sativa*) and to beech forest (*Fagus sylvatica*) following the change from a xeric to an udic pedoclimate. Soil temperature regimes change accordingly from thermic to mesic. Pedons EUR03 and EUR04 are located respectively in Monte Venere and Caldera di S. Matteo on tephritic-phonolitic leucite-bearing lava, to represent soil development on lava with a large variety of tephrites, tephritic phonolites and slightly undersaturated trachytes (Lulli and Bidini 1978, Bidini et al. 1984, Quantin et al. 1988, Quantin and Lorenzoni 1992). These sites, and especially the EUR03 soil, are very little disturbed by human activity.

Laboratory methods

The studied profiles were sampled by Working Group 5 of the COST-622 action and profile descriptions are given in the attachments to this book.

All samples were treated with H_2O_2 to remove organic matter. Afterwards, the sand fraction (0.25–1 mm) was separated from the H_2O_2 treated <2 mm fraction by sieving over a 50 μm sieve, following a 15-min ultrasonic pre-treatment (20 kHz and 200 W). After dispersion, the clay fraction (<2 μm) was separated from the <50 μm fraction by sedimentation in water. It was K-saturated saturated with a 0.5 M 1 M KCl solution (Jackson 1974).

Fe, Al, and Si were extracted from the clay fraction by sodium dithionite citrate bicarbonate (Fe_d, Al_d, Si_d) (Mehra and Jackson 1960) and by ammonium oxalate (Fe_o, Al_o, Si_o), (Schwertmann 1964). The suspension was centrifuged for 15 min at 2500 rpm, with three drops of 'superfloc' and the supernatant was filtered before analysis. The concentration of Si, Al, and Fe were determined in the extracts by a Perkin Elmer 3030 B Atomic Absorption Spectrometer (AAS), equipped with deuterium-arc background correction in acidic samples (Buurman et al. 1996). The allophane content

was calculated from the results of the selective dissolution extracts according to Parfitt and Wilson (1985) and Parfitt (1990). The allophane Al/Si molar ratio is estimated from (Al_o/Si_o). The allophane content is calculated by multiplying Si_o by a factor depending on the Al/Si molar ratio, assuming that allophanes with Al/Si=1 contain 20% Si_o and allophanes with Al/Si=3.5 contain 6.25% of Si_o (Dahlgren 1994). Intermediate Si_o contents of allophanes with intermediate Al/Si molar ratios are determined assuming a linear relationship between Si_o and Al/Si molar ratios of 1 and 3.5 (See 'The physico chemical data base (this volume) for a comment on these calculations).

The mineralogy of the sand fraction (particle size 0.25–1 mm) was investigated with Rigaku Geigerflex D/Max IIIC X-ray diffractometer (XRD) equipped for Co-Kα and Cu-Kα radiation, generated at 40 kW, 30 mA, using a scan speed of 0.5 ° 2 θ/min. A semi-quantitative analysis was carried out on the basis of integrated intensities of diagnostic peaks obtained with divergent receiving and antiscatter slits at 1°, 0.5 mm and 1°. Integrated intensities were calculated from the multiplication of intensities for width (calculated at half height) that were obtained after Gauss deconvolution with the data processing procedure of the D/Max-B system software Version 3.0 using the Rigaku FP-6000 computer. The mineral percentages were calculated on randomly oriented aggregates by the matrix-flushing and adiabatic principle according to the operating procedures proposed by Wilson (1987). Following weighting factors were used: biotite 0.75, sanidine (0.377 nm) 0.45, quartz 2.89, leucite 0.25, plagioclase 0.55, pyroxenes 0.7 and Fe-oxides 0.85. A value of 1 was attributed to the boehmite reflections that were used as a reference. To enhance the diffraction intensity of the poorly ordered mineral phases (allophane), the X-ray diffractometer traces were always the summation of eight separate runs of each sample and the differential X-ray diffraction pattern (DXRD) was also based on 8 summed signals (Malucelli et al. 1999).

Thin sections (10×5×0.003 cm) were produced after impregnation and hardening with polyester Crystic resin. They were described in transmitted light according to Stoops (2003); the terms *matrix* and *aureoles* refer to FitzPatrick (1984). Detailed micromorphological descriptions and photograph are presented in Stoops et al., (this book) where also a glossary of micromorphological terms is given. Volcanic glass was identified and quantified optically in the sand fraction (Stoops and Van Driessche this book).

In optical microscopy (OM), quantitative analyses on thin section are made by standard point counting. There have been doubts about the reliability of point counting for pedological features in thin sections because of: (i) the assumption that neighbouring counts are spatially independent

(Finke et al. 1991), (ii) the hypothesis that different features have the same apparent density (Murphy and Kemp, 1984), and (iii) the assumption that different people perceive and quantify different features in the same way. For the purpose of this investigation, which relies on a simple comparison of similar features in different horizons, the combination of numbers counts and grid spacing is satisfactory because the same fundamental errors apply to all samples. 400 points were counted on each thin section.

Selected areas of the thin sections were examined with a Zeiss DSM 940 scanning electron microscope (SEM) equipped with a Link System INCA Energy Dispersive X-Ray Analyser (EDS). The samples were mounted with colloidal carbon on aluminium stubs and coated with carbon. X-ray intensities at 25 kV using a working distance of 2.5 mm and a spot size of 5 μm were converted to weight percentages of elements applying the ZAF standard matrix correction procedure. About 10–20 EDS analyses were performed on each of the chosen micro sites. To evaluate significant relationships between EDS chemical composition of selected micro samples from different locations and soil weathering, descriptive statistics and Pearson's correlation coefficients were calculated. Element maps of selected areas representative of the major soil processes were produced with a time of acquisition of about 10 min at about 0.5 million counts per second. Samples for transmission electron microscopy (TEM) were prepared by evaporating a dilute suspension on carbon-coated Formvar films supported by copper grid and subsequently coating these with C to enhance conductivity. Microscope observations were conducted with a TEM Philips CM12 transmission electron microscope operating at 100 KV.

Results and discussion

Study sites and soils

The main morphological features of the four profiles EUR01, EUR02 (Gauro volcano) and EUR03, EUR04 (Vico volcano) are given in Table 1. The Gauro profile EUR01 is located on a man made terrace developed on pyroclastic trachytic ash deposits. It is characterised by weak horizon differentiation, abundance of primary minerals, light yellow colour (1Y), and high friability and is particularly well drained. Profile EUR02 is located on a gentle upper crest slope (15% gradient), with concave slopes to the W and E. It is characterised by a moderate horizon differentiation and a large quantity of primary minerals, and it is moderately deep. The differences in morphological properties between the two profiles are related to differ-

ences in soil management; profile EUR01 showing higher anthropogenic perturbation. Because of its geomorphic setting, the EUR02 profile is subject to surface erosion resulting in continuous rejuvenation. The Vico profiles (EUR03, EUR04) are developed on strongly weathered tephritic-phonolitic and leucititic lava. The profiles are moderately deep with a good horizon differentiation and they are well drained. The colour of the profiles is moderately yellow (8–9Y) for EUR03 to light reddish brown (10YR) for EUR04. The geomorphic setting (20–40% gradient) indicates an unstable landscape with little (EUR03) to strong (EUR04) evidences of colluviation.

Table 1. The main macromorphological and pedological features of the studied profiles.

Profile	Horizon	Depth (cm)	Colour*	Colour**	Texture	Structure
EUR01	Ap	0–16	1Y 7/3	10YR 3/3	Sandy loam	Very fine to fine subangular blocky
	Bw1	16–54	1Y 6/2	10YR 5/6	Loamy sand	Very fine, subangular blocky
	Bw2	54–95	1Y 7/3	10YR 6/6	Loamy sand	Granular
	BC	95–120/130	1Y 7/3	10YR 6/6	Loamy sand	Granular
	2C	>120/130	1Y 7/3	10YR 7/4	Very fine sand	No structure
EUR02	O	0				
	Ah	0–3/6	9YR 5/2	10YR 2/2	Sandy loam	No structure
	Bw	3/6–26	1Y 5/2	10YR 4/4	Sandy loam	Angular blocky
	BC1	26–31/51	2Y 7/2	2.5YR 7/4	Loamy fine sand	Granular
	BC2	31–51/71	2Y 7/2	2.5YR 7/3	Loamy sand	10% fine granular s
	C1	71–93	2Y 7/2	2.5 YR 7/2	Loamy sand	No structure
EUR03	O	2	8YR 5/2			
	Ah1	0–22	9Y 4/2	10YR 2/2	Silty loam	No structure
	Ah2	22–48	10Y 5/2		Silty loam	Very fine to fine granular
	2AB	48–70	10Y 6/3	10YR 2/2	Loamy fine sand	30% very fine granular
	2Bw1	70–98	9Y 6/3	2.5YR 7/3	Silty loam	No structure
	2Bw2	98–127	9YR 6/3	2.5YR 7/3	Loam	No structure
EUR04	O	0–2				
	Ah1	2–10	8YR 4/1	10YR 2/2	Silty loam	Very fine angular blocky
	Ah2	10–27	9YR 4/2	7.5YR 2/0	Silty loam	Fine granular
	Ah3	27–45	10YR 4/2	10YR 2/2	Silty loam	Subangular blocky
	Bw1	45–72	1Y 6/2	10YR 4/6	Sandy loam	Fine, angular blocky
	Bw2	72–107/142	1Y 6/2	10YR 5/6	Sandy loam	Very weak, fine, angular blocky
	C	107/142–182		10YR 6/6	Loamy sand	No structure

* Colour dry, spectrofotometric measurement.
** Colour humid, visive measurement.

Sand fraction mineralogy

Gauro volcano: EUR01-EUR02 pedons

Quantitative optical microscopy (OM) analyses of the 250–500 µm fraction (see also Table 1 in Stoops and Van Driessche this book) indicate that

on average one third of the grains consists of rock fragments and one third of volcanic glass, whereas in the 50–250 µm fraction the glass content varies between 50 and 80%. The glass is in general colourless or slightly coloured, pointing to a rather acid composition. In the 250–500 µm fraction a much higher content of opaque grains is observed in transmitted light than is evident in XRD analysis of the 250–1000 µm fraction. This suggests that part of the opaque grains are very dark rock fragments (tachylite), appearing opaque because of their relative thickness, or that a concentration of ore minerals occurs in the finer fraction.

Table 2. Sand mineralogy of the studied profiles by XRD.

Profile	Horizon	Biotite	K-Feldspars (sanidino)	Quartz	Leucite (albite	Plagioclase anortite)	Pyroxenes (augite)	Fe-oxides (magnetite)
EUR01	Ap	0	58	6	-	15	16	6
	Bw1	9	49	4	-	22	11	4
	Bw2	8	56	5	-	16	11	4
	BC	10	53	2	-	19	11	4
	2C	5	71	2	-	9	9	3
EUR02	O							
	Ah	0	55	4	-	21	14	5
	Bw	5	62	4	-	10	14	4
	BC1	5	67	6	-	11	8	4
	BC2	7	65	7	-	12	5	5
	C1							
EUR03	O							
	Ah1							
	Ah2	10	39	0	19	3	22	6
	2AB	9	36	0	22	4	23	6
	2Bw1	12	23	0	37	5	16	7
	2Bw2	6	24	0	19	35	10	7
EUR04	O							
	Ah1							
	Ah2							
	Ah3	0	32	3	25	17	14	9
	Bw1	0	20	3	27	34	8	8
	Bw2	0	27	2	22	33	10	7
	C	5	23	0	42	25	8	7

X-ray analyses of the EUR01 and EUR02 sand fraction show the specific reflections of biotite, sanidine, plagioclase and pyroxenes along with minor amounts of quartz and zeolite minerals such as phillipsite and analcime (Table 2; Figures 2ab). Zeolite minerals show only very weak reflections and the peaks were not used for quantitative determination. In the EUR02 profile the strong reflections at 0.377 (130 lattice), 0.323, 0.299 and 0.295 nm reflections of sanidine are dominant. The very weak 004 reflection of plagioclase at 0.318–0.319 nm is indicative of intermediate

forms of albite/anortite with a large variation in chemical composition (Brindley and Brown 1980). The 0.404 nm peak is attributed to Na-rich feldspars (albite) rather than to cristobalite because no other diagnostic peaks of cristobalite were observed (Violante and Wilson 1983, Figure 2b). Pyroxene, in particular augite, was identified by a strong reflection at 0.295 nm which is used for quantitative analysis rather than the 0.324 (100), 0.257 and 0.217 reflections because it does not overlap with the 0.299 nm reflection of sanidine (Wilson 1987). Also magnetite and maghemite were detected. A small amount of quartz, increasing with depth, was observed in Pedon EUR01, whereas it decreases with depth in EUR02. In Pedon EUR02, X-ray patterns indicate more crystalline material. A moderate amount of biotite was observed in the BC horizon of both Gauro pedons suggesting a discontinuity between the BC and 2C horizons, as observed by Buurman et al, 2004. Plagioclase and pyroxenes are generally more common in the top layers while in the rest of the profile feldspar and Fe-oxides show a similar distribution throughout the horizons (Table 2).

Vico volcano: Monte Venere (EUR03) and Caldera of San Matteo (EUR04)

Rock fragments represent in EUR03 three fourth and in EUR04 two third of the total grains counted by optical methods. Volcanic glass is absent, which is confirmed by micromorphology. The biotite revealed by XRD is observed only in EUR03 (Figure 3a). Its optical characteristics, especially its colour, confirm that it is an oxybiotite. Leucite, clearly detected by XRD at 0.325 nm, is less prominent in the grain mounts. The X-ray patterns of the sand fraction show a large difference between EUR03 and EUR04. Reflections of sanidine, leucite and plagioclases are more irregular and broad in the EUR04 profile (Figure 3b). Although the large amount of K-feldspars, in particular sanidine, obscures many of the leucite reflections, the 0.344 nm reflection of leucite is found useful for quantitative analysis. Another important leucite reflection is observed at 0.325 nm (Wilson 1987). EUR03 shows more and better-resolved reflections of these minerals and the sharp and well-defined peaks indicate a higher degree of crystallinity. The sand fraction mineralogy suggested a discontinuity between the Bw1 and Bw2 horizons observed in EUR03 (Buurman et al. 2004). Obviously, leucite is present in the parent material of both profiles, but extremely weathered in EUR04. X-ray diffractograms further show significant amounts of Fe-oxides that decrease with depth (Table 2).

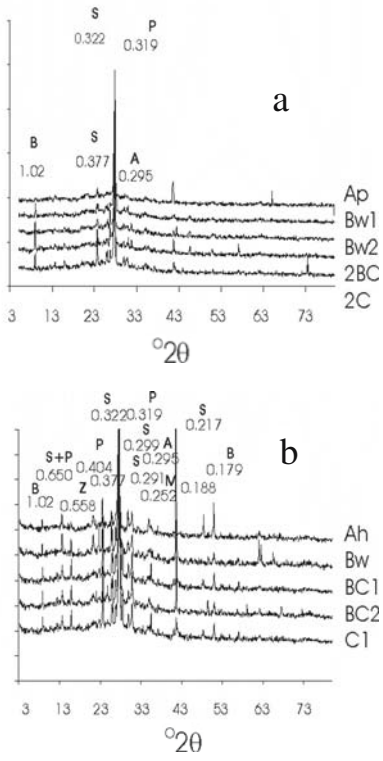

Figure 2. X-ray diffraction pattern (Cu-Kα of randomly oriented sand fraction (250–2000 µm) of the EUR01 profile (a) and EUR02 (b). B = biotite, S = sanidine, P = plagioclase, A = augite, M = maghemite/magnetite, Z = zeolites.

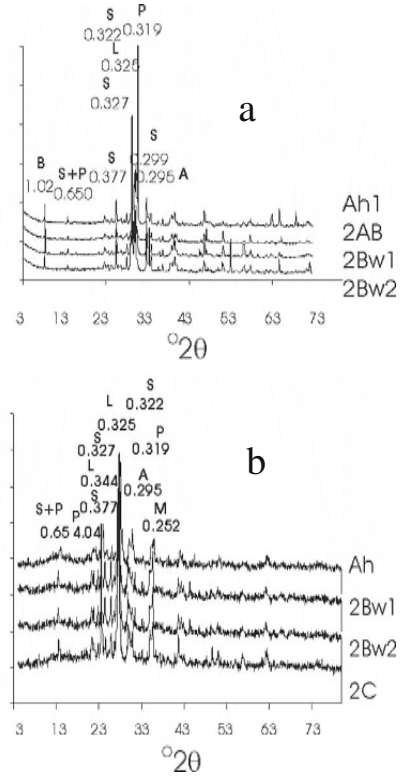

Figure 3. X-ray diffraction pattern (Cu-Kα of randomly oriented sand fraction (250–2000 µm) of the EUR03 profile (a) and EUR04 (b) from Vico Volcano. B = biotite, L = leucite, S = sanidine, P = plagioclase, A = augite, M = maghemite/magnetite.

Micromorphological analysis

For the systematic micromorphological description of these profiles the reader is referred to Stoops et al. (this book) where also the micrographs (Photo) can be found.

The microstructure of EUR01 is enaulic to granular throughout the profile, with a tendency to an angular blocky secondary microstructure in the Bw1 (Photo 2) and a vughy one in the BC. Compared to EUR01 the mi-

crostructure of EUR02 is less granular in depth (Photo 6 and 7). In the Ah1 a crumb and bimodal granular microstructure, associated with biological activity is present (Photo 4). In the Bw and BC2, a subangular blocky microstructure dominates over the granular, but the C horizon shows only granular structures. The Bw is characterised by a compaction and partial welding of the granular microstructure to angular blocky, however without loss of the intrapedal granular aspect.

The coarse material of the two pedons of the Gauro volcano is dominated by rounded, gravel and coarse sand-sized pumice fragments with considerable amounts of sand sized, hypocrystalline pyroclasts and angular grains of feldspar and pyroxene, and less fine glass splinters, as confirmed by the optical sand analysis. In EUR01 the amount of volcanic glass increases below the Bw horizon. In several horizons oxybiotite is observed. Especially in the upper part of EUR01 phytoliths occur. In general the abundance of pumice is lower in EUR02. In EUR01 weathering of chlorite is observed in some pyroclasts. Fresh excrements are observed in both profiles (Micrograph 5), attesting to a strong biological activity. Fungal hyphae in the upper horizons suggest a relatively acid humus.

In EUR01 a limpid yellowish micromass is observed, except for the Ap where organic pigment colours the clay. Its undifferentiated b-fabric is explained by the dominance of short-range order components. In EUR02 a speckled, greyish brown micromass occurs in all horizons with a weakly speckled b-fabric pointing to the presence or early development of phyllosilicate minerals as observed by XRD. Throughout EUR01, pyroclasts bear a dense coating of fine material (micromass). Pumice grains have in addition an internal hypocoating of the same material (Micrograph 1). In EUR02 the internal hypocoatings are better expressed than the coatings.

The C1 of EUR02 consists of a stratified material, containing denser layers of more reddish, coarse isotropic clay. Morphologically they can be considered as old surface crusts (Micrograph 8) pointing to a discontinuity in the profile. Below these crusts the packing pores are covered by strongly developed limpid illuviation coatings of yellowish clay with high and strong interference colours (Micrographs 9 and 10).

Whereas pedon EUR01 seems rather homogeneous, the micromorphology of EUR02 suggests the presence of an older profile, with surface crusts, covered by a colluvial material, as can be deduced from the characteristics of the micromass: a speckled limpidity, a greyish brown colour, both resulting from admixture of fine organic components, and a weakly speckled b-fabric, indicating the admixture of phylosilicates. The lithological discontinuity was also identified by Buurman et al. (2004), but these authors did not interpret it as a buried profile.

Throughout both Vico profiles the microstructure is granular (Micrographs 11 and 14) to enaulic, with an overprint of angular blocky secondary microstructure in the Bw horizons. The granular microstructure has a bimodal aggregate size, especially in the upper horizons, pointing to different processes of formation and/or faunal activity. Relative large amounts of organ and tissue residues, root sections and fungal hyphae (Micrograph 12) indicate a well-developed vegetation. The high amount of excrements is related to a high biological activity, which may be responsible for part of the granular microstructure in the surface horizons.

The parent material of the Vico profiles consists mainly of dense, hypocrystalline pyroclasts (Micrographs 12 and 13) with a variable degree of weathering. In addition to angular grains of augite a few oxybiotite flakes occur, as confirmed by both the optical and the XRD analysis of the sand fraction (Figures 3ab). In EUR03 the quantity of porous pyroclasts increases with depth. In the deeper part of EUR04 a fine-grained volcanic rock (andesite) with large phenocrysts of augite, feldspar and weathered leucite is observed. The latter is completely transformed to a light yellowish, limpid, isotropic material (Micrographs 16–19). Fragments of this material are also found in the Ah1.

In EUR03 the micromass is yellowish brown, becoming darker and dotted towards the surface. In EUR04 it is dark brown and speckled in the Bw, whereas yellowish zones are detected in the Ah1. The b-fabric is always undifferentiated.

Coatings of fine material (micromass) surround pyroclasts in all horizons. In the Ah1 of EUR04 these coatings have a lighter colour than the micromass in the granules.

The increase of porous pyroclasts and oxybiotite with depth in EUR03 indicates a gradual change in parent material. The coatings of lighter, fine material on weathered pyroclasts in the Bw suggest an admixture of materials from deeper horizons (e.g. from 2Bw2) by biological activity.

In EUR04 the Ah1 contains material similar to the C (pyroclasts with weathered leucite); which is absent in the Bw2. Therefore following sequence of events could be suggested, based on micromorphological evidence only: C-material developed in leucite bearing andesitic rock covered by a different volcanic deposit (Bw horizon), which in turn is covered by a material similar to the C, probably eroded from a Bw or C-horizon of a higher located profile. This is supported by the fact that the micromass in the Ah1 is light coloured around the free coarse grains, but dark brown in the granules. The change in parent material from Ah3 to Bw1 is confirmed by grain-size and chemical analysis (Buurman et al. 2004).

Submicroscopic analysis (SEM and EDS)

Micromorphological analysis reveals the presence of specific features such as pumice weathering, coatings of fine material (especially silt), and leucite weathering (in the EUR04). Figure 4 reports the frequency of such features in the four soils by means of point counting procedure. The coatings of such fine material around the grains seem to be important in all the investigated soils regardless the age of the soil and the stage of soil development. Instead, aggregates of fine material are mostly present in the BC and C horizons. This suggests that the latter are primary and not pedogenic.

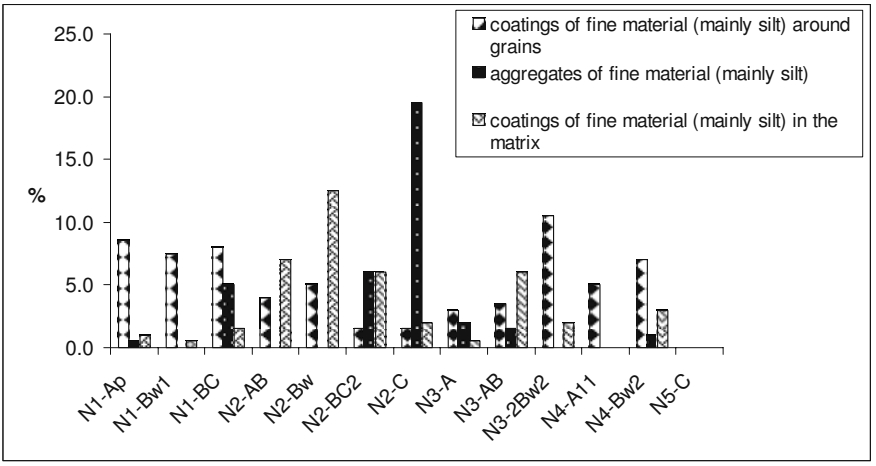

Figure 4. Frequency distribution (point counting) of the features formed by fine, mainly silt sized, materials in the studied horizons, expressed as volume % of total thin section.

In order to characterise these features, 198 EDS microanalyses have performed on selected thin sections, aiming an understanding of the overall geochemistry of the following units: (i) the unweathered interior of pumice and scoria fragments; (ii) the soil matrix (micromass); (iii) coatings of fine material (mainly silt) around grains and pumice and (iv) clay coatings (optically anisotropic, therefore consisting of well crystalline clay minerals) found in the ashy C horizon of EUR02. The descriptive statistics of the chemical composition of these features are given in Table 3; the Pearson bivariate correlation (r) between the elements is given in Table 4, and a multivariate hierarchical classification has been attempted and reported in Figure 5.

Table 3. EDS descriptive statistics and weathering index.

	Element	Na	Mg	Al	Si	K	Ca	Ti	Mn	Fe	Si/Fe	Weathering index (Si+Na+K+Ca+Mg(/ (Fe+Mn+Ti)
Pumice: unweathered interior (EUR01; EUR02)	Minimum	0.91	0	6.64	51.85	0.05	1.93	0.34	0	0.28	10.85	15
	Maximum	6.53	15.19	34.5	67.78	9.33	15.61	0.67	0.3	5.13	185.46	236
	Mean	3.59	2.75	21.58	60.23	4.46	5.7	0.48	0.19	2.39	51.95	63
	Std. deviation	2.12	5.07	8.21	5.42	3.34	5.19	0.11	0.15	1.44	60.62	78
Coatings of fine material (mainly silt) around pumices and grains (EUR01; EUR02).	Minimum	0.24	0.45	15.7	48.02	0.57	0.53	0.41	0.16	1.65	6.09	6
	Maximum	5.25	1.52	45.31	69.56	7.19	4.75	1.5	0.52	10.26	33.11	36
	Mean	1.56	1.06	30.85	56.96	3.07	1.48	0.85	0.3	4.83	16.18	17
	Std. deviation	1.59	0.4	11.45	6.74	2.64	1.43	0.42	0.16	2.99	8.96	10
Soil matrix (mainly micromass) (EUR01; EUR02)	Minimum	0.44	0.53	14.85	46.03	0.55	0.78	0.29	0.21	1.61	4.45	5
	Maximum	8.46	2.62	43.92	75.02	8.09	3.96	1.03	0.27	12.49	41.51	49
	Mean	3.01	1.39	21.26	62.51	4.97	2.05	0.64	0.24	4.95	17.84	19
	Std. deviation	2.39	0.67	7.79	7.09	2.34	0.78	0.23	0.03	3.55	10.45	12
Coatings of silt and clay in ash layers (EUR02)	Minimum	0.51	0.06	15.86	61.18	5.12	0.16	0.24	0	0.42	5.69	6
	Maximum	4.04	2.67	18.89	71.27	12.65	1.17	1.37	0.23	10.76	156.95	194
	Mean	2.28	1.32	17.31	65.11	7.17	0.86	0.84	0.1	5.19	37.87	42
	Std. deviation	1.41	0.96	0.79	2.54	2.25	0.39	0.37	0.08	3.74	51.62	63
Leucite pseudomorph (EUR04)	Minimum	0	0	4.24	14.01	0	0	0	0	0	1.15	2
	Maximum	12.2	17.16	69.99	68.38	28.21	21.89	6.03	1.55	26.33	270	316
	Mean	3.44	1.87	26.36	52.66	6.74	4.64	0.62	0.395	3.49	56.60	64
	Std. deviation	3.37	2.96	12.75	12.31	7.42	6.11	0.91	0.37	5.1	58.61	67

Table 4. Correlation coefficient of EDS analysis.

		Na	Mg	Al	Si	K	Ca	Ti	Mn	Fe
Weathering features of EUR01 EUR02 (pumice unweathered; coatings of fine material; matrix; clay and silt coatings)	Na	1.00								
	Mg	–0.18	1.00							
	Al	–0.08	–0.27	1.00						
	Si	0.27	–0.19	–0.76	1.00					
	K	–0.08	–0.24	–0.80	0.66	1.00				
	Ca	–0.12	0.55	–0.08	–0.29	–0.30	1.00			
	Ti	–0.40	0.11	–0.22	–0.17	0.01	0.00	1.00		
	Mn	–0.48	0.03	–0.08	–0.26	–0.55	0.09	0.36	1.00	
	Fe	–0.46	0.20	–0.31	–0.08	0.11	–0.12	0.80	0.66	1.00
		Na	Mg	Al	Si	K	Ca	Ti	Mn	Fe
Leucite weathering features of EUR04	Na	1.00								
	Mg	–0.21	1.00							
	Al	–0.22	–0.26	1.00						
	Si	0.60	–0.37	–0.56	1.00					
	K	–0.42	–0.42	–0.13	0.15	1.00				
	Ca	–0.34	0.75	0.02	–0.68	–0.53	1.00			
	Ti	–0.07	0.52	–0.45	–0.19	–0.38	0.65	1.00		
	Mn	–0.47	0.22	–0.52	–0.70	–0.06	0.51	0.75	1.00	
	Fe	–0.24	0.68	–0.47	–0.29	–0.34	0.77	0.84	0.80	1.00

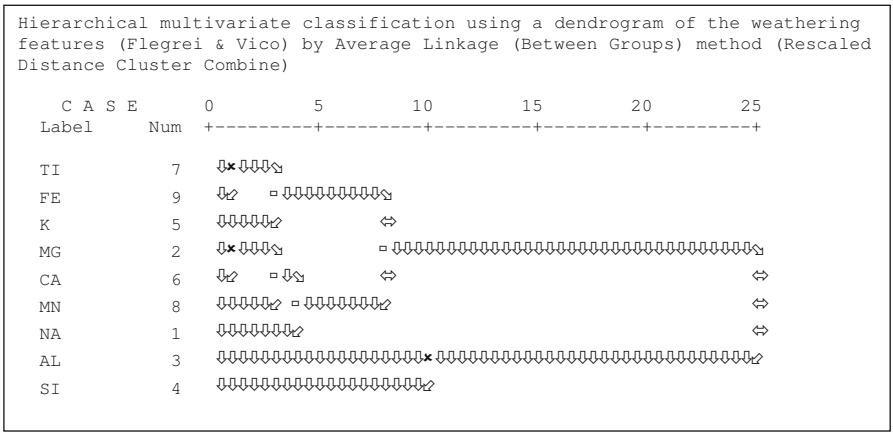

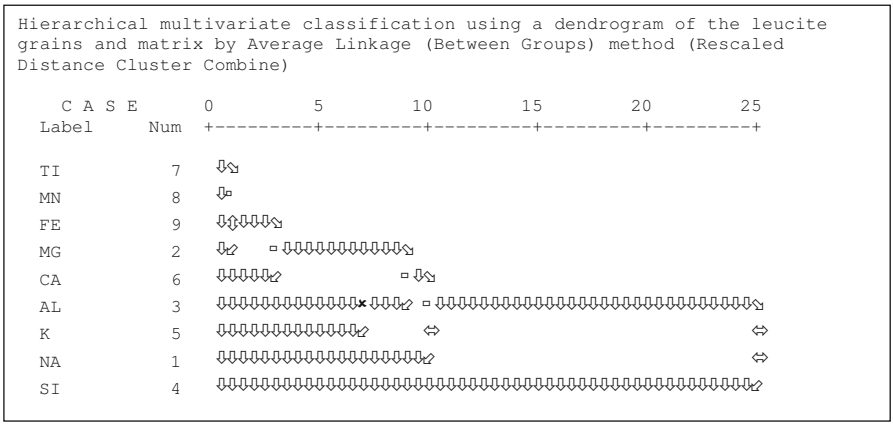

Figure 5. Hierarchical multivariate classification of the total elements of SEM-EDS chemical data.

The results of EDS analyses confirm that silica is the main constituent of the features, ranging from 60% in the unweathered pumice to 56–65% in the coatings of fine material (clay and silt) around pumice in the C horizons of EUR02 (Table 3). The second major component is aluminium, which accounts for about 21% in the unweathered pumice to 17–21% in the coatings of fine material around pumice. The Si/Fe ratio ranges from 63 in the unweathered pumice to 17% in the coatings (mainly silt) of the EUR02 samples. Other major elements are present in much smaller quantities, showing a significant difference between the units analysed, and indicating a strong variability in the chemical composition of the volcanic material (Table 3). Considering the type of analysis and the different units in-

vestigated, the results do not show a very large variability. Si, which is a strongly leached element in this Mediterranean environment, has a positive correlation with K (0.66) and Na (0.27), and a negative correlation with Fe, Mn and Ti. Fe, Mn and Ti are all very well correlated mutually, with r ranging between 0.66 and 0.80 (Table 4). This similarity is confirmed by a hierarchical multivariate classification of the whole data set, which shows the degree of relationship between the elements. Such analysis shows that Ti and Fe are highly related while Si and Al are far apart. On the base of these results, we have attempted to define an index of weathering based on the ratio between the most leached elements (Si, bases) and the well-correlated residual elements (Fe, Mn, Ti) / (Si+Na+K+Ca+Mg)/(Fe+Mn+Ti). As a soil becomes more weathered, mobile cations are removed and immobile cations show a relative accumulation. (Birkeland 1999, Malucelli et al. 1999). The index decreases in the following sequence (i) unweathered interiors of a pumice (ii) coatings of fine material around grains and pumice and (iii) the soil matrix (micromass) (Figure 6). The index indicates that the interior of pumice fragments is rich in Si and bases, which decrease with respect to Fe and Mn towards the coating around the pumice. A stronger enrichment of Fe and Mn compared to Si and bases is seen in the soil matrix (micromass). Soil features constituted by fine material, dominated by silt sized material, are found in all profiles (Figure 7). In a few cases (i.e. Figures 7ac) present day and past illuviation of fine material appears to be the cause of such features.

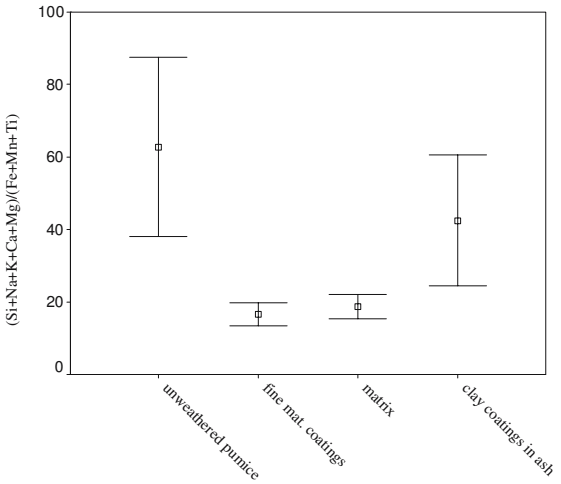

Figure 6. Example of weathering indexes on the basis of SEM-EDS chemical data applied to a transect starting from the inner part of a pumice to the outer shell and the soil matrix from Pedon EUR01.

The fine material features consist of (i) coatings in proximity of pores or located in the matrix (generally relicts of old coatings) (Figure 7a), (ii) coatings of fine material (both internal hypocoatings and coatings) tightly

or loosely packed around pumice and other mineral grains (Figures 7bcdfh il) and finally (iii) aggregates made by homogenous fine material (mainly silt) (Figures 7eg).

The detailed frequency (point counting) analysis, already reported in Figure 5, gives some further information on such fine material features.

The peak distribution of aggregates made by homogenous fine material (mainly silt) in the lower and less developed horizons of EUR01 and EUR02 may indicate that the biological activity is not the forming factor of these features while, possibly, illuviation processes play a much more relevant rule. In EUR01, the large concentration of aggregates made of silt sized homogeneous fine material in the lower horizons (BC, C) and the absence of coatings of recently illuviated fine material on the pore walls (especially in the surface horizons) indicates that the fine material ag-gregates and coatings around the grains were already present in the volcanic ash parent material. Actually, primary processes forming coatings of fine material around a volcanic core (ash or grain) are well known, producing as final product well rounded ashy aggregates (pisoliths) during many Plinian eruptions (e.g. 79 AD Pompeii eruption); this must be related to the effect of the reorganisation of the mineral material affected by the high turbulence and the high energy of the pyroclastic fluxes.

The fine material aggregates disappear towards the soil surface, possibly because of physical weathering. In the surface horizons of both EUR01 and EUR02 only the coatings (both interior hypocoatings and coatings) around the grains (aureola) are reported. The overall picture can be explained by a very large dynamics of fine material, and especially silt, in these soils, caused by its common occurrence in the parent material and its in situ redistribution or/and illuviation during soil development. In order to better understand such findings, an optical microscopy analysis of specific sites has been performed (Figures 7a-l; Figures 8ab).

These fine material features seem to undergo a process of physical weathering with (mainly) silt moving in the soil, bridging grains (Figure 7c) and forming aggregates (Figure 7e), or forming different generations of silt coatings around grains (pumice in Figure 7d). Therefore some silty features are, most likely, formed by primary processes (mainly ash deposition) (e.g. Figures 7fg) while other silty features are formed by secondary pedogenic (i.e. fine material redistribution) processes (i.e. Figures 7ab). On the base of such observations, we can assume that the inner dense compacted coatings of Figure 7d reflect a primary process (possibly contemporary) to ash deposition (such as in surge) and the loose outer shell reflects silt illuviation. Similar features related to silt coatings are also found in the EUR03 and EUR04 soils (Figures 7hil).

The presence of a horizontal layer of optically anisotropic (and therefore consisting of crystalline material) clay coatings (Figures 8ab) in the C horizon of EUR02, related to a discontinuity in microstructure, is very interesting. Such pedogenic crystalline clay materials, too little in quantity to be mineralogically identified, were obviously produced by precipitation from solution and subsequent illuviation of crystalline clay. None of these processes have been found in the horizons overlying the C.

To acquire a better understanding of the chemistry of this fine clay, a further SEM-EDS analysis has been performed on pumice from the Bw horizon of EUR02. In Figures 9ab the EDS map of Al, Si, Ca and K of such a pumice grain, surrounded by a fine material coating shows a large variability, possibly reflecting the different mineral phases in the volcanic parent material. Based on element mapping, an innovative map showing directly the values of the weathering index (Si+Na+K+Ca+Mg)/(Fe+Mn+Ti) was prepared (Figure 9c). In this map, the areas correspond to different degrees of weathering where the bright points refer to a very low index (strong alteration) while the dark points refer to weak alteration. From Figure 9c is clear that the strongest weathering occurred in the outer coating of the pumice. This feature is therefore pedogenic, but it is not possible to confirm whether the coating was formed by in-situ weathering, by redistribution, or by illuviation.

Figure 7. Micromorphological features from EUR01, EUR02 and EUR03 soils, caused by concentration of fine, mainly silt sized material.

(a) fragment of a large coating in the groundmass; there is no evidence of recent movement of fine material in the pores. Plane polarized light (PPL). EUR01, BC;
(b, c) coatings and internal hypocoatings, tightly or loosely compacted around pumice grains; in (c) the coating bridges two pumice grains. (PPL). EUR01, A horizon;
(d) different generations of coatings around a pumice grain. (PPL). EUR01 A horizon;
(e) aggregate of fine material showing a homogeneous particle size distribution and a layering. (PPL). EUR01, BC horizon;
(f) thick coating around an ash aggregate. The coating seems to have been formed before or during deposition. There is no evidence of further illuviation. (PPL). EUR02 C1 horizon;
g) subrounded aggregate including fine ash material. (PPL). EUR02, C1 horizon;
h, i) coatings around a scoria in EUR03. The light line at the border with the rock fragment in XPL refers to a strong orientation of anisotropic fine material. PPL and crossed polarised light (XPL). EUR03, 2Bw2 horizon;
l) coatings around a scoria showing physical disintegration. (PPL). EUR03 2Bw2 horizon.

Some pumice grains in EUR02 profile have a very low alkali content and Si/Al ratios >2 with an Al percentage between 6 and 53%; others have lower Si/Al ratios and larger alkali content. The EDS analyses of the pumice show that most of these pedogenic features have a low degree of weathering. The negative correlation between Si and Mn and Fe is possibly related to an accumulation of poorly-ordered Fe oxides outside the pumice.

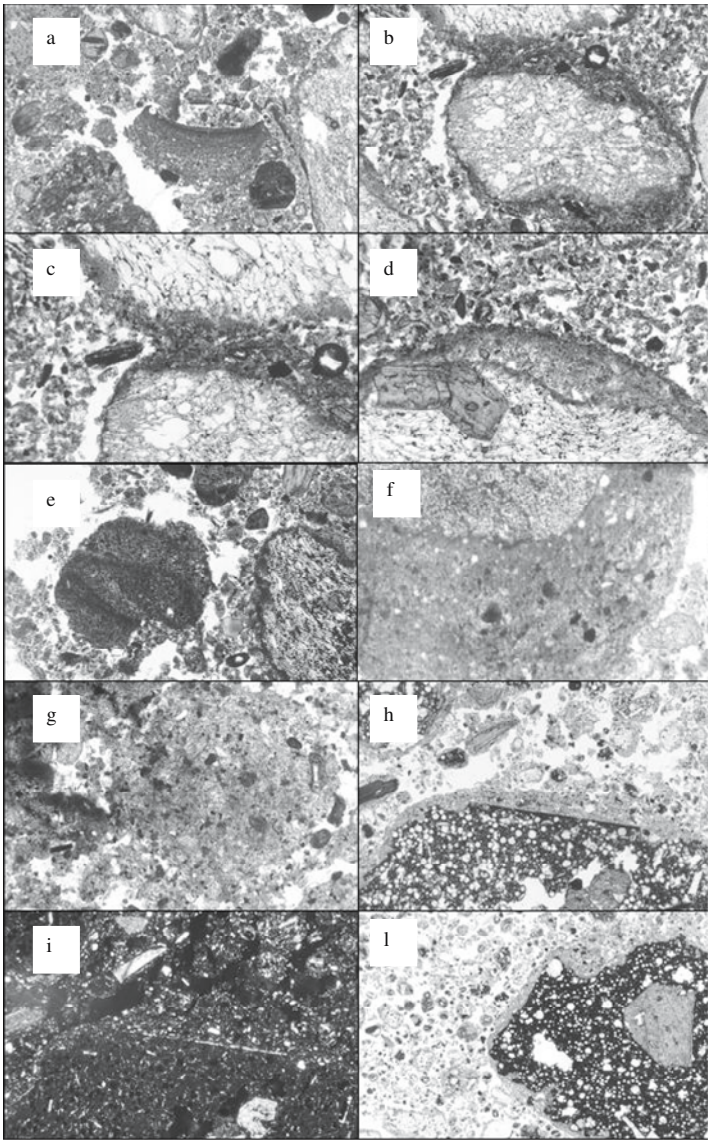

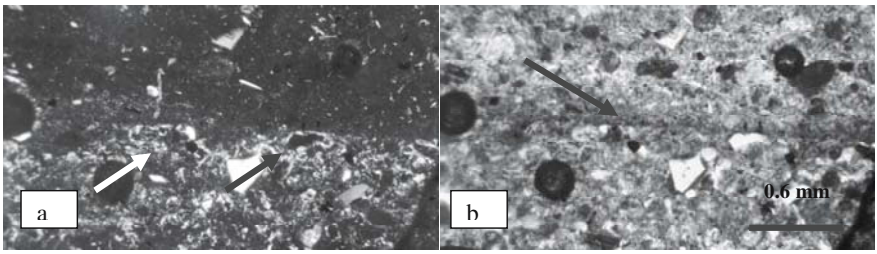

Figure 8. Micrograph of clay illuviation coatings in the lower zone of the sub-horizontal layered parts. The coatings are optically anisotropic in XPL, revealing that the clay minerals have a crystalline nature. C horizon of Pedon EUR02. (a): PPL, (b): XPL.

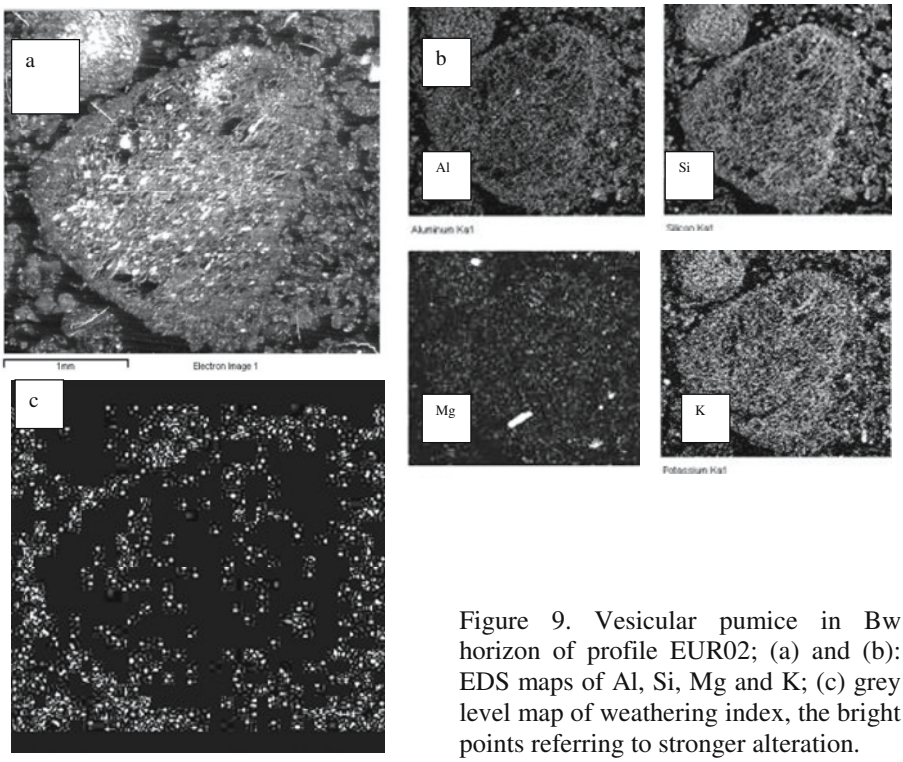

Figure 9. Vesicular pumice in Bw horizon of profile EUR02; (a) and (b): EDS maps of Al, Si, Mg and K; (c) grey level map of weathering index, the bright points referring to stronger alteration.

SEM-EDS analysis was also used to quantify element distributions in leucite pseudomorphs in the tephritic lava observed in the C horizon of EUR04 (Table 3). The chemical composition of the leucite particles shows a large variability related to the degree of weathering of the rock. The main

elements are Si (53%), Al (about 26%) followed by of K (6.74%), Ca (4.64%) and finally Na (3.44%). The excess of Ca and Na is indicative of analcime formation, with a large variation in chemical composition associated with a decrease of K in the leucititic lava. Leucite is the most widespread feldspathoid in high K-saturated rocks. It occurs as large phenocrysts and is the major component of the groundmass. Small amounts of late-stage, interstitial Ca-rich plagioclase crystals – together with Na-sanidine – are common in the groundmass of tephritic-phonolitic lava (Quantin et al. 1988, Quantin and Lorenzoni 1992). Table 4 shows good linear correlations of most elements measured in leucite pseudomorphs. It is very interesting that K is negatively correlated with Ca and Na and positively with Si. Ca is positively correlated with Mg and Fe with Mn. The Si/Fe ratio shows a high mean value of 64, similar to the unweathered pumice of the EUR02 samples, but ranging from 1.6 to 270 with a high standard deviation, suggesting that leucite pseudomorphs have a high but uneven degree of weathering. The variable content of alkaline cations and the negative correlation of K versus Ca and Na, emphasise that the weathering of leucite is very heterogeneous, but an increasing amount of Ca and Na might indicate a consistent trend with a higher loss of K from the system. Table 3 and Figure 10 give the main results of the EDS analyses and of the morphological analyses of leucite alteration and fragmentation observed in thin sections. More specifically, Figure 10a gives an example of the physical fragmentation of leucite The EDS maps of Al and Si are shown in Figures 10bc). Figure 10d presents the distribution of the weathering index (Si+Na+K+Ca+Mg)/(Fe+Mn+Ti) in the same microscopic field as Figure 10a. The bright points refer to a very a low index (strong alteration) while the dark points refer to a weak alteration. The figure clearly shows that, even in a leucite pseudomorph, the highest weathering occurs at the outer surface. In particular Figure 10 shows details of strongly weathered Fe-rich latitic lava in thin section (10e) and EDS maps of Al, Si, Ca and K (Figures 10fghi) indicating clearly the highest weathering and physical fragmentation of the rock. The distributions of Al, Si, Ca and K do not coincide, suggesting that elements have a more heterogeneous distribution within the pseudomorph and that relatively mobile cations (K and Ca) were lost more easily. This is also clearly visible in the strong alteration of the particle surfaces observed with SEM (Figures 10 lmn).

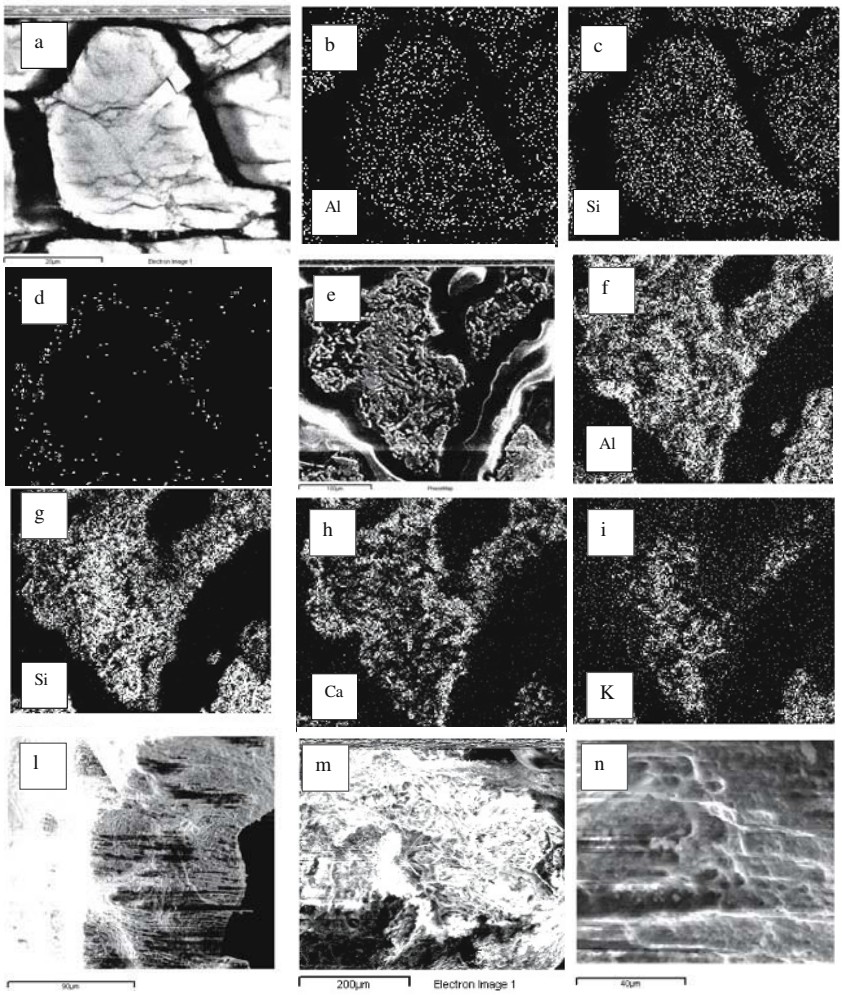

Figure 10. Leucite weathering in the C horizon of profile EUR04. (a) SEM micrograph of strongly weathered leucite; (b,c) EDS maps of Al, Si, (d) grey level map of weathering index, the bright points referring to high alteration); (e) strongly weathered Fe-rich latitic lava in thin section (f,g,h,i) EDS maps of Al, Si, Ca and K; (l,m,n) SEM of the weathered surface of leucite pseudomorph.

Mineralogy of thy clay fraction

Table 5 shows the amounts of Fe, Al and Si extracted by dithionite and oxalate in the <2 μm clay fractions. The amounts of DCB-extractable Fe and Al may be considered as indicators of iron-rich phases associated with allophanic materials (Dahlgren and Ugolini 1991, Malucelli et al. 1999, Adamo et al. 2001). According to the data shown in Table 5, the Al/Si ratio of the extracted material ranges between 1.3 to 6.3 for the Gauro profiles and between 1.5 to 8.2 for the Vico profiles. Applying the conversion factors provided by Parfitt (1990), the concentration of allophane varies from 0.5 to 40% of the clay fraction, with the highest values in the Vico profiles and more specifically in the 2Bw1 and 2Bw2 horizons of EUR03. Allophane may form by dissolution of glass through desilication, or by precipitation from the weathering solutions (Wada 1989). The mean Al/Si molar ratio is 3.4 and 2.5 for EUR01 and EUR02 respectively and 2.1 to 1.5 for EUR03 and EUR04 respectively. The Fe_o/Fe_d ratio for the Vico profiles indicates the dominance of non-crystalline iron oxides and a moderate amount of ferrihydrite (about 2.5%) mainly concentrated in the bottom part of EUR03.

Table 5. Chemical extractions of the clay fractions of the studied profiles.

Soil profile	Horizon	Depth (cm)	Al DCB extraction (%)	Fe DCB extraction (%)	Si DCB extraction (%)	Al Oxalate extraction (%)	Fe Oxalate extraction (%)	Si Oxalate extraction (%)	Al_o/Si_o	Fe_o/Fe_d	Allophane/ imogolite (%)
EUR01	Ap	0–16									
	Bw1	16–54	-	0.7	-	0.5	0.3	0.1	6.3	0.4	0.5
	Bw2	54–95	-	0.7	-	0.4	0.3	0.2	2.3	0.4	1.3
	BC	95–120/130	-	0.7	-	0.4	0.3	0.3	1.6	0.4	1.7
	2C	>120/130									
EUR02	O	0									
	Ah	0–3/6	1.4	1.6	1.8	1.2	0.5	0.4	3.1	0.3	4.8
	Bw	03/06/2026									
	BC1	26–31/51	0.5	1.2	2.2	0.4	0.2	0.2	2.2	0.2	1.4
	BC2	31–51/71	0.6	1.5	2.4	0.4	0.2	0.1	4.2	0.1	1.2
	C1	71–93	0.6	1.6	2.5	0.4	0.2	0.4	1.3	0.1	2.0
EUR03	O	2									
	Ah1	0–22	4.6	3.6	2.1	6.5	1.2	2.2	3.0	0.3	26
	Ah2	22–48									
	2AB	48–70	3.7	1.7	1.8	7.8	1.4	3.8	2.1	0.8	27
	2Bw1	70–98	3.7	1.4	2	9.9	1.1	5.5	1.8	0.8	39
	2Bw2	98–127	4.2	1.5	3	8.8	1.4	5.7	1.5	0.9	40
EUR04	O	0–2	-	1.5	-	2.8	1.1	2.1	1.3	0.7	15
	Ah1	2–10	-	2.4	-	6.2	1.1	0.8	8.2	0.5	11
	Ah2	10–27	-	2.5	-	7.2	1.3	2.9	2.4	0.5	21
	Ah3	27–45	-	2.5	-	6.4	1.1	3.6	1.8	0.4	25
	Bw1	45–72	-	1.3	-	6.4	0.7	3.7	1.7	0.5	26
	Bw2	72–107/142	-	1.1	-	5.8	0.7	3.1	1.9	0.6	22

X-ray analysis of the clay fraction reveals in profile EUR02 a broad reflection centred at 0.79 nm, indicating a small amount of poorly ordered 0.7 nm halloysite in the Bw and BC1 horizons (Figure 11). The clay fractions show clear strong reflections of sanidine at 0.377, 0.324 and 0.299 nm, which are apparently higher in the Ah horizon (Wilson 1987). In the bottom horizons, zeolites (phillipsite and analcime) are identified by the 0.713 nm and 0.560 nm reflections. The clay fraction of EUR02 shows badly resolved reflections of secondary minerals that clearly indicate a low degree of crystallinity. Diffuse, broad reflections at about 0.44 and 0.32 nm reflect the presence of pyroclastic glass. Violante and Wilson (1983), Adamo et al. (2001) and Vacca et al. (2003) found the same set of clay minerals in soils formed from volcanic materials with different chemical compositions in the Roccamonfina district, which is also part of the Lazio - Campanian volcanic province. This suggests that the chemical composition of the volcanic parent materials does not very much affect the crystalline weathering products.

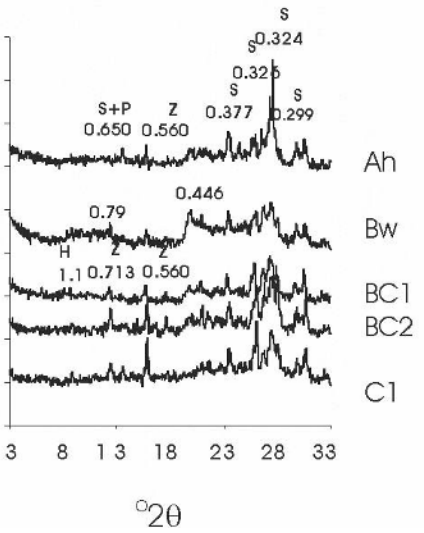

Figure 11. X-ray diffraction pattern (Cu-Kα) of randomly oriented clay fraction (<2 μm) of Pedon EUR02 from Gauro Volcano. H = halloysite, L = leucite, P = plagioclase, S = sanidine, Z = zeolite.

X-ray patterns of the EUR03 and EUR04 clay fraction are similar for both the studied pedons (Figures 12ab). They are generally poorly resolved because of the abundance of allophane (Table 5). Small reflection of hydrated halloysite at 1 nm together with those of sanidine and leucite and minor amounts of zeolite minerals are detected in all horizons. Leucite is easily identified by its 0.344 nm reflection, principally in the EUR04 pedon (Figure 12b). Formation of hydrated halloysite in all horizons appears to be related to weathering of leucite (Quantin et al. 1988). The differential

X-ray diffraction (DXRD) diagrams obtained by subtracting the pattern of the ammonium oxalate-treated clay from the pattern of the untreated clay indicate that allophane is present in the 2AB and BW2 horizons of the EUR03 profile. The DXRD shows broad reflections at 0.33 and 0.22 nm (Figure 13) of poorly ordered aluminosilicates (Dahlgren 1994).

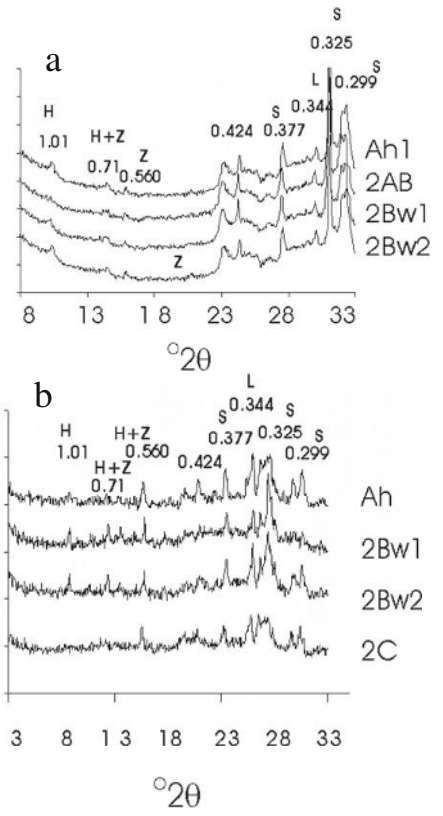

Figure 12. X-ray diffraction pattern of randomly oriented clay fraction (<2 μm) of the of the EUR03 profile (Co-Kα) (a) and of EUR04 (Cu-Kα) (b) from Vico Volcano. H = halloysite, L= leucite, S= sanidine, Z = zeolite.

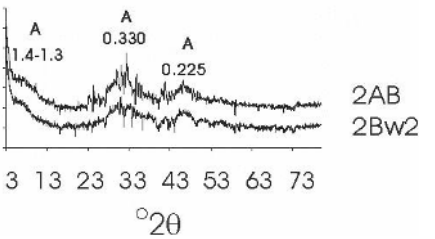

Figure 13. Differential X-ray diffraction pattern (DXRD) Cu-Kα radiation from the untreated and oxalate treated clay fraction. 2AB and 2Bw2 horizon of EUR03 profile. A = allophane.

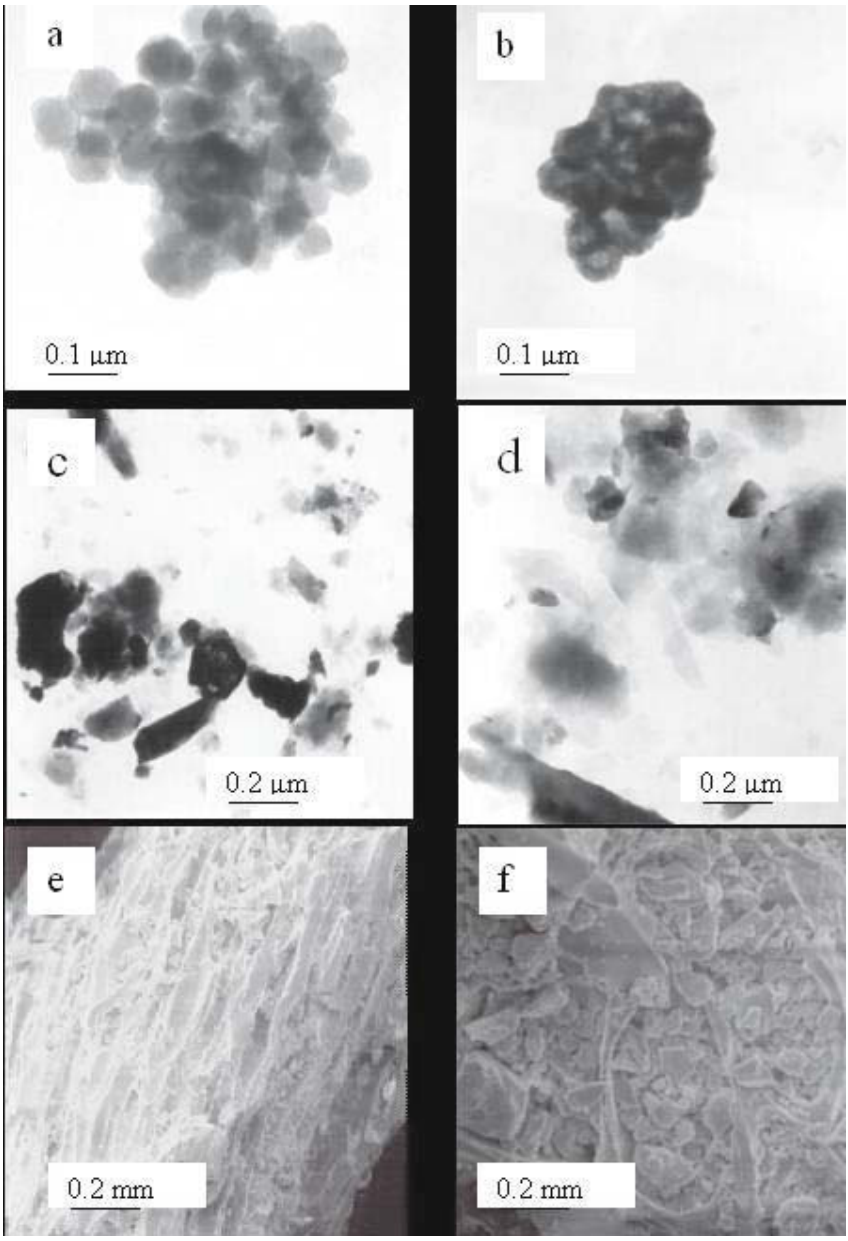

Figure 14. TEM of the clay (a–d) and SEM of the sand fraction (e & f) of selected horizons of EUR02: (a) and (b) aggregates of spherical shaped particles of allophane; (c) and (d) aggregates of C1 horizon showing amorphous material without any specific crystal morphology; (e) and (f) SEM of the sand fraction of the same horizon showing the weathered surface with cavities of vesicular pumice.

Transmission electron microscopy (TEM) confirms the results obtained by selective dissolution and XRD analysis. The Gauro profiles show poorly expressed spherical particles surrounded by apparently amorphous material without any specific crystal morphology, as commonly observed in volcanic ash soils (Figures 14abcd). In the Vico profiles (EUR03) some particles show a fibrous morphology specific of imogolite, varying in diameter from 5 to 15 nm and extending up to several micrometers in length (Figure 15a) Spheroidal particles (about 100 nm wide) (Figure 15c) and aggregates of particles without any specific crystal morphologies of allophane with lengths of 50 to 100 nm (Figures 15bd) are also found. The poorly expressed aggregate shapes are consistent with the DXRD patterns that show significative amount of poorly ordered alumino-silicates (Dahlgren 1994).

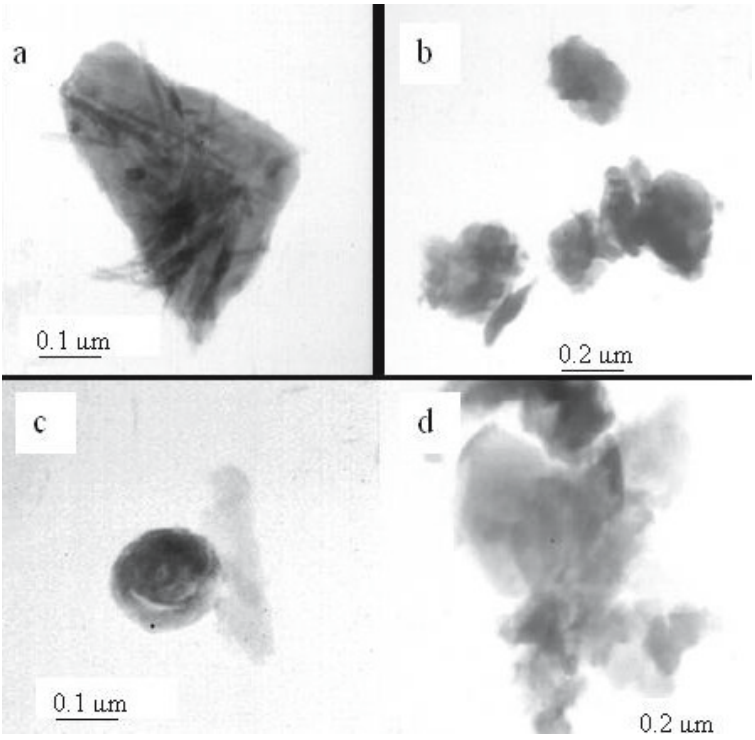

Figure 15. TEM of the clay fraction of selected horizons of EUR03: (a) subspherical shaped particles of halloysite and amorphous material without any specific crystal morphology; (b)(c) aggregate of fibrous imogolite in the A1 horizon; (d) aggregates of poorly ordered particles of allophane in the AB horizon.

Conclusion

The pedogenic environment of the studied soils is especially complex because of the heterogeneity of the stratified pyroclastic materials. If such stratification is a general condition in many volcanic areas (such as in the soils from Tenerife and Azores described in this book), it hardly produces very different pedogenic scenarios, at least in the analysed case studies. Other factors such as duration of pedogenesis, human impact and soil climate appear to play a much more important role.

The four profiles show different degrees of soil development, ranging from very young (EUR02) to moderately weathered (EUR03). Despite such differences, all the soils exhibit common features such as the pedogenic redistribution of fine material (mainly silt coatings). This process seems very important and is possibly underestimated in research on volcanic soils, but further research is needed to ascertain whether this process is an in situ reorganisation and/or illuviation process, or possibly a of primary (geogenic) coating formed during the ash deposition.

Pedogenesis in Campania district (Phlegraean Fields), in an ustic pedoclimate, appears to depend primarily on duration and secondly on the kind of pyroclastic material. In the deep and porous soils formed from younger volcanic ash, one of the most important pedogenic process is the formation of low amounts of short-range aluminosilicates with the development of non-allophanic soils. XRD and optical data of the sand fraction prove the vitreous nature of the parent materials of the Gauro volcano, which is more expressed in EUR01 than in EUR02. This can be explained by the combination of an abundance of pumice, fragment of scoria, and unconsolidated tuffs together with incipient weathering. Rapid weathering of biotite and sanidine in Ap horizons might be related to a more porous and more permeable soil structure. From a mineralogical viewpoint, the Gauro soils consist mainly of primary minerals, glass (30–50%) with minor amounts of allophane and zeolites. The presence of zeolites even in the fine clay fractions indicates a young stage of weathering. The negligible halloysite content points to both (i) young pedogenesis and (ii) a strongly leaching environment with high desilication (Parfitt et al. 1984, Parfitt and Wilson 1985, Wada 1989, Ugolini and Dahlgren 1991). In the Gauro profiles the small amount of allophane in the clay fraction could also be related to (i) a young pedoenvironment and (ii) a strong drainage that removes Si from the soil solution limiting the neogenesis of short-range-order aluminosilicate minerals (Parfitt et al. 1984, Parfitt and Wilson 1985, Violante and Wilson 1983). The leaching of relative mobile cations (Na, K, Mg, and Ca) and Si results in a higher Si and bases content in the interior of the pumice

and a decrease of Si and bases with respect to Fe and Mn towards the exterior of the pumice. In the Gauro soils, the loss of bases during leaching could be continuously compensated by the steady supply of bases from weathering of zeolites, glass and other minerals. This provides a chemical environment that could prevent the formation of poorly ordered aluminosilicates. In such an environment, a very contrasting micromorphological soil feature was found: the presence of a horizontal layer of crystalline clay coatings in the C horizon of EUR02, related to a discontinuity in microstructure. It is important to notice that the crystalline clay, although clearly visible in thin section, represents too small a quantity to be detected by standard XRD techniques. This emphasises (i) that the bulk sample is usually larger than the representative elementary volume (REV concept, Bear 1972) and this may results in an inappropriate sampling and analysing scheme, and (ii) that many analytical tools (i.e. XRD) have severe detection limits for small quantities of minerals. As a result, a fine layer of clay coatings, which may be very important for the functioning of an ecosystem (e.g. water movement, water availability, CEC, etc.) is easily overlooked.

The formation of soils in the Latium district (Vico volcano) is characterized by neogenesis of poorly ordered aluminosilicates (allophane and imogolite), ferrihydrite and a few crystallized clay minerals. The EUR03/04 pedons have formed in an udic pedoclimate on trachytic leucititic lava and on consolidated tuffs that are older, less porous, and less permeable than ash. The volcanic glass content is very low in these soils because of its low content in the parent rock and the long period of pedogenesis. Selective dissolution and micromorphological data indicate that the Vico profiles are characterized by short-range aluminosilicate minerals in the fine fraction mainly derived by the weathering of leucite, as indicated by previous research (Quantin et al. 1985, 1988, Quantin and Lorenzoni 1992, Lorenzoni et al. 1995). As compared to the Gauro soils, the less permeable environment is likely to increase the Si concentration in the soil solution and in this condition halloysite may form (Violante and Wilson 1983, Parfitt and Wilson 1985, Parfitt and Kimble 1989, Shoji et al. 1993). The same set of clay minerals has been observed in soils formed from volcanic materials with different bulk chemical compositions in other areas of the Roman and Campanian volcanic provinces (Lorenzoni et al. 1995, Vacca et al. 2003). Leucite seems to play an important role in this pedoenvironment because its weathering makes aluminum easyly available stimulating the formation of short-range-order aluminosilicate minerals.

Analysing the factors of pedogenesis determining the limited allophane formation in the Gauro soils (EUR01/02) in comparison to the more allophanic Vico soils (EUR03/04), it can be concluded that rather than topog-

raphy (similar volcanic slope), vegetation (woodland in 3 soils) and parent material, the main factors responsible for the different allophane content, and therefore for the soil type, are the duration of pedogenesis (too short in Gauro), the degree of human disturbance (too high in Gauro) and the climate (ustic in Gauro and udic in Vico). The other differences observed between the EUR01-EUR02 Gauro soils and EUR03-EUR04 Vico soils can be related to smaller differences (i) in parent material (different layering) and (ii) in land use. All these factors may have played a significant role in determining the various mineralogical trends.

Acknowledgments

We are grateful to the anonymous referees for interesting and helpful discussion of the results. Thanks are due to Dr. Lucia Maiuro (CSIM) of Molise University for her valuable assistance with the scanning electron microscope (SEM) and energy dispersive spectroscopic analyses (EDS). This paper was financially supported by FAR (Fondo per la ricerca di Ateneo) of Molise University.

References

Adamo P, Violante P, Wilson MJ (2001). Tubular and spheroidal halloysite in pyroclastic deposits in the area of the Roccamonfina volcano Southern Italy. Geoderma 99:295–316

Barberi F, Buonasorte G, Cioni R, Fiordelisi A, Foresi L, Iaccarino S, Laurenzi MA, Sbrana A, Vernia L, Villa IM (1994). Plio-Pleistocene geological evolution of the geothermal area of Tuscany and Latium. Mem Descr Carta Geol It 49:77–134

Barbieri M, Peccerillo A, Poli G, Tolomeo L (1988). Major, trace element and Sr isotopic composition of lavas from Vico volcano central Italy and their evolution in an open system. Contrib Mineral Petrol 99:485–497

Bear J (1972). Dynamics of fluids in porous media. New York, Dover

Bidini D, Dabin B, Lorenzoni P, Lulli L, Quantin P, Raglione M (1984). The soils of Vico, an extinct volcano to the north of Rome, an example of the most typical italian pedogenesis on volcanic materials. Comun Congr Int Suelos Volcanicos, Dep Edaf, Univ La Laguna, Tenerife (Islas Canarias). Ser Inf 13:334–340

Birkeland PW (1999). Soils and Geomorphology, 3rd edn. Oxford University Press, Oxford, p 430

Brindley GW, Brown G (1980). Crystal Structures of Clay Minerals and their X-ray Identification. Mineralogical Society, London, pp 41–406

Buurman P, van Lagen B, Velthorst EJ (eds) (1996). Manual for Soil and Water Analysis. Backhuys Publishers, Leiden, The Netherlands, p 314

Buurman P, García Rodeja E, Martínez Cortizas A, van Doesburg JDJ (2004). Stratification of parent material in European volcanic and related soils studied by laser-diffraction grain-sizing and chemical analysis. Catena 56:127–144

Dahlgren RA (1994). Quantification of Allophane and Imogolite. Quantitative Methods in Soil Mineralogy. SSSA miscellaneous Publication, S.S.S.A., Madison, WI, pp 430–450

Dahlgren RA, Ugolini FC (1991). Distribution and characterisation of short-range-order minerals in Spodosols from the Washington Cascades. Geoderma 48:391–413

de' Gennaro M, Cappelletti P, Langella A, Perrotta A, Scarpati C (2000). Genesis of zeolites in the Neapolitan Yellow Tuff: geological, volcanological and mineralogical evidences. Contr Mineral Petrol 139:17–35

De Vivo B, Rolandi G, Gans PB, Calvert A, Bohrson WA, Spera FJ, Belkin AE (2001). New constraints on the pyroclastic eruption history of the Campanian volcanic plain (Italy). Mineral Petrol 73:47– 65

Di Vito MA, Isaia R, Orsi G, Southon J, de Vita S, D'Antonio M, Pappalardo L, Piochi M (1999). Volcanism and deformation in the past 12 ka at the Campi Flegrei caldera (Italy). J Volcanol Geotherm Res 91:221–246

Finke PA, Mucher HJ, Witter JV (1991). Reliability of point counts of pedological properties on thin sections. Soil Science 151:249–253

FitzPatrick EA (1984). Micromorphology of Soils. Chapman and Hall, London, pp 433

Jackson ML (1974). Soil chemical analysis. Advanced Course, 2nd edn. M.L. Jackson, Madison, WI

Lorenzoni P, Mirabella A, Bidini D, Lulli L (1995). Soil genesis on trachytic and leucitic lavas of Cimini volcanic complex (Latium, Italy). Geoderma 68:79–99

Lulli L, Bidini D (1978). Guida alla escursione dibattito sui suoli dei vulcani Roccamonfina e Vulture. (In Italian). Centro Gen Class Cart Suolo, CNR, Univ Firenze. Pubbl 51. CNR, Firenze, Italy

Lulli L, Bidini D, Quantin P (1988). A climo and litho soil-sequence on the Vico volcano (Italy). Cah ORSTOM Ser Pedol 24:49–60

Malucelli F, Terribile F, Colombo C (1999). Mineralogy, micromorphology and chemical analysis of andosols on the Island of Sao Miguel (Azores). Geoderma 88:73–98

Mehra OP, Jackson ML (1960). Iron oxide removal from soils and clays by dithionite-citrate systems buffered with sodium bicarbonate. 7th Nat Conf Clay Minerals, pp 317–327

Murphy CP, Kemp RA (1984). The over-estimation of clay and under-estimation of pores in soil thin sections. Journal of Soil Science 35:481–495

Parfitt RL (1990). Allophane in New Zealand – A review. Aust J Soil Res 28:343–360

Parfitt RL, Saigusa M, Cowie JD (1984). Allophane and halloysite formation in a volcanic ash bed under different moisture conditions. Soil Sci 138:360–364

Parfitt RL, Wilson AD (1985). Estimation of allophane and halloysite in three sequences of volcanic soils, New Zealand. In: Fernandez Caldas E and Yaalon DH (eds) Volcanic soils. CA-TENA Suppl. 7. Braunschweig. Catena Verlag, Desdedt, Germany, pp 1–8

Parfitt RL, Kimble JM (1989). Conditions for formation of Allophane in soils. Soil Sci Soc Am J 53:971–977

Quantin P, Dabin B, Bouleau A, Lulli L, Bidini D (1985). Characteristics and genesis of two Andosols in Central Italy. In: Fernandez Caldas E and Yaalon DH (eds) Volcanic soils. CATENA Suppl 7. Braunschweig. Catena Verlag, Desdedt, Germany, pp 107–117

Quantin P, Gautheyoru J, Lorenzoni P (1988). Halloysite formation through in situ weathering of volcanic glass from trachytic pumices, Vico's volcano, Italy. Clay Miner 23:423–437

Quantin P, Lorenzoni P (1992). Weathering of leucite to clay minerals to tephrite of the Vico volcano. Miner Petrog Acta 35:289–296

Rosi M, Sbrana A (1987). The Phlegraean Fields. CNR Quad. Ricerca Sci 114:1–175

Scandone R, Bellucci F, Lirer L, Rolandi G (1991). The structure of the Campanian Plain and the activity of the Neapolitan volcanoes (Italy). J. Volcanol Geotherm Res 48:1–31

Schwertmann U (1964). Differenzierung der Eisenoxide des Bodens durch Extraktion mit Ammoniumoxalat-losung. Z Pflanzenernahr Dung Bodenk 105:194–202

Shoji S, Nanzyo M, Dahlgren RA (1993). Volcanic ash soils: Genesis, properties and utilization. Developments in Soil Science 21. Elsevier, Amsterdam, p 288

Sollevanti F (1983). Geologic, volcanologic and tectonic setting of the Vico-Cimino area, Italy. J Volcanol Geotherm Res 17:203–217

Stoops G (2003). Guidelines for the Analysis and Description of Soil and Regolith Thin Sections. SSSA. Madison, WI, p 184 + CD

Stoops G, FitzPatrick EA, Gérard M (2006). Micromorphological description of thin sections of volcanic ash soils of COST-622 reference profiles. In: Arnalds O, Bartoli F, Buurman P, Garcia-Rodeja E, Oskarsson H, Stoops G (eds) Soils of Volcanic Regions of Europe. Springer Verlag (in preparation)

Stoops G, Van Driessche A (2006). Mineralogy of the sand fraction. Results and problems. In: Arnalds O, Bartoli F, Buurman P, Garcia-Rodeja E, Oskarsson H, Stoops G (eds) Soils of Volcanic Regions of Europe. Springer Verlag (in preparation)

Ugolini FC, Dahlgren RA (1991). Weathering environments and occurrence of imogolite/allophane in selected Andisols and Spodosols. Soil Sci Soc Am J 55:1166–1171

Vacca A, Adamo P, Pigna M, Violante P (2003). Genesis of Tephra-derived Soils from the Roccamonfina Volcano, South Central Italy. Soil Sci Soc Am J 67:198–207

Violante P, Wilson MJ (1983). Mineralogy of some Italian Andosols with special reference to the origin of the clay fraction. Geoderma 29:157–174

Wada K (1985). The distinctive properties of Andosols. Advances of Soil Science, vol. 2. Springer-Verlag, New York 2:173–228
Wada K (1989). Allophane and imogolite. In: Dixon JB and Weed SB (eds) Minerals in Soil Environments, 2nd edn – SSSA Book Series, no.1. Madison, WI, pp 1051–1087
Wilson MJ (1987). A Handbook of determinative methods in clay mineralogy. Blackie and Son Ltd. Glasgow, pp 308

Classification of the Reference Pedons: World Reference Base for Soil Resources and Soil Taxonomy

P. Quantin and O. Spaargaren

Introduction

The soil classification systems used are the *World Reference Base (WRB) for Soil Resources* (Driessen et al. 2001) and the USDA *Keys to Soil Taxonomy* (Soil Survey Staff 2003); in addition the French pedons EUR16 & 17 have also been classified according to the *Référentiel Pédologique Français* (AFES 1995). WRB is currently under revision, including the Andosols. In the discussion attention will be given to the proposed revisions in WRB (FAO-ISRIC-IUSS, *in preparation*), in particular to the new diagnostic criteria for the andic, vitric, and fulvic horizons, which provide better correlation with Soil Taxonomy.

The Reference Pedons of European Volcanic Soils are mostly Andosols (WRB, RPF) or Andisols (ST). However, in Greece Regosols (WRB) or Entisols (ST) occur, whereas in Hungary Phaeozems and Umbrisols (WRB) or Haploxerolls and Haploxerepts (ST) are found.

The Andosol classification for the French 'Référentiel Pédologique' and the World Reference Base for Soil Resources are fairly well correlated, at least at the higher levels. The WRB draft, after a first presentation to the 15th World Congress of Soil Science (Quantin 1994), and some remarks by Shoji et al. (1996), some adjustments were made by Berding (1997) for the first edition (FAO-ISRIC-ISSS 1998); then it was revised (Driessen et al. 2001). But after remarks of some COST Action 622 contributors and recent 'proposed revisions' of Takahashi et al. (2004), the definitions of diagnostic horizons Andic/Vitric and Fulvic/Melanic are currently under revision (FAO-ISRIC-IUSS in preparation), in view of a better correlation with the Soil Taxonomy.

The definition of Andosols (AFES 1995, Driessen et al. 2001) or Andisols (Soil Survey Staff 2003) is essentially based upon 'andic soil properties', briefly: - for the Andic horizon: $Al_o + ½Fe_o$ at least 2%, P-retention at least 70% (in <2 mm fraction), and bulk density at most 0.9 g dm^{-3}; - for the Vitric horizon: $Al_o + ½Fe_o$ of 0.4–2% and a P-retention of at least 25%. In addition, WRB requires for a Vitric horizon a volcanic glass content of

at least 10%, whereas the Andic horizon should have less than 10% volcanic glass, as well as 10% or more clay.

Contrary to Soil Taxonomy, WRB and RPF do not use soil moisture and soil temperature regimes, such as aquic, cryic, udic, ustic, xeric, etc., as dividing criteria at the suborder level. WRB recognises only two levels: the Major Reference Group (MRG) level and the qualifier level (FAO-ISRIC-IUSS 1998, Nachtergaele et al. 2002). Each MRG has its own ranked listing of qualifiers. In Andosols the list of qualifiers is headed by Vitric, Silandic and Aluandic, which correlate in RPF with Vitrisol, Silandosol and Aluandosol. Then follow characteristics typical of Andosols, viz. Eutrisilic, Melanic, Fulvic and Hydric. The list is completed by qualifiers as Histic, Mollic, Umbric, Placic, Pachic, etc. If buried diagnostic horizons occur, like Melanic or Mollic, the modifier Thapto may be used, e.g. Thaptomelanic or Thaptomollic. WRB also offers the opportunity to use modifiers to indicate the position of certain horizons in the soil, e.g. Epi- for an occurrence within 50 cm from the soil surface, and Endo- for a presence between 50 and 100 cm depth, or to indicate weak or strong development (Hypo- or Hyper-).

Methods and materials

The Reference Pedons of European Volcanic Soils have been described in the field according to the Guidelines for Soil Description (FAO-ISRIC 1990). The accompanying samples were distributed, after homogenisation, amongst six laboratories participating in the COST 622 Action (Gödöllö, Lisbon, Nancy, Santiago de Compostella, Tenerife and Wageningen). Each laboratory analysed a specific set of characteristics of importance for studying and understanding Andosols.

The following characteristics are used in the classification and subdivision of Andosols (WRB) or Andisols (ST):

- Clay content (WRB: to identify the andic horizon);
- Bulk density (WRB, ST);
- Acid oxalate extractable aluminium and iron (WRB, ST);
- Acid oxalate extractable silicon (WRB: to discriminate between Silandic and Aluandic Andosols);
- Phosphate retention (WRB, ST);
- Volcanic glass content of the fine earth fraction (WRB);
- Moisture content (WRB, ST);
- Organic C and melanic index (WRB, ST);
- ECEC (WRB, ST: to identify Acroxic/Acrudoxic qualifiers/subgroups);

- Sum of exchangeable bases (ST: to identify Eutric subgroups);
- Thickness of the horizons (WRB) or layers with andic properties (ST).

As some laboratories analysed the same characteristics (e.g. clay content by Nancy and Wageningen, moisture content by Lisbon and Santiago, organic C by Santiago, Lisbon and Nancy, P-retention by Tenerife and Lisbon, acid oxalate extractable Al, Fe and Si by Santiago and Nancy), it was necessary, for reasons of comparison and correlation, to select from the duplicate/triplicate data sets one to be used in the soil classification exercise.

Nancy used samples different from the other laboratories (pers. comm. Buurman), therefore only their bulk density data have been used. For the other duplicate analytical data, the following data sets were selected, also taking into account the analytical methods required for classification purposes – for WRB the "Procedures for Soil Analysis" (Van Reeuwijk 2002), for Soil Taxonomy the "Soil Survey Laboratory Methods Manual" (USDA in press):

- Clay content: Wageningen;
- Oxalate extractable aluminium, iron and silicon: Santiago;
- Phosphate retention: Lisbon, because all samples were analysed in contrast to the data set from Tenerife, which contains data of only part of the samples;
- Moisture content: Lisbon, because all samples were analysed in contrast to the data set from Santiago, which contains data of only part of the samples;
- Organic C: Santiago, because all samples were analysed in contrast to the data set from Lisbon, which contains data of only part of the samples.

Mineralogical data, in particular the volcanic glass content, are available only for the profiles EUR 01 to 12. It should be noted that the mineralogical analysis comprised the fractions 50–250 and 250–500 μm, not the entire fine earth fraction as required for the WRB classification.

Where textural requirements had to be considered, e.g. for establishing a cambic horizon according to WRB 2001, the field assessment has been taken as the particle size distribution data for sand, silt and clay are incomplete, or derived using other methods than prescribed.

Results and discussion

The following classifications of the Reference Pedons are based on the World Reference Base for Soil Resources (Driessen et al. 2001) and the Ninth Edition of the Keys to Soil Taxonomy (Soil Survey Staff 2003). In addition, the two French Reference Pedons have been classified according to the Référentiel Pédologique Français (AFES 1995).

For WRB a comparison will be made of the present classification and the proposed revisions (FAO-ISRIC-IUSS in preparation), to test their applicability and usefulness.

Classification according to WRB 2001, Soil Taxonomy 2003, and RPF 1995

Italy

EUR01:

WRB (2001): ochric horizon (0–16 cm); no cambic horizon because of loamy sand texture between 16 and 95 cm and only weakly developed soil structure (WRB 2001 requires for a cambic horizon a texture of sandy loam or finer, and at least moderately developed soil structure); no andic or vitric horizon ($Al_o + ½Fe_o$ <0.4, phosphate retention <25%); humic (mean org. C is 1.38% between 0 and 50 cm depth); tephric soil material; eutric (BS >50%; ESP <6); no Arenosol because of sandy loam texture in the surface horizon:

Humi-Tephric Regosol (Eutric)

ST (2003): ochric epipedon (0–16 cm); cambic horizon (16–95 cm); no andic soil properties (phosphate retention <25%); $[(Al_o + ½Fe_o) \times 60] +$ % volcanic glass content ≥30; less than 35% rock fragments and loamy fine sand or coarser texture in the particle-size control section (25–100 cm); glass content assumed to be 30% or more in the 0.02–2.0 mm fraction (26–44% in 0.5–0.25 mm, 58–80% in 0.05–0.25 mm); xeric soil moisture regime; thermic soil temperature regime:

Ashy, glassy, thermic Vitrandic Haploxerept

EUR02:

WRB (2001): ochric horizon (0–3/6 cm); cambic horizon (3/6–25 cm); no vitric horizon (only 0–26 cm fulfils the requirements, but is too thin to be a vitric horizon, which requires 30 cm thickness); mean org. C most likely

>1% between 0 and 50 cm; BS >50%; ESP below 25 cm between 6 and 15:

Hyposodi-Humic Cambisol

ST (2003): ochric epipedon (0–3/6 cm); cambic horizon (3/6–25 cm); andic soil properties (0–26 cm); no Andisol, because only 43% of the soil within 60 cm have andic soil properties (requirement is 60% or more); $[(Al_o + ½Fe_o) \times 60]$ + % volcanic glass content ≥30; glass content assumed to be 30% or more in the 0.02–2.0 mm fraction (15–32% in 0.5–0.25 mm, 50–68% in 0.05–0.25 mm); xeric soil moisture regime; mesic soil temperature regime:

Ashy, glassy, mesic Vitrandic Haploxerept

EUR03:

WRB (2001): melanic horizon (0–43 cm; MI 1.64–1.65; sufficient org. C according to Santiago figures (mean org. C 6.5%); andic horizon (0–125 cm); mean Si_o 1,46% (Santiago figures); BS <50% but >20% in all parts between 50 and 100 cm, near 50% in top soil (2–50 cm):

Melani-Silandic Andosol (Dystric)

ST (2003): melanic epipedon (0–43 cm; MI 1.64–1.65; sufficient org. C according to Santiago figures); andic soil properties (0–125 cm); mean Si_o 1.46%, mean Fe_o 0.42 between 0 and 100 cm depth, 8x Si_o + 2x Fe_o >5, 8x Si_o >2x Fe_o (Santiago figures); sum of bases <25 cmol kg^{-1} between 25 and 75 cm; udic soil moisture regime; mesic soil temperature regime:

Ashy, amorphic, mesic Typic Melanudand

EUR04:

WRB (2001): melanic horizon (8–43 cm; MI 1.43–1.59; organic C >6%); andic horizon (0–105 cm); mean Si_o 1.65%; BS <50% in at least some part between 20 and 100 cm, but >20% in all parts between 20 and 100 cm:

Melani-Silandic Andosol (Dystric)

ST (2003): melanic epipedon (8–43 cm; MI 1.43–1.59; organic C >6%); andic soil properties (0–105/140 cm); mean Si_o 1.65%, mean Fe_o 0.71% between 0 and 100 cm, 8x Si_o + 2x Fe_o >5, 8x Si_o > 2x Fe_o (Santiago figures); sum of bases <25 cmol kg^{-1} between 25 and 75 cm; udic soil moisture regime; mesic soil temperature regime:

Ashy, amorphic, mesic Pachic Melanudand

Azores

EUR05:

WRB (2001): ochric horizon (0–10 cm); the buried soil between 30 and 90 cm depth does not have a buried umbric horizon because colour between 45 and 65 cm has a too high value for umbric (7.5 YR 4/3, moist); andic horizon (0–145 cm); Si_o >0.6% between 30 and 100 cm; ECEC <2 cmol kg^{-1} between 45 and 65 cm and between 90 and 110 cm, totalling exactly the 30 cm required within 1 m depth for the Acroxic qualifier; BS <20% throughout:

Acroxi-Silandic Andosol (Hyperdystric)

ST (2003): ochric epipedon (0–25 cm); andic soil properties (0–145 cm); mean Si_o 1.16%, mean Fe_o 1.23% between 0 and 100 cm, 8x Si_o + 2x Fe_o >5, 8x Si_o > 2x Fe_o (Santiago figures); BS <20% in all parts; ECEC <2 cmol kg^{-1} between 45 and 65 cm and between 90 and 110 cm, totalling exactly the required 30 cm between 25 and 100 cm depth; udic soil moisture regime; mesic soil temperature regime:

Medial, amorphic, mesic Acrudoxic Hapludand

EUR06:

WRB (2001): umbric horizon (0–35/40 cm); no melanic horizon (MI >1.7); no fulvic horizon because of too high colour value; no buried fulvic horizon either because of too high colour value; andic horizon (0–140 cm); Si_o >0.6% between 0 and 100 cm; hydric, moisture content more than 200% between 35 and 100 cm; ECEC <2 cmol(+) kg^{-1} fine earth between 70 and 100 cm; BS <20% throughout:

Hydri-Silandic Andosol (Umbric and Acroxic)

ST (2003): umbric epipedon (0–35/40 cm), depth, thickness and organic-carbon requirements for the melanic epipedon are met; MI >1.7; buried fulvic horizon (60–100 cm), however, colour value remains the same compared to the overlying horizons and the organic C content decreases regularly with depth; andic soil properties (0–140 cm); moisture content more than 200% between 35 and 100 cm; ECEC <2 cmol(+) kg^{-1} fine earth between 70 and 100 cm; 8x Si_o + 2x Fe_o >5; 8x Si_o > 2x Fe_o, except in the first two horizons (covering 0–30 cm) according to Wageningen/Nancy figures; udic soil moisture regime; mesic soil temperature regime:

Hydrous, amorphic, mesic Acrudoxic Hydrudand[1]

[1] The combination of Hydrous and Hydrudand does not seem to be excluded in Soil Taxonomy.

Iceland

EUR07:

WRB (2001): no histic or folic horizon (org. C content less than 20%); vitric horizon between 5 and 90/100 cm (P-retention >80%; Al_o + ½Fe_o >2.0; BD <0.9, throughout); no andic horizon because of too high volcanic glass content; BS <50% between 17 and 90/100 cm throughout:

Orthidystri-Vitric Andosol

ST (2003): no histic or folistic horizon (org. C content less than 20%); andic soil properties between 0 and >90/100 cm; 8x Si_o + 2x Fe_o >5, 8x Si_o > 2x Fe_o, except for AC (17–35/50 cm); 0–35/50 cm fulfils depth, thickness and organic carbon requirements for a melanic epipedon, but not the colour requirement; Al (KCl) <2.0 cmol(+) kg^{-1}; udic soil moisture regime; cryic soil temperature regime:

Ashy, amorphic Eutric Pachic Fulvicryand

EUR08:

WRB (2001): ochric horizon (O + Ah1 + Ah2 too thin to constitute together a mollic horizon); no andic horizon (too high glass content between 21/27 and 59/62 cm) starting within 25 cm; vitric horizon at least between 21/27 and 59/62 cm; no cryic horizon assumed between 26/34–37/42 cm despite cryoturbation features ((soil) temperature >0°C); BS <50% in some part between 20 and 100 cm (47% between 37/42–59/62 cm):

Dystri-Vitric Andosol

ST (2003): ochric epipedon (O + Ah1 + Ah2 too thin to constitute together a mollic horizon); andic soil properties (0– >59/62 cm); moisture content less than 15% throughout; no permafrost or gelic materials within 100 cm; 8x Si_o + 2x Fe_o >5, 8x Si_o > 2x Fe_o; udic soil moisture regime, cryic soil temperature regime:

Ashy, amorphic Typic Vitricryand

EUR09:

WRB (2001): umbric horizon (0–55 cm); vitric horizon (0–55 cm; no sufficient volcanic glass data, but assumed to be more than 10%); histic and vitric horizon (60–95 cm); no cryic horizon assumed between 0 and 55 cm despite cryoturbation features (soil temperature >0° C):

Thaptohisti-Vitric Andosol (Umbric and Pachic)

ST (2003): umbric epipedon (0–55 cm; fulfils depth, thickness and organic carbon requirements for a melanic epipedon, but not colour; MI=1.86); andic soil properties (0–100 cm); buried organic soil material (>18% org.

C, with fibric macrostructure and andic properties) between 60 and 95 cm; 8x Si_o + 2x Fe_o >5, 8x Si_o > 2x Fe_o; Al (KCl) <2.0 cmol(+) kg^{-1}; udic soil moisture regime; cryic soil temperature regime:

Ashy, amorphic Eutric Pachic Fulvicryand

Tenerife

EUR10:

WRB (2001): umbric horizon (0–40/50 cm); andic horizon (0–85/90 cm) vitric horizon (85/90–220 cm); Si_o >0.6%; BS <50% between 15 and 100 cm throughout and <20% between 40 and 100 cm:

Umbri-Silandic Andosol (Hyperdystric)

ST (2003): umbric epipedon (0–40/50 cm); andic soil properties (0–220 cm); 8x Si_o + 2x Fe_o >5, 8x Si_o > 2x Fe_o; water retention <15% in the Ah (0–40 cm); udic soil moisture regime; mesic soil temperature regime:

Ashy, amorphic, mesic Humic Udivitrand

EUR11:

WRB (2001): ochric horizon (0–10 cm); vitric horizon (0→55 cm); 50 and >70% coarse fragments; BS >50%, but <80% throughout:

Skeleti-Vitric Andosol (Orthieutric)

ST (2003): ochric epipedon (0–10 cm); andic soil properties (0→55 cm); more than 35% pumice-like (basalt lapilli) coarse fragments; more than 70% glass in 0.05–0.5 mm fraction; xeric soil moisture regime, mesic soil temperature regime:

Ashy-pumiceous, glassy, mesic Typic Vitrixerand

EUR12:

WRB (2001): umbric horizon[2] (0–65 cm); vitric horizon (0–100/130 cm; Al_o + ½Fe_o vary from 0.7–1.5); BS <20% between 15/20 and 100 cm:

Umbri-Vitric Andosol (Pachic and Hyperdystric)

ST (2003): umbric epipedon (0–65 cm); andic soil properties (0→100/130 cm); glass content between 65 and 95% in 0.05–0.5 mm fraction; water retention <15 percent throughout 0/130 cm; BS <20% and Al KCl >2 cmol kg^{-1} between 15–120 cm; udic (perudic) soil moisture regime; mesic soil temperature regime:

Ashy, glassy, mesic Humic Udivitrand[3]

---

[2] Colour indication Ah2 15/20–65 cm is lacking but it is assumed to be dark enough to be umbric.

Greece

EUR13:

WRB (2001): ochric horizon (0–40 cm); vitric horizon (0–40 cm; >10% volcanic glass assumed; BD >0.9 kg dm^{-3}, but P-retention is 2–3% and Al_o + ½Fe_o is only 0.1%!); calcaric soil material (40– >100 cm); no Arenosol because of >35% coarse fragments between 0 and 40 cm; ESP below 40 cm >6:

Endocalcari-Vitric Andosol (Hyposodic)
(if >10% volcanic glass is assumed)

ST (2003): ochric epipedon (0–40 cm); no andic soil properties; Psamment because texture is assumed to be loamy fine sand or coarser in the particle-size control section (very fine sand fraction not determined, but it is unlikely that there is 50% or more very fine sand); glass content is not determined but is assumed to be 24%[4] or more; xeric[5] soil moisture regime; thermic soil temperature regime:

Ashy, mixed, calcareous, thermic Vitrandic Xeropsamment
(if volcanic glass content is 24% or more)

EUR14:

WRB (2001): ochric horizon (0–30 cm); no vitric horizon (BD <0.9 kg dm^{-3}, but P retention 1–3% and Al_o + ½Fe_o 0.1%); no Leptosol because of <90% coarse fragments between 0 and 30 cm; no Arenosol because of >35% coarse fragments between 7 and >30 cm; BS >80% throughout; ESP >6 throughout:

Skeleti-Tephric Regosol (Hyposodic)

ST (2003): ochric epipedon (0–30 cm); no Psamment because of >35% rock fragments in the particle-size control section (25–100 cm); less than 10% fine earth between 30 and >95 cm; glass content is not determined but is assumed to be 24%[4] or more; xeric soil moisture regime; thermic soil temperature regime:

Pumiceous, mixed, nonacid, thermic Vitrandic Xerorthent
(if volcanic glass content is 24% or more)

---

[3] An abrupt contact between Ah and Bw horizons, marked by a charcoal bed dated 9000 BP, suggests a recent ash-fall deposit on the Bw, although of the same basaltic composition. The abundance of halloysite in Bw and 2Bw explains the low values of P retention and Al_o + ½Fe_o, as well as high clay content and Al KCl >2 cmol kg^{-1}.

[4] Derived from the formula [(Al_o + ½Fe_o) × 60] + % volcanic glass ≥30.

[5] Pedogenic lime, high percentage of Na+ and high pH suggest an aridic rather than xeric soil moisture regime.

EUR15:

WRB (2001): ochric horizon (0–20 cm); no vitric horizon (BD 0–20 cm >0.9 kg dm^{-3}, too thin for vitric); no Leptosol because of <90% coarse fragments between 0 and 50 cm; no Arenosol because of >35% coarse fragments between 0 and 50 cm; BS >80% throughout; ESP >6 throughout:

Skeleti-Tephric Regosol (Hyposodic)

ST (2003): ochric epipedon (0–20 cm); no vitric horizon; no Psamment because of >35% rock fragments in the particle-size control section (25–100 cm); glass content is not determined but is assumed to be 24%[6] or more; xeric soil moisture regime; thermic soil temperature regime:

Pumiceous, mixed, nonacid, thermic Vitrandic Xerorthent
(if volcanic glass content is 24% or more)

France

EUR16:

WRB (2001): umbric horizon (0–55 cm); andic horizon (0–120 cm); Si_o >0.6% throughout; >35% gravel below 55 cm; BS >50% below 55 cm:

Umbri-Silandic Andosol (Pachic and Endoskeletic)

ST (2003): umbric epipedon (0–55 cm); no melanic epipedon because MI is 2.07–2.14 and colour requirement is not met; andic soil properties (0–120 cm); Al (KCl) <2.0 cmol(+) kg^{-1}; 8x Si_o + 2x Fe_o >5, 8x Si_o > 2x Fe_o; udic soil moisture regime; frigid soil temperature regime:

Medial over ashy-pumiceous, amorphic, frigid Eutric Pachic Fulvudand

RPF (1995): silandic horizons 0–90 cm; dark humic horizon >6% org. C, 0–45 cm and dark Bw 5–5.8% org. C, 45–55 cm; eutric SB >15 mol kg^{-1}, 0–45 cm and BS >50%, 55–120 cm:

Eutric (near Humic) Silandosol on recent basaltic cinders

EUR17:

WRB (2001): umbric horizon (0–50 cm); aluandic horizon (0–35 cm); silandic horizon (35– >90 cm); ECEC <2.0 cmol kg^{-1} fine earth between 70 and 100 cm:

Epialuandi-Silandic Andosol (Umbric and Pachic)

ST (2003): umbric epipedon (0–50 cm); 0–50 cm fulfils depth, thickness and organic carbon requirements for a melanic epipedon but not the colour

[6] Derived from the formula $[(Al_o + ½Fe_o) \times 60] +$ % volcanic glass ≥30.

requirement; MI is 2.10–2.13; andic soil properties (0– >95 cm); KCl-extractable Al >2.0 cmol(+) kg^{-1} between 0 and 50 cm and <2.0 cmol(+) kg^{-1} between 50 and 90+ cm; mean Si_o 0.89%, mean Fe_o 1,23%, both between 0 and 100 cm; 8x Si_o + 2x Fe_o >5, 8x Si_o > 2x $Fe_{o;}$ udic soil moisture regime; frigid soil temperature regime:

Medial, amorphic, frigid Acrudoxic Fulvudand

RPF (1995): andic horizons 0–100 cm; aluandic horizon 0–32 cm; silandic horizons 32–100 cm; dark humic horizon >6% org C, 0–50 cm; BS <20% 0–100 cm and Al KCl >2 cmol kg^{-1}, 0–50 cm:
Hyperdystric Humic Aluandosol from glacial sediment over Miocene basalt lava

Hungary

EUR18:

WRB (2001): mollic horizon (0–70 cm); possibly vitric[7] horizon (0–70 cm; bulk density <0.9 kg dm^{-1}, Al_o + ½Fe_o >0.4%; P-retention >25%, but no data on volcanic glass content); tephric soil material at 70 cm +:

Molli-Vitric Andosol (Pachic)
(if vitric horizon is present)
more likely: Pachi-Endotephric Phaeozem (Siltic)
(if there is no vitric horizon)

ST (2003): mollic epipedon (0–70 cm); andic soil properties if 60% of the layer between 0 and 70 cm contains at least 26% volcanic glass (amount not determined); 0–70 cm does not fulfil the organic carbon requirement for a melanic epipedon; xeric soil moisture regime; mesic soil temperature regime:

Medial (?), mixed, mesic Humic Vitrixerand
(if sufficient volcanic glass is present)
more likely: Fine-loamy, mixed, superactive, mesic Vitrandic Haploxeroll
(if there is 5% or more volcanic glass)
Fine-loamy, mixed, superactive, mesic Pachic Haploxeroll
(if there is less than 5% volcanic glass)

EUR19:

WRB (2001): umbric horizon (0–25 cm), near mollic (7–25 cm, black, org. C 0.7%, BS 51%); no vitric horizon (Ah1 + Ah2 <30 cm thick); >40%

[7] The coarse angular blocky macrostructure, the high clay content (>30%, assumed to be smectite) and the high sum of bases (32 cmol kg^{-1}) do not concur with typical vitric horizons.

rock fragments below 25 cm; continuous hard rock at 50 cm depth; evidence of alteration by cultivation practices[8]:

Endolepti-Anthric Umbrisol (Episkeletic)

ST (2003): umbric epipedon (0–25 cm); andic soil properties if 60 percent of the layer between 7 and 30 cm contains at least 25% volcanic glass[9] (volcanic glass content not determined); BS >60% between 25 and 75 cm; >35% coarse fragments below 25 cm; xeric soil moisture regime; mesic soil temperature regime:

Ashy over loamy-skeletal, mixed, mesic Humic Vitrixerand
(if there is 25% or more volcanic glass)
more likely: Loamy-skeletal, mixed, mesic Vitrandic Haploxerept
(if there is 5% or more volcanic glass)
Loamy-skeletal, mixed, mesic Humic Haploxerept
(if there is less than 5% volcanic glass)

EUR20:

WRB (2001): mollic horizon (0–47 cm); cambic horizon (47–62 cm); no vitric horizon (Ah2 meets P-retention, but not $Al_o + ½Fe_o$ requirement, and is too shallow to be vitric); >40% silt between 2 and 47 cm; continuous rock at 62 cm depth:

Silti-Endoleptic Phaeozem

ST (2003): mollic epipedon (0–47 cm); cambic horizon (47–62 cm); no andic soil properties ($Al_o + ½Fe_o$ <0.4%); CEC/clay between 0.8 and 1.4; xeric soil moisture regime; mesic soil temperature regime:

Fine-silty, mixed, superactive, mesic Vitrandic Haploxeroll
(if volcanic glass content is 13% or more[9])
probably: Fine-silty, mixed, superactive, mesic Ultic Haploxeroll
(if volcanic glass content <13%)

---

[8] Additional information received from Hungary indicates that this soil has been cultivated for a long time. Until the end of the 19th century is was under vineyard. A overview of the cultivation characteristics, tested against the diagnostic requirements of the Hortic horizon, is given below:

Criteria	Deep working	Colour	OC%	BS%	P_2O_5 (Olsen) more than 100 mg kg^{-1}
Ah1 0–7 cm	+	+	+	– (43%)	+
Ah2 7–25 cm	+	+	+	+ (50.8%)	+
A/R 25–50 cm	+	+	+	+ (65.3%)	(+)

[9] Derived from the formula $[(Al_o + ½Fe_o) \times 60] +$ % volcanic glass ≥30.

Slovakia

SK1:

WRB (2001): ochric horizon (0–43 cm; colour chroma AB too high for mollic or umbric horizon); silandic horizon (43–73 cm); vitric (depending on volcanic glass content) horizon (3–43 cm); >40% coarse fragments below 43 cm; BS <50% between 3 and 73 cm:

Silandi-Vitric Andosol (Endoskeletic and Epidystric)

ST (2003): ochric epipedon (0–43 cm); cambic horizon (43–123 cm); andic soil properties between 3 and 143 cm; KCl-extractable Al >2.0 cmol(+) kg^{-1} is assumed to occur between 25 and 50 cm because of high total acidity; udic soil moisture regime; frigid soil temperature regime:

Medial, mixed, frigid Alic Hapludand

SK2:

WRB (2001): umbric horizon (0–67 cm); vitric horizon (2–92 cm); no andic horizon because of clay content <10%; >40% coarse fragments between 17 and 92 cm:

Umbri-Vitric Andosol (Pachic and Skeletic)

ST (2003): umbric epipedon (0–67 cm); cambic horizon (67–92 cm); andic soil properties between 2 and 97 cm; KCl-extractable Al >2.0 cmol(+) kg^{-1} is assumed to occur between 25 and 50 cm because of high total acidity; >35% coarse fragments between 17 and 92 cm; 0–67 cm fulfils depth, thickness and organic carbon requirements for a melanic epipedon; udic soil moisture regime; frigid soil temperature regime:

Medial-skeletal, mixed, frigid Pachic Fulvudand

SK3:

WRB (2001): folic horizon 0–10 cm; mollic horizon[10] (10–50 cm); vitric horizon assumed although volcanic glass content is not determined: Al_o + ½Fe_o 0.9–1%, P-retention 65–70%, BD 0.7–0.9 g dm^{-3} between 2–92 cm:

Molli-Vitric Andosol

ST (2003): mollic epipedon (10–50 cm); cambic horizon (63–110 cm); andic soil properties (10–110 cm); udic soil moisture regime; frigid soil temperature regime:

Medial, mixed, frigid Humic Udivitrand

[10] BS>50% does not concur with pH H_2O (5.2–5.0) and total acidity (11.4–9.6 cmol kg^{-1}).

SK4:

WRB (2001): umbric horizon (0–45 cm); vitric horizon (5– >85 cm) assumed although volcanic glass content is not determined: $Al_o + ½Fe_o$ 0.7–3.3%, P-retention 61–99%, BD around 0.7 g dm^{-3}; no andic horizon because clay content <10%; >40% coarse fragments below 45 cm depth; BS <50% throughout and <20% between 5 and 45 cm:

Umbri-Vitric Andosol (Endoskeletic and Hyperdystric)

ST (2003): umbric epipedon (0–45 cm); no melanic epipedon because melanic index is more than 1.7 between 5 and 35 cm (all other requirements apply); mean org. C >6% 5–55 cm; andic soil properties (5– >85 cm); udic soil moisture regime; frigid soil temperature regime:

Medial, mixed, frigid Pachic Fulvudand

Comparison between WRB 2001 and the proposed revisions (FAO-ISRIC-IUSS in preparation)

Currently the World Reference Base for Soil Resources is under revision after 6 years of testing. Numerous proposals have been received for improving WRB, which are being incorporated as much as possible. Major changes may be expected in the definitions of andic, argic, cambic, fulvic, and vitric horizons, all of which affect the present classification of the Reference Pedons of European Volcanic Soils.

The main proposed changes are as follows:

- *Andic horizon*: clay content of 10% or more to be deleted; volcanic glass requirement to be omitted; phosphate retention requirement to be increased to 85%; bulk density limit to be 0.9 g dm^{-3} or less;
- *Argic horizon*: provision is made to accommodate truncated argic horizons; exchangeable sodium percentage (ESP) of less than 15 to be added to the diagnostic requirements;
- *Cambic horizon*: textural requirement to be changed from sandy loam to very fine sand, loamy very fine sand, or finer; soil structural requirement to be changed to include weakly developed soil structure as well; more explicit colour requirements to include wet cambic horizons;
- *Fulvic horizon*: colour value or chroma of more than 2;
- *Vitric horizon*: 5% or more volcanic glass, glassy aggregates and other glass-coated primary minerals, either in the sand fraction (0.05–2 mm), or in the coarse silt, very fine sand and fine sand fraction (0.02–0.25 mm); both phosphate retention of more than 25% and $Al_o + ½Fe_o$ of 0.4 or more; BD requirement to be deleted; no overlap permitted with andic horizon.

Moreover, the qualifier level of the revised WRB will be reorganised into two sets: *prefix* qualifiers, always to be used before the name of the Major Reference Group (MRG), and *suffix* qualifiers, always to be used behind the MRG name. Prefix qualifiers will be those that are typical or unique for the MRG, and that represent intergrades to other MRGs; suffix qualifiers will be composed of those that indicate extragrades, specific chemical, mineralogical or material characteristics, and colour.

For Andosols the listing of prefix and suffix qualifiers in the revised WRB may be:

Prefix qualifiers	Suffix qualifiers
Vitric	Turbic
Aluandic	Gelic
Eutrisilic	Gelistagnic
Silandic	Stagnic
Melanic	Placic
Fulvic	Pachic
Hydric	Acroxic
Folic	Calcaric
Histic	Sodic
Technic[11]	Thixotropic
Leptic	Skeletic
Gleyic	Dystric
Mollic	Eutric
Petroduric	Thapto-[12]
Duric	
Umbric	Endo-, Epi-, Hyper-, Hypo-,
Arenic	Orthi-[13]

The consequences of the proposed revisions for the classification of the Reference Pedons of European Volcanic Soils can be summarised as follows:

No.	WRB 2001	Proposed WRB (FAO, 2004)
EUR01	Humi-Tephric Regosol (Eutric)	Haplic Cambisol (Humic and Tephric)
EUR02	Hyposodi-Humic Cambisol	Haplic Cambisol (Humic and Hyposodic)
EUR03	Melani-Silandic Andosol (Dystric)	Melani-Silandic Andosol (Dystric)

11 New qualifier; it refers to soil with technic (man-made) soil material.

12 Thapto is used here with any horizon buried deeper than 50 cm.

13 It is proposed that modifiers are to be used with the suffix qualifiers only (FAO-ISRIC-IUSS in preparation).

EUR04	Melani-Silandic Andosol (Dystric)	Melani-Silandic Andosol (Dystric)
EUR05	Acroxi-Silandic Andosol (Hyperdystric)	Silandic Andosol (Acroxic and Hyperdystric)
EUR06	Hydri-Silandic Andosol (Umbric and Acroxic)	Hydric Fulvi-Silandic Andosol (Acroxic and Hyperdystric)
EUR07	Orthidystri-Vitric Andosol	Fulvi-Silandic Andosol (Gelistagnic and Orthidystric)
EUR08	Dystri-Vitric Andosol	Silandic Andosol (Turbic and Dystric)
EUR09	Thaptohisti-Vitric Andosol (Umbric and Pachic)	Histic Fulvi-Silandic Andosol (Turbic)
EUR10	Umbri-Silandic Andosol (Hyperdystric)	Umbri-Silandic Andosol (Hyperdystric)
EUR11	Skeleti-Vitric Andosol (Orthieutric)	Vitric Andosol (Skeletic and Orthieutric)
EUR12	Umbri-Vitric Andosol (Pachic and Hyperdystric)	Umbri-Vitric Andosol (Pachic and Hyperdystric)
EUR13	Endocalcari-Vitric Andosol (Hyposodic)	Haplic Regosol (Tephric and Endocalcaric)
EUR14	Skeleti-Tephric Regosol (Hyposodic)	Haplic Regosol (Tephric and Skeletic)
EUR15	Skeleti-Tephric Regosol (Hyposodic)	Haplic Regosol (Tephric and Skeletic)
EUR16	Umbri-Silandic Andosol (Pachic and Endoskeletic)	Fulvi-Silandic Andosol (Endoskeletic)
EUR17	Epialuandi-Silandic Andosol (Umbric and Pachic)	Fulvic Aluandi-Silandic Andosol (Endoacroxic)
EUR18	Pachi-Endotephric Phaeozem (Siltic)	Haplic Phaeozem (Endotephric and Pachic)
EUR19	Endolepti-Anthric Umbrisol (Episkeletic)	Lepti-Anthric Umbrisol (Episkeletic)
EUR20	Silti-Endoleptic Phaeozem	Leptic Phaeozem (Siltic)
SK1	Silandi-Vitric Andosol (Endoskeletic and Epidystric)	Silandi-Vitric Andosol (Endoskeletic and Epidystric)
SK2	Umbri-Vitric Andosol (Pachic and Skeletic)	Fulvi-Aluandic Andosol (Skeletic)
SK3	Molli-Vitric Andosol	Mollic Foli-Vitric Andosol
SK4	Umbri-Vitric Andosol (Endoskeletic and Hyperdystric)	Fulvic Silandi-Vitric Andosol (Endoskeletic and Hyperdystric)

Discussion

The classification of the Reference Pedons of European Volcanic Soils using the very comprehensive data set is in many cases fairly straightforward. However, some problems remain for several pedons, in particular EUR08 in Iceland, EUR12 in Tenerife, EUR18, 19 and 20 in Hungary, and SK3 in Slovakia.

The first problem arises from still inadequate definitions of andic/vitric and melanic/fulvic horizons in WRB (Driessen et al. 2001), although these were an improvement compared to WRB (FAO-ISRIC-ISSS 1998). In particular the requirements for volcanic glass and clay content in andic horizons results in unsatisfactory placement of a number of soils with the vitric groups (EUR07, 08, 09, and SK2 and 4). Moreover, the too strict colour requirements for the fulvic horizon prevents recognising from this horizon in the name of many pedons (EUR06, 07, 09, 16 and 17, and SK2 and 4).

Secondly, arbitrary limits of ranking or priority listing, which differentiate one soil unit, group or subgroup from another, result proper sequencing to characterise the soils best. An example is the priority of Silandic over Aluandic (EUR17). Such problems were already noted by Nachtergaele et al. (2002).

Thirdly, other problems are due to possible misunderstanding of soil horizon descriptions (EUR12 and 18), or sometimes lack of important data, like clay mineral constituents, water retention capacity on un-dried moist samples, content in volcanic glass (either unknown (Hungary) or not accurate or probably misinterpreted (EUR12). Some diagnostic data, like for the vitric horizon in EUR18, do not seem to correspond with other data like high CEC and sum of bases (probably related to an important smectite clay content), as well a strong angular blocky macrostructure. Also in SK3, a mollic horizon/epipedon does not seem to be related to its acid (pH and total acidity) properties.

It appears that the proposed revisions in the definitions of the andic, fulvic and vitric horizons (FAO-ISRIC-IUSS in preparation) solve most of these issues. However, the lack of important data remains, in particular the moisture characteristics, and a reliable assessment of the volcanic glass content.

Conclusion

A world-wide system of soil classification is necessary to establish a common denomination of the Reference Pedons of European Volcanic Soils. The World Reference Base for Soil Resources provides a sound basis for such a common denomination, in particular if one takes into account the revisions recently proposed.

Some improvements, however, still may be considered:

- The aluandic horizon should get preference over the silandic horizon, to establish an Aluandic Andosol subgroup, even if it overlies a silandic

horizon, because this is very frequently the case (EUR17), as noted by Poulenard and Herbillon (2000) as well.
- Glass content must be used with precaution, because of the difficulty of its determination; it seems easy to observe the abundance of glass in the field, or to check if vitric or andic criteria fit well with other field observations or laboratory data.
- Range limits of andic/vitric diagnostic criteria could be more flexible, for example, if P-retention is at least 85% and BD <0.9 g dm^{-3}, the percentage $Al_o + ½Fe_o$ could be, exceptionally, between 1.5 and 2% (case of Si-rich allophane soils) so that the horizon would become andic rather than a vitric horizon.
- The Eutrisilic qualifier: sum of bases >25 cmol kg^{-1} seems too high and could be lowered to 15, as in the "Référentiel Pédologique Français".
- Thapto- is useful in case of buried horizons, either melanic, fulvic, histic or argic (kandic or ultic for ST) etc, throughout 30–120 cm. In the proposed revision of WRB the thapto- modifier should therefore also be permitted with prefix qualifiers, not only with suffix qualifiers.
- A Turbic (for obvious cryoturbation as in EUR08 and 09), and Stagnic qualifier should also be permitted in Andosols (as well as in other Major Reference Groups).

However, for land use, soil mapping and soil genesis interpretation, more comprehensive and adapted studies are necessary. Other systems, like that recommended by E.A. Fitzpatrick (2005a,b), may be more convenient to express all properties of each pedon, and constitute a basis for recording soil information as a whole.

References

AFES (1995). Référentiel Pédologique. INRA Ed, Paris p 328

Berding FR (1997). Third level modifiers for the major soil groups of Andosols, Phaeozems and Podzols. Working Paper. FAO/AGLS. Rome

Driessen P, Deckers J, Spaargaren O, Nachtergaele F (eds) (2001). Lecture notes on the major soils of the world. FAO World Soil Resources Reports 94. Rome p 334

FAO-ISRIC (1990). Guidelines for soil description. 3rd edn. Soil Resources, Management and Conservation Service, Land and Water Development Division. FAO, Rome

FAO-ISRIC-ISSS (1998). World reference base for soil resources. World Soil Resources Report 84. FAO, Rome

FAO-ISRIC-IUSS (in preparation). World reference base for soil resources. Rev. edn. World Soil Resources Report 84, Rev 1. FAO, Rome, http://www.fao.org/waicent/FaoInfo/Agricult/AGL/AGLL/WRB/news.stm

FitzPatrick EA (2005a). Horizon identification – reference point system – CD. Interactive Soil Science, Aberdeen, UK, http://www.interactivesoils.com

FitzPatrick EA (2005b). Classification of soils according to "Horizon Identification – reference point system"

Nachtergaele FO, Berding FR, Deckers J (2002). Pondering hierarchical soil classification systems. Soil Classification 2001. FAO-EUR Com 2002:71–79

Poulenard J, Herbillon AJ (2000). Sur l'existence de trois catégories d'horizons de référence dans les andosols. C R Ac Sci, Ser 2, 331:651–657

Quantin P (1994). The Andosols. Trans. 15th World Congress of Soil Science, Acapulco, vol 6a:848–859

Shoji S, Nanzyo M, Dahlgren RA, Quantin P (1996). Evaluation and proposed revisions of criteria for Andosols in the World Reference Base for Soil Resources. Soil Sc 161:604–615

Soil Survey Staff (2003). Keys to Soil Taxonomy, 9th edn. USDA-NRCS, Washington

Takahasi T, Nanzyo M, Shoji S (2004). Proposed revisions to the diagnostic criteria for Andic and Vitric Horizons and Qualifiers of Andosols in the World Reference Base for Soil Resources. Soil Sci Plant Nutr 50:431–437

Van Reeuwijk LP (ed) (2002). Procedures for soil analysis. 6th edn. ISRIC Technical Paper 9. Wageningen

Classification of the soils according to 'Horizon Identification – the Reference Point System'

E.A. FitzPatrick

This paper attempts to classify the COST 622 (COperation europèenne dans le domaine de la recherché Scientifique et Technique) soils with the 'Horizon Identification – Reference Point System' (HI-RPS) which uses computer technology to identify horizons (FitzPatrick 2005). The horizons are given symbols that can be put into formulae which make fundamental statements about soils. This is followed by a variable system of soil classification whereby different operators can construct individual systems to suit their specific requirements. This is achieved by filtering the formulae to bring together those soils that have the desired common attributes.

Thus this system is fundamentally different from other systems such as WRB (ISSS Working Group RB, Deckers et al. 1998) and Soil Taxonomy (Soil Survey Staff 2003) most of which require a large degree of personal memory and many have numerous either/or possibilities. For example, it is necessary to know the definitions of horizons before the keys can be used. In this programme the objective in really, is in the first place, to identify horizons using all of the available data about their properties. This gives an unprecedented degree of accuracy in defining horizons and almost unlimited versatility in classification. The underlying concept is that the properties are coordinates and theoretically there are an infinite number of coordinates. Values of these coordinates intersect in hyperspace to create an infinite number of conceptual points. In addition to the coordinates such as particle size analysis and pH, there are other coordinates such as time and degree of physical mixing to accommodate very old soils and crotovinas. About 300 of these conceptual points are chosen in a subjective manner as 'reference' points. These reference points form a universe of points with varying distances one from the other. These points are given names ending with 'on' and based on one or more conspicuous properties. E.g. the pale coloured upper point is the albons with the symbols Aba. Radiating out from the albon the points form continua sequences in space and time to other reference points. These are albons and designated Abb, Abc etc.

In addition the properties of a given reference point may be superimposed on those of another point to create a 'compound point'. This is usually due to an environmental change such as climate or vegetation. In the

field contiguous points form volumes or horizons which derive their name from the points. Thus there are reference horizons composed of contiguous reference points and compound horizons composed of contiguous volumes of compound points. Further, an horizon may be composed of discrete volumes of different reference or compound horizons, thus forming a 'composite horizon'.

The system attempts to place unknown horizons or soil volumes within the universe of points based upon a calculated score. This is achieved by creating spreadsheets with the properties arranged vertically and points arranged horizontally. Thus the fundamental theoretical units are conceptual points with a single value for each property.

The identification of horizons is based on the concept of the closest match or Euclidian distance between the unknown and fixed values. It should be stressed that this system uses single fixed values and not value ranges as used in other systems. This allows a certain degree of overlap or fuzziness. Perhaps it should be pointed out that these reference points are created at a specific moment in time.

Many Luvisols have had a climatic change to drier conditions with the consequent accumulation of calcium carbonate in the argillon (argic horizon). This is a compound horizon and should be designated {Cca+Ara} and is dominantly a calcon.

Similarly there are gibbsitic concretionary horizons that have become impregnated with opal. These are also compound horizons and should be designated {Dua+Spa} but are simply termed durons. In the arctic the frozen subsoil is permafrost (cryon). When it thaws, it retains some of the features and becomes an ison. Further development of this horizon will depend on many factors. In a dry environment calcium carbonate may accumulate and is a compound horizon and should be designated {Cca+Isa}. Therefore it seems that all horizons are constantly changing and are thus intergrades but there may be long periods when the change is negligible. Hence it is possible to recognise three different types of horizon.

Types of horizon

Reference horizons

These are composed of a contiguous reference point, and has a single set of dominant properties as a result of progressive development but they may have been through a number of distinct phases. A Podzol horizon may have passed through a Cambisol stage.

Compound horizons

These have a combination of properties of two or more reference points. These properties are usually contrasting and develop as a result of either contrasting seasonal processes or they have one set of properties superimposed upon an earlier set of properties. The designation of the seasonally compound horizons is based on the dominant summer process. For example, a strongly reduced horizon that freezes during the winter would be regarded as a type of cerulon and designated Crd. The designation of a compound horizon resulting from climatic change or progressive soil evolution would show the symbols of both horizons. For examle, an argillon may become calcified as a result of climatic change. These are designated by putting the symbols in curly brackets thus {Ccc+Ara}. This indicates that the calcite has been superimposed on an argillon. It may take detailed research to identify these situations which might otherwise be regarded as calcons.

Composite horizons

These have discrete volumes of two or more horizons. These are designated by placing the horizon symbols in round brackets and separated by a plus sign. One of the best examples is found in Chernozems, which have crotovinas and designated as follows: (Cha+2Cz-) where Cha is the symbol for a chernon and *2Cz*- is the symbol for moderately calcareous loess.

There are a very large number of composite horizons in the arctic and more than occur anywhere else in the world. This is the result of soil mixing due to the large amount of solifluction and cryoturbation that takes place.

Continuum horizons

Many points occur at some distance from those that have been chosen. Previously these have been regarded as intergrades, more correctly they are part of the soil continuum. An unknown in these areas will have a high score and designated by combining its symbol with the next highest and placed in round brackets thus: (Pzc-Cba). This horizon is close to the Pzc.

Classification of COST 622 profiles

Three classifications are given below. WRB and ST are given in an extended form in an other paper (Quantin and Spaargaren this book), here only the final soil name is given. For HI-RPS, the formulae and names are given for each of the soils, these are followed by a brief definition of the horizon symbols. Since they are very brief they may not be mutually exclusive but the data in the spreadsheets used to calculate the closest match are.

Italy

EUR01

WRB – Humi-Tephric Regosol (Eutric)
ST – Ashy, glassy, thermic Vitrandic Haploxerept
HI-RPS – Htb16~Vtg79#Vtd25~*I-P-z* – Hortic Vitrosol
Htb – Horton: upper, dark, continuously cultivated with the addition of organic wastes, tephra present.
Vtg – Vitron: middle, weakly weathered with dominant tephra, high rainfall and medium to high temperatures.
Vtd – Vitron: middle or lower with dominant tephra.
I-P-z: Intermediate pyroclastic silt.

EUR02

WRB – Hyposodi-Humic Cambisol
ST – Ashy, glassy, mesic Vitrandic Haploxerept
HI-RPS – Htb5~Vth22#Vtg52~Glg – Hortic gleyic Vitrosol
Htb – Horton: upper, dark, continuously cultivated with the addition of organic wastes, tephra present.
Vth – Vitron: middle, weakly weathered with dominant tephra, medium rainfall and medium to high temperatures.
Vtg – Vitron: middle, weakly weathered with dominant tephra, high rainfall and medium to high temperatures.
Glg – Gleyon: middle or lower strong yellow mottling with tephra.

EUR03

WRB – Melani-Silandic Andosol (Dystric)
ST – Ashy, amorphic, mesic Eutric Melanudand
HI-RPS – (Mlh-Umb)46~Ana60~(Ana-Vtg) – Mullic Silandic Andosol

Mlh – Mullon: natural, upper, dark to very dark intimate mixture of organic and mineral material with granular or vermicular structure with tephra.
Umb – Umbron: upper, dark to very dark intimate mixture of organic and mineral material as a result of long continuous cultivation.
Ana – Andon: silandic, friable to fluffy with granular to blocky structure, high allophane, high extractable silica.
Vtg – Vitron: middle, weakly weathered with dominant tephra, high rainfall and medium to high temperatures.

EUR04

WRB – Melani-Silandic Andosol (Dystric)
ST – Ashy, amorphic, mesic Eutric Pachic Melanudand
HI-RPS – Mlh2~(Mlh-Umb)8~(Umb-Mlh)35~Ana62 – Mullic Silandic Andosol
Mlh – Mullon: natural, upper, dark to very dark intimate mixture of organic and mineral material with granular or vermicular structure with tephra.
Umb – Umbron: upper, dark to very dark intimate mixture of organic and mineral material as a result of long continuous cultivation.
Ana – Andon: silandic, friable to fluffy with granular to blocky structure, high allophane, high extractable silica.

Azores

EUR05

WRB – Hyperdystri-Silandic Andosol
ST – Medial, amorphic, mesic Typic Hapludand
HI-RPS – (Umd-Mlh)10~Vtd20#(Umd-And)15~Anc20~Ana25#*I-P-cl* – Umbric Andosol
Umd – Umbron: thick, upper, dark to very dark mixture of organic and mineral material with abundant tephra.
Mlh – Mullon: natural, upper, dark to very dark intimate mixture of organic and mineral material with granular or vermicular structure with tephra.
Vtd – Vitron: upper, very lowly weathered with dominant tephra with high rainfall and low temperatures.
Ana – Andon: silandic, friable to fluffy with granular to blocky structure, high allophane, high extractable silica.
I-P-cl: intermediate pyroclastic clay loam

EUR06

WRB – Hydri-Silandic Andosol (Umbric and Acroxic)
ST – Hydrous, amorphic, mesic Acrudoxic Hydrudand
HI-RPS – Apd35~Hyb15~Anc80#*B-P-cl* – Amorphic Hydric Andosol
Apd – Amorphon dark brown to black, amorphous, well decomposed organic matter, permanently saturated with water, contains tephra.
Hyb – Hydroandon: upper, very dark, containg organo-aluminium complexes and high melanic index low extractable Si and low pH.
Anc – Andon: aluandic, friable to fluffy with granular to blocky structure, low allophane, high aluminium low extractable silica with winter freezing.
B-P-cl: basic pyroclastic clay loam.

Iceland

EUR07

WRB – Orthidystri-Vitric Andosol
ST – Ashy, amorphic Eutric Pachic Fulvicryand
HI-RPS – Apd5~Umd12#Luc48#Ana21~Vtk9#Mbd – Gleyic Andosol
Apd – Amorphon: dark brown to black, amorphous, well decomposed organic matter, permanently saturated with water, contains tephra.
Umd – Umbron: thick, upper, dark to very dark mixture of organic and mineral material with abundant tephra
Luc – Luton: upper, dark with very low iron staining around roots, carbonates absent with tephra.
Ana – Andon: silandic, friable to fluffy with granular to blocky structure, high allophane, high extractable silica.
Vtk – Vitron: middle, weakly weathered, dominant tephra with winter freezing, high rainfall and low temperatures.
Mbd – Marblon middle or lower, yellow to brown with marbled pattern and faint mottling and winter freezing.

EUR08

WRB – Dystri-Vitric Andosol
ST – Ashy, amorphic Typic Vitricryand
HI-RPS – Fmb3~Luc8~Umd10~Vtk5#Vtj33#Vtf~*I-scl* – Lutic Vitrosol
Fmb – Fermenton: fibrous, partially decomposed organic materials with aerobic conditions and winter freezing
Luc – Luton: upper, dark with very low iron staining around roots carbonates absent with tephra.

Umd – Umbron: thick, upper, dark to very dark mixture of organic and mineral material with abundant tephra.
Vtj – Vitron: middle, weakly weathered with dominant tephra with winter freezing, high rainfall and low temperatures.
Vtk – Vitron: middle weakly weathered with dominant tephra with winter freezing, medium rainfall and low temperatures.
Vtf – Vitron: weakly weathered with dominant tephra, silt cappings and winter freezing.
I-scl: Intermediate sandy clay loam.

EUR09

WRB – Umbri-Vitric Andosol (Pachic and Orthidystric)
ST – Ashy, amorphic Eutric Pachic Fulvicryand
HI-RPS – Vte55~*B-P-ls* #Fmc16~*B-P-ls*5#Vte – Vitrosol
Vte – Vitron: weakly weathered, upper with dominant tephra, medium rainfall, low temperature.
B-P-ls - Basic pyroclastic loamy sand.
Fmc – Fermenton: fibrous partially decomposed organic materials with aerobic conditions, tephra present.

Tenerife

EUR10

WRB – Umbri-Silandic Andosol (Hyperdystric)
ST – Ashy, amorphic, mesic Humic Udivitrand (Lisbon)
Ashy, amorphic, mesic Vitric Hapludand (Santiago)
HI-RPS – Umd45~Ana166#Vtk – Silandic Andosol
Umd – Umbron: thick, upper, dark to very dark mixture of organic and mineral material with abundant tephra.
Ana – Andon: silandic, friable to fluffy with granular to blocky structure, high allophane, high extractable silica.
Vtk – Andon: middle weakly weathered with dominant tephra with winter freezing, medium rainfall and low temperatures.

EUR11

WRB – Skeleti-Vitric Andosol (Orthieutric)
ST – Ashy-pumiceous, glassy, mesic Typic Vitrixerand
HI-RPS – Vtb10~*B-P-s-2D*#Ana27#*B-P-s-3D* – Vitric Andosol
Vtb – Vitron: upper, very lowly weathered with dominant tephra, medium rainfall and medium to high temperatures.

Ana – Andon: silandic, friable to fluffy with granular to blocky structure, high allophane, high extractable silica.
B-P-s-2D: Basic pyroclastic sand 2 cm fragments dominant.
B-P-s-3D: Basic pyroclastic sand 3 cm fragments dominant.

EUR12

WRB – Umbri-Vitric Andosol (Pachic and Hyperdystric)
ST – Ashy, glassy, mesic Humic Udivitrand
HI-RPS – Mea65~Ana55#Mea-Anb – Melanic Andosol
Mea – Melanon: upper, very dark, high allophane, low melanic index (<1.7) high extractable Si and moderate pH.
Ana – Andon: silandic, friable to fluffy with granular to blocky structure, high allophane, high extractable silica.
Anb – Andon: silandic, middle, friable to fluffy with granular to blocky structure, high allophane, high extractable silica, clay coatings.

Greece

EUR13

WRB – Endocalcari-Vitric Andosol (Hyposodic)
(if >10% volcanic glass is assumed)
Endocalcari-Tephric Regosol (Hyposodic)
(if <10% volcanic glass is assumed)
ST – Ashy, mixed, calcareous, thermic Vitrandic Xeropsamment
HI-RPS – Mlh40~*B-P-sl-2O* – Mullic Vitrosol
Mlh – Mullon: natural, upper, dark to very dark intimate mixture of organic and mineral material.
B-P-sl-2O: Basic pyroclastic sandy loam with 2 cm fragments occasional.

EUR14

WRB – Skeleti-Tephric Regosol (Hyposodic)
ST – Pumiceous, mixed, nonacid, thermic Vitrandic Xerorthent
HI-RPS – Vtb7~*B-P-s-7A* – Lithic Vitrosol
Vtb – Vitron: upper, very weakly weathered with dominant tephra, medium rainfall and medium to high temperatures.
B-P-s-7A: Basic pyroclastic sand 7 cm fragments abundant.

EUR15

WRB – Skeleti-Tephric Regosol (Hyposodic)
ST – Pumiceous, mixed, nonacid, thermic Vitrandic Xerorthent

HI-RPS – Hmd10~Vtb20~*B-P-s-2D* – Hamadic Vitrosol
Hmd – Hamadon: surface accumulation of large rock fragments.
Vtb – Vitron: upper, very weakly weathered with dominant tephra, medium rainfall and medium to high temperatures.
B-P-s-2D: Basic pyroclastic sand 2 cm fragments dominant.

France

EUR16

WRB – Umbri-Silandic Andosol (Endoskeletic and Endoeutric)
ST – Medial over ashy-pumiceous, amorphic, mesic Eutric Pachic Fulvudand
HI-RPS – (Fva-Umd)45~Ana10#*I-P-s* – Flavic Andosol
Fva – Flavon: upper, very dark, contains allophane and high melanic index (>1.7), high extractable Si and moderate pH extractable silica.
Umd – Umbron: thick, upper, dark to very dark mixture of organic and mineral material with abundant tephra.
Ana – Andon: silandic, friable to fluffy with granular to blocky structure, high allophane, high.
Vtd – Vitron: middle or lower with dominant tephra.
I-P-s: Intermediate pyroclastic sand.

EUR17

WRB – Epialuandi-Silandic Andosol (Umbric and Endoacroxic)
ST – Medial, amorphic, mesic Pachic Fulvudand
HI-RPS – Hfb8~Vta52~Ana40#Ana59+ – Humic silandic Andosol
Hfb – Humifon: very dark brown to black, strongly decomposed, aerobic, organic matter, winter freezing.
Vta – Vitron: upper, very lowly weathered with dominant tephra, high rainfall and medium to high temperatures.
Ana – Andon: silandic, friable to fluffy with granular to blocky structure, high allophane, high extractable silica.

Hungary

EUR18

WRB – Molli-Vitric Andosol (Pachic)
(if vitric horizon is present)
Pachi-Endotephric Phaeozem (Siltic)
(if there is no vitric horizon)

ST – Medial (?), mixed, mesic Humic Vitrixerand
(if sufficient volcanic glass is present)
Fine-loamy, mixed, superactive, mesic Vitrandic Haploxeroll
(if there is 5% or more volcanic glass)
Fine-loamy, mixed, superactive, mesic Pachic Haploxeroll
(if there is less than 5% volcanic glass)
HI-RPS - Mlh35#Vtg35~*B-P-s-5D* – Mullic Vitrosol
Mlh – Mullon: natural, upper, dark to very dark intimate mixture of organic and mineral material with granular or vermicular structure with tephra.
Vtg – Vitron: middle with dominant tephra.
B-P-s-5D: Basic pyroclastic sand with 5 cm fragments dominant.

EUR19

WRB – Skeletic Umbrisol
ST – Ashy over loamy-skeletal, mixed, mesic Humic Vitrixerand
(if there is 25% or more volcanic glass)
Loamy-skeletal, mixed, mesic Vitrandic Dystroxerept
(if there is 5% or more volcanic glass)
Loamy-skeletal, mixed, mesic Humic Dystroxerept
(if there is less than 5% volcanic glass)
HI - RPS – Mlh25#*B-P-zcl-5A* – Mullic Regosol
Mlh – Mullon: natural, upper, dark to very dark intimate mixture of organic and mineral material with granular or vermicular structure with tephra.
B-P-zcl-5A: Basic pyroclastic silty clay loam 5 cm fragments abundant.

EUR20

WRB – Silti-Endoleptic Phaeozem
ST – Fine-silty, mixed, superactive, mesic Vitrandic Haploxeroll
(if volcanic glass content is 13% or more)
Fine-silty, mixed, superactive, mesic Ultic Haploxeroll
(if volcanic glass content <13%)
HI-RPS – Mlh47~(Seg-*I-F-2w*)15~*I-F-2w* – Mullic Sepiosol
Mlh – Mullon: natural, upper, dark to very dark intimate mixture of organic and mineral material with granular or vermicular structure with tephra.
Seg – Sepion: brown, middle or lower, strongly weathered, loam, high CEC, low TBC, high silty:clay ratio, none to very low concretions.
I-F-2w: Intermediate fine grained rock moderately weathered.

Grouping of formulae

1. Htb16~Vtg79#Vtd25~*I-P-z* – Hortic Vitrosol
2. Htb5~Vth22#Vtg52~Glg – Hortic gleyic Vitrosol
3. (Mlh-Umb)46~Ana60~(Ana-Vtg) – Mullic Silandic Andosol
4. Mlh2~(Mlh-Umb)8~(Umb-Mlh)35~Ana62 – Mullic Silandic Andosol
5. (Umd-Mlh)10~Vtd20#(Umd-And)15~Anc20~Ana25#*I-P-cl* – Umbric Andosol
6. Apd35~Hyb15~Anc80#*B-P-cl* – Amorphic Hydric Andosol
7. Apd5~Umd12#(Mea-Umd)33~Luc3#Ana8~Vtk9#Mbd – Gleyic Andosol
8. Fmb3~Luc8~Umd10~Vtk5#Vtj33#Vtf~*I-scl* – Lutic Vitrosol
9. Vte55~*B-P-ls* #Fmc16~*B-P-ls*5#Vte – Vitrosol
10. Umd45~Ana166#Vtk – Silandic Andosol
11. Vtb10~*B-P-s-2D*#Ana27#*B-P-s-3D* – Vitric Andosol
12. Mea65~Ana55#Mea-Anb – Melanic Andosol
13. Mlh40~*B-P-sl-2O* – Mullic Vitrosol
14. Vtb7~*B-P-s-7A* – Lithic Vitrosol
15. Hmd10~Vtb20~*B-P-s-2D* – Hamadic Vitrosol
16. (Fva-Umd)45~Ana10#*I-P-s* – Flavic Andosol
17. Hfb8~Vta52~Ana40#Ana59+ – Humic silandic Andosol
18. Mlh35#Vtg35~*B-P-s-5D* – Mullic Vitrosol
19. Mlh25#*B-P-zcl-5A* – Mullic Regosol
20. Mlh47~(Seg-*I-F-2w*)15~*I-F-2w* – Mullic Sepiosol

These formulae can be put into a table in Excel and filtered to arrive at one or more classifications to suit individual users. For example all the soils with andons (andic horizons can easily be grouped by filtering for ‘An’ or more specifically for ‘Ana’ or ‘Anc’. Perhaps it would be interesting to determine whether any of the soils show gley characteristics then they could be filtered for ‘Gl’ horizons. It might be argued that this could be discovered by going to the original descriptions; however this would take considerably longer than a filtration. By filtering for a specific horizon it is possible to see whether there are any specific relationships. There could be a fixed relationship or there might be an either or situation. In this group of soils there is clearly no relationship between ‘An’ and any other horizon either above or below.

Every attempt has been made to work within WRB thus the main comparisons will be made with that system.

1. The computer analysis shows that the upper horizon in EUR01 is hortic. It might not meet the specific WRB depth criteron for hortic but it does have all the other properties especially as it is completely man made.

Because the system finds the closest match, all the criteria do not have to fit thus allowing a certain amount of fuzziness. I prefer to regard it as hortic. As far as I can see there is no indication in WRB that the whole soil is anthropogenic.

2. The lowest horizon in EUR02 is gleyed but this is not shown in the classification.
3. EUR07 has >20% C.
4. EUR08 has features that most definitely indicate freezing and possibly permafrost. In fact none of the WRB names indicate the cold climatic conditions. Eg EUR08 is a Dystri-Vitric Andosl and could occur almost anywhere. The lowest horizon is a vitron Vtf with silt cappings that is formed by freezing. That is one of the virtues of having a horizon based system that can depict many of the subtleties in soils.
5. EUR09 This soil is stated as having both an umbric and a vitric horizon 0–55 cm, surely it has to have one or the other. Again no indication of cryoturbation in the title, whereas Vtc is the vitron that has a high organic matter content and shows cold climate phenomena.

Most if not all of these soils are stratified yet this is not reflected in the classification. This can be indicated without going to the descriptions by using a formula, either using the ABC system or more accurately and specifically using the coordinate system with a change in material being designated with #. The suggestion is to give the formula which gives the details of the soil and a two or three word name to give a general idea about the soil. Longer titles are confusing – thus Humic-Tephric Regosol (Dystric) becomes: Htb16~Vtg104~Vtg – Hortic Vitrosol. An immediate response might be that Htb etc mean nothing to the present soil community. My reply is that the terms we use at present have become familiar with usage as with all terms present and in the future. In this system it must be pointed out to the beginner and even the professional that the meanings of the terms do not need to be remembered, they are quickly discovered by a few clicks.

Every attempt has been made to work within the framework of WRB and to introduced few class names outside WRB except for Vitrosols which seems logical since many so-called Andosols do not have andons (andic horizons).

There are fundamental differences;

1. In both WRB and ST an attempt is made to give what is tantamount to a mini description of the soil in the name. This produces extremely long names with little or no indication of the sequential arrangement of the horizons. With HI-RPS the horizon formula is the basic statement about the soil showing all the horizons and their juxtarelationships. Further

with HI-RPS, thicknesses of the horizons are shown and more particularly with soils derived from volcanic materials and other sedimentary materials discontinuities are clearly shown. In HI-RPS, the soil name is meant to indicate in a general manner where the soil occurs in multidimensional space. Usually the class name is preceded by one or more descriptors which do not indicate any sequential relationship such as EUR02 – Hortic gleyic Vitrosol. If sequential relationships are required between the whole formulae and class names then the subclass formulae can be used for EUR02 it is [Ht~Vt~Gl]. Thus the systems are fundamentally different. WRB and ST attempt to give both a descriptive statement and classification in the same term while HI-RPS makes a definitive statement by means of a formula showing all the horizons, their depths and sequential relationships. One of the advantages of formulae is that they can be put into a table and filtered to show different relationships. For most readers the first requirement is the general classification and then to require more specific information; for this the formula seems to be the ideal intermediate step to the full description and analytical data. Please note that the formula is not merely descriptive since the horizons are characterised by all properties.

References

Deckers JA, Nachtergaele FO, Spaargaren OC (eds) (1998). World Reference Base for Soil Resources. Acco Leuven

FitzPatrick EA (2005). Horizon Identification – Reference Point System – CD. Interactive Soil Science, Aberdeen, UK, www.interactivesoils.com

Quantin P, Spaargaren O (2006). Classification of the Reference Pedons. WRB and Soil Taxonomy. In: Arnalds O, Bartoli F, Buurman P, Garcia-Rodeja E, Oskarsson H, Stoops G (eds) Soils of Volcanic Regions of Europe. Springer Verlag (this book)

Soil Survey Staff (2003). Keys to Soil Taxonomy. 9th edn. USDA-NRCS. Washington pp 332

III. Reference Pedons: chemical and biological characteristics

Ed.: P. Buurman

Introduction: Chemistry of European volcanic soils

P. Buurman

The studies in this chapter are largely based on the chemical and physical analyses carried out on the twenty COST-622 European volcanic reference soils. Most analyses were carried out on identical sub-samples of the same bulk samples.

European volcanic soils vary considerably in parent material, climate, soil development, anthropic interference, oceanic influence, and a large number of other factors. The reference soils represent a cross section of this variation, which means that most reference soils are essentially different in many aspects. Treating such soils as one data set will logically yield a few results that are valid for the whole set, and quite a few others that must be explained by deviating parameters.

Analysing many properties on the same soil samples has the obvious advantage that correlations between soil properties can be studied that remain otherwise hidden through absence of adequate data. This is one of the main purposes of the research presented here. Although the database is rather small, some interesting new results have surfaced. Nevertheless, many relations are so complex that single-factor correlations do not properly describe the system. Interactions between non-crystalline components remain to be quantified in a proper way, but this can only be done with a larger database. Analysis of the chemical results clearly indicates that the mineralogical and physical information of Chapters 2 and 4 are critical for a correct understanding.

We are aware that we have not fully explored the possibilities of the present data set and that, e.g., relations between exchange properties, selective dissolution data, heavy metal adsorption, mineralogy, could be investigated in more detail. We provide the data base and all additional information to allow others to further mine our data. Much can still be learnt from samples that do not conform to general trends.

The papers in this chapter are related as follows. First, Buurman et al. describe the database and the methods used for the various analyses. This chapter also addresses the problem of calculating allophane contents. Martinez et al. and Taboada et al. analyze chemical compositions that relate to parent material and to weathering status. The following papers by Garcia Rodeja et al., and the two papers by Madeira et al. deal with specific prop-

erties that relate to soil functioning. The second paper by Martinez et al. is the last paper in this section that deals with all reference soils together. In a statistical analysis, the relation between many variables is explored, and criteria for the present subdivision of volcanic soils in international classification are evaluated.

The final three papers deal with much smaller data sets. Buurman and Nierop and Nierop and Buurman studied the organic matter of the two Azores reference soils, and finally Tanneberg and Jahn analysed heavy metal sorption of some widely different reference samples.

Buurman et al. indicate that calculations of allophane or imogolite are hindered by a seeming continuum of chemical properties. Although allophane and imogolite are readily identified by electron microscopy – and somewhat less readily by infrared adsorption – quantification of these components separately is virtually impossible. As a proxy, Al/Si ratios of extracted matter are used, but these cannot characterize mixtures. Further, because most extractants also extract unknown amounts of crystalline Al-containing minerals, a real quantification is still impossible. This is a setback for the interpretation of, e.g., adsorption of cations, phosphate, and heavy metals. In various cases the presence of different phases of extractable Al-silicates is indicated by the data, and this appears to coincide with different behaviour in other properties.

Because the parent materials of the investigated soils vary considerably, bulk chemical composition will first of all reveal these differences (Martinez et al). Stratification in parent materials is easily detected, and generally coincides with subdivisions based on laser-diffraction grain-size analysis and micromorphology. Weathering is detected both by principal components analysis of the bulk chemical composition and by solute composition in equilibrium with ground soil. Surface additions by human activity or cyclic salt (in the Atlantic islands) are readily detected.

Weathering studies in the laboratory (Taboada et al.) first of all reflect the parent material, but also demonstrate buried soils and surface rejuvenation. Of the various weathering indices (based on bulk chemistry), the normalized Chemical Index of Alteration was most useful; it was strongly correlated with the relative amount of oxalate-extractable aluminium in andic and vitric horizons. Application of principal components analysis and discriminant analysis, however, render the use of weathering indices obsolete.

Al and Fe fractions obtained by selective dissolution techniques (Garcia Rodeja et al.) remain very important for the interpretation of other Andisol properties, but the inadequacy of a single extraction if large amounts of extractable matter is present, was clearly demonstrated (see also Meijer et al., Chapter 2). Although the usefulness of the pyrophosphate extraction is a

matter of recurring discussion, the high correlation between pyrophosphate-extracted and $CuCl_2$-extracted aluminium appears to validate both extractions. The fact that Al_{Cu} is a fixed proportion (30%) of Al_p suggests that the former extracts all but the most strongly bound aluminium from organic complexes, but a full understanding is still lacking. The exchange/complexation capacity of organic matter is strongly influenced by its state of decomposition.

In most soils, NaOH and oxalate extract similar amounts of Al and Si. Exceptions are some alu-andic horizons, in which the Al/Si ratio in oxalate extract is higher than that in NaOH extract. This deviation still needs to be explored in more detail, but a stronger extraction of amorphous SiO_2 phases by NaOH may be an explanation. Soils from which NaOH extracts more Al than oxalate tend to contain gibbsite. Although there is a good correlation between oxalate extractable Al_o or (Al_o-Al_p) and Si_o, this obscures the fact that there is a wide range of Al/Si ratios in the investigated soils. The increase of the Al_p/Al_o ratio with increasing organic C content supports the anti-allophanic effect of organic matter.

$LaCl_3$ and KCl-extracted aluminium is highly dependent on soil pH and therefore more difficult to interpret.

The adsorption complex of volcanic soils is largely defined by variable charge components: organic matter, allophane and imogolite, ferrihydrite (Madeira et al.). The charge behaviour of such components is largely known from experiments on synthetic compounds that cannot be easily extrapolated to field conditions. One indication for this problem is that allophane in the investigated soils appears to have a lower Point of Zero Charge than indicated by literature, which implies that it may have considerable negative charge at field conditions.

Another consequence of the variability of charge is, that CEC determined at pH=7 is well above normal values in the field, and exaggerates the actual exchange capacity. Consequently, soils that are virtually base-saturated under field conditions seem heavily under-saturated. The unbuffered CEC determined by compulsive exchange or by sum of basic cations is a more suitable alternative. Blocking of CEC by binding of organic matter functional groups to allophane is a common feature. AEC clearly depended on Al/Si ratio of the extractable fraction, but amorphous Al-silicates with essentially different AEC appear to exist. This is another unexplored field. At field pH, allophane-rich soils retain anions more effectively than cations.

Because of its practical implications, phosphate sorption is one of the key properties used to identify andic soil materials or horizons. Madeira et al. indicate that, although the kinetic parameter *phosphate retention* adequately identifies most andic horizons, it does not describe the maximum

phosphate fixation capacity of the soil and partially depends on the amount of P already bound to the soil. The maximum phosphate fixation capacity, P_{max} is linearly correlated with oxalate-extractable Al (or Al+½Fe) and is more useful in agricultural evaluation of andic materials. In the investigated soils, extractable iron plays a negligible role in phosphate fixation and variable charge development. Because soils on volcanic materials are hardly ever phosphate-saturated, the various methods to extract P, although mutually correlated, are not well correlated with other soil properties. Kinetics of P-retention (the steepness of the adsorption isotherm) remains virtually unexplained. More data on extractability of the amorphous Al-silicates (and iron compounds), e.g. by sequential extraction, may be needed to solve this problem. Neither P-retention, nor P_{max} were essential criteria for the distinction between vitric, andic and non-andic horizons (Martinez et al.).

Multivariate analysis of the whole set of chemical data (Martinez et al.) results in a number of principal components that are related to weathering, vertical profile differentiation, iron fractionation (crystallinity, binding to organic matter), and effect of organic matter. Principal component analysis readily distinguishes silandic, aluandic and non-andic soil horizons, but discriminant analysis indicates that this can be done with far fewer variables than commonly used in soil classification.

In an era where quantification of soil properties is a basis for soil classification, and where clear and not-so-clear chemical criteria proliferate, it is useful to investigate how many measurements are really necessary to identify the differences that soil classification deems essential. Discriminant analysis indicates that to distinguish Andisols from non-Andisols far fewer properties are necessary than are usually determined. Sometimes a classification criterion functions adequately while it tells us less about soil behaviour than a related parameter. Although the data set is too small for the confident extrapolation of these results, this is a clear indication that chemical criteria for classification of Andisols need to be re-evaluated. This reduction of necessary data cannot be applied to the understanding of interactions in volcanic soils. So far, analytical data – or data handling – have been inadequate for the understanding of such complex relations.

Molecular research on soil organic matter in volcanic soils still shows more gaps than information. The two papers co-authored by Buurman and Nierop – and related research that is currently under way – places serious doubts on the so-called protection mechanisms, such as complexation between allophane and organic matter, that are supposed to slow down the mineralization of plant-derived organic components. The research presented here, and in related papers, suggests that organic matter in andic horizons is rapidly and strongly degraded and that high organic matter con-

tents may be due to a high production of primary and secondary organic components rather than to a strong preservation of primary ones. Components that are relatively stable in other soils, such as lignin fragments and long-chain aliphatic molecules, are readily degraded in allophane-rich horizons and strongly decrease with depth. Unpublished research on a volcanic toposequence in Costa Rica further suggests that the organic matter in allophane-rich horizons is more strongly decomposed than that in non-allophanic ones. Obviously, we have to rethink our theories on this matter.

Finally, Andisols strongly adsorb heavy metals. Only organic matter appears to be responsible for this adsorption, but blocking of organic matter sites by adsorption to allophane may reduce both heavy metal adsorption and the non-desorbable fraction (Tanneberg and Jahn). Adsorption capacity for heavy metals varied considerable between samples, but the database was too small to yield meaningful correlation with measured soil properties.

The present research is a large step towards a better understanding of the relation between the properties that are so typical for volcanic ash soils. Nevertheless, there are still major gaps in our knowledge. The result is that we can describe – and roughly understand – soil behaviour, but we cannot yet predict it with our current understanding of non-crystalline Al-Si phases, organic matter, iron compounds, reactive crystalline minerals, and their interactions. In some cases, such as heavy metal adsorption, there is too little information for extrapolation; in some others our understanding is inadequate. The present papers clearly indicate where gaps exist in our knowledge and where additional research could improve our understanding.

The physico-chemical data base

P. Buurman, F. Bartoli, A. Basile, G. Füleky,
E. Garcia Rodeja, J. Hernandez Moreno and M. Madeira

Introduction

To allow for better correlation between properties and to obtain a homogeneous data set, all soil samples were analysed by the same laboratories. All results are given in the file *chemical data base.xls* (on CD) and readers can choose to reprocess these data after unlocking the files.

Homogenization and distribution of samples

All samples were sent to the Laboratory of Soil Science and Geology, Wageningen University, The Netherlands. In Wageningen, the samples were sieved over a 2 mm sieve. The fine earth fraction was homogenized and split into sub-samples. Each of the participating laboratories received about 200 g of homogenized sample. The remaining samples are stored in Wageningen (ask ISRIC) and part is still available upon request.

Samples of the profiles EUR01–EUR06 were kept field moist and distributed in moist state. Because this procedure was too time consuming, samples of profiles EUR07–EUR20 were air dried before homogenization, splitting and distribution. The participating laboratories and the methods employed are given below.

Remarks regarding the data base

Remarks in green

If sampling or analytical methods deviate from the standard, this is indicated by a numbered remark in a green frame. The remarks are found at the bottom of the table.

Color codes of chemical properties

To make the table easier to read, grouping of properties is indicated by color codes. Within each group, the same property may have been measured by different laboratories.

Unlikely figures

In some cases, the analytical results are not internally consistent. This is the case in some pyrophosphate and oxalate extractions of Fe and Al and in where the Sum of exchangeable cations exceeds the measured CEC. Inconsistent numbers have been indicated in red.

Profile codes

The original profile numbers started with N. Because some double numbers appeared in the numbering of the Greek and French profiles, it was decided to change all codes into EUR. The table below gives both codes.

Old Code	New Code	Country	Location	Altitude
N1	EUR01	Italy	Gauro	103
N2	EUR02		Gauro	225
N3	EUR03		Vico	700
N4	EUR04		Vico	722
N5	EUR05	Azores	Faial	510
N6	EUR06		Pico	400
N7	EUR07	Iceland	Route 1	40
N8	EUR08		Audkuluheidi	
N9	EUR09		Hella	600
N10	EUR10	Tenerife	Tacoronte	1130
N11	EUR11		Boca Tauce	1675
N12	EUR12		Las Mercedes	1000
N13	EUR13	Santorin	Vlychada	
N14	EUR14		Profitis Ilias	300
N14A	EUR15		Mavro Vouno	230
N15	EUR16	France	Puy de la Vache	1000
N16	EUR17		Buron de Perle	1080
N17	EUR18	Hungary	Tihany	162
N18	EUR19		Badacsony	420
N19	EUR20		Tokaj	482

Horizon coding

The first column gives horizon codes as designed in the field during description and sampling. These codes are also used in the profile descriptions (on CD). In some cases, chemical and mineralogical data indicates sedimentary stratification. For the first twelve profiles, revised codes were suggested by Buurman et al. (2004). For the other profiles, the codes were slightly revised during a meeting on soil (micro)morphology in Paris (2004) and a subsequent meeting of Working Group IV in Santiago de Compostela (2004).

Melanic index

This index was determined exclusively for horizons that might have melanic properties.

Subdivision of Andosols

The subdivision into *vitric, alu-andic, sil-andic,* and *non-andic* is based on chemical properties and (incomplete) sand mineralogy. The subdivision is provisional.

Wet/dried soil samples

Both Nancy and Naples analysed bulk and undisturbed wet soil samples, collected very near to the soil volumes sampled for the joint chemical analysis. The reported results from both Nancy and Naples can therefore be correlated with the other chemical and grain-size results.

For oxalate and pyrophosphate extractions, all laboratories used field moist samples of the profiles EUR01–06. Of the later profiles, Nancy analyzed moist samples and the other laboratories air-dried samples. Observed discrepancies between the results should be attributed to a dilution effect when the extractions were carried out on wet soils and to a possible decrease of colloid accessibility when the extractions were done on dried soils in case they shrink (see section 4 of the book).

Grain-size fractions

The weight fraction >2 mm was only determined for part of the samples. For most soils, the organo-mineral clay was determined and also the laser-

diffraction grain-size fractions <2 and <20 μm (volume fractions). The latter were obtained after removal of organic matter (for a detailed discussion see Buurman and van Doesburg, this volume). For the Hungarian soils, the fraction <50 μm is given instead of <20 μm, because these soils contain no allophane and have a considerable admixture of loess.

Apart from the specificities of the Na resin dispersion method or the removal of organic matter or poorly-ordered minerals before water dispersion, particle size analysis of the profiles EUR07–20 was carried out on either field-moist soil samples (Nancy) or air-dried soil samples (Wageningen), with possible irreversible aggregation for some dried soils due to shrinkage, although this was not evident from the results. Nancy used the Robinson pipette/sedimentation method (Stokes law). Both pipette method and laser diffraction use an equivalent particle diameter that does not apply to platy particles (clay minerals). Pipette method results are reported as weight percentages (obtained by gravimetry) and laser diffraction results as volume percentages. This should normally provide a good correlation between the two, but because the measurements are essentially different, correlations between clay fractions obtained by the two methods are usually satisfactory, but deviate from unity (Buurman et al. 1997, 2001).

Oxalate extractions

The Santiago data form a consistent data set. Wageningen performed a number of sequential extractions on the same samples (see Meijer et al. this volume). The oxalate-Si,Al,Fe values reproduced under 'Wageningen' are the sum of the first two extractions.

Pyrophosphate extractions

Because Na-pyrophosphate is a strong surfactant, all extracts have been centrifuged *and* filtered.

Allophane-Parfitt

These 'allophane' contents were calculated using the formula published by Mizota and Van Reeuwijk (1989), as follows:

$$\% \text{ allophane} = 100/y \times \%Si_o,$$

in which $y = -5.1x + 23.4$, and $x = (Al_o - Al_p)/Si_o$.

This formula was based on regression analysis of a number of allophane-bearing samples with Al/Si ratios between 1 and 2.5. Data and graphs for the calculations are given in the file *allophane graphs.xls* on CD. The table below shows that for some groups there is a good correlation between the two allophane values, but the Al/Si ratios are obviously different between the groups. The correlations have not been reproduced out for the soils with very low amounts of extractable material and/or low correlation coefficients.

Allophane (Parfitt) = a × allophane (14% Si)		
Group	a	R^2
Azores	1.68	0.35
Azores without outlier	1.35	0.95
Iceland	0.952	0.98
Tenerife	1.155	0.96

Figure 1 shows that although the general correlation is good, there are some remarkable outliers. In Figure 2, the difference between the two allophane calculations (Parfitt - 14% Si) is plotted against the $(Al_o\text{-}Al_p)/Si_o$ ratio for all but the three samples with the largest difference (the full graph is in the file *allophane graphs.xls*). Figure 2 shows that serious deviations between the two calculations start at Al/Si ratios above 2. Because the 'Parfitt method' puts all extracted Al and Si into the allophane, there is the obvious problem of extracted gibbsite. Especially the soils in which the presence of gibbsite has been demonstrated show excessive contents of allophane(Parfitt).

Participating laboratories

France

Most analyses were carried out at the Centre de Pédologie Biologique CNRS, 54505 Vandoeuvre les Nancy Cedex, France. This centre is now closed and the group that carried out the analyses moved to the Laboratoire Sols et Environnement UMR 1120 ENSAIA – INPL/INRA, BP 172, 54505 Vandoeuvre les Nancy Cedex, France.

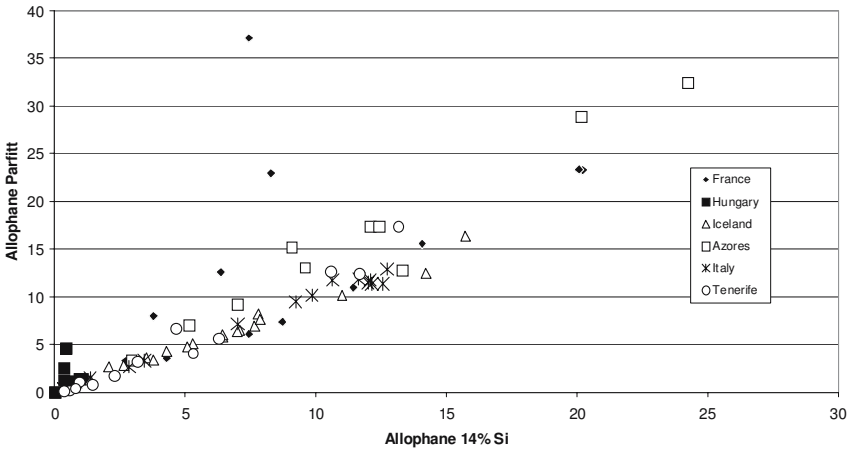

Figure 1. Plot of calculated allophane with 14% against allophane with variable Al/Si ratio (allophane-Parfitt).

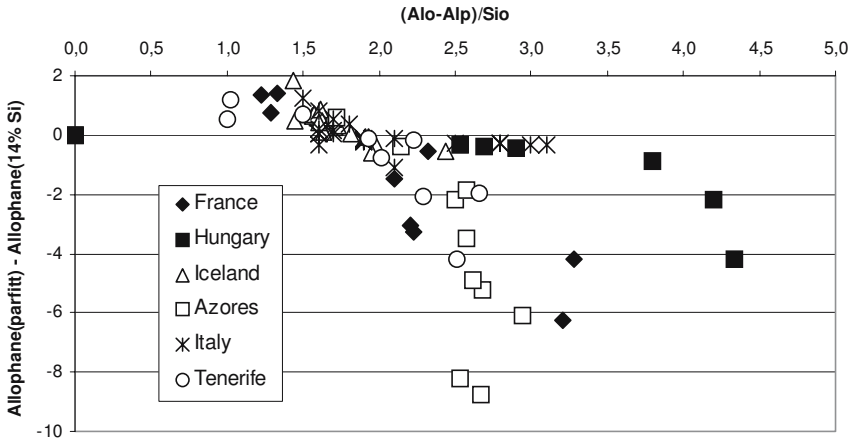

Figure 2. Deviation between allophane(Parfitt) and allophone (14% Si) in relation to Al/Si ratio.

Hungary

Most of the soil analyses and the hot water percolation, phosphate and atrazine adsorption experiments were carried out in the Agrochemistry Laboratory of the Department of Soil Science and Agricultural Chemistry, Szent István University Gödöllő. The Si, Al and Fe were determined in the

Central Laboratory of the Szent István University Gödöllő. Atrazine was determined at the Analytical Chemistry Department of the Institute for Veterinary Medicinal Products, Budapest.

Italy

Institute for Mediterranean Agricultural and Forest Systems (ISAFoM) – National Council of Research (CNR), P.O Box 101, 80040 San Sebastiano al Vesuvio (NA).

The Netherlands

Laboratory of Soil Science and Geology, Dept. of Environmental Sciences, Wageningen University. P.O. Box 37, 6700 AA Wageningen.

Portugal

Analyses were carried out in the soil laboratory of the Departamento de Ciências do Ambiente, Instituto Superior de Agronomia, Tapaada da Ajuda, 1349-017, Lisboa.

Spain-Santiago

Departamento de Edafología y Química Agrícola, Facultad de Biología, Universidad de Santiago de Compostela (USC). Rúa Lope Gómez de Marzoa s/n, Campus Sur, 15782 Santiago de Compostela.

Methods

Department of Soil Science and Agricultural Chemistry, Faculty of Biology. University of Santiago de Compostela

All measurements were performed by duplicate except when a different number of replicas is indicated.

All results are referred to oven dry weight (105ºC).

Moisture content and moisture correction factor

Moisture content was obtained following the procedure described by Buurman et al. (1996). When applicable, moisture correction factors were used to calculate the results of soil analysis on oven-dry basis.

pH measurement

The soil pH were measured in H_2O and 1 M KCl using a 1:5 soil:solution ratio following the procedure described by Buurman et al. (1996).

pH in NaF

The pH in NaF was measured using 1 M NaF and a soil:solution ratio of 1:50 after 2 minutes of equilibration, following the procedure described by Buurman et al. (1996).

Total C, N and S

Total C and N were determined by combustion using an elemental analyser LECO CHN-1000, following the standard procedures described in the instruction manual of the analyser. Between 0.1 and 0.2 g of wet soil sample were introduced in the combustion oven in a tin capsule. The following C and N standards were used for calibration: Leco-EDTA 502-092, Leco-SOIL 502-309 and Leco-SOIL 502-308.

For the total S content measurement an elemental analyser LECO SC-144DR was used, following the standard procedures described in the instruction manual. Calibration was obtained with the following standards: Leco-SOIL 502-309, Leco-SOIL 502-308 and Leco-COAL 501-005. A quantity of wet soil sample ranging from 0.5 to 0.7 g was directly introduced in the combustion oven in a ceramic capsule.

All total C, N and S measurements were performed in triplicate.

Exchangeable Al (Al KCl extractable)

The extraction of Al with 1 M KCl was as follows: 5 g of soil were shaken for 30 min with 30 ml of the extracting solution; then the suspension was centrifuged for 15 min at 3000 rpm and the supernatant transferred through a filter to a 200 ml volumetric flask. The procedure was repeated another four times. After the last extraction the filter was washed twice with 10 ml

of the extracting solution and the volume of the flask made up with 1 M KCl (Buurman et al. 1996).

$LaCl_3$ extractable Al

The extraction is based in the method proposed by Hargrove and Thomas (1981). The extraction solution used was 0.33 M $LaCl_3$ (pH 4.0). For the extraction 10 g of soil were shaken for 2 h with 50 ml of the extracting solution; then the suspension was filtered through acid-washed paper and washed with $LaCl_3$ to a volume of 100 ml.

$CuCl_2$ extractable Al

The extraction is based in the method proposed by Juo and Kamprath (1979). The extraction solution was 0.5 M $CuCl_2$ (pH 2.8). For the extraction 5 g of soil were shaken for 5 min with 50 ml of the extracting solution; then the suspension was allowed to equilibrate for 12 h and was shaken again for 30 min, filtered through acid-washed paper and the soil in the filter washed with $CuCl_2$ to a volume of 100 ml.

Pyrophosphate extractable Al and Fe

Aluminium and Fe were extracted with 0.1 M Na-pyrophosphate (pH10) using a soil:solution ratio 1:100 and shaking for 16 h. The suspension was centrifuged (15 min at 2500 rpm, with 3 drops of 0.2% 'superfloc') as described by Buurman et al. (1996). Before the measurement of Fe and Al, the supernatant was pre-filtered through an acid washed paper filter (7–11 μm pore size) and through a 0.45 μm pore size filter.

Acid oxalate extractable Al, Fe, Si and Mn

Aluminium, Fe, Si and Mn were extracted with 0.2 M ammonium oxalate - oxalic acid at pH 3 using a soil:solution ratio 1:50 and shaking for 4 h in the dark as described by Buurman et al. (1996). Before the measurements the suspension was centrifuged for 15 min at 2500 rpm, with 3 drops of 0.2% 'superfloc' and the supernatant was pre-filtered through an acid washed paper filter (7–11 μm pore size) and through a 0.45 μm pore size filter.

Dithionite extractable Al, Fe, Si and Mn

Aluminium, Fe, Si and Mn were extracted with Na citrate (17%) + Na dithionite (1.7%) (Holmgren 1967) using a soil:solution ratio 1:60 and shaking for 16 h as described by Buurman et al. (1996). Before the measurements the suspension was centrifuged for 15 min at 2500 rpm, with 3 drops of 0.2% 'superfloc' and the supernatant was pre-filtered through an acid washed paper filter (7–11 μm pore size) and through a 0.45 μm pore size filter.

Aluminium and Si extraction with NaOH

Aluminium and Si were extracted with 0.5 M NaOH using a soil:solution ratio of 1:100 and shaking for 16 h (Borggaard 1985). Before the measurements the suspension was centrifuged for 15 min at 2500 rpm, with 3 drops of 0.2% 'superfloc' and the supernatant was pre-filtered through an acid washed paper filter (7–11 μm pore size) and through a 0.45 μm pore size filter.

Aluminium, Fe, Si and Mn in all the extracts were measured using flame atomic absorption spectrometry (Perkin-Elmer 1100 B) following the standard procedures described in the instruction manual. The results, which are the mean of duplicate analysis that are less than 10% apart, are expressed to oven dry weight (105ºC).

Melanic Index

Melanic index was calculated following the method described by Honna et al. (1988).

Native and water soluble sulphate

Native and water-soluble sulphate were determined following a modification of the method proposed by Johnson and Henderson (1979). Sulphate was extracted with ultra-pure water (water soluble) and 0.016 M KH_2PO_4 (native). In both cases a suspension of 4 g of soil and 40 ml of the extractant was allowed to equilibrate for 1 h, shaken for 14 h, left 1 h for settling and filtered through a 0.45 μm pore size filter. The sulphate in the filtered extracts was measured using ionic chromatography.

Retained sulphate was calculated as native – water soluble sulphate.

Total major and trace elements

Silicon, Al, Na and Mg were measured using XRF (Siemens SRS 3000).

Calcium, K, Ti, Fe, Cr, Mn, Ni, Cu, Zn, Ga, As, Se, Br, Rb, Sr, Y, Zr, Pb, Th and U were analysed using XRF Energy-dispersive Miniprobe Multielement Analyzer (EMMA) at Key Analytical (Canada). The EMMA and its application for element analysis is described elsewhere (Cheburkin and Shotyk 1996, Weiss et al. 1998, Shotyk et al. 2000). Detection limits for the elements were: 0.01% for K, Ti and Fe; 0.05% for Ca; 0.7 µg g^{-1} for Se; 1 µg g^{-1} for Rb and Ga; 1.5 µg g^{-1} for Sr; 2.0 µg g^{-1} for Zn and Br; 2.5 µg g^{-1} for Y and Pb; 3 µg g^{-1} for Cu; 4 µg g^{-1} for Th and U; 5 µg g^{-1} for Ni, As and Zr; 30 µg g^{-1} for Mn and 50 µg g^{-1} for Cr.

Mercury was analysed with a LECO-ALTEC AMA-254, a single purpose atomic absorption spectrophotometer for Hg determination in liquid and solid samples, with a detection limit of 0.01 ng of Hg and a working range from 0.05 to 600 ng. Each sample was analysed in triplicate.

The instruments were calibrated using certified standard reference materials.

Abrasion pH and abrasion solution composition

Abrasion pH was measured in per-oxidized samples (to minimize the homogenizing effect of organic matter in the pH values) following the method of Grant (1969) that consists of measuring the pH of a soil (20 g): distilled water (40 ml) suspension after a grinding period of 2¼ min (+ 2 min for settling) in an agate mortar. After centrifugation of an aliquot of the suspension, Ca, Mg, Na, K, Fe, Mn, Si and Al were measured by atomic absorption spectrophotometry.

Centre de Pédologie Biologique CNRS, 54505 Vandoeuvre les Nancy Cedex, France Nancy

Bulk density

Bulk density was the mean of three soil core replicates (cylinders of internal diameter of 2.65 cm and internal height of 5 cm, volume of 28.6 cm^3) dried at 105°C for 48 hours.

Organo-mineral clay

The amounts of total organo-mineral clay were determined by Na cation-exchange resins, which are recommended dispersants for strongly aggregated soils such as Oxisols and Andisols (Bartoli et al. 1991).

A specific methodology was designed for the reference COST 622 soils, as follows: 500 mg of field wet soil was added to 200 ml demineralised water, ultrasonicated and wet-sieved at 200 and 50 µm. The <50 µm soil suspension was then added to 100 ml of Na Amberlite IR-120 (500 µm mesh) resin and shaken for 16 hours in an end-over-end shaker at 40 rpm. The resin was collected by wet sieving at 50 µm and the <50 µm soil suspension was finally transferred to a 250 ml beaker of 37.5 mm internal diameter and 226 mm height and made up to a volume of 250 ml with demineralised water. The amount of clay (expressed with respect to 105°C dried soil) was determined using the Robinson pipette method.

For the Greek soils the dispersant used was Na hexametaphosphate: ten g of <2 mm air-dried sample was added to 25 ml HMP solution (124 g l^{-1}) and 175 ml demineralised water and shaken for 16 hours in an end-over-end shaker at 40 rpm. Sieved at 200 µm and then at 50 µm the suspension was transferred to a 1 l beaker and made up to a volume of one litre with demineralised water. Amount of clay (expressed in proportions of 105°C dried soil) was determined using the Robinson pipette method.

Elementary carbon and nitrogen

Elementary organic analysis by dry combustion of the ground <2 mm air-dried soil using a Carlo Erba NA 1500 auto-analyser (mean of two replicates).

Oxalate and pyrophosphate extractions

Extractions on field-moist soils were done following the standard procedures (see above) with Al, Fe and Si analyses by atomic adsorption.

Calcium carbonate

Calcium carbonate (Greek soils) was determined using a Carmograph 8, as follows: 1 g of <2 mm dried soil was ground and put into a hermetically-closed reactor, 10 ml of HCl 6N was then added in this reactor where the soil suspension was magnetically shaken. Standardization of the results

(variation of electric conductivity of a NaOH N/25 solution due to CO_2) was made using a $CaCO_3$ reference.

Institute for Mediterranean Agricultural and Forest Systems (ISAFoM-CNR)

Bulk density

Bulk density was measured on undisturbed soil samples dried at 105°C for 24–48 hours. The soil was collected in cylinders (diameter = 7.25 cm, height = 7.00 cm) filled up to about 200 cm^3.

Volumetric water content

Two characteristic values have been reported: at 0 kPa and at 33 kPa of pressure head. Both derive from an interpolation of the measured data of the soil water retention curve. The 4-parameter van Genuchten equation (van Genuchten 1980) was used in the fitting procedure by applying a least squares analysis method.

Agrochemistry Laboratory of the Department of Soil Science and Agricultural Chemistry, Szent István University Gödöllő. Central Laboratory of the Szent István University Gödöllő. Analytical Chemistry Department of the Institute for Veterinary Medicinal Products, Budapest

Hot Water extraction

30 g fine earth (<2 mm) was put into the container of the HWP instrument. Hot water (about 102–105°C) was percolated through the soil sample for some minutes collecting 100 cm^3 solution. C, N, K, Na, Ca, Fe, Mn, Zn, Cu, Ni, Pb content and pH were determined.

Phosphate sorption

1 g fine earth (<2 mm) was equilibrated in 10 cm^3 solution with 0, 50, 100, 500, 1000, 3000, 5000 and 10000 mg kg^{-1} P as KH_2PO_4, respectively for 24 hours.

Atrazine sorption

2 g fine earth (<2 mm) was equilibrated in 20 cm^3 solution of 0.5–15.0 mg dm^{-3} atrazine for 16 hours. Atrazine content was determined with high performance liquid chromatography.

Instituto Superior de Agronomia – Departamento de Ciências do Ambiente

pH (H_2O, KCl, NaF),

The soil pH was measured in H_2O, 1 M KCl and 1 M NaF, following the procedures used in the Department of Soil Science and Agricultural Chemistry of the University of Santiago de Compostela.

Organic C

Organic carbon was measured by wet oxidation, following the method described by De Leenheer and Van Hove (1958).

Phosphorus retention

Phosphorus retention was determined on fine earth (<2 mm) using the Blakemore method as described by Buurman et al. (1996).

Extractable ("available") phosphorus

P was extracted by distilled water and by 0.01 M $CaCl_2$, shaking the samples for 1 h and 2 h, respectively, at a soil to solution ratio of 1:10 (Self-Davis et al. 2000). Extractable P in fine earth (<2 mm) was determined by the Olsen and Bray methods as described by Buurman et al. (1996). Extractable P was also assessed by the Egner-Riehm and the Mehlich methods, using the methodology described, respectively, by Riehm (1958) and by (Mehlich (1984).

Cation exchange capacity and exchangeable bases

The cation exchange capacity (CEC) was determined by the 1 M NH_4OAc method using continuous leaching of 5 g of fine earth (<2 mm) with 100 ml of 1 M NH_4OAc adjusted to pH 7. The leachate was used to determine

the exchangeable bases by atomic absorption spectroscopy (AAS). The adsorbed NH_4^+ was displaced with acidified 1 M KCl and the NH_4^+ in the leachate was then measured for CEC using the Kjeldahl standard method. The results were expressed on an oven dry basis (105°C).

The cation exchange capacity was also determined by the compulsive exchange procedure (CEC_{CE}). Basic cations and Al were extracted by shaking 2 g of fine earth (<2 mm) with 2 ml of a mixture of 0.1 M $BaCl_2/NH_4Cl$ for 2 h, and the bases were measured in the extract by AAS. Then, the soil was saturated with $BaCl_2$ at a solution ionic strength of 0.002 M followed by the addition of 0.05 M $MgSO_4$. Magnesium remaining in the solution was used to determine the compulsive cation exchange capacity. The amount of Cl^- in the solution was measured using the silver nitrate titration method for the determination of anion exchange capacity (AEC). The CEC_{CE} and the AEC (dried soil basis) were calculated as described by Gillman and Sumpter (1986).

Laboratory of Soil Science and Geology, Wageningen University, the Netherlands

Grain-size characteristics

Grain-size distributions and stability of aggregates were measured by laser-diffraction. The method is described in detail by Buurman and Van Doesburg (this volume).

Sequential extractions

Sequential extractions with oxalate-oxalic acid are described in detail by Meijer et al. (this volume).

References

Bartoli F, Burtin G, Herbillon A (1991). Disaggregation and clay dispersion of Oxisols: Na resin, a recommended methodology. Geoderma 49:301–317

Borggaard OK (1985). Organic matter and silicon in relation to the crystallinity of soil iron oxides. Acta Agriculturae Scandinavica 35:398–406

Buurman P, van Lagen B, Velthorst EJ (eds) (1996). Manual for Soil and Water Analysis. Backhuys Publishers, Leiden, The Netherlands pp 314

Buurman P, Pape Th, Muggler CC (1997). Laser grain-size determination in soil genetic studies. 1. Practical problems. Soil Science 162:211–218

Buurman P, Pape Th, Reijneveld JA, de Jong F, van Gelder E (2001). Laser-diffraction and pipette-method grain-sizing of Dutch sediments: correlations for fine fractions of marine, fluvial and loess samples. Netherlands Journal of Geosciences 80:49–57

Cheburkin AK, Shotyk W (1996). An energy dispersive miniprobe multielement analyzer (EMMA) for direct analysis of Pb and other trace elements in peats. Freis Jour Anal Chem 345:688–691

De Leenheer L, Van Hove J (1958). Determination de la teneur en carbone organique des sols. Etudes critiques des methods titrimétriques. Pédologie 8:39–77

Gilman GP, Sumpter EA (1986). Modification to the compulsive exchange method for measuring exchange characteristics of soils. Australian Journal of Soil Research 24:61–66

Grant WH (1969). Abrasion pH, an index of chemical weathering. Clays and Clay Minerals 17:151–155

Hargrove WL, Thomas GW (1981). Extraction of aluminium from aluminium-organic matter complexes. Soil Science Society of American Journal 45:151–153

Holmgren GS (1967). A rapid citrate-dithionite extractable iron procedure. Soil Science Society of American Proceedings 31:210–211

Honna T, Yamamoto S, Matsui K (1988). A simple procedure to determine the melanic index that is useful for differentiating Melanic from Fulvic Andisols. Pedologist 32:69–75

Johnson DW, Henderson GS (1979). Sulfate adsorption and sulfur fractions in a highly weathered soil under a mixed deciduous forest. Soil Science 127:34–40

Juo AS, Kamprath EJ (1979). Copper chloride as an extractant for estimating the potentially reactive aluminium pool in acid soils. Soil Science Society of American Journal 43:35–38

Mehlich A (1984). Notes on Mehlich 3 soil test extractant: a modification of Mehlich 2 extractant. Comm Soil Sci Plant Anal 15:1409–1416

Mizota C, van Reeuwijk LP (1989). Clay mineralogy and chemistry of soils formed in volcanic material in diverse climatic regions. International Soil Reference and Information Centre Soil Monograph 2:1–185. ISRIC, Wageningen

Riehm H (1958). Die ammoniumlaktatessigsäure Methode zur Bestimmung der leichtlöslichen phosphorsäure in karbonathaltigen Böden. Agrochimica 3:49–65

Self-Davis ML, Moore, PA Joern BC (2000). Determination of water and/or dilute salt-extractable P. In GM Pierzynski (ed) Methods of phosphorus analysis for soils, sediments, residuals and waters. Southern Cooperative Series Bull. No. 296, USDA-CSRRES Regional Committee, USA

Shotyk W, Blaser P, Grünig A, Cheburkin AK (2000). A new approach for quantifying cumulative, anthropogenic, atmospheric lead deposition using peat cores from bogs: Pb in eight Swiss peat bog profiles. Science of the Total Environment 249:257–280

van Genuchten M Th (1980). A closed-form equation for predicting the hydraulic conductivity of unsaturated soils. Soil Sci Soc Am J 44:892–898

Weiss D, Shotyk W, Cheburkin A (1998). Determination of Pb in ashed peat plants using and energy-dispersive miniprobe multi-element analyzer (EMMA). Analyst 123:2097–2102

Appendix materials on CD-Rom

Physico-Chemical data base.xls
Allophane graphs.xls

Elemental composition of Reference European Volcanic Soils

A. Martínez-Cortizas, J.C. Nóvoa, X. Pontevedra,
T. Taboada, E. García-Rodeja and W. Chesworth

Introduction

The content and distribution of elements in soils depend on a number of factors: (1) the nature of the parent material from which they develop, (2) the weathering processes dominating in the soil environment, (3) biocycling, (4) additions via atmospheric deposition due to natural sources and (5) human activity. The importance of each of these main factors depends on the degree of soil evolution – in weakly evolved soils the imprint of the parent material is more important than in strongly evolved ones – and the mobility of the specific element in the soil environment. But it also depends on external factors (land use, vegetation, proximity to pollution sources). Human activity may have direct impacts, such as fertilization, or indirect ones such as atmospheric pollution.

The elemental composition of soils is of great interest for pedogenetic interpretation since it provides a good way to decipher the relevance of each of the main factors affecting soil evolution; but it is also important in soil fertility, acidity neutralization, weathering, and clay mineralogy. As Kurtz et al. (2000) have stated, weathering profiles are complex open geochemical systems that, stripped to their essence are chromatographic columns.

Studies on the elemental composition of volcanic soils are particularly scarce (Laurelle and Stoops 1967, Kobayashi 1979, Rahman et al. 1996, Fujikawa et al. 2000, Palumbo et al. 2000, Meijer and Buurman 2003). In this chapter we describe the results of the analysis of 26 elements (Na, Mg, Al, Si, P, Cl, K, Ca, Ti, Cr, Mn, Fe, Ni, Cu, Zn, Ga, As, Rb, Br, Sr, Y, Zr, Hg, Pb, Th, and U) in the fine earth fraction (<2 mm) of the soils. The main objectives are: (1) to provide a data base of some major and trace elements in volcanic soils from different European countries, (2) to describe their vertical distribution and (3) to relate it to the main factors affecting element concentrations.

Material and methods

Within the framework of the EU-COST Action 622, twenty soils (EUR01 to EUR20) developed on volcanic materials from Azores Islands, Canary Islands, France, Hungary Greece, Iceland, and Italy were described, sampled and analyzed for a large number of properties. Information on location, parent material, climate and soil properties can be found in the different chapters of this book. Only part of this information will be presented later when discussing the role of parent material and degree of weathering on elemental composition.

Subsamples of fine earth (<2 mm) from each soil horizon were air-dried, finely milled, homogenized, and all elements except Hg were determined by XRF analysis. Mercury was measured with a LECO-ALTEC AMA-354 Hg analyzer, which is a single-purpose atomic absorption spectrophotometer for solid and liquid samples. No sample pretreatment was done for any of the determinations. These techniques and the detection limit for each element are described in the corresponding chapter of this book.

The considerably large number of samples (92) analyzed demanded a multivariate statistical approach. Thus we performed both hierarchical cluster analysis (HCA) and principal components analysis (PCA) to get insight into the structure of the variance of the population and the main controlling factors. HCA was performed in two ways: (1) in the variable mode to get information on the association of the different elements and (2) in the sample mode, to establish the compositional affinity of the horizons and soils. HCA data were standardized using Z scores ($Z_i=(x_i–M)$/SD; were x_i is the content of element x in sample i, M is the mean value of x in the total population and SD is the standard deviation of the mean) to avoid the scale effect resulting from the different orders of magnitude in elemental concentrations. Statistical analyses were performed using SPSS software.

Because of the largely different nature of the organic and mineral horizons, a certain bias can be expected in the statistical analyses. To check this possibility we performed both PCA and HCA with and without organic horizons and found no significant changes in the association of the mineral ones. As it will be shown later, the few organic horizons (four O and two H) studied here showed a closer link to the mineral horizons of the same soil than to other O horizons.

Results and discussion

In the dendrogram of Figure 1A it can be seen that K, Rb, U, As, Pb and Th are closely related; Sr is linked to this group. Silicon, Na and Cl form a second group and Y joins both K and Si groups at a larger distance. The metallic elements also show a close association in two subgroups: one including Ti, Cr, Fe and Ni and another one with Al, Ga and Zr. Br and Hg show shorter distances to the metallic elements, and P, Mn and Zn join at a higher hierarchical level. Ca, Mg, and Cu also link to the metallic elements at large distances.

PCA analysis is consistent with these results (Figure 1B). The loadings of each individual element on the first six components (those with eigen values greater than 1) are in Table 1. They account for 79% of the total variance. The variation in the first principal component (PC1) is dominated by the very high positive loadings of Rb, K, Si, As, U, Pb, Na and Th (0.85–0.61) and high negative loadings of Fe, Ti, Cr and Ni (–0.87 to –0.60). Variation in PC2 is mainly associated with Al, Zr, Th and Ga (0.77–0.67) versus Ca content (–0.63); in PC3 to Sr and P (0.62, 0.56) versus Y (–0.43); in PC4 to Cu, Mg and Ca (0.56–0.55) versus Br (–0.39); in PC5 to Cl, Mn, Cu and Hg (0.52–0.47) versus Sr (–0.34); and in PC6 is almost exclusively due to Zn (0.71).

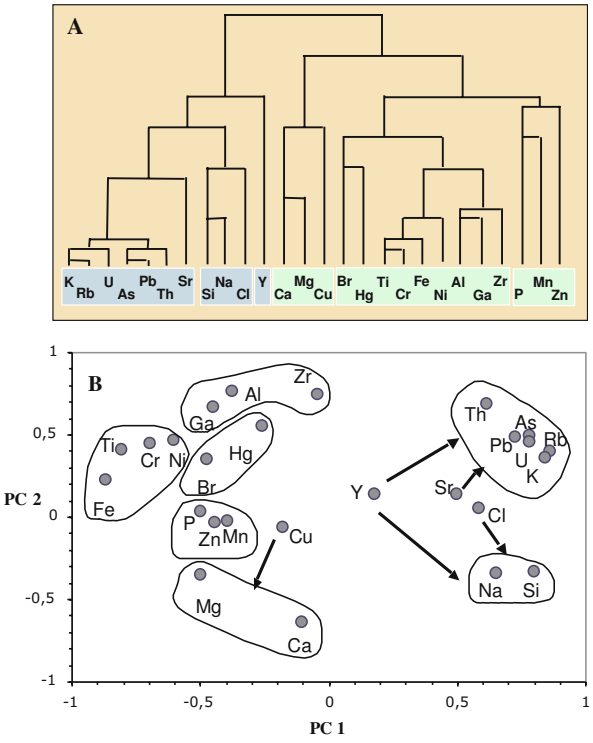

Figure 1. (A) Dendrogram of the HCA analysis of the elements analyzed in this study. (B) PC1/PC2 projection of elements loadings of the PCA analysis.

Table 1. PCA loadings of the first six principal components (eigen values greater than 1) accounting for 79% of the total variance. In bold the variables with major contributions to each component.

	PC1	PC2	PC3	PC4	PC5	PC6
Na	**0.652**	–0.340	–0.336	–0.090	0.033	0.161
Mg	–0.499	–0.345	0.231	**0.557**	0.003	–0.022
Al	–0.381	**0.774**	0.041	0.136	–0.287	0.041
Si	**0.796**	–0.328	–0.376	0.038	–0.110	–0.012
P	–0.504	0.037	**0.560**	–0.220	0.095	0.194
Cl	0.580	0.053	–0.329	0.037	**0.519**	–0.096
K	**0.837**	0.367	–0.024	0.077	0.197	0.082
Ca	–0.106	**–0.635**	0.273	**0.550**	0.006	0.079
Ti	**–0.809**	0.416	–0.087	0.170	–0.041	–0.067
Cr	**–0.700**	0.448	–0.132	0.196	0.147	–0.304
Mn	–0.395	–0.020	0.226	0.022	**0.516**	–0.139
Fe	**–0.872**	0.226	0.065	0.203	0.135	–0.065
Ni	**–0.604**	0.475	–0.244	0.275	–0.103	–0.322
Cu	–0.181	–0.057	–0.126	**0.565**	**0.444**	0.193
Zn	–0.448	–0.033	0.108	–0.070	0.173	**0.712**
Ga	–0.452	**0.671**	–0.268	–0.070	–0.212	0.273
As	**0.776**	0.499	0.275	0.110	0.077	–0.040
Br	–0.474	0.354	0.135	**–0.390**	0.160	0.011
Rb	**0.856**	0.407	0.100	0.088	0.146	–0.058
Sr	0.497	0.148	**0.625**	0.251	**–0.342**	0.217
Y	0.178	0.142	**–0.430**	**0.403**	0.093	0.380
Zr	–0.044	**0.746**	–0.370	0.084	–0.204	0.267
Pb	**0.723**	0.489	0.256	0.041	0.179	–0.090
Hg	–0.260	0.555	0.077	–0.320	**0.474**	0.141
Th	**0.610**	**0.693**	0.190	0.128	–0.121	–0.087
U	**0.776**	0.460	0.187	0.203	0.044	–0.023
Variance (%)	34.7	19.1	7.7	6.8	5.8	4.8
Cumulative		53.8	61.5	68.3	74.1	78.9

This set of six principal components explains almost all the variation in the concentration of Si, As, Rb, Zr and Th (>90%); a large proportion of the variation in Al, K, Ca, Ti, Cr, Fe, Ni, Ga, Sr, and Pb (80–90%), and also of Mg, Cl, Zn and Hg (70–80%); moderate proportions for Na, P, and Cu (60–70%); and a relatively low proportion for Mn, Br, and Y (45–50%) (Figure 2).

Most elements seem to group by geochemical affinity. For example, K-Rb or Al-Ga have similar ionic radius so the trace elements (Rb, Ga) frequently substitute the major elements (K, Al) in minerals; Pb, Th and U form a radioactive series; Si and Na are common in alkaline rocks; while metallic elements (Fe, Cr, Fe, Ni) are closely related. This suggests that the

main source of variation is the geological/mineralogical nature of the volcanic material combined with the complex stratigraphy in many soil profiles. The latter obscures to a great extent the variations in the vertical distribution and limits the identification of chemical trends (enrichments or depletions) for most elements. These facts support the idea that pedogenesis is in general terms weak to moderate, although some particular profiles show a greater degree of development – see also the chapter by Taboada et al. (this book) and Table 3.

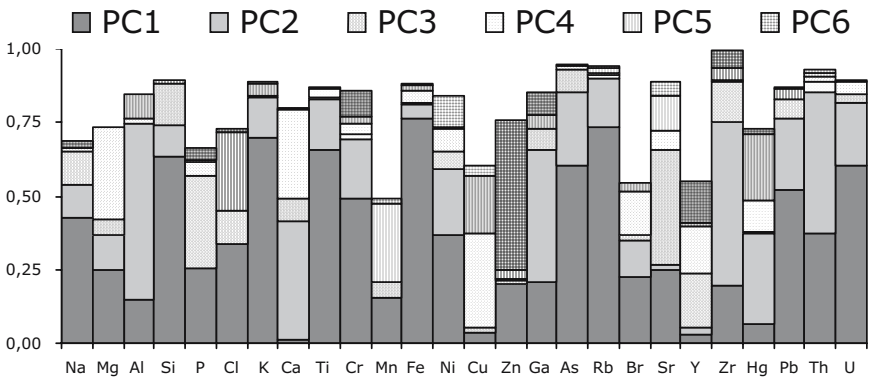

Figure 2. Fraction of total element variance explained by the first six principal components.

Volcanic area: the geological imprint

PCA analysis reveals large compositional differences among the volcanic areas, as also supported by the summarized concentration data presented in Table 2. In the PC1/PC2 projection of samples (Figure 3) soils from Italy, Greece, Azores Islands and Canary Islands (with the exception of EUR11) form well separated groups, while those from Iceland, France and Hungary cluster together.

The soils from Italy (EUR01–EUR04) show the highest concentrations of elements of the K group (maximum values: Cl 0.32, and K 8.6%; Rb 423, As 30, Pb 122, Th 82, and U 23 μg g^{-1}), particularly for U and As since these elements are below or close to the detection limit of XRF in the rest of the volcanic soils (see annexed file). The later elements do not show differences between the two sampled areas (Gauro: EUR01–02, and Vico: EUR03–04); Th only shows relatively lower values in EUR01. But K and Rb concentrations are somewhat higher in the soils developed in the de-

posits of the Gauro than those of the Vico volcano. While Pb concentrations are lower in EUR03, compared to the other Italian soils.

Table 2. Relative elemental composition of soils from the different volcanic areas. Values in bold and italics are the maximum and minimum concentrations of all horizons, respectively. A plus sign (+) indicates relatively rich and a minus sign (-) relatively poor in the corresponding element. (Si, Al, Ca, Mg, Na, K, P, Cl, Ti and Fe are in % and the rest of the elements in µg g^{-1} except for Hg which is in ng g^{-1}).

	Na	Mg	Al	Si	P	Cl	K	Ca	Ti	Cr	Mn	Fe	Ni	Cu	Zn	Ga	As	Rb	Br	Sr	Y	Zr	Hg	Pb	Th	U
Italy	+	-			-	**0.32**	**8.6**	-	-	*<dl*	-	*1.2*	-	**259**	-		**30**	**423**		**1260**	*12*			**122**	**82**	**23**
Azores Islands		+	+	*6.3*	+	-		-	+	+	+	+	+		**205**	+		-	**653**	-			+	-		-
Iceland	-	**3.3**	-			-	-	+			**19353**	**19.6**		+	+			*<dl*	*7*		-	**84**	-	-	*<dl*	*<dl*	-
Canary Islands	*0.1*		**19.7**	-	**1.9**			*0.1*	**10.1**	**1565**			**384**		+	**42**	+		+	*20*		**1136**	**637**	+	+	-
Greece	**3.0**	*0.2*	*6.0*	**32.9**	*<dl*	+		**8.5**	*0.2*		*399*	-	*<dl*	-	*44*	*8*	-		*3*	-	-	*67*	*3*			-
France	-	+	+	-	+		*0.5*	+										-		+		-		-	-	
Hungary	-	+	-	+		-		-				-		-			+	+	-		-	-		+	-	-

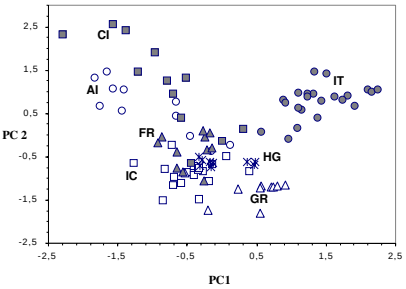

Figure 3. PC1/PC2 projection of the PCA loadings of the soil horizons.

The other soils have much lower contents of all elements in the K-group than those from Italy. Soils from Iceland (EUR07–09) are those with the lowest concentrations. The soils from the Canary Islands (EUR10–12) are richer in Th than those from Iceland, Azores Islands (EUR05–06), Greece (EUR13–15), France (EUR16–17) and Hungary (EUR18–20). Soils from Azores and Canary Islands, in particular EUR06 (AZ) and EUR10 (CI), show very large Ti, Fe, Cr and Ni concentrations (up to 10%, 19.6%, 1565 µg g^{-1} and 384 µg g^{-1} respectively), and plot to the left upper side of the PC1/PC2 projection. They also have high contents of Al, Ga and of Zr in the Canary Islands (Table 3). The lowest concentrations of this group of elements are found in soils from Italy, Greece and Hungary.

Table 3. HCA groups and summarized information for the European volcanic soils presented in this chapter. Parent material is assigned based on the available data from field descriptions (COST) and as proposed in the chapter on chemical weathering (1); Climate: temperature and humidity regimes (Th: thermic, Ms: mesic; Cr: cryic; Fr: frigid; Xr: xeric; Ud: udic); DW: degree of weathering based on the NCIA described in the mentioned chapter (W: weak; M: moderate; S: strong). Cluster: group each horizon belongs to in the hierarchical cluster analysis (see also Figure 4).

	Soil	Parent material COST	Parent material[1]	Climate	DW	Cluster
Italy	EUR01	Pyroclastic trachytic ash	Leucite-trachyte	Th/Xr	W	**L2:** Ap-Bw1-Bw2 **L1:** (2)BC-2C
	EUR02	Pyroclastic trachytic ash	Leucite-trachyte	Th/Xr	W	**K2:** O-Ah **L1:** 2BC1-2BC2-2C1
	EUR03	Tephritic-phonolite with leucite	Tephri-phonolite	Ms/Ud	M	**K2:** O **K1:** Ah1-Ah2-2AB-2Bw1-3Bw2
	EUR04	Tephritic-phonolite with leucite	Tephri-phonolite	Ms/Ud	M	**K2:** O **K1:** Ah1-Ah2-Ah3-2Bw1-2Bw2
Azores Islands	EUR05	Pyroclastic material	Leucite-tephrite and basanite	Ms/Ud	S	**C3:** Ah-3C **J1:** 2Ahb-2Bwb-2Bw/2C1
	EUR06	Balsaltic pyroclastic material	Basalt	Ms/Ud	S	**I:** Ah-AB1-AB2 **J2:** 2Bw1-2Bw2-2Bw3
Iceland	EUR07	Basaltic aeolian and tephra deposits with rhyolitic tephra layers	Basalt (Ah1-2Ah2-2Ah3, 4Bw3-4B/Cg), Andesite (3Bw1-3Bw2)	CrFr/Ud	W	**E:** O-Ah1 **M:** 2Ah2 **C4:** 2Ah3-3Bw1-3Bw2-4Bw3 **D1:** 4B/Cg
	EUR08	Aeolian volcanic ash	Basalt (Ah1-Ah2-Bw1, 3BwC-4C), Dacite (2Bw2)	Cr/Ud	W	**C4:** Ah1-Ah2-Bw1 **F:** 2Bw **D1:** 3BwC-4C
	EUR09	Aeolian, tephra and organic materials	Andesite (A1, 3C-4H), dacite (3H)	CrFr/Ud	W	**C4:** A1-3H-4H **D1:** 3C
Canary Islands	EUR10	Basaltic ash	Basalt	Ms/Ud	S	**J2:** Ah1 **H:** 2Bw-2Bwb1 **N:** 3Bwb2 **O:** 4Bwb3
	EUR11	Basaltic scoria and basaltic lapilli	Tephribasanite (Ah1), nephelinite (2C1), Trachybasalt (3Bwb-4BCb)	Ms/Xr	W	**G:** 1Ah **D2:** 2C1 **C1:** 3Bwb-4BCb
	EUR12	Basaltic ash over weathered basaltic lava	Basalt	Ms/Ud	S	**J2:** Ah1-Ah2-Bw-2Ahb
Greece	EUR13	Pumice	Dacite	Th/Xr	W	**A1:** Ah1-Ah2-C1-Ck
	EUR14	Pumice, volcanic ash	Andesite (Ah), rhyolite (2AC-2C)	Th/Xr	W	**B:** Ah **A1:** 2AC-2C
	EUR15	Pumice	Andesite (Ah), basalt (2C1)	Th/Xr	W	**A1:** Ah **B:** 2C1
France	EUR16	Volcanic scoria	Nephelinite	Ms/Ud	M	**C2:** Ah2-Ah3-2Bw **D2:** 2C/R-2R/C-3R
	EUR17	Trachy-andesitic colluvium	Trachyandesite	Ms/Ud	M	**C3:** Ah1-Ah2-Ah3-Bw1-2Bw2
Hungary	EUR18	Basaltic tuff	Basaltic andesite	Ms/Xr	M	**C5:** Ah1-Ah2-AC
	EUR19	Pyroclasticbasaltic tuff	Basaltic andesite	Th/Xr	W	**C5:** Ah1-Ah2-A/R
	EUR20	Andesitic material	Dacite	Th/Xr	W	**A2:** Ah1-Ah2-Bw/R

Soils from Greece are characterized by high Si (up to 32.9%), Na (up to 3.0%) and Ca (up to 8.5%) contents, but concentrations of most of the other elements are very low (the lowest concentrations for Mg, Al, P, Ti, Mn, Ni, Zn, Ga, Br, Zr and Hg were obtained in the Greek soils). Although

not well separated in the PC1/PC2 projection, Icelandic soils show a distinctive compositional signature as mentioned above, with the lowest contents of elements in the K group and relatively high concentrations of Ca, Mg, Y, Fe and Mn. Soils from France have high contents of Al, Ca and P, and moderately high values of Ti and Fe.

Despite soils from each country tend to show a closer association between them than to other, there is variability within countries due to the particular volcanic region where they develop. In Italy, the soils developed on the Gauro deposits (EUR01–02) are richer in K, Rb and Sr and poorer in Al than those developed on the Vico deposits (EUR03–04). In the Azores Islands EUR06 is richer in metallic elements (Ti, Fe, Cr, Mn, Cu), Th and Y, and poorer in Si, Al, Na and K than EUR05. In the Canary Islands, the three soils show remarkable differences: EUR11 is richer in Si, Na, K, Ca, Mg, Sr and P, and poorer in Pb and Th than the other two; while EUR10 is richer in Ti, Fe, Cr, Ni, Zr and Y than EUR10 and EUR12. In Greece EUR14 separates from EUR13 and EUR15 (it is richer in Al, Fe, Ca, Mg, Mn, Cu and Zn, and poorer in Si, Na, K and Zr); in France EUR17 is richer in Ti, Fe, Cr, Ca, Mg, Sr and poorer in Rb, Zr, Ga and As than EUR16; and in Hungary EUR18 is richer in Al, Ni and Cr and poorer in Pb than EUR19 and EUR20, while EUR19 is richer in P and Zn and EUR20 is poorer in Ca, Fe, Cr, Ni. Soils from Iceland show similar concentrations for all elements.

The dendrogram of Figure 4 shows the main groups (identified by capital letters) and subgroups (identified by numbers) resulting from the HCA analysis. These are also found in Table 3, together with the parent material, climate and degree of weathering of the soils. As shown by PCA the HCA analysis corroborates the volcanic area as the main factor, evidenced by the separation of Italian soils in clusters K and L. But it also shows some other linkages, as for example the close association between soil EUR20 from Hungary (cluster A2) with the Greek soils (EUR13–15), all developed from sub-alkaline Si-rich rocks (dacite, andesite and rhyolite). Cluster C is composed by the soils from Iceland (EUR07–09), France (EUR16–17) and the other two Hungarian profiles (EUR18–19), as well as the Ah and 3C horizons of EUR05 from Azores Islands. Clusters H, I and J correspond to the most strongly weathered soils (EUR10–12 from the Canary Islands and EUR06 and most of the horizons of EUR05 from Azores Islands).

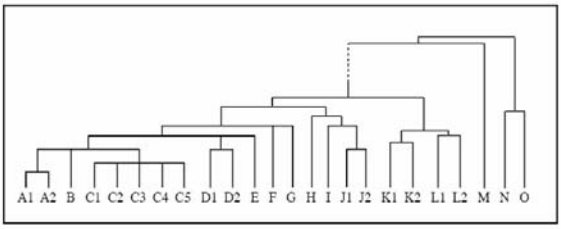

Figure 4. Dendrogram of the HCA analysis showing the main groups and subgroups for the soil horizons. The codes are used in Tables 3 and 4.

At a profile scale the grouping of the basal cycles of the Icelandic soils (EUR07–09) also suggests a similar (basaltic) parent material for the three. These horizons show a composition close to that of the horizon 2C1 of soil EUR11 from the Canary Islands.

Stratigraphic discontinuities

Many soils have irregular concentration profiles, with large shifts between consecutive horizons as a result of lithological discontinuities in the parent material. This aspect was already noted for some soils during field sampling and incorporated into the profile coding (see elsewhere in this book and the annexed file), and was also corroborated by laser-diffraction grain-sizing and chemical composition in previous works (Buurman et al. 2004, Martínez Cortizas et al. 2003). Table 4 shows the elements involved in the geochemical discontinuities, as well as in the other factors responsible for the observed differences in the HCA grouping.

Only six profiles can be considered as truly homogeneous from the compositional point of view: EUR12 from Canary Islands, EUR13 from Greece, EUR17 from France and the three Hungarian soils (EUR18–20). Soils EUR03 and EUR04 from Italy may also be considered as homogenous since the main chemical changes are attributed to the O horizons.

The most heterogeneous profiles contain up to four layers with different chemical composition: EUR07 and EUR10. Four soils have at least three recognizable chemical layers (EUR05, EUR08, EUR09, and EUR11) and the other six have two (EUR01, EUR02, EUR06, EUR14, EUR15, and EUR16). In some cases these chemical layers conform to the discontinuities described in the field, as in profiles EUR05, EUR06, EUR08, EUR09 and EUR11. In other cases parent material layering recognized in the filed is not accompanied by significant changes in chemical composition (EUR03, EUR12, EUR17 and part of soil EUR07); while in others the large changes in chemical composition suggest the presence of more discontinuities than those noted in the field – notably in EUR10 and EUR16.

Element depletion

Most elements (Si, Al, Fe, Na, K, Mg, Ti, Cr, Ni, Ga, As, Rb, Sr, Y, Th, U) show a more or less clear trend of decreasing concentration from the bottommost horizon to the organic-rich surface ones (O and A) – with the exceptions and limitations imposed by soil stratification, as mentioned before. This is largely due to the dilution effect of the organic matter. The ratio X_h/X_{bh} (where X_b is the concentration of a given horizon and X_{bh} that of

the bottom, organic-matter poorest horizon), which is a measure of the relative change in concentration in the fine earth fraction of the soil, shows negative correlations to the C content. The slope of the regression equations (–1.34 to –2.28) is close to the van Bemmelen factor (1.724), which expresses the proportion of C in soil organic matter.

Table 4. Synthesis of the main factors affecting the elemental composition of the COST volcanic soils (GD: geochemical discontinuities; WP: weathering and pedogenesis; EC: external cycles (surface enrichment). Volcanic areas: IT: Italy; AI: Azores Islands; IC: Iceland; CI: Canary Islands; GR: Greece; FR: France; HG: Hungary).

EUR01 IT	Ap	L2	**EC**: Cu, Pb, Hg **WP**: K, Rb, U
	Bw1	L2	
	Bw2	L2	
	(2)BC	L1	
	2C	L1	
EUR02 IT	O	K2	**GD**: Fe, Ca, Mg, Ti, Mn, Sr **WP**: Si, Al, Na, K, Ga, Y, Zr, Th, U, Rb **EC**: Zn, Br
	Ah	K2	
	2BC1	L1	
	2BC2	L1	
	2C1	L1	
EUR03 IT	O	K2	**WP**: Ga, Y, Zr, Th **EC**: Pb, Zn
	Ah1	K1	
	Ah2	K1	
	2AB	K1	
	2Bw1	K1	
	3Bw2	K1	
EUR04 IT	O	K2	**GD**: Ca, Mn, Ni, P, Zn **WP**: Si, Al, Mg, Ti, Ga, Sr, Y, Zr, Th **EC**: Pb
	Ah1	K1	
	Ah2	K1	
	Ah3	K1	
	2Bw1	K1	
	2Bw2	K1	
EUR05 AI	Ah	C3	**GD**: Na, Ca, As, Sr, Al, Mg, Ti, Ni, Zn, Ga, Th **EC**: Hg, Br
	2Ahb	J1	
	2Bwb	J1	
	2Bwb/2C	J1	
	3C	C3	
EUR06 AI	Ah	I	**GD**: Al, Cu, Zn, Ga, Zr, Mg, P, Cr, Mn **EC**: Br
	AB1	I	
	AB2	I	
	2Bw1	J2	
	2Bw2	J2	
	2Bw3	J2	
EUR 07 IC	O	E	**GD:** Si, Na, Sr, Fe, K, Ti, Cr, Mn, Th **EC:** Br, Zn, Hg
	Ah1	E	
	2Ah2	M	
	2Ah3	C4	
	3Bw1	C4	
	3Bw2	C4	
	4Bw3	C4	
	4B/Cg	D1	
EUR08 IC	Ah1	C4	**GD:** Si, Na, Sr, Fe, K, Ti, Cr, Mn, Th, Ca, Mg **EC:** Br
	Ah2	C4	
	Bw1	C4	
	2Bw	F	
	3BwC	D1	
	4C	D1	
EUR09 IC	A1	C4	**WP:** horizon 3C is less weathered
	3H	C4	
	3C	D1	
	4H	C4	
EUR10 CI	Ah1	J2	**GD:** K, Mg, Cu, As, Rb, P, Ni, Fe, Ti, Cr, Zr, Th, Si
	2Bw	H	
	2Bwb1	H	
	3Bwb2	N	
	4Bwb3	O	
EUR11 CI	Ah1	G	**GD:** Al, Na, K, Ca, Mg, Mn, Ni, Cu, Zn, Rb, Sr, Zr, Pb, Th, U **EC:** Hg
	2C1	D2	
	3Bwb	C1	
	4BCb	C1	
EUR12 CI	Ah1	J2	**Homogeneous**
	Ah2	J2	
	Bw	J2	
	2Ahb	J2	
EUR13 GR	Ah1	A1	**Homogeneous**
	Ah2	A1	
	C1	A1	
	Ck	A1	
EUR14 GR	Ah	B	**GD:** Si, Al, Na, Ca, Mg, As, Rb, Y, Zr, Th **WP:** K, Ti, Ga **EC:** Pb, Hg, Br
	2AC	A1	
	2C	A1	
EUR15 GR	Ah	A1	**GD:** Si, Fe, Na, K, Ca, Cr, Mn, Ni, Cu, Ga, Rb, Y, Zr, Pb, Th **WP:** Ca, Mg, Ti, P; **EC**: Hg, Br
	2C1	B	
EUR16 FR	Ah1	C2	**GD:** Si, Al, Fe, Ca, Ti, P, Mn, Ni, Cu, Rb, Th; **EC:** Pb, Hg, Br
	Ah2	C2	
	Ah3	C2	
	2Bw	C2	
	2C/R	D2	
	2R/C	D2	
	3R	D2	
EUR17 FR	Ah1	C3	**Homogeneous**
	Ah2	C3	
	Ah3	C3	
	Bw1	C3	
	2Bw2	C3	
EUR18 HG	Ah1	C5	**Homogeneous**
	Ah2	C5	
	AC	C5	
EUR19 HG	Ah1	C5	**Homogeneous**
	Ah2	C5	
	A/R	C5	
EUR20 HG	Ah1	A2	**Homogeneous**
	Ah2	A2	
	Bw/R	A2	

Apart from this apparent dilution effect, the lower concentrations in the surface horizons may also be the result of element mobility. Martínez Cortizas et al. (2003) indicate that Ca, K, Sr, Zr, Th and U show significant depletion in the Italian soils. Calcium, K, and Sr (and to some extent Rb) are very mobile elements and they tend to be leached rapidly from the more weathered horizons. But also Zr mobilization was reported for volcanic soils (De Paepe and Stoops 1969), with net losses increasing with water availability (Kurtz et al. 2000). The relative increase in the Ti/Zr ratios from the deeper to the surface horizons can also be taken as an indication of a greater degree of weathering. But despite these overall weathering trends, most soils seem to be weakly to moderately evolved.

Figure 5 shows the relation between the normalized weathering index (NCIA, see chapter by Taboada et al. this book) and the concentrations of the elements – only those showing a trend have been included. Although the complex stratigraphy of the volcanic soils makes it difficult to assess the mobility of the elements from their vertical distribution profiles, the plotting of all samples against the NCIA gives quite a relevant information. Silicon, Na and to different extents K, Ca, Rb and Sr show a decreasing concentration with increasing degree of weathering supporting the interpretation that they are mobile in andic soils – it is worth to remind that the non-andic soils are those with the lowest degree of weathering of those we have studied. It is also noticeable that the general trend shown by Zr and Th for all soils does not coincide with what we described for Italian soils. These two elements tend increase in concentration with degree of weathering, suggesting they are immobile. In both cases the Italian soils (and Zr in soil EUR11 from the Canary Islands) fall well outside the trend. Excluding the Italian soils in the HCA analysis also suggest that Zr and Th are immobile since they link at very short distances to Al and Ga (data not shown).

Element enrichment

Phosphorus, Hg, Cl and Pb in almost all soils, and Cu, Zn and Br in some of them, show the highest concentrations in the surface horizons and are thus enriched with respect to the parent material. The biogeochemical cycles of these elements share two basic aspects: (1) they are mainly incorporated to the soils by external fluxes (atmospheric deposition and human activity) and (2) they show a high affinity to organic matter.

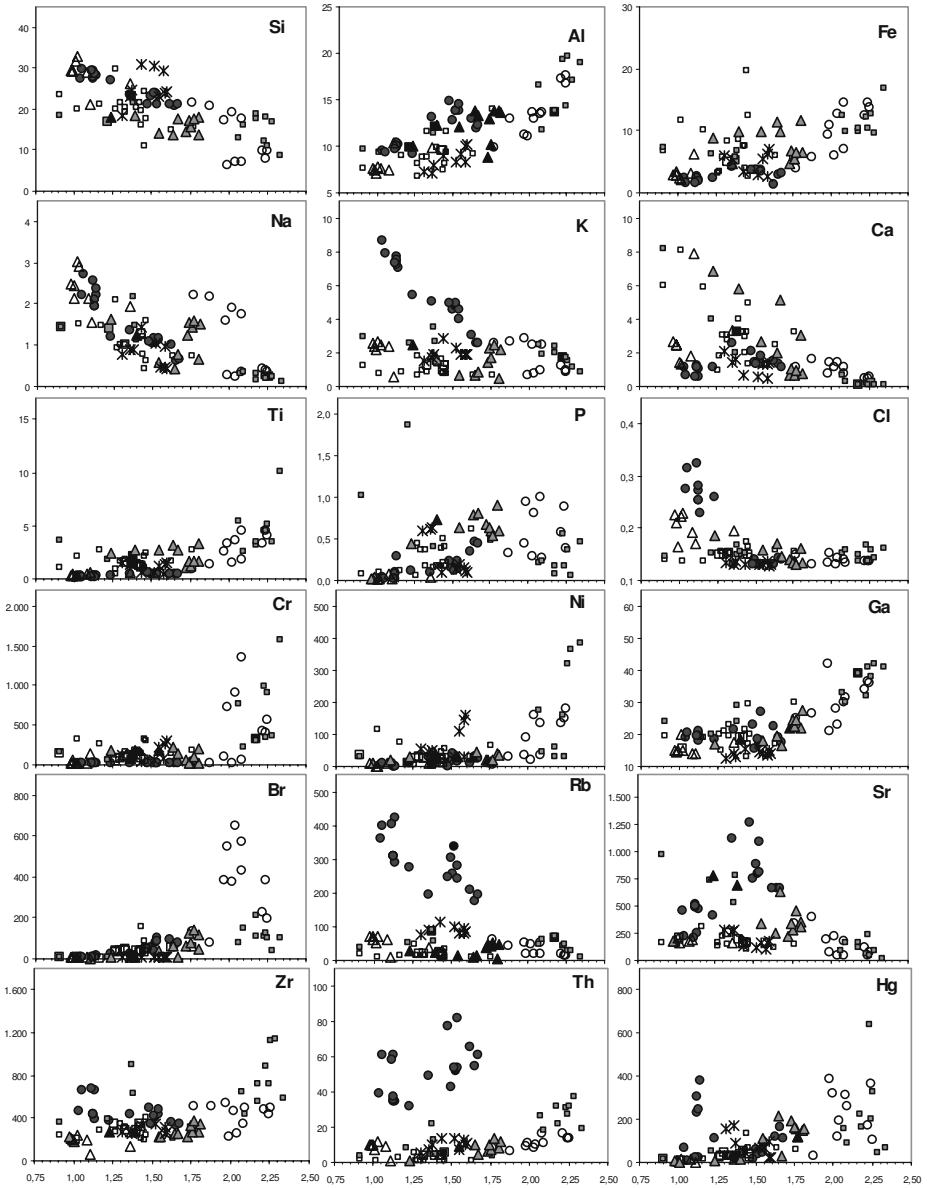

Figure 5. Relation between the normalized weathering index (NCIA, see chapter by Taboada et al., this book) and the concentrations of the elements. Only elements showing a trend have been included. (Filled circles: Italy; open circles: Azores Islands; open squares: Iceland; filled squares: Canary Islands; open triangles: Greece; filled triangles: France; asterisks: Hungary).

Phosphorus shows relatively high concentrations (>0.5%) in the soils from France (EUR16–17), in EUR11 (CI, up to 2%), EUR06 (AZ) and EUR19 (HG). Very low concentrations were found in soils from Italy (EUR01–03), Iceland (EUR08), Canary Islands (EUR12), Greece (EUR13–15) and Hungary (EUR18 and EUR20). This element is highly correlated with total C and thus it is assumed to be mainly in the form of organic P in the soils (P:C ratios 0.01–0.02). Only in EUR10 and EUR16 P is not correlated to C and the highest values were found in the B horizons, suggesting that in these cases part of the P can be present in a mineral phase. With the exception of soils from the Canary Islands, P concentrations tend to increase with weathering (Figure 5), which may be related to its fixation by soil components following the increase of reactive amorphous Al inorganic compounds. This is also supported by two facts: (1) that the proportion total Al extracted with ammonium oxalate presents a high correlation to the normalized weathering index (Taboadata et al. this book) and (2) that the soils from the Canary Islands do not conform with this trend.

Chlorine is another element with a slight increase in the surface horizons. Although until very recently halogens were considered as mobile elements not retained by soils, research has demonstrated that they are in fact retained through enzymatic incorporation into soil organic matter (van Pée and Unversuch 2003), and that halogenation is an ubiquitous process in nature. The larger concentrations of Cl in the surface horizons of most soils are consistent with this finding and also with its biocycling. The main Cl source is the ocean, so we would expect soils from the islands to have higher concentrations. But in fact the largest contents were found in soils developed from the Gauro deposits (Italy) and in soils from Greece (EUR13–14); even more, in these cases Cl concentrations decrease upwards and with increasing degree of weathering (Figure 5). In both cases (soils developed on the Gauro deposits and from Greece) are located in areas with thermic/xeric climate, which suggests that climate aridity can be responsible for the high content of this element. Two of the Hungarian soils (EUR19–20) are also on arid environments but show no particular changes on Cl concentrations, probably due to their inland situation, far from marine sources. On the other hand, the type of volcanism cannot be ruled out as a source of variation.

The large Cl concentrations obtained in soils from Italy may also be the reason for this element plotting/linking to the Si and K group (Figure 1), and not to the other halogen measured (Br). But the elimination of the Italian soils in the HCA analysis does not change the relation of Cl to Si and Na, although the linkage distance increases. So it is not clear why Cl in the analyzed soils is related to Si and Na. Sodium can have an important com-

ponent from marine sources as well as weathering and has also been found to contribute to stabilization of soil organic matter (Buurman et al. 2002), so the link may arise from an indirect effect of both elements depending on processes related to the transformations of the soil organic matter.

Bromine shows the largest concentrations in the most oceanic areas (Azores and Canary Islands, 100–640 μg g^{-1}) and the lowest in the continental ones (<10 μg g^{-1}, Hungary). This source effect is observable even at smaller scales: in Italy soils EUR03–04 (with udic moisture regime) have higher Br concentrations than EUR01–02 (with xeric moisture regime) and in France soil EUR17 has larger contents than EUR16. It may also be responsible for the apparent statistical link to Hg and the metallic group (Figure 1). But in contrast to Cl, Br profiles do not tend to show its maximum in the surface layer of the soil (see for example the profiles of EUR05 and EUR06 from Azores Islands) suggesting that other factors must be involved in Br retention. For example, Martínez Cortizas et al. (2003) indicated that age, stratigraphy and moisture regime may be involved in the differences observed between the Italian soils.

Elevated concentrations of Hg (200–640 ng g^{-1}) were found in soils from the Canary Islands (EUR10, EUR12), Azores Islands (EUR05–06) and Italy (EUR01). This element is mostly incorporated to the soils through atmospheric deposition, its main source being is degassing of the Earth's crust and the oceans (Anderson 1979). The latter is consistent with the elevated concentrations in soils from islands; but the kind of volcanism – volcanoes are known to emit large amounts of Hg –, forest fires and fossil fuel burning also contribute to Hg atmospheric deposition. Mercury shows a high affinity to organic matter, particularly organic sulphur groups (Craig 1986, Meili 1991, Schuster 1991, Xia et al. 1999), resulting in its large enrichments in the surface horizons. The largest enrichments (calculated using Ti as conservative reference element, as in Martínez Cortizas et al. 2003) range between 10 and 30 times those of the parent materials (in EUR02–04, EUR07–08, EUR10, EUR14 and EUR16).

Bromine and Hg plot together in the PCA projection and the HCA dendrogram (Figure 1) because they have large concentrations in the soils from the Canary Islands and Azores Islands. This may be related to both sharing a main source (the oceans) and a main mechanism of retention in soils (organic matter) as indicated above. But Figure 5 suggests that the degree of weathering may also play an indirect role, perhaps through increased colloid-humus interactions. For example, in the Canary Islands strongly weathered soils (EUR10 and EUR12) have high Br and Hg concentrations while the weakest evolved soil (EUR11) has very low concentrations of both elements.

Chromium and Ni show a similar pattern, with large concentrations in the most intensely weathered soils (Figure 5). In this case the effect of weathering is difficult to assess because the high values are found in the soils with the largest metallic contents and there is no clear trend for the other soils, so it can be a compositional effect. This may be a likely situation, since other metallic immobile elements like Fe and Ga show a continuous increase in concentration with the intensity of weathering (Figure 5), and not the sharp separation seen for Cr and Ni.

Pb, Zn and Cu do not present a clear trend with degree of weathering although they show enrichments in the surface horizons. Martínez Cortizas et al. (2003) reported a superficial enrichment of Pb in the Italian soils, although indicating that the calculation of enrichment factors in volcanic soils is seriously limited by their inherent stratigraphic and chemical heterogeneity. This is exemplified by soil EUR16, for which the enrichment factor of Pb in the A horizon (calculated using Ti as reference element) is 36 while its concentration is only 4 times that of the rock (29.3 and 7.5 respectively).

With the present larger database we have found that Pb and Th are highly correlated for the subsurface horizons (r^2=0.98), with an almost constant Pb/Th ratio of 1.27; suggesting that in this particular case Th can reasonably be used as reference element for Pb (also supported by the increase in Th concentrations with weathering and it plotting with Ga and Al when the Italian soils are excluded of the HCA analysis). Enrichments calculated in this way – $[Pb_s/Th_s]/[Pb_r/TTh_r]$, where s and r refer to individual soil horizon and the reference bottommost one respectively – are largest in the A horizons of EUR19 (EF=5.4) and EUR17 (EF=3.4); followed by the soils from Italy (EUR01–04, EF=2.0–2.8) and Greece (EUR13–15, EF=1.6–1.8). Soil EUR16 shows a moderate surface Pb enrichment (EF=1.5), while soils from the Azores Islands, Iceland, the Canary Islands and France show EF lower than one in all or part of the subsurface horizons, due to the fact that either Pb or Th are close or below the detection limit of the XRF.

Zinc shows relatively high concentrations in soils from the Azores Islands, Iceland, Canary Islands and EUR19 from Hungary. A large number of the profiles analyzed have the highest concentrations in the upper most horizon (EUR01–04, EUR05, EUR07, EUR10–12, EUR14, EUR17, EUR20). Maximum enrichments are between 2–3, and again point to biocycling, atmospheric deposition and organic matter binding as the main processes involved in Zn distribution in these soils.

The highest Cu concentrations were found in the Icelandic soils, but only the Italian ones show Cu enrichment. The maximum EFs vary between 4 and 29 and occur in the topmost horizons. Copper as well as the

other elements mentioned in this section have a high affinity for organic matter. As stated by Reimann and De Caritat (2005), the surface enrichment of many elements is due to the fact that they easily form organometallic compounds and their biogeochemical cycles are responsible for the high EF shown by the surface, organic-rich soils horizons. This is supported by the fact that concentrations of these elements usually show high correlations between the B and C horizons on one hand, and the O and A horizon on the other; but not between the O and B or the O and C horizons (Reimman et al. 2001). Based on this behavior Reimann and De Caritat (2005) suggest that the biogeochemical cycles are responsible for the geochemical decoupling of the mineral and organic horizons of the soils – different geochemical processes tend to dominate in different compartments of the soil ecosystem.

Of the soils analyzed in this study the largest Cu EF value was detected in EUR01, the orchard soil, which also has significant enrichments of P, Pb and Hg. The extent of the enrichment found in the A and O horizons of this and other profiles suggests that soil management (i.e. fertilizing) and atmospheric metal pollution may be significant sources of some elements to the soils. So, at least in some cases several processes may be responsible for the observed distribution of the elements.

Conclusions

The results presented in this chapter suggest that the elemental composition of the European volcanic soils analyzed here is largely dependent on the mineralogy and chemical composition of the parent material, as already suggested in previous studies (Buurman et al. 2003, Martínez Cortizas et al. 2003). But also as found by Martínez Cortizas et al. (2003) pedogenesis, organic matter content, climate conditions and soil management by humans are other important factors in the distribution of some elements.

A combination of PCA and HCA analysis revealed geochemical discontinuities in most of the soil profiles, in agreement with their complex stratigraphy. Some soils show major geochemical discontinuities, as for example EUR01, EUR05, EUR07, EUR08, EUR09, EUR10 and EUR11; while a few of them showed a more homogeneous elemental composition throughout the soil profiles (EUR12, EUR13, EUR16, EUR17, EUR18, EUR19).

Very mobile elements (Ca, K, Sr) and even Zr, Th and U – in the Italian soils – seem to have been leached; while Cu, Zn, Pb and Hg show elevated concentrations in the organic-rich horizons, suggesting a role by organic

matter in their retention in the soils. On the other hand, Br is more dependent on its external source (the ocean) and the dominant climatic conditions, since the highest concentrations are found in the more oceanic (Azores) and rainy areas (as it happens for the Italian soils). Finally, the degree of enrichment in Cu, Pb and Hg in some soils (as for example EUR01) indicates that soil management (i.e. fertilization and use of biocides) and atmospheric metal pollution are also significant sources of some elements.

Acknowledgements

We thank Peter Buurman and Randy Dahlgren for their comments on a previous version of this chapter which largely helped to improve it.

References

Andersson A (1979). Mercury in soils. In: Nriagu, JO (ed) The Biogeochemistry of Mercury in the Environment. Elsevier/North Holland Biomedical Press:Elsevier 79–112

Buurman P, García-Rodeja E, Martínez Cortizas A, van Doesburg JDJ (2003). Stratification of parent material in European volcanic and related soils studied by laser-diffraction grain-sizing and chemical analysis. Catena 56:127–144

Buurman P, van Lage B, Picolo A (2002). Increase in stability against thermal oxidation of soil humic substances as a result of self association. Organic Geochemistry 33:367–381

Craig PJ (1986). Organometallic compounds in the environment. Essex, pp 362

Fujikawa Y, Fuki M, Kudo A (2000). Vertical distributions of trace elements in natural soils from Japan: Part 1. Effect of soil types. Water Air and Soil Pollution 124:1–21

Kobayashi S (1979). Studies on the occurrence of copper and zinc and their plant availability in Andisols. PhD Thesis, Faculty of Agriculture, Tohoku University, Japan

Kurtz A, Derry LA, Chadwick OA, Alfano MJ (2000). Refractory element mobility in volcanic soils. Geology 28:683–686

Laurelle J, Stoops G (1967). Minor elements en Galapagos soils. Pedologie 17:232–258

Martínez Cortizas A, García-Roeja E, Nóvoa Muñoz JC, Pontevedra Pombal X, Buurman P, Terribile F (2003). Distribution of some selected major and trace elements in four Italian soils developed from the deposits of the Gauro ad Vico volcanoes. Geoderma 117:215–224

Meijer EL, Buurman P (2003). Chemical trends in a perhumid soil catena on the Turrialba volcano (Costa Rica). Geoderma 117:185–201

Palumbo B, Angelone M, Bellanca A, Dazzi C, Hauser S, Neri R, Wilson J (2000). Influence of inheritance and pedogenesis on heavy metal distribution in soils of Sicily, Italy. Geoderma 95:247–266

Meili M (1991). The coupling of mercury and organic matter in the biogeochemical cycle – towards a mechanistic model for the boreal forest zone. Water Air Soil Pollut 56:333–348

Rahman S, Takaki H, Tamai M, Nagamoto Y (1996). Distribution of zinc, manganese, copper, cobalt and nickel in andosol profiles. Soil Sci Plant Nutr 42:881–891

Reimann C, De Caritat P (2005). Distinguishing between natural and anthropogenic sources for elements in the environment: regional geochemical surveys versus enrichment factors. Science of the Total Environment 337:91–107

Reimann C, Kashulina G, De Caritat P, Niskavaara H (2001). Multi-element, multi-medium regional geochemistry in the European arctic: element concentration, variation and correlation. Applied Geochemistry 16:759–780

Schuster E (1991). The behaviour of mercury in the soil with special emphasis on complexation and adsorption processes – a review of the literature. Water Air Soil Poll 56:667–680

van Pée KH, Unversuch S (2003). Biological dehalogenation and halogenation reactions. Chemosphere 52:299–312

Appendix materials on CD-Rom

elements.xls

Chemical weathering of Reference European Volcanic Soils

T. Taboada, C. García, A. Martínez-Cortizas, J.C. Nóvoa,
X. Pontevedra and E. García-Rodeja

Introduction

Volcanic rocks are an important component of the weathering regime. They contribute to the geochemical cycles of many elements and are locally significant as a source of nutrient elements in agricultural soils (Chesworth et al. 2004). Geochemistry makes use of major element data in different ways, as for example in rock classification (Rollinson 1993) and in rock and soil material weathering. During weathering and pedogenesis, elements are removed from the parent material or selectively accumulated. So, in homogeneous materials differences in chemistry between samples may simply reflect variation in extent of weathering. Consequently, chemical weathering indices are commonly used for characterizing weathering and soil profiles (Price and Velbel 2003). Chemical weathering indices convert bulk major element contents into a single value for each sample. Weathering indices are typically plotted versus depth in the soil profile, providing a visual representation of changes in bulk chemistry with presumed increase or decrease in weathering. In homogeneous parent rocks, changes of weathering indices with depth are usually gradual and systematic, reflecting continuous leaching of elements as weathering progresses. Due to the frequent burial by new volcanic materials and/or by the gradual or repeated deposition of fresh materials that causes rejuvenation of topsoils, volcanic materials, however, do not always produce systematic trends with depth of elemental composition.

The weathering rate of volcanic materials depends on their chemical composition and texture. Volcanic material of rhyodacitic composition weathers at lower rates than material of andesitic or basaltic composition (Kirkman and McHardy 1980). Fine volcanic materials show little resistance to weathering in comparison to other types of parent materials (Shoji 1986). In addition to the parent material, climatic conditions and the age of weathering are important factors.

Additionally, Malpas et al. (2001) studying pyroclastic volcanic rocks in Hong Kong, showed that the type and abundance of sesquioxides and clay

minerals can significantly modify the geochemical signature of weathering. For this reason, in addition to the chemical weathering indices more frequently reported in literature, we have also measured the abrasion pH, a parameter used as an indicator of rock weathering (Grant 1969) that has been proposed by Ferrari and Magaldi (1983) as an index of potential fertility of soils. The abrasion pH is obtained by grinding soil material in distilled water. Its value is affected by the quantity of cations released from primary minerals and by the amount and type of clay minerals. Consequently, higher abrasion-pH values are expected in soils that are rich in fresh and weatherable minerals. As weathering proceeds and the clay content of the soil increases, the abrasion pH tends to decrease.

Table 1. Weathering indices used in this study. All ratios refer to molecular proportions.

Index	Formula	Optimum fresh value	Optimum weathered value	Ideal trend of index	Reference
WIP	$100*(2Na_2O/0.35+MgO/0.9+2K_2O/0.25+CaO/0.7)$	>100	0	Negative	Parker 1970
CIA	$100*Al_2O_3/(Al_2O_3+CaO+Na_2O+K_2O)$	≤ 50	100	Positive	Nesbitt & Young 1982
CIW	$100*Al_2O_3/(Al_2O_3+CaO+Na_2O)$	≤ 50	100	Positive	Harnois 1988
PIA	$100*(Al_2O_3-K_2O)/(Al_2O_3+CaO+Na_2O-K_2O)$	≤ 50	100	Positive	Fedo et al. 1995
R	SiO_2/Al_2O_3	>10	0	Negative	Ruxton, 1968
STI	$100*SiO_2/Al_2O_3/(SiO_2/TiO_2+SiO_2/Al_2O_3+Al_2O_3/TiO_2)$	>90	0	Negative	Jayawardena & Izawa 1994

Methods

Major elements composition of the fine-earth fraction has been determined for all COST profiles (see *the physico-chemical data base*, this book). Si, Al, Na and Mg were measured by X-ray Fluorescence (XRF). Ca, K, Ti, Fe and Mn, were analysed using XRF Energy-dispersive Miniprobe Multielement Analyzer (EMMA). The contents of elements and oxides were corrected for the dilution by organic matter and the recalculated oxide contents for each element are presented in the excel files belonging to this

chapter. The chemical weathering indices calculated and used in this study are presented in Table 1. The Weathering Index of Parker (WIP) is based on the proportions of alkali and alkaline earth metals (Na, K, Ca, and Mg), which are the most mobile of the major elements. The Chemical Index of Alteration (CIA), the Chemical Index of Weathering (CIW) and the Plagioclase Index of Alteration (PIA) are based on the ratio of a group of mobile oxides to immobile ones (these indices assume that Al is immobile) and they are interpreted as a measure of the extent of conversion of feldspars to clays. The Silica-Titania index is based on the ratio of a group of the immobile elements and the Ruxton ratio (R) is a ratio of two oxides only (Table 1). The values of these chemical weathering indices are in the excel files belonging to this paper. All are plotted against depth, but only those that present clear trends are discussed in the text. Field descriptions of the soils and the modifications of horizon codes proposed for part of the soils by Buurman et al. (2004) and García-Rodeja et al. (2004) were used to understand soil evolution and to draw the graphs.

Because weathering of volcanic rocks (the 'andosolization process') causes removal of basic cations and Si and relative accumulation of Al and Fe, the evolution towards the residual system is analyzed using the diagram proposed by Chesworth (1973). Finally, the SiO_2-Al_2O_3-Fe_2O_3 diagram is used to illustrate the behaviour of the residual elements. These figures together with the abrasion pH data are included in the excel files accompanying this chapter.

Results and discussion

On the basis of the chemical composition of the least weathered samples (those from the deeper horizon) the parent material compositions were plotted in a bivariate oxide-oxide major element plot, the total alkali-silica diagram (TAS; Le Maitre et al. 1989), one of the most useful classification schemes available for volcanic rocks (Rollinson 1993). In this diagram we added the subdivision between alkaline and subalkaline (tholeiite) rocks by plotting coordinates given by Irvine and Baragar (1971).

Results are presented in Figure 1, which shows major differences between the studied materials. Parent materials have chemical compositions similar to phonolite, trachyte, tephrite, basanite, nephelinite, basalt, trachybasalt, basaltic-trachyandesite, basaltic-andesite, andesite, dacite and rhyolite. Due to their high weathering, soils EUR06 and EUR10 could not be plotted in this fresh-rock based diagram.

The studied soils were developed from parent materials with different textures (lava flows, pyroclastic materials, volcanic till and eolian sediments), under different climatic conditions (from cryic to thermic and from udic to xeric) and also differ in age, vegetation and land use history. These factors, in combination with differences in parent material, make comparison of geochemical changes that occurred during weathering difficult.

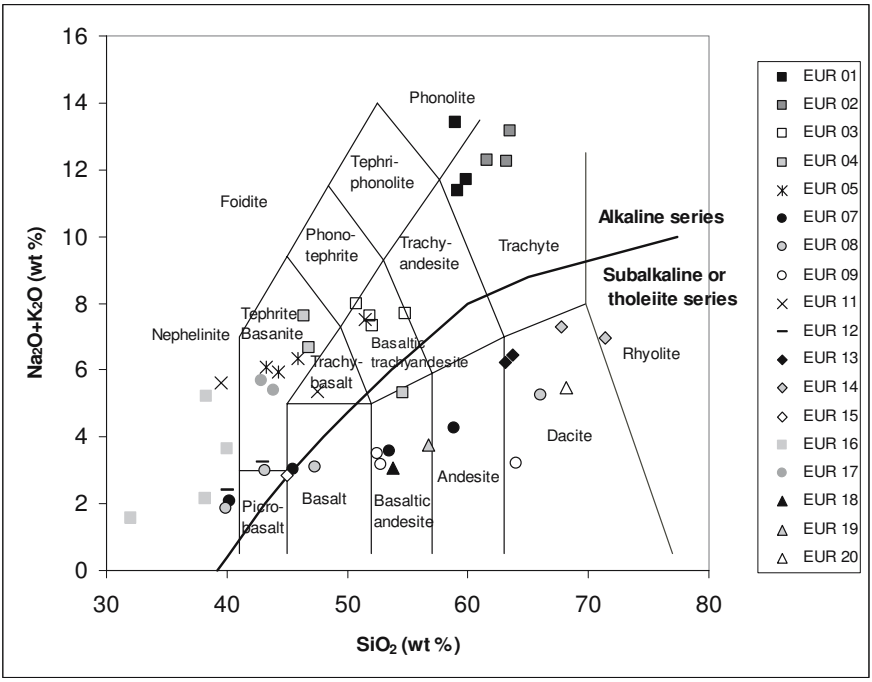

Figure 1. Total alkali versus silica diagram (TAS). Plotted points are C and R horizons of European volcanic reference soils.

Chemical weathering indices

Soils from Italy

EUR01 and EUR02

The deepest horizons of the soils from the Gauro volcano in the TAS diagram (Figure 1) project in the field of alkaline volcanic rocks with a composition close to phonolites and trachytes. Their richness in K_2O (around 10%) indicates that they are leucitophyre and K-trachytes, which are more precise terms to designate ultrapotassic volcanic rocks. Therefore, the

mean value of four chemical analyses of leucite-trachytes, given by Nockolds et al. (1978), was used as a reference for the chemical composition of the fresh rock of both soils.

The different weathering indices show that the mineral fraction of all horizons had a very low geochemical evolution because their values fall very close to those calculated for the leucite-trachyte (Figure 2). The WIP gives more information, indicating besides a small loss of bases from both soils, the possible influence of rejuvenation in the topsoil of EUR01 (Figure 2B). The low degree of evolution of these materials is also shown in the Chesworth and SiO_2-Al_2O_3-Fe_2O_3 diagrams, where all samples cluster in the same area (Figures 3 and 4). The youth of parent material (Astroni eruption, 3700 BP) and the low leaching associated with the xeric soil moisture regime, explain the low pedological evolution of both soils.

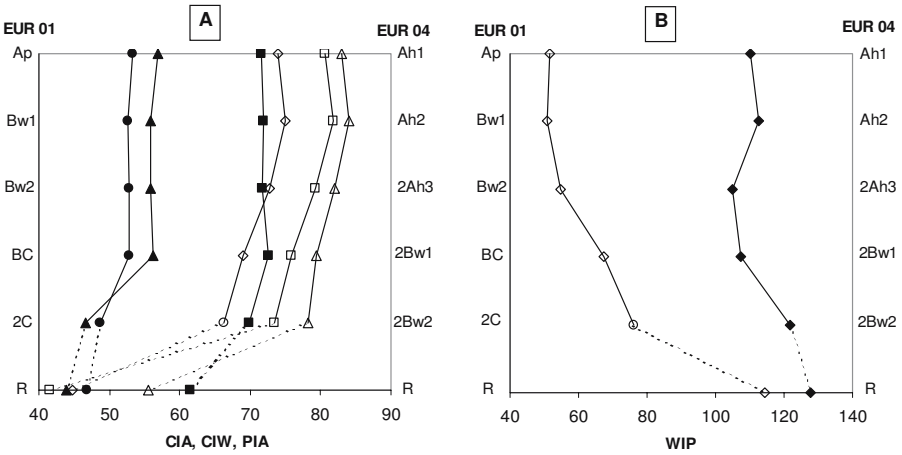

Figure 2. Chemical weathering indices of EUR01 (filled symbols) and EUR04 (open symbols): (A) CIA (circles), CIW (squares), PIA (triangles), (B) WIP.

EUR03 and EUR04

According to field soil descriptions (Van Oort 2000), the soils EUR03 and 04 are developed from leucite-bearing tephritic-phonolitic lava flows. The average composition of the tephri-phonolite lavas from Monte Venere, in the Vico Volcano area, given by Perini et al. (2004) was used as a reference for the unweathered parent material. The Al-Fe-Si diagram indicates that the profiles are slightly richer in Al than the reference rocks (Figure 4).

A steep gradient of depletion of base cations is found in the deepest horizons of both (EUR03-3Bw2/2Bw2 and EUR04-2Bw2/Bw2), more intense in the latter. This is apparent in all weathering indices. Weathering increases further towards the soil surface but with a lower gradient (Figure

2). The WIP shows a slight rejuvenation in the Ah2 horizon of EUR03, which is also reflected in the soil description by the presence of a thin stone line at the base of the horizon.

In EUR03 and 04 all horizons plot very close in the Chesworth and the SiO_2-Al_2O_3-Fe_2O_3 diagrams. The plot of the horizons of EUR04 shows a slight trend towards the residual corner (SiO_2-Al_2O_3-Fe_2O_3) (Figure 3) in spite of a certain silica leaching that can be observed when the three components of the system are compared (Figure 4).

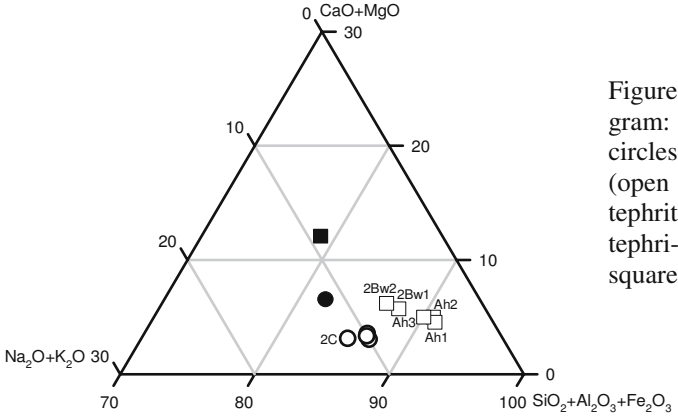

Figure 3. Chesworth diagram: soil EUR01 (open circles), soil EUR04 (open squares), leucite tephrite (filled circle) and tephri-phonolite (filled square).

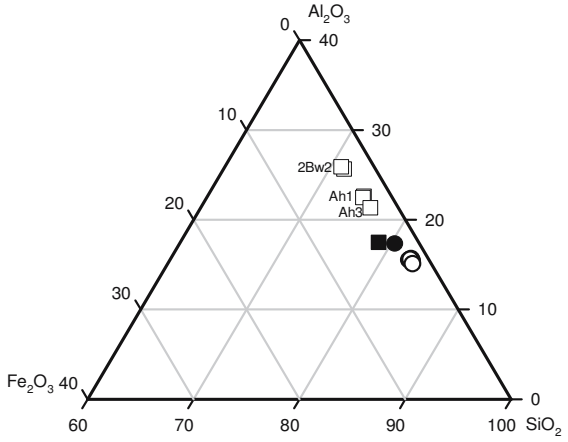

Figure 4. SiO_2-Al_2O_3-Fe_2O_3 diagram: soil EUR01 (open circles), soil EUR04 (open squares), leucite tephrite (filled circle) and tephri-phonolite (filled square).

Soils from the Azores

The parent material of soil EUR05 is constituted of pyroclastic materials, but there is no reference to its composition in the field description. The lower samples of this profile project in the basanite field of the TAS diagram (Figure 1). If this would reflect the real parent material, it must have been more alkaline than the average of the basanites compiled by Le Maitre (1976), and its composition would probably be closer to the average composition of the leucite tephrite and basanite given by Nockolds (1978). The Al-Fe-Si diagram shows that the soil has more Al than the reference material. In this soil, the reference rock has CIA, CIW and PIA indices between 30 and 40 and a WIP of 112 (see files on CD). Weathering caused and increase of the indices to 70 in the 3C/2C horizon. Except for an increase towards the soil surface, there are no major differences in weathering degree between the horizons. All indices also show rejuvenation in the upper part of the soil, consistent with a discontinuity observed in the field and with the presence of fresh pyroclasts identified in thin sections (Stoops and Gerard 2004). Due to the similar evolution, all samples group together in the Chesworth diagram.

Soil EUR06 was developed in pyroclastic basaltic material. The average composition of basalts as compiled by Le Maitre (1976) give weathering indices of about 40 for fresh rock. The CIA, CIW and PIA indices increase to about 90 in the 2Bw horizons. The WIP decreases from 78.8 in the average basaltic rock to around 20 in these horizons. The intense weathering of the basaltic material reflected by these indices can be explained by the climatic conditions (mesic and udic soil regimes) and probably also by the age of the soil. All indices also show a slight rejuvenation associated with the upper soil formation cycle.

The projection of the horizons in the Chesworth diagram confirms the trends observed from the chemical weathering indices showing the addition of fresh materials in the upper soil, but also a trend towards the residual system in the buried soil that indicates a more advanced stage of weathering and soil formation.

Soils from Iceland

One of the most significant features in the soils of Iceland is the frequent deposition of volcanic and aeolian tephric materials on the soil surface (Arnalds 2004). This is clear in the three studied soils, which are formed in stratified deposits with different composition (Figure 1). The deeper hori-

zons of soils EUR07 (3/4Bw3 and 4BCg) and EUR08 (3BwC and 4C), which correspond to oldest cycles of pedogenesis in both profiles, are developed from glacial till of basaltic composition. Over this till, younger pedogenetic cycles are marked by a clear change in composition. In EUR07, the 3Bw1 and 3Bw2 have an andesitic composition, and the Bw1 and 2Bw2 of EUR08 are developed in rhyodacitic to dacitic tephra layer richer in SiO_2 that forms the base of the surface soil and the second layer. The surface horizons of both soils (0–65 cm in EUR07 and 0–21/27 cm in EUR08), were developed from basaltic material similar to that of the glacial till at the base.

Despite the high content in organic matter of EUR09, the stratification of the parent materials is evident. Horizons 4H and 3C have a basaltic-andesite composition; in the 3H horizon, the composition is richer in silica and similar to dacite or rhyodacite, and in the surface Ah horizons the composition is again similar to that of the deeper horizons. The discontinuities found in these soils are mainly due to the deposition of fresh inorganic materials with different composition. This causes an irregular variation of chemical weathering indices and absence of a weathering trend.

The soils from Iceland (together with those from Greece) are the least developed ones because their formation took place under cold climatic conditions (cryic/frigid soil temperature regime and udic soil moisture regime). The dispersion of the horizons in the Chesworth diagram is again a consequence of stratification.

Soils from Tenerife (Canary Islands)

The three soils from Tenerife are developed from basaltic materials. Nevertheless, the chemical composition of the deeper horizons shows some variation (Figure 1). Soils EUR10 and EUR12 developed from basalts and EUR11 from a trachy-basalt. The soils differ in weathering degree: EUR11 is weakly developed, while EUR10 and 12 are intensely weathered. The chemical weathering indices show differences between the soils and within each profile. The high degree of weathering and the polygenetic character of these two soils is also clear in micromorphological studies (Stoops and Gerard 2004).

In horizons 3Bwb2/Bwb2 and 4Bwb3/2Bwb3 of EUR10, the WIP has very low values (15.6) while CIA, CIW and PIA are close to 100, the characteristic values of these indices for materials with a high weathering degree (Table 1). The chemical weathering indices of the other horizons indicate a lower weathering due to a shorter time of evolution.

In the Bw and 2Ahb horizons of EUR12, the weathering indices are not as extreme as in EUR10. Especially the WIP, the index that better reflects small variations, reaches values of 23.2 and 30.9 respectively in these horizons. As in EUR10, weathering in the Ah horizons is not so intense.

The high weathering degree of the soils EUR10 and EUR12 is reflected in the Chesworth diagram, where all horizons cluster very close to the apex of the residual oxides. In addition, the SiO_2+Al_2O_3+Fe_2O_3 diagram shows significant silica leaching and the consequent residual enrichment in Al and Fe in the buried horizons of the soil EUR10.

In EUR11, developed from a more alkaline material and less developed, the more remarkable feature is the abrupt decrease in the chemical weathering in the 2C1/C horizon, which is described as a thin layer of fine to coarse, fresh and slightly altered gravel (vitric lapilli).

Soils from Greece

Parent materials of EUR13 and EUR14 from Greece are pumice. In the horizons of EUR13 there is between 10% and 30% of unweathered gravel described as a mixture of basalt (70%) and pumice (30%). In EUR14, gravel is more abundant (30–95%) and its nature is rhyodacitic. The projection of the C-horizons in the TAS diagram fall in the field of SiO_2-rich rocks type dacite-rhyodacite and rhyolite, respectively. The composition of the parent material of EUR15, described as black scoria with andesitic composition, is closer to basalt (Figure 1).

In all horizons of EUR13, the values of CIA, CIW and PIA are between 47 and 55, indicating a low weathering degree related to the dry climatic conditions. A slight rejuvenation in the surface horizon with materials of similar composition can be also deduced from these indices.

Soil EUR14, with a clearly polycyclic profile, is more complex. The subsurface horizons (2AC, 2C) have a low degree of weathering, with indices similar to those of EUR13, while the surface A-horizon is richer in Ca and Mg due to a secondary enrichment in these elements from limestone of the Profitis Ilias area (Moustakas and Georgoulias 2005).

When the samples of EUR13 and 14 are projected in the Chesworth diagram, all horizons group close to the SiO_2+Al_2O_3+Fe_2O_3 corner due to their high SiO_2 content. The different composition of the Ah-horizon of EUR14 is evident. In EUR15, which is also slightly weathered, the difference between the andesitic material of the Ah horizon and the basaltic one of the 2C is clear in the Chesworth diagram.

Soils from France

The chemical analysis of the parent material of EUR16, described as 'coarse black bluish lapilli' falls in the field of nephelinites, and its composition is similar to the average of ten samples of this type of volcanic rock given by Nockolds (1978).

The well-known composition of parent material of this soil permits a better insight in the weathering processes. The values of the weathering indices progress from the rock to the surface horizon. The values of CIA, CIW and PIA are close to 40 in the parent material and they increase progressively to values close to 80 in the Ah3 horizon. The WIP is 78 in the rock and decreases to 28 in Ah3. In the Ah2 and Ah1 horizons the trend changes to a less weathered material. The progressive loss of bases that occurs upon weathering and pedogenesis and the slight rejuvenation in Ah1 and Ah2 are corroborated in the Chesworth diagram. Silica leaching and enrichment in Al and Fe can be easily deduced from the SiO_2-Al_2O_3-Fe_2O_3 diagram.

Using the average composition of trachyandesites (Nockolds 1978) as the reference parent material, a significant geochemical evolution at the weathering front can be seen in EUR17. From the parent rock to the 2Bt/2Bw2 horizon, the WIP decreases from 93 to 56. There is no significant increase in weathering in the overlying horizons. This absence of weathering trend in the solum is confirmed by the ternary diagrams where all samples group together.

Soils from Hungary

Parent materials of soils EUR18 and EUR 19 are described as basaltic tuff, but the projection of the chemical analysis of the AC and A/R horizons in the TAS diagram are more consistent with a basaltic-andesitic rock (Figure 1). The weathering indices of both soils indicate low weathering. In EUR18, the index values are similar for all horizons. In EUR19 there is a change in the values of the Ah1 horizon, also reflected in the Chesworth diagram, probably due to the effect of an allochthonous material richer in Ca, Fe, Ti and Al. For this soil Buurman and van Doesburg (this book) mention an admixture of loess.

The field description of EUR20 identifies the parent material as andesitic volcanic scoria, but the Bw/R horizon falls in the field of dacites of the TAS diagram (Figure 1), which are richer in SiO_2. Although weathering is not very intense in this soil, all chemical weathering indices indicate

a slight loss of bases from the Bw/R to the soil surface. This weathering trend is not reflected in the Chesworth diagram where, due to the high silica content and only slight geochemical evolution, all samples group close to the corner that represents the residual composition.

Abrasion pH

The results showed a wide range of abrasion pH values (4.5–7.7), with the lower values in the soils from Azores (4.5–5.3) and the higher ones in those from Santorini and Hungary (>7), a difference that is related to the climatic conditions (udic versus xeric) determining weathering and pedogenesis. In some cases, variations within the profile are small (EUR01, 02, 05, 06, 14 and 20) while the lower values for each soil tend occur in the A horizons. In other soils, the variation of abrasion pH down the profile is more complex and associated to discontinuities in the parent material or to different cycles of soil formation. For example, EUR03 has a more acid abrasion pH in the subsurface horizons than in the upper part of the profile with the transition located at a discontinuity marked by a stone line. In EUR08, 10, and 12 the buried horizons, with higher degree of weathering and pedological evolution, also have lower pH.

Weathering degree of soils

Although all studied soils have in common that they have been formed from volcanic parent materials, they differ in texture and chemical composition (Figure 1) making comparison of their weathering degree difficult. Furthermore, there are large differences in the environmental conditions that regulated their evolution, from the cold climate of Iceland, where weathering and pedogenesis are limited by the low temperatures, to the Mediterranean areas of Greece, where weathering is conditioned by the scarcity of water, to the wet and temperate climates of the Azores and the Canary Islands that favour weathering. Additional problems are that the age of soil formation – basic information for understanding weathering speed and intensity – has not been documented for most soils, and that the history of land use in the studied areas is widely different.

Nevertheless we tried to find a weathering index useful for comparison of the degree of evolution of the different soils. To make comparison of weathering on different rocks more easy, the value of some chemical weathering indices has been normalized with respect to their value in the parent material ($NCIA=CIA_{Hor}/CIA_{FR}$, $NCIW=CIW_{Hor}/CIW_{FR}$, $NPIA=PIA_{Hor}/PIA_{FR,}$ in which Hor: horizon; FR: fresh rock; data on CD). Thus,

values close to 1 of the normalized indices indicate a low weathering degree and they increase with the weathering stage of the horizon. In stratified soils, the normalization for each horizon was done with reference to its parent material. All normalized indices have a similar behaviour and, consequently, the following comments are based on the NCIA alone. Using the NCIA values, three groups of samples can be distinguished (Figure 5):

1. Soil materials with a low degree of weathering (NCIA<1.5): soils EUR01, 02, 08, 09, 11, 13, 14, 15, 19, 20 and the surface horizons of EUR07.
2. Soil materials with an intermediate degree of weathering (1.5<NCIA<2.0): EUR03, 04, 16, 17, 18, the surface horizons of EUR05 and the buried soil of EUR07.
3. Soil materials with a high degree of weathering (NCIA>2.0): soils EUR06, 10, 12 and the buried soil of EUR05.

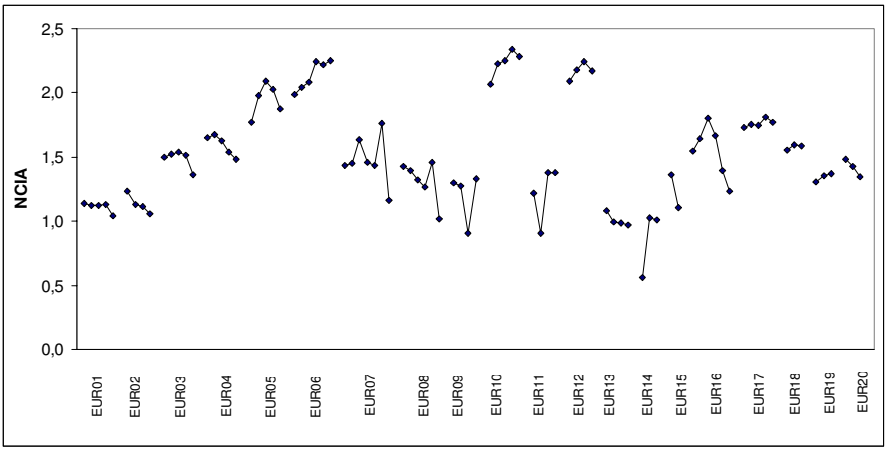

Figure 5. Normalized Chemical Index of Alteration (NCIA) values for the European volcanic reference soils.

This classification based on the NCIA coincides with the interpretation of thin sections of these soils by Stoops and Gerard (2004). The low degree of weathering of the soils in group 1 is mainly related to the environmental conditions, since most of them correspond to dry areas with a xeric moisture regime (EUR01, 02, 11, 13, 14, 15, 19, 20) or to very cold regions, with a cryic/frigid temperature regime (EUR07, 08, 09). The effect of dry climates is reinforced if parent materials are rich in silica, as in some of these soils, and the vitric properties tend to persist for a long time. The weak weathering may explain the absence or the low content of short-

order secondary minerals such as allophane and imogolite, and the lack of andic horizons. In fact, soils EUR01, 02, 13, 14, 15, 19 and 20 are not classified as Andosols in the World Reference Base of Soil Resources (FAO, 1998) while EUR07, 08, 09 and 11 are Vitric Andosols.

Disregarding EUR18, the soils with intermediate degree of weathering are from regions that nowadays have wet and temperate climates with udic moisture regime and mesic soil temperature regime. The leaching that takes place under such environmental conditions enhances the weathering of tephra and the formation of short-order materials that are characteristic of andic horizons. In fact, most Andosols in the world are found under these environmental conditions (Wilding 2000). Differences between the soils of these group are mainly attributed to diversity in texture and chemical composition, together with different intensity of the weathering processes that are, at the same time, dependent on the time of evolution. EUR18 is formed in a dry climate where the amount of rainfall and water availability are important features determining not only mineral weathering but also the type of secondary minerals. The lack of humidity decreases the persistence of short-order components (e.g. Chadwick et al. 2003) and explains the existence of relatively high quantities of smectite in this soil.

Finally, the soils with higher degree of evolution are those formed from the most weatherable parent materials under wet and temperate climates: those of basaltic composition and with a longer time of evolution. The climatic conditions and rock type favour rapid weathering and formation of allophane, imogolite and ferrihydrite (Stefansson and Gislason 2001).

In most of the studied soils there is a good correlation between the NCIA and the content of reactive Al estimated by oxalate extraction (Al_o, see García-Rodeja et al. this volume). This indicates that as weathering progresses there is an increment of the reactive components that are characteristic of Andosols: Al-humus complexes, allophane and imogolite. Exceptions are the soils from Hungary (without andic or vitric horizons) and EUR10 and 12 from Tenerife that have high weathering indices but lower quantities of Al_o. In these soils crystalline phyllosilicates are dominant (Hungary), discernible (EUR10) or well developed (EUR12) (see Monteiro et al. this volume).

Disregarding the above-mentioned soils, the NCIA values are significantly correlated (R^2=0.831) with the percentage of total Al extracted by acid oxalate ($100 \times Al_o/Al_t$) (Figure 6). Soils EUR10 and particularly EUR12 are richer in crystalline halloysite and gibbsite (Tejedor and Jiménez 2000), and in these soils NaOH extracts more Al and/or Si than acid oxalate (García-Rodeja et al. this volume). These soils probably represent the transition of andosols with allophane and imogolite or Al-humus com-

plexes to those with more crystalline phases as halloysite, gibbsite or 1:1–2:1 mixed layer clays.

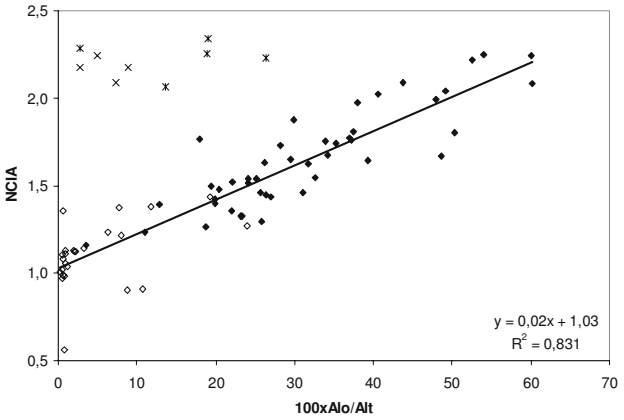

Figure 6. Relationship between the NCIA value and the relative amount of total Al extracted by acid oxalate ($100 \times Al_o/Al_t$). Filled symbols correspond to andic horizons and open ones to vitric horizons. EUR10 (*) and EUR12 (x) were not included in the regression equation.

Conclusions

The study of the chemical composition of the 20 volcanic European Reference Volcanic Soils together with the use of different chemical weathering indices demonstrates the importance of climate, parent material and soil age in the weathering and pedogenetic evolution of soils formed from volcanic materials in Europe. The main conclusions are:

1. The geological nature of the parent materials, deduced from the chemical composition of the least weathered horizons, shows the wide heterogeneity of the volcanic materials included in this particular set of volcanic soils.
2. The chemical weathering indices reveal the existence of gradual or repeated processes of soil burial and deposition of fresh tephra that caused vertical variations in the profiles and the presence of younger materials in the surface soil. In most cases the discontinuities indicated by weathering indices are coincident with those described in the field and those based on cluster analysis of chemical composition or grain-size characteristics.
3. The normalized Chemical Index of Alteration (CIA, Nesbitt and Young 1982) is a very useful parameter for comparison of the weathering degree of the studied soils. Based on its value three groups of soils with different weathering intensity were distinguished:

a. The soils with the lower degree of weathering (NCIA<1.5) are developed under dry or very cold conditions and frequently the parent materials are the most siliceous. They do not have andic horizons but some have vitric horizons. This group includes the soils from the Gauro Volcano in Italy (EUR01, 02), from Iceland (EUR08, 09, and the surface horizons of EUR07), from Greece, EUR19 and 20 from Hungary and EUR11 from Tenerife.
b. The group with an intermediate degree of weathering (1.5<NCIA <2.0) includes the soils from the Vico Volcano (EUR03, 04), from France (EUR16, 17), EUR18 from Hungary, the surface soil of EUR05 and the buried soils of EUR07. These soils are formed under wet and temperate climatic conditions but differ in parent material, in intensity of leaching and in time of weathering and pedogenesis.
c. The soils with a higher degree of weathering (NCIA>2.0) are those formed under the most favourable conditions for alteration and for the formation and persistence of short-order components. They are formed from basaltic tephra in a wet and temperate climate without distinct dry season. These are soils EUR06 and the subsurface horizons of EUR05 from Azores together with EUR10 and 12 from Tenerife. The maturity of the latter two is probably due to a longer time of evolution.

4. Excluding the most weathered soils (EUR10 and 12) where the short-order components have been transformed to halloysite and gibbsite, the values of the NCIA are significantly and positively correlated to the relative amount of oxalate-extractable Al, indicating that both the NCIA and the ratio Al_o/Al_t, can be used as weathering indices to compare the degree of evolution of vitric and andic soils.

Acknowledgments

We thank to Peter Buurman for his comments on a previous version of this chapter which significantly helped to improve it.

References

Arnalds O (2004). Volcanic soils of Iceland. Catena 56:3–20

Buurman P, García-Rodeja E, Martínez Cortizas A, van Doesburg JDJ (2004). Stratification of parent material in European volcanic and related soils studied by laser diffraction grain-sizing and chemical analysis. Catena 56:127–144

Chadwick OA, Gavenda RT, Kelly EF, Ziegler K, Olson CG, Crawford EW, Hendricks DM (2003). The impact of climate on the biochemical functioning of volcanic soils. Chem Geol 202:195–223

Chesworth W (1973). The residual system of chemical weathering a model for the chemical breakdown of silicate rocks at the surface of the Earth. J Soil Sci 24:69–81

Chesworth W, Dejou J, Larroque P, García-Rodeja E (2004). Alteration of olivine in a basalt from central France. Catena 56:21–30

FAO (1998). World Reference Base for Soil Resources. World Soil Resources Report 84, FAO, Rome

Fedo CM, Nesbitt HW, Young GM (1995). Unraveling the effects of potassium metasomatism in sedimentary rocks and paleosols, with implications for paleoweathering conditions and provenance. Geology 23:921–924

Ferrari GA, Magaldi. D (1983). Degree of soil weathering as determined by abrasion pH: Applications in soil study and paleopedology. Pedologie 33:93–104

García-Rodeja E, Nóvoa JC, Pontevedra X, Martínez-Cortizas A, Buurman P (2004). Aluminium fractionation of European volcanic soils by selective dissolution techniques. Catena 56:155–183

Grant WH (1969). Abrasion pH, an index of chemical weathering. Clays and Clay Miner 17:151–155

Harnois L (1988). The CIW index: A new chemical index of weathering. Sediment Geol 55:319–322

Irvine TN, Baragar WRA (1971). A guide to the chemical classification of the common volcanic rocks. Can J Earth Sci 8:523–548

Jayawardena US, Izawa E (1994). A new chemical index of weathering for metamorphic rocks in tropical regions: a study from Sri Lanka. Engineering Geol 36:303–310

Kirkman JH, McHardy WJ (1980). A comparative study of the morphology, chemical composition and weathering of rhyolitic and andesitic glass. Clay Min 15:165–173

Le Maitre RW (1976). The chemical variability of some common igneous rocks. J Petrol 17:589–673

Le Maitre RW, Bateman P, Dudek A, Keller J, Lameyre Le Bas MJ, Sabine PA, Schmid R, Sorensen H, Streckeisen A, Woolley AR, Zanettin B (1989). A classification of igneous rocks and glossary of terms. Blackwell, Oxford

Malpas J, Duzgoren-Aydin NS, Aydin A (2001). Behaviour of chemical elements during weathering of a pyroclastic rocks, Hong Kong. Environ Inter 26:359–368

Moustakas NK, Georgoulias F (2005). Soils developed on volcanic materials in the island of Thera, Greece. Geoderma 129:125–138

Nesbitt HW, Young GM (1982). Early Proterozoic climates and plate motions inferred from major element chemistry of lutites. Nature 299:715–717

Nockolds SR, Knox RW O'B, Chinner GA (1978). Petrology for students. Cambridge University Press, Cambridge
Parker A (1970). An index of weathering for silicate rocks. Geol Mag 107:501–504
Perini G, Francalanci L, Davidson JP, Conticelli S (2004). Evolution and genesis of magmas from Vico Volcano, Central Italy: Multiple differentiation pathways and variable parental magmas. J Petrol 45:139–182
Price JR, Velbel MA (2003). Chemical weathering indices applied to weathering profiles developed on heterogeneous felsic metamorphic parent rocks. Chem Geol 202:397–416
Rollinson H (1993). Using geochemical data: evaluation, presentation, interpretation. Longman Group U.K. Limited, London
Ruxton BP (1968). Measures of the degree of chemical weathering of rocks. Journal of Geology 76:518–527
Shoji S (1986). Mineralogical characteristics: I. Primary minerals. In Wada K (ed) Ando Soils in Japan. Kyushu University Press, Fukuoka, Japan 21–40
Stefansson A, Gislason SR (2001). Chemical weathering of basalts, southwest Iceland: effect of rock crystallinity and secondary minerals on chemical fluxes to the ocean. American Journal of Science 301:513–556
Stoops G, Gerard M (2004). Micromorphology of the volcanic ash soils of the COST-622 reference profiles. Rala Report 214:12–13
Tejedor M, Jiménez C (2000). Field Guide Tenerife. COST 622 Action, Internal Report. University of La Laguna, Tenerife, Spain
Van Oort F (2000). Report on the first four Working Group 5 meetings in Italy, Portugal, Iceland and Spain. COST 622 Action, Internal Report. INRA, Versailles
Wilding LP (2000). Introduction: General characteristics of soil orders & global distributions. In Sumner ME (ed) Handbook of Soil Science. CRC Press, New York, E175-183

Appendix materials on CD-Rom

Chemical weathering-Azores.xls	profiles EUR05, EUR06
Chemical weathering-France.xls	profiles EUR16, EUR17
Chemical weathering-Greece.xls	profiles EUR13, EUR14, EUR15
Chemical weathering-Hungary.xls	profiles EUR18, EUR19, EUR20
Chemical weathering-Iceland.xls	profiles EUR07, EUR08, EUR09
Chemical weathering-Italy.xls	profiles EUR01, EUR02, EUR03, EUR04
Chemical weathering-Tenerife.xls	profiles EUR10, EUR11, EUR12

Aluminium and iron fractionation of European volcanic soils by selective dissolution techniques

E. García-Rodeja, J.C. Nóvoa, X. Pontevedra,
A. Martínez-Cortizas and P. Buurman

Introduction

Soils developed from volcanic materials are characterized by mixture of short range order components such as allophane, imogolite, ferrihydrite, opaline silica, Al(Fe)-humus complexes and volcanic glass, in addition to the crystalline minerals halloysite, gibbsite, goethite, and aluminised 2:1 phyllosilicates. The accumulation of highly reactive components formed upon rapid weathering of volcanic rocks is the main cause for the unique physical and chemical properties of Andosols (Shoji and Fujiwara 1984, Dahlgren and Saigusa 1994). Depending on the dominant forms of Al, two kinds of Andosols are distinguished: 'allophanic' (Al in allophane and/or imogolite predominates) and 'non allophanic' (Al mainly in complexes with humus) (Shoji and Fujiwara 1984). When these components are less abundant, in the presence of volcanic glass, soils on volcanic materials are called 'vitric' (FAO 1998).

Allophane and imogolite are formed preferentially at pH about 5. In more acid conditions, Al-humus complexes tend to be dominant (Shoji and Fujiwara 1984, Nanzyo et al. 1993). At pH<5, complexation of Al by organic matter exerts an anti-allophanic effect (Shoji et al. 1993), leaving no Al available to react with silica to form allophane or imogolite. The high organic carbon content of many of these soils is explained by protection exerted by non-crystalline alumino-silicates (Mizota and Van Reeuwijk 1989) or by a stabilizing effect of Al and to a lesser extent Fe on soil organic matter (Higashi 1983).

Many properties of volcanic soils (phosphate retention, reactivity to NaF, water holding capacity, smeary consistence, etc.) are related to their active Al and Fe pools. Though mainly consisting of Al(Fe)-humus complexes, short-range ordered alumino-silicates (allophane or imogolite) and ferrihydrite, the pool may include other Al fractions, such as salt-exchangeable Al, Al substituted in free iron oxides, hydroxy-Al polymers in interlayer positions of 2:1 layer silicates, and poorly crystallized gibbsite

(Dahlgren and Walker 1993). In addition, Meijer and Buurman (1997) and Meijer et al. (this volume) suggested the presence of cation-depleted Al-silicate skeletons that may act as a source of active Al.

Al-humus complexes play a major role in pH buffering and in the regulation of Al activity in the soil solution (Bloom et al. 1979ab, Cronan et al. 1986, Mulder and Stein 1994, Takahashi et al. 1995). Extractions with unbuffered salts, such as $CuCl_2$ (Juo and Kamprath 1979) or $LaCl_3$ (Bloom et al. 1979b, Hargrove and Thomas 1981), have been proposed as alternative methods for estimating the organic fraction of soil Al.

Another fraction of interest is 1M KCl-exchangeable Al (Lin and Coleman 1960, Kamprath 1970). Although this is the standard method to measure 'exchangeable' Al, this interpretation was questioned for variable charge soils (Wada 1987ab, Dahlgren and Walker 1993, 1994), for organic matter rich soils (Ponnette et al. 1996), and for soils in which Al-humus complexes are abundant (Takahashi and Dahlgren 1998).

In this chapter we evaluate several selective dissolution methods (SDM) for Al, Fe and Si, their use in the characterization of soil components in volcanic soils and their relation to some of the characteristic properties of these soils. García-Rodeja et al. (2004) have previously studied the fractionation of Al in part of the COST622-Reference European volcanic soils, those from Italy, Azores, Iceland and Tenerife.

Material and methods

The soils

The twenty COST 622 reference soil profiles from different European volcanic regions (Italy, Azores, Iceland, Tenerife, Greece, France and Hungary) were used for this study. Following the criteria (disregarding horizon thickness) used in the World Reference Base for Soil Resources (WRB) (FAO 1998) the 94 soil horizons were separated into 'andic' (48 horizons, 3 aluandic and 45 silandic), 'vitric' (32 horizons) and 'non-andic' (12 non-andic nor vitric horizons, including 3 organic horizons). The aim was to separate samples according to properties that are mainly related to the non-crystalline alumino-silicates and iron oxyhydroxides, Al(Fe)-humus complexes or other components (volcanic glass or organic matter content). The data used for this classification, including horizons classification, are presented in the '*The physico-chemical database*' (Buurman et al. this volume).

Methods

The extractions of Al, Fe and Si were performed on the fine-earth fraction using air-dried samples for the soils from Iceland, Tenerife, Greece, Hungary and France, and field moist samples from Italy and the Azores. The following selective dissolution methods (SDM) were used:

1. Extraction with 0.5 M NaOH (Al_n, Si_n).
2. Extraction with Na dithionite-citrate (Fe_d).
3. Extraction with 0.2 M ammonium oxalate - oxalic acid at pH 3 (Al_o, Fe_o, Si_o).
4. Extraction with 0.1 M Na-pyrophosphate (pH 10) (Al_p, Fe_p).
5. Extraction with 0.5 M $CuCl_2$ (pH 2.8) (Al_{Cu}).
6. Extraction with 0.33 M $LaCl_3$ (pH 4.0) (Al_{La}).
7. Extraction with 1 M KCl (Al_K).

In addition, total contents of the studied elements were determined by XRF (Al_t, Fe_t, Si_t).

The methods used for the quantification of Al, Fe and Si pools are described in the chapter '*The physico-chemical data base*' (Buurman et al. this volume). These are standard procedures that use a single extraction for the quantification of each element in a given pool. All results are given in the file *physico-chemical data base.xls* (on CD). All extracts were prefiltered through an acid-washed paper filter (7–11 μm pore size) and through a 0.45 μm pore size filter. The results are expressed with respect to oven-dry weight (105ºC); duplicate analyses are less than 10% apart.

The need for more than a single extraction to quantify the amorphous components in soils with high contents of these constituents is considered by Meijer et al. (this volume) for the oxalate extraction in a selection of COST soils.

The interpretation of selective dissolution methods (SDM)

Extraction with 0.5 M NaOH (Hashimoto and Jackson 1960, Borggaard 1985) is used to estimate the so-called *total free Al* pool, because it can dissolve Al and Si in allophane, imogolite, gibbsite and opaline silica but also from 1:1 phyllosilicates with weak crystallinity (Wada 1980, Darke and Walbridge 1994).

Different selective dissolution methods (DSM), such as extractions with acid ammonium oxalate, Na-pyrophosphate or dithionite-citrate (DC), are commonly used in the quantification of Al and Fe fractions for classification purposes in modern soil classification systems and to characterize some specific soil components (Paterson et al. 1993). The usefulness of

these methods is limited by the continuum between very short-range ordered and crystalline components and by the weaker tendency of Al than Fe to form oxyhydroxides. Although the SDM used are not always specific for a given pool of Al, Si or Fe, some of them are reasonably specific for most soils (see Parfitt and Childs 1988).

In order to differentiate Al-humus complexes non buffered salts ($CuCl_2$, $LaCl_3$ and KCl) were used. Oates and Kamprath (1983ab) compared extractions by these chlorides in several soils, showing an efficiency in displacing Al from organic matter in the order Cu>La>K.

Following commonly used interpretations, the Al, Si, and Fe pools were grouped as follows:

Al_n: Total free Al pool (also Al in poorly ordered 1:1 phyllosilicates).
Al_n-Al_o: Al in gibbsite (also Al in poorly ordered 1:1 phyllosilicates).
Al_o-Al_p: Al in allophane and imogolite.
Al_p-Al_{Cu}, Al_{Cu}-Al_{La}, Al_{La}-Al_K: Al bound to organic matter, in order of decreasing stability.
Al_K: 'Exchangeable' Al.
Si_n: Total free Si pool (also Si in poorly ordered 1:1 phyllosilicates).
Si_n-Si_o: Si in opaline silica (also Si in poorly ordered 1:1 phyllosilicates).
Si_o: Si in allophane and imogolite (including opaline silica).
Fe_d: Total free Fe pool.
Fe_d-Fe_o: crystalline Fe oxyhydroxides (goethite, magnetite,...).
Fe_o: Fe in ferrihydrite and Fe-humus complexes (Fe in allophane).
Fe_p: Fe in Fe-humus complexes and in 'active' Fe oxyhydroxides.

Results and discussion

Total 'free' Al, Si and Fe: Al_n, Si_n and Fe_d

The results of the extractions of Al and Si with cold NaOH (Al_n, Si_n) and Fe with citrate dithionite (Fe_d) are given in Table A and Figure A (on CD). The percentage of the total content of Al, Si and Fe extracted by these SDM are represented in Figure B (on CD).

The quantity of Al extracted by NaOH is quite variable, ranging from values under 0.5% in the soils from Greece and Hungary and in most horizons of EUR01 and EUR02 (Italy) to values exceeding 6% in some horizons of the soils from the Azores (10.2% in 2Bwb of EUR06), France and EUR10 from Tenerife. Sodium hydroxide dissolved less than 5% of total Al (Al_t) in the soils from Greece, Hungary and in EUR01 and EUR02 from Italy. In the remaining soils, Al_n represented >10% and frequently >20% of

Al_t. In soils from France and the Azores, the dissolved Al fraction was 25 to 55% of total element content.

Silica extracted with NaOH ranged from 0.12 to 3.02%, as Al with higher values in andic horizons. The lowest percentage of total Si extracted by NaOH is found in the same soils as for Al: soils from Greece (<1%), Hungary (1–4%) and EUR01 and EUR02 from Italy (2–4%). In EUR05, Si_n represents from 18 to 30% of total Si, in EUR10 from 16 to 20%, and between 10 and 15% in several horizons of soils from France, Iceland and Azores (EUR06). The quantities of extracted Al and Si were well correlated with the percentage of extraction of the total element content (R^2=0.689 and 0.726 respectively).

The Al_n/Si_n molar ratios ranged from less than 1 to more than 6, indicating a wide range of Al and Si bearing components. In the less evolved soils from Italy (EUR01, EUR02) and in the soils from Greece, the components dissolved by NaOH were Si-rich (Al_n/Si_n<1), while they were Al-rich in many horizons of soils from the Azores, Tenerife and France, with Al/Si molar ratios >5 in the surface horizons of EUR06.

The difference between NaOH and acid oxalate extraction can be used to estimate the crystalline or 'less reactive' pool of Al. There is a good correlation between Al extracted by both methods for all samples (R^2=0.960) and the regression is close to the 1:1 line (slope=0.96). It further improves if soils EUR10 and EUR12 are omitted (R^2=0.986, slope=0.99) (Figure 1a). For the samples of EUR10 and EUR12, both Al pools are well correlated (R^2=0.996) but the slope is lower (slope=0.79) because NaOH extracts clearly more Al than oxalate. Similar good correlations are found for the soils of each region and for the different types of horizons (Table 1), indicating that, in these soils, the crystalline Al pool is very small and the sources of the extracted Al are mainly allophane, imogolite and Al-humus complexes. There are exceptions to this general trend. In several cases oxalate extracted more Al than NaOH, the larger differences occurred in the horizons EUR16-Bw (Al_n-Al_o= –0.6%) and EUR17-Ah3 (Al_n-Al_o= –1.18%). Smaller but significant negative differences (Al_n-Al_o< –0.3%) also occur in organic C-rich horizons of soils from Italy (EUR03 and EUR04) and Iceland (EUR07, EUR08, EUR09). The contrary occurs with the soils EUR10 and EUR12 from Tenerife and two subsurface horizons (Bw, 2Bt) from EUR17, where Al_n clearly exceeds Al_o. Gibbsite was found in all the reference soils from Tenerife (Tejedor and Jiménez 2000, Meijer et al. this book). It is especially abundant in EUR10, except in the 2Bwb3 horizon where halloysite is an important component. In the Bw and 2Bt horizons from EUR17, the presence of a smectite-allophane association has been described. In these soils, the Al_n/Si_n molar ratio is higher than 3 in most horizons; with excep-

tion of the buried 2Ahb horizon of profile EUR12 and the halloysite rich 2Bwb3 horizon of EUR10.

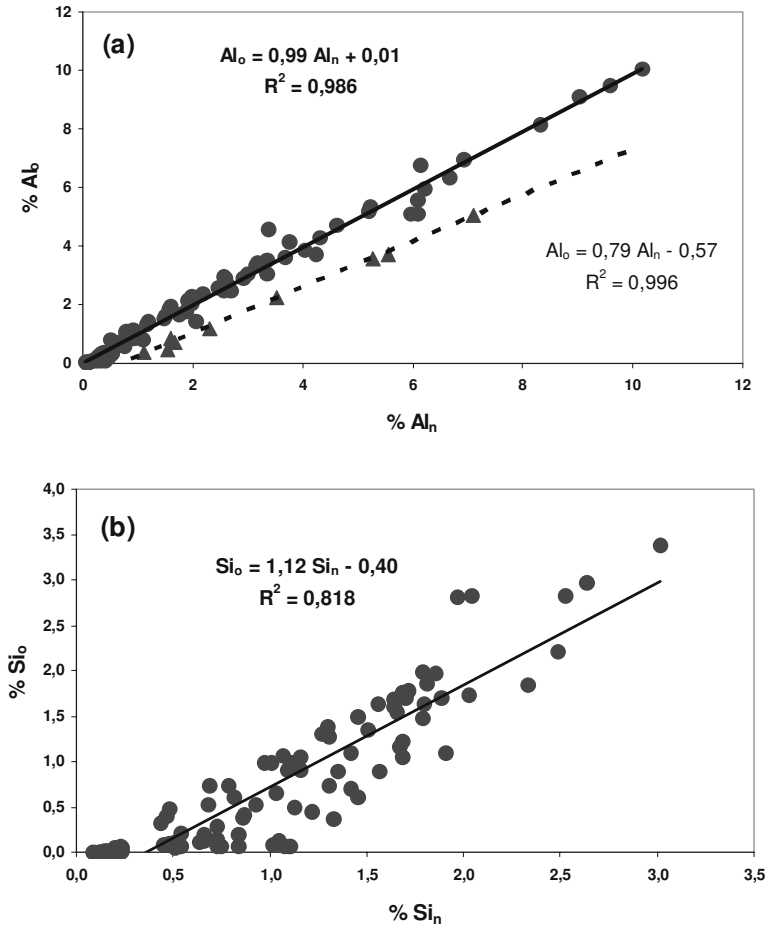

Figure 1. Relations between acid oxalate and sodium hydroxide-extractable Al (a) and Si (b). Regression lines and equations for all samples except horizons from EUR10 and 12 (●) and EUR10 and 12 (▲) samples.

The relation between Si extracted by NaOH and acid oxalate (Figure C, on CD) is similar to that obtained for Al (R^2=0.818, slope 1.12, Figure 1b), although the correlations are not so good for low concentrations (Table 1). In the soils from Italy, both extractions yielded similar quantities of Si in the soils EUR03 and EUR04 (R^2=0.996, slope=1.07). In EUR01 and EUR02, where zeolites (analcime and philippsite) are abundant and halloysite was identified in the clay fraction (Colombo et al. 2004), Si_n is

clearly larger than Si_o. If aluandic horizons are disregarded, Si_n and Si_o are similar in the soils from the Azores, France, EUR08 from Iceland, and the silandic horizons of EUR10, while in those from Greece and Hungary the Si_o content is negligible. NaOH tends to extract more Si than acid oxalate, mainly in vitric and non-andic horizons, but also in aluandic and other organic C-rich horizons. This is a consequence of the high pH of the former extractant, which causes dissolution of silica from components not extractable with acid oxalate. High values for Si_n-Si_o may be attributed to the dissolution in NaOH of components such as opaline silica, volcanic glass, weathered plagioclase (Meijer et al. this volume), and poorly crystalline kaolinite or halloysite. Phytoliths and diatom skeletons, identified in some soils from Iceland (Stoops and Gerard 2004), can also contribute to Si_n.

Table 1. Comparison between Al and Si extracted with acid oxalate and cold NaOH. Regression coefficients and equations. * Data sets with low values of Al or Si. Soils from Greece not included.

Aluminium		
Italy EUR01, 02*	R^2=0.837	Al_o=0.96Al_n–0.18
Italy EUR03, 04	R^2=0.948	Al_o=0.89Al_n–0.34
Azores	R^2=0.996	Al_o=1.00Al_n–0.17
Iceland	R^2=0.980	Al_o=0.99Al_n+0.20
Tenerife	R^2=0.972	Al_o=0.72Al_n–0.23
France	R^2=0.924	Al_o=0.93Al_n+0.31
Hungary*	R^2=0.687	Al_o=0.99Al_n–0.05
Andic	R^2=0.930	Al_o=0.91Al_n+0.27
Vitric	R^2=0.706	Al_o=0.62Al_n+0.03
Non-andic	R^2=0.946	Al_o=1.53Al_n–0.24
All soils	R^2=0.960	Al_o=0.95Al_n–0.03
Silicon		
Italy EUR01, 02*	R^2=0.005	
Italy EUR03, 04	R^2=0.996	Si_o=1.07Si_n–0.06
Azores	R^2=0.967	Si_o=1.27Si_n–0.51
Iceland	R^2=0.730	Si_o=1.05Si_n–0.34
Tenerife	R^2=0.828	Si_o=0.91Si_n–0.31
France	R^2=0.746	Si_o=1.63Si_n–1.06
Hungary*	R^2=0.903	Si_o=0.22Si_n–0.01
Andic	R^2=0.785	Si_o=1.22Si_n–0.48
Vitric	R^2=0.394	Si_o=0.36Si_n–0.06
Non-andic	R^2=0.332	Si_o=0.33Si_n–0.02
All soils	R^2=0.818	Si_o=1.12Si_n–0.40

In general, the Al/Si molar ratios obtained from both extractions are similar for most andic horizons (Figure 2) (R^2=0.859, slope=0.95), except for a group of seven organic carbon-rich horizons, which includes the 3 aluandic and EUR07-2CB, EUR09-Ah and 4H, and EUR17-Ah3, with Al_o/Si_o ratio twice Al_n/Si_n. This suggests that oxalate more readily dissolves Al from organic complexes than NaOH and the higher solubility of Si components in alkaline solutions. For most vitric and non-andic horizons Al_o/Si_o is clearly greater than Al_n/Si_n, with the largest difference in the soil EUR20. This is probably due to stronger dissolution of volcanic glass in NaOH.

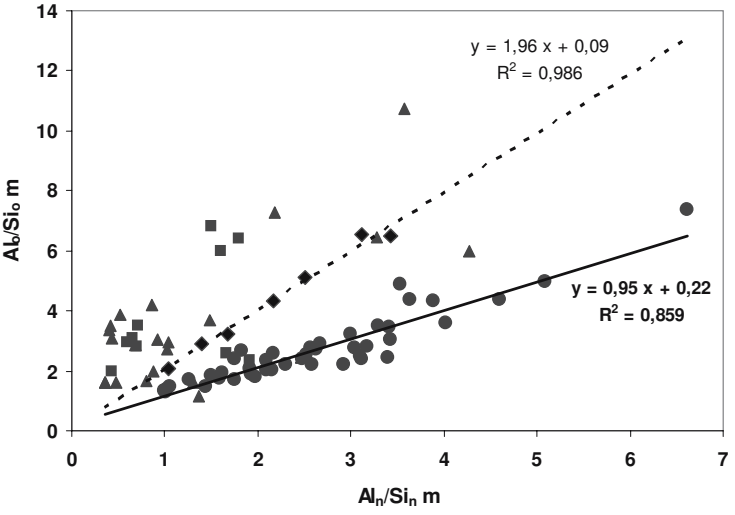

Figure 2. Relations between Al/Si molar ratios in the acid oxalate and cold sodium hydroxide extractions. Regression lines for andic (●) and some organic C-rich andic (♦) horizons (see text for details). Vitric (▲) and non-andic (■) horizons.

The dithionite-citrate extraction is useful to quantify the pool of free Fe in soils, although it may extract some Fe from layer silicates such as biotites and nontronites, and also from fine-sized chlorites. It cannot be used for total non-crystalline Al or Si because it fails to extract non-crystalline alumino-silicates and gibbsite (Dahlgren and Saigusa 1994). Nevertheless, Al and Si extracted with dithionite-citrate can in some cases be used to estimate the presence of Al and Si in the structure of crystalline Fe oxides. It is not discussed here because this extraction yielded lower quantities of Al and Si than acid oxalate.

The amount of free Fe extracted with dithionite-citrate (Fe_d), varied from very low in the soils from Greece or EUR01 and 02 from Italy (<0.5%) to more than 8% in some horizons from the soils EUR06, EUR07 and EUR10 (Table A – Figure A, on CD). Fe_d represents from less than 15% of total Fe in the soils from Greece and the subsurface horizons of many other soils to more than 55% in EUR06 and some horizons of EUR05, EUR07, EUR08 and EUR10 (Table A – Figure B, on CD). The ratio Fe_d/Fe_t has been interpreted in terms of weathering degree or pedogenesis at profile scale (Ndayiragije and Delvaux 2004). Following this interpretation the most weathered soils are EUR06 and the Bw, Bwb1 and Bwb2 horizons from EUR10, followed by some horizons from EUR05, EUR16 and EUR12. The high Fe_d/Fe_t values of some horizons of the soils from Iceland can be related to iron accumulation due to gleying upon water saturation caused by frost blockage and/or freeze-thawing processes described in the field and in the micromorphological studies (Stoops and Gerard 2004). The least weathered are the soils from Greece and the subsurphace horizons from EUR01 and 02.

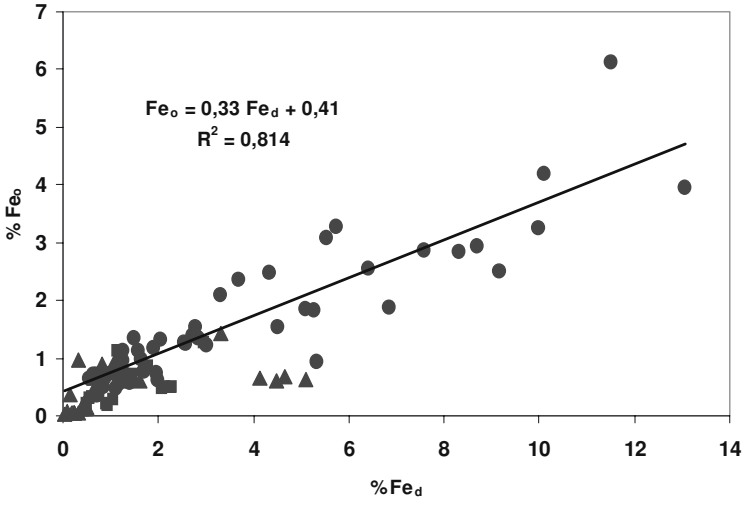

Figure 3. Relation between acid oxalate and citrate dithionite extractable Fe. Regression line and equation for andic horizons. Andic (●), vitric (▲), and non-andic (■) horizons.

Dithionite-citrate extracts more Fe than acid oxalate although there is a clear relation between both extractions for all samples (R^2=0.797) and, particularly, for andic horizons (R^2=0.814) (Figure 3). The exceptions are the horizons EUR09-3C and EUR10-2Bwb3, where Fe_o exceeds Fe_d, but with low quantities of extractable Fe. Figure D (on CD), where the Fe_o/Fe_d ra-

tios for all soils are presented, shows the predominance of crystalline Fe oxides (Fe_o/Fe_d<0.5) in the soils from Hungary and in EUR05, EUR10 and especially EUR12 (with Fe_o/Fe_d<0.2), together with some horizons EUR07 and 08 from Iceland. In the other soils the ratio Fe_o/Fe_d is >0.5, indicating the dominance of non-crystalline Fe components. The effect of oxalate extraction on minerals like magnetite or lepidocrocite, and the need of more than one extraction to dissolve all amorphous Fe oxides must be taken into account to interpret these results. In EUR06, the second oxalate extraction is more effective than the first one, suggesting that part of the Fe is incorporated in or enveloped by allophane (see Meijer et al. this volume).

The non crystalline components: acid oxalate extraction

Acid oxalate is commonly used to dissolve short-range order hydroxides and oxihydroxides of Al and Fe, Al and Fe bound to organic matter, Al and Si in allophane and imogolite, and opaline Si (McKeague and Day 1966, McKeague et al. 1971, Kodama and Schnitzer 1971, Higashi and Ikeda 1974, Wada 1977, Theng et al. 1982). The amounts extracted by oxalate are used to estimate the ferrihydrite, imogolite and allophane contents (Higashi and Ikeda 1974, Parfitt and Wilson 1985, Parfitt and Childs 1988). Oxalate can also extract a portion of the hydroxy-Al interlayer material from 2:1 layer silicates (Iyengar et al. 1981, Farmer et al. 1988, Paterson et al. 1993), and partly extract Fe from minerals such as magnetite (Baril and Bitton 1969, Walker 1983), maghemite (Taylor and Schwertmann 1974), lepidocrocite (Schwertmann 1973, Jeanroy 1983), chlorites, and biotites.

The results of the acid oxalate extractions are represented for Al in Figure E and for Fe in Figure F (both on CD). For comparison these figures also include Al_n and Fe_d values. The extraction of Si with acid oxalate is presented in Figure C (on CD) and was discussed in the previous section. Because of their very low contents of non-crystalline components, the soils from Greece and Hungary and the profiles EUR01–02 from Italy will not be discussed here.

The largest contents of Al_o and Si_o are found in B-horizons of profile EUR06 from the Azores. In general Al_o and Si_o are more abundant in andic horizons than in the vitric or non-andic ones (Figures C and E, on CD) and are well correlated (R^2=0.812, Figure 4). In most cases the surface horizons have also the lowest Al_o and Si_o contents in each soil. The ratio Al_o/Al_t, can be used as a weathering index to compare the degree of evolution of vitric and andic soils (see Taboada et al. this volume).

Comparison of Al_o and Al_p values ($Al_p/Al_o<0.5$) indicates that, in most soils, the reactive Al pool is dominated by inorganic constituents (Figure G, on CD). The only exceptions are the superficial horizons of the soils EUR05, EUR06, EUR11 and EUR17. In spite of the abundance of organic C in many A and B-horizons, (Figure E, on CD), much of the Al_o can be ascribed to the dissolution of allophane and/or imogolite.

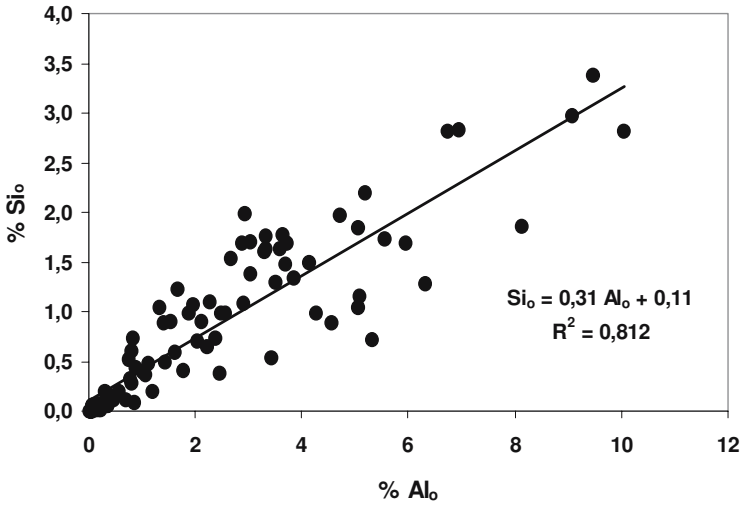

Figure 4. Relation between acid oxalate-extractable Al and Si.

According to Parfitt and Henmi (1982), a molar Al_o/Si_o ratio close to 2 indicates allophane. Figure 5 shows that Si_o increases with (Al_o-Al_p), the molar ratio corrected for organically bound Al. Disregarding the horizons of EUR12, from Tenerife, from which pyrophosphate extracted more Al than oxalate, the (Al_o-Al_p)/Si_o ratio is virtually constant for the total data set. The correlation gives a general molar ratio of 2.34 (R^2=0.908) for the non-crystalline inorganic constituents. The average Al/Si ratio of these constituents is 2.50 (R^2=0.819) in the andic horizons, 1.36 (R^2=0.882) in the vitric and 1.34 (R^2=0.970) in the non-andic ones. From these values, differences in composition of the inorganic amorphous fraction in the areas studied, and also between horizons from the same profile, become apparent. The regression lines give average (Al_o-Al_p)/Si_o molar ratios of 2.63 (R^2=0.993) for andic horizons from the Azores, 2.15 (R^2=0.907) for those from Tenerife (soil EUR10), 1.72 (R^2=0.916) for Iceland and 1.47 (R^2=0.773) for Italy. The soils from France have large differences, with Al/Si ratios of 2.85 (R^2=0.996) in EUR16 and 4.33 (R^2=0.966) in EUR17 (see also '*The physico-chemical database*' – this book – for a discussion

on allophane calculation). The non-crystalline aluminosilicates of the studied soils therefore vary from alumina-rich (Azores, Tenerife, France) to silica-rich (Italy, Iceland) (see also Meijer et al. this book). In the soils from Hungary the low pool of amorphous constituents are also rich in alumina, but because extracted amounts were low, the ratios are unreliable.

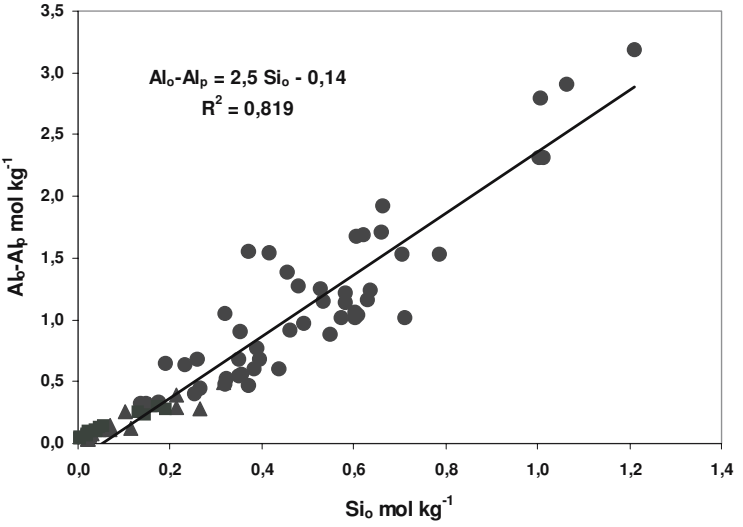

Figure 5. Relation between Si extracted with acid oxalate (Si_o) and the pool of 'amorphous inorganic' Al (Al_o-Al_p). Regression line and equation for andic horizons. Andic (●), vitric (▲) and non-andic (■) horizons.

With regards to Fe (Figure F, on CD), acid oxalate extracted the largest quantities in some horizons from the soils EUR05, EUR06, EUR10 and EUR16, reaching the highest content (6%) in the AC horizon of the soil EUR07. The lowest contents were found in EUR01–02 and in the soils from Greece. There is a general positive relation between Al_o or Si_o and Fe_o for the whole set of samples (R^2=0.678 and 0.540 respectively, EUR07-AC not included), but the dispersion is high. Given that – in absence of reduction and oxidation – both allophane and ferrihydrite are rather immobile weathering products, a positive correlation between the two appears logical. Good correlations of the non-crystalline pools are found in individual pedons and in the soils of a given region (R^2>0.8 for the soils from Gauro and Vico volcanoes in Italy, EUR08–09 from Iceland and EUR16–17 from France).

Acid oxalate generally extracts more Fe than pyrophosphate, although there are several cases where Fe_p is larger than Fe_o (EUR05-2Ahb,

EUR06-Ah and AB, EUR20-2CB and all the horizons of EUR12). Excluding these horizons, the ratios Fe_p/Fe_o (Figure G, on CD) have values from 0.05 to 1, with a poorly-defined trend to increase with organic C content. In spite of the lack of selectivity of pyrophosphate for Fe bound to humus, there is a relatively good relation between the Al_p/Al_o and Fe_p/Fe_o ratios for the whole population (R^2=0.507), and much better ones for separate soils (R^2=0.946 for EUR03–04; 0.902 for EUR06; 0.954 for EUR08–09; 0.838 for EUR10–11; 0.937 for the soils from France). This indicates that not all Fe extracted with oxalate can be allocated to inorganic amorphous components and, consequently to use it to estimate ferrihydrite contents without correction for Fe_p is unrealistic. Sequential oxalate extractions (Meijer et al. this book) indicate that in EUR06, a single oxalate extraction is not a good measure for Fe_o. This complicates the interpretation of such data.

Disregarding the above mentioned limitations and following the common use of acid ammonium oxalate extractions, the amounts of allophane (+ imogolite) and ferrihydrite, were calculated (Figure H, on CD). For a discussion of allophane calculations see also '*The physico-chemical database*' (this book). The contents of allophane, estimated according to Mizota and van Reeuwijk (1989), are well correlated with allophane contents estimated from Si_o (R^2=0.93). They ranged from negligible in the soils from Greece, Hungary and Italy (EUR01 and 02) to more than 20% in some horizons from France and Azores. Ferrihydrite content has the same distribution as Fe_o because it has a linear relationship with this value.

Allophane formation is limited when soil pH<5, and allophanic andosols often have pH in the range 5.5–6.5 (Nanzyo et al. 1993) although higher values may occur when fresh basic parent materials buffer the pH by release of basic cations upon weathering (Arnalds 2004a). In this set of soils, maximum allophane and ferrihydrite contents are in the pH-H_2O range 5.4–6.8 (pH-KCl 4.8–5.8), similar to that reported by Arnalds (2004b), although there are horizons with more than 10% of allophane that have a more acid pH (Figure I on CD, which also includes Al_o, Al_o-Al_p and Si_o). The samples with significant quantities of calculated ferrihydrite and high pH values are the subsurface horizons of EUR16, probably indicating the action of acid oxalate on crystalline, but oxalate-soluble, Fe minerals (see also Meijer et al. this book, for multiple oxalate extraction of Fe).

The organically bound Fe and Al: pyrophosphate extraction

Aluminium extracted with Na-pyrophosphate (Al_p) is used as a proxy for Al in organic complexes (assuming negligible extraction of hydrous oxides, allophane and imogolite). Pyrophosphate is less specific for Fe- than

for Al-humus complexes due to the trend of particulate Fe to stay in suspension and to its capacity to dissolve ferrihydrite (Kassim et al. 1984) and other non-crystalline hydroxides and iron-rich smectites (Higashi et al. 1981).

In spite of the dominance of the inorganic Al reactive pool in most of the studied soils, pyrophosphate extracts a considerable amount of reactive Al from many samples (Figure E, on CD). Though Al_p tends to increase with organic C in mineral horizons, this is not true for the horizons of soil EUR12, which have more Al_p than Al_o and very low C/Al_p ratios, for the surface horizons of EUR02, EUR03 and EUR11 and for the Ah horizons of EUR07. The low Al_p content of soil EUR07 may be explained by a low humification degree caused by temperature regime and poor drainage. Excluding these samples, organic C and Al_p are well correlated in non-andic horizons and vitric horizons (R^2>0.8) and relatively well in the andic ones (Figure 6a). This relationship is very significant in the soils from Italy (R^2>0.97 in the andic and vitric horizons), Azores (R^2=0.803), Tenerife (R^2>0.95) and Iceland (R^2>0.95, disregarding the subsurface horizons of EUR07) and also in many individual soils. The increase of the Al_p/Al_o ratio with organic C content in the andic horizons (Figure 6b) supports both the anti-allophanic effect of organic matter and the specificity of the pyrophosphate extraction.

Metal-humus complexes tend to dominate in andosols with pH<5. In soil classification, a pH of 5.5 is used as a limit to separate aluandic (more acidic) and silandic (less acidic) andosols. In the studied soils, the quantities of Al_p and Fe_p are negligible when pH-H_2O>6.0 (pH-KCl>5.5), while contents over 1% of both elements are only found in soils with pH-H_2O<6.1 (pH-KCl<5.7) (Figure J, on CD).

Although the C/Al_p molar ratio strongly depends on humification degree and chemistry of soil organic matter, it can provide a measure of the degree of Al-saturation of humus. The values of this ratio ranged from 9 to 58 in andic horizons (Figure K, on CD) but most are close to the range of 10–20, reported by Takahashi et al. (1995) for Japanese Andosols or those of the Andisol TU database (Shoji et al. 1993) with a mean value of 13. Most of the andic horizons from Iceland had higher C/Al_p ratios (31–50), which shows a lower Al saturation that may be due to the lower complexing power of the less decomposed organic matter, related to poor drainage and cold conditions. The C/Al_p ratio is also high in the organic matter-rich surface horizons from France. The opposite occurs in those from the Azores (with C/Al_p ratios <10 in most cases), that have a high Al saturation of the organic matter. For the vitric horizons with larger quantities of organic C and Al_p the ratio was generally >40, which might reflect a low availability of aluminium in these rather unweathered soils. In EUR12, the

anomalously high Al_p content caused very low values (<5) of the C/Al_p ratio in subsurface horizons.

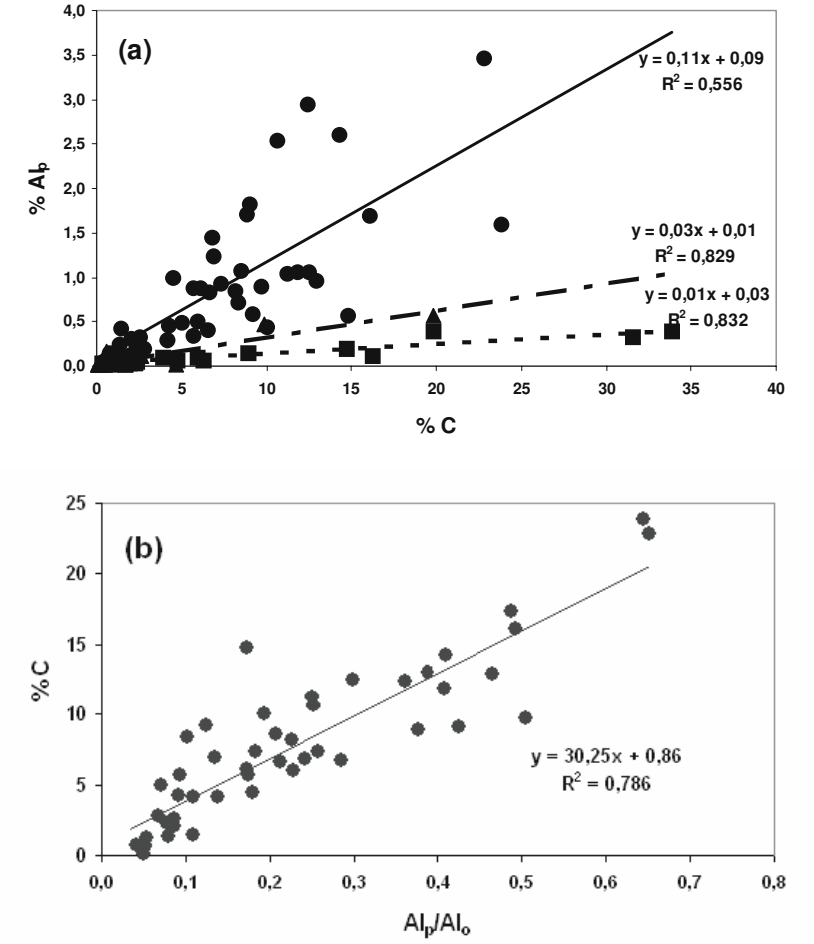

Figure 6. Relations of organic C with Al_p for andic (●), vitric (▲) and non-andic horizons (■) (a), and with the Al_p/Al_o ratio for andic horizons (b).

In O-horizons, C/Al_p ratios were very high (115–222) due to the high content of unhumified organic C. The ratios of the soils from Greece and Hungary are also high, in this case as a consequence of their high pH and very low content of active Al. In many andic horizons the $C/(Al_p+Fe_p)$ molar ratios are close to the C/Al_p ones due to the relatively low contents of Fe_p.

Unbuffered salts

For a better characterization of the Al pool, the soils were extracted with unbuffered $CuCl_2$ or $LaCl_3$, in addition to the commonly used KCl extraction. The results of these extractions for the soils of each country are presented in Figure L (on CD).

Copper chloride

Copper chloride was proposed by Juo and Kamprath (1979) as an extractant for 'potentially reactive non-exchangeable' Al. The difference between Al_{Cu} and Al_K was attributed mainly to organo-Al complexes. The high efficiency of $CuCl_2$ in extracting Al has been related to the low pH of 0.5 M $CuCl_2$ solutions (2.7–3.3) and the strong complexing power of the cation (Oates and Kamprath, 1983a, Conyers 1990). The low pH can induce depolymerization of Al-hydroxides, and thus extraction of Al from Al-interlayered clay minerals (Juo and Kamprath 1979, Hargrove and Thomas 1981). However, $CuCl_2$ has been considered as a better extractant for Al-humus complexes than pyrophosphate (Kaiser and Zech 1996). García-Rodeja et al. (2004) showed, in a subset of the soils studied here, that the amount of Al extracted with unbuffered KCl and $LaCl_3$ increased with decreasing soil pH, but there was no similar relationship with unbuffered $CuCl_2$. The effect of soil pH in $CuCl_2$ extraction is showed in Figure M (on CD). Low values of Al_{Cu} are found for pH-H_2O>7 (pH-KCl>6) and the maximum Al_{Cu} values correspond to the soil pH-H_2O range 4.3–6.2 (pH-KCl 4.0–5.7).

The quantity of Al extracted with $CuCl_2$ ranged from 13 to 121 $cmol_c\ kg^{-1}$ in andic, and from 3 to 28 in non-andic horizons, with the higher values for the latter group in the organic horizons. In the vitric horizons the values ranged from <1 to 27, with the exception of the horizons of EUR12 with high Al_{Cu} content (30–91). In accordance with the small pyrophosphate-Al pools, the soils from Greece and the subsurface horizons of EUR01 and EUR02 had low Al_{Cu} contents (<1.5 and 6–9 $cmol_c\ kg^{-1}$, respectively).

In several horizons with low C contents, $CuCl_2$ extracted more Al than pyrophosphate. In most cases the difference was small (<3 $cmol_c\ kg^{-1}$) or between 4 and 6 $cmol_c\ kg^{-1}$ in EUR01 and EUR02 subsurface horizons. Thus a similar extraction capacity for both methods, possibly with a slight contribution of Al from mineral phases, can be concluded.

Pyrophosphate generally extracted more Al than $CuCl_2$, with differences ranging from 4 to 264 $cmol_c\ kg^{-1}$. Al_{Cu} increases with Al_p (Figure 7) in all

soils (Al_{Cu}=0.30Al_p–0.05; R^2=0.906), disregarding EUR10 and the buried B-horizons of EUR12. In the andic horizons, $CuCl_2$ again extracts about 30% of Al_p (Al_{Cu}=0.30Al_p–0.06; R^2=0.889), while it reaches about 50% of Al_p in the vitric (Al_{Cu}=0.52Al_p–0.03; R^2=0.873) and non-andic horizons (Al_{Cu}= 0.49Al_p–0.02; R^2=0.753). For most andic horizons, the fraction of Al_p not extracted by $CuCl_2$ is about 70% (Al_p-Al_{Cu}=0.69Al_p–0.06; R^2=0.959). In comparison, Takahashi et al. (1995) reported that Al_{Cu} was 40–50% of Al_p in A horizons from Andosols and Dahlgren and Walker (1993) gave values between 50–80% for podzol B-horizons. This correlation suggests that $CuCl_2$ extracts a very specific portion of Al that may be used to describe complexation characteristics of the organic matter. It is not unlikely that $CuCl_2$ would extract all but the trivalently bound Al. Nevertheless, in the B-horizons from soils EUR10–11, $CuCl_2$ extracted significantly more Al than pyrophosphate (differences up to 59 $cmol_c\ kg^{-1}$, or 0.53%). In these horizons, with C content between 1.89 and 4.22%, the contribution of an Al-phase with greater solubility in $CuCl_2$ (at low pH) than in pyrophosphate (at high pH) must be considered. It is possible that this is the Al-fraction of weathered plagioclases mentioned by Meijer et al. (this volume).

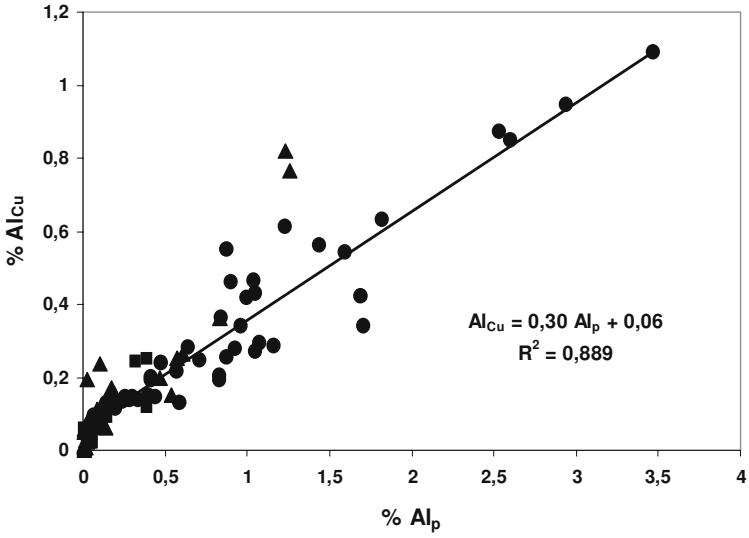

Figure 7. Relations between pyrophosphate and $CuCl_2$ extractable Al. Regression lines and equations for andic horizons. Andic (●), vitric (▲) and non-andic (■) horizons.

In non-andic horizons, Al_{Cu} is strongly correlated with organic C (R^2=0.926), and this trend holds true for the other horizons, but with higher dispersion. Nevertheless, both properties are well-correlated for the soils of given region or for individual profiles: andic (R^2=0.968) and vitric (R^2=0.897) horizons from Italy, vitric horizons from Iceland (R^2=0.916), or the horizons of the soils EUR06 (R^2=0.827), EUR08 (R^2=0.848), EUR12 (R^2=0.879) and EUR17 (R^2=0.979). A similar correlation (R^2=0.96) was reported by Soon (1993) in organic matter-rich horizons using a sequential extraction procedure and a weaker $CuCl_2$ solution (0.1 M) with higher pH (4.2). The Al_{Cu} for organic C=0%, calculated from the regression equations, is low (<10 $cmol_c\ kg^{-1}$) in vitric and non-andic horizons and in the andic horizons from Italy and Iceland, which may indicate that all Al_{Cu} is organic-matter bound. On the other hand, the cut-off values >20 $cmol_c\ kg^{-1}$ in the andic horizons from France and Azores (51 $cmol_c\ kg^{-1}$ in EUR06) and in EUR12 suggest the presence of an additional source. In fact, Urrutia et al. (1995) reported that $CuCl_2$ extracted Al from inorganic amorphous constituents in soils with andic properties from gabbros and basalts and in podzol Bs-horizons.

For the soils studied here, Al_{Cu} is highly correlated with an approximation of the CEC of organic matter and allophane (Al_{Cu}=3*%C + 1.5*%allophane). The R^2 of this correlation is 0.972 in the andosols from Italy, 0.858 for the Azores soils, 0.879 for the Icelandic soils (R^2=0.879), and 0.830 and 0.993, respectively, for the French soils EUR16 and EUR 17. These may indicate that Al extracted with $CuCl_2$ is related to the reactive surfaces with Al and explain why, in some cases, Al_{Cu} content is better explained by a combination of allophane and carbon contents, than only by C content, as previously reported by García-Rodeja et al. (2004) for a subset of the samples studied here. It supports the conclusion by Madeira et al. (this book) that allophane may be negatively charged at soil pH. In soils with low allophane contents there is also a good relation between Al_{Cu} and CEC at pH7 (R^2=0.915 for EUR01 and EUR02; 0.801 for EUR16; 0.971 for EUR17. The R^2 is >0.6 for the soils from Azores and Iceland, which is in agreement with the conclusions of Cronan et al. (1986) who stated that Al_{Cu} can be considered as the more labile Al-humus fraction, responsible for regulating activities of dissolved Al in organic matter-rich soils, or with those of Oates and Kamprath (1983ab) who reported that Al content from $CuCl_2$ extraction was a better parameter than Al_K to calculate lime requirements because it also includes potential acidity. These conclusions should be extended to soils with allophane or imogolite.

The molar ratio C/Al_{Cu} varied from 23 to 65 in the andic horizons from Italy and Azores, and most are within the range of 23–46 reported by Takahashi et al. (1995) for A horizons of Andosols. Higher ratios are found

in the soils from Iceland and France (85–156), with maximum values in the Ah-horizons. This reflects a lower Al saturation (C/Al_p ratios were also high) but probably also greater stability of Al-humus complexes, because, in many of the horizons of these soils, $CuCl_2$ extracted <30% of Al_p. As with Al_p, the C/Al_{Cu} ratios for organic horizons were very high (178–373) because of the low degree of evolution of the organic matter and possibly the low availability of aluminium. The Bw horizons of EUR10, with $Al_{Cu}>Al_p$, has very low C/Al_{Cu} ratios (5–13), which may indicate the dissolution of Al from non-organic sources (see above). As Soon (1993) and Berggren and Mulder (1995) proposed, this possibility must be taken into account if this extraction is used as an estimate of Al complexed or chelated by organic matter in soils with allophane or imogolite.

Lanthanum chloride

Lanthanum chloride is more efficient than KCl in extracting Al from Al-humus complexes (Bloom et al. 1979ab) and very effective in removing the less hydroxylated and less polymerized Al species from organic matter-rich soils, an Al fraction that correlates well with titrable acidity (Hargrove and Thomas 1984). Although $LaCl_3$ does not extract a well-defined Al fraction, in addition to the exchangeable pool, it can probably dissolve significant amounts of Al potentially available to plants (Darke and Walbridge 1994). This can clarify the potential acidity of soils that have little Al extracted by KCl, but frequently show symptoms of Al toxicity (Saigusa et al. 1980).

The quantity of Al extracted by $LaCl_3$ decreased with increasing soil pH (Figure M, on CD). Values were <2 $cmol_c\ kg^{-1}$ for pH-H_2O>6.0 (pH-KCl>5.5). In more acid andic horizons, Al_{La} ranged from 2 to 19 $cmol_c\ kg^{-1}$ (the higher values in EUR06-Ah and EUR07-Ah1). Both, Al_{La} and the fraction of Al specifically extracted by $LaCl_3$ (Al_{La}-Al_K) tended to increase with organic C content (R^2=0.727 and 0.721 respectively, Figure 8) although values were very low for horizons with less than 4% of organic carbon. A similar trend was found in non-andic horizons (R^2=0.737) but not in the vitric ones. Due to the fact that organic C and pH are also related (higher C content at low pH, see Figure M on CD) the relation of Al_{La} and C is difficult to interpret.

The fraction of Al_{Cu} extracted by $LaCl_3$ is very variable, from <1% to more than 50%, with the higher percentages in the silandic horizons, in the H horizons of EUR09, and in the non-andic horizons of the soils EUR19–20. Disregarding these soils from Hungary, $LaCl_3$ extracted less than 14% and frequently <1% of Al_p. These results agree with those reported by Ur-

rutia et al. (1995), who found that $LaCl_3$ extracts most Al from podzol-B horizons and least from andic Ah horizons that have more stable complexes of organic matter with Al. Although this would indicate that Al extracted with $LaCl_3$ can be interpreted in terms of the stability of Al-humus complexes, this is obscured by the effect of soil pH on Al extraction with an unbuffered salt, and by the relation between soil pH and C content.

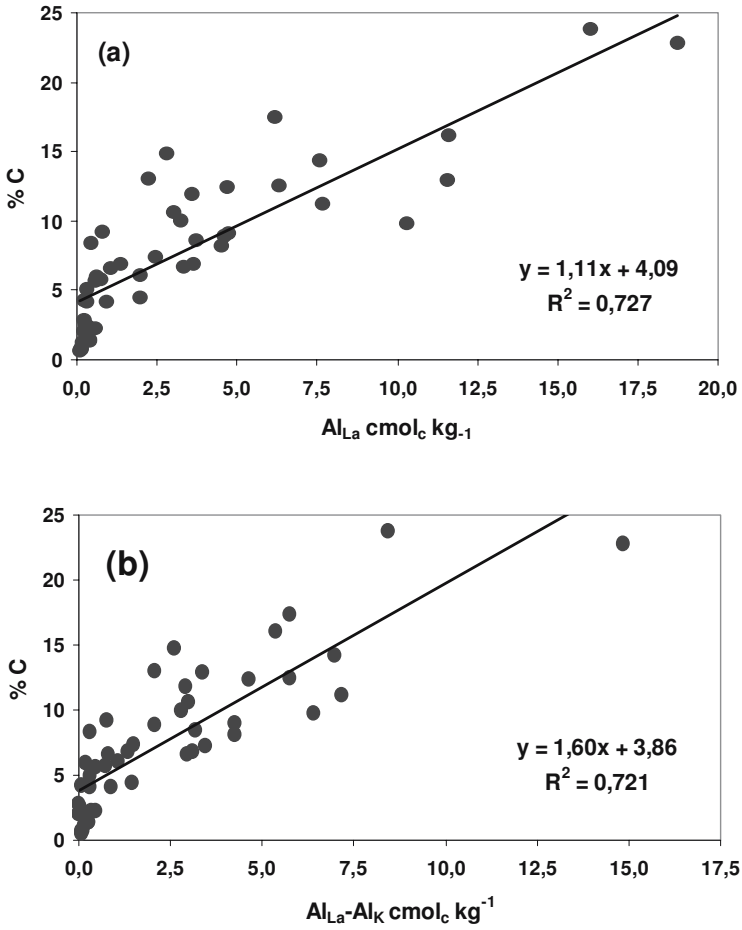

Figure 8. Relations of organic C with Al_{La} (a) and with the Al pool specifically extracted by $LaCl_3$ (Al_{La}-Al_K) (b) for andic horizons.

Potassium chloride

Al extracted with KCl is generally interpreted as exchangeable Al (Lin and Coleman 1960), and it is the standard method for determining salt-exchangeable forms of Al for use in modern soil classification (FAO 1998, Soil Survey Staff 1999) but it does not extract the reactive Al associated with organic matter. Many studies have shown the problems that arise from its use in variable charge soils (see also Madeira et al. this book).

Only horizons with pH-H_2O<5.5 (pH-KCl<4.5) had Al_K>1 $cmol_c\ kg^{-1}$ (Figure M on CD), and Al_K contents >3 $cmol_c\ kg^{-1}$ were found only in the more acid, organic matter rich aluandic or nearly aluandic horizons (EUR05-Ah1, EUR06-Ah, EUR17-Ah1, Ah2, EUR09-2H with the highest Al_K, and EUR12-2Ahb). These low Al_K contents are in agreement with the virtual absence of Al_K in Andosols containing allophane and imogolite (Wada 1987a).

Al_{La}-Al_K was very small (<2 $cmol_c\ kg^{-1}$) in horizons with high pH (pH-H_2O>6) and/or relatively low organic C contents (<3%). It was larger in A and B-horizons with lower pH and organic C contents >6%. In each profile it decreased with depth, as pH increases and organic C decreases.

From the results for the extraction of Al with unbuffered Cu, La and K chlorides, and its comparison with the total organic Al pool (Al_p), the general sequence of extraction efficiency was: Al_p>Al_{Cu}>Al_{La}≥Al_K. A few exceptions occurred in horizons poor in Al and with low degree of development. Interpretation of Al_K and Al_{La} in terms of soil formation remains difficult.

Pyrophosphate always extracted about three times more Al than $CuCl_2$. In organic matter-rich mineral horizons, Al_{La}, Al_{Cu} and Al_p tend to increase with the organic carbon content, showing the relation of the Al extracted with these methods with the binding sites provided by organic matter.

The sequence above indicates the solubility of Al compounds in the soils and these methods can be useful for comparing the stability of Al-humus complexes. The use of unbuffered salts may also help to assess the limitations in the interpretation of Al_p. $LaCl_3$ extraction may estimate the most labile Al pool, including a fraction of Al-humus complexes.

Conclusions

The use of selective dissolution methods to study the components of 20 European volcanic soils shows the validity of these kind of methods to compare soils formed from different parent materials and varied environ-

mental conditions, and to characterize their reactive Al and Fe pools. In addition, the Al_o/Al_t ratio can be used as a weathering index to compare the degree of evolution of vitric and andic horizons (see Taboada et al. this volume). Nevertheless, these methods can render anomalous values that limit their use to characterize soil components. This was the case of the soil EUR12, where pyrophosphate extracted more Al than oxalate, and the B-horizons from EUR10 and 11 where $CuCl_2$ was more effective than pyrophosphate in the extraction of Al. Another problem arises from the inadequacy of standard procedures to quantify the different Fe, Al and Si pools when the active components are very abundant (see Meijer et al. this volume), or when they extract these elements from crystalline mineral phases. The main conclusions that can be drawn from this study are:

1. The soils from Greece, Hungary and from the Gauro Volcano in Italy (EUR01, 02) are poor in extractable Al and Si and their contents in allophane are negligible. On the contrary, the soils from Azores and France are allophane-rich. The soils from Greece and Italy have also very low quantities of extractable iron, that is more abundant in the other soils, especially in those from Azores, Iceland (EUR07, 08), Tenerife (EUR12) and France (EUR16). Crystalline Fe oxides only predominate in the soils from Hungary and in EUR12 from Tenerife.
2. In most soils NaOH and acid oxalate extracted similar quantities of Al indicating that the extractable crystalline Al pool is very small. However, in the soils from Tenerife (EUR10, 12) and in the Bw and 2Bt horizons from EUR17 there are differences between both methods attributable to the dissolution of gibbsite and/or halloysite. Due to its high pH, NaOH extracts more Si than acid oxalate because it can dissolve silica from components such as opaline silica, volcanic glass, weathered plagioclase, poorly crystalline 1:1 phyllosilicates and, possibly, zeolites.
3. The non crystalline inorganic Al pool (Al_o-Al_p) and the Si extracted with acid oxalate show large differences between soils from different geographical regions: allophane is in average Al rich in the andosols from Azores, Tenerife and France and silica rich in the soils from Iceland and Italy. Even when disregarding the surface horizons of EUR05, 06, 11 and 17, in which the organic active Al is the dominant pool, many soils have a considerable fraction of Al in complexes with organic matter. This pool is largest in the soils from the Azores, where climatic conditions favour the accumulation of organic matter and, in contrast, is very small in the soils developed under warmer (Italy, Greece), colder (Iceland) or drier (Greece, Hungary) conditions. Metal-humus complexes are negligible when pH-H_2O>6.0.

4. Both, allophane and ferrihydrite reach maximum values in the pH-H_2O range 5.4–6.8. The ratios Fe_p/Fe_o and Al_p/Al_o tend to increase with organic C content supporting both the anti-allophanic effect of organic matter and the effectiveness of the pyrophosphate extraction. Because not all Fe extracted with oxalate can be allocated to inorganic amorphous components, its use to estimate ferrihydrite is unrealistic.
5. In organic matter-rich mineral horizons, Al_{La}, Al_{Cu} and Al_p increase with organic C indicating than these Al fractions are associated with organic matter. Both Al_p and Al_{Cu} tend to decrease with depth, as organic C decreases. $CuCl_2$ extracts a very specific portion of Al_p in andic and vitric horizons suggesting that it can be used to describe complexation characteristics of the organic matter. For most andic horizons, there is a good relationship between Al_{Cu} and the components that determine the CEC of the soils (organic matter and allophane). The maximum Al_{Cu} values correspond to the soil pH-H_2O range 4.3–6.2.
6. The Al extracted with $LaCl_3$ and KCl is highly dependent on soils pH and difficult to interpret in terms of soil formation. Nevertheless the use of unbuffered salts, including $CuCl_2$, may help to assess the limitations in the interpretation of Al extracted with pyrophosphate. In spite of limitations, the quantities of Al extracted with $CuCl_2$ and with $LaCl_3$ may be useful for practical purposes as they represent labile fractions of Al that are potentially important for plant toxicity.

References

Arnalds O (2004a). Volcanic soils of Iceland. Catena 56:3–20

Arnalds O (2004b). Icelandic volcanic soils. Rala Report 214:27–28

Baril R, Bitton G (1969). Teneurs élevées de fer libre et l`identification taxonomique de certain sols du Québec contenant de la magnetite. Canadian Journal of Soil Science 59:1–9

Berggren D, Mulder J (1995). The role of organic matter in controlling aluminum solubility in acidic mineral soil horizons. Geochimica et Cosmochimica Acta 59:4167–4180

Bloom PR, McBride MB, Weaver RM (1979a). Aluminum organic matter in acid soils: buffering and solution aluminum activity. Soil Science Society of America Journal 43:488–493

Bloom PR, McBride MB, Weaver RM (1979b). Aluminum organic matter in acid soils: salt-extractable aluminum. Soil Science Society of America Journal 43:813–815

Borggaard OK (1985). Organic matter and silicon in relation to the crystallinity of soil iron oxides. Acta Agriculturae Scandinavica 35:398–406

Colombo C, Di Cerce A, Sellito MV, Palumbo G, Terribile F (2004). Genesis and formation of volcanic soils in Fegrean Fields. Rala Report 214:61–62

Conyers M (1990). The control of aluminium solubility in some acidic Australian soils. Journal of Soil Science 41:147–156

Cronan CS, Walker WJ, Bloom PR (1986). Predicting aqueous aluminium concentrations in natural waters. Nature 324:140–143

Dalhgren RA, Saigusa M (1994). Aluminum release rates from allophanic and non allophanic Andosols. Soil Science and Plant Nutrition 40:125–136

Dahlgren RA, Walker WJ (1993). Aluminium release rates from selected Spodosol Bs horizons: effect of pH and solid-phase aluminium pools. Geochimica et Cosmochimica Acta 57:57–66

Dahlgren RA, Walker WJ (1994). Solubility control of KCl extractable aluminum in soils with variable charge. Communications in Soil Science and Plant Analysis 25:2201–2214

Darke AK, Walbridge MR (1994). Estimating non-crystalline and crystalline aluminum and iron by selective dissolution in a riparian forest soil. Communications in Soil Science and Plant Analysis 25:2089–2101

FAO (1998). World Reference Base for Soil Resources. World Soil Resources Report 84. FAO, Rome

Farmer VC, Smith BFL, Wilson MJ, Loveland PJ, Payton RW (1988). Readily-extractable hydroxyaluminium interlayers in clay- and silt-sized vermiculite. Clay Minerals 23:271–277

Fieldes M, Perrot KW (1966). The nature of allophane in soils: 3. Rapid field and laboratory test for allophane. New Zealand Journal of Science 9:629–639

García-Rodeja E, Nóvoa JC, Pontevedra X, Martínez A, Buurman P (2004). Aluminium fractionation of European volcanic soils by selective dissolution techniques. Catena 56:155–183

Hargrove WL, Thomas GW (1981). Extraction of aluminum from aluminium-organic matter complexes. Soil Science Society of America Journal 45:151–153

Hargrove WL, Thomas GW (1984). Extraction of aluminum from aluminium-organic matter in relation to titratable acidity. Soil Science Society of America Journal 48:1458–1460

Hashimoto IM, Jackson ML (1960). Rapid dissolution of allophane and kaolinite and halloysite after dehydration. Clays and Clay Minerals 7:102–113

Higashi T (1983). Characterisation of Al/Fe-humus complexes in dystrandepts through comparison with synthetic forms. Geoderma 31:277–288

Higashi T, de Connick F, Gelaude F (1981). Characterization of some spodic horizons of the Campine (Belgium) with dithionite-citrate, pyrophosphate and sodium hydroxide tetraborate. Geoderma 25:131–142

Higashi T, Ikeda H (1974). Dissolution of allophane by acid oxalate solution. Clay Science 4:205–211

Iyengar SS, Zelazny LW, Martens DC (1981). Effect of photolitic oxalate treatment on soils hydroxyinterlayered vermiculites. Clays and Clay Minerals 29:429–434

Jeanroy E (1983). Diagnostique des forms de fer dans les pédogenèses tempérées. Evaluation par les reactives chimiques d'extraction et apports de la spectrométrie Mössbauer. Thèse. Université Nancy

Juo AS, Kamprath EJ (1979). Copper chloride as an extractant for estimating the potentially reactive aluminium pool in acid soils. Soil Science Society of America Journal 43:35–38

Kaiser K, Zech W (1996). Defects in estimation of aluminum in humus complexes of podzolic soils by pyrophosphate extraction. Soil Science 161:452–458

Kamprath EJ (1970). Exchangeable Al as a criterion for liming leached mineral soils. Soil Science Society of America Proceedings 34:252–254

Kassim JK, Gafoor SN, Adams WA (1984). Ferrihydrite in pyrophosphate extracts of podzol B horizons. Clay Minerals 19:99–106

Kodama H, Schnitzer M (1971). Evidence for interlamellar adsorption of organic matter by clay in a podzol soil. Canadian Journal of Soil Science 51:509–512

Lin C, Coleman MT (1960). The measurement of exchangeable aluminum in soils. Soil Science Society of America Proceedings 24:444–446

McKeague JA, Brydon JE, Miles NM (1971). Differentiation of forms of extractable iron and aluminum in soils. Soil Science Society of America Proceedings 35:33–38

McKeague JA, Day JH (1966). Dithionite and oxalate extractable Fe and Al as aids in differentiating various classes of soils. Canadian Journal of Soil Science 46:13–22

Meijer EL, Buurman P (1997). Factor analysis and direct optimization of the amounts and properties of volcanic soil constituents. Geoderma 80:129–151

Mizota C, van Reeuwijk LP (1989). Clay Mineralogy and Chemistry of Soils Formed Under Volcanic Materials in Diverse Climatic Regions. Soil Monograph 2, ISRIC, Wageningen, The Netherlands

Mulder J, Stein A (1994). The solubility of aluminum in acidic forest soils: long-term changes due to acid deposition. Geochimica et Cosmochimica Acta 58: 85–94

Nanzyo M, Dahlgren RA, Shoji S (1993). Chemical characteristics of volcanic ash soils. In: Shoji S, Nanzyo M, Dahlgren RA (eds) Volcanic Ash Soils. Genesis, Properties and Utilization. Developments in Soil Science 21, Elsevier, Amsterdam, pp 145–187

Ndayiragije S, Delvaux B (2004). Selective sorption of potassium in a weathering sequence of volcanic soils from Guadeloupe, French West Indies. Catena 56:185–198

Oates KM, Kamprath EJ (1983a). Soil acidity and liming: I. Effect of the extracting solution cation and acidity on the remove of extractable aluminum from acid soils. Soil Science Society of America Journal 47:686–689

Oates KM, Kamprath EJ (1983b). Soil acidity and liming: II. Evaluation of using aluminum extracted by various chloride salts for determining lime requirements. Soil Science Society of America Journal 47:690–692

Parfitt RL, Childs CW (1988). Estimation of forms of Fe and Al: a review, and analysis of contrasting soils by dissolution and Mössbauer methods. Australian Journal of Soil Research 26:121–144

Parfitt RL, Henmi T (1982). Comparison of an oxalate-extraction method and an infrared spectroscopic method for determining allophane in soil clays. Soil Science and Plant Nutrition 28:183–190

Parfitt RL, Wilson AD (1985). Estimation of allophane and halloysite in three sequences of volcanic soils, New Zealand. In: Fernandez Caldas E, Yaalon DH (eds) Volcanic Soils. Weathering and Landscape Relationships of Soils on Tephra and Basalt. Catena Supplement 7, Elsevier, Amsterdam, pp 1–8

Paterson E, Clark L, Birnie C (1993). Sequential selective dissolution of iron, aluminium, and silicon from soils. Communications in Soil Science and Plant Analysis 24:2015–2023

Ponette Q, André D, Dufey JE (1996). Chemical significance of aluminium extracted from three horizons of an acid forest soil, using chloride salt solutions. European Journal of Soil Science 47:89–95

Saigusa M, Shoji S, Takahashi T (1980). Plant root growth in acid Andosols from north-eastern Japan. Exchange acidity Y1 as a realistic measure of aluminum toxicity potential. Soil Science 130:242–250

Schwertmann U (1973). Use of oxalate for Fe extraction from soils. Canadian Journal of Soil Science 53:244–246

Shoji S, Fujiwara Y (1984). Active aluminum and iron in the humus horizons of Andosols from north-eastern Japan: their forms, properties and significance in clay weathering. Soil Science 137:216–226

Shoji S, Nanzyo M, Dahlgren RA (eds) (1993). Volcanic ash soils. Genesis, Properties and Utilization. Developments in Soil Science 21, Elsevier, Amsterdam

Soil Survey Staff (1999). Soil taxonomy. A basic system of soil classification for making and interpreting soil surveys. Agriculture Handbook 436, 2nd edn. US Government Printing Office, Washington, DC

Soon YK (1993). Fractionation of extractable aluminium in acid soils: a review and a proposed procedure. Communications in Soil Science and Plant Analysis 24:1683–1708

Stoops G, Gerard M (2004). Micromorphology of the volcanic ash soils of the COST-622 reference profiles. Rala Report 14:12–13

Takahashi T, Dahlgren RA (1998). Possible control of aluminum solubility by 1 M KCl treatment in some soils dominated by aluminium-humus complexes. Soil Science and Plant Nutrition 44:43–51

Takahashi T, Fukuoka T, Dahlgren RA (1995). Aluminum solubility and release rates from soil horizons dominated by aluminium-humus complexes. Soil Science and Plant Nutrition 41:119–131

Taylor RM, Schwertmann U (1974). Maghemite in soils and its origin. I. Properties and observations on soil maghemites. Clays and Clay Minerals 10:289–298

Tejedor M, Jiménez C (2000). Field Guide Tenerife. COST 622 Action, Internal Report. University of La Laguna, Tenerife, Spain

Theng BKG, Russell M, Churchman GJ, Parfitt RL (1982). Surface properties of allophane, imogolite and halloysite. Clays and Clay Minerals 30:143–149

Urrutia M, Macías F, García-Rodeja E (1995). Evaluación del $CuCl_2$ y del $LaCl_3$ como extractantes de aluminio en suelos ácidos de Galicia. Nova Acta Científica Compostelana (Bioloxía) 5:173–182

Wada K (1977). Allophane and imogolite. In: Dixon JB, Weed SB (eds) Minerals in Soil Environments. Soil Sci Soc Am, Madison, WI, USA, pp 603–638

Wada K (1980). Mineralogical characteristics of Andisols. In: Theng BKG (ed) Soils with Variable Charge. New Zealand Society of Soil Science, Lower Hutt, New Zealand, pp 87–107

Wada SI (1987a). Critical evaluation of 1M KCl-extraction method for determining exchangeable Al ions in variable charge soils. Soil Science and Plant Nutrition 33:153–160

Wada SI (1987b). Adsorption of Al(III) on allophane, imogolite, goethite and non crystalline silica and the extractability of the adsorbed (AlIII) in 1M KCl solution. Soil Science and Plant Nutrition 33:487-491

Walker A (1983). The effects of magnetite on oxalate- and dithionite-extractable iron. Soil Science Society of America Journal 47:1022–1026

Appendix materials on CD-Rom

Table A.	TableA, Figure A. Total free Al, Fe and Si (%).
	Table A, Figure B Percentage of total Al, Si and Fe extracted with NaOH (Al_n, Si_n) and dithionite-citrate (Fe_d)
Figure C.	Silica extracted with cold NaOH (Si_n) and with acid oxalate (Si_o)
Figure D.	Fe_o/Fe_d ratios (Fe_o/Fe_d=1 when Fe_o slightly exceeds Fe_d). Soils with Fe_d<0.5% not included
Figure E.	Aluminium extracted with NaOH (Al_n), acid oxalate (Al_o) and pyrophosphate (Al_p)
Figure F.	Iron extracted with citrate-dithionite (Fe_d), acid oxalate (Fe_o) and pyrophosphate (Fe_p)
Figure G.	Al_p/Al_o and Fe_p/Fe_o ratios. Soils with low X_o and with $X_p>X_o$ not represented
Figure H.	Percentages of allophane and ferrihydrite
Figure I.	Allophane, ferrihydrite and soil pH
Figure J.	Pyrophosphate extraction and soil pH
Figure K.	C/Al and C/(Al+Fe) molar ratios
Figure L.	Al extractions with unbuffered salts
Figure M.	Extraction of Al with unbuffered salts and soil pH

Phosphate sorption of European volcanic soils

M. Madeira, Gy. Füleky and E. Auxtero

Introduction

Due to the presence of active and amorphous Al- and Fe-compounds (allophane/imogolite, ferrihydrite), Al- and Fe- organic matter complexes and high variable charge in the soil colloidal system, a high ability to adsorb P is one of the characteristics of volcanic soils (Mizota and Reeuwijk 1989, Shoji et al. 1993). Therefore, the phosphate retention percentage is one of the requirements of andic soil properties in Soil Taxonomy (SSS 2003) and of the diagnostic andic horizon of WRB (Driessen et al. 2001). However, this parameter corresponds to a single determination that reflects P-adsorption kinetics rather than capacity and that does not adequately reflect differences between Andisols with regard to P availability and the risk of P losses. Wide differences of P-sorption in volcanic soils were recently reported by Van Ranst et al. (2004) from a sequence of Andisols from the island of Java (Indonesia). These authors characterized the reactivity of these soils by the P-sorption maximum and by P-bonding energy, calculated from the fitted Langmuir adsorption isotherm, considering that the simple Langmuir equation is more suitable and able to fit the P-sorption data than the formerly used Freundlich equation. They found a close relationship between the P-sorption maximum and allophane content, oxalate soluble Al (Al_o) and Al_o+½Fe_o contents (R^2=0.82, 0.92, and 0.95, respectively). Similar strong correlations were observed between the bonding energy (k value) and the allophane, Al_o, and Al_o+½Fe_o contents. Furthermore, Balkovic and Slivkova (2002) observed that P-sorption in andic horizons was also positively influenced by soil pH, and that the measured P-sorption maximum may reach 10 g kg^{-1}. These authors also studied the effect of different Al_o, Al_p and Fe_o concentrations on P-retention at pH 4.65, and concluded that phosphate was immobilized both on non-crystalline Al/Fe colloids and on Al/Fe humic complexes. Espino-Mesa et al. (1993) reported that active Al_o is positively correlated with cation exchange capacity determined by 1 M ammonium acetate at pH 7.

In volcanic soils, phosphorus is often a growth-limiting nutrient for crops, given the ability of these soils to strongly bind phosphate. On the other hand, because of the risk of eutrophication of water bodies, the loss

of adsorbed P from intensively managed volcanic soils, through surface runoff and infiltration, is an environmental concern (Pinheiro et al. this book). Evaluation of soil behavior with respect to P availability to crops, and to P desorption is therefore of utmost importance. At a given P content, extractable P is influenced by soil constituents, but also highly dependent on the extraction method (Kuo 1996, Monteiro 2005). Hence, more information regarding the ability of different methods to extract P from volcanic soils is needed.

Within this context, a study was carried out on twenty pedons of European volcanic soils to assess: (i) the P retention percentage; (ii) the phosphate sorption isotherms and the influence of soil characteristics which determine the maximum phosphate sorption capacity; and, (iii) the amounts of extracted P by several methods and the relationships between these amounts and soil properties.

Materials and methods

P-retention values were determined in all samples of twenty European volcanic soil profiles, as described in *The physico-chemical data base* (this book). In addition to these soils, samples from other Hungarian volcanic soils were used to assess the phosphate sorption isotherms, bringing the total number of samples to 114. To determine the adsorption isotherm and the P adsorption maximum, samples were equilibrated for 24 hours with 10 cm^3 of 0, 50, 100, 500, 1000, 3000, 5000 and 10000 mg kg^{-1} P solutions. The Langmuir equation (Füleky and Tolner 1990), used to fit the data, was;

$$Pads = \frac{P_{\max} kc}{1 + kc},$$

where P_{max} is the maximum amount of phosphate which could be adsorbed (and used as a soil characteristics in further statistical analysis), k is a constant related to the adsorption energy, and c the P concentration in the solution. All data of the EUR soils are in *The physico-chemical data base* (this book) and they are also compiled in *phosphate data.xls* attached to this chapter.

Extractable P was obtained for each sample in four replicates. Extraction of P by distilled water and 0.01 M $CaCl_2$ extractions involved shaking the sample for 1 h and 2 h, respectively, at a 2:20 soil: solution ratio (Self-Davis et al. 2000). Extractable P by the Bray 2 method (BR) was obtained by shaking 2 g soil with 20 ml 0.03 N NH_4F + 0.1 N HCl solution at pH 2.6 for 40 sec (Bray and Kurtz 1945). Phosphorus by the Mehlich 3

method (ME) was extracted using a soil:solution (0.013 M HNO_3 + 0.02 M CH_3OOH + 0.015 M NH_4F + 0.025 M NH_4NO_3 + 0.001 M EDTA) ratio of 2:20 at pH 2.5, and shaking for 30 min (Mehlich 1984). Extractable P determined by the Egnér-Riehm method (ER) was obtained by shaking 1 g of soil with 20 ml of $K(SbO)C_4H_4O_6$,½H_2O solution at pH 3.7 to 3.8 for 2 h (Riehm 1958). A 2:20 soil to solution (0.5 M $NaHCO_3$) ratio at pH 8.5 and 30 min shaking was used to extract P by the Olsen (OL) method (Olsen et al. 1954). Phosphorus was determined in filtered extracts by the molybdate blue coloring method (Murphy and Riley 1962), using a spectrophotometer (adsorbance at 882 nm).

Correlation coefficients were obtained for single and multiple correlations between variables, using Statistica 6.0.

Results and discussion

Phosphate retention

As expected, samples corresponding to non-Andisols (EUR01–02, EUR13–15, EUR18–20) showed lower P-retention values throughout the soil profile (2.0–42.6%, Figure 1), than the threshold percentages of 85% and 70% used by Soil Taxonomy (SSS 2003) or WRB (Driessen et al. 2001), respectively, to recognize andic soil properties or the diagnostic andic horizon (Figure 1). This is in agreement with the low content of Al in the forms of Al-humus complexes and allophane in these soils. Nevertheless, P-retention values were strongly correlated with Al_o ($r=0.838$; $p<0.01$) and Al_o+½Fe_o ($r=0.916$; $p<0.01$) contents.

Relationships between P-retention values and Al_o+½Fe_o or Al_o contents are shown in Figure 1. Pedons classified as Andisols mostly showed P-retention values higher than 85% for Al_o+½Fe_o or Al_o contents higher than 2.0%. Above this content, P-retention was always higher than 70%. Some exceptions should be taken into account, as horizons with Al_o and Al_o+½Fe_o contents >2% may show P-retention values lower than 85%, and P-retention values of 85% or more were observed in horizons with low contents of Al_o and Al_o+½Fe_o. For example, pedon EUR03 with high contents of Al_o (2.49–3.33%), allophane (7.1–11.8%) and Al_o+½Fe_o (2.52–3.61%) showed P-retentions ranging from 80.5 to 84.5%. This pedon also had a much lower anion exchange capacity than the other studied soils (Madeira et al. this book). This characteristic may contribute to a lower the phosphate adsorption potential. Conversely, pedon EUR12 with low contents of Al_o (1.21%) and Al_o+½Fe_o, (1.55%) and no allophane, showed a P-retention of 86%. This is in line with data reported by Madeira et al.

(1994) for non-allophanic soils from Madeira Island, which in spite of their low Al_o content (1.2–1.4%, mostly as Al-humus complexes) showed a high P-retention (96–98%). Retention values higher than 85% were also reported by Shoji et al. (1985) for Andisols with Al_o>1%. Finally, very low P retention values were found in some horizons of pedon EUR11. This may be due to the extremely high extractable P, by water and other extractants, which is much higher than in other studied pedons (see section P extraction).

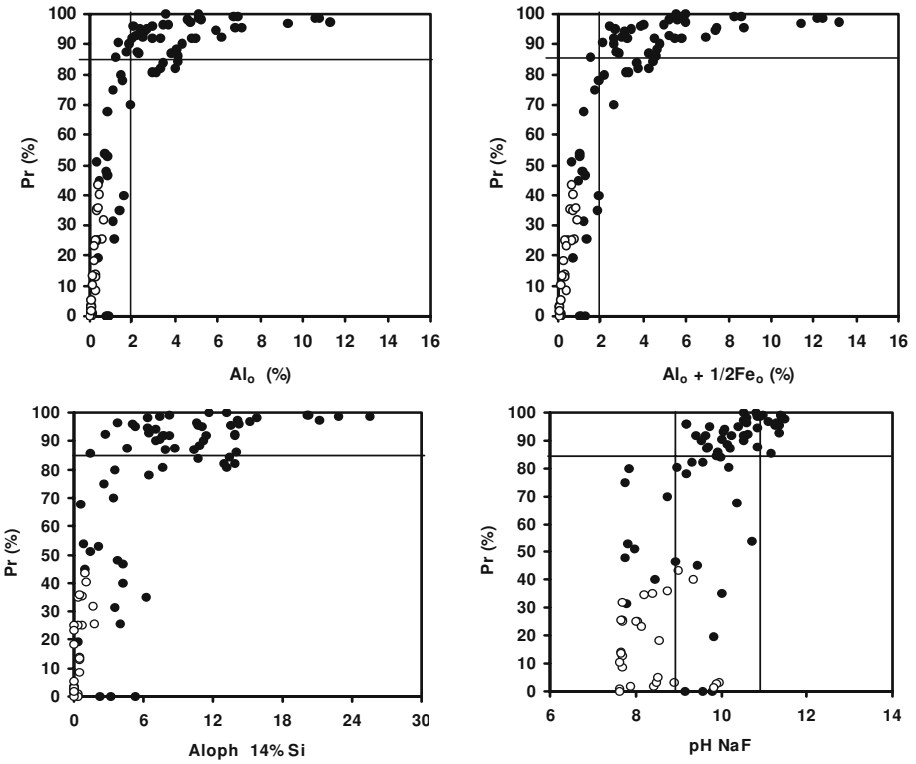

Figure 1. P-retention in studied volcanic soils in relation to Al_o, Al_o+½Fe_o and allophane contents, and to pH-NaF values. Black and open dots correspond, respectively, to Andisols and to non-Andisols.

P-retention increased with the calculated allophane content (Figure 1), but the relationship was much less clear than that observed for the Al_o and Al_o+½Fe_o contents. Values higher than either 70 or 85% were obtained for a wide range of allophane contents (1.4–24.2%), which indicates that constituents other than allophane (e.g., Al-humus complexes) also adsorb P. Values of pH-NaF did not adequately discriminate andic horizons from

non-andic ones (Figure 1), and are not well-correlated with P-retention in Andisols. Although all horizons with a P-retention higher than 85% showed a pH-NaF between 9 and 12, some other horizons with similar high pH values (9–11) had lower P-retention.

Maximum P-sorption

The studied soils showed a wide range of P-sorption values (see *The physico-chemical data base*, this book and *phosphate data.xls*). In horizons without andic properties (non-Andisols) the values were lower than 2000 mg kg^{-1}, while in the A and B horizons of Andisols values ranged from 2215 to 10.200 mg kg^{-1}. This range is within that reported by Van Ranst et al. (2004) for Andisols from Java, and by Auxtero et al. (2005) for Andisols from the Azores.

The P_{ret} value does not indicate a maximum adsorbed amount but a value relative to the offered amount. Soils with high phosphate fixing capacity can adsorb much more phosphate than 5000 mg kg^{-1}, the concentration for P_{ret} determination. At the same time, the k-value, which is correlated with the bonding energy, could explain differences in the steepness of curves at lower concentrations of soils with similar P_{max} (Figure 2).

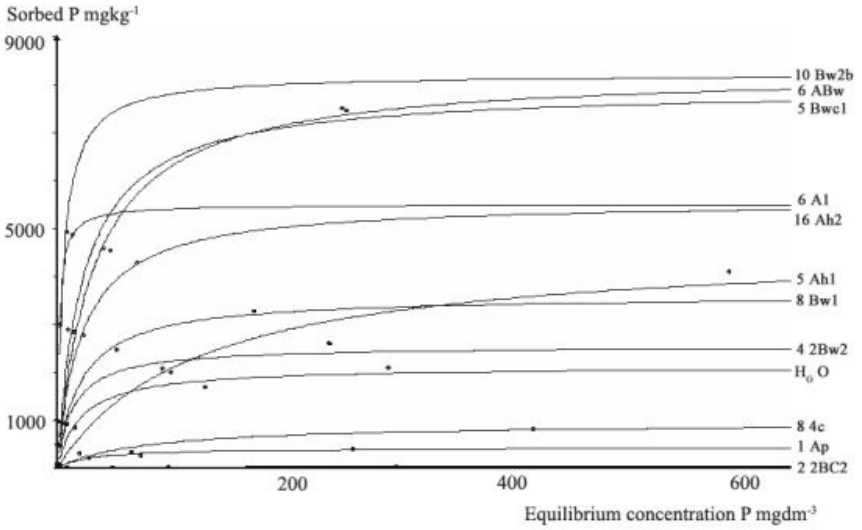

Figure 2. Phosphate sorption isotherms of selected horizons. The number before the horizon code indicates the EUR profile.

The maximum amounts of phosphate (P_{max}) sorbed by the European volcanic soils, as calculated from the Langmuir adsorption isotherms, are shown in *phosphate data.xls* (on CD). The calculated phosphate sorption maxima ranged from 0 to 10000 mg P kg^{-1} soil. At low concentrations, some of the volcanic soils sorbed a large fraction of the added phosphate, some of them somewhat less. This difference in phosphate binding kinetics causes the differences observed in the shape of Langmuir adsorption isotherms (Figure 2).

Soil characteristics that determine the rate of phosphate sorption are shown in Table 1. In some cases, there are inner correlations between the soil characteristics, such as Fe_o and Al_o, Al_d and Al_o.

Table 1. Linear correlation between some soil characteristics and the phosphate sorption maximum, n=114.

Soil characteristic	R^2	Soil characteristic	R^2	Soil characteristic	R^2
Al_o%+½Fe_o	0.753	P-retention %	0.555	Base sat.% (n=64)	0.609
Al_o%	0.734	Allophane (Parfitt)	0.514	CEC-NH_4OAc	0.256
Al_o%-Al_p%	0.574	Fe_o%	0.514	Sum of Bases	0.202
Al_d%	0.711	Fe_d%	0.478	Organic C%	0.139
Al_p%	0.443				

The most significant positive correlation was obtained between the maximum phosphate sorption (P_{max}) and Al_o+½Fe_o% (Figure 3). 75% of phosphate sorption ability of soils is explained by the Al_o+½Fe_o content, and 73% by the Al_o content alone. The correlation between P_{max} and Al_o%-Al_p% was closer (0.574) than that for Al_p (0.443). Both relationships demonstrate the predominance of non-crystalline Al oxi-hydroxides (Al_o) in phosphate fixation compared with that of humus-bound Al. For the subset of andic horizons, the correlation between phosphate sorption ability and Al_o (R^2=0.57) and Al_o+½Fe_o (R^2=0.59) contents was weaker than for the whole data set, which was also observed by Auxtero et al. (2005) for Andisols from the Azores Islands. The base saturation, excluding soils above 100% saturation (most of the non-Andisols), showed a close negative correlation with the phosphate sorption (R^2=0.609) (Figure 4). This is probably an indirect relation. In fact, base saturation in studied Andisols showed a significant negative correlation with the contents of allophane and Al-humus complexes (Madeira et al. this book).

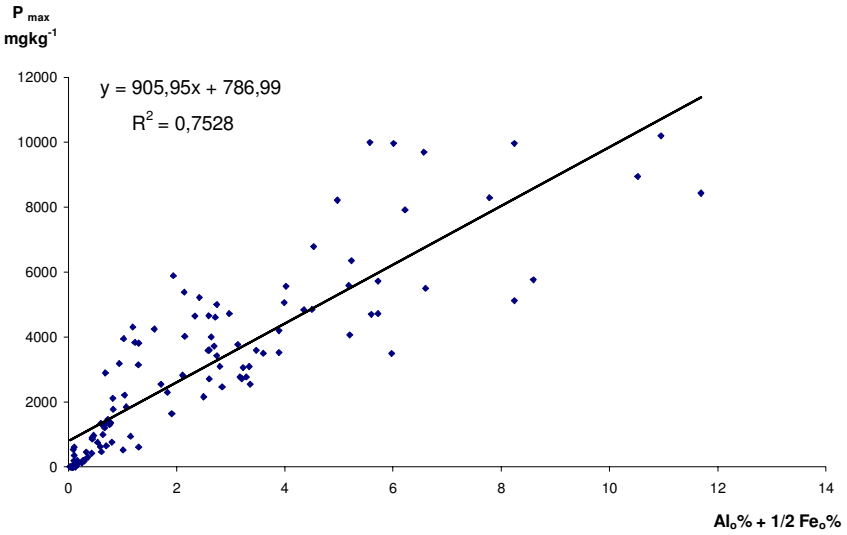

Figure 3. Linear relationship between Al_o+½Fe_o content and phosphate sorption maximum, n=114.

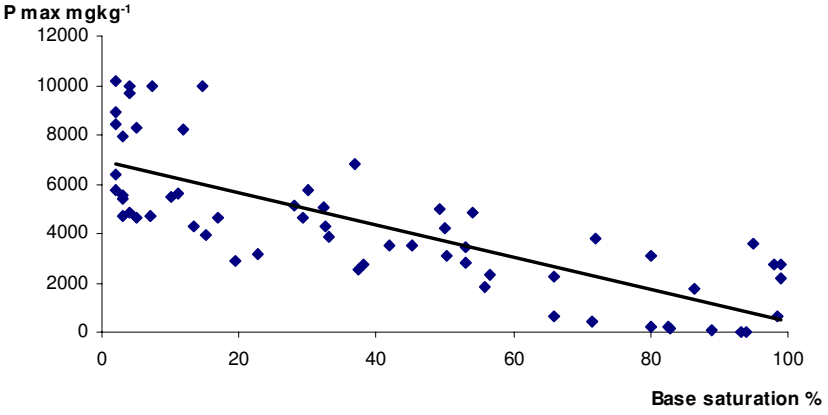

Figure 4. Linear relationship between phosphate sorption maximum (P_{max}) and base saturation (n=64) .

Extractable P

P extracted by H_2O and $CaCl_2$ were determined because they correspond to a measurement of P in solution that correlates well with the concentration of dissolved reactive P in runoff (Self-Davis et al. 2000), corresponding

then to a measurement of P in solution, and are independent of soil type (Monteiro 2005). Methods estimating the amount of sorbed P were also used. The Bray (BR), Mehlich (ME), and Egnér-Riehm (ER) methods are commonly used in acid soils, while the Olsen (OL) method, which is mostly used in neutral and alkaline soils but also in acid soils, is less dependent on soil type than the other methods.

Extractable P in non-Andisols varied considerably between soils and methods, and it may reflect differences in land use. Amounts extracted by the BR method were greater (24.6–291.6 mg kg^{-1}) than those determined by the other methods (0–197.6 mg kg^{-1}), and amounts extracted by the ER and ME methods were about double those obtained by the OL method (Figure 5). The large quantities of P extracted from pedons EUR01 and EUR19 by Bray (259–292 mg kg^{-1}) and by Olsen (97–109 mg kg^{-1}) methods are noteworthy. These high values are also associated with large amounts of P extracted by H_2O (5.8–24.7 mg kg^{-1}) and by $CaCl_2$ (4.0–24.2 mg kg^{-1}), suggesting that high amounts of P could be released to the soil solution. This may be related to anthropic influence, as pedon EUR19 is in the site of a Bronze Age settlement found at the profile description, and pedon EUR01 is located in a man-made terrace (with pot shards) used for apple tree orchards (see Profile descriptions, this book). We may emphasize that the Olsen-P values in those pedons are far beyond the limit (21 and 57 mg kg^{-1}) found for soils with similar amounts of oxalate-extractable Fe and Al, in which P losses increase from soil to drainage water, and from soil to runoff (Monteiro 2005).

In Andisols, the amounts of extracted P varied widely with soil type and method. As observed in *The physico chemical data base*, the extracted P was generally lower than in non-Andisols (Figure 5), especially in the subsurface horizons. As observed for the non-Andisols, P extracted by the BR method was usually higher than that extracted by the other methods, and it was usually higher in the topsoils (Ah, O) than in the subsurface horizons. This decrease with soil depth was more pronounced in P-fractions obtained by the ER and ME methods. Pedon EUR11 showed very high P values by the BR (460.2 mg kg^{-1}), ER (172.6 mg kg^{-1}) and OL (67.6 mg kg^{-1}) methods, which coincides with high amounts extracted by H_2O and $CaCl_2$ (5.9 and 5.5 mg kg^{-1}, respectively). As this pedon is under forest, apparently there is not a relation between high P values and anthropic influence; instead, these high P values might be related to natural conditions as the parent material corresponds to superposed basaltic scoria and layers of basaltic lapilli (see Soil descriptions, this book). High P values in H_2O were also measured in the topsoil of pedons EUR03 (4.3 mg kg^{-1}), EUR04 (4.0 mg kg^{-1}) and EUR07 (13.6 mg kg^{-1}), which may be associated with the high amounts of partly decomposed organic matter observed in these layers.

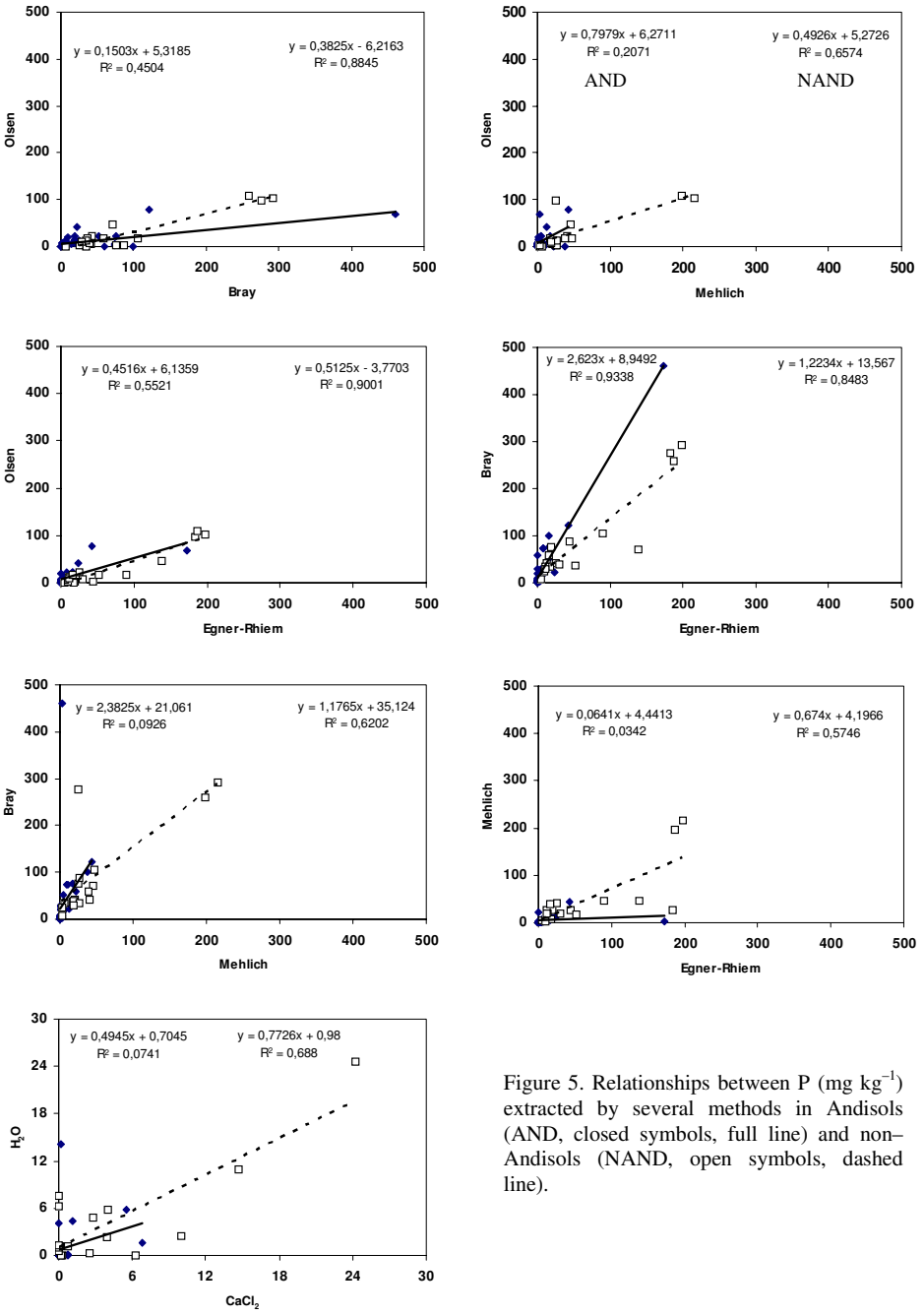

Figure 5. Relationships between P (mg kg^{-1}) extracted by several methods in Andisols (AND, closed symbols, full line) and non–Andisols (NAND, open symbols, dashed line).

Extractable P and soil characteristics

The amounts of P obtained by the various methods showed different relationships with soil type and constituents (Table 2). In the whole set of studied soils, P extracted by the different methods showed a weak negative correlation with P_{max}, and the correlation coefficient (r; $p<0.05$) varied between –0.33 and –0.44. However, in Andisols the amounts of P extracted by the different methods were not correlated with values of P_{max}. The lack of this relationship may be explained by the fact that soils are not P-saturated and the extracted fraction is therefore an accidental part of the total adsorption capacity. On the other hand, the extractable P was negatively correlated with P-retention (PR) values, with correlation coefficients (r) of –0.70, –0.65, –0.57, –0.53, –0.43 and –0.39, respectively, for the BR, EG, OL, ME, WT and CA extractions. This correlation was expected, because P-retention is decreased by the part of the binding sites that is already occupied by phosphate, which is in agreement with the fact that the best correlation was with the strongest extractant (BR method). P extracted by the Olsen method was negatively correlated with Al_o (–0.34), Si_o (–0.34), allophane (–0.34) and Al_o+½Fe_o (–0.34) contents, and positively with organic C content (0.53). The latter correlation corroborates the fact that P adsorbed on metal-organic matter complexes is one of the P Olsen sources (Monteiro 2005). A similar pattern was observed for P extracted by the ME method. Conversely, amounts obtained by the BR and EG methods were not correlated with the above mentioned soil constituents. As also observed for the Olsen extraction, amounts of P extracted by H_2O were weakly and negatively correlated with Al_o (–0.33) and Al_o+½Fe_o (–0.32), and positively with organic C (0.43) contents, while the fraction extracted by $CaCl_2$ was not significantly correlated to measured soil properties. The similar behaviour observed for both H_2O and OL methods is in line with findings of Kuo et al. (1988), who reported that P extracted by the OL is a function of the fraction of P coverage on the surfaces of soil particles, reflecting P in soil solution rather than sorbed P.

Contrarily to Andisols, P extracted by the different methods from non-Andisols was not correlated with P-retention. This pattern may be related to the low sorption capacity shown by these soils, being the extracted P mostly dependent on the amount of P retained by soil. It is noteworthy that P extracted by the OL and ME methods was positively correlated ($p<0.05$) with both organic C (r=0.56, 0.63) and Fe_o (r=0.60, 0.67) contents. Extractable P by the ER method was positively correlated (0.50) with Fe_o content alone, while that extracted by the BR method did not show any correlation with soil constituents. P extracted by H_2O and $CaCl_2$, as ob-

served for the OL and ME methods, was positively correlated ($p<0.05$) with organic C (0.56) content, and that extracted by $CaCl_2$ was also correlated with Fe_o (0.56) content. The positive correlation between extractable P and Fe_o contents, as well as the lack of a negative effect of Al_o and allophane on P extraction, do not follow the general pattern observed for Andisols in this study, suggesting that these constituents (in low amounts) in non-Andisols are of great importance to soil P availability.

Table 2. Coefficients (R) of correlations between P-fractions extracted by various methods and some soil properties. Numbers in bold are significant at $p<0.05$.

Extraction method	P_{max}	P_{ret}	Al_o	Fe_o	Al_o+½Fe_o	Allophane	Org. C
Andisols (n=41)							
H_2O	**–0.332**	**–0.435**	**–0.333**	–0.153	**–0.319**	–0.298	**0.434**
$CaCl_2$	–0.180	**–0.392**	–0.241	–0.09	–0.229	–0.260	0.176
Olsen	–0.259	**–0.572**	**–0.340**	–0.186	**–0.337**	**–0.339**	**0.532**
Mehlich 3	–0.052	**–0.534**	–0.283	–0.252	–0.302	**–0.322**	**0.583**
Egner-Riehm	–0.216	**–0.647**	0.255	–0.173	–0,259	–0.268	0.199
Bray 2	–0.161	**–0.700**	–0.258	–0.234	–0.277	–0.288	0.166
Non-Andisols (n=17)							
H_2O	–0.135	0.077	0.032	0.397	0.188	–0.164	**0.556**
$CaCl_2$	0.090	0.293	0.179	**0.559**	0.348	0.007	**0.540**
Olsen	0.046	0.393	0.335	**0.595**	0.462	0.109	**0.560**
Mehlich 3	0.043	0.306	0.242	**0.671**	0.436	–0.004	**0.630**
Egner-Riehm	–0.062	0.272	0.207	**0.504**	0.344	0.006	0.427
Bray 2	–0.046	0.253	0.227	0.479	0.345	0.043	0.372

Relationships between methods

In non-Andisols, P extracted by H_2O (Table 3 and Figure 5) was positively correlated ($p<0.05$) with that extracted by $CaCl_2$ ($r=0.87$), and also with that extracted by the ME, OL, BR and EG methods ($r=0.81$, 0.75, 0.72 and 0.68, respectively). Correlations with P extracted by $CaCl_2$ and the other methods were stronger than for H_2O ($r=0.81$, 0.84, 0.75 and 0.77, respectively). This proportionality between desorbed P by those methods and by H_2O or dilute $CaCl_2$ suggests that P losses from the soil to water might be estimated from any of these values. Amounts of P extracted by the ME, OL, BR and EG methods were positively correlated (Figure 5). The amount of P extracted by the OL method was strongly correlated with that obtained by the BR ($r=0.94$) and the ER (0.95) methods; P by the BR and ER methods were also strongly correlated (0.92). Correlations between

these methods have been found among soils, especially when they are of the same type (Kuo 1996, Monteiro 2005).

Table 3. Coefficients (R) of correlation between P-fractions extracted by various methods. Numbers in bold are significant at $p<0.05$.

Extraction method	**H_2O**	$CaCl_2$	Mehlich 3	Olsen	Bray 2	Egner-Riehm
All EUR soils (n=58)						
H_2O		**0.75**	**0.58**	**0.72**	**0.57**	**0.67**
$CaCl_2$	**0.75**		**0.64**	**0.71**	**0.57**	**0.72**
Mehlich 3	**0.58**	**0.64**		**0.56**	**0.49**	**0.56**
Olsen	**0.72**	**0.71**	**0.56**		**0.80**	**0.89**
Bray 2	**0.57**	**0.57**	**0.49**	**0.80**		**0.88**
Egner-Riehm	**0.67**	**0.72**	**0.56**	**0.89**	**0.88**	
Non-Andisols (n=17)						
H_2O		**0.87**	**0.61**	**0.75**	**0.72**	**0.68**
$CaCl_2$	**0.87**		**0.90**	**0.84**	**0.75**	**0.77**
Mehlich 3	**0.81**	**0.90**		**0.81**	**0.78**	**0.75**
Olsen	**0.75**	**0.84**	**0.81**		**0.94**	**0.95**
Bray 2	**0.72**	**0.75**	**0.78**	**0.94**		**0.92**
Egner-Riehm	**0.68**	**0.77**	**0.75**	**0.95**	**0.92**	
Andisols (n=41)						
H_2O		0.26	0.04	**0.56**	**0.35**	**0.45**
$CaCl_2$	0.26		–0.04	**0.44**	**0.55**	**0.61**
Mehlich 3	0.04	–0.04		0.03	0.13	0.00
Olsen	**0.56**	**0.44**	0.03		**0.67**	**0.74**
Bray 2	**0.35**	**0.55**	0.13	**0.67**		**0.96**
Egner-Riehm	**0.45**	**0.61**	0.00	**0.74**	**0.96**	

In Andisols, in contrast to the previous, P extracted by H_2O was not correlated with that extracted by $CaCl_2$. (Table 3, Figure 5) The former was correlated with P extracted by the OL (0.56) and ER (0.45) methods, whereas the latter showed stronger correlations with P extracted by the ER (0.61) and BR (0.55) methods. This means that in Andisols the value of such data for estimating P losses from soil to water is smaller than in non-Andisols. Correlations between the OL, ME, ER and BR methods were less significant than in soils without andic soil properties. For example, extractable P by the ME method was not correlated with that determined by the other methods, but a correlation was observed between the OL and BR (0.67) and the OL and ER (0.74) methods. In addition, P extracted by the BR method showed a strong correlation with that obtained by ER method

(0.96) (Figure 5). Correlations between methods were less significant in Andisols (ME and OL methods were not correlated) than for non-Andisols, which may result from the larger heterogeneity of soil constituents in the former than in the latter.

Ass commonly reported, the BR extracted more P than the ME, ER OL methods in both Andisols and non-Andisols (Kuo 1996, Monteiro 2005). OL extracted less P than ME and ER, but differences were more pronounced in non-Andisols than in Andisols (Figure 5). The combination of its strong acidity with the effect of fluoride on the formation of Al complexes may explain why the BR method extracted more P than the other methods (Jackson 1958). The effectiveness of ME and ER extractions in comparison to OL may also be based on the high acidity of the extractant and on the role of acetate fluoride and lactate anions in solubilizing or complexing cations (Ca, Al, Fe) and in desorbing P from active surfaces.

Conclusions

1. The P-retention percentage discriminates Andisols from non-Andisols. However, the lower limit of 85% does not correspond exactly to the threshold values of Al_o+½Fe_o 2.0%.
2. The Langmuir isotherm properly describes the phosphate sorption in volcanic soils of Europe at 0–600 mg dm^{-3} P concentration interval.
3. Because P_{ret} does not assess the total capacity of the soil to bind phosphate, the estimated phosphate adsorption maximum (P_{max}) is a better property for the characterization of the surface activity of soils developed on volcanic parent material.
4. Oxalate-soluble Al is the main factor explaining the observed variations (73%) of P_{max}.
5. Soils showed a wide variation of extractable P for each of the extractors. In non-Andisols, amounts of P extracted by H_2O, $CaCl_2$ and other methods were correlated, whereas in Andisols correlations were weaker. As Andisols are not P-saturated and the extractable fraction is an accidental part of the total adsorption capacity, extracted P was not correlated with P_{max} values. It was, however, negatively correlated with P-retention values.
6. In Andisols, P extracted by the Olsen and Mehlich methods was positively affected by soil organic constituents, and negatively by mineral constituents (Al_o, allophane). Contrarily to Andisols, low amounts of Fe_o in non-Andisols may increase the amount of extractable P.

7. The BR method extracted more P than the other methods, which may be explained by the combination of strong acidity and by the effect of fluoride on the formation of Al complexes.

Acknowledgements

E. Auxtero gratefully acknowledges the award of a post-doctoral research fellowship by the Fundação para a Ciência e a Tecnologia. The authors express their appreciation to Isabel Meireles and Ana Batista for technical assistance in the laboratory, to Paulo Marques for preparation of the manuscript, and to Prof. Ana Carla Madeira for improving the language.

References

Auxtero E, Madeira M, Sousa E (2005). Extractable P as determined by different tests and P adsorption capacity of selected Andisols from the Azores, Portugal. Revista de Ciências Agrárias 28:119–132

Balkovic J, Slivkova K (2002). Phosphorus retention in volcanic soils of Slovakia. Phytopedon (Bratislava) 1:78–85

Bray RH. Kurtz LI (1945) Determination of total organic and available forms of phosphorus in soils. Soil Sci 59:39–45

Driessen P, Deckers J, Spaargaren O, Nachthtergaele F (eds) (2001). Lecture Notes on the Major Soils of the World. FAO, Rome. (World Soils Resources Reports, 94)

Espino-Mesa M, Arbelo CD, Hernandez-Moreno JM (1993). Predicting value of diagnostic soil properties on actual and potential cation exchange capacity (CEC) in andisols and andic soils. Commun Soil Sci Plant Anal 24:2569–2584

Füleky Gy, Tolner L (1990). Gemeinsames Modell der P-adsorption und P-desorption in Boden. Tagungberich Nr. 289 Justus von Liebigs Werk – Wegbereiter der wissenschaftlich begründeten Düngung, Adl Berlin 291–298

Jackson ML (1958). Soil chemical analysis. Prentice-Hall, Inc., Englewood Cliffs, NJ

Kuo S (1996). Phosphorus. In: Sparks DL (ed) Methods of soil analysis: Chemical methods, Part 3. Soil Science Society of America Book Series, SSSA, ASA, Madison, Wisconsin, USA

Kuo S, Jellum EJ, Pan WL (1988). Influence vof phosphate sorption parameters of soils on the desorption of phosphate by various extractants. Soil Sci Soc Am J 52:974–979

Madeira M, Furtado A, Jeanroy E, Herbillon A (1994). Andisols of Madeira Island (Portugal). Characteristics and classification. Geoderma 62:363–383

Mechlich A (1984). Notes on Mehlich 3 soil test extractant: a modification of Mehlich 2 extractant. Commun Soil Sci Plant Anal 15:1409–1416

Mizota C, van Reeuwijk LP (1989). Clay mineralogy and chemistry of soils formed in volcanic material in diverse climatic regions. ISRIC, Wageningen

Monteiro MC (2005). La disponibilidad de fósforo evaluado por el método de Olsen en suelos ácidos de Portugal: significado agronómico y ambiental. PhD Thesis, Universidad de Córdoba, Córdoba

Murphy J, Riley JP (1962). Modified single solution method for the determination of phosphate in natural waters. Anal Chim Acta 27:31–36

Olsen SR, Cole CV, Watanabe FS, Dean LA (1954). Estimation of available P in soils by extraction with sodium bicarbonate. USDA Department of Agriculture Circular 939, Washington

Riehm H (1958). Die ammoniumlaktatessignäure Methode zur bestimmung der leichtlöslichen phosphorsäure in karbonathaltigen böden. Agrochimica 3:49–65

Self-Davis ML, Moore PAJr, Joern BC (2000). Determination of water and/or dilute salt-extractable P. In: Pierzynski GM (ed), Methods of phosphorus analysis for soils, sediments, residuals and waters. Southern Cooperative Series Bull. no. 396, USDA-CSREES Regional Committee, USA

Shoji S, Ito T, Saigusa M, Yamada I (1985). Properties of non-allophanic andosols from Japan. Japan. Soil Sci 140:264–277

Shoji S, Nanzyo M, Dahlgren R (1993). Productivity and Utilization of Volcanic Ash Soils. Genesis, Properties and Utilization. Elsevier Science Publishers, Amsterdam

Soil Survey Staff (SSS) (2003). Keys to Soil Taxonomy (9th edn). United States Department of Agriculture, National Resources Conservation Service, Washington

Van Ranst E, Utami SR, Vanderdeelen J, Shamshuddin J (2004). Surface reactivity of andisols on volcanic ash along the Sunda arc crossing Java Island, Indonesia. Geoderma 123:193–203

Appendix materials on CD-Rom

phosphate data.xls

Exchange complex properties of soils from a range of European volcanic areas

M. Madeira, E. Auxtero, F. Monteiro,
E. García-Rodeja and J.C. Nóvoa-Muñoz

Introduction

Most Andisols show a complex colloidal fraction, in which variable charge constituents (allophane/imogolite, ferrihydrite and Al- and Fe-humus complexes) can be predominant. These components have a charge that depends both on pH and on ionic strength of the solution. In volcanic soils, only the pH is of influence. The main contributor to negative charge is the dissociation of functional groups in soil organic matter. Dissociation is virtually zero around pH 3, while at pH 7 organic matter may contribute a negative charge of up to 0.4 $cmol_c\ g^{-1}$. The surface charge of allophane, imogolite, and ferrihydrite is positive at low pH and negative at higher ones. Parfitt (1980) gives zero-charge pH values of 6.5 for allophane and imogolite, 6.9 for ferrihydrite, and 4.4 for an Andisol. Above this pH, net charge is negative. The influence of pH-dependent charge components on cation exchange capacity (CEC) and anion exchange capacity (AEC) is of considerable importance for the retention and leaching of both cations and anions in Andisols. The values obtained for these properties are highly dependent on the method of determination. The CEC measured by the 1 M NH_4OAc at pH 7 (CEC7) is commonly used as a reference, among others, in international Soil Classifications Systems (Driessen et al. 2001, SSS 2003). The sum of bases by 1 M NH_4OAc at pH 7 and of the extractable Al (by 1 M KCl), alone or together, are used to subdivide Andisols at the sub-group level (SSS 2003) and to establish qualifiers of soil units in the WRB system (Driessen et al. 2001). However, it is recognized that the ammonium acetate method overestimates the CEC of Andisols, as the measurement is carried out at a pH higher than that at field conditions. Therefore, it is more convenient to measure the CEC at pH conditions similar to those prevailing in the field.

We studied the European reference volcanic soils collected by the COST-622 Action and determined (1) the cation exchange capacity and the anion exchange capacity, (2) the exchangeable cations, the extractable Al in KCl, and the effective cation exchange capacity. Finally, we assessed

the influence of various components of the soil colloidal systems on CEC and AEC.

Materials and methods

Determinations were carried out on the fine earth fraction (<2 mm) of air-dried samples. The results were expressed on an oven dry basis (105°C). The cation exchange capacity (CEC7) and the amount of exchangeable basic cations were determined by the 1 M NH_4OAc standard method. The effective cation exchange capacity (ECEC) was calculated by adding the sum of bases to the 1 M KCl-extractable Al.

The cation exchange capacity was also determined by the compulsive exchange procedure (CEC_{CE}) following methodology described by Gillman and Sumpter (1986). Basic cations and Al were extracted by shaking 2 g of fine earth (<2 mm) with 2 ml of a mixture of 0.1 M $BaCl_2/NH_4Cl$ for 2 h, and the bases were measured in the extract by AAS. Then, the soil was saturated with 0.002 M $BaCl_2$, followed by the addition of 0.05 M $MgSO_4$. The magnesium remaining in the solution is used to calculate the compulsive cation exchange capacity (CEC_{CE}). The amount of Cl^- in solution was measured using the silver nitrate titration method and used to calculate the anion exchange capacity (AEC). CEC_{CE} and AEC (oven-dried soil basis) were calculated as described by Gillman and Sumpter (1986).

All data used here are in *The physico-chemical data base* (this book). For the present purpose, organic soil horizons (organic C content >25%) and R, R/C, and C layers were not taken into account. Data analysis was done for the whole set and for the Andisol and non-Andisol subsets. The non-Andisol profiles are EUR01, 02, 13–15, 18–20). Samples of surface horizons (A, A/B, A/C) of Andisols were also separated from those of subsurface horizons (B, B/C). Data of Andisols and non-Andisols are presented separately. Data were subjected to statistical analysis, and correlation coefficients between variables were determined in single and multivariate correlation analysis, using the programmes Statistica 6.0 and Microsoft Excel.

Results and discussion

Exchangeable basic cations

Exchangeable Ca varied strongly among the studied soils. Andisols with high allophane content and/or organic C contents, i.e. pedons EUR05 and 06 (Azores), and EUR17 (France) showed the lowest values, both in the surface (0.35–4.03 $cmol_c\ kg^{-1}$) and subsurface (Bw) horizons (0.40–0.56 $cmol_c\ kg^{-1}$). In the other Andisols the values were 7.0–30.5 $cmol_c\ kg^{-1}$ and 2.4–13.6 $cmol_c\ kg^{-1}$, and the highest values were measured in pedons EUR04 (21.7 $cmol_c\ kg^{-1}$), EUR07 (30.5 $cmol_c\ kg^{-1}$), EUR11 (22.4 $cmol_c\ kg^{-1}$) and EUR16 (25.0 $cmol_c\ kg^{-1}$), which contain high amounts of weatherable materials and possibly calcite (Stoops and Gérard 2004). A similar pattern was observed for exchangeable Mg, which was strongly correlated with exchangeable Ca ($r=0.862$; $p<0.01$). These data are in agreement with results reported by Madeira et al. (2003) for a set of Andisols from the Azores, which included a wide range of Andisols, and by Espino-Mesa et al. (1993) for Andisols from the Canary Islands.

Exchangeable K, which may depend on the nature of the volcanic material, was also quite variable, and in some cases (non-Andisol pedons EUR01 and 02, Italy) values were very high (6.7–25.0 $cmol_c\ kg^{-1}$) and similar to those of Ca. In the Andisols from Italy (EUR03 and 04) the values were also rather high (0.8–2.3 $cmol_c\ kg^{-1}$). This may be attributed to significant amounts of K-bearing minerals, e.g. micas, sanidine, and especially leucite observed both in the sand (Colombo et al. 2004) and clay fractions of these soils (Monteiro et al. this book). The high proportion of micas in the clay fraction of the topsoils of pedons EUR18, 19 and 20 (non-Andisols, Hungary) also caused high contents of extractable K (1.2–2-1 $cmol_c\ kg^{-1}$) in these soils. Values of extractable K were not significantly correlated with those of Ca, Mg and Na.

Exchangeable Na did not show a clear relation with soil type, but was weak and positively correlated with exchangeable Mg ($r=0.48$; $p<0.01$). This suggests a common origin, probably from cyclic salt, which would explain the high exchangeable Na content in pedons EUR05 and 06 (Azores), and EUR10–12 (Tenerife). Noteworthy is the high exchangeable Na content in the subsurface horizons of pedon EUR02, which may be assigned to the presence of analcime (Colombo et al. 2004).

In the Andisol subset, the sum of basic cations (SB) was positively correlated ($p<0.01$) with values of both exchangeable Ca ($r=0.987$) and Mg ($r=0.926$), which were predominant in the soil exchange complex, but not with K and Na. Values of SB higher than 25 $cmol_c\ kg^{-1}$ were only found in some horizons of EUR04, 07, 11 and 16.

In pedons without andic properties (non-Andisols), contents of exchangeable Ca (6.0–53.4 $cmol_c\ kg^{-1}$) and Mg (0.7–14.3 $cmol_c\ kg^{-1}$), were mostly within the range observed for most of the studied Andisols, and also related to the relative abundance of weatherable materials (Stoops and Gérard 2004).

Extractable Al

Extractable Al values (by 1 M KCl) in non-Andisols were very low (mostly nil) and the maximum was 0.55 $cmol_c\ kg^{-1}$ (Table 1). Values were also low in most of the studied Andisols. In the subsurface horizons of the Andisols, Al_{KCl} values were much less than 2 $cmol_c\ kg^{-1}$, with the exception of one buried horizon of EUR09 (8.2 $cmol_c\ kg^{-1}$) and of two subsurface horizons (Bw and 2Ahb) of EUR12 (2.3–2.4 $cmol_c\ kg^{-1}$). High values of extractable Al were only measured in the Ah horizons of EUR05 (3.9 $cmol_c\ kg^{-1}$) and EUR06 (3.9 $cmol_c\ kg^{-1}$), from the Azores, and in the Ah1, Ah2 and Ah3 horizons (7.6, 6.2, and 2.5 $cmol_c\ kg^{-1}$, respectively) of EUR17 (France), which meets the requirements of the *alic* subgroup (SSS, 2003). In the Ah1 and Ah2 horizons of EUR12 (Tenerife), the values were lower and reached, 1.7 and 2.4 $cmol_c\ kg^{-1}$, respectively.

Effective cation exchange capacity

The effective cation exchange capacity (ECEC), is defined as the sum of the exchangeable basic cations and KCl-extractable Al. It is supposed to be similar to the CEC at field-pH (Sumner and Miller 1996), and it is useful to estimate cation exchange capacity in soils that do not contain salts or carbonates. As extractable Al values were mostly low, values of ECEC were similar to those of SB ($r=0.98$, $p<0.001$). Values in Andisols were higher in the surface (2.4–43.4 $cmol_c\ kg^{-1}$) than in the subsurface (1.0–20.2 $cmol_c\ kg^{-1}$) horizons (Table 1). The highest values were found in the O and Ah1 horizons (42.74 and 43.44 $cmol_c\ kg^{-1}$, respectively) of pedon EUR07, and in the surface horizons of EUR04, 11 and 16 (27.06–30.80 $cmol_c\ kg^{-1}$), which also showed the highest amounts of exchangeable Ca. The lowest ECEC values (1.0–2.1 $cmol_c\ kg^{-1}$) were measured in the subsurface horizons of pedons EUR05 and 06 (Azores) and EUR17 (France). The latter profile showed very low amounts of both base cations and extractable Al (Table 2), and meets the criteria of the acrudoxic subgroup (SSS 2003). Also in these soils, ECEC values were higher in the top soil (8.7–11.4 $cmol_c\ kg^{-1}$) than in the subsurface horizons, and were within the range observed for the other studied soils.

Table 1. Range of values of exchange properties in non-Andisols (NAND) and Andisols (AND). CEC7=CEC in ammonium acetate at pH7; CEC_{CE} = Unbuffered CEC by the compulsive exchange method; SB = Sum of base cations; AEC = Anion exchange capacity, Al_{KCl} = Al extracted in 1 M KCl; ECEC (effective CEC) = Sum of base cations + Al_{KCl}.

Pedons	CEC7	Al_{KCl}	Sum Bases	CEC_{CE}	AEC	CEC7-CEC_{CE}	CEC7-ECEC	AEC/CEC_{CE}
				$cmol_c\ kg^{-1}$				
Surface horizons								
NAND								
EUR01,02,13,14,15,18,19,20	5–63	0.1–0.5	8–63	3–27	**<0.1**	1–38	**–28–+8**	**0**
AND								
EUR07,08,09,11,16	29–60	0.1–1.1	11–43	10–22	4–6	8–42	11–37	0.2–0.5
EUR03,04	20–50	0–0.5	9–19	7.5–18	**0.2–0.8**	13–36	11–31	<0.1
EUR12	47–59	**1.7–2.4**	6–19	11–18	5–7	37–41	38–39	0.3–0.6
EUR10	40	0.4	12	-	-	-	28	-
EUR05	29–38	**0.5–4**	**4.0–4.8**	**3.1–3.6**	7–13	26–35	20–34	**2.3–3.7**
EUR06	**56–74**	**0–4**	**2.4–7.5**	**3.3–5.8**	4–8	**53–68**	**53–65**	**1.2–1.4**
EUR17	37–50	**3–8**	**0.9–3.5**	**2–8**	4.6–9.2	36–42	34–36	**0.6–4.2**
Subsurface horizons								
NAND								
EUR01,02,13,14,15, 8,19,20	13–40	<0.1	14–38	5–11	**<0.5**	2–35	**–2–+43**	**<0.1**
AND								
EUR07,08,09,11,16	11–66	0.1–8.2	5.9–19.7	7–22	3.3–6.0	4–45	7–46	0.2–0.8
EUR03,04	13–19	≤0.1	5.1–6.8	3.5–5.6	**0.3–0.7**	8–14	8–12	0.1–0.2
EUR12	24	**2.3–3.4**	3.6–4.7	6–10	**4.5–6.3**	14–19	16–18	0.5–1.1
EUR10	37–55	0.1–0.8	3.7–8.5	**2.0**	**8–12**	**49–51**	44–47	**4–6**
EUR05	27–51	0.5	**0.8–1.6**	3.5–4.3	**6–7**	22–48	25–49	**1.5–2.0**
EUR06	**59–83**	<0.1	**1.1–1.3**	**0.6–1.1**	**12–16**	**59**	**58–81**	**15–19**
EUR17	36–37	0.9	**0.8–1.0**	**0.7–2.1**	**5.4–7.4**	35	34–35	**3–11**

In Andisols, a significant negative relation was observed between values of ECEC and the Al_o content (Figure 1A), which indicates that ECEC decreases with the progression of weathering. In Figure 1A, some samples have ECEC values clearly above the general trend. These are surface and subsurface horizons of pedons EUR07 (the highest values), 04 and 16. ECEC values were positively correlated with the organic C content ($r=0.51$; $p<0.01$) (Table 2), as organic matter contributes significantly to the soil negative charge, and thus to the amounts of cations (base cations plus Al) that can be stored. In non-Andisols, ECEC values varied from 9.3–62.9 $cmol_c\ kg^{-1}$, and were not significantly correlated with other soil properties.

Table 2. Relationships between cation exchange capacity by ammonium acetate (CEC7) and by the compulsive exchange method (CEC_{CE}), ECEC, CEC7-ECEC, and AEC and soil constituents.

Equations	R^2	p
Andisols		
CEC7 = 27.6 + 1.80 Org. C	0.408	<0.01
CEC7 = 3.6 + 29.40 Al_o	0.252	<0.01
CEC7 = 31.6 + 6.95 Fe_o	0.258	<0.01
CEC7 = 30.24 + 13.67 Al_p	0.389	<0.01
CEC7 = 27.81 + 38.28 Al_{Cu}	0.395	<0.01
CEC7 = 13.8 +3.8 Al_o + 1.9 Org. C	0.689	<0.001
CEC7 = 18.3 + 0.64 Allophane + 2.05 Org. C	0.580	<0.001
CEC7 = 12.8 + 3.5 (Al_o+½Fe_o) + 1.8 Org. C	0.718	<0.001
ECEC = 6.13 + 0.86 Org. C	0.261	<0.001
CEC7-ECEC = 9.35 + 1.49 Org. C	0.158	<0.01
CEC7-ECEC = 14.19 + 17.29 Al_p	0.568	<0.01
CEC7-ECEC = 9.67 + 52.37 Al_{Cu}	0.675	<0.001
CEC7-ECEC = 9.49 + 5.62 Al_o	0.558	<0.01
CEC7-ECEC = 16.8 + 8.18 Fe_o	0.327	<0.01
CEC7-ECEC = –4.6 + 7.0 Al_o + 1.0 Org. C	0.749	<0.001
CEC7-ECEC = –5.1 + 6.0 (Al_o+½Fe_o) + 1.0 Org. C	0.763	<0.001
CEC_{CE} = 16.16 – 1.47 Al_o	0.222	<0.01
CEC_{CE} = 16.25 – 1.30 (Al_o+½Fe_o)	0.185	<0.01
CEC_{CE} = 15.05 – 0.36 allophane	0.202	<0.01
AEC = 2.75 + 0.60 (Al_o+½Fe_o)	0.195	<0.01
Andisols-Surface horizons		
CEC7-ECEC = 17.7 + 0.996 Org. C	0.139	<0.01
CEC7-ECEC = 13.3 + 5.14 Al_o	0.382	<0.01
CEC7-ECEC = 12.2 + 4.40 (Al_o +½Fe_o)	0.424	<0.01
CEC7-ECEC = –1.7 + 5.6 Al_o + 1.2 Org. C	0.579	<0.001
CEC7-ECEC = –1.1 + 4.6 (Al_o+½Fe_o) + 1.1 Org. C	0.594	<0.001
Andisols-Subsurface horizons		
CEC7-ECEC = 15.3 + 3.09 Org. C	0.268	<0.01
CEC7-ECEC = 5.14 + 6.1 Al_o	0.694	<0.01
CEC7-ECEC = 3.5 + 5.5 (Al_o +½Fe_o)	0.729	<0.01
CEC7-ECEC = 0.71+ 5.5 Al_o + 1.6 Org. C	0.758	<0.001
CEC7-ECEC =–1.1 + 4.9 (Al_o+½Fe_o) + 1.7 Org. C	0.799	<0.001
AEC = 2.66 + 0.75 Al_o	0.330	<0.01
AEC = 3.14 + 0.17 allophane	0.272	<0.01
AEC = 1.96 + 0.84 (Al_o+½Fe_o)	0.414	<0.01
Non-Andisols		
CEC7 = 19.7 + 1.9 Org. C	0.248	<0.05
CEC7 = 8.8 + 79.8 Al_o	0.516	<0.001
CEC7 = 8.6 + 70.2 Al_o + 0.62 Org. C	0.534	<0.001
CEC7 = 10.5 + 38.8 (Al_o+½ Fe_o) + 0.64 Org. C	0.486	<0.05

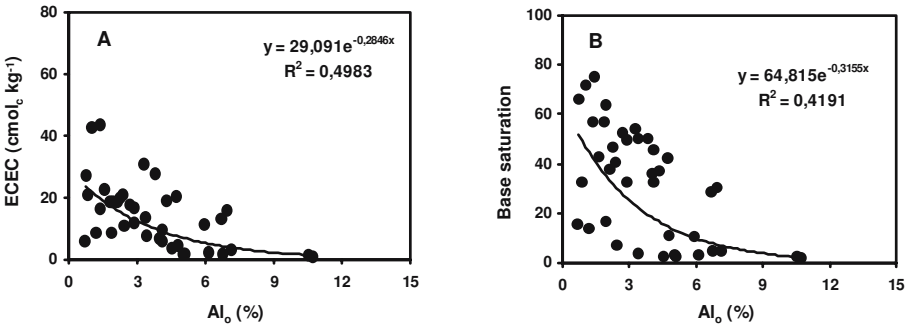

Figure 1. Relationship between Al_o content and effective cation exchange capacity (ECEC) (A) and between Al_o content and base saturation (Sum Bases/CEC7) (B) of the Andisol subset.

Cation exchange capacity by NH_4OAc (CEC7)

The CEC7 values for all horizons of Andisols (Figure 2A) showed a wide variation (13.5–83.1 $cmol_c\ kg^{-1}$), which coincided with that observed in subsurface horizons (20.9 to 73.7 $cmol_c\ kg^{-1}$). The highest values were measured in the surface and subsurface horizons of pedon EUR06 (Azores), which showed both high contents of organic C and allophane (see The physico-chemical data base, this book), and low or negligible amounts of crystalline clay minerals (Monteiro et al. this book). The measured values for studied Andisols are similar to those reported by Madeira et al. (2003), for a wide range of Andisols from the Azores, by Shoji et al. (1985) for non-allophanic soils from Japan, and by Espino-Mesa et al. (1993), for Andisols from the Canary Islands.

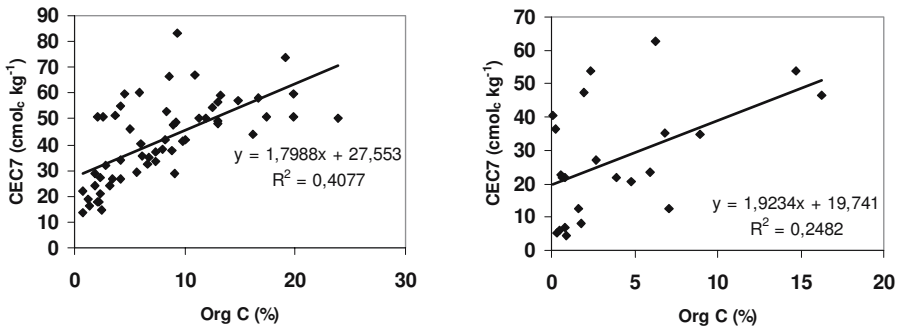

Figure 2. Relationship between the values of cation exchange capacity (CEC7), and organic C contents in Andisols (A) and non-Andisols (B).

The maximum values of CEC7 did not coincide with the highest organic C contents, but a positive relation (r=0.64; p<0.01) was observed between CEC7 values and the organic C content (Figure 2A), which is in agreement with data obtained for soils from the Azores (Pinheiro et al. 2001, Madeira et al. 2003). A similar positive correlation (p<0.01) between these values and Al_p (r=0.62) and Al_{Cu} (r=0.63) contents was also observed (Table 2), suggesting that these forms of Al are indeed related to organic components responsible for the negative charge measured at pH 7 (García-Rodeja et al. 2004). The correlation between CEC7 and Al_o content (Table 2) was also positive (r=0.50; p<0.05), but weaker. The combination of organic C and Al_o contents (multivariate correlation) accounted for 69% of the total variability of CEC7 values (Table 2), whereas the combination of organic C and Al_o+½Fe_o accounted for 72%. Organic C and allophane together explained only 58% of the variation in CEC7. In Figure 2A, samples corresponding to horizons of pedons EUR07 and 09 (Iceland) and 17 (France) combine high organic matter contents with relatively low CEC7, suggesting a low degree of humification. This is in agreement with a cryic soil temperature regime (Arnalds 2004, Quantin 2004) of those pedons, and with the observation of weakly decomposed organic material in micromorphology (Stoops and Gérard 2004). Conversely, some samples of pedons EUR06, 05 and 10 are far above the general trend, which is in agreement with their high contents of allophanic constituents. Both deviations are also observed in Figures 3A and 3B, respectively for surface and subsurface horizons. If the outliers in Figure 2 are omitted, the correlation line is steeper and the part of CEC7 attributable to organic C amounts to approximately 0.4 $cmol_c\ g^{-1}$, which is a realistic value. The intercept on the Y-axis of Figure 2A should be due to CEC of the mineral phase (allophanic constituents and clay minerals).

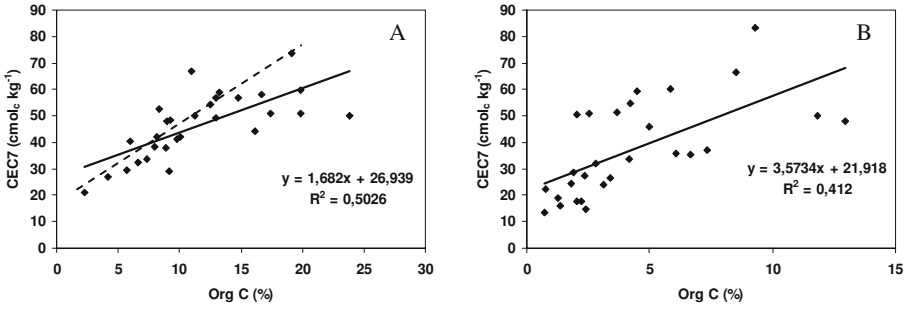

Figure 3. Cation exchange capacity (CEC7) and organic C in surface (A) and subsurface (B) horizons of the Andisol subset. Dashed line: approximate correlation after removal of outliers with low humification.

In the surface horizons of Andisols, the positive correlation between CEC7 values and the organic C content (Figure 3A) was stronger than in subsurface horizons (Figure 3B), and positive correlations between CEC7 values and Al_p (0.57) and Al_{Cu} (0.51) contents were observed, but not with the Al_o and the Al_o+½Fe_o contents. Contrarily, in the subsurface horizons, the correlations of CEC7 with Al_o ($r=0.73$; $p<0.01$) and Al_o+½Fe_o ($r=0.75$; $p=0.01$) contents were similar to those observed with Al_{Cu} ($r=0.75$), and Al_p ($r=0.70$) contents, and stronger than with organic C. Differences between surface and subsurface horizons are related to higher organic C and complexed Al in the surface horizons versus higher contents of inorganic Al compounds (allophane/imogolite, ferrihydrite) in the subsurface ones.

In the non-Andisols, CEC7 values showed a wide variation and ranged between 4.6 and 62.6 $cmol_c\ kg^{-1}$. CEC7 increased with organic C content ($r=0.50$; $p<0.05$) (Figure 2B). The intercept on the Y-axis should be due to clay minerals and is in agreement with the predominance of phyllosilicates in the clay fraction, while the scatter (larger than in Andisols) should be due to differences in clay content and mineralogy (Monteiro et al. this book). Also in non-Andisols, CEC7 values were correlated with Al_o content ($r=0.72$; $p<0.01$) (Table 2). However, given the low Al_o content, the correlation might be an indirect effect of clay content. The combination of the organic C and Al_o contents (multiple correlation) accounted for 53% of the total variability of CEC7 values in non-Andisols (Table 2).

Cation exchange capacity measured by compulsive exchange

Values of the cation exchange capacity determined by the compulsive exchange method (CEC_{CE}) for both Andisols and non-Andisols also showed a wide variation (Table 1), and were much lower than CEC7, especially in Andisols very rich in allophane and organic C. CEC_{CE} values varied from 0.2 to 21.6 $cmol_c\ kg^{-1}$, in Andisols, and from 1.3 to 26.7 $cmol_c\ kg^{-1}$, in non-Andisols. Values for CEC7 and CEC_{CE} were not correlated because the latter value is determined at a different pH for each sample.

In Andisols, CEC_{CE} values of surface horizons were usually higher (2.6–22.0 $cmol_c\ kg^{-1}$) than those of subsurface horizons (0.2–21.5 $cmol_c\ kg^{-1}$). The latter were especially low (0.2–2.1 $cmol_c\ kg^{-1}$) in pedons EUR06 (Azores), EUR17 (France) and EUR10 (Tenerife), which have high contents of allophanic constituents. As reported by Auxtero et al. (2004) for similar soils of the Azores, the lower field-pH reduces the negative charge of organic matter, while the positive charge of allophane, imogolite and ferrihydrite at the prevailing pH may cause partial blocking of this negative charge through complexation. The combined effect leads to low

CEC_{CE} values. Under these circumstances, and especially under udic and perudic conditions, the limited retention capacity may cause significant leaching of nutrient cations.

Similar to the ECEC, CEC_{CE} values decreased with the progression of weathering as they showed a weak negative correlation ($p<0.05$) with Al_o ($r= –0.32$), $Al_o+½Fe_o$ ($r= –0.30$), and allophane ($r= –0.34$) contents, and a positive correlation ($r=0.29$) with organic C content. In the Andisols (Table 2), the correlation values of CEC_{CE} with Al_o, $Al_o+½Fe_o$ and allophane were –44, –0.43, and –0.45, respectively (Table 2), but correlation with the organic C content was not significant. Similar trend was observed for Andisols from the Azores (Madeira et al. 2003) and from Canary Islands (Espino-Mesa et al. 1993). Probably the pH-effect on CEC_{CE} obscures the effect of organic C.

As reported by Gillman and Hallman (1988) for Andisols, values of CEC_{CE} were positively correlated ($p<0.01$) with ECEC ($r=0.79$) and Sum of Bases ($r=0.81$) (Figure 4). Correlations in non-Andisols were weaker ($r=0.68$). The relationship for Andisols between the CEC_{CE} and the sum of bases is illustrated in Figure 4A. Most of the points are close to the 1:1 line, suggesting that the Sum of Bases is close to the CEC_{CE}, which indicates complete saturation of the CEC at soil-pH. Some horizons with high content of Ca and Sum of Bases (e.g. EUR04, 07, 11 and 16) showed a significant departure from the 1:1 line, indicating that high amounts of non-exchangeable basic cations were extracted. Similarly, Madeira et al. (2003) found that CEC_{CE} in Andisols with a eutric character (or high content of bases) is much lower than the Sum of Bases and the ECEC. This trend was even stronger in (calcareous) non-Andisols, whose CEC_{CE} values were always lower than the Sum of Bases (see The physico-chemical data base, this book).

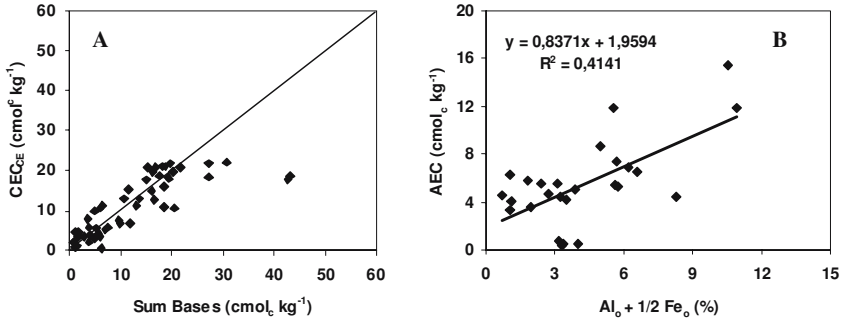

Figure 4. Relationship between the cation exchange capacity determined by the compulsive exchange method (CEC_{CE}) and the Sum of Bases for Andisols (A), and relationship between the anion exchange capacity (AEC) and the ($Al_o+½Fe_o$) content for subsurface horizons of Andisols (B).

The difference between the CEC7 and the ECEC strongly varied with soil type (Figure 5, Table 2). Values in non-Andisols, with pH higher than 7 (EUR13–15 and EUR18), were negative, as ammonium acetate extracted some Ca from calcite (Economou 2004), which renders the ECEC values meaningless. In spite pH values below 7, pedons EUR19–20 (Hungary) also showed small negative CEC7-ECEC values, which can be attributed to analytical uncertainty. In profiles EUR01 and 02, the difference was mostly positive, but smaller than in Andisols.

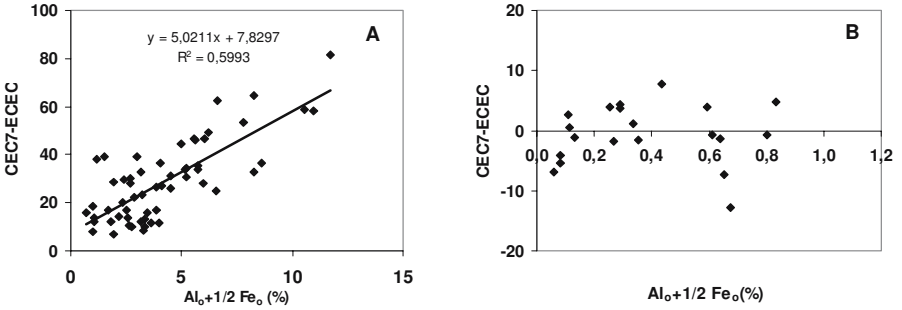

Figure 5. The difference between the cation exchange capacity and the effective cation exchange capacity (CEC7-ECEC) in relation to Al_o+½Fe_o content in Andisols (A) and non-Andisols (B).

In Andisols, CEC7-ECEC was always positive (Table 1), especially in those with high contents of allophane and organic C. Difference values showed a strong positive correlation with Al_o and Al_o+½Fe_o contents (Figure 5A, Table 2) and a weak correlation with the organic C content ($r=0.32$; $p<0.05$), suggesting that Al_o causes positive charge which blocks the negative charge through complexation with organic matter. This blocking may be undone when Al in complexes hydrolyses at higher pH (e.g. pH=7). The combination of the organic C and Al_o contents (multivariate correlation) accounted for 75% of the total variability of CEC7-ECEC values (Table 2), whereas the combination of organic C and Al_o+½Fe_o contents accounted for 76%.

In surface horizons, the correlation (r) between CEC7-ECEC and organic C, Al_o and Al_o+½Fe_o contents were 0.37 ($p<0.05$), 0.62 ($p<0.01$) and 0.65 ($p<0.01$), respectively. The highest multiple correlation coefficient was found for organic C and Al_o+½Fe_o contents ($r=0.77$, $p<0.01$), which was similar to that obtained with the organic C and Al_o contents (0.76, $p<0.01$). In the subsurface horizons, the correlations with organic C, Al_o, and Al_o+½Fe_o contents were 0.52 ($p<0.05$), 0.83 ($p<0.01$) and 0.85 ($p<0.01$) and the multiple correlation coefficient with organic C and

Al_o+½Fe_o contents (r=0.89; p<0.01) was similar to that obtained for the organic C and Al_o contents (0.87, p<0.01). This indicates that at the prevailing pH, Fe_o hardly contributes to the positive charge of the soil, which is in agreement with the low correlation between CEC7-ECEC and Fe_o content (Table 2). This is not in agreement with a high AEC and a PZC of 6.9 for ferrihydrite as reported by Parfitt (1980). Possibly, the iron phases in the studied soils have much less charge than the synthetic ones on which such estimates are based. Thus, the difference CEC7-ECEC, especially in the subsurface horizons, is mostly related to Al constituents (Figure 5A). Because Al-phases have a positive charge at the prevailing pH, and this charge increases with decreasing pH, while organic matter, the main contributor to negative charge, has a CEC that increases with pH, the correlation with Al_o can be explained by the blocking of negative charge on organic matter through complexation of Al.

As the Andisol samples had pH<7, CEC7 overestimates the CEC under field conditions. Similarly, CEC7 underestimates the base saturation (2 to 75%) under the same conditions. Base saturation on CEC7 was extremely low in pedons with high amounts of Al_o or allophane (Figure 1B), indicating that values decrease from the less to the more weathered soils. Therefore, in Andisols the base saturation based on CEC7 does not reflect field conditions, and the base saturation on CEC_{CE} is a more realistic estimate.

Anion exchange capacity

The values of anion exchange capacity (AEC), as determined by the compulsive exchange method, that is approximately at field pH conditions, showed a wide variation according to soil type and characteristics. The values were very low (<0.54 $cmol_c\ kg^{-1}$) or nil for both surface and subsurface horizons of non-Andisols, i.e. soils from volcanic areas of Greece, Hungary and EUR01 and 02 from Italy. This is in agreement with the very low content of variable charge constituents (e.g. allophane and Al_o contents) found in these soils (The physico-chemical data base, this book).

AEC values determined for pedons EUR03 and 04 (Italy), in spite of their significant amounts of allophane (7–12%), were smaller than in other pedons with andic soil characteristics and varied between 0.25 and 0.84 $cmol_c\ kg^{-1}$ (Table 2). It is unlikely that low AEC values are due to low allophane contents or to high pH values, as these are similar to those of other pedons with high AEC values. As the Al/Si ratio of allophane strongly affects the amount of positive charge (Greenland and Mott 1978), it is hypothesised that low AEC values of those pedons could be in relation with the Al_o/Si_o ratio of the extractable alumino-silicates, which is lower than in

the other pedons (García-Rodeja et al. 2004). Parfitt (1980) suggests that allophanes with Al/Si=1 have lower AEC than those with ratio 2:1, but the cited AEC values are uncertain. Our data indicate that AEC increases with increasing $(Al_o\text{-}Al_p)/Si_o$ ratio, and the allophanic samples appear to separate into two groups. In the other pedons, AEC values were much higher and ranged between 4.09 and 15.45 $cmol_c\ kg^{-1}$. Values above 6.5 $cmol_c\ kg^{-1}$ were only found in surface and subsurface horizons of pedons EUR05 and 06 (Azores), EUR10 (Spain-Tenerife), and EUR17 (France), which also showed the highest allophane contents. According to their colloidal composition, these soils are expected to have a net positive charge at field-pH (Auxtero et al. 2004), The high AEC measured for pedon EUR17 (France) is attributable to its low pH (4.2–5.5, in water) compared to that of other soils (5.4–6.2). Accordingly, it is to be expected that significant amounts of electrostatically adsorbed anions such as nitrates can be retained in these horizons, as has been reported for similar Andisols from the Azores (Auxtero et al. 2004). This would be beneficial for crops and diminish leaching of mobile anions. It is notable that pedon EUR12, with negligible amounts of allophane (<1%), and with a low C/Al_p ratio (García-Rodeja et al. 2004), showed AEC values (4.5–7.0 $cmol_c\ kg^{-1}$) similar to those exhibited by pedons with significant contents of allophane (3–23%, allophane Parfitt). This stresses that Al-humus complexes, as reported by Auxtero et al. (2004) for non-allophanic Andisols from the Azores, may also cause significant positive charge and retention of anions in non-allophanic Andisols. Additionally, AEC values might be high when large amounts of partially weathered plagioclases are present (Tenerife horizons, sample 7; Meijer et al. this book).

As reported for soils of the Azores Archipelago (Auxtero et al. 2004), values of AEC for all soils showed a wide variation and were positively correlated ($p<0.01$) with Al_o (r=0.62), $Al_o+½Fe_o$ (r=0.67) and allophane (r=0.54) contents. In the subset of Andisols, these correlations were absent in surface horizons, whereas in the subsurface horizons, with higher contents of allophanic constituents, r-values were 0.52, 0.57 and 0.64 (Table 1; Figure 4B). In Figure 4B, the AEC values that plot far below the general trend correspond to pedons EUR03 and 04 (Italy). With or without the samples from these two profiles, the correlation does not go through 0. There is still a significant amount of AEC at low Al_o contents (pedon EUR12 and some samples of EUR7–9), which supports the contribution of Al-organic complexes to AEC.

The AEC/CEC_{CE} ratio was less than one for most of the studied soils (Table 2). It was greater than one in both surface and subsurface horizons of pedons EUR05 and 06 (Azores), in subsurface horizons of pedon EUR10 (Tenerife), and in most of the horizons of the pedon EUR17

(France). This means that in Andisols with high contents of allophanic materials, at field-pH, the AEC becomes more important than the CEC, so that soils can retain lower amounts of cations than anions. In such conditions, a low retention of cations, notwithstanding the high organic C content, may be due to the blocking of the negative charge of organic matter by formation of Al-humus complexes and by sorption to allophanic constituents, as suggested by the negative correlation between CEC_{CE} values and Al_o contents (Table 2).

Exchange complex properties and soil grouping

Based on their exchange characteristics, and especially those of subsurface horizons, the studied soils can be subdivided into three groups (Table 1).

i. The group formed by Andisol pedons EUR05, 06, 10 and 17, which have high contents of allophanic constituents, is distinguished from the others by the lowest values of cation exchange capacity at soil pH (CEC_{CE}), sum of bases, and effective cation exchange capacity, and on the other hand the highest values of the anion exchange capacity (AEC), which is higher than CEC_{CE}.
ii. The second group includes pedons that are Andisols, but differing in characteristics from the first set. Within this set, some variations should be stressed. Firstly, pedons EUR03–04 differ from other Andisols in that they show an AEC as low as in non-Andisols; secondly, pedon EUR12 is exceptional because, although having low amounts of Al_o and being non-allophanic, it has an AEC similar to other Andisols.
iii. The third set includes pedons corresponding to non-Andisols, which show zero or negligible AEC and a base saturation mostly higher than 100%.

Conclusions

1. Exchange complex properties of soils from European volcanic areas showed a wide variation. Amounts of exchangeable basic cations (Ca, Mg, K and Na) were extremely variable among soils, and varied according to climate, kind of volcanic material, and weathering progression.
2. Extractable Al was mostly low, and consequently the ECEC was closely related to the sum of bases (SB).

3. Cation exchange capacity as determined by ammonium acetate (CEC7) was mostly related with the content of organic C and with Al pools related to the organic matter. The CEC7 of surface horizons of Andisols is more dependent on organic C content than on Al_o content, while the reverse is observed in the subsurface horizons.
4. Amorphous aluminium silicates appear to contribute to CEC at a lower pH values than is suggested by the Point of Zero Charge values from literature.
5. The CEC_{CE} values were much lower than those of CEC7 and the values were not correlated, but the CEC_{CE} was strongly correlated with SB and ECEC. CEC7 gave an overestimate with respect to field conditions, so that the respective base saturation does not reflect field conditions. The CEC_{CE} better reflects field conditions, and the similarity between this value and the sum of bases indicates that soils in field conditions are virtually base-saturated.
6. In Andisols, CEC7-ECEC values were positively correlated with Al_o and Al_o+½Fe_o, suggesting that aluminous constituents cause positive charge which blocks the negative charge through complexation with organic matter.
7. Values of AEC varied widely among studied soils and were highest in soils with high Al_o and allophane contents, but positive correlation with these constituents was only observed in the subsurface horizons. A correlation with the Al/Si ratio appears to exist, but also Al-organic complexes contribute to AEC.
8. AEC values did not clearly separate Andisols and non-Andisols, as low values were found in soils with significant amounts of allophane, while significant values were observed for non-allophanic soils, with low content of Al_o.
9. At field-pH conditions, Andisols that are rich in allophane are more effective in retaining anions than cations, especially in the subsurface horizons.
10. Properties of the exchange complex were useful in subdividing soils with andic properties.

Acknowledgements

E. Auxtero gratefully acknowledges the award of a post-doctoral research fellowship by the Fundação para a Ciência e a Tecnologia. The authors express their appreciation to Isabel Meireles and Ana Batista for technical as-

sistance in conducting laboratory work, and Paulo Marques for the manuscript preparation. Prof. Edgar de Sousa is also acknowledged for comments and English style improvement.

References

Arbelo Rodrigues CD, Espino-Mesa M, Hernandez JM (1991). Determinacion de capacidad de cambio y cationes extraibles con Arg-tiourea en Andosoles. Suelo y Planta 1:257–268

Arnalds O (2004). Volcanic soils of Iceland. Catena 56:3–20

Auxtero E, Madeira M, Sousa E (2004). Variable charge characteristics of selected Andisols from the Azores, Portugal. Catena 56:111–125

Colombo C, Di Cerci A, Sellitto MV, Palumbo G, Terribili F (2004). Genesis and formation of volcanic soil in Fregrean Fields. Volcanic Soil Resources in Europe, Cost Action 622 final meeting. Abstracts. Rala Report no. 214. Agricultural Research Institute, Reykjavík, Iceland

Driessen P, Deckers J, Spaargaren O, Nachtergaele F (eds) (2001). Lecture Notes on the Major Soils of the World. FAO, Rome. (World Soils Resources Reports, 94)

Economou A, Pateras D, Michopoulos P, Vavoulidou E (2004). Properties of soil derived from different volcanic parent material in Greece. Volcanic Soil Resources in Europe, Cost Action 622 final meeting. Abstracts. Rala Report no. 214. Agricultural Research Institute, Reykjavík, Iceland

Espino-Mesa M, Arbelo, CD, Hernandez JM (1993). Predicting value of diagnostic soil properties on actual and potencialcation exchange capacity (CEC) in andisols and andic soils. Communications in Soil Science and Plant Analysis 24(19):2569–2584

Greenland DJ, Mott, CJB (1978). Surface of soil particles. In: Greenland DJ and Hayes MHB (eds) The Chemistry of Soil Constituents, pp 321–353. John Wiley & Sons, Chichester

García-Rodeja E, Nóvoa JC, Pontevedra X, Martinez-Cortizas A, Buurman P (2004). Aluminium fractionation of European volcanic soils by selective dissolution techniques. Catena 56:155–183

Gillman GP, Hallman MJ (1988). Measurement of exchange properties of Andosols by the compulsive exchange method. Soil Sci Soc Am J 52:1196–1198

Gillman GP, Sumpter EA (1986). Modification to the compulsive exchange method for measuring exchange characteristics of soils. Australian Journal of Soil Research 24:173–192

Madeira M, Auxtero E, Sousa E (2003). Cation and anion exchange properties of Andisols from the Azores, Portugal, as determined by the compulsive exchange and the ammonium acetate methods. Geoderma 117:225–241

Parfitt RL (1980). Chemical properties of variable charge soils. In: Theng BKG (ed) Soils with Variable Charge. New Zealand Society of Soil Science, Lower Hutt, pp 167–194

Pinheiro J, Madeira M, Monteiro F, Medina J (2001). Características e classificação dos Andossolos da Ilha do Pico (Arquipélago dos Açores). Rev Ciências Agrárias 24(3–4):48–60

Quantin P (2004). Volcanic soils of France. Catena 56:95–109

Shoji S, Ito T, Saigusa M, Yamada I (1985) Properties of nonallophanic Andosols from Japan. Soil Science 140(4): 264–277

Stoops G, Gérard M (2004). Micromorphology of the volcanic ash soils of the COST-622 reference profiles.Volcanic Soil Resources in Europe, Cost Action 622 final meeting. Abstracts. Rala Report no. 214. Agricultural Research Institute, Reykjavík, Iceland

Sumner ME, Miller WP (1996). Cation exchange capacity and exchange coefficients. Methods of Soil Analysis: Part 3. Chemical Methods. SSSA, vol. 5. Madison, USA

Soil Survey Staff (SSS) (2003). Keys to Soil Taxonomy (9th edn). United States Department of Agriculture, National Resources Conservation Service, Washington

Multivariate statistical analysis of chemical properties of European volcanic soils

A. Martínez-Cortizas, J.C. Nóvoa, X. Pontevedra,
T. Taboada, E. García-Rodeja and P. Buurman

Introduction

Within the framework of EU-COST action 622 twenty soils developed on volcanic materials from Italy (IT: EUR01 to EUR04), Azores Islands (AI: EUR05, EUR06), Iceland (IC: EUR07 to EUR09), Canary Islands (CI: EUR10 to EUR12), Greece (GR: EUR13 to EUR15), France (FR: EUR16 and EUR17) and Hungary (HG: EUR18 to EUR20) were described, sampled and analyzed for a large number of physico-chemical soil properties by different research groups. This database provides a good opportunity for the application of multivariate statistical methods, although the number of samples is moderate (94 horizons). In this chapter we applied two different approaches for the explanation of the variance structure of the chemical properties of the European volcanic soils: (1) an exploratory analysis using principal component analysis (PCA) aimed to identify the major trends and processes in these soils, and (2) a confirmatory analysis based on PCA separation and knowledge on andic properties using discriminant analysis (DA) to identify the minimum set of properties that enable a good separation of the different types of horizons (non-andic, vitric, andic).

Material and methods

The properties used in this study are summarized in Table 1 and all were measured in the fine earth fraction (<2 mm). They include properties related to particle size, organic matter, exchange complex and reactive soil components. All methods are described in *The physico-chemical data base* (this book).

Not all measurements were done for all samples, so the number of available cases (i.e. horizons) for analysis varies depending on the proper-

ties that have been included. Here we will preferentially describe the results obtained in the analysis including all (or almost all) soil horizons. Only in specific cases we performed analyses on a reduced data set. This is the case for the clay content, since the resin method was done only on the soils from Italy, Iceland, Azores Islands and Canary Islands (and not for all horizons: 42 out of 59). This method was not used for soils from Greece, France and Hungary.

The principal component and discriminant analysis were performed using the SPSS statistical software.

Table 1. Physicochemical properties used in this study for the characterization of the European volcanic soils.

Property	Description of the property
Granulometry	
$Clay_L$ $Clay_R$	Clay content (method: L laser, R resin) %
Soil reaction	
pH_w	pH in water
pH_k	pH in 1 M KCl
ΔpH	pH_w–pH_k
Organic matter	
C	Total soil organic carbon %
Exchange complex	
CEC	Cation exchange capacity (NH_4-Acetate at pH 7) $cmol_c\ kg^{-1}$
SB	Sum of bases $cmol_c\ kg^{-1}$
V	Base saturation %
Reactive components	
Al_t, Fe_t	Total Al and Fe content %
Al_n	Al extracted in NaOH %
Al_o, Fe_o	Al and Fe extracted in NH_4-oxalate %
Al_p, Fe_p	Al and Fe extracted in Na-pyrophosphate %
Al_{Cu}	Al extracted in $CuCl_3$ (low stability Al-humus complexes) %
Fe_d	Fe extracted in dithionite-citrate-bicarbonate (total free Fe) %
Si_o	Si extracted in NH_4-oxalate (amorphous Si-compounds) %
pH_f	pH in NaF
P_{mx}	Maximum P-retention mg kg^{-1}
P_{ret}	Percentage of P-retention
Calculated variables of reactive comp.	
Al_o/Si_o	Ratio of Al to Si extracted in NH_4-oxalate
$(Al_{o\text{-}p})/Si_o$	Ratio of (Al_o-Al_p) to Si extracted in NH_4-oxalate
Al_o+½Fe_o	Sum of Al and Fe extracted in NH_4-oxalate
Alloph.	Allophane content (Parfitt's method) %
Al_{ia}	Al_o-Al_p: inorganic amorphous Al %
Fe_{ia}	Fe_o-Fe_p: Fe in amorphous inorganic compounds %
Fe_c	Fe_d-Fe_o: crystaline free iron %
$Al_{o/t}$	Al_o/Al_t: proportion of Al in amorphous compounds
$Al_{p/o}$	Al_p/Al_o: proportion of amorphous Al in humus complexes
Al_{hs}	Al_p-Al_{Cu}: Al in high stability humus complexes
$Fe_{d/t}$	Fe_d/Fe_t: proportion of total free Fe
$Fe_{o/t}$	Fe_o/Fe_t: proportion of the total Fe as amorphous compounds
$Fe_{o/d}$	Fe_o/Fe_d: proportion of total free Fe as amorphous compounds

Results and discussion

PC analysis of the whole data set

PC1: weathering and pedogenesis

Seven principal components (PCs) have eigen values greater than 1 and account for an 87.6% of the total variance (Table 2). A large proportion of the variance is explained by the first PC (PC1: 45.8%) and is related to the contents of reactive components (extractable Al (Al_n, Al_o), Fe (Fe_d, Fe_o) and Si (Si_o)), amount of inorganic amorphous Al (Al_{ia}) and amount of low/moderate stability Al-humus complexes (Al_{Cu}), P retention (P_{ret} and P_{mx}) and degree of weathering ($Al_o/_t$, Fe_d/Fe_t) (Figure 1). On the opposite side of PC1/PC2 projection plot, with moderate loadings, the base saturation (V) and pH_w, indicating that both decrease with increasing amounts of reactive components. This suggests that PC1 represents the intensity of weathering and pedogenesis – development of andic properties.

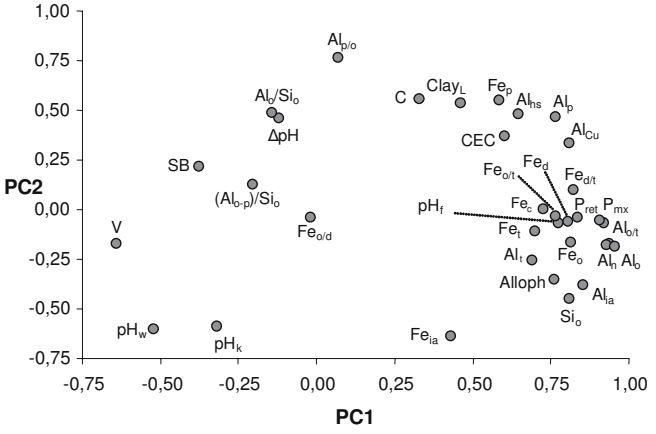

Figure 1. PC1/PC2 projection of loadings of physico-chemical properties of the European volcanic soils. The codes of the properties are in Table 1.

This trend of increasing weathering is clearly seen in Figure 2, where we have plotted the scores of each soil sample on PC1 through PC4. The highest scores on PC1 are found in soils EUR06 (Azores Islands), EUR10 (Canary Islands) and EUR16–17 (France) followed by moderate values in EUR03–04 (Italy), EUR07–08 (Iceland) and EUR12 (Canary Islands). The lowest scores correspond to the soils from Greece (EUR13–15), Hungary (EUR18–20) and those from Italy developed on the Gauro deposits (EUR01–02). These results are in agreement with the degree of weathering proposed by Taboada et al. (this book) for these volcanic soils, and is sup-

ported by the significant correlation between the PC1 scores and the normalized weathering index (NCIA) as shown in Figure 3.

Table 2. Loadings of physicochemical properties in the PCA analysis. In bold the properties with higher loadings for each principal component.

	PC1	PC2	PC3	PC4	PC5	PC6	PC7
$Clay_L$	0.46	0.53	0.11	–0.11	–0.24	0.06	0.36
pH_w	–0.52	**–0.61**	0.36	0.06	0.13	–0.34	0.11
pH_k	–0.32	**–0.59**	0.45	0.18	0.35	–0.29	–0.02
ΔpH	–0.12	0.45	–0.19	–0.34	**–0.48**	–0.01	0.11
C	0.33	**0.56**	–0.23	**0.62**	0.18	0.03	–0.04
CEC	0.62	0.37	–0.12	**0.57**	–0.08	0.06	0.22
SB	–0.38	0.21	–0.05	**0.79**	–0.05	0.15	0.29
V	**–0.64**	–0.18	0.36	0.20	0.33	–0.15	0.05
Al_t	**0.69**	–0.26	0.05	–0.34	–0.28	0.03	0.33
Al_n	**0.94**	–0.18	–0.01	–0.12	0.14	0.02	0.18
Al_o	**0.93**	–0.18	–0.08	–0.06	0.24	0.01	0.13
Al_p	**0.77**	0.47	0.02	–0.05	0.31	–0.25	–0.08
Al_{Cu}	**0.81**	0.33	0.18	–0.06	–0.00	–0.16	0.08
Fe_t	**0.70**	–0.11	0.36	0.01	–0.39	–0.08	–0.29
Fe_d	**0.81**	–0.06	0.47	0.13	–0.27	0.01	–0.13
Fe_o	**0.82**	–0.17	0.21	0.21	–0.16	0.03	–0.38
Fe_p	0.59	**0.55**	0.27	–0.05	0.21	–0.27	–0.20
Si_o	**0.81**	–0.45	–0.18	–0.01	0.08	0.07	0.13
Al_o/Si_o	–0.14	0.49	0.42	–0.26	0.28	**0.60**	–0.09
$(Al_{o-p})/Si_o$	–0.20	0.12	0.32	–0.20	**0.43**	**0.75**	–0.12
$Al_o+½Fe_o$	**0.95**	–0.19	–0.03	–0.01	0.17	0.02	0.03
Alloph.	**0.76**	–0.36	–0.10	–0.08	0.15	0.15	0.24
$Al_{p/o}$	0.07	**0.76**	0.23	–0.11	–0.16	–0.22	0.01
$Al_{o/t}$	**0.92**	–0.07	–0.20	0.02	0.29	–0.02	–0.02
Al_{hs}	**0.65**	0.48	–0.07	–0.04	**0.43**	–0.27	–0.16
Al_{ia}	**0.86**	–0.38	–0.11	–0.06	0.17	0.10	0.18
$Fe_{d/t}$	**0.82**	0.10	0.32	0.18	–0.14	0.18	0.04
$Fe_{o/t}$	**0.77**	–0.04	–0.30	0.24	0.06	0.14	–0.27
$Fe_{o/d}$	–0.02	–0.04	**–0.63**	–0.21	–0.10	–0.05	**–0.42**
Fe_{ia}	0.43	**–0.64**	0.01	0.27	–0.35	0.26	–0.27
Fe_c	**0.73**	0.00	**0.58**	0.07	–0.31	–0.01	0.02
pH_f	**0.77**	–0.07	0.06	–0.24	0.16	–0.18	0.05
P_{mx}	**0.91**	–0.06	–0.06	–0.07	–0.03	–0.03	0.03
P_{ret}	**0.84**	–0.04	–0.28	0.03	–0.04	0.05	–0.07
Explained Variance (%)	45.8	13.4	7.4	6.3	6.1	4.9	3.7
Cumulative explained variance %	45.8	59.2	66.6	72.9	79.0	83.9	87.6

The loadings of some soil properties are affected by the fact that there are sets of horizons/soils showing a departure of the main trend in PC1. This is particularly evident for the clay ($Clay_L$), iron (Fe_d and Fe_c), proportion of non-crystalline Al ($Al_{o/t}$) and phosphorous retention (P_{ret}). The clay content shows two different groups in PC1 (Figure 4A), one composed mainly by

horizons classified as andic (A) and the other by the non-andic and most vitric horizons (NA-V). In both cases the content increases with the PC loading, in agreement with the fact that the clay content usually increases with degree of weathering. The slope of the linear functions fitting PC1 loadings and clay content is 8 for the andic group (r=0.77) and 25 (r=0.87) for the non-andic/vitric group. For the set of samples for which the clay content was determined by the resin method the slope is 14 (r=0.82). This result suggests that the laser method underestimated the clay content, perhaps due to the presence of very small aggregates that were not broken with pretreatment (see also Buurman and van Doesburg this book).

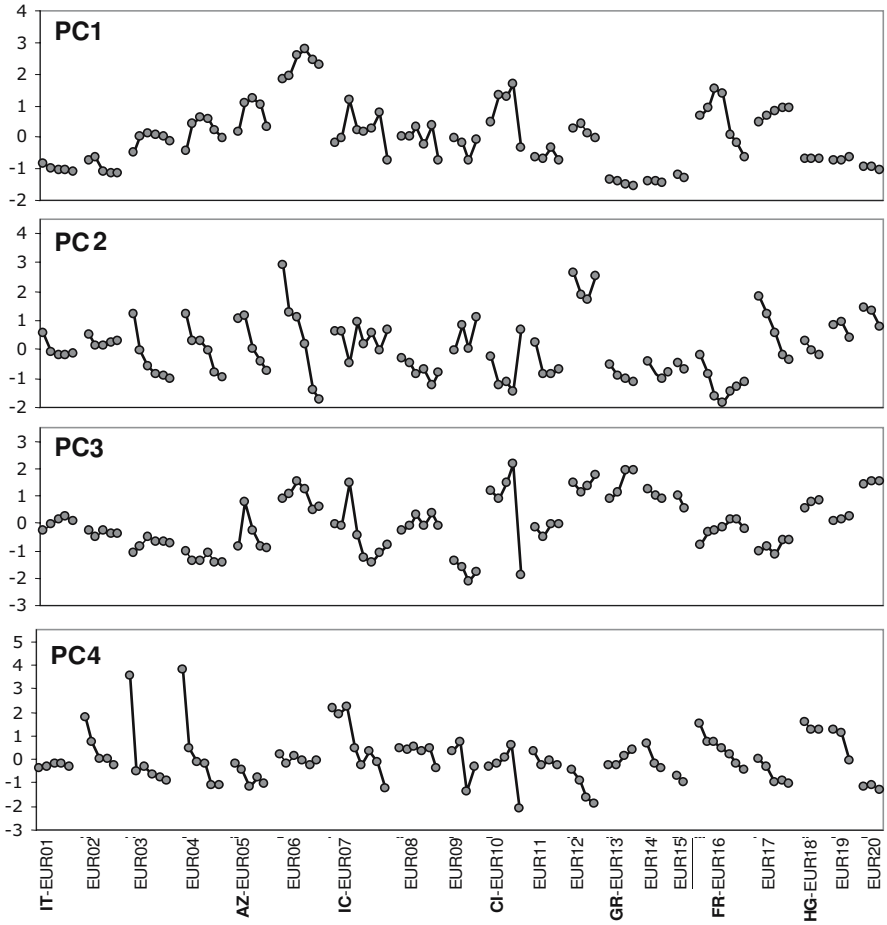

Figure 2. Factor scores of the first four principal components for the different soils and horizons.

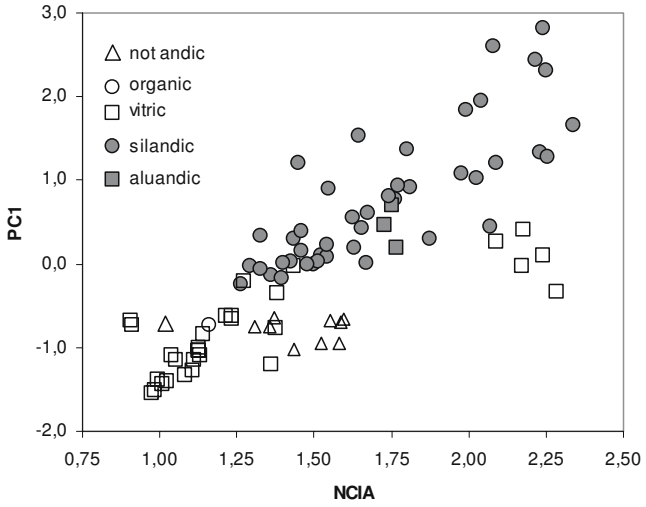

Figure 3. Relationship between the normalized weathering index (NCIA, Taboada et al. this book) and the PC1 factor scores of soil horizons.

As for Fe and Al, two facts are evident: (1) soils from Greece and Hungary plot together at the lowest PC1 loadings and show almost no trend (Figure 4B,C), and (2) soils EUR10 and EUR12 from the Canary Islands and a few horizons of soils EUR07 (2Ah2) and EUR08 (Bw1 and 3BwC) form a separate group although showing an increase in Fe and Al with PC1 loading (Figure 4B,C,E). Both the increase in total free Fe and proportion of non-crystalline Al are related to the degree of weathering (see Taboada et al. and Martínez Cortizas et al. this book), so this reflects a relatively greater proportion of crystalline phases of Fe and Al in the soils from the Canary Islands than in soils with a similar degree of weathering (e.g., EUR06). This is corroborated by results of multiple oxalate Fe-extractions of some Tenerife samples and by the fact that the Tenerife samples contain significant amounts of gibbsite and extractable weathered plagioclase (Meijer et al. this volume). The lower Al_o/Si_o ratio in the Tenerife samples is significant in this respect. The lower content of non-crystalline Al may also be the reason for the separation of the horizons of EUR12 with regard to phosphorus retention (Figure 4D).

PC2: profile differentiation

The second principal component (PC2) extracted a 13.4% of the total variance and reflects profile differentiation related to soil organic matter and properties associated with it. The highest positive loadings correspond to the non-crystaline Al and Fe bound to organic matter ($Al_{p/o}$, 0.76; Fe_p,

0.55) and carbon content (C, 0.56), while pH (pH_w, –0.61; pH_k, –0.59) and inorganic Fe (Fe_{ia}, –0.64) show the more negative loadings (Table 1 and Figure 1). Thus it reflects a trend to an increase in Fe-Al bound to organic matter, carbon content and decreasing pH and inorganic Fe. As for PC1, the explained variance for pH is limited by the fact that there are two different groups of samples (Figure 4F). The soils from Greece and, to some extent, those from Hungary form a group with a similar convergent trend but a different initial slope from the rest of the soils, which is related to their higher pH due to the presence of carbonates.

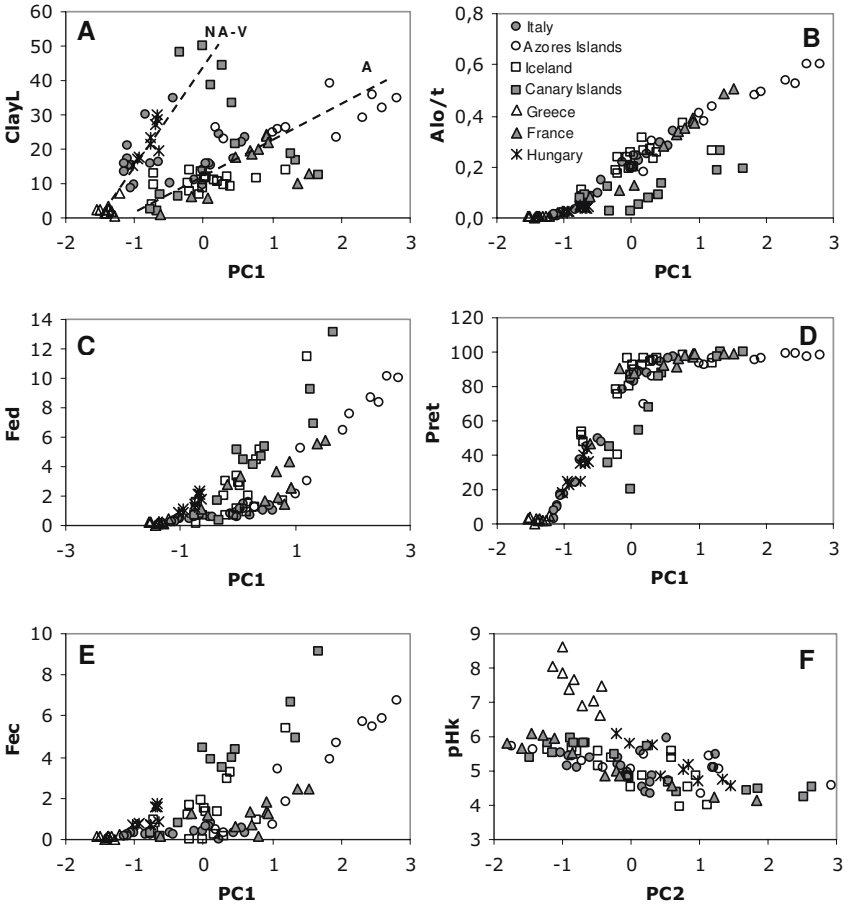

Figure 4. Relationship between $Clay_L$, Fe_d, Fe_c, $Al_{o/t}$ and P_{ret} and the PC1 factor loadings, and between pH_k and the PC2 factor scores showing deviations from the main trends. (NA-V: not-andic and vitric horizons; A: andic horizons).

The vertical differentiation is more obvious in the variation of the PC2 loadings for each soil (Figure 2). The values typically increase from the bottom horizons to the surface ones. The most intense differentiation is found in soils EUR06, EUR03, EUR04, EUR05 and EUR17.

PC3: Fe fractionation

PC3 extracted 7.4% of total variance that is almost exclusively related to Fe fractionation. Crystalline Fe (Fe_c) and total free Fe (Fe_d) have positive, although moderate (0.58 and 0.47 respectively), loadings while the proportion of non-crystalline Fe ($Fe_{o/d}$) shows a negative loading (–0.63) (Table 1). So the variation in PC3 scores for each soil profile (Figure 2) can be taken as a relative index of the dominance of inorganic crytalline (low values) versus non-crystalline (high values) Fe. Crystalline Fe dominates in the soils EUR06 (AZ), EUR10 (CI, except the horizon 4Bwb3), EUR12 (CI), the soils from Greece (EUR13–15) and Hungary (EUR18–20), while non-crystaline Fe dominates in EUR09 (IC), horizon 4Bwb3 of EUR12 (CI), EUR03–04 (IT), the basal horizons of EUR07 (IC, 3BC, 3CB, 4Bw, 4B/Cg) and soil EUR17 (FR). For the Azores, the dominance of well-crystalline Fe compounds is corroborated by the multiple oxalate extractions. A single oxalate extraction extracted only a small fraction of Fe_d in most samples (Meijer et al. this volume).

PC4: effects of organic matter on CEC and nutrient cycles

PC4 extracted 6.3% of the total variance that depends on the sum of bases (SB), the cation exchange capacity (CEC) and the carbon content (C) (Table 1). The factor scores of the horizons for each soil (Figure 2) indicate that this variance is associated with the organic-rich surface horizons, as for example the O horizons of soils EUR02, EUR03, EUR04 and EUR07. This suggests that this principal component reflects the role of organic matter on cation exchange capacity and nutrient cycling (biocycling, mineralization, higher nutrient content) in the surface horizons.

PC5 to PC7: residual variance

The other three principal components with eigen values >1 account for 6.1, 4.9 and 3.7% of the variance (PC5, PC6 and PC7, respectively). The factor

loadings of the properties are low in these PCs except for PC6 that has relatively high loadings for the ratios Al_o/Si_o and Al_{o-p}/Si_o, which refer to the nature of the non-crystalline alumino-silicates. Nevertheless this principal component, as well as the other two, describe anomalies rather than trends. For example, almost all the variation for PC6 is related to very high loadings of soil EUR20 (HG), which has also anomalously large values for the ratios (17–23 for Al_o/Si_o and 13–14 for Al_{o-p}/Si_o). Because the total extracted amounts of Al and Si in these soils are close to the detection limit, the ratios have no meaning and neither has the related PC.

PCA on a smaller set of samples

As it was mentioned previously, some soil properties were not measured in all soil samples. This is the case for the clay content determined by the resin method ($Clay_R$), which is available for only 42 horizons (less than half of the total) distributed as follows: 1 non-andic, 1 organic, 12 vitric, 27 silandic and 1 aluandic horizon. So the PCA analysis for this set of horizons is only representative for the vitric and andic ones.

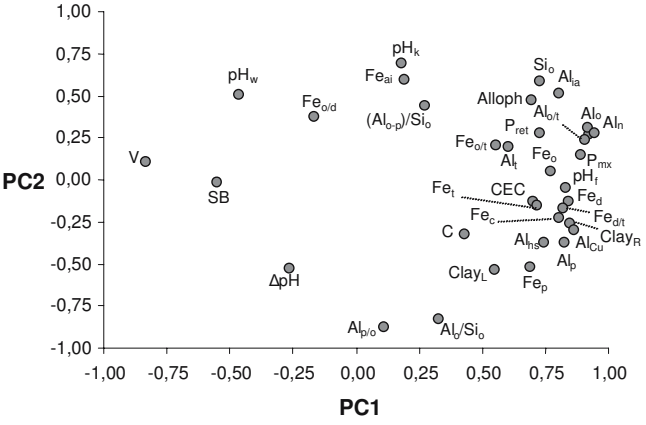

Figure 5. PC1/PC2 projection of loadings of physico-chemical properties of the 42 soil horizons for which the $Clay_R$ was determined. The codes of the properties are in Table 1.

The greater homogeneity of this reduced dataset resulted in only 6 components with eigen values >1 and in a small increase in the variance explained by the first principal component (from 45.8 in the large dataset to 48.1 in the reduced one). In Figure 5 it can be seen that most soil properties kept similar loadings as in the previous analysis (note that the sign of variables in PC2 has changed because the axis has rotated) indicating that they are dominated by the same trends and factors described before. The communality (proportion of the variance of each variable explained by the

set of significant principal components) of ΔpH, proportion of non-crystalline Fe ($Fe_{o/d}$), base saturation (V), proportion of non-crystalline Al bound to organic matter ($Al_{p/o}$) and reactivity to NaF (pHf) is between a 10 and a 20% larger (Figure 6), as a result of the greater homogeneity in the type of horizons included in the analysis. At the same time the communalities of the pH and the ratio $Al_{o\text{-}p}/Si_o$ decreased by 9 and 24%, respectively. This is due to the fact that the soils with higher pH (EUR13–15 from Greece) and the soil with the anomalously high $Al_{o\text{-}p}/Si_o$ ratios (EUR20 from Hungary) were not included in this PCA.

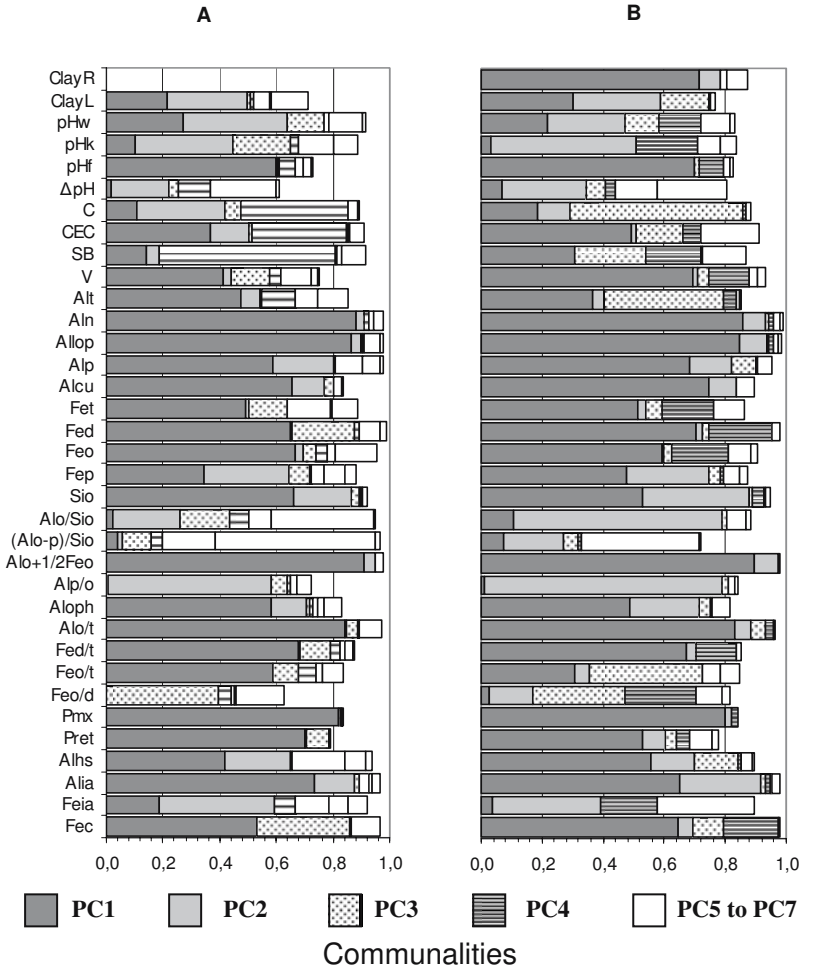

Figure 6. Communalities for the (A) large (94 horizons) and (B) reduced (42 horizons) datasets of physico-chemical properties.

In the PC1/PC2 projection, $Clay_R$ plots to the right of the first axis, indicating that it increases with weathering and pedogenesis (Figure 5). In fact, $Clay_R$ shows a number of significant correlations (r=0.7–0.75) to indices of the degree of weathering, such as the $Fe_{d/t}$ and $Al_{o/t}$ ratios, and other soil properties related to reactive Al (Al_n, Al_p, Al_{Cu}, Al_o+½Fe_o, pH_f) and to phosphorus retention (P_{mx}). It also shows a significant negative correlation with base saturation (V, r= –0.72), but one should be aware that in these soils V decreases with increasing weathering and pedogenesis.

PCA and type of soil horizon

Figure 7 represents the distribution of soil horizons in the PC1/PC2 projection of the PCA for the large dataset. Andic horizons (silandic and aluandic) have slightly negative to positive scores on PC1, while the other (not-andic, organic and vitric) have negative factor scores; the few aluandic horizons appear towards the upper part with larger scores on PC2 than the silandic horizons, in agreement with the association of the Al_p/Al_o ratio to this component. The non-andic, organic and vitric horizons are not well separated in this projection. Most vitric horizons spread from the lower left corner, where the soils from Greece cluster together, to the middle upper part where EUR12 (CI) projects.

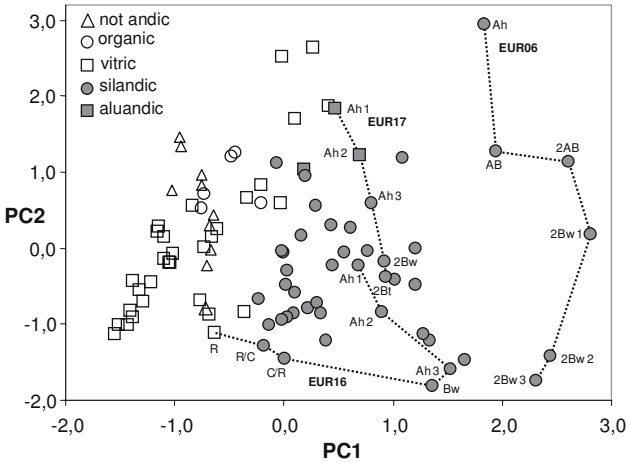

Figure 7. PC1/PC2 plot of the factor scores of the soil horizons.

All horizons of soil EUR06 (AZ) appear at the right of the diagram, indicating the highest degree of soil evolution (weathering and pedogenesis). From top to bottom the horizons follow the profile vertical distribution, in agreement with the profile differentiation character we have attributed to

PC2. Between the AB and the 2AB horizons there is a shift suggesting that the second soil cycle is more evolved than the superficial one. A similar distribution is found for soil EUR17 (FR) although there is almost no change in PC1 and almost all the variation is accounted for by PC2 (Figure 7), and thus it is related to organic matter and properties associated to it. This is also the case for soils EUR10 and EUR11 from the Canary Island and, although with very minor increases in PC2 loading, for the soils from Greece (EUR13–15) and Hungary (EUR18–20).

Another typical pattern is shown by soil EUR16 (FR): the degree of evolution increases from the bottom-most vitric horizon to the base of the A horizon (Ah3, silandic) with negligible contribution of PC2 and then shows a moderate decrease while increasing the contribution of PC2 to the surface soil horizons (Figure 7). This pattern is also found in soil EUR05 (AZ), EUR03 and EUR04 (IT) and highly attenuated in EUR02 (IT).

Soils from Iceland (EUR07–09) and soils EUR10 and EUR12 from the Canary Island have more complicated distributions of PCs scores originating from their complex stratigraphy.

Discriminant analysis

In general terms, the PCA shows a transition from weak developed soils to highly weathered ones, which implies a varying degree of expression of the andic properties. This result suggests that PCA can be complemented with a discriminant analysis (DA), used in a confirmatory way. In DA, each sample is assigned to a known class (vitric, siliandic, alu-andic, organic, non-andic) and the statistics enable to identify a minimum set of variables necessary to support the original classification. In our case the samples are the soil horizons, the classes are the types of horizon and the variables are the physico-chemical properties. Due to the limited number of organic and aluandic horizons, we defined three classes: non-andic (non-andic and organic), vitric, and andic (silandic and aluandic).

Two canonical functions (CFs) explained the observed variance and included seven predictor variables: pH_f, SB, V, Fe_p, $Al_{o\text{-}p}/Si_o$, $Al_{o/t}$ and $Fe_{o/t}$ (Table 3). These two CFs are sufficient for an almost perfect separation of the defined types of horizons (Figure 8), with 95.7% of correctly classified horizons. Only four horizons have a higher probability to belong to a group different from the assigned one: the 4B/Cg of EUR08 and the A/R of EUR18 which were classified as non-andic and appear chemically closer to the vitric; and the 3H of EUR09 and the 2Bwb of EUR11, which were classified as vitric and are chemically more similar to andic.

Table 3. Variables necessary to discriminate between soil groups.

Variable	Andic, vitric and non-andic groups	Andic and non-andic groups
pH-water		X
pH-NaF	X	
Sum Bases	X	
Base saturation	X	
CEC		X
Fe_p	X	
Si_o		X
$(Al_o\text{-}Al_p)/Si_o$	X	
Al_o/Al_t	X	
Fe_o/Fe_t	X	
P-retention		X
% correctly classified horizons	95.7	96.8

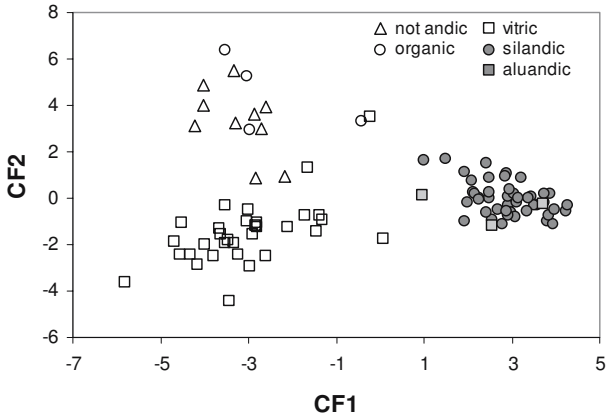

Figure 8. Projection of the soil horizons in the space defined by the two canonical functions obtained by discriminant analysis.

If the classification is simplified two only two groups, non-andic and andic, the percentage of correct classification only increases to 96.8%, but the number of variables necessary to support the classification is reduced to four: pH_w, CEC, Si_o and P_{ret} (Table 3). In both cases the results are consistent with the nature of andic soils and with the criteria required for their characterization.

Conclusions

Multivariate statistical analysis of the physico-chemical properties available in the database of COST action 622 enabled the identification of the

main trends of the pedogenesis in European volcanic soils. Through PCA we determined four main factors affecting the variance: weathering and pedogenesis, profile differentiation, Fe fractionation, and the role of soil organic matter on CEC and nutrient cycles. A residual part of the variance was related to particular soils and soil horizons with anomalous properties.

These factors are related to the development and intensification of the andic nature, that is to say, to the formation of silandic and aluandic horizons. The results of the discriminant analysis indicated that a limited set of chemical properties is sufficient to separate, and thus characterize, the different types of horizons: seven properties if three classes are considered (non-andic, vitric and andic) and only four properties if only two classes are defined (non-andic and andic). These chemical properties are consistent with the criteria currently used in the classification for andic soils.

Although these results are promising, some aspects can be improved to strengthen the analysis: (1) the database of andic volcanic soils must be enlarged, in particular for aluandic and organic horizons; (2) the inclusion of non-volcanic andic soils will potentially enable to define with greater precision the pathways for the development of andic properties; and (3) it is recommended to use other statistical methods which take advantage of the large redundancy of the soils properties like reverse modeling or structural equation modeling (see for example Pugesek et al. 2003).

References

Buurman P, van Doesburg JDJ (2005). Laser-diffraction grain-size analyses of reference profiles (this book)

Martínez Cortizas A, Nóvoa JC, Pontevedra X, Taboada T, García-Rodeja E, Chesworth W (2005). Elemental composition of Reference European Volcanic Soils (this book)

Meijer EL, Buurman P, Fraser A, García-Rodeja E (2005). Extractability and FTIR-characteristics of poorly-ordered minerals in a collection of volcanic ash soils (this book)

Pugesek H, Tomer A, von Eye A (2003). Structural equation modeling. Applications in ecological and evolutionary biology. Cambridge University Press, p 409

Taboada T, García C, Martínez Cortizas A, Nóvoa JC, Pontevedra X, García-Rodeja E (2005). Chemical weathering of Reference European Volcanic Soils (this book)

Appendix materials on CD-Rom

Physico-chemical database.xls (see that chapter)

NaOH and Na-$Na_4P_2O_7$-extractable organic matter in two allophanic volcanic ash soils of the Azores Islands – quantified pyrolysis-GC/MS data and factor analysis

P. Buurman and K.G.J. Nierop

Introduction

In a previous paper (Nierop et al. 2005) we described the general results of pyrolysis-GC/MS of the Azores Andosols EUR05 and EUR06. This previous paper was based on visual comparison of pyrolysis-GC/MS results by chemical group. We found that polysaccharide-derived compounds dominated the chemistry of organic matter in these two allophanic Andosols. Three groups of organic compounds that tend to be important in humus of other soils, i.e. moieties derived from lignin, from lipids and from aliphatic biopolymers such as cutin and suberin were relatively scarce. On the other hand, chitin moieties were present in significant amounts, which is rare in most soils.

The aforementioned study was based mainly on molecular fragments that are commonly found in pyrolysis-GC/MS results. When we interpreted the mass spectra in more detail, we found a large number of polysaccharide-derived and N-containing fragments that are not commonly identified in pyrolysates of soils. We therefore decided to carry out a more detailed analysis, to quantify the pyrolysis products, and to analyze the quantified results by principal components analysis so that differences that are otherwise not apparent would be made visible. Additionally, this might also bring out differences in NaOH- and $Na_4P_2O_7$-extracts that are not evident from visual comparison, and elucidate binding mechanisms in allophanic soils. The present detailed study is based on the same samples and pyrograms as that by Nierop et al. (2005).

Materials and methods

We analysed all samples of the Azores soils EUR05 and EUR06. The samples were first extracted with 0.1 M NaOH and subsequently with 0.1

M $Na_4P_2O_7$. Both extractions were carried out in a N_2 atmosphere to prevent oxidation during extraction. In both the first and the second extraction, the samples were shaken for 24 hours, after which the suspensions were centrifuged for 1 hour at 2200 *g* and decanted to collect the extracts. The extracts were acidified with HCl (to pH=2), dialysed against demineralized water, and freeze-dried. If ash contents were higher than 10%, the material was redissolved, treated with a 0.1 M HF + 0.1 M HCl mixture and dialysed again till neutral pH. All analysed samples had less than 10% ash content.

Curie-point pyrolysis was carried out using a Horizon Instruments Curie Point pyrolyser. Samples were pressed onto Curie Point alloy rods and heated for 5 s at 600°C in a helium atmosphere. The pyrolysis unit was connected to a Carlo-Erba gas chromatograph and the products were separated on a fused silica column (Chrompack, 25 m, 0.25 mm i.d.) coated with CP-Sil-5 (film thickness 0.40 μm). Helium was used as a carrier gas. The initial oven temperature (40°C) was raised at a rate of 7°C min^{-1} to 320°C and maintained at that temperature for 20 minutes. The column was coupled to a Fisons MD-800 mass spectrometer (mass range *m/z* 45–650, ionization energy 70 eV, cycle time 1 s).

Pyrolysis-GC/MS data were obtained for both extracts of all samples. To be able to judge representativity of the results, a number of samples was pyrolysed several times. We made eight repetitions of sample 445(NaOH), three of 445($Na_4P_2O_7$), and two each of 450($Na_4P_2O_7$) and 455($Na_4P_2O_7$). Altogether, 33 pyrograms were obtained. Of these 33 pyrograms, ten were interpreted in detail to obtain the full range of chemical fragments and their retention times. The detailed interpretation yielded some 500 different chemical fragments. After eliminating most of the unidentified ones and those that occurred only once, we chose 192 fragments for quantification. The list of fragments and their retention times is given in Table 1 (on CD). All fragments have been classified according to probable origin or character, which is indicated by codes. All aliphatic biopolymers are identified by their chain length and alkane (e.g. 15:0) or alkene (e.g. 15:1) character. The same holds true for methylketones (Mk) and part of the lipids (Lp). Further codes are Ar= aromatics; Ca= catechols; Ch= chitins; FA= fatty acids; Lg= lignins, N= nitrogen compounds other than chitins; PA= polyaromatics; Ph= phenols; Ps= polysaccharides. Within the groups, numbers are given in order of appearance in the pyrogram.

All fragments are quantified using two characteristic ions. These ions are indicated in Table 1 (on CD). The quantification carried out by the software of the mass spectrometer was carefully checked and corrected if necessary. The total ion current (TIC) of the quantified products was set as

100% and relative amounts were calculated with respect to this sum. This quantification indicates the relative abundance of each of the products, and not their weight percentages.

Principal components analysis using Statistica software (Statsoft) was carried out for the matrix of 33 samples and 192 pyrolysis products. In a second approach, all products with a mean relative abundance of ≤ 0.1% were omitted and the analysis was repeated on the remaining 92, which are indicated in bold type in Table 1.

Results and discussion

All quantified data are on CD (File: *Azores quant.xls*). If the sums of quantified pyrolysis fragments are grouped by chemical origin and character (Table 2), there is no significant difference between the NaOH and $Na_4P_2O_7$ extracts. Comparison of these data with those of agricultural, grassland and forest soils (e.g., Saiz Jimenez and de Leeuw 1986, van Bergen et al. 1997, 1998ab, Bull et al. 1998, 2000, Nierop and Buurman 1998, 1999, Nierop and Verstraten, 2003, Nierop et al. 1999, 2001), peat (Buurman et al. 2005b) and podzols (Buurman et al. 2005a), brings out a few major differences. Most soils have much higher contents of aliphatic biopolymers, lignin pyrolysis products, methyl ketones and phenol-derived compounds. On the other hand, both number of fragments and contents of chitin pyrolysis markers (Stankiewicz et al. 1996) and other N-compounds are exceptionally high in the two Andosols and also polysaccharides are significantly higher. Although quantified pyrolysis data on soil humus are scarce, this suggests that the Andosol humus is considerably different from

Table 2. Average contents (% of Total Ion Current) and standard deviations of chemical groups in NaOH and $Na_4P_2O_7$ extracts.

	NaOH-extract		NaPyr-extract	
Chemical group	Mean	s.d.	Mean	s.d.
Aliphatics	2,28	0,89	2,69	1,60
Aromatics	3,12	0,85	2,68	1,32
Catechols	2,23	0,95	2,54	1,04
Chitins	3,40	0,56	3,47	0,72
Fatty acids	0,70	0,24	1,49	0,74
Lignins	3,17	2,40	1,88	1,70
Lipids	0,25	0,14	0,23	0,15
Methylketones	0,05	0,03	0,14	0,27
N-compounds	10,29	1,86	12,03	1,63
Poly-aromatics	0,07	0,12	0,05	0,06
Phenols	3,66	1,39	3,43	1,50
Polysaccharides	70,73	7,07	69,32	6,58

that encountered in other soils. In the Andosols investigated here, there is no sign of burning or the related increase of (poly)aromatics as observed by Hiradate et al. (2004) on melanic Andosols of Japan. A large number of the compounds encountered by us, especially chitin fragments, N-containing compounds, and some polysaccharide fragments do not appear to be common to other soils. The number of N-containing compound is exceptionally high. Although C/N ratios of the soil humus are not exceptionally low (10–17), the total number of identified N-compounds was 90, of which we selected only 37 for quantification. As Stankiewicz and van Bergen (1998) state, nitrogen-containing compounds in soils are a relatively unexplored area and of many pyrolysis fragments the origin is unknown. Also Schnitzer and Schulten (1998) in their review on soil organic nitrogen give few exclusive sources for nitrogen-containing pyrolysis products.

Notwithstanding the fact that the means of the quantified data show very few significant differences between NaOH and $Na_4P_2O_7$ extracts, factor analysis using all individual compounds gives a completely different picture. In both the total and the reduced data set, three factors explain about 61% of the total variance while eight factors explain 80%. Figure 1 (reduced data set, all fragments >0.1%) shows that all $Na_4P_2O_7$ extracts plot in the upper half of the diagram while all NaOH extracts plot in the lower half. The exception is sample 449(NaOH), which plots in the upper half. This appeared to be a rather poor pyrogram in which many of the minor compounds cannot be recognized. We had no opportunity to repeat this sample, so we will omit it from further discussion. All replicates plot very close in the diagram. Two repetitions of sample 445 (445aN, 445bN) plot at some distance from the other replications, but these pyrograms were clearly of lesser quality than the others so that the main cluster of replicates is more reliable. Both in NaOH and in $Na_4P_2O_7$ extracts, the topsoils of the two profiles (samples 445 and 450) plot towards the left and the subsoils more or less cluster in the right half of the diagram. In both extracts, samples 452 and 453 plot below the other horizons. Buurman et al. (2004) indicate a buried profile beginning either with sample 451 or with 452, and the deviating position of the two samples in the diagram could reflect deviating properties of a buried (top) soil.

Figure 2 gives the factor loadings underlying the differentiation observed in Figure 1. The circle indicates the rather undecomposed lignin, aliphatic (n-alkanes and n-alkenes), and levosugar components. The polysaccharide components Ps17 (3-furancarboxylic acid, methylated) and Ps30 (1,4:3,6-dianhydro-alpha-D-glucopyranose), N compounds N3 and N4 (C1-pyrroles), N14 (benzeneacetonitrile), N21 (2-butyl-4,5-dimethyl-oxazole), N25 (1,3-dihydro-(2H)-indol-2-one), N28 (1-(2,4,6,-trimethyl-

phenyl)-methyl-1H-imidazole), and N33 (diketopiperazine derivative), toluene (Ar2), aliphatics n-C29:1 alkene and n-C33:0 alkane, and finally the chitin fragments Ch2 (4-acetylpiridine), Ch4 (unknown compound), Ch11 (3-acet-amido-5-acetyl-furan) and Ch12 (alpha-D-galactopyranoside/acetylamine compound) plot also in the circle. Most of these compounds have been encountered in pyrolysates of other soils. The nitrogen compounds N1,2,3,4,29 were found in pyrolysates of plant residues after acid hydrolysis (van Bergen et al. 1998). Outside the circle in Figure 2, fragments with negative loadings on Factor 2 are mostly polysaccharide moieties and a few N- and chitin compounds. Most chitin and other N-containing compounds have positive loadings on F2, together with a number of polysaccharide-derived fragments, a large number of which is not common to soils. Especially the smaller polysaccharide pyrolysis products have negative loadings on Factor 2. In podzols, relatively high amounts of such small fragments indicated stronger decay of plant remains (Buurman et al. 2005a). NaOH-extracts plot in the lower half of Figure 1, which may indicate a higher degree of decomposition in the NaOH-extractable material.

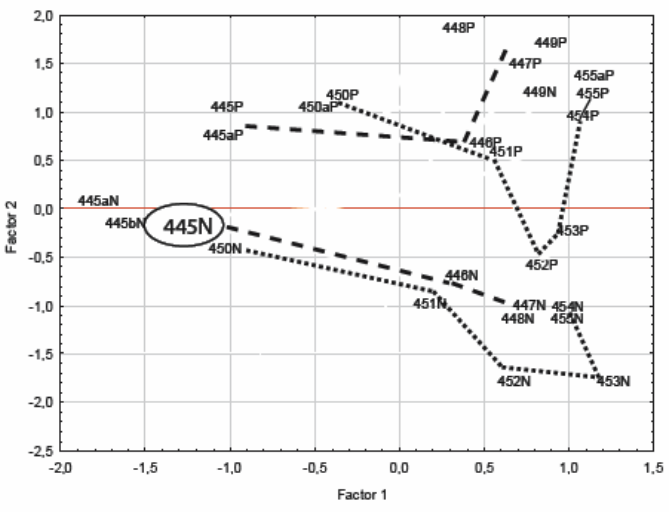

Figure 1. Factor scores in F1F2 space; reduced data set. Dotted line: EUR 06; dashed line: EUR 05. P= $Na_4P_2O_7$ extracts; N=NaOH extracts. The oval contains all but two of the replications of sample 445N.

It is evident that the positions of the surface horizons in Figure 1 reflect the presence in these horizons of relatively fresh plant remains. A shift to the right in Figure 1 obviously represents the effects of decomposition and, because many of the encountered fragments are not clearly plant-derived, a probable influence of microbial and mesofaunal contribution.

The relative importance of the compounds outside the circle is clear from the quantified data (Table 3). In the NaOH extracts, the proportion of

fragments associated with rather undecomposed plant material is between 23 and 28% in Ah horizons and around 14% in the subsoil horizons. In this respect there is little difference between NaOH and $Na_4P_2O_7$ extracts.

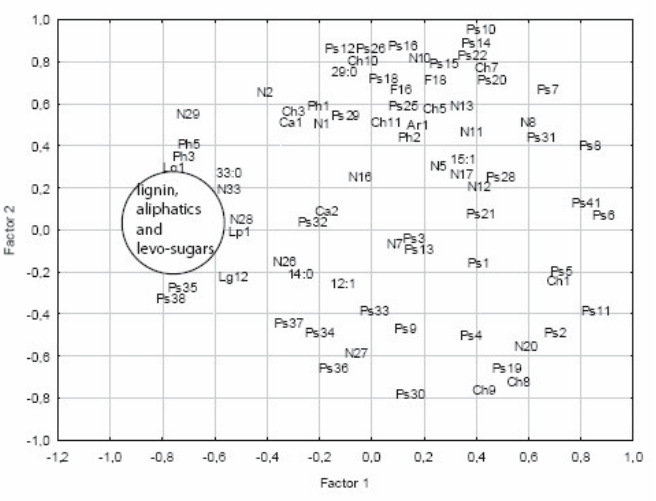

Figure 2. Factor loadings in F1F2 space belonging to Figure 1. Codes of compounds are given in Table 1. Some labels have been slightly displaced to eliminate overlap.

Table 3. Relative proportion of components in left hand cluster of Figure 1 (% of TIC). All components with a score of < –0.4 on Factor 1 have been included.

	Proportion (%) of components in cluster	
	NaOH-extract	$Na_4P_2O_7$-extract
A horizon 445 (EUR 05)	27.9 (3.1)	25.7
A horizon 450 (EUR 06)	23.7	21.6
Subsurface horizons	13.8 (4.9)	13.7 (4.2)

To judge whether the division found in Factor1-Factor2 space was due to decomposition of plant material, we checked whether the various compounds in the right-hand side of Figure 2 were related either with extracts or with residues in peat samples investigated by Buurman et al. (2005b), but we found no clear division. In the upper right part of the diagram plot most polysaccharide, nitrogen-containing, and chitin fragments that were not encountered in peat. When the factor loadings were plotted in F1F3 space, however (Figure 3), there was a clear division between compounds that – in peat – were related to NaOH-extractable material and residues. Virtually all of the compounds that had a positive loading on Factor 3 were either connected to unextractable residues in peat or were not found in peat

samples, while virtually all fragments that had a negative loading on Factor 3 were related to the extractable fraction in peat. This is also true for the total data set. This suggests that negative scores of samples on Factor 3 represent decay of primary plant-derived compounds, while positive scores indicate remnants of native plant material and secondary metabolites contributed by microbial and mesofaunal biomass. The fact that chitin moieties plot in the upper half sustains this interpretation.

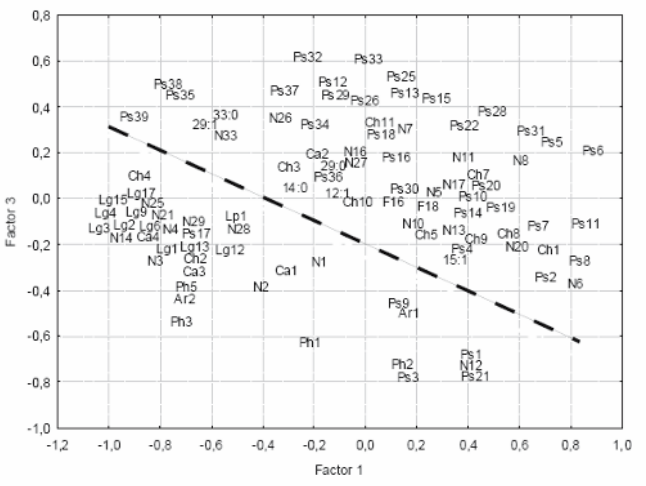

Figure 3. Factor loadings in F1F3 space, reduced data set. Codes of compounds are given in Table 1. Some labels have been slightly displaced to avoid overlap. For explanation of line, see text.

In F1F3 factor space, Ah horizons plot in the left half of the diagram (Figure 4). $Na_4P_2O_7$ extracts of these horizons plot higher and to the right in the diagram, indicating lower contents of undecomposed, plant-derived moieties. All samples of deeper horizons plot to the upper right of a diagonal line.

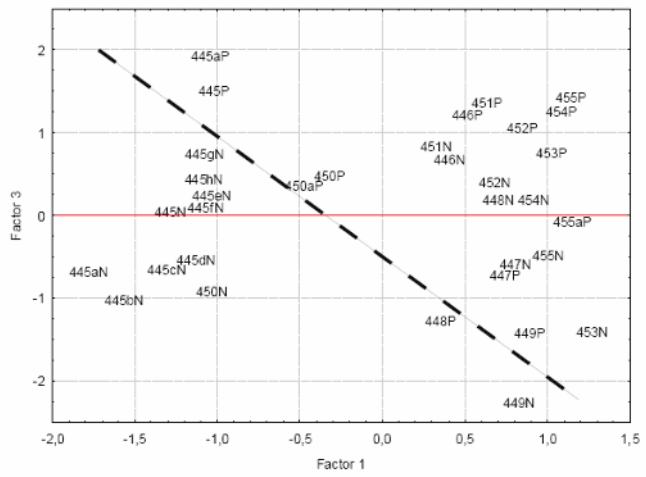

Figure 4. Factor scores in F1F3 space, reduced data set. For explanation of line, see text.

Conclusions

In studies of kaolinitic and smectitic clays, there was evidence that $Na_4P_2O_7$-extracted organic matter had a higher mean age (and thus a slower turn-over time) than NaOH-extractable OM (Wattel et al. 2004). In allophanic soils, the organic fraction extracted by $Na_4P_2O_7$ *after* NaOH extraction was expected to be more strongly bound to the mineral fraction. The present results do not support this thesis. The differences between $Na_4P_2O_7$- and NaOH-extracted material are in relative amount rather than in kind of pyrolysis fragments, so that specific binding is not supported by these data. The fact that unequivocally plant-derived moieties such as lignin fragments and *n*-alkanes/alkenes are of minor importance in these soils contradicts the existence of chemical protection through binding to allophane, Al^{3+} or Fe^{3+} of plant-derived organics. It appears that decay of plant-derived organics is extremely efficient and that microbially and mesofauna-derived moieties represent a large fraction of the soil organic matter. The question arises whether the microbial organic matter is protected against further decay or is constantly replenished. This question still needs to be answered.

References

van Bergen PF, Bull ID, Poulton PR, Evershed PR (1997). Organic geochemical studies of soils from the Rothamsted Classical Experiments – I. Total lipid extracts, solvent insoluble residues and humic acids from Broadbalk Wilderness. Organic Geochemistry 26:117–135

van Bergen PF, Flannery MB, Poulton PR, Evershed RP (1998a). Organic geochemical studies of soils from Rothamsted Experimental Station: III Nitrogen-containing organic matter in soil from Geescroft Wilderness. In: Stankiewicz BA and van Bergen PF (eds) Nitrogen-containing macromolecules in the Bio- and Geosphere. ACS Symposium Series 707:321–33. Oxford University Press, New York

van Bergen PF, Nott CJ, Bull ID, Poulton PR, Evershed RP (1998b). Organic geochemical studies of soils from the Rothamsted Classical Experiments – IV. Preliminary results from a study of the effect of soil pH on organic matter decay. Organic Geochemistry 29:1779–1795

Bull ID, van Bergen PF, Poulton PR, Evershed RP (1998). Organic geochemical studies of soils from the Rothamsted Classical Experiments – II, Soils from the Hoosfield Spring Barley Experiment treated with different quantities of manure. Organic Geochemistry 28:11–26

Bull ID, van Bergen PF, Nott CJ, Poulton PR, Evershed RP (2000). Organic geochemical studies of soils from the Rothamsted classical experiments – V. The

fate of lipids in different long-term experiments. Organic Geochemistry 31:389–408

Buurman P, García Rodeja E, Martínez Cortizas A, van Doesburg JDJ (2004). Stratification of parent material in European volcanic and related soils studied by laser-diffraction grain-sizing and chemical analysis. Catena 56:127–144

Buurman P, van Bergen PF, Jongmans AG, Meijer EL, Duran B, van Lagen B (2005a). Spatial and temporal variation in podzol organic matter studied by pyrolysis-gas chromatography/mass spectrometry and micromorphology. European Journal of Soil Science 56:253–270

Buurman P, Nierop KGJ, Pontevedra Pombal X, Martínez Cortizas A (2005b). Molecular chemistry by pyrolysis-GC/MS of selected samples of the Penido Vello peat deposit, Galicia, N.W. Spain. In: Martini I.P, Martinez Cortizas A, Chesworth W (eds) Peatlands as regulators and monitors of Holocene environmental and atmospheric changes. Elsevier, Amsterdam in press

Hiradate S, Nakadai T, Shindo S, Yoneyama T (2004). Carbon source of humic substances in some Japanese volcanic ash soils determined by carbon stable isotopic ratio, $\delta^{13}C$. Geoderma 119:133–141

Nierop KGJ, Buurman P (1998). Composition of soil organic matter and its water-soluble fraction under young vegetation on drift sand, central Netherlands. European Journal of Soil Science 49:605–615

Nierop KGJ, Buurman P (1999). Water-soluble organic matter in incipient podzols: accumulation in B horizons or in fibers? European Journal of Soil Science 50:701–711

Nierop KGJ, Verstraten JM (2003). Organic matter formation in sandy subsurface horizons of Dutch coastal dunes in relation to soil acidification. Organic Geochemistry 34:499–513

Nierop KGJ, Buurman P, de Leeuw JW (1999). Effect of vegetation on chemical composition of H horizons in incipient podzols as characterized by ^{13}C NMR and pyrolysis-GC/MS. Geoderma 90:111–129

Nierop KGJ, van Lagen B, Buurman P (2001). Composition of plant tissues and soil organic matter in the first stages of a vegetation succession. Geoderma 100:1–24

Nierop KGJ, van Bergen PF, Buurman P, van Lagen B (2005). NaOH and $Na_4P_2O_7$-extractable organic matter in two allophanic volcanic soils of the Azores Islands – a pyrolysis-GC/MS study. Geoderma 127:36–51

Saiz Jimenez C, de Leeuw JW (1986). Chemical characterization of soil organic matter fractions by analytical pyrolysis-gas chromatography-mass spectrometry. Journal of Analytical and Applied Pyrolysis 9:99–119

Schulten HR, Schnitzer M (1998). The chemistry of soil organic nitrogen: a review. Biology and Fertility of Soils 26:1–15

Stankiewicz BA, van Bergen PF, Duncan, IJ, Carter JF, Briggs DEG, Evershed RP (1996). Recognition of chitin and proteins in invertebrate cuticles using analytical pyrolysis/gas chromatography/mass spectrometry. Rapid Communications in Mass Spectrometry, 10,1747–1757

Stankiewicz BA, van Bergen PF (1998). Nitrogen and N-containing macromolecules in the bio- and geosphere: an introduction. In: Stankiewicz BA, van

Bergen PF (eds) Nitrogen-containing macromolecules in the Bio- and Geosphere ACS Symposium Series 707,1–12, American Chemical Society, Washington

Wattel-Koekkoek EJW, Buurman P (2004). Mean residence time of kaolinite and smectite-bound organic matter in Mozambiquan soils. Soil Science Society of America Journal 68:154–161

Appendix materials on CD-Rom

Table 1. Quantified pyrolysis fragments arranged according to chemical group
Azores quant.xls: Excel table of quantified pyrolysis results

Thermally assisted hydrolysis and methylation of organic matter in two allophanic volcanic ash soils from the Azores Islands

K.G.J. Nierop and P. Buurman

Introduction

Andosols contain large amounts of organic carbon, often between 5–25% even at 1 m depth (Andreux 1996). The high contents of soil organic matter (SOM) at relatively great depth is partially the result of burial of soils by additions of volcanic ash, but also surface soils and B horizons tend to have higher C contents than other soils. This latter property is usually ascribed to the formation of complexes of SOM with minerals such as allophane, ferrihydrite and imogolite, and Al/Fe-organic matter interactions (Dahlgren et al. 2004). The SOM-mineral bonds are supposed to stabilize SOM against decomposition, resulting in much longer mean residence times than in any other soil type (Wada and Aomine 1973, Torn et al. 1997) and, consequently, in higher SOM contents.

Only very few studies have focused on SOM composition in volcanic ash soils at the molecular level. Naafs et al. (2004) studied organic solvent extractable lipids, ester-bound moieties were investigated by Naafs and van Bergen (2002ab) and results of analytical pyrolysis were reported by Naafs (2004) and Nierop et al. (2005). These authors reported that lignin was a very minor constituent of SOM and that polysaccharides, and particularly chitin, were present in relatively large amounts as compared with other soils. Lipids were used as source indicator of plants, and ester-bound compounds, especially those derived from cutin and suberin, provided useful information on the contribution of various plant parts to SOM. Together with waxes and sometimes cutan, cutin forms the cuticle of all aerial parts of higher plants, such as leaves, fruits, flowers and seeds. All protective and wound-healing layers of all other plants parts, including barks, woody stems and underground parts (roots, tubers, stolons), contain suberin (Kolattukudy 2001). In some simple cases in terms of vegetation cover, the cutin and suberin composition in soil horizons allow semi-quantitative information on the extent of bioturbation (Nierop and Verstraten 2004).

In this paper, we used Thermally assisted Hydrolysis and Methylation (THM) to study the same Azores profiles (EUR05 and EUR06) as Nierop et al. (2005). We analysed total soil samples instead of NaOH and $Na_4P_2O_7$ extracted SOM, because lipids in particular are less extractable with these solutions than most other SOM constituents. As mentioned above, the conventional pyrolysates of the NaOH and $Na_4P_2O_7$ extracted SOM of these profiles were dominated by polysaccharide-derived products, whereas both lignin and lipids were low in abundance (Nierop et al. 2005). THM using tetramethylammonium hydroxide (TMAH) is a technique complimentary to (conventional) pyrolysis as it methylates hydroxyl and carboxyl groups making the usually very polar compounds that bear these functional groups better GC amenable (Challinor 2001). As a result, this method is well suited to study lignin and lipids with multiple functional groups even at relatively low abundance (e.g. del Río et al. 1998, Nierop 2001). In addition, this technique is less time consuming than hydrolysis-based methods to analyse ester-bound moieties in Andosols (Naafs et al. 2005).

Materials and methods

Site and soil description

We analysed the highly allophanic soils EUR05 and EUR06 (previously N5 and N6) from the Azores Islands (See the Physico-chemical database for inorganic analyses of these profiles).

Profile EUR05 consists of two superposed profiles developed in three ash layers. It is located in extensively grazed grassland on the Island of Faial, Azores. The altitude is 510 m a.s.l. and the parent material is pyroclastic. The temperature regime is mesic and the moisture regime is udic.

Profile EUR06 is developed in two superposed ash layers. It is located on the Island of Pico, Azores, in a plantation forest of *Cryptomeria japonica* with undergrowth of *Pittosporum undulatum, Erica azorica, Rubus* sp., and ferns. The altitude is 400 m a.s.l. and the parent material consists of basaltic pyroclastics similar to profile EUR05. The temperature regime is mesic and the moisture regime is udic. According to Soil Taxonomy (SSS 1999), profile EUR05 is classified as a Medial amorphic mesic Typic Hapludand. Profile EUR06 is a Hydrous amorphic mesic Acrudoxic Hydrudand.

Thermally assisted Hydrolysis and Methylation (THM)

Prior to Thermally assisted Hydrolysis and Methylation (THM), the dried and ground samples were pressed onto Curie-point wires, after which a droplet of a 25% solution of tetramethylammonium hydroxide (TMAH) in water was added to the samples, which were subsequently dried by a Philips 100 W halogen lamp. THM was performed by pyrolyzing the sample for 5 s at 600°C. The Horizon Instruments Curie-Point pyrolyser was connected to a ThermoQuest Trace GC 2000 gas chromatograph and the products were separated by a fused silica column (J & W, 30 m, 0.32 mm i.d.) coated with DB-1 (film thickness 0.50 µm). Helium was used as carrier gas. The oven was initially kept at 40°C for 1 min, next it was heated at a rate of 7°C/min to 320°C and maintained at that temperature for 15 min. The column was coupled to a Finnigan Trace MS quadrupole mass spectrometer (Electron Ionization, ionization energy 70 eV, mass range *m/z* 45–600, cycle time 1 s). With THM, hydrolysable bonds are cleaved and the resulting carboxylic acid and hydroxyl groups are *in situ* transformed into their corresponding methyl esters and methyl ethers (e.g. Challinor 2001). Identification of the compounds was carried out by interpretation of their EI spectra and by their GC retention times.

Results and discussion

Aromatics

The THM results of the Ah horizon of EUR05 shows the presence of aromatic and lipid-derived moieties. The aromatic products included methyl esters of *p*-methoxybenzoic acid, 3,4-dimethoxybenzoic acid and 3,4,5-trimethoxybenzoic acid and those of *p*-methoxycinnamic acid and 3,4-dimethoxycinnamic acid (Figure 1 and Table 1). Most likely, these compounds are mainly derived from lignin (e.g. Clifford et al. 1995). In the pyrolysates of the NaOH and $Na_4P_2O_7$ extracted SOM of this horizon, lignin-derived compounds were prominently present, and their distribution suggested that grasses were the main source (Nierop et al. 2005). However, other polyphenols, such as tannins may also produce such aromatics upon THM (Garnier et al. 2003).

In the THM-GC trace of the Ah horizon of EUR06, the lignin-derived aromatics were dominated by the methyl esters of *p*-methoxybenzoic acid, 3,4-dimethoxybenzoic acid and 3,4,5-trimethoxybenzoic acid. Compared with EUR05, EUR06 contained virtually no *p*-coumaric acid and ferulic acid, which reflects the forest vegetation covering EUR06 as opposed to

the grass vegetation of EUR05. Other compounds that may be related to polyphenols included methoxybenzene, *p*-methoxytoluene, C_2-methoxybenzene and 1,4-dimethoxybenzene (Garnier et al. 2003). All these aromatic compounds were hardly or not identified in the THM-GC traces of the lower horizons of both profiles, which confirms the very low abundance of lignin and tannins in these volcanic ash soils. Combined with the lack of other lignin-derived compounds, such as those with a fully methylated glycerol unit (e.g. Filley 2003) in the Ah horizons, which are usually encountered in THM results of plants and soils, this all indicates the high degree of oxidation of the lignin remnants in the Andosols studied.

Table 1. Aromatic compounds and lipids identified upon THM with retention times and characteristic mass fragments.

Compound	Retention time (min)	Mass fragments*
Methoxybenzene	7.05	65, 78, <u>108</u>
4-Methoxytoluene	9.20	77, 91, 107, 121, <u>122</u>
1,3,5-Trimethylhexahydro-1,3,5-triazine	9.23	57, 86, <u>128</u>
4-Ethyl-1-methoxybenzene	9.43	<u>121</u>, 136
1,2-Dimethoxybenzene	12.00	77, 95, 123, <u>138</u>
1,4-Dimethoxybenzene	12.48	95, <u>123</u>, 138
1,2,4-Trimethoxybenzene	16.57	125, <u>153</u>, 168
4-Methoxybenzoic acid, methyl ester	16.78	<u>135</u>, 166
3,4-Dimethoxybenzoic acid, methyl ester	20.50	165, <u>196</u>
4-Methoxycinnamic acid, methyl ester	22.07	133, <u>161</u>, 192
3,4,5-Trimethoxybenzoic acid, methyl ester	22.78	155, 195, 211, <u>226</u>
3,4-Dimethoxycinnamic acid, methyl ester	25.22	191, 207, <u>222</u>
Alkanoic acid, methyl ester		<u>74</u>, 87, [M-15], [M]
1-Methoxyalkane		<u>55</u>, 57, …., [M-15], [M-32]
ω-Methoxyalkanoic acid, methyl ester		<u>74</u>, 87, 98, [M-47], [M-32], [M-15]
α,ω-Alkanedioic acid, dimethyl ester		74, <u>98</u>, 111, [M-105], [M-73], [M-31]

* Underlined mass fragment is base peak.

Only one prominent aromatic fragment, 1,2,4-trimethoxybenzene, which is generally attributed to polysaccharides (Fabbri and Helleur 1999, Schwarzinger et al. 2002), was identified throughout both soil profiles upon THM. Other typical products that were present in the THM-GC traces of all soils and which originate from carbohydrates included the isomers of methylpentenoic acid, methyl ester and tri-O-methyl-3-deoxy-aldaric acids, dimethyl esters and tetra-O-methyl-3-deoxyhexonic acids, methyl esters (Fabbri and Helleur 1999, Tanczos et al. 2003). As they are not the focus of this study, these polysaccharides-derived compounds are not indicated in the Figures. With depth the polysaccharide-derived THM products decreased relatively, which contradicts the results of conventional

pyrolysis (Nierop et al. 2005). However, it may well be that the differences in sensitivity of both techniques towards various compounds may explain this apparent discrepancy; i.e. THM is much more sensitive to, for example, long-chain lipids than conventional pyrolysis. 1,3,5-Trimethylhexahydro-1,3,5-triazine is probably a by-product of the reaction of TMAH with SOM.

Lipids

The aliphatic compounds in both profiles were dominated by methyl esters of *n*-alkanoic acids (C_{14}–C_{34}), with an even-over-odd predominance (Figures 1 and 2). Other prominent compounds were the methyl esters of C_{16}, C_{22} and C_{24} ω-methoxyalkanoic acids, which are typical products of cutin and suberin upon THM (e.g. del Río et al. 1998, Nierop 2001). In addition, dimethyl esters of α,ω-alkanedioic acids, with the same chain lengths as the methylated ω-hydroxyalkanoic acids, were identified. In contrast to ω-hydroxyalkanoic acids, α,ω-alkanedioic acids are derived from suberin only (Kolattukudy 2001). In the Ah horizon of EUR05, the lack of di- and trihydroxyalkanoic acids (diagnostic for grass cutin but generally not present in suberin of grasses), strongly suggests that root contribution exceeded that of surface litter. Similarly, the Ah horizon was the only horizon of EUR06 that contained appreciable amounts of cutin- and suberin-derived ω-hydroxyalkanoic acids and α,ω-alkanedioic acids. Here, and in contrast to EUR05, the predominance of the C_{16} member over C_{22} and C_{24} within the ω-hydroxyalkanoic acids suggests an input of cutin rather than of suberin.

Another prominent product encountered after THM of the Ah horizon of EUR05 was methylated C_{26} alkanol, which is typical of grass foliar material (Nierop et al. 2001). Although clearly present, its abundance with respect to e.g. ω-hydroxyalkanoic acids is far lower than in that of fresh grass leaves (Nierop et al. 2001), thereby confirming the rather low input of grass foliar material to the Ah horizon.

Only small amounts of cutin- and suberin-derived compounds were present in the 2Ahb (EUR05) and AB1 horizons (EUR06), while all deeper horizons lacked these compounds as determined by THM. The absence of these plant-derived biopolymers agrees with our results from conventional pyrolysis that showed hardly any (plant-derived) lipids and lignin below the Ah horizon (Nierop et al. 2005). Such a small contribution of cutin and suberin-derived lipids in the lower horizons of the Azores profiles contrasts with data of Andosols from Madeira studied by Naafs et al. (2005). These authors found cutin and suberin throughout the whole soil profile,

with a relative increase of suberin with depth. The higher pH of the Azores profiles may have caused the lower abundance of lipid-derived compounds in EUR05 and EUR06 as lipids accumulate with decreasing soil pH (e.g. Nierop et al. 2003). Other factors, such as different climatic conditions, might also induce differences in lipid stability between Azores and Madeira Andosols.

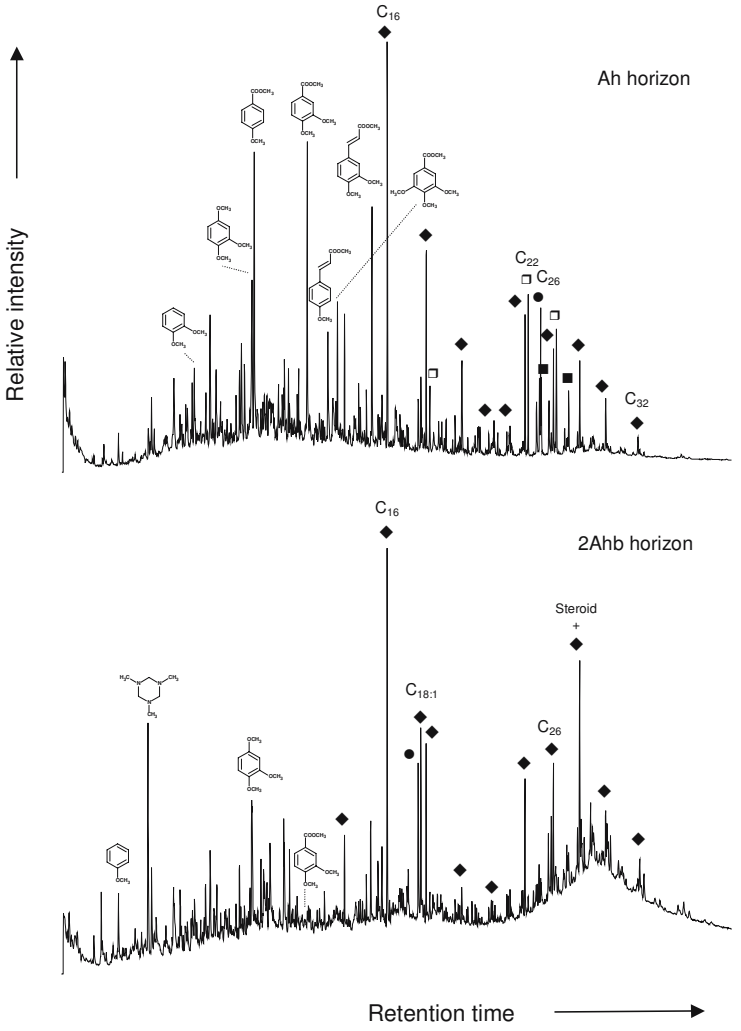

Figure 1. Gas chromatogram of the thermally assisted hydrolysis and methylation products of EUR05 (Ah and 2Ahb horizon). Legend: ◆: alkanoic acid; ●: 1-alkanol; ❐: ω-hydroxyalkanoic acid; ■: α,ω-alkanedioic acid. $C_{n:1}$: indicates chain length, and when appropriate the number of double bonds. All compounds measured as methyl esters and/or ethers.

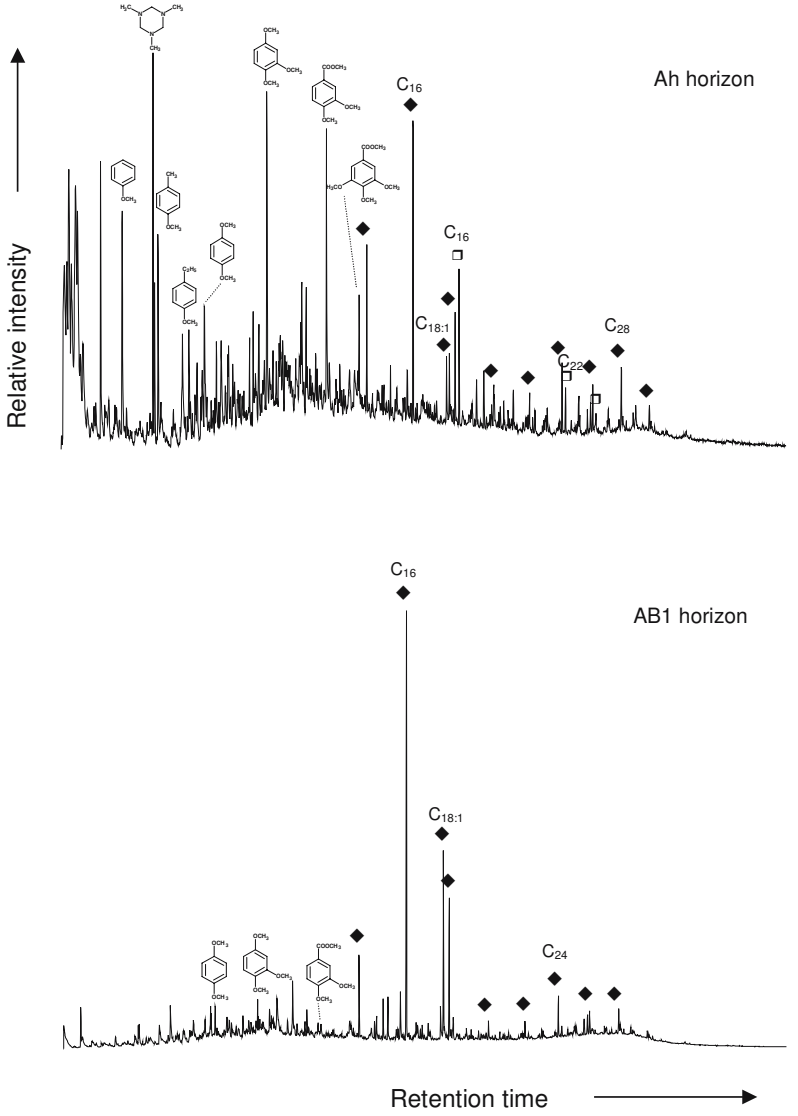

Figure 2. Gas chromatogram of the thermally assisted hydrolysis and methylation products of EUR06 (Ah and AB1 horizon). For legend, see Figure 1.

In EUR05, the contribution of even numbered long-chain alkanoic acids (>C_{20}) decreased with depth relative to the short-chained ones (C_{14}–C_{18}) (Figure 3). The short-chain alkanoic acids can have multiple sources including plants and microbes, while the longer ones are probably mainly derived from plants or insects (Amblès et al. 1994). As we found mainly

non-plant derived SOM in the lower horizons, including many chitin markers (Nierop et al. 2005), these long-chain acids may, for a significant part, be derived from insects.

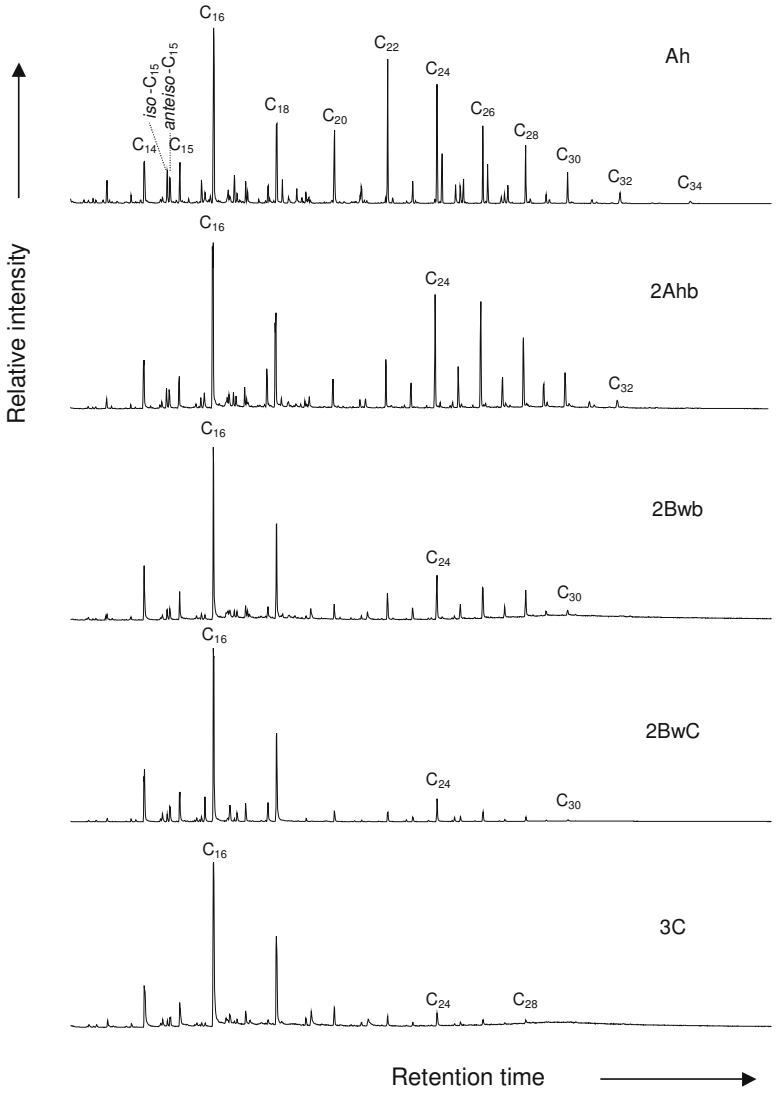

Figure 3. Partial mass chromatogram of methyl esters of alkanoic acids (*m/z* 74+87) of EUR05 profile. C_n indicates chain length.

EUR06 showed a different behaviour of the relative abundance of even-numbered long-chain alkanoic acids with respect to the C_{14}–C_{18} alkanoic acids (Figure 4). From the Ah to AB2 horizon they decreased, but further down to the 2Bw3 horizon they increased relatively. This change can probably be ascribed to the fact that the horizons below the AB2 represent a buried profile. The horizon designated as 2Bw1 may in fact be a buried Ah horizon. Apart from the present Ah horizon, the distribution of C_{20}–C_{30} maximized at C_{24}. This maximum was also present in all horizons below the Ah horizon of EUR05. In addition, the Ah horizon of EUR06 showed a relatively high contribution of unsaturated C_{16} and C_{18} alkanoic acids, which decreased with depth. These unsaturated acids are the main constituents of mono-, di- and triacylglycerides (Amblès et al. 1994). Their decrease with depth most likely reflects a combination of a decreasing input of plant material combined with a more rapid degradation in soil of unsaturated compounds compared to saturated ones (Mouçawi et al. 1981).

Next to the even-numbered acids, odd numbered alkanoic acids (C_{15}–C_{31}) were identified in both profiles. Together with the corresponding *iso*- and *anteiso* isomers, the C_{15} and C_{17} alkanoic acids are associated with bacteria. These branched acids decrease relatively with depth, which is in accordance with Nierop et al. (2005), but increase relatively compared with long-chain acids ($>C_{20}$). Odd-numbered alkanoic acids with chain lengths greater than C_{21} are typical of higher plants. They may have been derived from oxidized alkanes, which were converted into the corresponding acids (Amblès et al. 1994).

Overall, the relative abundance of lipids decreased with depth in comparison with other compounds. Such a decrease was also observed by Naafs et al. (2004) in an andic profile from Madeira island and ascribed to a lower input of lipids due to lower input of plant material with depth, to selective degradation of lipids and to a possible incorporation of lipids into macromolecular entities. As THM as used in our study, i.e. performed at 600°C, cleaves also macromolecular SOM, the latter possibility is not very likely.

Conclusions

Thermally assisted Hydrolysis and Methylation was used to analyse in more detail the aromatic and aliphatic building blocks of the organic matter of two soil profiles from the Azores. Both Ah horizons showed significant contributions of lignin, tannins, cutin and suberin, which were virtually absent from the underlying horizons. Alkanoic acids were present

throughout both soil profiles, with long-chain acids (>C_{20}) decreasing with depth in comparison with short-chain acids in EUR05, whereas having a relative minimum in AB2 and 2Bw1 horizons in EUR06. Despite the huge potential of Andosols to store carbon, the studied soils did not exhibit a great preservation potential of *plant*-derived molecules (lignin, cutin/suberin-derived lipids, C_{26} alkanol) in comparison with other soils as studied by THM. By contrast, bacterial-derived branched alkanoic acids are better preserved than the plant-derived alkanoic acids, which confirms the high degree of microbial and insect-derived OM in the Andosols studied.

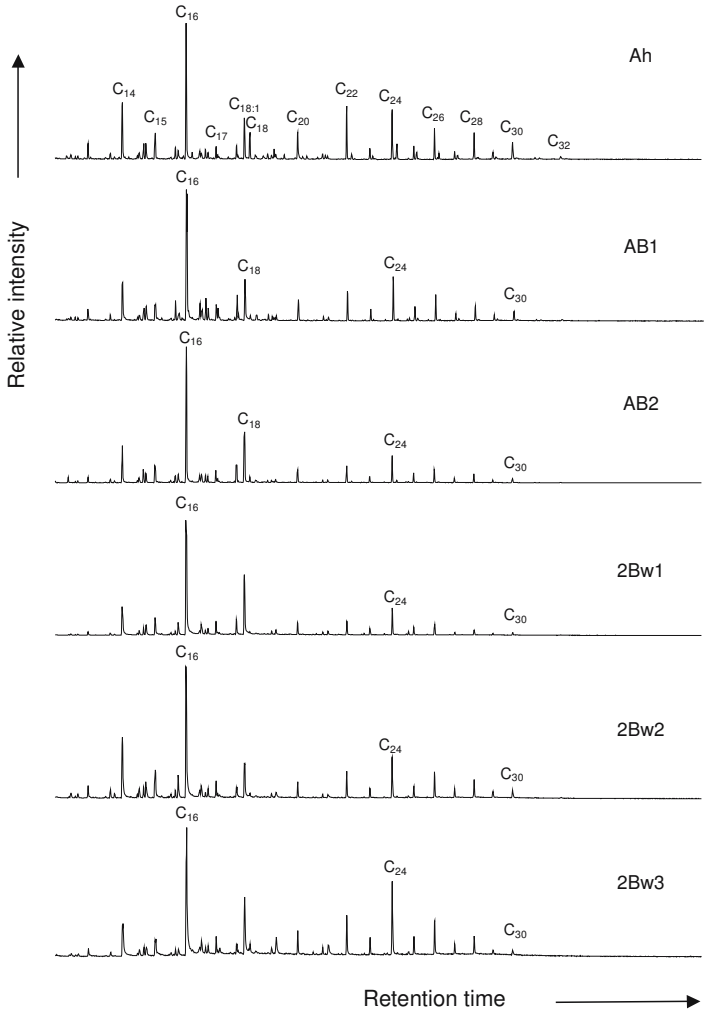

Figure 4. Partial mass chromatogram of methyl esters of alkanoic acids (*m/z* 74+87) of EUR06 profile. C_n indicates chain length.

References

Amblès A, Jambu P, Parlanti E, Joffre J, Riffe C (1994). Incorporation of natural monoacids from plant residues into an hydromorphic forest podzol. European Journal of Soil Science 45:175–182

Andreux F (1996). Humus in world soils. In: Piccolo A (ed) Humic substances in terrestrial ecosystems. Elsevier, Amsterdam, pp 45–100

Challinor JM (2001). Review: development and applications of thermally assisted hydrolysis and methylation reactions. Journal of Analytical and Applied Pyrolysis 61:3–34

Clifford DJ, Carson DM, McKinney DE, Bortiatynski JM, Hatcher PG (1995). A new rapid technique for the characterization of lignin in vascular plants: thermochemolysis with tetramethylammonium hydroxide (TMAH). Organic Geochemistry 23:169–175

Dahlgren RA, Saigusa M, Ugolini FC (2004). The nature, properties and management of volcanic soils. Advances in Agronomy 82:113–182

del Río JC, McKinney DE, Knicker H, Nanny MA, Minard RD, Hatcher PG (1998). Structural characterization of bio- and geo-macromolecules by off-line thermochemolysis with tetramethylammonium hydroxide. Journal of Chromatography A 823:433–448

Fabbri D, Helleur R (1999). Characterization of the tetramethylammonium hydroxide thermochemolysis products of carbohydrates. Journal of Analytical and Applied Pyrolysis 49:277–293

Filley TR (2003). Assessment of fungal wood decay by lignin analysis using tetramethylammonium hydroxide (TMAH) and ^{13}C-labeled TMAH thermochemolysis. In: Goodell B, Nicholas DD, Schultz TP (eds) Wood deterioration and preservation: advances in our changing world. ACS Symposium Series 845:119–139

Garnier N, Richardin P, Cheynier V, Regert M (2003). Characterization of thermally assisted hydrolysis and methylation products of polyphenols from modern and archaeological vine derivatives using gas chromatography-mass spectrometry. Analytica Chimica Acta 493:137–157

Kolattukudy PE (2001). Polyesters in higher plants. In: Scheper T (ed) Advances in Biochemical Engineering/Biotechnology, vol. 71, Springer-Verlag, Berlin Heidelberg, pp 1–49

Mouçawi J, Fustec E, Jambu P, Jacquesy R (1981). Decomposition of lipids in soil: free and esterified fatty acids, alcohols and ketones. Soil Biology and Biochemistry 13:461–468

Naafs DFW (2004). What are humic substances? A molecular approach to the study of organic matter in acid soils. PhD Thesis, University of Utrecht, p 162

Naafs DFW, van Bergen PF (2002a). A qualitative study on the chemical composition of ester-bound moieties in an acidic andosolic forest soil. Organic Geochemistry 33:189–199

Naafs DFW, van Bergen PF (2002b). Effects of pH adjustments after base hydrolysis: implications for understanding organic matter in soils. Geoderma 106:191–217

Naafs DFW, van Bergen PF, Boogert SJ, de Leeuw JW (2004). Solvent extractable lipids in an acid andic forest soil – variations with depth and season. Soil Biology and Biochemistry 36:297–308

Naafs DFW, Nierop KGJ, van Bergen PF, de Leeuw JW (2005). Changes in the molecular composition of ester-bound aliphatics with depth in an acid andic forest soil. Geoderma 127:130–136 (doi:10.1016/ j. geoderma. 2004.11.022)

Nierop KGJ (2001). Temporal and vertical organic matter differentiation along a vegetation succession as revealed by pyrolysis and thermally assisted hydrolysis and methylation. Journal of Analytical and Applied Pyrolysis 61:111–132

Nierop KGJ, Pulleman MM, Marinissen JCY (2001) Management induced organic matter differentiation in grassland and arable soil. A study using pyrolysis techniques. Soil Biology and Biochemistry 33:755–764

Nierop KGJ, Naafs DFW, Verstraten JM (2003). Occurrence and distribution of ester-bound lipids in Dutch coastal dune soils along a pH gradient. Organic Geochemistry 34:719–729

Nierop KGJ, Verstraten JM (2004). Rapid molecular assessment of the bioturbation extent in sandy soil horizons under pine using ester-bound lipids by online thermally assisted hydrolysis and methylation-gas chromatography/mass spectrometry. Rapid Communications in Mass Spectrometry 18:1081–1088

Nierop KGJ, van Bergen PF, Buurman P, van Lagen B (2005). NaOH and $Na_4P_2O_7$ extractable organic matter in two allophanic volcanic ash soils of the Azores Islands – a pyrolysis-GC/MS study. Geoderma 127:36–51 (doi: 10.1016/j.geoderma.2004.11.003)

Soil Survey Staff (1999). Soil Taxonomy, a Basic System of Soil Classification for Making and Interpreting Soil Surveys, 2nd edn. Agriculture Handbook 436, US Dept. of Agriculture, Washington DC

Schwarzinger C, Tanczos I, Schmidt H (2002). Levoglucosan, cellobiose and their acetates as model compounds for the thermally assisted hydrolysis and methylation of cellulose and cellulose acetate. Journal of Analytical and Applied Pyrolysis 62:179–196

Tanczos I, Schwarzinger C, Schmidt H, Balla J (2003). THM-GC/MS analysis of model uronic acids of pectin and hemicelluloses. Journal of Analytical and Applied Pyrolysis 68–69:151–162

Torn MS, Trumbore SE, Chadwick OA, Vitousek PM, Hendricks DM (1997). Mineral control of soil organic carbon storage and turnover. Nature 389:170–173

Wada K, Aomine S (1973). Soil development on volcanic material during the Quaternary. Soil Science 116:170–177

Heavy metal sorption by andic and non-andic horizons from volcanic parent materials

H. Tanneberg and R. Jahn

Introduction

Due to large and chemically reactive inner and outer surfaces, soils in general have huge capacities to bind heavy metals (HM), either naturally inherited from the parent rock or from anthropogenic sources. Heavy metals, compared to other harmful substances, have a high persistence in ecosystems and can accumulate over long periods of time.

Metals may precipitate or adsorb to humic substances, clay minerals, oxides and hydroxides. Mechanisms of metal binding in soil include specific and unspecific adsorption, ionic exchange, complexation and precipitation at surfaces as well as chemical precipitation (Roehl 1997). Adsorption of trace elements, governed by ion association, ion exchange and rapid sorption usually occurs within seconds to a few hours (Sparks 2000). Some metals bind so strongly that they become more or less unavailable to plants. Depending on the type of metal and the soil properties, soils may release a portion of the metals they contain into the soil solution. Metals dissolved in the soil solution are available to plants and organisms (bioavailable) and can be transported to ground and surface water.

Although vitally important for environmental protection in many regions of the world, information on reaction of metals in soils derived from volcanic parent materials (Andosols) is scarce. For these soils, typically having large contents of organic matter, in general a large sorption capacity for heavy metals can be assumed. In addition to organic complexes, many trace metals can also form surface complexes with aluminol and silanol groups at the surfaces of Si and Al oxides. Similar reactions can be assumed for allophane and imogolite, but few studies have addressed these minerals (Clark and Mc Bride 1984). The large contents of organic matter as well as of allophane, allophane-like phases, and oxides result in a dominance of variable charge sites in Andosols. Thus, the sorption of trace elements likely is highly pH-depended (Abd-Elfattah and Wada 1981). In order to predict the fate of heavy metals in Andosols, we carried out batch

experiments. In particular, we aimed at estimating the binding and release of metals at different pH values

Materials and methods

Horizons of COST profiles without vitric or andic properties EUR01 (Italy; Eutric Humi-Tephric Regosol) and with andic properties EUR03 (Italy, Dystric Fulvi-Silandic Andosol); and EUR06 (The Azores, Umbric and Acoxic Hydri-Silandic Andosol) were selected for major differences in contents of organic matter and short-range ordered minerals (Figure 1). For comparison, an Ap-horizon of a Siltic Chernozem (Germany) without short range ordered minerals was included. Whereas the Siltic Chernozem has an illitic clay fraction, EUR01 and EUR06 (EUR03 no data) contain only very small amounts or traces of phyllosilicates. In EUR01, the recognisable phyllosilicates were very small amounts of illite and kaolinite with negligible amounts of vermiculite (Ap and Bw2) and traces of halloysite in Bw2, while EUR06 contained very low amounts of a vermiculite-like phase, a 1.0 nm mineral and kaolinite in (Monteiro et al. this book).

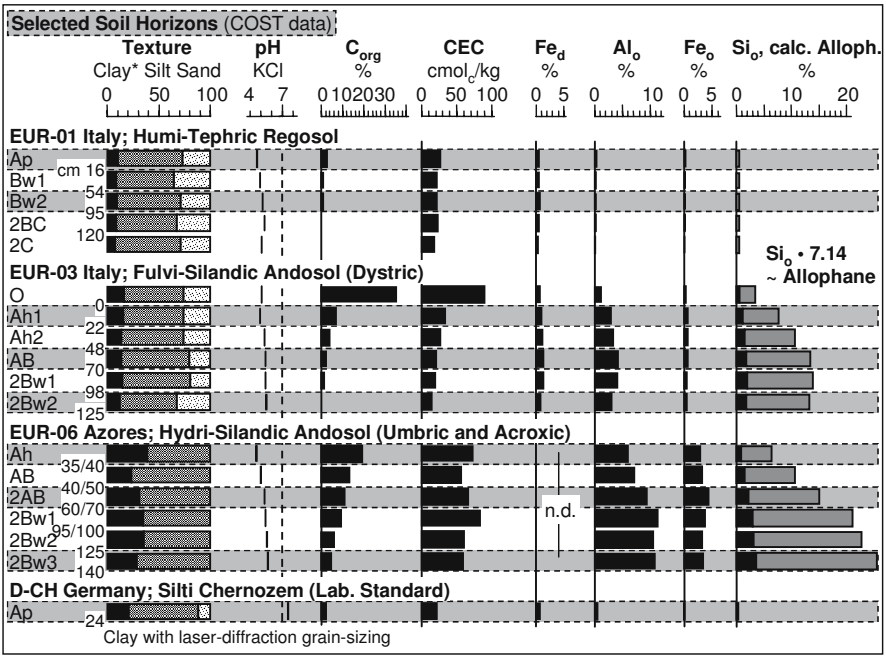

Figure 1. Selected data of the investigated soil samples.

Results of adsorption and desorption experiments depend strongly to experimental conditions. In general, we followed the experimental design as outlined in the OECD Guideline 106 (OECD 1981), using a soil-to-solution ratio of 1 to 5 and a 0.01M $CaCl_2$ background solution. The methods were slightly modified to cope with the limited materials available. We used field moist samples (stored in plastic bags) with known water content. All results were normalized to oven-dry (105ºC) soil mass.

For testing the sorption kinetics, 50 ml 0.01 M $Ca(NO_3)_2$ solution containing 300 mg l^{-1} of Cd, Pb, Cu, Ni, and Cr as nitrates were added at ambient pH to 2 g of soil material (based on dry weight). After 0.17, 0.33, 0.5, 0.67, 1.3, 2.7, 5.3, 10.7, 21.3, 45.3, 69.3 and 117 hours of shaking the suspensions were centrifuged and 0.5 ml of the supernatant was removed for determination of metal concentrations.

The pH-dependent sorption of heavy metals was tested in batch experiments at pH 7, ambient pH and pH 4. Samples equivalent to 2 g oven-dry soil were first equilibrated in $Ca(NO_3)$ solutions for 2 days after adjusting the of pH of the suspensions to 7 or 4 by adding either NaOH or HCl. Then $Ca(NO_3)_2$ solutions containing nitrate salts of Cd, Pb, Cu, Ni, and Cr were added and the pH of the suspension was readjusted. The final concentrations of heavy metals in solution were 1, 5, 10, 20, 50, 100, 200 and 300 mg l^{-1}. Total solution amounted to 10 ml. Samples where shaken for 48 hours, then centrifuged, the supernatants filtered and analysed for metals.

Desorption was evaluated on the samples with the highest metal loading. Samples were consecutively shaken 10 times for 24 hours in 20 ml 0.01 M $Ca(NO_3)_2$. Concentration of metals was measured in the supernatants after centrifuging and filtering.

Determination of the metals was carried out by flame-atomic absorption spectrophotometry and inductively coupled plasma-optical emission spectroscopy (ICP-OES).

Results and discussion

Kinetics of adsorption

Adsorption can be distinguished into fast processes that take place within seconds to hours and slow processes that need hours to days (Sparks 2000). Fast sorption is due ion association and ion binding whereas slow sorption processes include diffusion into micropores and interlayer spaces as well as the formation of surface precipitates.

The sorption capacity varies from metal to metal and from horizon to horizon (Figure 2, Table 1). In general, we found high sorption capacities

and no clear sorption maximum (see next section). The sorption by the COST samples at ambient pH, with soil pH values ranging from 4.6 to 5.7, was always smaller and slower than that of the reference sample (Chernozem Ap, pH 7.5).

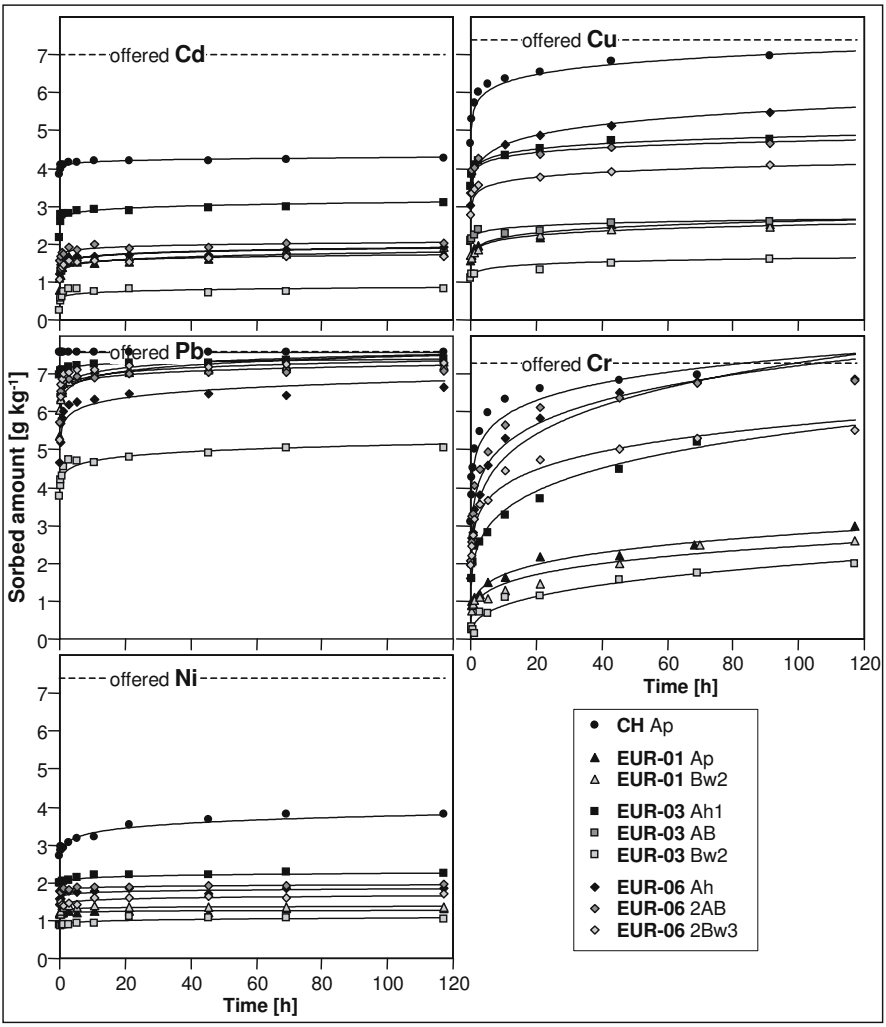

Figure 2. Time dependent sorption of Cd, Pb, Ni, Cu and Cr (2 g soil in 50 ml 0.01 M $Ca(NO_3)_2$ solution containing 300 mg HM l^{-1}, ambient pH).

The rapid sorption kinetics suggests that, in all samples, ion association, ion exchange and rapid sorption govern the sorption of HM. On average, sorption within the first 10 minutes accounted for 59% Cd, 79% Pb, 87%

Ni and 68% Cu of the total amount sorbed over 117 hours (nearly 5 days) by the COST-samples. Only for Cr the sorption was distinctly slower for all samples (27%), especially in EUR03-Bw2 (12%), which is probably due to the formation of inner-sphere surface complexes. The exchange of water molecules from hydrated Cr^{III} is known to be a slow process (Fukushima et al. 1995), and consequently the formation of inner-sphere surface complexes is delayed. Jin et al. (1987) reported that the sorption of Cr^{III} onto humic substances in batch experiments did not reach equilibrium within seven days.

Table 1. Time-dependent sorption of Cd, Pb, Ni, Cu and Cr (2 g soil in 50 ml 0.01 M $Ca(NO_3)_2$ solution containing 300 mg HM l^{-1}, ambient pH).

	pH	Sorbed in 117 h					In % of offered					$Sorbed_{10\ min}$ in % $sorbed_{117\ h}$				
	(KCl)	Cd	Pb	Ni	Cu	Cr	Cd	Pb	Ni	Cu	Cr	Cd	Pb	Ni	Cu	Cr
		---------- g kg^{-1} ----------					---------- % ----------					---------- % ----------				
CH Ap	7.5	4.26	7.56	3.82	6.98	7.01	61	100	52	94	96	90	100	70	67	44
EUR-01 Ap	4.7	1.78	7.32	1.31	2.60	2.99	25	97	18	35	41	45	73	91	60	33*
EUR-01 Bw2	5.2	1.92	7.23	1.35	2.50	2.59	27	96	18	34	36	58	84	88	68	29*
EUR-03 Ah1	4.9	3.09	7.39	2.24	4.82	5.79	44	98	30	65	79	70	94	88	73	28*
EUR-03 AB	5.4	n.b.	n.b.	n.b.	2.67	n.b.	n.b.	n.b.	n.b.	36	n.b.	n.b.	n.b.	n.b.	79	n.b.
EUR-03 Bw2	5.5	0.82	5.05	1.04	1.65	1.99	12	67	14	22	27	32	75	84	68	12*
EUR-06 Ah	4.6	1.92	6.66	1.84	5.58	6.86	27	88	25	75	94	63	70	85	54	23
EUR-06 2AB	5.4	2.02	7.09	1.96	4.72	6.83	29	94	27	64	94	78	81	91	71	30
EUR-06 2Bw3	5.7	1.66	7.30	1.72	4.07	5.51	24	96	23	55	76	65	72	82	68	36
Average EUR	5.2						27	91	22	48	64	59	79	87	68	27

* 20 min.

Neglecting the Chernozem with a much higher ambient pH and the general high sorption of Pb, the different sorption values after 117 hours of Cu and Cr at ambient pH show a fairly high correlation with the content of organic carbon (R^2=0.81 and 0.72) reflecting a higher affinity of these elements to organic matter than for Ni and Cd (Alloway 1995).

Adsorption isotherms

The adsorption of HM at different pH (Figure 3) was described by the Freundlich approach and the adsorption coefficient K_F (Table 2) was calculated. In contrast to the model of Langmuir (1918), the empirical Freundlich model describes systems with multiple layers of molecule adsorbed on surfaces. For small sorbate additions, where sorption sites are not limited, both models give similar results but they differ at higher sorbate additions. Freundlich isotherms are widely used to describe the sorption of HM in soils (e.g. Gerth and Brümmer 1979, Buchter et al. 1989,

Michenfelder 1993, Filius 1993, Swarup et al. 1994, Welp and Brümmer 1998, Krauss et al. 2002) and allow, under defined conditions, comparison of soils with different properties. The Freundlich coefficient K_F reflects the affinity of a certain metal to a given soil (at an equilibrium concentration of 1 mg l^{-1}). The Freundlich model correctly described the sorption of HM to the studied samples at all pH values, except for Cr and for Pb and Cu at pH 7. If the Freundlich isotherms cannot be calculated, precipitation processes have interfered with the adsorption behaviour. K_F values for adsorption and desorption of the studied metals and soils are listed in Table 2.

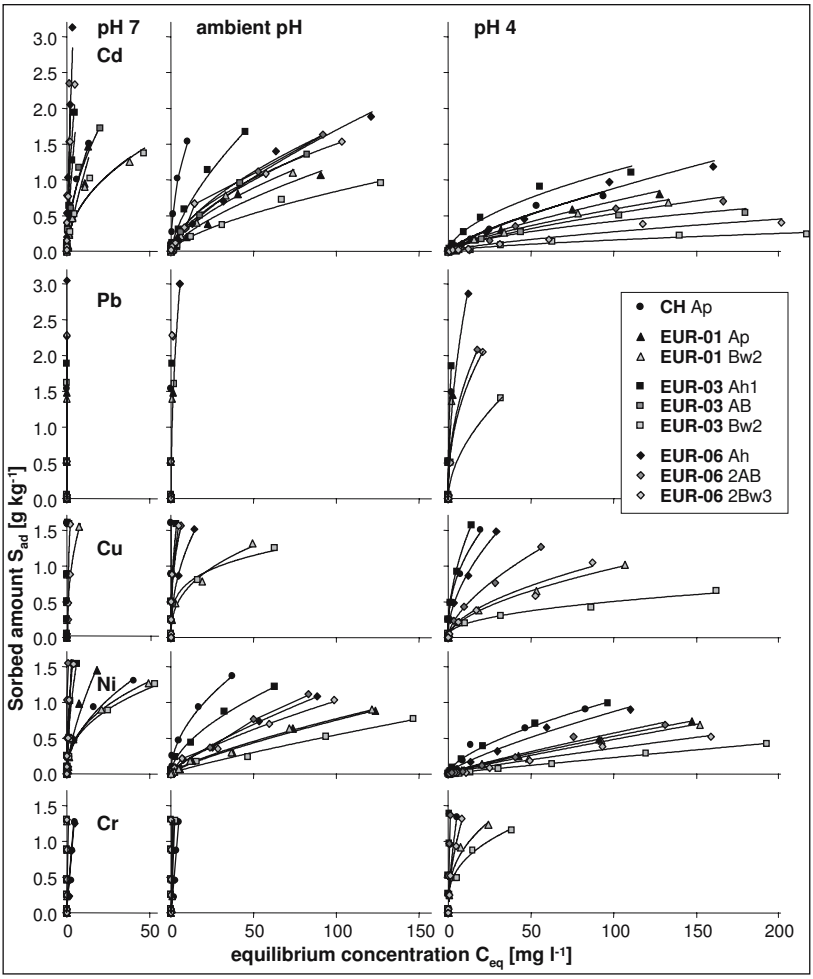

Figure 3. Adsorption isotherms for Cd, Pb, Cu, Ni and Cr at different pH (2 g soil in 10 ml 0.01 M $Ca(NO_3)_2$ solution containing up to 300 mg HM l^{-1}).

Table 2. Freundlich-constants (KF) for adsorption and desorption of Cd, Pb, Cu, Ni and Cr (2 g soil in 10 ml 0.01 M $Ca(NO_3)_2$ solution containing up to 300 mg HM l^{-1}).

Horizon	K_F Cd_{ad}	K_F Cd_{des}	K_F Pb_{ad}	K_F Pb_{des}	K_F Cu_{ad}	K_F Cu_{des}	K_F Ni_{ad}	K_F Ni_{des}	K_F Cr_{ad}	K_F Cr_{des}
pH 7										
CH Ap	332	762	n.c.	n.c.	n.c.	n.c.	208	923	97	7806
EUR01 Ap	171	416	n.c.	n.c.	n.d.	n.d.	222	669	n.d.	n.d.
EUR01 Bw2	229	301	n.c.	n.c.	n.c.	n.c.	249	714	n.c	4320
EUR03 Ah1	499	663	n.c.	n.c.	n.c.	n.c.	555	715	n.c.	7582
EUR03 AB	366	396	n.d.	n.d.	n.d.	n.d.	n.d.	n.d.	n.d.	n.d.
EUR03 Bw2	234	264	n.c.	n.c.	1227	1586	243	604	n.c.	2805
EUR06 Ah	1195	751	n.c.	n.c.	n.c.	n.c.	568	483	363	8247
EUR06 2AB	1383	713	n.c.	n.c.	n.c.	n.c.	1609	788	n.c.	n.c.
EUR06 2Bw3	853	638	n.c.	n.c.	n.c.	n.c.	800	698	n.c.	7392
Ambient pH										
CH Ap	448	857	7336	10506	n.c.	n.c.	209	1024	54	9203
EUR01 Ap	53	236	1747	8232	n.d.	n.d.	19	n.d.	n.d.	n.d.
EUR01 Bw2	76	222	2410	8314	279	798	22	280	949	4972
EUR03 Ah1	138	330	2779	6843	931	1419	109	287	n.c.	7515
EUR03 AB	85	242	n.d.	n.d.	n.d.	n.d.	n.d.	n.d.	n.d.	n.d.
EUR03 Bw2	40	214	1594	3053	412	822	10	323	16	3468
EUR06 Ah	64	359	1704	5705	443	1082	33	202	n.c.	9034
EUR06 2AB	99	202	2689	4573	763	1209	37	195	n.c.	8980
EUR06 2Bw3	118	224	3698	5858	936	1327	37	268	n.c.	n.c.
pH4										
CH Ap	29	182	2155	6366	402	1114	54	377	420	3960
EUR01 Ap	21	142	1276	6981	n.d.	n.d.	9	298	n.d.	n.d.
EUR01 Bw2	22	120	1320	6576	70	440	7	280	330	2897
EUR03 Ah1	78	193	1580	5276	408	1227	51	270	n.c.	5326
EUR03 AB	26	47	n.d.	n.d.	n.d.	n.d.	n.d.	n.d.	n.d.	n.d.
EUR03 Bw2	7	48	502	1303	67	390	3	284	258	2266
EUR06 Ah	25	137	888	5025	231	1018	24	171	n.c.	8388
EUR06 2AB	18	15	607	2564	101	630	9	179	n.c.	8257
EUR06 2Bw3	10	18	339	3165	18	869	6	159	374	5577

n.c. = Not possible to calculate; n.d. = Not determined; Cr_{des} with 2000 mg l^{-1}.

Sorption was strongest for Pb and Cu, especially at pH 7. For all tested metals and horizons, no clear adsorption maximum was found, even when HM concentrations were increased to 2000 mg l^{-1} (results not shown). This suggests the formation of multiple molecule layers on surfaces in all horizons. In most cases, the Chernozem reference sample exhibited the highest K_F values while the lowest were found for the EUR03-Bw2 (Table 2). A distinct decrease of adsorption with pH can be observed for all HM and horizons, especially for Cd, Ni and Cu (Figure 3).

Figure 3 shows a strong effect of pH on the sorption, which is most prominent for Cd and Ni. At pH 7, strong binding of Pb, Cu and Cr occurred for all horizons. Sorption of Cr and Pb was little affected by changes of pH. Due to the limited number of investigated samples, correlations of sorption variables and of sorption in a solution with a concentra-

tion of 300 mg HM l^{-1} with other soil variables (Table 3) resulted in low values for R^2. However, for Cd a relation between K_F values and Fe_o, CEC, clay content and C_{org} seems to exist at pH 7 (Table 3). This agrees with findings of other authors. According to Alloway et al. (1985) and Alloway (1995) pH is a key factor that controls the adsorption and solubility of Cd, in conjunction with organic matter and hydroxides. Correlations of sorbed Cd with contents of organic matter, clay and CEC showed increasing R^2 values with increasing pH, indicating the importance of exchange processes even in soils with variable charge.

Table 3. Coefficient of determination (R^2) of linear correlations of K_F and sorbed HM from a 300 mg l^{-1} solution (300_{ad}) with selected soil properties.

	Cd_{ad}		Pb_{ad}		Cu_{ad}		Ni_{ad}		Cr_{ad}	
	K_F	300_{ad}	K_F	300_{ad}	K_F	300_{ad}	K_F	300_{ad}	K_F	300_{ad}
pH 7										
Clay content	0.85	0.87	0.00	0.86	0.08	0.19	0.40	0.46	0.43	0.32
C_{org}	0.71	0.87	0.05	0.87	0.01	0.03	0.26	0.52	0.59	0.38
CEC	0.90	0.88	0.13	0.85	0.12	0.08	0.56	0.72	0.24	0.11
Fe_o	0.91	0.66	0.14	0.64	0.19	0.14	0.78	0.55	0.05	0.00
Calc. allophane*	0.13	0.15	0.23	0.19	0.56	0.26	0.20	0.19	0.06	0.20
Ambient pH										
Clay content	0.01	0.69	0.01	0.86	0.00	0.37	0.00	0.18	0.31	0.30
C_{org}	0.03	0.64	0.07	0.86	0.08	0.19	0.02	0.09	0.16	0.42
CEC	0.04	0.58	0.04	0.86	0.13	0.31	0.07	0.07	0.14	0.64
Fe_o	0.05	0.37	0.02	0.66	0.13	0.20	0.09	0.02	0.17	0.52
Calc. allophane*	0.09	0.03	0.02	0.20	0.17	0.02	0.10	0.02	0.22	0.24
pH	0.79	0.00	0.86	0.12	0.84	0.06	0.59	0.28	0.01	0.52
pH 4										
Clay content	0.02	0.11	0.12	0.83	0.00	0.18	0.01	0.03	0.39	0.46
C_{org}	0.02	0.43	0.06	0.92	0.02	0.29	0.01	0.19	0.72	0.47
CEC	0.01	0.15	0.25	0.84	0.04	0.14	0.02	0.02	0.49	0.48
Fe_o	0.07	0.00	0.43	0.56	0.16	0.01	0.09	0.02	0.41	0.26
Calc. allophane*	0.08	0.28	0.61	0.11	0.31	0.14	0.15	0.34	0.00	0.00

* $Si_o \cdot 7.14$.

Above pH 5.5, Cr precipitates more or less completely, forming largely insoluble hydroxides and oxides (Grove and Ellis 1980). Excluding the reference sample, only two of the investigated horizons have their ambient pH in that range. All other soil samples are more strongly acidic. Similarly, the immobilisation of Cu^{2+} is more strongly controlled by the pH of the soil solution than by cation exchange capacity or clay content (Pickering 1979). Also for Ni retention in soil, pH is assumed to be a stronger control than other factors like clay content and Fe and Mn oxides (Anderson and Christensen 1988). Ni is generally the least sorbed HM in the soils tested,

probably due to the mostly acidic pH (Willaert and Verloo 1988, Kiekens 1983).

No significant correlations were found between K_F values or the sorbed HM in a solution of 300 mg HM l^{-1} at any pH and the calculated allophane content, indicating that other soil constituents may be more important for HM-binding than allophane. But with increasing allophane content, a weak decrease of Pb-sorption and a strong decrease of Cd- and Ni-sorption were found between pH 7 and 4. The general lower level of Cd- and Ni-sorption at pH 4 indicate that other variable charge sites than from allophanes or precipitates at higher pH may contribute to the lower HM-binding at pH 4 (Figure 4).

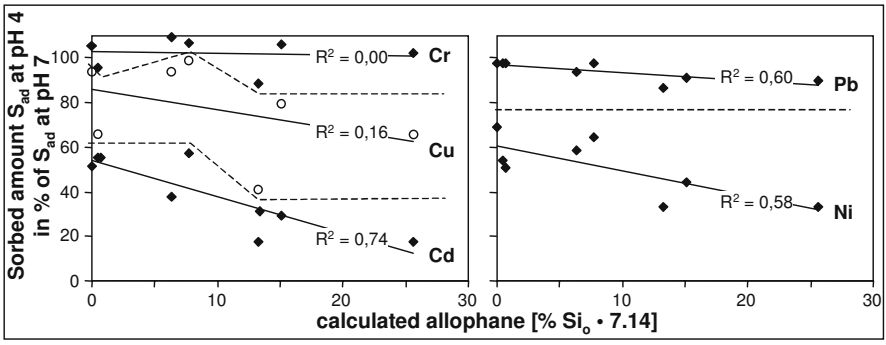

Figure 4. Relation of calculated allophane content to sorption decrease from pH 7 to pH 4 (sorbed from a solution of 300 mg l^{-1} HM).

For Pb, Cu and Cd, K_F correlated closely to the equilibrium pH in experiments under ambient pH conditions. In the profile EUR03, sorption increased with the C_{org} content (Figure 5 centre) while in profiles EUR01 (Figure 5 left) and EUR06 (Figure 5 right) the trend is indifferent or reverse. The strong adsorption of Pb can be however explained by the high contents of organic matter in horizons developed from volcanic materials. Zimdahl and Skogerboe (1977) found that Pb mostly binds to organic matter and that pH and CEC are less important controls.

For the experiments at pH 4, it was possible to calculate K_F-values for all horizons and HM loadings. This may indicate that at higher pH precipitation of HM took place. At pH 4, the topsoils clearly adsorbed HM stronger than the subsoils. Again, EUR03-Bw2 showed the weakest HM adsorption of all tested samples.

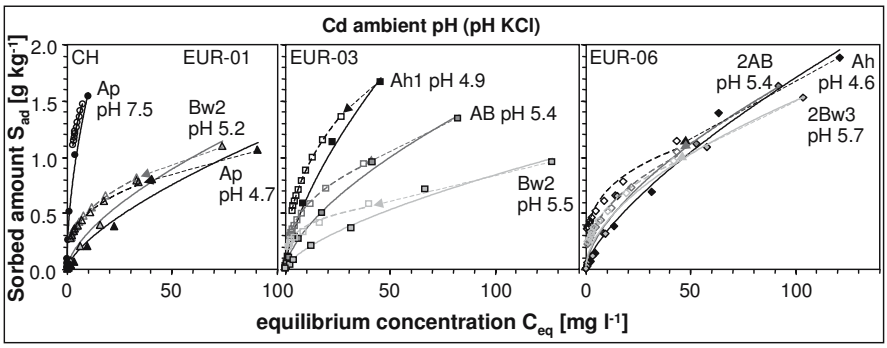

Figure 5. Adsorption and desorption isotherms for Cd at ambient pH (2 g soil in 10 ml 0.01 M $Ca(NO_3)_2$ solution containing up to 300 mg HM l^{-1}; 10 times washing of the highest HM loading).

To distinguish soils according to their capability to retain HM, Kukowski (1989) suggested five classes based on the K_F-value: <2 = very low, 2–20 = low, 20–50 = intermediate, 50–200 = strong and >200 = very strong adsorption. According to this system, all tested horizons, at ambient (and higher) pH, can be classified as strong to very strong sorbents for HM, except for Ni. The only exception is the EUR03-Bw2, which showed a weaker adsorption of Cd. Even at pH 4, all horizons except EUR06-2Bw3 were strong to very strong sorbents for Pb and Cu.

Desorption isotherms

For samples with the highest HM loading as described above, desorption was analysed. The comparison of adsorption and desorption isotherms reveals hysteresis of HM binding (Figure 5). Strong hysteresis is characteristic for strong binding, whereas weak hysteresis is indicative for weak binding and possible re-mobilisation. Because of the strong hysteresis, we conclude that sorption was not fully reversible, thus much of the adsorbed HM were not extractable even after 10 desorption cycles.

In general, the proportion of irreversibly bound HM decreases with pH. For Cd, the proportion that was not desorbable at pH 7 ranged from 40 to 70% and dropped to 10 to 30% at pH 4. The K_F values for desorption were on average 1 to 2 times larger than of the adsorption K_F at pH 7 but many times larger for ambient pH and pH 4 (Table 2). The decrease of the non-desorbable portion with pH seems to be more pronounced for horizons with high amounts of calculated allophane. Figure 6 indicates a lower portion of remaining Cd in allophane rich samples at ambient pH and at pH 4 in comparison to pH 7.

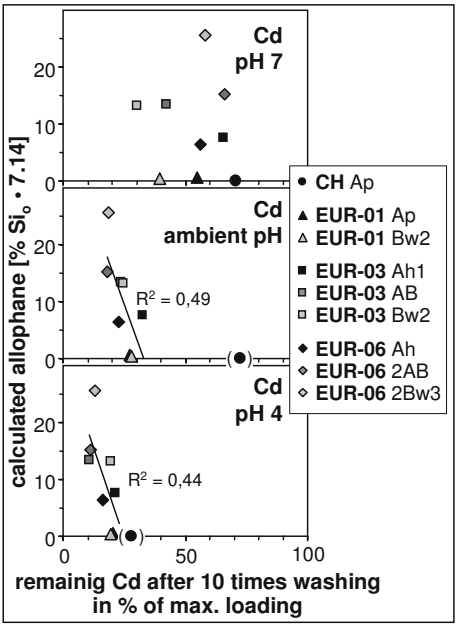

Figure 6. Non-desorbable Cd at different pH after 10 times washing.

Conclusions

Volcanic soils exhibit a high to very high sorption capacity for heavy metals at different pH-values. In particular, they exhibit strong sorption of Pb and Cr at all tested pH values. Sorption of Cd and Ni was found to be strongly pH dependent. A clear relation of adsorption and desorption to the content of allophane was not found, but with increasing allophane contents, Pb-sorption decreased weakly and Cd- and Ni-sorption decreased strongly from pH 7 to pH 4. It appears that, at ambient pH and at pH 4, Cd desorbs more completely with increasing allophane content. The general high sorption capacity of the studied soils, thus, appears to be caused mainly by organic matter.

Acknowledgements

We are grateful to Mrs. Polcher for carrying out the laboratory work and to Dr. K. Kaiser who carefully improved the manuscript.

References

Abd-Elfattah A, Wada K (1981). Adsorption of lead, copper, zinc, cobalt and cadmium by soils that differ in cation-exchange materials. J Soil Sci 32:271–283

Alloway BJ, Tills AR, Morgan H (1985). In: Hemphill DD (ed) Trace Substances in Environmental Health, Bd 18. Univ. Missouri, Columbia/MO, S 187–201

Alloway BJ (1995). Herkunft von Schwermetallen in Böden. In: Alloway BJ (ed) "Schwermetalle in Böden", Springer, Berlin

Anderson PR, Christensen TH (1988). Distribution Coefficients of Cd, Co, Ni and Zn in Soils. J Soil Science 39:15–22

Buchter B, Davidoff B, Amacher MC, Hinz C, Iskandar IK, Selim HM (1989). Correlation of Freundlich Kd and n retention parameters with soils and elements. Soil Sci 148:370–379

Clark CJ, Mc Bride MB (1984). Chemisorption of Cu(II) and Co(II) on allophane and imogolite. Clays Clay Miner 32:300–310

Filius A (1993). Schwermetall-Sorption und -verlagerung in Böden. Dissertation Technische Universität Carolo-Wilhelmina, Braunschweig

Fukushima M, Nakayasu K, Tanaka S, Nakamura H (1995). Chromium(III) binding abilities of humic acids. Anal Chim Acta 317:195–206

Gerth J, Brümmer GW (1979). Quantitäts-Intensitäts-Beziehungen von Cadmium, Zink und Nickel in Böden unterschiedlichen Stoffbestandes. Mitteilgn Dtsch Bodenkund. Gesellsch 29:555–566

Grove JH, Ellis BG (1980). Extractable Chromium as related to soil-pH and applied Chromium. Soil Sci Soc Am J 44:238–242

Jin X, Bailey GW, Yu YS, Lynch AT (1996). Kinetics of single and multiple metal ion sorption processes on humic substances. Soil Science 161:509–520

Kiekens L (1983). In: Utilisation of Sewage Sludge on Land Rates of Application and Long-Term Effects of Metals, Proc. Summary of Commission of the European Communities, Uppsala, Sweden

Krauss M, Wilcke W, Kobza J, Zech W (2002). Predicting heavy metal transfer from soil to plant: potential use of Freundlich-type functions. J Plant Nutr Soil Sci 165:3–8

Kukowski H (1989). Untersuchungen zur Ad- und Desorption ausgewählter Chemikalien in Böden. PhD Thesis, Kiel University

Langmuir I (1918). The adsorption of gases on plane surfaces of glass, mica, and platinum. J Am Chem Soc 40:1361–1403

Michenfelder A (1993). Labor- und Geländeuntersuchungen zum Transportverhalten und Rückhaltevermögen landwirtschaftlich genutzter Böden gegenüber Schwermetallen und Pflanzenschutzmitteln. Schr Angew Geol 27, Karlsruhe

OECD (Organization for Economic Co-Operation and Development) (1981). OECD-Guideline for testing of chemicals 106. Adsorption and Desorption, pp 1–23

Pickering WF (1979). In: Nriagu J.O. (ed) Copper in the Environment, Part I: Ecological Cycling. Wiley, New York, pp 217–253

Roehl KE (1997). Experimentelle Untersuchungen zu Retardation und Bindungsformen von Schwermetallen in tonigen Deponiebarrieren. Schr Angew Geol Karlsruhe 46:27–29
Sparks D (2000). New frontiers in elucidating the kinetics and mechanisms of metal and oxyanion sorption at the soil mineral/water interface. J Plant Nutr Soil Sci 163:563–570
Swarup A, Beese F, Ulrich B (1994). Movement of Zn, Pb and Cd through an undisturbed soil column of a soil under forest. J Indian Soc Soil Sci 42:182–184
Welp G, Brümmer GW (1998). Adsorption and solubility of ten metals in soil samples of different composition. J Plant Nutr Soil Sci 162:155–161
Willaert G, Verloo M (1988). Biological effects of nickel species and their determination in plant and soil. Plant and Soil 107:285–292
Zimdahl RL, Skogerboe RK (1977). Behavior of lead in soils. Environ Sci Technol 11:1202–1207

Appendix materials on CD-Rom

Heavy Metal Data Jahn-Tanneberg.ex

IV. Reference Pedons: physical characteristics

Ed.: F. Bartoli

Application of Diffuse Reflectance Spectroscopy (DRS) to study European Volcanic Soils: a preliminary examination

V.M. Sellitto, V. Barrón, G. Palumbo and C. Colombo

Introduction

Volcanic soils recently recognized as a pedological unit have been named "Andosoils" (Andosols (FAO-WRB) or Andisols (Soil Taxonomy)) which comes from the Japanese roots "*An"* meaning dark and *Do* meaning soil. Andosoils appear darker in the upper horizons while deep horizons appear lighter, which is related to the chemical composition of the parent material (Wada 1985, Shoji et al. 1993). However, a systematic study of the color of European Andosoils has yet to be made.

A wide range of information can be obtained from color in terms of the nature and chemical composition of soil material (Baumgardner et al. 1985, Escadafal et al. 1988, 1989, Bédidi et al. 1992, Bédidi and Cervelle 1996). In particular, soil color has long been known to reflect the content and nature of the organic matter (Shields et al. 1966, 1968, Stoner and Baumgardner 1981, Schulze et al. 1993) and mineral constituents, especially Fe oxihydroxides (Torrent et al. 1983, Franzmeier et al. 1983, Barrón and Torrent 1984, 1986, Torrent and Schwertmann 1987, Scheinost and Schwertmann 1999). For example, the variety of colors shown by the Fe oxides results from different types of electronic transitions (Shermann and Waite 1985). Fe oxides adsorb strongly in the ultraviolet (UV) and blue spectral regions but are strongly reflecting in the red and infrared regions (IR). There are marked differences in color among individual oxides, from yellow in goethite (α-FeOOH) to purple red in some hematites (α-Fe_2O_3). Orange hues in soil are often caused by ferrihydrite or lepidocrocite (γ-FeOOH), whose identification is crucial in many soils as they indicate active or recent redox processes (Schwertmann 1993, Madeira et al. 1997, Scheinost and Schwertmann 1999). Qualitative and quantitative analysis of soil Fe oxides is of great pedological interest because Fe oxide content reflect duration and intensity of pedogenesis (Cornell and Schwertmann 1996). Andosoils are good soil candidates for validating these relationships between soil color and soil organic and mineral constituents because they are rich in both organic materials and ferrihydrite

(Shoji et al. 1993). In addition, soil color may vary as a function of soil physical properties: porosity, drainage conditions, moisture and kind of aggregation. It is therefore reasonable to consider that the patterns of soil color variation observed are the cumulative result of several physical processes acting together, a process at one scale (e.g. wetness of soil aggregates) having a feedback to an action at another scale (e.g. amount and nature of soil mineral and organic constituents). The subject is therefore complex. In addition, estimation of soil color is also dependant of the methodology used.

The usual method for measuring soil color requires visual matching of a sample with standard color chips (Marcus 1998, Soil Survey Division Staff 1999). Most studies on soil color employ the Munsell Color System because of its ease of use, ready availability, and historical importance to soil science (Shields et al. 1966, Escadafal et al. 1988, Munsell Color 1994). The Munsell system represents a perceptually uniform color space and is based on careful psychophysical observation and experimental measurements (Marcus 1998). Munsell Color Space is conceptualized as cylindrical coordinates where the variables *Hue* (the attribute of a color perception denoted by blue, yellow, red, and so on), *Value* (the lightness of a color), and *Chroma (*the degree to which a stimulus differs from an achromatic, i.e. gray, stimulus). The Munsell Books of Color (available through Munsell Color, New Windsor, NY) present color chips arranged on constant-hue charts. The visual method is limited by a subjective match and by the number of Munsell color chips (Baumgardner et al. 1985, Post et al. 1993), leading to large color variability, significant errors in the application of color criteria to soil classification and poor correlations between soil color and many soil properties (Shields et al. 1966). Lighting conditions and observer experience are two factors known to limit visual matching techniques (Torrent and Barrón 1993, Soil Survey Division Staff 1999). These limitations can be eliminated by using a tristimulus colorimeter, which is an instrument capable of providing both accurate and precise color data (Torrent and Barrón 1993). Another alternative is to obtain the color from diffuse reflectance spectrophotometers (DRS). The spectral reflectance (SR) data given by these instruments are easily converted to the three figures, tristimulus values (X,Y,Z), that define the color perceived by the human eye. In turn, tristimulus values can be transformed to Munsell notation and other color space CIELAB. This color system uses three coordinates: L* (similar to Munsell value), a* (denoting hue on the red–green axis), and b* (which denotes hue on the yellow–blue axis). CIELAB is less familiar to soil scientists, but has been used for some studies of soil color because it has some advantages in multivariate analysis of soil data (Fernandez and

Schulze 1987, Bédidi et al. 1992, Marcus 1998, Scheinost and Schwertmann 1999, Sánchez Marañón et al. 2004, Vodyanitskii et al. 2005).

The first aim of this research was a color study on a large set of European volcanic soil samples by diffuse reflectance spectroscopy (DRS) and their comparison with visual measurements taken *in situ* using the Munsell charts. The second objective was to attempt to relate the color parameters obtained from the reflectance spectra to soil organic matter and soil mineralogy.

Materials and methods

We examined a total of 91 samples from 20 soil profiles in different European countries (Italy, Portugal, Iceland, Spain, Greece, France and Hungary). The soils were the reference pedons of the European funded scientific action entitled "COST-622: Soil Resources of European Volcanic Systems" (Table 1). Fe, Al, and Mn were extracted by sodium dithionite-citrate (Fe_d, Al_d, Mn_d), ammonium oxalate (Fe_o, Al_o, Mn_o) and pyrophosphate sodium (Fe_p, Al_p and Mn_p). The suspension was centrifuged at 2500 rpm for 15 min, with three drops of 'superfloc' and the supernatant was filtered before AAS determination (Buurman et al. 1996). Total organic carbon content was determined using a LECO CHN 1000 Analyser. Soil chemical extraction and organic carbon data come from the soil chemical data base of the reference pedons (Buurman et al. this Volume). Visual color estimation in the field was carried out under natural solar light by comparison to the Charts from the Munsell Books of Color (Munsell Color 1994). This was done by two expert observers belonging to the COST 622 Working Group for Soil Description and Sampling. Color measurements on dry soil samples sieved at <2 mm were also made in the laboratory by two expert observers using the Charts from the Munsell Books of Color. In the laboratory, diffuse reflectance measurements were obtained by using a Jasco 560 UV-visible spectrophotometer, equipped with an integrating sphere, according to the method proposed by Torrent and Barrón (1993). Briefly, air-dried soils, previously sieved at <2 mm, were vigorously ground in an agate mortar for at least 10 minutes in order to exclude the influence of micro-aggregation. Then, the samples were gently pressed in a special circular hole (diameter of 10 mm) against unglazed white paper in order to avoid undesired particle orientation and also to prevent some of the samples pouring out into the integrating sphere. This sphere of reflectance has a particular geometry that simultaneously allows the measurement of sample and white standard (polytetrafluorinethylene), whose re-

flectance was adjusted, in all the range of wavelengths, to 100%. We ran the reflectance spectra from 350 to 900 nm with a resolution of 0.5 nm. From the diffuse reflectance curve we calculated the color parameters according to CIE and afterwards converted into the Munsell system and CIE-Lab (CIE Commission Internationale de L'Eclairage 1978). A useful tool for converting between different color systems can be downloaded from the Munsell web page (www.munsell.com). Data acquisition, processing and conversion between different color systems were performed by Jasco software (Model VWTS-581 – Color Analysis Program – version 2.00A). Furthermore, a "spline algorithm" was used in order to reduce the instrumental noise (Press et al. 1992). A yellow index "b" from the C.I.E.-Lab notation was used to evaluate possible relationships between soil color and the content and mineralogy of Fe oxihydroxides. All our color data are listed in Table 2.

Table 1. Location, site characteristics and classification of the COST 622 reference pedons (partly from Garcia Rodeja et al. 2004).

Profiles	Country	Location	Soil depth (cm)	Altitude (m)	Climate: temperature moisture regime	Parent material	Soil Classification WRB
EUR01	Italy	Gauro	120	103	Thermic xeric	Pyroclastic trachytic ash deposits	Humi-Tephric Regosol (Eutric)
EUR02	Italy	Gauro	92	225	Mesic xeric	Pyroclastic trachytic deposits	Eutri-Humic Cambisol
EUR03	Italy	Vico	125	700	Mesic udic	Lava, tephritic-phonolitic with leucite	Fulvi-Silandic Andosol (Dystric)
EUR04	Italy	Vico	105	722	Mesic udic	Lava, tephritic-phonolitic with leucite	Fulvi-Silandic Andosol (Dystric)
EUR05	Portugal	Azores-Faial	145	510	Mesic udic	Pyroclastic material	Hyperdystri-Silandic Andosol
EUR06	Portugal	Azores- Pico	140	400	Mesic udic	Basaltic pyroclastic material	Hydri-silandic Andosol (Umbric and Acroxic)
EUR07	Iceland	Route 1	100	40	Cryic/Frigid udic	Eolian and basaltic tephra sediments	Orthidystri-Vitric Andosol
EUR08	Iceland	Audkuluheidi	65	400	Cryic udic	Eolian and volcanic ash	Dystri-Vitric Andosol
EUR09	Iceland	Hella	230	50	Cryic/ Frigid udic	Eolian, tephra and organic materials	Umbri-Vitric Andosol (Pachic and Orthidystric)
EUR10	Spain	Tenerife- Tacoronte	220	1130	Mesic udic	Basaltic ashes	Umbri-Silandic Andosol (Hyperdystric)
EUR11	Spain	Tenerife- T.-G. de Isora	50	1675	Mesic xeric	Basaltic scoria and layers of lapilli	Skeleti-Vitric Andosol (Orthieutric)
EUR12	Spain	Tenerife-M. Mercedes	130	1000	Mesic udic	Basaltic ashes with weathered basaltic lava.	Umbri-Vitric Andosol (Pachic and Hyperdystric)
EUR13	Greece	Santorini, Vlychada	100	80	Thermic xeric	Pumice	Endocalcari-Tephric Regosol
EUR14	Greece	Santorini, Profitis Ilias	95	300	Thermic xeric	Pumice and volcanic ash	Skeleti-Tephric Regosol (Hypereutric)
EUR15	Greece	Santorini, Mavro Vounó	70	230	Thermic xeric	Pumice and coarse pyroclastic sediment	Skeleti-Tephric Regosol (Hypereutric)
EUR16	France	Puy de La Vache.	120	1000	Mesic udic	Volcanic scoria	Umbri-Silandic Andosol (Endoskeletic and Endoeutric)
EUR17	France	Buron du Perle	90	1080	Mesic udic	Colluvium of trachyandesitic rock	Aluandi-Silandic Andosol (Umbric and Acrudoxic)
EUR18	Hungary	Tihanny Peninsula	70	180	Mesic xeric	Basaltic tuff	Molli-Vitric Andosol (Pachic)
EUR19	Hungary	Badacsony	50	420	Mesic xeric	Pyroclastic deposits; basaltic tuff	Skeletic Umbrisol
EUR20	Hungary	Tokai	62	482	Mesic xeric	Andesitic rock	Silti-Endoleptic Phaeozem

Table 2. Laboratory color parameters of the studied soil samples according to Munsell, CIE Tristimulus and CIE-Lab system obtained on dry samples with spectrophotometer measurements.

Profile	Location	Horizon	Depth cm	Munsell Hue	Value	Chroma	Tristimulus X	Y	Z	Lab L	a*	b*
EUR01	Italy	Ap	0–16	0.5 Y	7.1	2.8	44.2	44.2	35.3	72.4	2.4	18.8
		Bw1	16–54	1.4 Y	6.3	2.4	43.0	44.2	35.7	72.4	1.8	18.2
		Bw2	54–95	1.0 Y	7.1	2.7	33.3	33.5	27.1	64.6	1.5	16.5
		BC	95–120	0.7 Y	7.0	2.9	43.2	43.3	34	71.7	2.0	19.3
		2C	120+	1.3 Y	7.1	2.5	44.8	45.2	37.5	73.0	1.2	17.1
EUR02	Italy	O	0–1	9.3 YR	5.1	1.5	21.1	21	19.6	53.0	2.4	9.0
		A	1–2/5	0.7 Y	5.3	2.3	22.8	22.7	18.2	54.7	2.4	14.8
		BC1	25–30/50	1.7 Y	7.3	2.0	47.5	48.3	42.6	75.0	0.4	14.6
		BC2	30/50–70	1.8 Y	7.3	2.0	47.1	47.9	42.3	74.7	0.4	14.5
EUR03	Italy	O	2	8.2 YR	4.9	1.7	18.9	18.6	16.7	50.2	3.6	9.8
		Ah1	0–22	9.6 YR	4.3	2.0	14.6	14.3	11.3	44.6	3.5	13.1
		Ah2	22–48	9.7 YR	4.9	2.2	18.8	18.5	14.9	50.1	3.3	13.8
		AB	48–70	9.6 YR	5.6	2.6	26.5	26.1	20.3	58.1	3.8	16.6
		2Bw1	70–98	9.3 YR	6.1	2.9	32.0	31.5	23.3	63.0	4.2	18.0
		3Bw2	98–125	9.2 YR	6.4	2.5	34.8	34.4	28.3	65.3	3.7	15.9
EUR04	Italy	O	2	8.1 YR	4.7	1.4	17.2	16.9	16	48.2	3.0	8.1
		Ah1	0–18	9.5 YR	3.8	1.9	11.2	11	8.7	39.5	3.5	12.0
		Ah2	18–25	9.6 YR	3.7	1.7	10.2	10	8.1	37.8	3.2	11.1
		Ah3	25–45	9.8 YR	4.1	1.8	13.0	13.0	10.4	42.5	3.0	12.0
		Bw1	45–70	1.0 Y	5.8	1.8	27.8	28	24.7	59.9	1.5	12.1
		Bw2	70–105	1.0 Y	6.1	1.7	31.2	31.5	28.5	62.9	1.3	11.6
EUR05	Portugal	Ah	0–25	0.3 Y	5.1	3.4	21.0	20.5	13.1	52.4	4.4	21.9
		A/C	25–30	9.1 YR	5.1	2.6	21.4	20.7	13.4	52.6	5.1	21.4
		2Ahb	30–45	0.5 Y	5.1	2.8	21.3	20.8	16.0	52.7	4.4	15.8
		2Bwb	45–65	9.7 YR	5.2	2.2	21.3	21.0	15.0	53.0	3.4	18.4
		2Bw/2	65–90	0.7 Y	6.0	1.8	21.5	21.3	17.4	53.0	3.4	18.3
EUR06	Portugal	Ah	0–35	9.6 YR	5.1	2.3	21.2	20.9	16.6	52.8	3.6	14.6
		1AB	35–50	0.3 Y	3.9	3.1	11.6	11.2	6.6	39.9	5.0	19.9
		2AB	50–70	9.3 YR	4.8	2.4	18.9	18.5	14.4	50.1	4.1	14.9
		2Bw1	70–100	8.3 YR	4.3	1.7	14.7	14.3	12.3	44.1	3.9	10.5
		2Bw2	100–125	9.8 YR	4.5	3.8	16.7	16	8.8	46.9	6.1	24.3
		2Bw3	125–140	9.3 YR	4.8	4.4	18.8	18	9.1	49.1	7.6	27.1
EUR07	Iceland	O	0–5	9.6 YR	4.0	2.7	12.7	12.2	8.2	41.6	4.7	17.2
		Ah1	5–17	9.4 YR	4.2	2.7	14.2	13.7	9.4	43.7	4.9	17.0
		2Ah2	17–35/50	9.1 YR	4.2	3.7	14.5	13.6	7.4	43.6	7.2	23.3
		2Ah3	35/50–65	9.6 YR	4.5	3.0	16.6	16	10.6	47.0	5.0	19.1
		3Bw1	65–73	0.3 Y	6.0	3.0	29.9	29.5	21.7	61.3	3.4	19.6
		3Bw2	73–82	9.4 YR	4.8	2.6	18.3	17.8	13.1	49.3	4.5	16.4
		4Bw3	82–90/100	0.1 Y	5.6	3.2	26.3	25.8	18	57.9	4.1	20.5
		4BCg	>90/100	1.8 Y	5.6	2.1	25.6	25.8	21.2	57.8	1.2	14.5
EUR08	Iceland	Ah1	0–8/16	0.2 Y	4.8	3.3	18.4	17.9	11.3	49.4	4.6	21.3
		Ah2	8/16–19/24	9.9 YR	4.7	3.3	17.7	17	10.7	48.3	5.1	21.0
		Bw1	19/24–23/31	0.4 Y	5.6	4.0	26.3	25.6	15.4	57.7	4.8	25.8
		2Bw	23/31–34/39	0.6 Y	6.1	3.6	32.0	31.6	21.3	63.0	3.6	23.2
		3BwC	34/39–56/59	0.8 Y	5.8	3.9	28.2	27.7	17.0	59.6	4.0	25.6
		4C	>56/59	2.7 Y	5.6	2.1	25.5	25.9	20.9	57.9	0.5	15.1
EUR09	Iceland	Ah	0–60	9.7 YR	5.5	2.2	24.9	24.6	20.5	56.7	3.1	13.8
		H	60–95	8.5 YR	5.1	2.1	21.1	20.6	17.6	52.3	4.0	12.3
		C	95–100	9.8 YR	5.1	1.4	20.5	20.4	19	52.3	2.1	9.0
EUR10	Spain	Ah1	0–40	7.8 YR	4.6	3.6	17.8	16.6	10.4	47.8	8.2	21.2
		Bw	40–85	8.1 YR	5.2	5.0	23.4	21.6	11.1	53.6	10.2	29.0
		Bwb1	85–110	8.9 YR	5.6	4.9	27.6	26.0	14.1	58.1	8.4	29.3
		Bwb2	110–220	8.4 YR	5.6	5.4	27.3	25.3	12.3	57.4	10.3	32.3
		2Bwb3	>220	8.6 YR	5.7	4.6	28.6	27.1	16.0	59.1	8.1	26.7
EUR11	Spain	C1	10–18	1.5 Y	4.7	2.0	17.2	17.2	13.7	48.5	1.8	13.6
		2Bwb	18–35	0.7 Y	5.9	3.1	28.9	28.7	20.6	60.5	3.0	20.2
		2BCb	35–45	1.5 Y	6.5	3.1	36.3	36.4	26.8	66.9	1.8	20.9
EUR12	Spain	Ah1	0–15	8.3 YR	3.7	2.7	10.6	10	6.6	37.8	6.3	16.1
		Ah2	15–65	8.5 YR	3.8	2.6	11.6	11	7.5	39.6	5.9	16.1
		Bw	65–90	8.5 YR	5.4	3.8	24.8	23.6	15.4	55.7	7.0	22.2
		2Ahb	90–100	7.2 YR	5.3	4.5	24.6	22.7	13.5	54.8	10.2	25.1

Continued

Profile	Location	Horizon	Depth cm	Munsell Hue	Munsell Value	Munsell Chroma	Tristimulus X	Tristimulus Y	Tristimulus Z	Lab L	Lab a*	Lab b*
EUR13	Greece	Ah1	0–7	9.3 YR	6.1	1.3	30.9	30.9	30.1	62.5	2.0	8.4
		Ah2	7–40	9.3 YR	6.6	1.2	37.8	38.0	38.0	68.0	1.7	8.0
		C1	40–65	9.4 YR	6.8	1.8	40.1	40.2	37.4	69.6	2.3	11.3
		C2	>65	9.4 YR	6.8	1.5	40.1	40.3	38.8	69.7	2.0	9.8
EUR14	Greece	A	0–7	9.7 YR	5.9	1.7	29.2	29.2	26.5	60.9	2.3	11.2
		AC	7–30	0.6 Y	7.3	1.4	47.5	48.1	46.8	74.9	1.0	9.8
EUR15	Greece	Ah	0–20	1.1 Y	5.4	2.1	23.5	23.5	19.4	55.6	1.9	14.1
		C1	20–50	1.5 Y	4.8	0.8	18.1	18.3	18.6	49.8	0.8	5.6
EUR16	France	Ah1	0–10	9.2 YR	5.1	2.0	21.4	21.1	17.8	51.8	4.5	23.1
		Ah2	10–25	9.2 YR	5.2	2.3	22.5	22.1	18.1	54.8	11.2	23.2
		Ah3	25–45	0.5 Y	5.0	3.6	20.5	20	12.2	57.8	0.9	19.2
		Bw	45–55	1.1 Y	5.3	3.5	23.1	22.8	14.3	57.2	0.3	14.0
		C/R	55–65	2.5 Y	5.6	2.8	25.4	25.7	18.6	53.2	0.3	9.6
		R/C	65–120	3.6 Y	5.4	2	23.6	24.1	19.9	56.2	–0.2	14.4
		R	>120	3.8 Y	5.2	1.3	20.7	21.2	19.5	53.2	–0.4	9.6
EUR17	France	Ah1	0–8	9.2 YR	5.1	1.8	21.0	20.7	18.3	47.2	4.1	19.4
		Ah2	8–32	9.4 YR	5.2	1.9	22.2	22	19.2	51.5	4.1	19.8
		Ah3	32–50	0.3 Y	4.6	3.0	16.6	16.2	10.6	49.6	4.7	21.4
		Bw1	50–90	0.3 Y	5.0	3.1	20.2	19.7	13.3	51.4	4.1	19.8
		2Bt	90+	0.2 Y	4.8	3.3	18.7	18.1	11.4	49.8	4.7	21.3
EUR18	Hungary	Ah1	0–15	0.4 Y	4.7	2.4	17.6	17.4	13.0	48.7	3.3	15.8
		Ah2	15–35	1.0 Y	5.0	2.4	20.2	20.1	15.4	52.0	2.4	15.9
		AC	35/40–70	0.9 Y	4.9	2.3	19	18.8	14.7	50.5	2.5	14.9
EUR19	Hungary	Ah1	0–7	7.2 YR	3.9	2.4	11.9	11.2	8.4	40.0	6.4	13.8
		Ah2	7–30	6.7 YR	4.0	2.9	12.7	12	9.1	41.2	6.1	13.5
		A/R	>30	7.3 YR	4.4	2.3	15.2	14.5	11.5	45.0	6.0	13.2
EUR20	Hungary	Ah1	0–12/20	9.6 YR	4.0	1.7	12.3	12.1	9.9	41.3	3.1	11.4
		Ah2	12/20–45	9.7 YR	4.1	1.8	12.9	12.7	10.3	42.2	3.0	11.6
		Bw/2R	45–60+	9.5 YR	5.3	2.1	23.2	23.0	19.3	55.0	3.2	13.1

Results and discussion

Color parameters

Visual color estimations carried out in the field (wet soil samples) or in the laboratory (dried soil samples) were related to spectrophotometric measurements done on dried grinded soil samples (Figure 1 and 2). The Figure 1 is a representation of the frequency distribution of a large set of laboratory soil color obtained by measuring with the Munsell color charts (chroma and values) on dry soil samples compared with diffuse reflectance spectroscopy (DRS) measurement. This distribution shows the shape of a normal curve for both the color system, in particular the mean of the Munsell chroma measures were similar while the mean of the values data obtained with spectrophotometric measurement shows an significative increase from 3.924 to 5.315. This data also indicated that visual measurements of the Munsell value (coefficient of variation of the mean of 42.5%) were more variable than the spectrophotometric measurement (coefficient of variation of the mean of 36%; Figures 1c and 1d). These relationships scattered but were often statistically significant (Figure 2). Scat-

tering was first attributed to discontinuous color measurement from Munsell color charts whereas color estimations were more continuously recorded by diffuse reflectance spectroscopy (DRS). Munsell color chips are so manufactured with intermediate hue each 2.5 units, while hues from the spectrophotometer measurements were determined with a precision of 0.1. Discrepancies could also be attributed to methodological differences (soil moisture, microaggregate or particle size, lighting conditions and observer experience). Further research is required on the drying effect on soil color which was well expressed for this wide range of European volcanic soils.

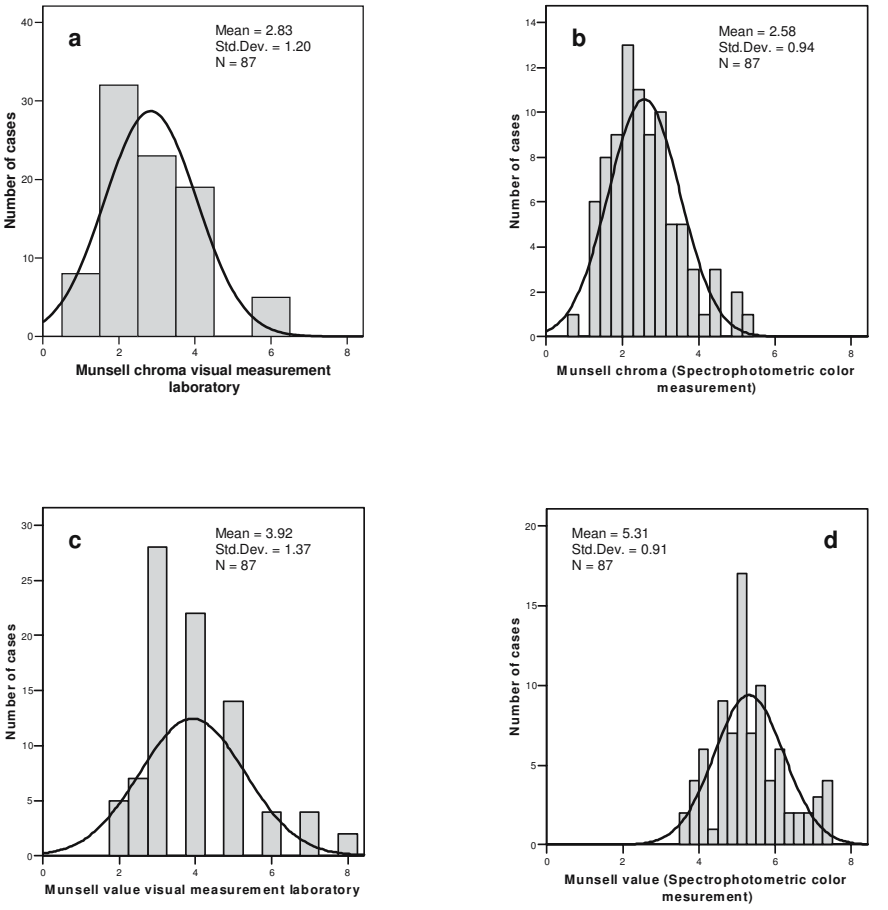

Figure 1. Histogram plot of the color parameters (Munsell chroma: (a) and (b), Munsell value: (c) and (d) visually estimated with the Munsell color charts on dry soil samples: (a), (c) in the laboratory on air-dried and ground soil samples: (c), (d) estimated by diffuse reflectance spectroscopy (DRS).

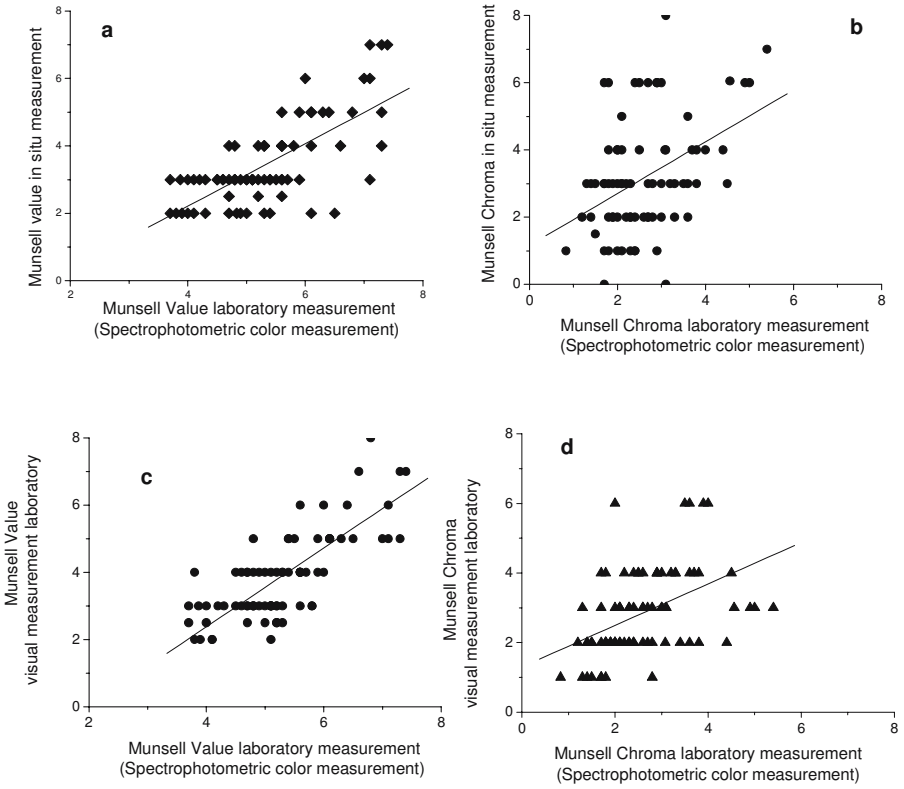

Figure 2. Relationships between the color parameters (Munsell value: (a) and (c), Munsell chroma: (b) and (d) visually estimated with the Munsell color charts (either in the field on wet soil samples: (a), (b) or in the laboratory on air-dried and ground soil samples: (c), (d) and their color parameter counterparts estimated by diffuse reflectance spectroscopy (DRS) carried out on air-dried and ground samples. Probability levels were <0.001 for all the linear regressions.

Moreover, visual estimates of Munsell values showed similar variations to those of their spectrophotometer value counterparts but there was less differentiation among similar colors. (Figure 2a). For example, visual estimates for a Munsell value of 3 correspond to spectrophotometer values ranging from 3.5 to 7. Our data showed that visual measurements of the Munsell value (coefficient of variation of the mean of 36.5%) were more variable when estimated in the field than in the laboratory (coefficient of variation of the mean of 18.1%). Therefore, the visual estimates are somewhat imprecise in determining color. Furthermore, being able to control particle size, aggregation and grain orientation in the laboratory improves color estimation *via* a better surface luminosity (Torrent et al. 1983, Barrón

and Torrent 1986, Bédidi et al. 1992, Fernandez and Schulze 1992, Madeira et al. 1997). Colors of Fe rich sediments were similarly improved after aggregate disruption by grinding, being very near those of the Fe oxides occurring in these sediments (Torrent et al. 1983, Barrón and Torrent 1986). This is why luminosity was slightly lighter (higher values) after soil drying and grinding than in wet field conditions (soil wet microaggregates).

Finally, shifts in Munsell chroma (the degree to which a stimulus differs from an achromatic grey color) occurred for some samples (n=79). Figure 2b showed that visual measurements of the Munsell chroma (coefficient of variation of the mean of 54.7%) were more variable compared with the laboratory color determination (Figure 2d, coefficient of variation of the mean of 35.9%) suggesting that the spectrophotometer measurement parameters (integrating sphere geometry, kind of illumination) was a better illumination standardized system that reduce the problem of the visual and subjective observation of soil color.

Relationships between color parameters and organic, organo-mineral and mineral soil constituents

Results of linear regression analyses between soil color parameters (Munsell, CIE and CIELab), soil organic matter and different forms of Fe, Al and Mn are listed in Table 3. First, Table 3 and Figure 3 showed significant relationships between the Munsell value and total organic carbon content. This was attributed to the specific behaviour of soil organic matter that absorbs energy and promotes lower reflectance intensity throughout the entire spectrum (Schulze et al. 1993). Moreover, the reflectance level of all soils decreased as organic carbon content increased but with two main data plots fittings. The color data plots from the Italian, Hungarian and Greek Andosoils showed a non-linear decrease as a function of organic carbon content whereas the color *vs* organic carbon relation was linear, with a moderate slope, for the Spanish and French Andosoils. The presence of a large amount of organic matter in the topsoils could mask the colors induced by Fe oxihydroxides and reduce diffuse spectra reflectance intensity (Schulze et al. 1993, Galvao et al. 1997). The measurements of the color obtained by using a spectrophotometer ranged from 3.8Y (yellow) to 6.7 YR hue (reddish yellow), 3.7 to 7.3 value, 1.5 to 5.4 chroma (Table 2). Minor changes in color were observed on samples with hues between 7.5YR and 10YR for considerable variations in the organic matter content (from 0.1% to 35%) while for samples with hues between 0.1Y and 4Y the organic matter caused substantial changes in color (Figure 4).

Table 3. Coefficent of linear correlation (r) among Munsell chromatic parameters (Hue, Value, Chroma), C.I.E (X, Y, Z and x_{min}, y_{min}) and C.I.E.-Lab (L, a, b) and soil organic matter (SOM); aluminum (Al_d), iron (Fe_d), manganese (Mn_d) extractactable with dithionite; aluminum (Al_o), iron (Fe_o), manganese (Mn_o) and silicon (Si_o) extractable with the oxalate; aluminum (Al_p), iron (Fe_p) and manganese (Mn_p) extractable with pyrophosphate. (** correlation is significant at the level 0.001, * correlation is significant at the level 0.01).

	Munsell System			Tristimulus (C.I.E)					C.I.E.-Lab		
	Hue	Value	Chroma	X	Y	Z	x_{min}	y_{min}	L	a	b (Yellow index)
SOM	0.36(**)	**–0.53(**)**	–0.13	–0.52(**)	–0.52(**)	–0.44(**)	0.08	–0.07	**–0.56(**)**	0.21(*)	–0.10
Al_d	0.15	–0.35(**)	–0.39(**)	–0.34(**)	–0.36(**)	–0.44(**)	0.50(**)	0.43(**)	–0.34(**)	0.40(**)	0.39(**)
Fe_d	0.17	–0.33(**)	**0.62(**)**	–0.32(**)	–0.34(**)	–0.48(**)	**0.70(**)**	**0.64(**)**	–0.31(**)	0.58(**)	**0.57(**)**
Mn_d	0.21(*)	–0.35(**)	0.26(**)	–0.31(**)	–0.32(**)	–0.35(**)	0.41(**)	0.25(**)	–0.34(**)	0.32(**)	0.225(*)
Al_o	0.10	–0.30(**)	0.32(**)	–0.32(**)	–0.33(**)	–0.40(**)	0.40(**)	0.39(**)	–0.28(**)	0.27(*)	0.32(**)
Fe_o	0.11	–0.33(**)	0.49(**)	–0.34(**)	–0.35(**)	–0.46(**)	0.58(**)	0.56(**)	0.31(**)	0.43(**)	0.48(**)
Mn_o	0.05	–0.18	0.35(**)	–0.22(*)	–0.23(**)	–0.33(**)	0.37(**)	0.41(**)	0.16	0.21(*)	0.34(**)
Si_o	0.19	–0.33(**)	0.15	–0.30(**)	–0.30(**)	–0.32	0.31(**)	0.26(**)	0.33(**)	0.22(**)	0.13
Al_P	0.24(*)	–0.38(**)	0.33(**)	–0.36(**)	–0.38(**)	–0.43(**)	0.44(**)	0.32(**)	–0.38(**)	0.51(**)	–0.32(**)
Fe_P	0.24(*)	**–0.64(**)**	0.22(*)	**–0.61(**)**	**–0.62(**)**	**–0.64(**)**	0.44(**)	0.32(**)	**–0.64(**)**	0.45(**)	0.22(*)
Mn_P	0.16	–0.43(**)	–0.07	–0.39(**)	–0.39(**)	–0.34(**)	0.11	0.05(*)	–0.43(**)	0.11	–0.20
Fe_d-Fe_o	–0.30	**0.63(**)**	–0.28	–0.31	–0.44(**)	**0.70(**)**	**0.61(**)**	–0.29	**0.64(**)**	0.56	0.19
Fe_o-Fe_P	0.02	–0.11	0.33	–0.14	–0.15	–0.25	0.32(**)	**0.36(**)**	–0.08	0.11	0.30

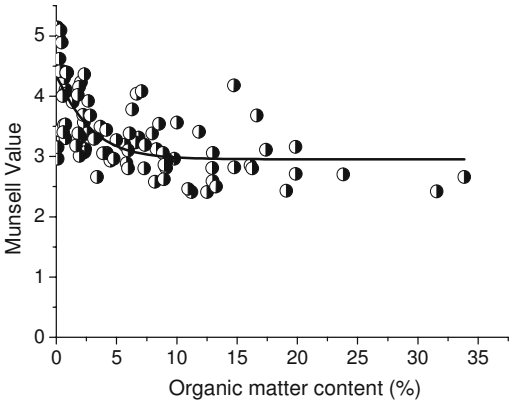

Figure 3. Non-linear relationship (r=0.53, p<0.001) between the Munsell value estimated on air-dried and ground samples by diffuse reflectance spectroscopy (DRS) and organic matter content.

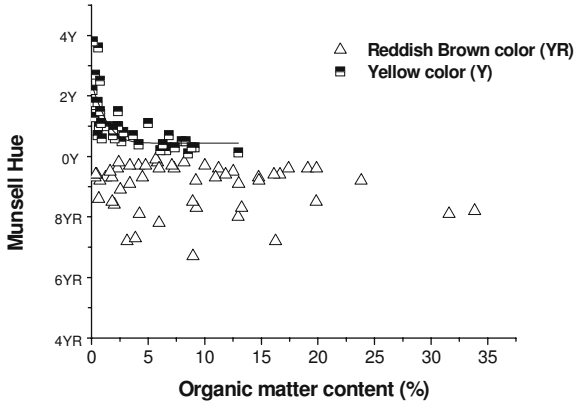

Figure 4. Relationships between the Munsell hue estimated on air-dried and ground samples by diffuse reflectance spectroscopy (DRS) and organic matter content.

We also evaluated the relationships between Munsell parameters obtained with laboratory color measurement (air-dried and ground samples) using diffuse reflectance spectroscopy (DRS) and mineralogy of Fe oxides, estimated by differential chemical dissolutions. The Fe and Al oxalate and dithionite extractions were produced in order to estimate the degree of weathering and the different phases and crystalline mineralogy of Fe oxydroxides (Schwertmann 1993, Cornell and Schwertmann 1996). In particular Fe_o-Fe_p was used as an approximation of ferrihydrite concentrations and the Fe_d-Fe_o was used as a measure of crystalline iron oxides (goethite and hematite). These parameters have been determined in order to obtain important information on the degree of weathering of the different horizons. Moderate correlations ($p<0.01$) were found between Munsell chroma or "b" CIE-Lab and pyrophosphate extractable organo-iron complexes (Fe_p) (Table 3). In contrast, significant correlations ($p<0.001$) were found between these color parameters and either Fe_o (organo-iron complexes and ferrihydrite) or, better, Fe_d and Fe_d-Fe_o (organo-iron complexes, ferrihydrite and crystallline oxihydroxides such as goethite, hematite) (Table 3, Figures 5 and 6). The difference Fe_d-Fe_o (crystallline oxihydroxides) and Fe_o-Fe_p (ferrihydrite) show different behaviour because a large fraction of Fe oxalate in top soil could be dissolved from poorly ordered aluminosilcates and from soil organic matter but were also closely linked to color parameter. Munsell chromas <2 could be considered as an indication of low Fe oxides content (Schwertmann 1993, Scheinost and Schwertmann 1999); nevertheless the significantly higher Fe oxide content of volcanic soils with ferrihydrite or goethite may contribute to their higher chroma (Shoji et al. 1993). Indeed Figure 6 shows that the yellow index was significantly correlated with iron extracted with dithionite citrate, confirming that not only soil organic matter but also some yellow Fe oxide minerals like goethite, strongly influence color (Fernandez and Schulze 1992, Scheinost and Schwertmann 1999). In addition, Figure 7 shows a significant correlation between the Munsell value determined in laboratory (air-dried and ground samples) using diffuse reflectance spectroscopy (DRS), and Mn and Al pyrophosphate extracted. These data clearly indicate that the color of volcanic soils is largely determined by different forms of Fe and Mn oxyhydroxides that are also closely linked to organic carbon. The high organic carbon content was responsible for the dark color although variation in this soil organic phase did not appreciably influence the color of the volcanic soil studied. This is due to the reduction in Munsell value by soil organic matter, and the reduction in Munsell chroma by the dilution of the Fe oxide pigments with the volcanic parent matrix (Table 1 and 2), which usually consists of primary minerals (i.e. pyroclastic materials) of high reflectance.

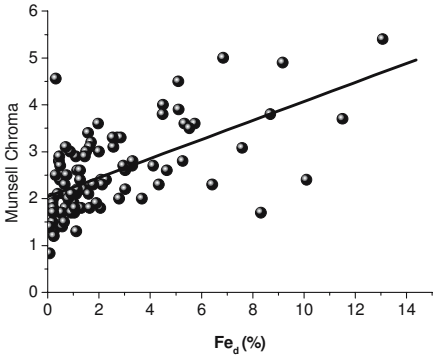

Figure 5. Linear relationship (r=0.61, p<0.001) between the Munsell chroma estimated on air-dried and ground samples by diffuse reflectance spectroscopy (DRS) and dithionite citrate-extractable Fe content (Fe_d).

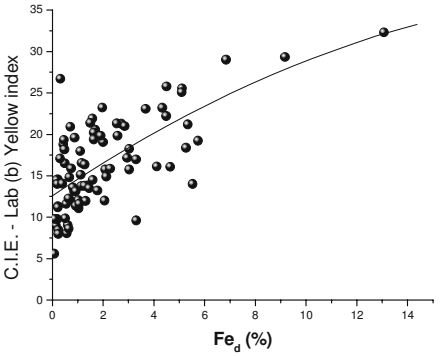

Figure 6. Linear relationship (r=0.57, p<0.001) between the yellow index (C.I.E.-Lab Parameter, b factor) estimated on air-dried and ground samples by diffuse reflectance spectroscopy (DRS) and dithionite citrate-extractable Fe content (Fe_d).

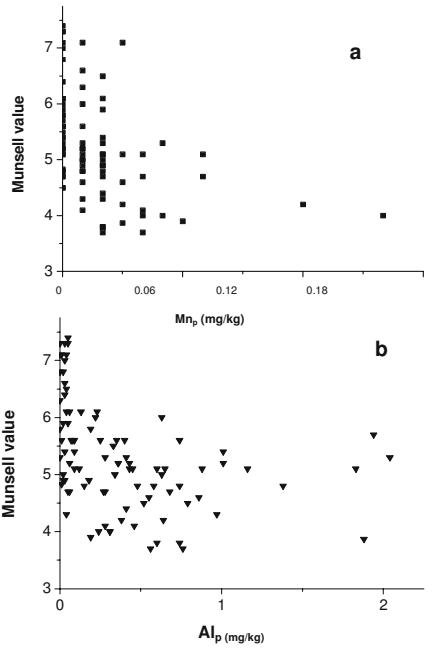

Figure 7. Relationships between the Munsell value estimated on air-dried and ground samples by diffuse reflectance spectroscopy (DRS) and either pyrophosphate-extractable Mn content (a) or pyrophosphate-extractable Al content (b).

Conclusion

This study shows that the use of spectrophotometer measurements gives precise, reproducible results, and solves the problem of the visual and subjective observation of soil color, influenced by factors such as the eye's

adaptability, background and illumination. The visual estimates of Munsell color value and the instrumental measurements were moderately correlated. Discrepancies between the two measurements originate from different lighting, sample preparation, soil moisture and particles size. The measurements of the soil color of volcanic European soil using a spectrophotometer method range from 3.8Y (yellow) to 6.7 YR hue (reddish yellow), 3.7 to 7.3 value, 1.5 to 5.4 chroma. Minor changes in color were observed on samples with Munsell hues between 7.5YR and 10YR for considerable variations in the organic matter content (from 0.1% to 35%) while for samples with Munsell hues between 0.1Y and 4Y the organic matter caused significant changes in soil color. The high organic carbon content was responsible for the dark color of the volcanic soil studied with the reduction in Munsell value. A significant positive correlation between soil Fe_d (extracted by dithionite solution) and Munsell chroma indicated that both poorly ordered and crystalline Fe oxide minerals are especially important for color development in volcanic soils. Munsell chromas <2 could be considered as an indication of low Fe oxides content, although soils with high chroma (>3) generally exhibited higher amounts of Fe and showed more intense weathering. Differential chemical dissolution data clearly indicate that the color of volcanic soils is largely determined by Fe_d and Fe_d-Fe_o (organo-iron complexes, ferrihydrite and crystallline oxihydroxides such as goethite, hematite). Poorly ordered Fe oxides estimated with Fe_o and Fe_o-Fe_p (organo-iron complexes and ferrihydrite) are closely linked to organic carbon. Although these results are only preliminary, they show solid evidence that diffuse reflectance spectroscopy (DRS) can be a useful method for determining color in volcanic soils. In particular, we demonstrated that the yellow index was significantly correlated with dithionite citrate-extracted iron, confirming that not only soil organic matter but also some yellow Fe oxide minerals like goethite, strongly influence the color of volcanic soils. Analysis of the Fe minerals played a special role in clarifying the type of weathering in volcanic systems. More specifically, the presence of hematite and goethite could provide essential insights to understand the rate of alteration processes. Knowledge of the spatial distribution of color can be used to obtain important information on soil properties in order to improve soil cultivation and conservation of volcanic soils. These results also suggest that soil color calculated by reflectance spectra could be used to study soil weathering processes.

Acknowledgements

We thank the permanent members of the Working Group for Soil Description and Sampling of COST 622 (François Bartoli, Angelo Basile, Martine Gérard, Toine Jongmans, Folkert van Oort and Fabio Terribile) for their valuable work. We also thank Peter Buurman for coordinating the COST 622 chemical data base and organic carbon and soil chemical extraction data were kindly provided by the Department of Soil Science and Geology of the University of Santiago, Spain (E. Garcia-Rodeja). We finaly thank the reviewer for useful comments on an early draft of the chapter.

References

Barrón V, Torrent J (1984). Influence of aluminium substitution on the color of synthetic hematites. Clays Clay Miner 32:157–158

Barrón V, Torrent J (1986). Use of the Kubelka-Munk theory to study the influence of iron oxides on soil colour. J Soil Sci 37:499–510

Baumgardner MF, Silva LR, Biehl LL, Stoner ER (1985). Reflectance properties of soils. Adv Agron 38:1–44

Bédidi A, Cervelle B (1996). Mesures spectrophotométriques de laboratoire (Spectromètrie optique). Photo-Interprétation 2:9–33

Bédidi A, Cervelle B, Madeira J, Pouget M (1992). Moisture effects on visible spectral characteristics of lateritic soils. Soil Sci 153:129–141

Buurman P, van Lagen B, Velthorst EJ (eds) (1996). Manual for Soil and Water Analysis. Backhuys Publishers, Leiden, The Netherlands

Buurman B, Bartoli F, Basile A, Füleky G, Garcia Rodeja E, Hernandez Moreno J, Madeira M (2006). The chemical data base. This volume

CIE (Commission Internationale de L'Eclairage) (1978). Recommendations on Uniform Colour Spaces, Colour-Difference Equations, Psychometric Colour Terms. Supplement no 2 to Publ no 15, Colorimetry, Bureau Central de la CIE: Paris, pp 1–21

Cornell RM, Schwertmann U (1996). The Iron Oxides, Wiley, New York, pp 604

Escadafal R, Girard M, Courault D (1988). La couleur des sols: apprècition, mesure et relations avec le propriètès spectrales. Agronomie 8:147–154

Escadafal R, Girard MC, Courault D (1989). Munsell soil color and soil reflectance in the visible spectral bands of Landsat MSS and TM data. Remote Sens Environ 27:37–46

Fernandez RN, Schulze DG (1987). Calculation of soil color from reflectance spectra, Soil Sci Soc Am J 51:1277–1282

Fernandez RN, Schulze DG (1992). Munsell colors of soils simulated by mixtures of goethite and hematite with kaolinite. Z Pflanzenernahr Bodenkd 155:473–478

Franzmeier DP, Yahner JE, Steinhardt GC, Sinclair Jr HR (1983). Color patterns and water table levels in some Indiana soils. Soil Sci Soc Am J 47:1196–1202

Galvao LS, Vitorello I, Formaggio AR (1997). Relationships of spectral reflectance and color among surface and subsurface horizons of tropical soil profiles. Remote Sens. Environ 61:24–33

Garcia Rodeja E, Nóvoa JC, Pontevedra X, Martinez Cortizasa A, Burrman P (2004). Aluminium fractionation of European volcanic soils by selective dissolution techniques. Catena 56:155–183

Madeira J, Bédidi A, Cervelle B, Pouget M, Flay N (1997). Visible spectrometric indices of hematite (Hm) and goethite (Gt) content in lateritic soils: the application of a Thematic Mapper (TM) image for soil mapping in Brasilia, Brazil. Int J Remote Sens 18:2835–2852

Marcus RT (1998). The measurement of color. In: Nassau, K. (ed.) Color for Science, Art and Technology. Elsevier, Amsterdam, pp 31–96

Munsell Color (1994). Munsell Soil Color Charts (1994). Rev. edn. Macbeth Division of Kollmorgen Instruments, New Windsor, NY

Post DF, Levine SJ, Bryant RB, Mays MD, Batchily AK, Escadafal R, Huete AR (1993). Correlations between field and laboratory measurements of soil color. In: JM Bigham, E Ciolkosz (eds) Soil color. SSSA Spec Publ 31. SSSA, Madison, WI, pp 35–49

Press WH, Teukolsky SA, Vetterling WT, Flannery BP (1992). Numerical recipes in fortran. The art of scientific computing. Press Syndicate of the University of Cambridge, pp 99–116

Sanchez Marañón M, Soriano M, Melgosa M, Delgado G, Delgado R (2004). Quantifying the effects of aggregation, particle size and components on colour of Mediterranean soils. Eur J Soil Sci 55:551–565

Scheinost AC, Schwertmann U (1999). Color identification of iron oxides and hydroxysulfates: use and limitations. Soil Sci Soc Am J 63:1463–1471

Schulze DG, Nagel JL, Van Scoyoc GE, Henderson TL, Baumgardner MF, Scott DE (1993). Significance of organic matter in determining soil colors. In: Bigham JM, Ciolkosz EJ (eds) Soil Color. Soil Science Society of America, Madison, WI, pp 71–90

Schwertmann U (1993). Relations between iron oxides, soil color, and soil formation. In: Bigham JM, Ciolkosz EJ (eds) Soil Color. Soil Science Society of America, Madison WI, pp 51– 70

Shermann DM, Waite TD (1985). Electronic spectra of Fe^{3+} oxides and oxide hydroxides in the near IR to near UV. Am Miner 70:1262–1269

Shields JA, St. Arnaud RJ, Paul EA, Clayton JS (1966). Measurement of soil color. Can J Soil Sci 46:83–90

Shields JA, Paul EA, St Arnaud J, Head WK (1968). Spectrophotometric measurement of soil color and its relationship to moisture and organic matter. Can J Soil Sci 48:271–280

Shoji S, Nanzyo M, Dahlgren R (1993). Volcanic ash soils: Genesis, properties and utilization. Developments in Soil Science 21. Elsevier, Amsterdam

Soil Survey Division Staff (1999). Soil taxonomy: a basic system of soil classification for making and interpreting soil surveys, 2nd edn. Agriculture Handbook, vol. 435. USDA, US government Printing Office, Washington DC

Stoner ER, Baumgardner MF (1981). Characteristic variations in reflectance of surface soils. Soil Sci Soc Am J 45:1161–1165

Torrent J, Schwertmann U (1987). Influence of hematite on the color of red beds. J Sediment Petrol 57:682–686

Torrent J, Barrón V (1993). Laboratory measurements of soil color: theory and practice. In: Bigham JM, Ciolkosz EJ (eds) Soil color. SSSA Spec Publ 31. SSSA, Madison, WI, pp 21–33

Torrent J, Schwertmann U, Fechter H, Alferez F (1983). Quantitative relationships between soil color and hematite content. Soil Sci 136:354–358

Vodyannitskii YN, Shishov LL, Vasilev AA, Sataev EF (2005). An analysis of the color of forest soils on the Russian Plain. Eur Soil Sci 38:11–22

Wada K (1985). The distinctive properties of Andosols. Advances of Soil Science, vol 2. Springer-Verlag, New York 2:173–22

Laser-diffraction grain-size analyses of reference profiles

P. Buurman and J.D.J. van Doesburg

Introduction

Previous studies on laser diffraction granulometry of volcanic soils indicate that (1) allophane causes the formation of fine-silt size aggregates that appear to increase in size with increasing allophane content, and (2) detailed grain-size data are equally effective as chemical analyses in detecting stratification of volcanic deposits (Buurman et al. 1997b, 2004). The second publication was based on the profiles EUR01–12.

The purpose of the present study is fourfold:

1. To judge the effect of organic matter and amorphous silicates on aggregation;
2. To judge the stability of aggregates <2 mm in a dynamic watery environment;
3. To study sedimentary stratification in profiles EUR13–20;
4. To find out whether the amounts of (a) extractable aluminium-silicate and iron-oxyhydrates and (b) Na-resin dispersed clay (Bartoli and Burtin this Section) can be estimated by comparison of grain-size distributions before and after removal of the amorphous fraction.

Because all the information and all graphs are available in the appended Excel files mentioned above, only a minimum of illustrations is included in this paper.

Sample preparation

Similar to the chemical analysis, samples of profiles EUR01–06 were analysed in field-moist condition while samples of EUR07–20 were analyzed after air-drying. The air-drying procedure did not appear to influence aggregation in the studied soils and with the current procedures.

The standard analyses were done after three pretreatments: shaking with distilled water, wet oxidation of organic matter, and extraction of amorphous silicates. In the water-shaken samples, stability of aggregates was

estimated by measuring the grain-size distribution after 1, 5, 15, and 30 minutes in the grain-sizer. The speed of the percolating suspension (12 l/min) and internal sonication cause disruption of aggregates that increases with time in the machine, and weakly aggregated particles will fall apart. The procedures were as follows:

Water-shaken samples: 1–2 grams of well-homogenized sample <2 mm was shaken overnight with 50 ml distilled water. With laser diffraction, the exact amount of sample need not be recorded. The total suspension was transferred to the cuvette of the LS230 (see below) and diluted to the correct obscuration while the suspension flow was on. 50 ml of 1% polyphosphate solution was added to the 1 l suspension volume to avoid flocculation (this addition has no effect on aggregate disruption). Measurements were carried out after 1, 5, 15, and 30 minutes in the cuvette. The change in texture during this treatment is an indication for the stability of fine aggregates.

Removal of organic matter: 1–2 grams of sample was treated with H_2O_2 to remove organic matter, following standard procedures. After peroxide treatment, the total suspension was transferred to the LS230 cuvette and diluted as required. 50 ml of polyphosphate was added to avoid flocculation.

Removal of amorphous silicates. A separate aliquot of 1–2 grams of sample was treated with H_2O_2 and afterwards extracted with ammonium oxalate/oxalic acid according to the extraction procedure for oxalate Al, Fe, Si (see section Methods in 'The chemical data base'; Section 3). After extraction, the sample was washed with distilled water, centrifuged, redispersed by sonication, and transferred to the measuring cuvette. 50 ml of polyphosphate solution was added to avoid flocculation.

Measurement

Measurements were carried out with a Coulter LS230 apparatus. The instrument measures 116 grain-size classes below 2000 μm. The lower size boundary is 0.04 μm, and each following boundary is 1.098 times the preceding one. The apparatus uses the Mie theory to calculate grain sizes from the intensity of the diffracted light. Constants were 1.33 for the refractive index of water, 1.56 for the refractive index of the solid phase (valid for quartz, feldspars and phyllosilicates), and adsorption coefficients of 0.15 for the 750 nm laser and 0.20 for the three polarized wave lengths of 450, 600, and 900 nm (Buurman et al. 1997a). The latter values were based on adsorption measurements on a number of natural and deferrated samples at

sediment concentrations as used in laser diffraction. Calculations included the PIDS measurements, but at an obscuration of 10% as used in the measurements, the adsorption values for the polarized wavelengths have little influence on the calculation of fractions.

Calculation of extracted grain-size fraction

If the amorphous (extractable) constituents are concentrated in the fine fraction, their amount can be estimated by comparison of grain-size distributions before and after removal of the extractable material (after wet oxidation of organic matter), using the coarse fraction as inert reference. Removal of amorphous material will cause a relative increase in the remaining fine and coarse fractions (the sum remains 100%). If one assumes that the fraction coarser than a specific limit is unaffected by the extraction, the amount of fine fraction removed by extraction can be calculated as follows:

$$\% \text{ Extracted fine fraction} = 100-(C_i+C_i/C_t*F_t) \quad (1)$$

in which C_i = % (coarse) fraction above reference limit in untreated sample; C_t = % (coarse) fraction above reference limit in treated sample; F_t = % (fine) fraction below reference limit in treated sample.

The calculation can also be written as:

$$\% \text{ Extracted fine fraction} = (F_i-F_t)*100/(100-F_t) \quad (2)$$

in which F_i = % (fine) fraction below reference limit in untreated sample.

For the present calculations, reference limits of 52.6 and 83.9 µm were used. This means that the fractions coarser than this limit are supposedly unaffected by the extraction of amorphous material. The boundary of 52.6 µm was chosen because it is closest to the sand/silt boundary. However, because the grain-size distributions in most samples are continuous at this value, the nearest low in the distribution (83.9 µm) was also chosen as a reference limit.

Results

Stratification and aggregate stability

All measurements and graphs are stored in Excel sheets on the accompanying CD (see last page). The grain-size distributions of profiles EUR01–12 have already been interpreted in terms of depositional discontinuities

(Buurman et al. 2004), and the horizon codes used here are based on that paper. For the remaining profiles, the field horizon codes are used. In the following, the discussions will start with the distributions after removal of amorphous silicates and organic matter, because such distributions most closely resemble those of the parent material. As in allophanic soils of Costa Rica (Buurman et al. 1997b), allophane causes silt-size aggregates to form, and oxalate extraction therefore strongly affects the silt fraction. Further, removal of organic matter and allophane may free layer silicate clay from aggregates so that it is transferred to the fraction <2 μm.

Italian profiles

Profiles EUR01 and EUR02. These profiles have low amounts of amorphous silicates, so that oxalate extraction does not result in significant mass loss. All oxalate-extracted samples have very similar distributions in the fractions below ±300 μm. The Ap through Bw2 horizons, however, have a considerable fraction larger than 300 μm. The clay fraction shows a broad superposed peak around 2 μm that ranges upward into the fine silt fraction. The peroxide-treated samples have lower clay contents than the oxalate-extracted ones, so that oxalate extraction appears to destroy aggregates that contain phyllosilicate clay. This is especially the case for the Ap, 2BC and 2C horizons. After peroxide treatment, EUR01 shows a clear maximum in the silt/fine sand range, but as this does not change significantly upon removal of amorphous silicates, it must be attributed to mineral particles and not to aggregates. In EUR02, oxalate extraction obliterates the fractions >500 μm.

Although aggregates coarser than 1 mm are readily destroyed by circulation in the grain-sizer, 30 minutes of circulation only slightly increases the clay- and fine silt contents of the water-shaken samples, which indicates that fine aggregates are stable.

Profiles EUR03 and EUR04. Both profiles have more than 10% of allophane in the lower horizons. The oxalate-extracted samples of EUR03 show a differentiation between the O, Ah1+Ah2, and lower horizons. A similar subdivision is found for EUR04. Both profiles have three grain-size maxima between 10 and 150 μm and little clay. The peroxide-treated samples of both profiles show peaks between 1 and 10 μm that disappear upon oxalate extraction (example in Figure 1) and should therefore be attributed to (aggregation by) amorphous silicates and iron compounds. In EUR04, clay contents after oxalate extraction are somewhat higher than after per-

oxide treatment. This may be a combined effect of (a) removal of allophane clay, (b) dispersion of phyllosilicate clay and (c) a relative increase due to removal of coarser fractions (the sum remains 100%). In EUR03, breakdown of aggregates as a result of oxalate extraction is clear in the upper three samples, but in the lower horizons that have little aggregation, this extraction results in a (relative) increase of fractions coarser than 500 μm. Similar effects are observed in EUR04. The fact that most horizons of EUR03 have lower clay contents after oxalate extraction suggests that the clay fraction contained allophane and ferrihydrite.

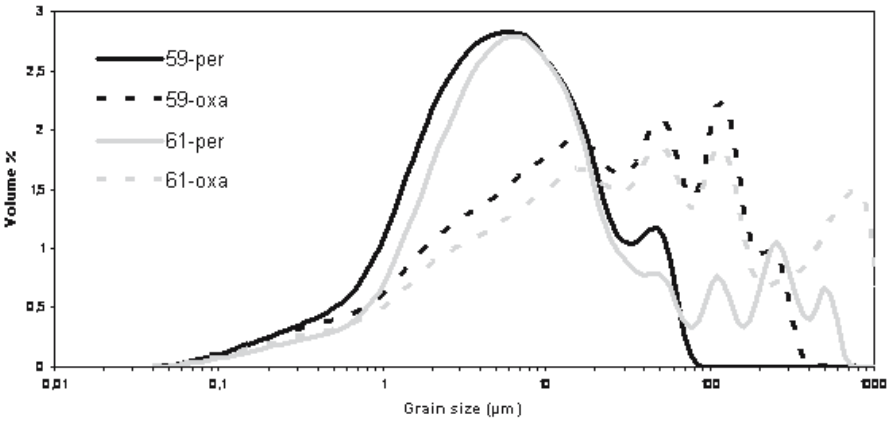

Figure 1. Grain-size distribution of peroxide- and oxalate-treated samples 59 and 61 from profile EUR04.

Comparison of water-shaken and peroxide-treated samples shows that there is significant aggregation by organic matter. In both EUR03 and EUR04, part of the coarse aggregation in the lower three horizons diminishes upon 30 minutes percolation in the grain-sizer. The aggregate peak around 60–80 μm, which decreases with depth, disappears upon removal or organic matter.

In EUR04 the difference between the water- and peroxide-distributions indicates that there is much aggregation by organic matter. Removal of organic matter brings about clear maxima in the fine silt fractions. In sample 58, the silt-fraction maximum disappears upon oxalate treatment, and a phyllosilicate peak appears at smaller grain size. All fractions coarser than 100 microns disappear and should therefore be allophane-bound aggregates. Also samples 59–61 loose part of the fine silt fraction upon oxalate extraction. Samples 62 and 63 are less affected.

Water-shaken series. Most samples have a rather broad distribution, with little fraction <2 μm. This fraction hardly increases during the measurement time.

Most samples show a loss of aggregates >500 μm with time. This loss is offset by a gain in smaller fractions, but the grain-size range in which the gain occurs may vary. In the four Italian profiles, the grain-size above which fractions decrease varies between 300–900 μm in EUR01, 60–200 μm in EUR02, 70–200 μm in EUR03 and 80–900 μm in EUR04 (O-horizons excluded). This indicates that 'stable' aggregate fraction varies considerably in size.

In profile EUR02, the distributions are similar to those of EUR01, but with less pronounced maxima. The boundary between stable and unstable aggregates appears to occur at smaller size than in EUR01. In most samples, all fractions below 200 microns increase with time. Sample 50 is an exception in that it hardly contains coarse aggregates and its distribution changes little with time.

In profile EUR03, the results suggest that the profile contains several superposed layers. The O-horizon (52) has a large stable coarse fraction, which is probably composed of organic particles (Figure 2). This is a large contrast with the Ah-horizon sample (53, Figure 3), which has a clearly defined maximum around 50 microns, and a decay with time in all size classes above 200 microns. The samples 54–57 have increasingly coarse distributions, of which the stability of the coarsest fractions (>1000 microns) increases with depth. This might be due to primary cementation of volcanic ash.

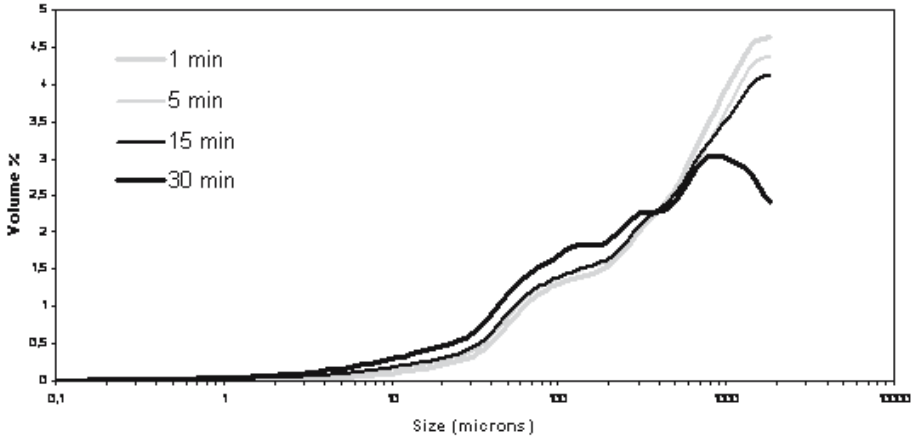

Figure 2. Aggregate decay in the water-shaken sample 52 (Profile EUR03).

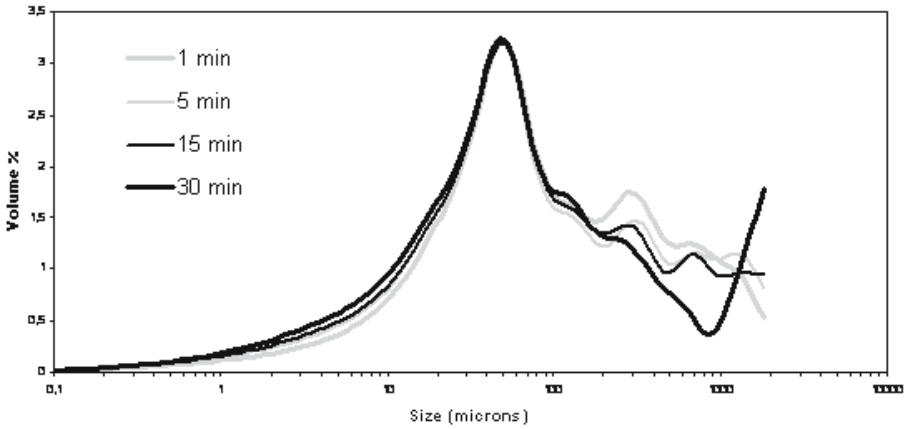

Figure 3. Aggregate decay in the water-shaken sample 53 (Profile EUR03).

The samples of Profile EUR04 suggest clear stratification or superposition of profiles. The O-horizon (sample 58) largely consists of coarse stable organic particles. Sample 59 is slightly less aggregated and shows a trend towards samples 60 and 61, which have distributions in the fine sand and silt ranges. The much coarser nature of 62 and 63 suggests that it is aggregated primary ash, or the top of a buried profile.

Azores profiles EUR05 and EUR06. Both Azores profiles have 10–20% of extractable alumino-silicates and this considerably affects their grain-size distributions. In profile EUR05, the oxalate-extracted material contains no fractions larger than 100 µm, but the shape of the upper boundary of the curves suggests that the high contents of fine silt in these samples may have obstructed the detection of coarser particles, as was also observed for high clay contents (see Buurman et al. 1997a). Except for a clear peak just above 10 µm in the topsoil samples, there is no significant difference between the samples. In profile EUR06, the residue after oxalate extraction was so small that the samples have been combined to obtain one single distribution. The result is similar to the distribution of sample 446, but with a slight peak below 1 µm. The fact that the grain-size distributions after peroxide treatment and oxalate extraction are rather similar may indicate that the extraction of amorphous material was incomplete. Sequential extraction of amorphous components suggests that the remaining amorphous material largely consists of iron compounds (Meijer et al. this volume). Comparison of the peroxide and oxalate-treated samples 446–448 indicates that oxalate removes the peak in the clay fraction and that the fine silt peak shifts from about 10 µm to slightly higher values. The water-shaken samples indicate consider-

able organic matter-induced aggregation in the upper two horizons, but not in the deeper ones where allophane dominates.

In profile EUR06, peroxide removes all aggregates larger than 100 μm, increases the fraction <1 μm, and shifts the fine silt peak to smaller grain sizes while coarse silt disappears. As in EUR05, aggregates coarser than 100 μm are restricted to the upper horizons. The combined distribution after oxalate extraction shows that the peak below 1 μm decreases but data are insufficient to support further conclusions.

Iceland profiles EUR07–EUR09. With the exception of samples 1050 (EUR07), 1054 and 1056 (EUR08), calculated allophane contents are below 10%. Organic C contents in profiles EUR07 and 09 are above 10% in most horizons.

The oxalate-extracted samples of EUR07 clearly show three different grain-size populations and four layers. Comparison of peroxide and oxalate treated samples indicates that oxalate removes a grain-size maximum between 1 and 10 μm in all samples except the bottom one (1051), while in samples 1044–1046 it also removes a peak below 1 μm. Both oxalate-extractable Fe and Al/Si compounds may be responsible for these changes. Oxalate extraction has no significant influence on coarser aggregation. Comparison of the water-shaken and peroxide-extracted samples indicates significant aggregation by organic matter. Except in bottom sample 1051, in the water-shaken samples most of the fraction <10 μm appears to be aggregated into sand-sized particles.

In EUR08, oxalate-treated samples show two grain-size populations. There is no maximum below 1 μm. Comparison with the peroxide-treated samples indicates that oxalate removes aggregate fractions smaller than 10 μm in all but the bottom sample (1057). In the latter, it removes some aggregation coarser than 500 μm. In sample 1057, amorphous fractions are probably still linked to the primary minerals and do not yet constitute separate fine fractions.

In EUR09, which is a hydromorphic profile, the oxalate-extracted upper two samples (1058 and 1059) have a single grain-size maximum. The lower two samples are slightly coarser. Comparison with the peroxide-treated samples shows that oxalate removes a fraction <10 μm in samples 1058 and 1061. The relation between this fraction and oxalate-extracted Al+Fe is better than that with calculated allophane. The water-shaken samples again show that most fine silt is aggregated into sand-size particles.

Tenerife profiles EUR10–EUR12. Of the Tenerife profiles, only EUR10 has appreciable amounts of extractable Fe and Al+Si. Organic carbon contents are highest in the topsoils of EUR11 and 12.

In EUR10, oxalate–extracted samples indicate the presence of considerable amounts of crystalline (phyllo)silicates in the clay fraction. The peroxide-treated samples show that most of the fine fraction is aggregated into particles of coarse silt – fine sand size, which are cemented by organic matter into larger particles. Only the bottom sample 0105 does not show aggregation by organic matter. The oxalate-extraction does not remove a clear size fraction but strongly reduces the fine sand and coarse silt fractions, freeing clay-size material.

In the weakly developed soil EUR11, grain-size distributions after the three treatments are almost similar, except for the coarsest fraction in 0108 and 0109 after peroxide treatment. Peroxide appears to destroy some aggregation and causes an increase in silt fractions that is somewhat affected by oxalate extraction.

In EUR12, oxalate extraction hardly affects the grain-size distributions. There is a slight decrease in the fraction <1 μm in some samples and perhaps some disaggregation in the fine silt fraction. The water-shaken samples show that aggregation by organic matter is especially strong in the upper two horizons, where the main peak is around 100 μm. In the subsoil samples, clay and fine silt fractions appear to be aggregated into larger units by organic matter.

The aggregate-stability test of the water-shaken samples (subsheet: *water-shaken*) shows significant differences between samples. In EUR10, sample 0101 shows hardly any influence of percolation time. Samples 0102 and 0103 first have a considerable fraction coarser than 1000 μm, which disappears after 30 minutes in the machine. This effect is faster in 0103 than in 0102. Sample 0104 shows some disaggregation of the coarsest fractions, while 0105 is hardly affected at all.

In the weakly developed profile EUR11, there is a very slight increase of finer fractions at the expense of coarser ones, but some of the coarser grains appear to be stable.

In EUR12, the topsoil (0111) shows a gradual aggregate decay over time, resulting in an increase in mainly silt fractions. The effect is smaller in sample 0112. In the subsoil samples 0113 and 0114, longer residence in the machine appears to induce some aggregation of fine particles, which may be due to the particular character (charge ?) of the extractable fraction in this soil (pyrophosphate extracts more Al and Fe than oxalate. See Physico-chemical data base, Section 3).

Greek profiles EUR13–15. The samples of the Greek profiles were air-dried. Because extractable iron and Al/Si compounds are negligible, most samples have only been measured after peroxide treatment. In all profiles, the grain-size distributions reflect the relatively fresh character of the ma-

terial. There are hardly any fine fractions, and grain-sizes >1000 μm constitute a considerable portion of the soil. In the topsoil of EUR14, oxalate extraction removes part of the coarse aggregation and the freed fines are distributed proportionally over the finer grain-size fractions. A pedogenic fine fraction is not visible.

In EUR13, the second horizon is finer than the overlying and underlying ones, which may indicate stratification. Chemistry of the layers, however, is similar (Martinez et al. Section 3). In EUR14 and 15, the topsoils (20, 23) are clearly finer than the subsoils (22, 24). In both soils, chemical properties also indicate that the Ah horizon is chemically (somewhat) different from the underlying ones.

French profiles EUR16–17. Because the samples were air-dried, the grain-size distributions upon shaking with water have not been measured for these profiles.

In EUR16, the oxalate-extracted samples have multiple maxima in the 20–500 μm range. Samples 29 and 30 also have a peak around 1000 μm. All samples lack a maximum below 10 μm. The distributions suggest that the profile consists of two separate layers; (Ah1)Ah2,Ah3,Bw – C/R,R/C (grain-size of the R was not measured), but the difference between the lower two horizons and the overlying ones may be due to differences in weathering. Chemical properties suggest a slightly different grouping: Ah1,Ah2,Ah3 – Bw,C/R, R/C – R (see Martinez et al. Section 3).

Comparison between the peroxide- and oxalate-treated samples shows that oxalate removes peaks in the regions 2–3 and <1 μm, which indicates that crystalline clays occur in minor amounts only (in laser-diffraction grain-sizing, phyllosilicate clays appear in the <1 μm fraction and there are excellent non-unity correlations between laser-diffraction and pipette-clay; Buurman et al. 2001). As a result of the removal of fine fractions upon oxalate extraction, the coarse fractions increase relatively.

EUR17 does not show any grain-size or chemical stratification in the parent material. In this profile, there is a decrease in the same fine fractions upon oxalate extraction but, in accordance with the lower amounts of oxalate-extractable material, the differences between the two measurements are smaller. Oxalate-extraction does not remove any coarse aggregation.

Hungarian profiles EUR18–20. The Hungarian profiles, although developed in volcanic materials, do not have andic properties. Organic matter contents are low and calculated allophane is generally lower than 1%. Grain-size distributions of the air-dried samples were determined after peroxide treatment and removal of carbonates. All profiles show admixture of loess, which is characterized by peaks around 50 and 100 μm. This ad-

mixture is minor in EUR20. The broad peaks in the grain-size distributions reflect aggregated parent material. Only EUR18 shows a significant peak of (phyllosilicate) clay below 1 μm. In each of the three profiles grain-size changes little with depth, but the top horizons have slightly more fraction <1 μm than the lowest horizons. There is no apparent grain-size or chemical stratification.

Comparison of extractable fraction estimates and Na-resin clay

The calculations, as mentioned in the methods section, use a reference grain-size value. The calculation method assumes that no amorphous material is extracted from grain-size fractions coarser than this value.

Estimates of extracted fine fraction using the calculation given in 4 are presented in Table 1. The table also gives calculated allophane and ferrihydrite (as FeOOH) based on Si_o and Fe_o contents, respectively. These data can be found in the Physico-Chemical data base (see Section 3). The Azores profiles EUR05–06 have been excluded because these show no coarse fraction in laser-diffraction analysis.

It is clear from Table 1, that there is a wide divergence between both estimates of the amorphous (extractable fraction). The results for a grain-size reference value of 52.6 μm are depicted in Figure 4. The graphs for the reference size of 83.9 μm are given in the file *allophane & grainsize.xls* (on CD). Although there is some correlation between the contents of extractable material calculated from grain-size distributions and from oxalate extraction, it is far from satisfactory. Very few observations are found on the 1:1 line. This implies that the conditions for which the estimates based on grain-size would be valid, are not met. The deviations in the estimates also indicate which suppositions were wrong.

Deviations. In many samples, the grain size-estimates are far higher than the extracted allophane. Considering equation (1)

$$\% \text{ Extracted fine fraction} = 100-(C_i+C_i/C_t*F_t),$$

been identified in profiles EUR4, 8, and 14 (see above), but may also occur in the other soils. It is clear that an underestimate would result when the coarse fraction after treatment (C_t) would be smaller than the original coarse fraction. This will happen when the coarse fraction contains extractable material, and even more strongly if the removal of extractable material disaggregates part of the coarse fraction. Extractable material in the coarse fraction has been identified in profiles EUR04, 08, and 14 (see above), but may also occur in other soils.

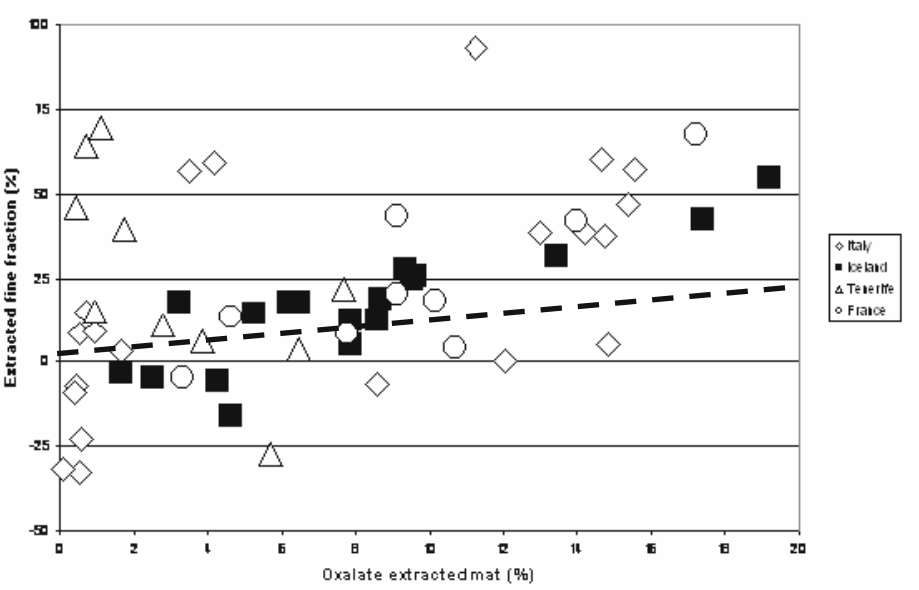

Figure 4. Scaled loss of fine fraction upon oxalate extraction (Reference 52.6 μm; volume %, Y-axis) versus contents of allophane + ferrihydrite (weight %) calculated from oxalate extraction. The dashed line indicates equal amounts.

A strong transfer of material to the fine fraction would cause both C_i/C_t and F_t to increase considerably, which may even cause negative values for 'Extracted fine fraction'. The graphs indicate that the deviation increases when the reference grain size is increased. An overestimate of the extracted particle-size fraction might also be caused by the difference between volume % (laser diffraction)

Table 1. Comparison of estimates of extractable fractions.

Profile	Sample	From oxalate extract			From grain size	
		Alloph	Ferrih	Sum	Ref. <52.6	Ref. <83.9
		%	%	%	%	%
Italy						
EUR01	41	0.6	0.1	0.7	15.0	14.7
	42	0.5	0.1	0.6	–23.1	–36.5
	43	0.5	0.1	0.6	8.7	9.4
	44	0.4	0.1	0.5	–56.1	–122.0
	45	0.4	0.1	0.5	–33.0	–78.8
EUR02	46	0.8	0.2	1.0	9.0	4.6
	47	1.4	0.3	1.7	3.2	–18.0
	49		0.1	0.1	–31.9	–69.8
	50	0.4	0.1	0.4	–7.1	–22.4
	51	0.3	0.1	0.4	–9.4	–26.0
EUR03	52	2.9	0.6	3.5	56.9	56.2
	53	7.0	1.6	8.6	–6.6	–30.0
	54	9.9	2.2	12.1	0.2	–18.6
	55	11.6	2.6	14.2	38.4	41.2
	56	12.6	2.8	15.4	46.8	50.9
	57	12.1	2.7	14.8	37.4	43.2
EUR04	58	3.4	0.8	4.2	59.2	56.0
	59	9.2	2.1	11.3	93.2	100.0
	60	10.6	2.4	13.0	38.5	28.4
	61	12.0	2.7	14.7	60.1	57.8
	62	12.7	2.8	15.5	57.2	56.9
	63	12.1	2.7	14.8	5.3	2.9

Continued

Profile	Sample	From oxalate extract			From grain size	
		Alloph	Ferrih	Sum	Ref. <52.6	Ref. <83.9
		%	%	%	%	%
Iceland						
EUR07	1044	2.6	0.6	3.2	17.9	15.3
	1045	3.5	0.8	4.3	–5.6	–27.1
	1046	6.4	1.4	7.9	12.7	–10.4
	1047	5.3	1.2	6.5	17.8	5.0
	1048	7.8	1.7	9.5	24.8	20.9
	1049	7.1	1.6	8.6	18.7	15.0
	1050	15.7	3.5	19.2	55.0	49.2
	1051	1.4	0.3	1.7	–3.4	–14.0
EUR08	1052	7.0	1.6	8.6	12.4	3.4
	1053	7.6	1.7	9.3	27.7	28.7
	1054	11.0	2.4	13.4	31.8	29.7
	1055	6.4	1.4	7.9	5.0	–11.7
	1056	14.2	3.2	17.4	42.6	46.6
	1057	3.8	0.8	4.6	–16.0	–32.2
EUR09	1058	7.9	1.7	9.6	25.9	26.5
	1059	4.3	1.0	5.2	14.5	10.3
	1060	2.1	0.5	2.5	–4.7	–8.3
	1061	5.1	1.1	6.2	17.8	15.9
Tenerife						
EUR10	1	4.6	1.0	5.7	–27.2	–15.9
	2	13.1	2.9	16.1		
	3	10.6	2.4	12.9	–270.0	–290.0
	4	11.6	2.6	14.2	–187.0	–120.0
	5	0.9	0.2	1.1	69.4	66.0
EUR11	6	2.3	0.5	2.8	11.1	10.9
	7	5.3	1.2	6.5	3.5	2.8
	8	6.3	1.4	7.7	21.8	24.4
	9	3.1	0.7	3.8	6.3	7.4
EUR12	11	0.6	0.1	0.7	64.2	63.6
	12	1.4	0.3	1.7	39.3	4.7
	13	0.8	0.2	1.0	15.1	15.7
	14	0.4	0.1	0.4	45.8	
France						
EUR16	25	11.4	2.5	14.0	41.9	38.5
	26	14.1	3.1	17.2	67.5	68.2
	27	20.2	4.5	24.7	45.7	61.7
	28	20.1	4.5	24.5	37.9	51.0
	29	8.7	1.9	10.7	4.2	–3.1
	30	7.4	1.7	9.1	43.2	46.3
EUR17	32	2.7	0.6	3.3	–4.6	–16.0
	33	3.8	0.8	4.6	13.5	8.0
	34	6.4	1.4	7.8	8.6	8.1
	35	8.3	1.8	10.1	18.6	10.4
	36	7.4	1.7	9.1	20.4	14.1

and weight % (oxalate extraction). Because the supposedly hollow and porous allophane particles have low particle density, the volume fraction may considerable overestimate the weight fraction. This effect is not found for layer silicate clays, which have particle densities close to those of sand minerals such as quartz and feldspars. A further possible cause for error is the fact that in grain-sizing in general, the coarsest fraction is determined with less reproducibility than finer ones because it may consist of very few grains.

Considering the problems encountered in the conversion of differential grain-size to extracted material, it is not surprising that the relation between calculated extracted material from grain-size curves and the measured Na-resin dispersible clay (Bartoli and Burtin this section) shows broad scattering (see graphs in *allophane & grain-size.xls*, on CD. Actually, the scattering is even worse than in the previous case. This is caused by several additional reasons: (1) Na-resin clay contains organic mater, which was removed for the grain-size determinations, (2) Na-resin clay contains both amorphous and crystalline clays and the latter are not extractable. It appears therefore that, although laser diffraction grain-size curves provide useful information on parent material, ag-

gregation, and weathering, they cannot be used to quantify the clay fraction or the extractable material.

Conclusions

Aggregation

1. Laser-diffraction grain-size studies after different treatments give insight in aggregation characteristics of the soils.
2. Aggregation in allophanic soils appears to consist of two hierarchies. Allophane and ferrihydrite cause the formation of fine silt-size aggregates that are combined into larger units by organic matter.
3. In well-developed soils, most allophane and ferrihydrite is present in both the fraction 1–10 μm and <1 μm. The dip around 1 μm in the distributions may be an artifact of the calculation module of the Coulter apparatus (Buurman et al. 1997) and the size distribution may be continuous instead of bimodal. In less weathered soils, allophane may occur in association with sand fraction minerals and cause aggregation in the sand fraction.
4. It is not clear from the data whether extractable iron oxyhydrates and extractable Al-silicates have size distributions of particles or aggregates in the same range.
5. Aggregation by organic matter is most readily observed in the coarse sand fractions, but it is effective also in the silt fractions. Its effect tends to decrease with depth.
6. In allophane-dominated samples, removal of organic matter does not always reduce aggregation. If coarse aggregates are affected by oxalate extraction, these are probably altered rock fragments.
7. As shown by the tests of water-dispersible aggregation in the Italian and Tenerife soils, there is considerable aggregation by organic matter, which decreases with depth, but a clear relation between aggregate stability and other soil properties was not found.

Stratification

8. Laser-diffraction grain-size characteristics are good indicators of sedimentary stratification. In addition to the stratified parent materials described by Buurman et al. (2004) for soils EUR01–12, stratification was also found in EUR14, 15, and 16.

Scaling

9. It appears not feasible to recalculate differential grain-size data to extracted fractions or clay-size material.

Acknowledgement

The authors thank Mr Th. Pape for the grain-size determinations on EUR01–EUR06.

References

Bartoli F, Burtin G (2006). Organo-mineral clay and physical properties in COST 622 European volcanic soils. This volume

Buurman P, Pape Th, Muggler CC (1997a). Laser grain-size determination in soil genetic studies. I. Practical problems. Soil Science 162:211–218

Buurman P, de Boer K, Pape Th (1997b). Laser diffraction grain-size characteristics of Andisols in perhumid Costa Rica: the aggregate size of allophane. Geoderma 78:71–91

Buurman P, Pape Th, Reijneveld JA, de Jong F, van Gelder E (2001). Laser-diffraction and pipette-method grain-sizing of Dutch sediments: correlations for fine fractions of marine, fluviatile, and loess samples. Netherlands Journal of Earth Sciences 80:49–57

Buurman P, García Rodeja E, Martínez Cortizas A, van Doesburg JDJ (2004). Stratification of parent material in European volcanic and related soils studied by laser diffraction grain-sizing and chemical analysis. Catena 56:127–144

Martínez Cortizas A, Nóvoa JC, Pontevedra X, Taboada T, García Rodeja E, Chesworth W (2006). Elemental composition of reference European volcanic soils. This volume

Meijer EL, Buurman P, Fraser A and García Rodeja E (2006). Extractability and FTIR characteristics of poorly ordered minerals in a collection of volcanic ash soils. This volume

Appendix materials on CD-Rom

grain-Azores.xls	profiles EUR05 and 06
grain-France.xls	profiles EUR16 and 17
grain-Greece.xls	profiles EUR13–15
grain-Hungary.xls	profiles EUR18–20
grain-Iceland.xls	profiles EUR07–09

grain-Italy.xls	profiles EUR01–04
grain-Tenerife.xls	profiles EUR10–12
allophane & grainsize.xls	comparison of estimates of extractable material and clay

Organo-mineral clay and physical properties in COST 622 European volcanic soils[†]

F. Bartoli and G. Burtin

Introduction

The particle-size distribution is undoubtedly a basic soil characteristic as useful in soil classification as it is in agronomy. Nevertheless, it is now well documented (see, e.g. the reviews of Nanzyo et al. 1993, Mizota and van Reeuwijk 1993) that Andosols (WRB 2001) fail to disperse completely when submitted to the dispersion agents that are utilized with success with other soils (e.g. sodium hexametaphosphate which is the recommended dispersant agent following the ISO international standards of soil particle-size analysis). The fact that sodium hexametaphosphate is not completely effective in obtaining dispersion should be attributed to the strong affinity of this dispersing agent for allophane, leading to edge to edge flocculated aggregates. Also, clay dispersability decreases when wet volcanic ash soils are dried. This is due to irreversible structural and mechanical changes occurring during drying (e.g. Kubota 1972, Nanzyo et al. 1993). Therefore, the common laboratory determined particle-size analysis of allophanic Andosols shows a low to very low clay content as compared with field determination (Ping et al. 1989), and particle-size/mineralogy modifiers such as ashy, medial and hydrous, based on 1500 kPa water retention, are used to replace the names of particle-size classes for Andisols in Soil Taxonomy (ST 1999).

The first aim of this study is therefore to adapt and develop the Na-resin method, without destruction of organic matter or/and poorly-ordered minerals, for obtaining most of the organo-mineral clay fraction. This Na-resin method was already recommended for strongly aggregated soils such as Oxisols and Andisols (Bartoli et al. 1991, Churchman et al. 1999).

The second aim of this study is to relate amounts of organo-mineral clay to physical soil properties such as bulk density, capillary porosity obtained by capillary rise, and total volumetric shrinkage of wet undisturbed soil cores at the end of controlled 40°C drying kinetics. As a matter of fact,

---

[†] This chapter is dedicated to the memory of late Gérard Burtin, co-author, who died in January 2004.

mineral, organic and organo-mineral colloidal soil constituents interact to give organo-mineral clay fractions (soil micro-property). In turn, organo-mineral clay coates and bridges coarser soil particles (soil aggregation) leading to soil structural features which vary with clay content and control soil macro-properties (enaulic coarse/fine related distribution pattern and granular microstructure, water retention and transport, aggregate stability and mechanical properties, shrinkage etc.).

This type of sequential scaling relationships has been widely reported for temperate cultivated soils, leading to, e.g., pedotransfer functions (prediction of water retention and hydraulic conductivity characteristics from particle-size data). Some of these expected relationships were already reported for Japanese volcanic ash soils: e.g., a linear relationship between retained water at 1500 kPa or liquid limit and organo-mineral clay content, mostly obtained by ultrasonication and pH adjustement (Nanzyo et al. 1993). However, such relationships have not been fully explored in volcanic soils, mostly because of the difficulty to disperse these strongly aggregated soils. In addition, European volcanic soils were much less studied than their American, Asian and New-Zealand counterparts.

Materials and methods

The following wet reference soil horizon samples (see the relevant Book Section 2 chapters) were analysed for particle-size distributions after Na-resin, sodium hexametaphosphate, or water treatment:

- EUR01 (Gauro Volcano, near Naples, Italy): *Humi-Tephric Regosol (Eutric)* (WRB 2001), *Ashy, glassy, nonacid, thermic Vitrandic Xeropsamment* (ST 1999): A_p (0–16 cm)*, B_w1 (16–54 cm)*, B_w 2 (54–95 cm), BC (95–125 cm)
- EUR02 (Gauro Volcano, near Naples, Italy): *Hyposodi-Humic Cambisol* (WRB 2001), *Ashy, glassy, mesic Vitrandic Haploxerept* (ST 1999): O_e + O_a (0.3–1 cm), A_h (1–6 cm)*, B_w (6–26 cm)*, BC1 (26–41 cm)
- EUR03 (Vico Volcano, near Rome, Italy): *Fulvi-Silandic Andosol* (Dystric) (WRB 2001), *Ashy, amorphic, mesic Eutric Fulvudand* (ST 1999): A_h1 (2–24 cm)*, 2 B_w1 (72–100 cm)*, 2 B_w2 (100–127 cm)
- EUR04 (Vico Volcano, near Rome, Italy): *Fulvi-Silandic Andosol (Dystric)* (WRB 2001), *Ashy, amorphic, mesic Eutric Pachic Fulvudand* (ST 1999): A_h1 (2–10 cm)*, B_w1 (45–72 cm)*, B_w2 (72–125 cm)
- EUR05 (Faial Island, Azores, Portugal): *Hyperdystri-Silandic Andosol* (WRB 2001), *Medial, amorphic, mesic Typic Hapludand* (ST 1999):

A_h1 (0–10 cm)*, 2 A_hb (30–45 cm)*, 2 B_wb (45–65 cm)*, 2 B_wb/2C (65–90 cm)

- EUR06 (Pico Island, Azores, Portugal): *Hydri-Silandic Andosol (Umbric and Acroxic)* (WRB 2001), *Hydrous, amorphic, mesic Acrudoxic Hydrudand* (ST 1999): A_h (0–37 cm)*, AB (37–45 cm), 2AB (45–65 cm), 2 B_wb (65–98 cm)*, 2 B_w2 (98–125 cm), 2 B_w 3 (125–140 cm)
- EUR07 (NW Iceland): *Orthidystri-Vitric Andosol* (WRB 2001), *Ashy, amorphic Pachic Fulvicryand* (ST 1999): A_h (5–17 cm)*, AC (17–38 cm)*, 2CB (38–65 cm)*, 3BC (65–73 cm), 3CB (73–82 cm), 4 B_w (82–95 cm)
- EUR08 (N Iceland): *Dystri-Vitric Andosol* (WRB 2001), *Ashy, amorphic Typic Vitricryand* (ST 1999): A_h1 (3–15 cm)*, B_w1 (24–30 cm)*, 2 B_w2 (30–40 cm)
- EUR09 (SW Iceland): *Umbri-Vitric Andosol (Pachic and Orthidystric)* (WRB 2001), *Ashy, amorphic Pachic Fulvicryand* (ST 1999): A_h (0–55 cm)*, 3H (60–95 cm)*
- EUR10 (Tenerife Island, Canary, Spain): *Umbri-Silandic Andosol (Hyperdystric)* (WRB 2001), *Ashy, amorphic, mesic Humic Udivitrand* (ST 1999): A_h (0–45 cm)*, B_w (45–88 cm)*,
- EUR 17 (Cantal, France): *Aluandi-Silandic Andosol (Umbric and Acroxic)* (WRB 2001), *Medial, amorphic, mesic Pachic Fulvudand* (ST 1999): A_h2 (8–32 cm)*, 2 B_w (50–90 cm)*

Asterisks (*) indicate that also wet undisturbed soil cores of 28.6 cm^3 (2.7 cm diameter, 5 cm height) have been sampled using rigid plastic pipes with bevelled edges to ease insertion. The core samples were capped at both ends with two parafilm sheets to minimize soil and evaporative loss and stored at 4°C until analysis.

Bulk density, field volumetric soil moisture and capillary porosity were estimated as follows. After removal of the two parafilm sheets, each wet soil core sample was weighed and placed on a brass sieve (height 70 mm, diameter 60 mm, mesh size 200 µm), which was placed on a PVC grid (mesh size 2×20 mm) located 10 mm above the bottom of a rectangular PVC box. Demineralised water was added to a height of 12 mm (2 mm of water above the lower limit of the soil cores) and the PVC box was closed by a PVC box top to avoid evaporation. Capillary rise occurred for 48 hours. Soil cores were weighed thereafter and wet soils were oven-dried at 105°C for 26 hours, allowing estimation of bulk density (weight of 105°C dried soil/core volume ratio), capillary porosity (volumetric water content after capillary rise calculated as the difference between weight of the wet soil core after capillary rise and after drying at 105°C, normalised to the soil core volume) and field volumetric soil moisture (difference in weight

of the field-wet soil core and that of the 105°C dried core, normalised to the soil core volume).

After the capillary rise experiments, a set of wet undisturbed soil cores (water-filled capillary porosity) was submitted to controlled 40°C drying for 39 to 51 h. During this 40°C drying, regular (mostly each hour) measurements of both total soil volume and volumetric soil moisture were carried out. Total volumetric shrinkage of wet undisturbed soil cores (water-filled capillary porosity) was estimated at the end of the 40°C drying period.

Mean aggregate water-stability (3 replicates) was estimated for both the field-wet aggregates and their 40°C dried aggregate counterparts using a home-made sieving machine and a methodology as described by Bartoli et al. (1991). Samples of either 4 g of wet aggregates or 2 g of 40°C dried aggregates were added to 200 ml demineralised water in this sieving machine (nine brass sieves), each sieve (diameter 60 mm, mesh size 200 µm) being immerged 20 mm deep in 200 ml demineralised water. Oscillations were sinusoidal, with an amplitude of 2 cm and a frequency of 98 oscillations/min; the time of disaggregation in water was 6 h. The water-stable aggregates were expressed as a fraction of the 105°C dried soil, after correction of the real coarse sand fraction determined in triplicate on each sample.

The bulk wet soil samples were used for particle-size distribution analyses, as follows:

First, the amount of total organo-mineral clay was determined by Na cation-exchange resin, which is the recommended dispersant for strongly aggregated soils such as Oxisols and Andosols (Bartoli et al. 1991, Churchman et al. 1999). A specific methodology was designed for the reference COST 622 soils, as follows: 1.5 to 3 g of field wet soil (equivalent to 1 g of 105°C-dried soil) was added to 200 ml demineralised water (resistivty of 18 microSiemens) and the soil suspension was ultrasonicated (3 708 J g^{-1} 105°C-dried soil using the North' method (1976) for ultrasonic energy calibration), and successively wet-sieved over 200 and 50 µm thereafter. The <50 µm soil suspension was added to 200 ml of Na Amberlite IR-120 resin (500 µm mesh, CEC of 2 eq l^{-1} or of 250 mol kg^{-1}) and shaken for 16 hours in an end-over-end shaker at 40 rpm. The resin was collected by wet-sieving over 200 µm whereas the <50 µm soil suspension was transferred to a 1 l beaker and made up to a volume of one liter with demineralised water.

Second, the ISO standard soil dispersant sodium hexametaphosphate (HMP) was used as follows: ten g of field wet soil sample was added to 25 ml HMP solution (124 g l^{-1}) and 175 ml demineralised water and shaken

for 16 hours in an end-over-end shaker at 40 rpm. After sieving over 200 and 50 μm, the suspension was transferred to a 1 l beaker and made up to a volume of one liter with demineralised water.

Third, dispersion in demineralised water was used as a reference as follows: ten g of field wet soil sample was added to 200 ml demineralised water and shaken for 16 hours in an end-over-end shaker at 40 rpm. After sieving over 200 and 50 μm, the suspension was transferred to a 1 l beaker and made up to a volume of one liter with demineralised water.

At the end of each of these three treatments, amounts of coarse silt (20–50 μm), fine silt (2–20 μm) and clay (<2 μm) were determined using the Robinson pipette method. All the aggregate and particle-size fractions were expressed as fractions of 105°C dried soil. Proportions of clay obtained after HMP or water treatment were also calculated as fractions of total organo-mineral clay (ultrasonic and Na-resin sequential treatment, often called Na-resin treatment for simplification).

Finally, bulk soil samples were air-dried for Al, Si and Fe oxalate-extraction and analysis, pH-H_2O and pH-KCl N (1/2.5 soil/solution ratio) and elementary organic analysis by dry combustion of the ground <2 mm air-dried soil using a Carlo Erba 1500 auto-analyser. All the results were also expressed with respect to 105°C dried soil.

Results and discussion

Aggregate and particle-size distributions as a function of the dispersion treatment

Figure 1 shows aggregate and particle-size distributions determined after each of the three dispersant treatments (water, sodium hexametaphosphate, ultrasonic and Na-resin sequential treatment) for representative vitric soil or Andosol wet samples (A_h and B_w horizons). As a complement, Figure 2 shows how clay content varied as a function of both the dispersant treatment and the andic index Al_o+½Fe_o.

All the soil suspensions were flocculated in water (Figures 1 and 2), being mainly composed of sandy and silty water-stable aggregates (Figure 1). In contrast, their soil suspension counterparts were relatively well dispersed after the Na-resin treatment (Figures 1 and 2). In the present study, the pH values of the soil-water suspensions varied from 4.3 to 6.9 whereas the range of the pH values of the soil suspensions was relatively narrow after the Na-resin treatment, from 5.8 to 7.0. Sodium hexametaphosphate (HMP) was also an efficient dispersant agent for the wet samples of the

vitric Andosols, so that similar aggregate and particle-size distributions were obtained after HMP and Na-resin treatment. By contrast, in the other wet Andosols samples, the HMP treatment disrupted only the sandy aggregates into fine silty aggregates, with low to very low clay dispersion (Figures 1 and 2). All the values of Na-resin clay content are included in the data base itself included in the accompanying CD of the present book (*physico-chemical data base.xls*).

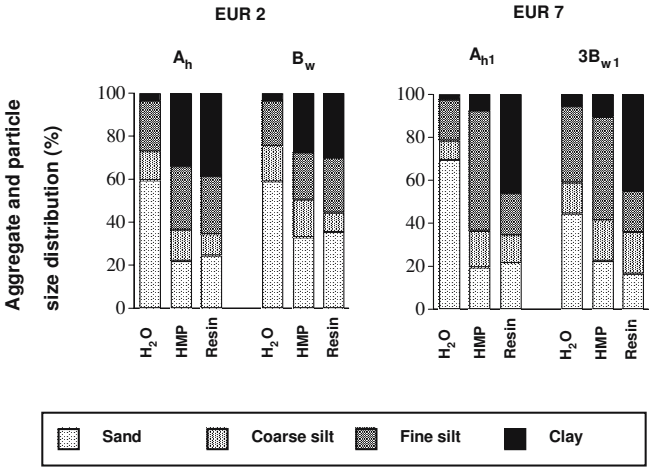

Figure 1. Aggregate and particle size distribution after dispersion by water (H_2O) or sodium hexametaphosphate (HMP) or by an ultrasonic and Na-resin sequential treatment (Resin) done on A_h and B_w horizon wet samples of two representative European vitric soil (Italy) and non-vitric Andosol (Iceland).

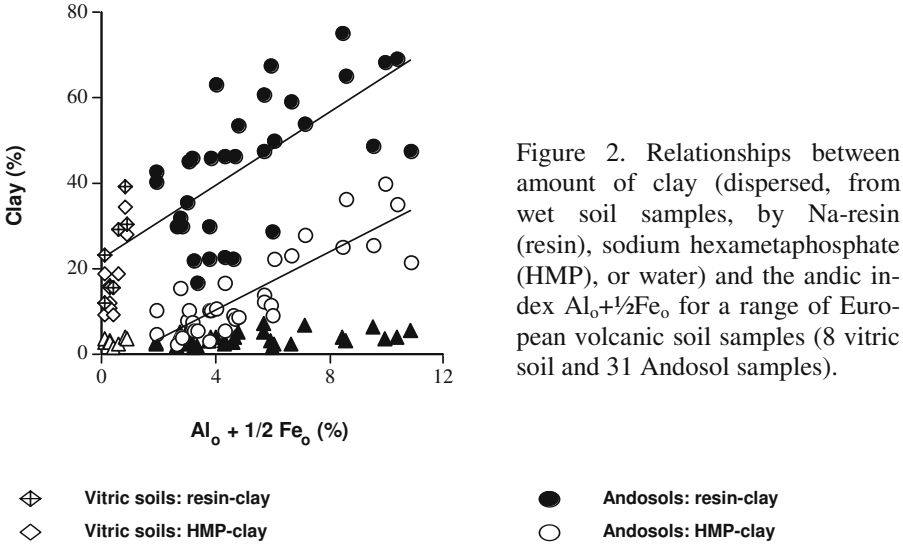

Figure 2. Relationships between amount of clay (dispersed, from wet soil samples, by Na-resin (resin), sodium hexametaphosphate (HMP), or water) and the andic index Al_o+½Fe_o for a range of European volcanic soil samples (8 vitric soil and 31 Andosol samples).

The very positive dispersant effect of the resin was already discussed by Bartoli et al. (1988, 1991) and by Churchmann et al. (1999), as follows. The maximum internal pressure due to air trapped in soil aggregates increases with soil wettability from hydrophobic soil to Na-resin hydrophilic soil. Na resin would be more efficient than Na salts for cation exchange, particularly for hydrated cations strongly hydrogen-bonded on the surfaces. The cation exchange process should also be rather stochiometric with the Na-resin whereas the standardized HMP concentration would be too high, leading to larger solute concentration and flocculation of clay. However, the role of the resin is complex because three processes occur: cation exchange (with an increase of affinity from monovalent to trivalent cations), Donnan equilibium, and resin swelling.

Total organo-mineral clay

Figure 2 shows that the Na-resin and HMP clay contents were very similar for the wet samples of vitric soils, but very different for the other wet Andosol samples, with a much better clay dispersion after the Na-resin treatment than after the HMP treatment.

Figure 2 also shows two positive but scattered linear relationships ($p<0.001$) between the Na-resin clay content (all volcanic soil samples) or the HMP clay content (only the non vitric Andosol samples) and the andic index $Al_o+½Fe_o$. This suggested that allophane, organo-aluminium associations and ferrihydrite are dispersed and part of the clay fractions. The more 'andic' the Andosol sample, the more statistically clayey it is. Most B_w horizons were then richer in total clay than the overlying horizons.

Na-resin clay content would therefore be as good a weathering and andic indicator, as the andic index $Al_o+½Fe_o$. For example, the EUR06 Andosol samples from the Pico Island (Azores) were more andic and clayey than the EUR07 and 08 Andosol samples from Iceland (Figure 3a). The climate of Pico Island is rather warm (monthly temperature range from 9 to 20°C) and very wet (mean annual rainfall of 2500 mm), leading to an intense weathering of the volcanic ash. By contrast in Iceland, a cryic temperature regime (–8 to 9°C and many freeze-thaw cycles in winter, particularly for the EUR08 reference pedon with frost and snow cover for 6–9 months and 3–7 months, respectively) and relatively dry udic moisture regime (mean annual rainfall of 550 mm and 800 mm for the EUR07 and 08 reference pedons, respectively), lead to moderate amounts of allophane and ferrihydrite.

On the other hand, the fact that most of the EUR06 Andosol samples (Pico Island) were more clayey than the EUR05 Andosol samples (Faial

Island) (Figure 3a) should be attributed to (i) a larger mean annual rainfall in the Pico Island (2500 mm) than in the Faial Island (1600 mm) and (ii) older pyroclastic materials and longer soil development in Pico Island (10,000 to 50,000 years BP) than in Faial Island (1600 to 5500 years BP).

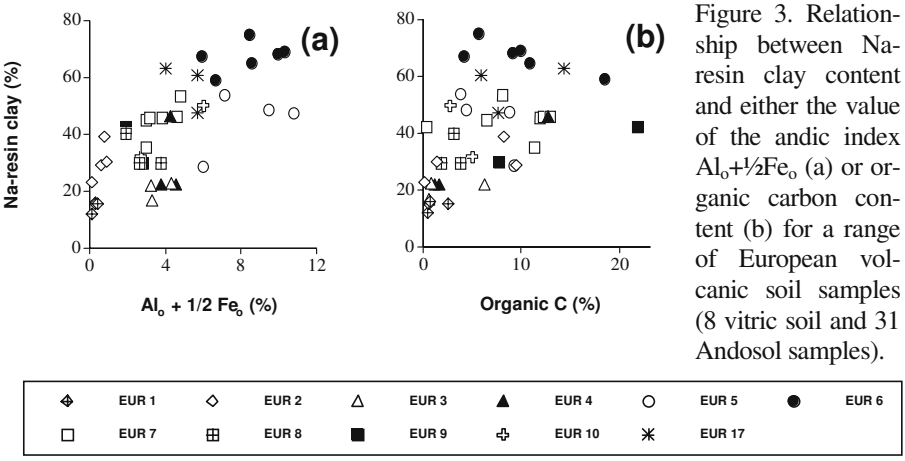

Figure 3. Relationship between Na-resin clay content and either the value of the andic index Al_o+½Fe_o (a) or organic carbon content (b) for a range of European volcanic soil samples (8 vitric soil and 31 Andosol samples).

Finally, Na-resin clay is a fine organo-mineral soil fraction, as indirectly shown by the positive relationships between Na-resin clay content and either Al_o+½Fe_o content (Figures 2 and 3a), allophane + ferrihydrite content (results not shown) or organic carbon content (Figure 3b, showing a positive but very scattered linear relationship). Previously, Nanzio et al. (1993) reported a similar relation between (allophanes + imogolite + ferrihydrite) content and organo-mineral clay content.

The Na-resin clay fractions of the representative EUR10 A_h and B_w samples (Tenerife Island, Canary) were analyzed in detail. They had 86 to 92% of total organic carbon, and 77 to 86% of total oxalate-extractable Al, Si and Fe (31.9 and 49.9% of total soil for the A_h and B_w samples, respectively). Most of the mineral, organic and organo-mineral colloids of the European reference volcanic soils should therefore be concentrated in the Na-resin clay fractions. Therefore, Na-resin clay content could be a useful indicator of weathering, organo-mineral interactions and soil development. However, further study on mineralogy and organic matter characteristics of the organo-clay fractions are needed to explain Figures 2 and 3.

Water-dispersible clay

Although clay was highly flocculated, it was possible to relate the proportion of organo-mineral clay dispersed by water to both soil organic matter and soil surface charges, as follows. The ratio Water-dispersible clay / Na resin clay decreased non-linearly as a function of organic carbon content ($p<0.001$, shown on Figure 4) whereas it decreased linearly with increasing ΔpH ($p<0.001$, see Figure 5).

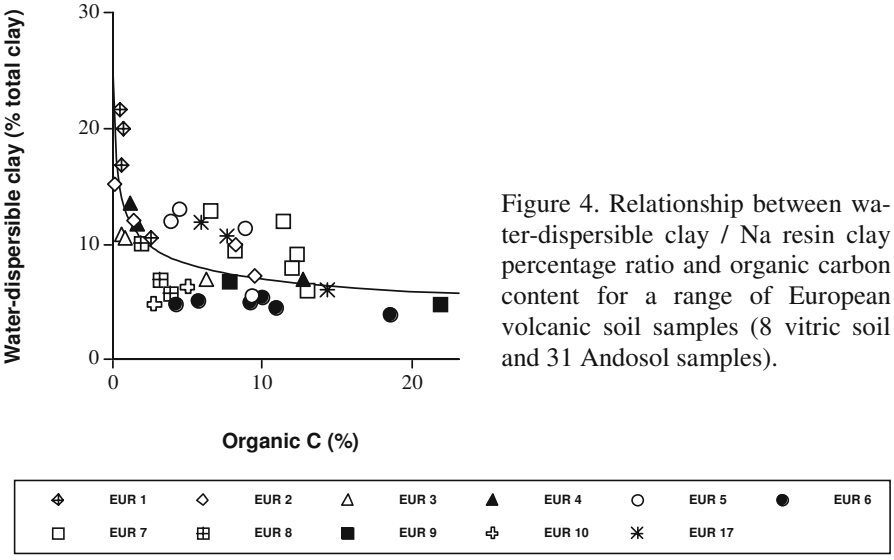

Figure 4. Relationship between water-dispersible clay / Na resin clay percentage ratio and organic carbon content for a range of European volcanic soil samples (8 vitric soil and 31 Andosol samples).

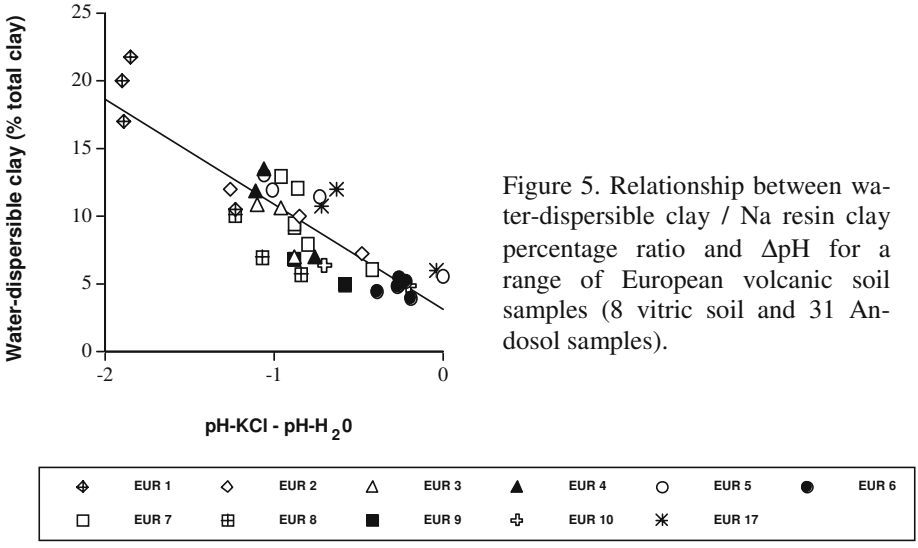

Figure 5. Relationship between water-dispersible clay / Na resin clay percentage ratio and ΔpH for a range of European volcanic soil samples (8 vitric soil and 31 Andosol samples).

ΔpH (pH-KCl N – pH-H_20) is related to negative and positive surface charges of soil constituents (e.g. Mekaru and Uehara 1972). The relationship between water-dispersible clay and ΔpH indicates that in the studied soils intra-aggregate bonding is mainly electrostatic, as was previously reported for Oxisols (e.g. Gillman 1974, Gillman and Bell 1976, Tessens 1984, Bartoli et al. 1992, Koutika et al. 1997).

As shown in Figure 5, most of the soil samples had a moderate net negative charge (ΔpH values from 0 to –1.2) and were relatively flocculated (only 6 to 16% of total clay was water-dispersible). The neutral to slightly negatively charged samples of EUR06 were most strongly flocculated whereas the negatively charged samples of the vitric soil EUR02 were most dispersed (Figure 4). Auxtero et al. (2004) recently characterized the surface charges of selected Andosols from Faial and Pico Islands (Azores). They found similar ΔpH values, mostly ranging from –0.2 to –0.9 (slightly to moderately negatively charged soil samples). The corresponding pH values of the point of zero net charge ranged from 4.2 to 5.7 and were positively correlated to both pH-KCl and allophane content.

Finally, we compared clay water-dispersability of the studied European Andosols to that of the also strongly aggregated Oxisols. Both Andosol and Oxisol B_w horizons are strongly flocculated in water whereas the studied Andosol A_h horizons are more flocculated (4–16% of total clay were water-dispersed, this study) than the Oxisol A_h horizons (often 20–40% of total clay were water-dispersible: Gillman and Bell 1976, Tessens 1984, Bartoli et al. 1992, Koutika et al. 1997). This discrepancy should be attributed to the stronger colloïdal character of the allophanes, ferrihydrite and organo-aluminium associations of the Andosols (e.g., very large specific surface areas, partly due to the microporosity of allophanes), as compared to that of the rather rigid and coarser kaolinite, gibbsite and goethite of the Oxisols. Organo-mineral interactions should also be stronger and more complex in Andosols than in Oxisols, often leading to specific hydrophobic properties (Poulenard et al. 2004).

Soil structure and water retention

Figure 6 shows a significant ($p<0.001$) but scattered power-law relationship between field soil moisture (weight %) and Na-resin clay content, with often larger soil moisture values (up to 250–280% for some Andosol samples particularly rich in organic and organo-aluminium colloïds) than those measured in other soil types where soil moisture values mostly range from 5 to 60%.

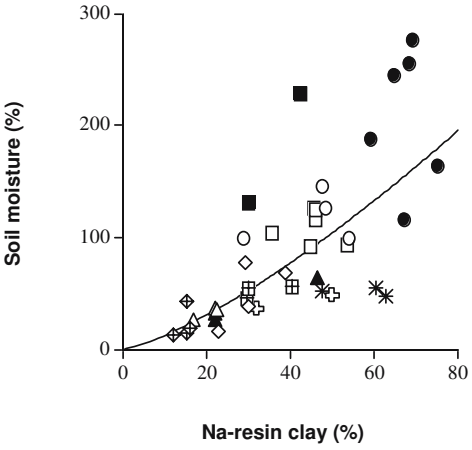

Figure 6. Relationship between proportion of field soil moisture (weight %) and organo-mineral clay content for a range of European volcanic soil samples (8 vitric soil and 31 Andosol samples).

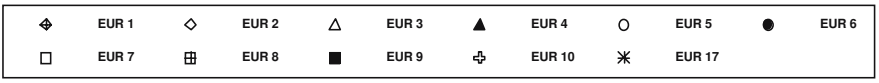

Maeda and Soma (1985), Warkentin et al. (1988) and Nanzyo et al. (1993) clearly point out that, besides allophanes, organic colloïds also also influence bulk density and soil water retention. Mizota and van Reeuwijk (1989), Pinheiro et al. (2001) and Poulenard et al. (2003) have described organic matter-rich, non-allophanic Andosols (*Hydric Melanudands* according to ST 1999) characterized by 1500 kPa water contents close to or far exceeding 100%.

However, interpretation of these authors, as most soil scientists who studied volcanic soils, are constituent-based and not physical-based. We have to keep in mind the causal relation between soil constituents to soil structure and then to soil hydric properties. This is why field volumetric soil moisture (soil plots not reported) or capillary porosity (Figure 7) and Na-resin clay content show significant ($p<0.001$) but scattered linear relationships.

The more clayey the soil, the larger its microporosity, and the more water it retains in its capillary porosity. This explains why most B_w horizons had higher water contents than the corresponding topsoils. However, water retention in the field is also controlled, in a complex way, by the various climatic, vegetative and pedoclimatic conditions occurring at the time of sampling. We will first focus on capillary and total porosity before coming back to field volumetric soil moisture.

The extremely large capillary porosity values of the studied volcanic soils (mostly from 0.6 to 0.8 $cm^3\ cm^{-3}$, Figure 7) are similar to those of

Histosols but are much larger than those of other soil types, which range mostly from 0.1 to 0.4 $cm^3\ cm^{-3}$.

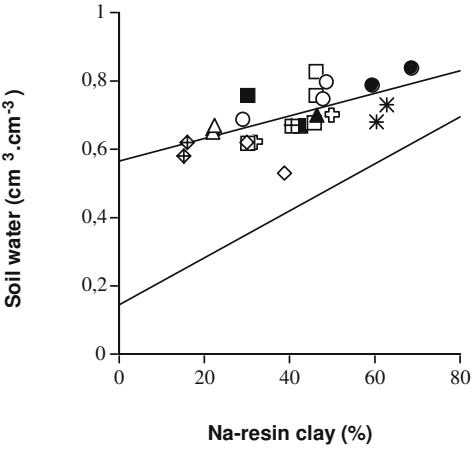

Figure 7. Relationships between capillary porosity (full line) or volumetric field soil moisture (dashed line without data plots) and organo-mineral clay content for a range of European volcanic soil samples (4 vitric soil and 20 Andosol A_h and B_w samples). Same symbols as those used in Figure 6.

This is mainly attributed to soil aggregation by the very reactive organo-mineral clay fraction which coated and bridged coarser particles, as shown indirectly by the capillary porosity *vs* organo-mineral clay relationship (Figure 7) and, directly, by soil micromorphology (Stoops and Gérard this book). Capillary porosity is also partly attributed to microporosity of pumice and ash, particularly for the vitric soils (as also described by Stoops and Gérard this book) and for a very small part, by the microporosity of allophane (quantified by nitrogen adsorption and use of the t-plot procedure allowing to estimate the volume and surface area of the micropores of diameters less than 1 nm, results not shown).

The question arises whether we can quantify the capillary porosity within the void network space. We can estimate total porosity from bulk density, ρ_b, and particle density, ρ_s (total porosity = $1 - \rho_b / \rho_s$). We measured bulk density and computed particle density from the linear relationship between particle density (measured by helium pycnometry) and organic carbon content which was recently obtained by Poulenard et al. (2003) on a wide range of allophanic and non-allophanic Andosols ($\rho_S = -0.004$ organic C + 2.678, $p<0.001$).

First, the measured bulk density decreased as a function of Na-resin clay content (Figure 8, showing a significant, $p<0.01$, but very scattered relationship).

Conversely but with a better physical meaning, a positive but scattered relationship between calculated total porosity and Na-resin clay content was identified (results not shown, also $p<0.01$). Calculated total porosity

varied from 0.69 to 0.74 cm^3 cm^{-3} for the vitric soil samples and from 0.72 to 0.87 cm^3 cm^{-3} for the non-vitric Andosol samples. Similar high total porosity values of 0.7 to 0.85 cm^3 cm^{-3} have been reported previously for Japanese Andosols (e.g. Nanzyo et al. (1993).

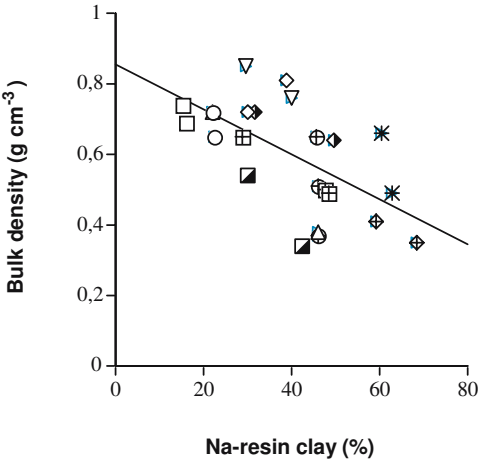

Figure 8. Relationship between bulk density and organo-mineral clay content for a range of European volcanic soil samples (4 vitric soil and 20 Andosol A_h and B_w samples).

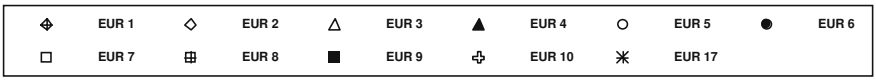

The key result is that capillary porosity represents 87–97% of total porosity for most non-vitric Andosol samples, with a negligible macroporosity, but 75–85% of total porosity for the vitric soil samples (Figure 9). For most other soil types, capillary porosity represents only 40–70% of total porosity, leading to the well-known hierarchical and bimodal porosity (e.g. Brewer 1964).

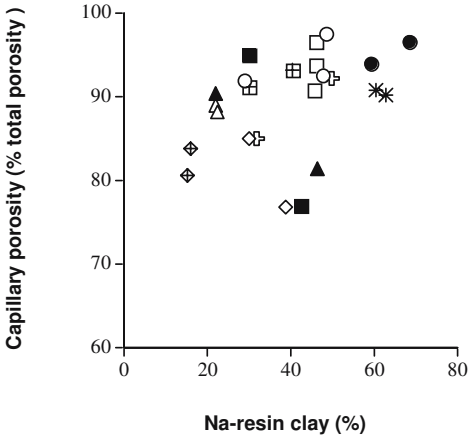

Figure 9. Relationship between proportion of total porosity that corresponds to capillary porosity and organo-mineral clay content for a range of European volcanic soil samples (4 vitric soil and 20 Andosol A_h and B_w samples). Same symbols as those used in Figure 8.

Let us now analyse again the results obtained on volumetric field soil moisture. Figure 10 shows that the H1 horizon sampled from the EUR09 *Umbri-Vitric Andosol (Pachic and Orthidystric)* (WRB 2001) was the only soil sample where capillary porosity was saturated. This validates field observation on this hydromorphic peaty soil horizon.

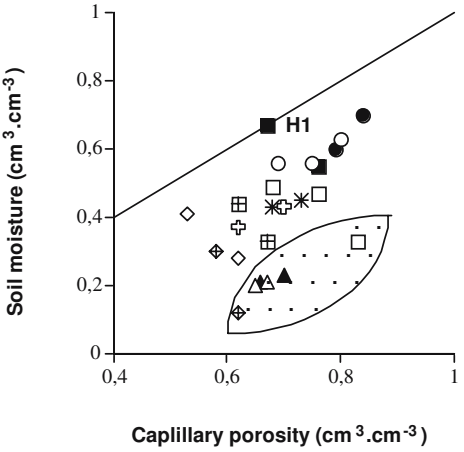

Figure 10. Relationships between volumetric field soil moisture and capillary porosity for a range of European volcanic soil samples (4 vitric soil and 20 Andosol A_h and B_w samples). Three categories of soil samples have been distinguished: the EUR09 H1 Andosol sample, with a data plot located on the saturation line (saturation of capillary porosity), the relatively dry soil samples with data plots located within the closed dotted area, and the relatively wet soil samples in between.

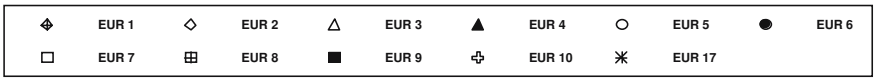

In most samples, 45–83% of the capillary porosity was filled by water, while in EUR05 and EUR06 samples the capillary porosity was filled for 75–83%. In the vitric soil samples these values were much lower and only amounted to 45–72% (Figure 10). This shows the high capacity of volcanic soils to retain water (particularly under the wet oceanic climate occuring in the Azores Islands) within their very large capillary porosity. By contrast, only a few samples were relatively dry at the time of sampling (Italian EUR03 and EUR04 Andosol samples, EUR07 topsoil sample and EUR01 vitric soil B_w horizon: Figure 10). For most of the studied soil samples, except the driest ones, the values of volumetric soil moisture from the field were also similar to those estimated from drainage at a suction value of 33 kPa as reported by Basile et al. in the next chapter of the present Book Section (results not shown).

A final question arises about the similarity between capillary porosity properly estimated by capillary rise (present study) and that estimated at a suction value of 33 kPa (see, e.g. the review of Nanzyo et al. 1993). Volumetric soil water of volcanic soils is often subdivided into three categories:

hygroscopic water (water content values at suction values more than 1500 kPa mainly referred to hygroscopic forces, micropores), capillary water available to plants (water content values at suction values from 1500 to 33 kPa mainly referred to capillary forces, mesopores) and gravitional water (water content values at suction values from 33 to 0 kPa mainly referred to gravitional forces, macropores). Nanzyo et al. (1993) reported water content values of nearly 30–35 vol%, 25 vol% and 30–10 vol% for hygroscopic, capillary and gravitational water, respectively, in the A_h and B_w horizons of a representative Andosol (*Alic Melanudand* according to ST 1989). This leads to 33 kPa capillary porosity values of nearly 0.55 to 0.6 cm^3 cm^{-3} which appear to be underestimates when compared to those measured by capillary rise on wet undisturbed soil cores 0.6 to 0.8 cm^3 cm^{-3} (this study).

It is therefore strongly recommended to estimate the capillary porosity by capillary rise on wet undisturbed soil cores rather than by measurement at a suction value of 33 kPa. The key result is that capillary porosity represents 87–97% of total porosity. This is exceptionally high for soils and has key consequences for physical properties of these volcanic soils. In a complex way, capillary porosity regulates water retention and also all processes in which capillary forces are involved, such as is shrinkage of fine-grained soils on drying.

Shrinkage

Despite previous work, shrinkage of Andosols has not been fully explored. The main results of the 40°C drying kinetics were as follows.

First, the studied soil samples were subdivided into two categories: those which dried without (or very moderate) shrinkage (e.g., EUR01 and 02 vitric soil samples from Italy, EUR08 Andosol samples from Iceland) and those which shrank, (often intensively, e.g., EUR05 and 06 Andosol samples from the Azores Islands) when submitted to controlled drying. Above a specific Na-resin clay content (20%) threshold value, total shrinkage increased as a function of either Na-resin clay content ($p<0.001$: Figure 11). The maximum shrinkage of 60–80% is exceptional for soils. The more clayey a volcanic soil, the more microporous it is and the more it shrinks upon drying. This is why the B_w horizons shrank more than the corresponding topsoils (Figure 12).

The relation between total shrinkage and initial capillary porosity ($p<0.001$: Figure 13) is physical-based. A similar relation between total shrinkage (40–75%) and initial void ratio was reported by Poulenard et al. (2002) for a range of Andosols from Central America, Japan and West Indies. The relation between total shrinkage and Na-resin clay ($p<0.001$:

Figure 11), however is an indirect relation, because soil aggregation is controlled by Na-resin clay (e.g. Figure 7).

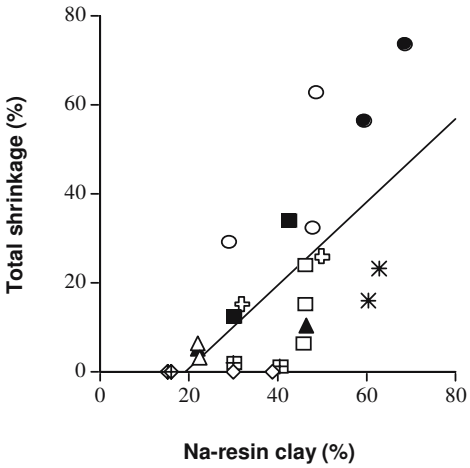

Figure 11. Relationship between total volumetric shrinkage at 40°C and Na-resin clay content for a range of European volcanic soil samples (4 vitric soil and 20 Andosol A_h and B_w samples).

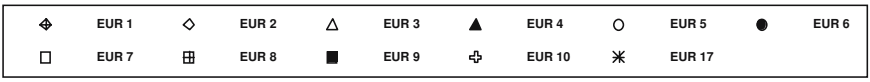

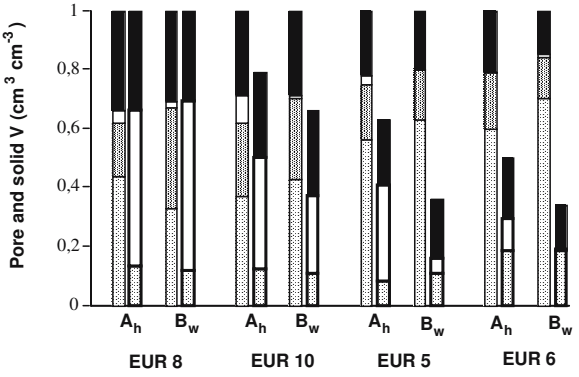

Figure 12. Void and solid volumes after water-filling of capillary porosity (initial state) and at the end of the controlled 40°C drying (final state) for a range of European Andosol A_h and B_w samples. Towards the right the samples show both larger clay content and stronger shrinkage. Capillary porosity – fw = field air-filled capillary porosity.

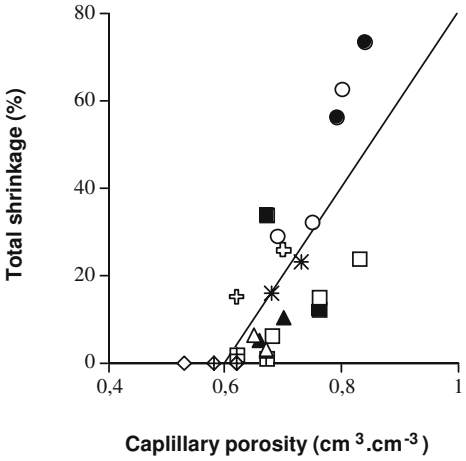

Figure 13. Relationship between total volumetric shrinkage at 40°C and capillary porosity for a range of European volcanic soil samples (4 vitric and 20 Andosol A_h and B_w samples).

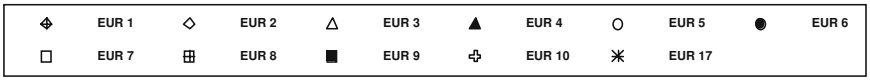

Figure 14 shows a typical shrinkage curve of a strongly shrinking sample. The drying starts at upper right. The first stage is a short loss of water without change in total volume. (the structural shrinkage domain of the Three Sraight Lines Model described, e.g., by Poulenard et al., 2002). This stage is followed by an intense combined water loss and shrinkage process with data points often located on the saturation line (Figure 14). This emphasizes the exceptional predominance of capillary porosity within the total solid and void volume of the studied samples (Figure 12), capillary porosity controlling such intense shrinkage. As a matter of fact, shrinkage of fine-grained and highly microporous Andosols on drying is caused by movement of microaggregates as a result of pore-water tension developed by capillary menisci.

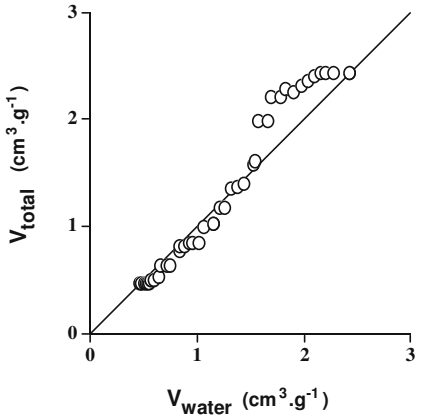

Figure 14. Shrinkage as change in total volume versus soil water volume for the undisturbed EUR06 $2B_w$b core (capillary porosity preliminarily filled by water by capillary rise for 48 h) during its controlled 40°C drying.

Many changes in physical properties are associated with this change of void volume. For example, the increase in water-stable aggregates upon drying was proportional ($p<0.001$) to volumetric shrinkage (Figure 15).

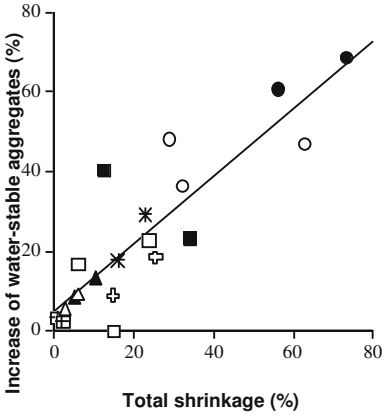

Figure 15. Relationships between the increase of mean proportion of water-stable aggregates occurring during drying and total volumetric shrinkage for a range of European Andosol A_h and B_w samples (n=20).

The more shrunken the soil, the more water-stable are the >200 μm aggregates. Such irreversible mechanical changes caused by drying have been previously reported for Japanese Andosols (e.g. Kubota 1972). The exceptional increase in the proportion of water-stable aggregates of 40–70% (of 105°C dried soil) estimated for the most clayey Andosol samples was attributed to the strong reduction of porosity occurring upon drying. This reduction in porosity is itself related to high values of initial capillary porosity (Figure 13). Further, the proportion of water-stable aggregates of the 40°C-dried soil was negatively related to its initial porosity, whereas this relationship was only a tendency for the wet samples (results not shown). We assume that capillary forces related to menisci of the residual water located between the solid phases are very high.

Conclusion

The main conclusions from the analyses carried out on a range of European volcanic soil samples can be summarised as follows:

Ultrasonic and Na resin sequential treatment, a recommended methodology for clay dispersion

The Na-resin method without destruction of organic matter or/and poorly-ordered minerals was specifically adapted for Andosols for obtaining most of the organo-mineral clay fractions. This relatively new methodology is recommended for characterizing particle-size distribution in Andosols. This opens new perspectives in this area, because many Andosols fail to disperse completely with sodium hexametaphosphate, as we clearly reported in this study. Na-resin clay content is a useful combined indicator of weathering, organo-mineral interactions and soil development.

Water-dispersible clay

Even with highly flocculated clay, a negative relation was found between the proportion of organo-mineral clay dispersed by water and soil surface charge estimated by ΔpH (pH-KCl N – pH-H_20). The studied Andosol A_h horizons were more flocculated (4–16% of total clay were water-dispersible) than Oxisol A_h horizons previously studied elsewhere (often 20–40% of total clay were water-dispersible). This difference should be attributed to the much more colloidal character of the allophanes, ferrihydrite and organo-aluminium associations occurring in Andosols, as compared to that of the rather rigid and coarser kaolinite, gibbsite and goethite occurring in the Oxisols. Organo-mineral interactions should also be stronger and more complex in the Andosols than in the Oxisols.

Organo-mineral clay and water retention

The more clayey the soil, the more microporous it is and the more water it retains in its capillary pores. This explains why most B_w horizons were wetter than the related topsoils.

The very large capillary porosity of the studied soils (mostly from 0.6 to 0.8 $cm^3\ cm^{-3}$) are similar to those of Histosols but are much more larger than those of other soil types (mostly from 0.1 to 0.4 $cm^3\ cm^{-3}$). This is mainly attributed to soil aggregation by the very reactive organo-mineral clay fraction which coats and bridges coarser particles leading to frequent granular microstructures for the non-vitric Andosols (Stoops and Gérard this book). Capillary porosity is partly attributed to pumice and ash microporosity, particularly for the vitric soils and, for a very small part, to the microporosity of allophane.

Capillary porosity represents 87–97% of total porosity for most Andosol samples – with a rather negligible macroporosity – but 75–85% of total porosity for the vitric soil samples. The high capacity of volcanic soils to retain water is clearly related to their very large capillary porosity. For most of the other soil types, capillary porosity represents only 40–70% of total porosity, leading to the well-known hierarchical and bimodal porosity.

Capillary porosity determined by capillary rise: a recommended methodology in the study of soil structure and water retention

It is recommended to estimate the physical-based capillary porosity by capillary rise on wet undisturbed soil cores rather than by the classical estimate at a suction value of 33 kPa (underestimation of capillary porosity).

Drainage and shrinkage on drying

The studied soil samples were subdivided into two categories: those which drained without (or very moderate) shrinkage and those which shrank, often intensively, when submitted to controlled 40°C drying. Moreover, above a specific Na-resin clay content (20%) or capillary porosity (0.6 cm^3 cm^{-3}) threshold value, total shrinkage increased as a function of either Na-resin clay content or initial capillary porosity. The maximum shrinkage values of 60–80% are exceptional for soils. Thus, the more clayey a volcanic soil, the more microporous it is and the more it shrinks upon pronounced drying. This is why B_w horizons shrank more than topsoils.

For the most shrunken Andosol samples, the shrinkage curve typically began by a very short-time predominance of water loss, followed by an intense combined drying and shrinkage process with data points often located on the saturation line. This emphasizes the exceptional predominance of capillary porosity within the total solid and void volume of the studied horizons, capillary porosity controlling such intense shrinkage caused by movements of microaggregates as a result of pore-water tension developed by capillary menisci.

An increase in the proportion of water-stable aggregates occurred when the wet soils were 40°C dried. This was positively correlated to total volumetric shrinkage. The exceptional increase in the proportion of water-stable aggregates of 40–70% (of 105°C dried soil) estimated for the most clayey Andosol samples from the Azores Islands was attributed to the strong reduction of porosity occurring from the wet to the 40°C dried state, itself related to exceptional values of initial capillary porosity.

General conclusion

To summarise, the sampling and methods used to characterise soil texture, soil structure and physical properties on a range of European volcanic soils enabled a much wider range of scales to be considered than is often the case. In particular, we related amounts of organo-mineral clay to physical soil properties such as bulk density, capillary porosity obtained by capillary rise and total volumetric shrinkage of wet undisturbed soil cores (with water-filled capillary porosity) at the end of controlled 40°C drying kinetics. We therefore validated that mineral, organic and organo-mineral colloidal soil constituents interact between them to give organo-mineral clay fractions (soil micro-property) and that, in turn, organo-mineral clay coates and bridges coarser soil particles (soil aggregation) leading to soil structural features which vary as a function of clay content and control soil macro-properties (capillary porosity, water retention, shrinkage, irreversible structural and mechanical changes upon drying).

Acknowledgements

We thank Luciani Lulli and Fabio Terribile (Vico and Gauro Volcanoes, Italy), Jorge Pinheiro and Manuel Madeira (Azores Islands, Portugal), Olafur Arnalds and Hlynur Oskarsson (Iceland), Marisa Tejedor and Jose Hernandez-Moreno (Tenerife Island, Spain) and Jean Dejou (Cantal, France) for the selection of the COST 622 reference profiles, Toine Jongmans (The Netherlands) and Folkert van Oort (France) for the soil and site description, Paul Quantin (France) for the ST and WRB soil classifications, Elisabeth Schouller and Bernadette Gerard for valuable technical assistance in shrinkage experiments and elementary organic analysis, respectively. Inorganic soil data and pH data were kindly provided by the Department of Soil Science and Geology of the University of Santiago, Spain (E. Garcia-Rodeja) and the Instituto Superior de Agronomia, Lisbon, Portugal (M. Madeira), respectively. Support and funding from the COST Action 622 “Soil resources of European volcanic systems” (1998–2004) are greatly appreciated. We finally thank the reviewers for their useful comments on an early draft of the chapter and Peter Buurman for his careful editing.

References

Auxtero E, Madeira M, Sousa E (2004). Variable charge characteristics of selected Andisols from the Azores, Portugal. Catena, 56 special issue (Volcanic soil resources: occurrence, development and properties, Arnalds O, Stahr K, eds), pp 111–125

Bartoli F, Philippy R, Burtin G (1988). Aggregation in soils with small amounts of swelling clays. I. Aggregate stability. J Soil Sci 39:593–616

Bartoli, F, Burtin G, Herbillon A (1991). Disaggregation and clay dispersion of Oxisols: Na resin, a recommended methodology. Geoderma 49:301–317

Bartoli F, Burtin G, Guerif J (1992). Influence of organic matter on aggregation in Oxisols rich in gibbsite or in goethite. II. Clay dispersion, aggregate strength and water-stability. Geoderma 54:259–274

Brewer R (1964). Fabric and Mineral Analysis of Soils. John Wiley & Sons, New York

Churchman GJ, Bartoli F, Burtin G, Rouiller J, Weismann D (1999). Comparison of methods using sodium for the size fractionation of soil. 11th Int Clay Conf Proc, June 15–21 1997, Ottawa (Canada), pp 331–338

Gillman GP (1974). The influence of net charge on water dispersible clat and sorbed sulphate. Australian J Soil Sci 12:173–176

Gillman GP, Bell LC (1976). Surface charge characteristics of six weathered soils from tropical North Qeensland. Austr J Soil Sc 14:351–360

Koutika LS, Bartoli F, Andreux F, Cerri CC, Burtin G, Chone T, Philippy R (1997). Organic matter dynamics and aggregation in soils under rain forest and pastures of increasing age in the eastern Amazon Basin. Geoderma 76:87–112

Kutoba T (1971). Aggregate-formation of allophanic soils: effect of drying on the dispersion of the soils. Soil Sci and Plant Nutr 18:79–87

Maeda T, Soma K (1985). Classification of Andisols in Japan based on physical properties. Int Clay Conf Proc (Schultz LG, van Olphen H, Mumpton FA, eds), The Clay Minerals Society, Denver, pp 174–178

Mekaru T, Uehara G (1972). Anion adsorption in ferragineous tropical soils. Soil Sci Soc Am Proc 36:296–300

Mizota C, van Reeuwijk LP (1993). Clay mineralogy and chemistry of soils formed in volcanic material in diverse climatic regions. Soil Monogr vol 2, ISRIC, Wageningen

Nanzyo M, Shoji S, Dahlgren R (1993). Physical characteristics of volcanic ash soils. In: Shoji S, Nanzio M, Dahlgren R (eds) Volcanic Ash Soils: Genesis, Properties and Utilization, Development in Soil Science vol 17, Elsevier, Amsterdam, pp 189–201

North PF (1976). Towards an absolute measurement of soil structural stability using ultrasound. J Soil Sci 27:451–459

Ping CL, Shoji S, Ito T, Takahashi T, Moore JP (1989). Characteristics and classification of volcanic-ash-derived soils in Alaska. Soil Sci 148:8–28

Pinheiro J, Madeira M, Monteiro F, Medina J (2001). Caracteristicas e classifiçao dos Andossolos da Ihla do Pico 'Arguipélago dos Açores). Rev Cienc Agrarias 24:48–60

Poulenard J, Bartoli F, Burtin G (2002). Shrinkage and drainage in volcanic soil aggregates: a structural approach combining air under vacuum drying kinetics and mercury porosimetry. Eur J Soil Sci 52:563–574

Poulenard J, Podwojewski P, Herbillon AJ (2003). Characteristics of non-allophanic Andisols with hydric properties from the Ecuadorian paramos. In: Bartoli F, Buurman P, Delvaux B, Madeira M (eds) Volcanic sols; properties and processes as a function of soil genesis and land use. Geoderma 117 special issue, pp 267–281

Poulenard J, Michel JC, Bartoli F, Portal JM, Podwojewski P (2004). Water repellency of volcanic ash soils from Ecuadorian Páramo: effect of water content and characteristics of hydrophobic organic matter. Eur J Soil Sci 55:487–496

ST (Soil Taxonomy), Soil Survey Staff (1999). Soil Taxonomy. A Basic System of Soil Classification for Making and Interpreting Soil Surveys. 2nd edn. USDA-NRCS. Agriculture Handbook No 436. Washington

Stoops G, Gérard M (2006). Micromorphology, this book (Section II)

Tessens E (1984). Clay migration in uplands soils of Malaysia. J Soil Sci 35:615–624

Warkentin BP, Maeda T, Soma K (1988). Physical characteristics for classification of Andisols. Proc of the 9th Int Soil Classification Workshop for Soil Management (Kinloch DJ, Shoji S, Beinroth FH, Eswaran H, eds), Support Service, Washington, pp 97–107

WRB (World Reference Base for Soil Resources, Driessen P, Deckers J, Spaargaren O, Nachtergaele F, eds) (2001). Lecture Notes on the Major Soils of the World. FAO World Soil Resources Reports 94. Rome

A comparative analysis of the pore system in volcanic soils by means of water-retention measurements and image analysis

A. Basile, A. Coppola, R. De Mascellis,
G. Mele and F. Terribile

Introduction

The soil pore system governs life in many terrestrial ecosystems. In this regard the case of volcanic soils, and especially Andosols, is of major interest since the unique properties of these soils, such as high water retention, low bulk density, high smeariness, etc., mainly depend on the overall organisation of the pore system.

Given such importance, this chapter addresses the characterisation of the porous system of the COST action 622 reference soils by means of two-well established techniques, namely the water retention curve and image analysis. This work will also attempt to address the complex issue of comparing the results obtained by these two methods.

Water retention measurements on volcanic soils were carried out, especially in soils of the circum-Pacific region, by Misono et al. (1953) for Japanese soils, Colmet-Daage et al. (1967, 1970) for soils from the Caribean, Central America and South America. Most of these measurements were performed on few points of the water retention curve, generally 30 and 1500 kPa (Maeda et al. 1977, Nanzyo et al. 1993).

In Europe, only recently, detailed water retention characteristics were measured on volcanic soils, although not emphasizing their distinct properties. Ciollaro and Romano (1995) combined geostatistics and an inverse method to derive hydraulic properties on a cultivated volcanic soil transect; Basile et al. (2003a) applied the hysteresis concept to the field-laboratory comparison.

More recently few authors took into account the distinct behaviour and characteristics of volcanic soils: Basile and De Mascellis (1999) reported results on the irreversible drying effect on water retention and transport parameters, Basile et al. (2003b) applied a water flow deterministic model to evaluate risk of debris flow triggering, Armas-Espinel et al. (2003) related hydraulic properties to specific andic properties of cultivated soils, Fontes et al. (2004) compared hydraulic properties in volcanic soils with different

methods, and Ritter et al. (2004) analysed measurement strategies for the inverse optimization of the hydraulic properties of a volcanic soil.

Soil pores range in size over several orders of magnitude. Many measurement methods are available in order to quantify pore size distribution, each giving best results in a specific pore size range. Nitrogen sorption at –196°C (Sills et al. 1973), for example, is a well-established method for determining specific surface area and pore size distribution in the range below 20 nm. Mercury intrusion porosimetry can rapidly provide pore size distribution ranging from 10 nm to 100 μm (Pagliai 1988). Soil water retention measurements allow estimation of equivalent pore size distribution between 200 nm to 1 mm. Image analysis methods can also be applied after using very different techniques (fluorescent resin impregnation, *x*-ray Tomography, NMR, etc.) which allow pore space to be visualized. In this latter case size limits depend on which technique is used.

Image analysis methods are generally laborious and time consuming but they can provide details about shape and arrangement of pore space that are not given by other methods (Marshall et al. 1996). Nevertheless, a pore system cannot be adequately characterized by using a single method (Lawrence 1977). Only a comparison of different types of measurements can give more complete representation of the soil structure. Moreover, measurements of the pore size distribution in volcanic soils taking into account their distinctive properties are scarce (Mele et al. 2000).

In the present chapter pore size distributions from water retention curves and from image analysis of resin impregnated soil blocks are compared for the representative soils of the COST action 622.

Materials and methods

Soil sample analysis

The soils subjected to analysis were sampled in the framework of the COST action 622. They are described in the two previous Sections of this book. The reader must refer to this material for a detailed morphological and chemical characterisation.

Undisturbed soil samples were collected for soil structure and hydrology analysis from the major horizons of the COST 622 soils with aluminium cylinders of diameter ranging between 50 and 90 mm.

For soil structure study based on image analysis, the undisturbed samples were kept at the field moisture content and then slowly saturated with acetone (Murphy 1985). The resulting acetone-water solution was treated

with zeolite molecular filters in order to extract the water from the solution; after removal of the water, the samples were treated with orthophthalic polyester resin and fluorescent dye (Uvitex OV). After full impregnation was achieved, the resin was left to harden; the samples were then cut to obtain a parallelepiped (soil block) with four exposing vertically oriented surfaces. Each of the four surfaces (7.2×5.4 cm large) was lightened with a UV lamp and four images were acquired with a Praktica digital scanner (3590×2700 pixels) reaching a resolution of 20 μm per pixel. The images were stored with a PC and then sent to a Silicon Graphics workstation Indigo2 having a CPU R10000 175 mhz, MG Impact, 640 Mb RAM and 18 Gb HD. The images were processed with software developed in C language (Moreau 1997) based on algorithms of mathematical morphology (Serra 1982, 1988). Sequential opening operator (Horgan 1998) was used to calculate pore size distribution. The reported results are averages from the processing of the four images for each of the soil blocks.

For soil hydrology analysis, the soil samples collected in the field were, in the laboratory, slowly saturated from the bottom to the top in different steps, till the external level of the water was higher then the top of the soil samples. Therefore, connected pores were assumed to be completely filled. Saturated hydraulic conductivity was measured by the variable head method (Klute and Dirksen 1986). The soil water retention curve $\theta(h)$ was determined by means of the Stakman apparatus (Klute 1986). Ten points of the curve ranging between saturation and –30.0 kPa of potential were measured, namely 0.0, –0.2, –0.4, –0.8, –1.6, –3.0, –6.0, –10.0, –15.0, –30.0 kPa. In addition, dryer points of the soil water retention curve, namely –100, –300, –800 and –1500 kPa, were measured by means of the pressure chamber method (Klute 1986).

Parametric models for hydraulic properties

The unimodal $\theta(h)$ relationship proposed by van Genuchten (1980) is expressed here in terms of the scaled water content, S_e, as follows:

$$S_e = \left[1 + \left(\alpha_{vg}|h|\right)^n\right]^{-m} \quad (1)$$

where $S_e=(\theta-\theta_r)/(\theta_0-\theta_r)$, and α [m^{-1}], n [–] and m [–] are curve-fitting parameters. In particular, α_{vg}^{-1} corresponds roughly to the so-called air entry pressure value for low m/n ratios, while for high m/n values it is roughly equal to the suction head at the inflection point of the curve (van Genuchten and Nielsen 1985). θ_0 [m^3m^{-3}] and θ_r [m^3m^{-3}] represent the maximum (at h=0) and the residual water content respectively, and may either be fixed or treated as parameters to be optimized.

In natural soils, the presence of aggregates frequently results in a water retention curve with at least two points of inflection (among others, Bruand and Prost 1987, Smettem and Kirkby 1990, Durner 1994, Coppola 2000). To explain such behaviour, a double porosity approach can be used which assumes that the pore space θ_0–θ_r consists of two pore size distributions, occupying respectively the fractions ϕ_1 and ϕ_2=1–ϕ_1 of that pore space (0≤ ϕ_1≤ 1).

For describing the behaviour of the "macro" fraction of the pore space, Ross and Smettem (1993) introduced the following simple one-parameter function:

$$S_e = \left(1 + a_{rs}|h|\right)\exp\left(-a_{rs}|h|\right) \tag{2}$$

where α_{rs} assumes a similar meaning of the α_{vg} parameter; these characterize the position of the inflection points for each water retention curve. Combining Eqs. (1) and (2), the bi-modal $S_e(h)$ relationship can be expressed as follows:

$$S_e = \phi_1\left(1 + a_{rs}|h|\right)\exp\left(-a_{rs}|h|\right) + \phi_2\left[1 + \left(\alpha_{vg}|h|\right)^n\right]^{-m} \tag{3}$$

Detailed description of the near-saturation part of the water retention is required not only for the water retention itself but also with a view to estimating the hydraulic conductivity through theoretical approaches (Mualem 1986). Mualem's widely used expression allows hydraulic conductivity to be calculated from the retention curve: the reliability of hydraulic conductivity estimation depends primarily on the accurate prediction of the pore size distribution toward the large pores, the model being particularly sensitive to the slope of the retention curve near saturation (van Genuchten and Nielsen 1985, Vogel and Cislerova 1988, Durner 1994 and Coppola 2000).

The parameters of the retention functions were obtained by minimizing the following objective function:

$$Z(P) = \sum_{j=1}^{N} \omega_j \left(\theta_j - \overline{\theta}\left(h_j, P\right)\right)^2 \tag{4}$$

in which P={ θ_0, θ_r, α_{vg}, n, ϕ_1, α_{rs}} is the parameter vector, N is the number of $\theta(h)$ data measured, θ_j and (h_j,P) are respectively the measured and estimated water contents at h_j. Assuming all data are of equal quality, for the least squares optimization, the weights were set at the same value ω_j=1/N ∀ j=1, …, N (ordinary least squares).

For the sake of having fewer parameters involved and to attain a consequent overall reduction in parameter uncertainty the parameter θ_0 was fixed at the measured θ_{sat} and m=1–1/n. In most cases when θ_r converged close to zero it was fixed at zero. When the parameter ϕ_1 was estimated at

less than 0.05, the optimization procedure was repeated fixing ϕ_1=0; in this case equation (3) becomes unimodal (Eq. (1)) and the θ_0 was optimized.

Water retention Indexes

The general idea behind this book is the multidisciplinary approach (Bartoli et al. Introduction of this book). Therefore, a synthetic description of hydraulic behaviour is required to find correlations with information from soil chemical analysis. Moreover, the comparison between hydraulic properties of soils formed under considerably different climatic and parent material conditions is complex in itself.

In light of the above, soil hydraulic behaviour was compared by means of two numeric indexes, defined in the following.

The first integrated parameter proposed, the Integral Retention Index, *IRI*, is defined by:

$$IRI = \frac{1}{wp} \int_0^{wp} \theta \, d\left(\log_{10} h\right) \tag{5}$$

where *wp*=4.2 is the logarithm of the pressure head at the wilting point. This adimensional index (0<*IRI*<1) represents the average value of the function $\theta(log_{10}\, h)$ on the interval [0, *wp*] and allows simple comparisons of the whole water retention by coalescing it in a single characteristic value.

The second index is the parameter ϕ_1, defined in Eq. (3), representing the fraction of the pore space occupied by macroporosity according to the modelling of Eq. (2). The reader should be aware that the structural information of the pore system included in the range of soil water potential near saturation determines most of the water flow behaviour in wet conditions. Neglecting such information may lead to overlooking the preferential flow path, widely expected in structured soils. Unlike the *IRI* parameter, which is more related to the static properties of the matrix fraction of the porous system, the parameter ϕ_1 mainly contains information on its dynamic behaviour.

Approaches to pore size analysis

Most of the pore size distribution methods used in image analysis are based on a classical "object" analysis approach (Figure 1a), that is pore objects are identified, and equivalent diameters and/or other shape parameters are calculated for each pore object (Pagliai et al. 1984). According to this

approach equivalent diameters are the diameters of the disks (spheres in 3D) having the same area (volume) as the pore objects identified.

In this work, a morphological opening algorithm has been used to calculate the pore size distribution (Serra 1982, Horgan 1998, Mele et al. 1999). This approach operates by producing a series of disks *i* (spheres in 3D) of increasing diameter D_i which run in the pore network and fill all the pore space between the opposite walls of the solid phase with a distance less than D_i (Figure 1b).

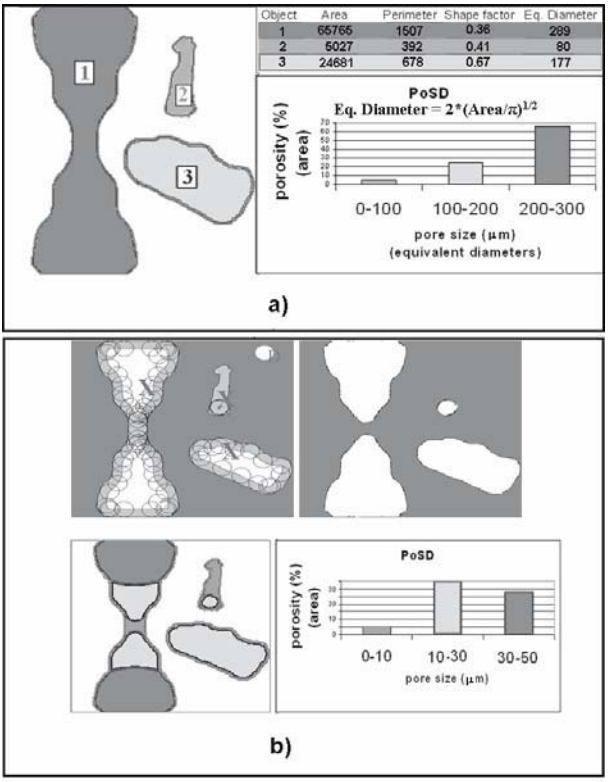

Figure 1. Pore size distribution by image analysis. (a) object approach: pore objects are identified; pore sizes are equivalent diameters; each pore contributes only to one size class. (b) opening algorithm approach: no objects are identified; a succession of circles *i* (spheres in 3D) with increasing diameters D_i sweeps the whole pore space and fills all the porous phase spaced less than D_i. The whole pore space is divided in size classes D_i–D_{i-1} wide; different parts of each pore can contribute to different size classes according to their shape.

Hence using this algorithm no single pore objects are identified and pore size distribution is determined according to the solid wall spacing. This approach produces results which can better relate with functional soil properties like fluid flow and solute transport than using the classical object-based image analysis approach.

In order to obtain pore size distributions from water retention curves the following procedure was used.

The scale of the soil water pressure head on the axis of the soil water retention curve (Eqs. (1) or (3)) was replaced by that of the diameter of the capillaries according to the capillarity law $|h| = 2\,\sigma \cos\gamma / r\rho_w g \approx 0.3/d$ for length units in cm. This procedure supplies the cumulative pore size distribution curve. The derivative of this curve is the curve of pore size density distribution and may be expressed by the following equation (Durner 1994):

$$f(h) = \frac{d\theta(h)}{d\log_{10} h} = \frac{[\log_e 10]h\,d\theta(h)}{dh} \tag{6}$$

or simply by the $f(h)=d\theta(h)/dh$ if log-scale is not applied.

Such a schematization, which assumes the simple conceptual model of the soil porous system as a bundle of parallel capillaries to be correct, leads to the derivation of the "equivalent" pore size distribution. In this manner the equivalent diameters are those of the bundle of capillary tubes which behave, in functional terms, as the soil sample. Therefore the frequency of an equivalent diameter is proportional to the number of capillary tubes constituting the conceptual bundle model, having that diameter.

Statistical analysis

Two statistics were applied (i) to test relationships between data produced and (ii) to investigate the normality of the proposed indexes.

(i) In order to compare pore diameter distribution as obtained from the water retention curve and image analysis, to evaluate the water retention curve's goodness of fit and to correlate *IRI* vs both andicity and pressure heads, Pearson's correlation coefficient was used:

$$r = \frac{k\sum xy - \sum x \sum y}{\left[k\sum x^2 - \left(\sum x\right)^2\right]\cdot\left[k\sum y^2 - \left(\sum y\right)^2\right]^{1/2}} \tag{7a}$$

where x, y are the pairs of data to correlate and k is the number of pairs (x,y). It measures the linear association between two variables. Values of the correlation coefficient range from –1 to 1. The sign of the coefficient indicates the direction of the relationship, and its absolute value indicates the strength, with larger absolute values indicating stronger relationships (Hays 1981). Significance of r has also been evaluated by calculating the probability level p of the statistic U_C which is t-student distributed with k–2 degrees of freedom (Amemiya 1985) being:

$$U_C = \frac{\hat{B}}{es(B)} = \frac{(k-2)\cdot\sum(x-\bar{x})\cdot(y-\bar{y})}{(1-r^2)\cdot\sum(y-\bar{y})^2} \tag{7b}$$

where $\hat{B}$ and *es(B)* are respectively the estimated value and the standard error for the angular coefficient *B* of the fitting line between (*x,y*) data points, $\bar{x}$ and $\bar{y}$ being mean values of *x* and *y* data respectively.

(ii) Statistical distributions of the parameter ϕ_1 and the *IRI* index were tested using the Box-Cox transformation (Box and Cox 1964):

$$T(Z,\lambda) = \begin{cases} (z^{\lambda}-1)/\lambda \text{.....} if \text{..} \lambda \neq 0 \\ \log(z) \text{.....} if \text{..} \lambda = 0 \end{cases} \tag{8}$$

where *Z* represents both ϕ_1 and *IRI* random variables, and *z* are the values.

The maximum likelihood log-function, log *L*:

$$\log L(Z,\lambda) \propto -\frac{n_d}{2}\log\sigma^2(T) + (\lambda-1)\sum_{i=1}^{n_d}\log(z_i) \tag{9}$$

was plotted at varying values of the parameter λ, n_d being the number of the data and σ^2 the sample variance of the transformed variable *T*. The maximum value of Eq. (9) supplies the best λ value which transforms, through Eq. (8), the *Z* variable into a Gaussian one (Box and Tiao 1973; Draper and Smith 1981). Closer to 1 is the best λ, closer to a Gaussian distribution is the untransformed variable *Z*.

Results

In Table 1 the hydraulic parameters of the COST soil horizons are reported, describing the retention curve by using Eqs.(1) and (3). Table 2 shows the correlation coefficient *r* between measured and fitted data of the water retention; high values resulted for both fitting of the bimodal and unimodal model with very low probability levels values ($p<0.0001$).

In the studied soils large differences arise in boundaries and shape of the water retention curve: the strongly physically based parameter θ_0 ranges from 0.475 to 0.883 m^3m^{-3}, the shape parameter α_{vg} ranges between three orders of magnitude and the parameter *n* varies from 1.059 to 3.279. Moreover, half of the investigated soils show a distinct unimodal behaviour ($\phi_1=0$) while the others have a significant fraction of the pore space occupied by macroporosity ($\phi_1>0.05$) as described by Eq. (2). This pore fraction ranges from 6% to 21%.

Table 1. Hydraulic parameters in equations (1) and (3) obtained by minimization of Eq. (4).

Profile	Horizon	θ_0 [m^3m^{-3}]	θ_r [m^3m^{-3}]	α_{rs} [m^{-1}]	ϕ_l [–]	α_{vg} [m^{-1}]	n [–]
EUR 01	Ap	0.563	0.161	1.352	0.08	0.010	1.847
EUR 01	Bw1	0.618	0.120	0.808	0.09	0.014	1.527
EUR 02	Bw	0.602	0.123	-	0	0.078	1.274
EUR 02	2BC1	0.699	0.000	1.136	0.09	0.037	1.241
EUR 03	Ah1	0.532	0.000	-	0	0.042	1.157
EUR 03	Ah2	0.708	0.000	3.139	0.09	0.018	1.169
EUR 03	2Bw1	0.729	0.000	0.781	0.08	0.015	1.389
EUR 04	Ah2	0.725	0.208	-	0	0.041	1.652
EUR 04	Bw1	0.674	0.248	0.845	0.13	0.046	1.376
EUR 05	2Ahb	0.812	0.000	0.827	0.06	0.044	1.094
EUR 05	2Bwb	0.762	0.000	-	0	0.379	1.099
EUR 05	C	0.860	0.000	-	0	0.070	1.096
EUR 05	3C	0.718	0.000	-	0	0.025	1.072
EUR 06	Ah	0.794	0.000	-	0	0.247	1.065
EUR 06	AB2	0.883	0.000	-	0	0.073	1.072
EUR 06	2Bw1	0.883	0.000	-	0	0.128	1.059
EUR 07	Ah1	0.863	0.000	-	0	0.116	1.254
EUR 07	2Ah2	0.718	0.000	-	0	0.007	1.431
EUR 08	Ah1	0.644	0.000	-	0	0.014	1.332
EUR 09	A1	0.729	0.000	0.030	0.20	0.002	3.279
EUR 10	Ah1	0.714	0.000	0.388	0.07	0.008	1.886
EUR 10	2Bw	0.735	0.000	-	0	0.011	1.350
EUR 10	3Bwb2	0.731	0.000	-	0	0.010	1.264
EUR 11	Ah1	0.502	0.000	-	0	0.095	1.467
EUR 11	3Bwb	0.531	0.000	0.381	0.13	0.024	1.581
EUR 13	Ah1	0.530	0.000	2.915	0.06	0.035	1.414
EUR 13	Ah2	0.475	0.000	2.193	0.09	0.029	1.393
EUR 14	2AC	0.753	0.000	2.121	0.07	0.078	1.294
EUR 16	Ah1	0.775	0.000	0.066	0.10	0.483	1.118
EUR 16	2Bw	0.806	0.000	1.468	0.06	0.018	1.427
EUR 16	2RC	0.739	0.000	0.389	0.21	2.913	1.158
EUR 17	Ah1	0.695	0.000	-	0	0.004	1.373

In Table 2 are also given the saturated hydraulic conductivity values, K_S, measured on selected horizons. In the last column total porosity values measured by image analysis are reported. These values are referred to the porosity above 20 μm, the pixel resolution, and therefore they represent only a small fraction of the total porosity estimated by the θ_0 values.

Table 2. *r* is the correlation coefficient between measured and fitted data of water retention, with * indicating probability level p<0.0001. K_S is the saturated water conductivity. *IRI* is the Integral Retention Index, defined in Eq. (5). The last column shows the total porosity (>20 μm) resulting from image analysis (N.A.= not available).

Profile	Horizon	*r*	K_S	*IRI*	Porosity by Image Analysis
		[–]	[m s^{-1} · 10^3]	[m^3 m^{-3}]	[m^3 m^{-3}]
EUR 01	Ap	0.996*	13.57	0.41	0.187
EUR 01	Bw1	0.998*	4.16	0.44	0.117
EUR 02	Bw	0.996*	0.59	0.43	0.270
EUR 02	2BC1	0.999*	1.58	0.47	N.A.
EUR 03	Ah1	0.998*	1.77	0.42	N.A.
EUR 03	Ah2	0.999*	N.A.	0.54	N.A.
EUR 03	2Bw1	1.000*	2.51	0.49	0.069
EUR 04	Ah2	0.996*	N.A.	0.50	N.A.
EUR 04	Bw1	0.997*	N.A.	0.49	N.A.
EUR 05	2Ahb	0.996*	N.A.	0.66	0.117
EUR 05	2Bwb	0.996*	N.A.	0.57	0.120
EUR 05	C	0.994*	N.A.	0.71	N.A.
EUR 05	3C	0.994*	N.A.	0.64	N.A.
EUR 06	Ah	0.999*	N.A.	0.66	0.140
EUR 06	AB2	0.994*	N.A.	0.76	0.077
EUR 06	2Bw1	0.988*	2.53	0.77	0.106
EUR 07	Ah1	0.998*	0.67	0.55	N.A.
EUR 07	2Ah2	0.995*	N.A.	0.54	N.A.
EUR 08	Ah1	0.997*	N.A.	0.47	N.A.
EUR 09	A1	1.000*	N.A.	0.50	N.A.
EUR 10	Ah1	0.999*	N.A.	0.46	0.058
EUR 10	2Bw	0.994*	N.A.	0.55	0.083
EUR 10	3Bwb2	0.943*	N.A.	0.58	0.058
EUR 11	Ah1	0.994*	N.A.	0.27	0.428
EUR 11	3Bwb	0.999*	N.A.	0.31	0.183
EUR 13	Ah1	0.998*	0.40	0.32	N.A.
EUR 13	Ah2	0.999*	N.A.	0.29	N.A.
EUR 14	2AC	0.999*	0.57	0.45	N.A.
EUR 16	Ah1	0.997*	0.84	0.53	N.A.
EUR 16	2Bw	0.998*	0.12	0.53	N.A.
EUR 16	2RC	0.997*	12.56	0.35	N.A.
EUR 17	Ah1	0.997*	0.0005	0.56	N.A.

In Table 2 and Figure 2 the values of the Integral Retention Index, IRI, are reported for all the investigated horizons. The index shows a strong relationship with the pedoenvironment. More specifically:

– the highest values are those of profiles EUR05 and EUR06 collected in the Azores;

- the lowest values refer to profiles EUR11, South of Tenerife and EUR13, Greece. These soils have on average less than 43% of the water retention shown by the soils from the Azores;
- slightly higher water retention (53–61% of the maximum) is shown by soils EUR01 and EUR02 of the Phlegrean fields (South Italy) while the more andic EUR03 and EUR04 from the Vico volcano (Central Italy) have values around 63% of the maximum;
- generally speaking the differences among the profiles are greater than those between the horizons in each of the profiles: this means that the *IRI* parameter is mainly affected by overall soil environment;
- in each profile, under cultivation conditions (EUR01, EUR02, EUR05), the surface horizons show lower *IRI* values than the deeper ones; but in natural conditions the trend seems to be the opposite. This behavior may be related to the change in the soil structure caused by the marked drying process typical of areas in arid and semi-arid climates, (i.e. EUR11);
- as shown in Figure 2, the *IRI* is correlated with $Al_o+½Fe_o$ (r=0.84, p<0.0001). This is very important because it states the relevance of low order clay minerals and/or Al and Fe organo-mineral complexes in governing the hydrological parameters and eventually the hydrological behavior of these soils. The relationship between andic properties and water retention parameters is well investigated for the driest zone (i.e. 1500 kPa) of the water retention curve (Maeda et al. 1977, Nanzyo et al. 1993), but very little is known in the range 1500–0.1 kPa (near saturation), which is indeed the most important zone of the water retention curve for plant life in many terrestrial ecosystems;
- in Figure 2 it is important to note that the soils that depart most from the regression line are those with the lowest $Al_o+½Fe_o$ (and also a high content in pumice). It seems therefore that in low andic environments the content of low order clay minerals and/or Al and Fe organo-mineral complexes is not the main factor governing hydrological parameters; other factors such as pumice content, organic carbon content and faunal activity may play a much more important role.

A correlation between the *IRI* and the water content at each single pressure head value of the soil water retention curve was calculated for all the analyzed horizons. In Figure 3, Pearson's correlation index vs the logarithm of the pressure head value is shown. As expected, at all the pressure head values, a considerable correlation with the *IRI* (r>0.83, p<0.0001) resulted. Two peaks can be distinguished: the first (r≈ 0.93), close to saturation, at around 6 cm (log|h|≈ 0.8) of pressure head and the second (r≈ 0.96) at around 400 cm (log|h|≈ 2.6) of pressure head.

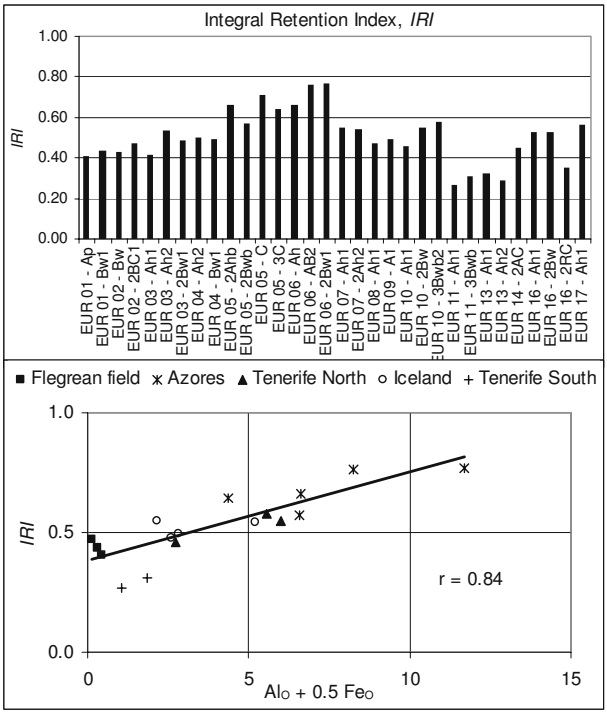

Figure 2. Integral Retention Index, *IRI*, for all the horizons investigated (upper graph) and correlation with the andicity expressed by $Al_o+½Fe_o$ (lower graph).

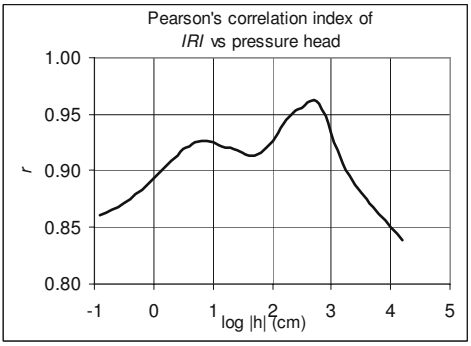

Figure 3. Correlation index of the Integral Retention Index, *IRI*, vs the logarithm of the pressure head value.

If only few points of the retention curve can be measured in order to infer the retention behavior of such soils, it seems reasonable to choose a point around these peaks. For these volcanic soils, the widely used wilting point ($\log|h| \approx 4.2$) seem to be less representative of the entire water retention behavior than near-saturation and field capacity values ($\log|h| \approx 2$ or alternatively $\log|h| \approx 2.5$).

In Table 1 parameter ϕ_l representing the fraction of the pore space occupied by macroporosity is also reported. Analysis of the distribution of this parameter shows no correlation with other parameters or with environmental factors. The only weak correlation found is with the maximum soil water content, which has to be reasonably ascribed to the retention model formulation and only partly to a real physical basis.

The water retention measurements allow to deduce the existence of two different pore systems. However, the lack of data doesn't permit to unequivocally identify the actual shape of the secondary pore system and therefore air entry point and the abruptness of water content release were determined with a high degree of uncertainty.

The fact that parameter ϕ_l is conceptually related to dynamic properties and the *IRI* index is related to static properties is explored by studying their distributions. The Box and Cox normality analysis of parameter ϕ_l and index *IRI* is reported in Figure 4. The *IRI* index has the best value λ=0.70 and therefore a distribution that can be roughly approximated to a Gaussian one, being λ equal to 0 and 1 for a log-normal and normal distribution, respectively. This result partially confirms that soil static properties are normally distributed (Hopmans and Overmars 1986, Horowitz and Hillel 1987). For parameter ϕ_l, λ was equal to –1.2, hence showing a distribution far from the Gaussian one, therefore confirming its dynamic character. More precisely, the asymmetric distribution of ϕ_l approximates the normality with an inverse transformation of the data, i.e. the Cauchy distribution (Patel and Read 1996).

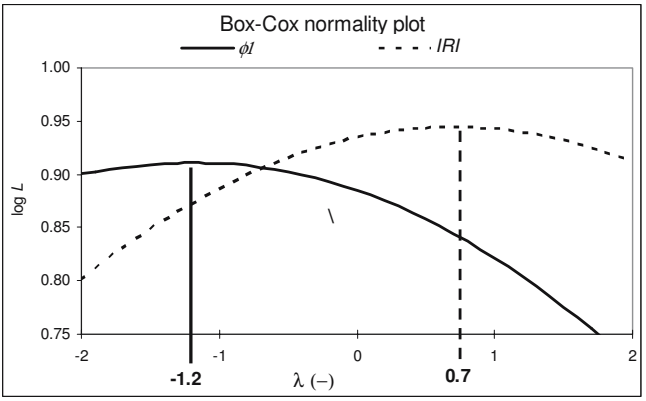

Figure 4. Box Cox normality analysis. Maximum likelihood log-function log *L* vs parameter λ of the Box-Cox transformations of variables ϕ_l and *IRI*.

Image analysis was applied on the soils from Italy, the Azores and Tenerife (last column of Table 2). The results are given in Figure 5 where the

% porosity vs pore diameter at intervals of 40 μm for both image analysis and hydrological measurements is represented. The hydrological derived equivalent pore size distribution was obtained from the water retention curve. The pore percentage to be assigned to each pore class of 40 μm was calculated as the difference from the previous class and this value was assigned to the central value of the class.

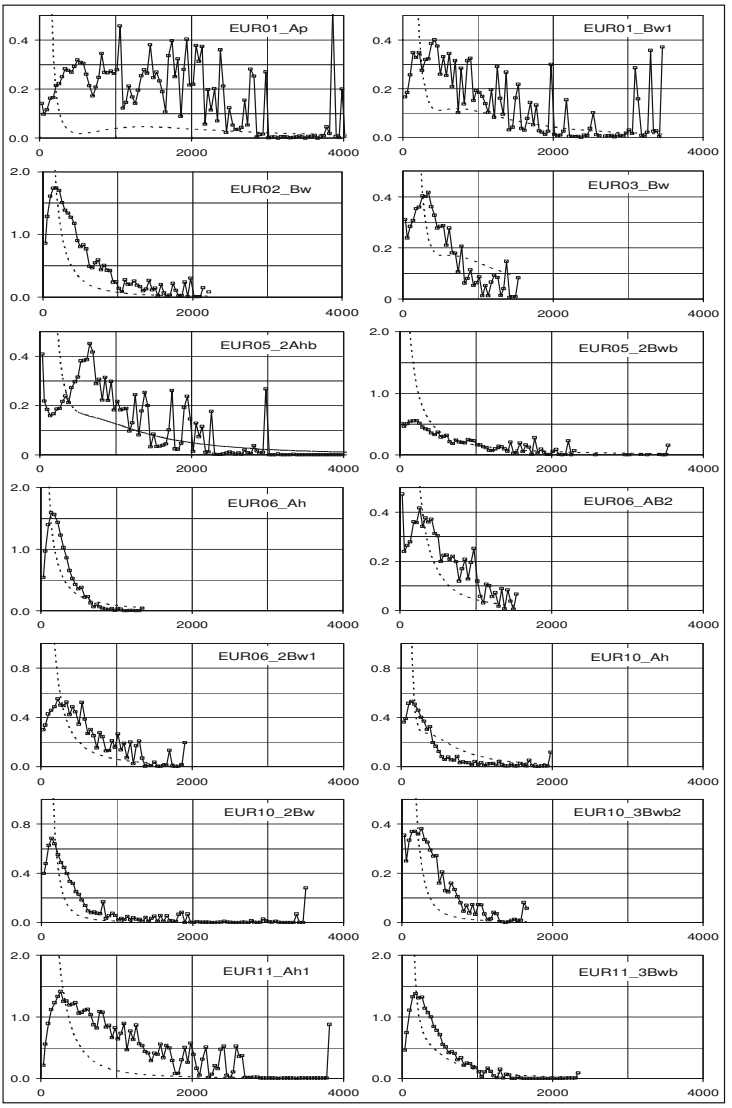

Figure 5. Pore size distributions: -------- from water retention curve (Eq. (6)); ——□—— by image analysis; pore diameter (μm) on X axis, porosity (%) on Y axis.

Pore size distributions by image analysis show a large variability in all the examples which indicate many different pore compartments and high physical fertility.

From Figure 5, it is clear that the image analysis results obtained from the many diverse volcanic soils suggest the importance of human activities in determining the complexity of the pore size distribution (PoSD). As human soil impact increases (EUR01, EUR02, EUR05), the PoSD becomes more complex and multimodal; with a decrease in soil impact the PoSD tends towards unimodality as already shown by Mele et al. (2000). If present, pumice can make a major contribution in determining PoSD complexity (i.e. EUR01; EUR11) especially in the range of the largest pore width.

The matching of the two techniques is very poor for some soils and better for others. Generally speaking, the pore size distributions detected with the two techniques are completely different for the classes of pore size finer than 500 μm. Such behavior cannot simply be due to the fact that pore size distribution on 2D images did not represent exactly the soil volume involved in the hydraulic measurement. Most volcanic soils have a well developed and uniform soil structure (Miyazaki 1993, Moldrup et al. 2003) and the pore size distribution resulting from the four 2D faces is very closely related to that obtainable from the whole 3D soil block (Mele et al. (2000) with respect to the analysis of EUR01 Ap). In fact 3D images are strictly required only when connectivity analyses must be performed.

The difference between image analysis and water retention analysis is, indeed, related to the very different physical principles which are behind these techniques.

While the hydrological method is based on measuring capillarity forces, the image analysis method is based on detecting photon emission energy from the fluorescent dye introduced in the pores. Therefore, while for pores finer than 500 μm capillarity forces are well established and dominant, photon emission energy detection is hindered by the decreasing quantity of fluorescent resin which fills those fine pores. The opposite happens for larger pore size classes, in which the capillary bundle model becomes less realistic while photon emission energy increases.

Moreover, the image analysis detects the real geometry of the porous system while the water retention curve determines a functional equivalent pore size distribution. This equivalence includes also the effects related to the pores connectivity, crucial for dynamic properties (i.e. hydraulic conductivity) but playing a minor role in the water retention characteristic (e.g. hysteresis effect).

It is worth noting that the more complex the pore system, the poorer the matching of the two techniques. In such cases hydrological analysis, which

describes the porous system well in functional terms, result in a poor description of pore architecture.

Numerical comparison of the two methods produced weak results as shown by the correlation coefficients reported in Table 3, column 1; this is especially caused by the influence of the pore size classes finer than 500 μm in determining a low correlation index between the methods. Considering such problem, in order to enhance the understanding of the dataset, it has been chosen to reiterate the calculation of the correlation coefficient after step-wise elimination of pore size classes starting from the smallest size. In Figure 6 the results of this procedure were shown for the two horizons (EUR01 Ap; EUR05 2Bwb) which represent the extreme cases in terms of correlation coefficient between the two methods. The first point was calculated considering all the *n* pairs while the *n*–1; *n*–2; …; *n*–15, etc. correspond to the successive elimination of the 1st, 2nd, …, 15th pairs of points starting from the smallest pore size classes.

Table 3. Correlation coefficients between the pore size distributions as derived from image analysis and from soil water retention curve: *r* was determined using the whole data set and *r*' excluding the first seven points. Data are ordered according to decreasing values of *r*'. Probability levels, p>0.0001 are reported in parenthesis. Parameter ϕ_1 derived from the water retention (see Table 1), representing the pore space occupied by macroporosity, is shown in the last column.

Horizons	*r* (n points)	*r*' (n–7 points)	ϕ_1
EUR11 3Bwb	0.396 (p=0.002)	0.989	0.13
EUR06 Ah	0.590	0.985	0
EUR02 Bw	0.606	0.951	0
EUR10 3Bwb2	0.423 (p=0.005)	0.919	0
EUR10 2Bw	0.470	0.902	0
EUR05 2Bwb	0.694	0.863	0
EUR06 2Bw1	0.393 (p=0.006)	0.859	0
EUR06 AB2	0.482 (p=0.002)	0.851	0
EUR03 2Bw1	0.273 (p=0.093)	0.827	0.08
EUR10 Ah1	0.403 (p=0.004)	0.803	0.07
EUR05 2Ahb	0.334	0.748	0.06
EUR11 Ah1	0.341 (p=0.001)	0.729	0
EUR01 Bw1	0.126 (p=0.246)	0.669	0.09
EUR01 Ap	0.008 (p=0.997)	0.504	0.08

The coefficients are stable after the first 7 points for all the curves (data not shown); therefore it was decided to use *n*–7 pairs of points for the correlation analysis.

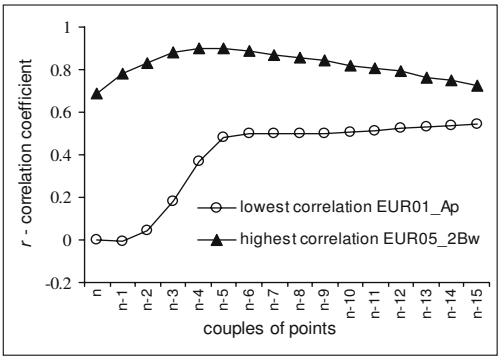

Figure 6. Trend of the correlation coefficient between water retention and image pore size distribution analysis consequent to the stepwise elimination of pore size classes starting from the smallest.

In Table 3 are reported, for each investigated horizon, the correlation coefficients *r*, between the PoSD measured by the two methods, the new correlation coefficient, called *r'*, using *n*–7 pairs of points and the parameters ϕ_1 derived from the water retention (also reported in Table 1). Data are ordered according to decreasing values of *r'* in order to help discussion. Interestingly, the general trend is that all the horizons showing the presence of macropores ($\phi_1 \neq 0$), have the lowest correlations *r'*. On the other hand, the best correlation between the two methods occurs when the unimodal pore size distribution was obtained by hydrological analysis. Only the EUR11 profile behaved oppositely, showing a high correlation index (*r'*=0.989) in presence of macroporosity (ϕ_1=0.13) for the 3Bwb horizon and low correlation index (*r'*=0.729) along with unimodal distribution, for the Ah1 horizon. Such differences can be related to the high vitric features of this soil (Al_o+½Fe_o: 1%), as compared to the other soils, and also possibly to the presence of a population of pores related to the occurrence of abundant pumice grains (especially in the Ah horizon).

Overall the general results in the case of complex porous systems like volcanic soils confirms that the image analysis approach is a powerful tool for its description while water retention rarely can infer such pore complexity. Results can be improved if water retention are properly parameterized taking into account that the choice of the most appropriate parameterization depends on the aim of the analysis. A more detailed description of the retention curve may be found preferable to a more simplified representation with well identified parameters and vice versa. This is the case when the aim of the interpolation could be the only best fitting of the water

retention measurements. However the data we reported show that, independently from the parameterization, the water retention approach is feasible in describing the only simple pore size distribution.

Conclusions

For the range of volcanic soils investigated, water retention analysis showed that near-saturation and field capacity water contents are more representative of the whole water retention behavior than the most commonly used "wilting point" water content. The Integral Retention Index, *IRI*, showed a strong relationship with the different environments; the index also showed a clear relationship with the andic properties (as estimated by Al_o+½Fe_o; r=0.84), the soils with the lowest Al_o+½Fe_o and also a high content in pumice departing from this linear relationship. This is especially relevant because *IRI*, has a very important physical meaning with respect to ecosystem fertility.

The fraction of the pore space occupied by macroporosity, inferred from the parameter ϕ_1, was relevant for half the soils investigated; however, it was not possible to detect any correlation with other environmental variables.

The *IRI* index, related to static hydrological properties, was approximately normally distributed. The distribution of the ϕ_1 parameters, related to dynamic hydrological properties, was far from normality as it was better approximated by others distributions (i.e. Cauchy) than the log-normal.

Image analysis showed the great complexity of the pore system of these volcanic soils which generally present multimodal pore size distributions.

Comparison between the results from these two techniques suggests that hydrological pore analysis is more suitable to represent pore systems in the size range lower than 500 μm while a much more detailed description is provided by image analysis for pores larger than 500 μm. Specifically, the water retention approach is feasible in describing only simple pore size distribution while fails in describing more complex porous systems with micro ad macropores.

The overall results reported in the present chapter confirm the necessity of different approaches in order to thoroughly understand the soil pore system, especially when complex volcanic material is examined.

Acknowledgements

The authors express their gratitude to Francois Bartoli from ENSAIA - INPL/INRA (Fr), Carlos Regalado from ICIA (Es) and the anonymous reviewer for their valuable comments that greatly enhanced this work.

References

Amemiya T (1985). Advanced Econometrics. Oxford, Basil Blackwell

Armas-Espinel S, Hernández-Moreno JM, Muñoz-Carpena R, Regalado CM (2003). Physical properties of "sorriba" cultivated volcanic soils from Tenerife in relation to diagnostic Andic parameters. Geoderma 117:297–311

Bartoli F, Arnalds O, Buurman P, Garcia-Rodeja E, Hernandez-Moreno J, Oskarsson H, Pinheiro J, Quantin P, Stoops G, Terribile F, van Oort F (2006). Introduction (this book)

Basile A, De Mascellis R (1999). Change of hydraulic properties and solute transport parameters. Modelling of transport processes in soils. Int Workshop of EurAgEng's Field of interest on Soil and Water. Feyen & K. Wiyo (ed), Leuven, pp. 267–275

Basile A, Ciollaro G, Coppola A (2003a). Hysteresis in soil water characteristics as a key to interpreting comparisons of laboratory and field measured hydraulic properties. Water Resources Res 39:1355–1366

Basile A, Mele G, Terribile F (2003b). Soil hydraulic behaviour of a selected benchmark soil involved in the landslide of Sarno 1998. Geoderma 117:331–346

Box GEP, Cox DR (1964). An Analysis of Transformations. Journal of the Royal Statistical Society, 211–243, discussion 244–252

Box GEP, Tiao GC (1973). Bayesian Inference in Statistical Analysis. John Wiley & Sons, New York

Bruand A, Prost R (1987). Effect of water content on the fabric of a soil material: an experimental approach. J Soil Sci 38:461–472

Ciollaro G, Romano N (1995). Spatial variability of the hydraulic properties of a volcanic soil. Geoderma 65:263–282

Colmet-Daage F, Cucalon F, Delaune M, Gautheyrou J, Gatheyrou M, Moreau B (1967). Cah ORSTOM. Ser Pedol 5:1–38

Colmet-Daage F, Gautheyrou J, Gatheyrou M, de Kimpe C, Sieffermann G, Delaune M, Fusil G (1970). Cah ORSTOM. Ser Pedol 8:113–172

Coppola A (2000). Unimodal and bimodal descriptions of hydraulic properties for aggregated soils. Soil Sci Soc Am J 64:1252–1262

Draper NR, Smith H (1981). Applied regression analysis. John Wiley & Sons, New York

Durner W (1994). Hydraulic conductivity estimation for soils with heterogeneous pore structure. Water Resources Research 30:211–223

Fontes J, Goncalves M, Pereira L (2004). Andosols of Terceira, Azores: measurement and significance of soil hydraulic properties. Catena 56:145–154

Hays W L (1981). Statistics. Holt, Rinehart and Winston, New York

Hopmans JW, Overmars B (1986). Presentation and application of an analytical model to describe soil hydraulic properties. Journal of Hydrology 87:135–143

Horgan GW (1998). Mathematical morphology for analysing soil structure from images. Eur J Soil Sci 49:161–173

Horowitz J, Hillel D (1987). A theoretical approach to the areal distribution of soil surface conductivity. Soil Sci 143:231–240

Klute A (1986). Water retention: Laboratory methods. In: Klute (ed) Methods of soil analysis, Part I, 2nd edn. Agron Monogr, 9, ASA and SSSA, Madison, pp 635–662

Klute A, Dirksen C (1986). Hydraulic conductivity and diffusivity: Laboratory methods. In: Klute (ed) Methods of soil analysis, Part I, 2nd edn. Agron Monogr, 9, ASA and SSSA, Madison, pp 687–734

Lawrence GP (1977) Measurement of pore sizes in fine-textured soils: a review of existing techniques. J Soil Sci 28:527–540

Maeda T, Takenaka H, Warkentin BP (1977). Physical properties of allophane soils. Adv Agr 29:229–264

Marshall TJ, Holmes JW, Rose CW (1996) Soil Physics, 3rd edn. Cambridge University press, Cambridge

Mele G, Basile A, Leone AP, Moreau E, Terribile F, Velde B (1999). The study of soil structure by coupling serial sections and 3D image analysis. Modelling of transport processes in soils. Int Workshop of EurAgEng's Field of inter on Soil and Water. Feyen & Wiyo (ed), Leuven, pp 103–117

Mele G, Terribile F, Moreau E (2000). Soil structure characterisation of selected European volcanic soils. Agricoltura Mediterranea 130:247–256

Misono S, Terasawa S, Kishita A, Sudo S (1953). Bull Natl Inst Agric Sci 2:95–124

Miyazaki T (1993). Water flow in soils. Marcel Dekker, New York

Moldrup P, Yoshikawa S, Olesen T, Komatsu T, Rolston DE (2003). Gas Diffusivity in Undisturbed Volcanic Ash Soils: Test of Soil-Water-Characteristic-Based Prediction Models. Soil Sci Soc Am J 67:41–51

Moreau E (1997). Etude de la morphologie et de la topologie 2D et 3D d'un sol argileux par analyse d'images. PhD Thesis. Université de Poitiers, France, pp 328

Mualem Y (1986). Hydraulic conductivity of unsaturated soils: Prediction and formulas. In: Klute (ed) Methods of soil analysis, Part I, 2nd edn. Agron Monogr, 9, ASA and SSSA, Madison, pp 799–823

Murphy CP (1985). Faster methods of liquid-phase acetone replacement of water from soils and sediments prior to resin impregnation. Geoderma 35:39–45

Nanzyo M, Shoji S, Dahlgren R (1993). Physical characteristics of volcanic ash soils. In: Shoji, Nanzio, Dahlgren (eds) Volcanic Ash Soils: Genesis, Properties and Utilization. Development in Soil Science, vol. 17, Elsevier, Amsterdam, pp 189–201

Pagliai M (1988). Soil porosity aspects. International Agrophysics 4:215–232

Pagliai M, La Marca G, Lucamente G, Genovese L (1984). Effects of zero and conventional tillage on the length and irregularity of elongated pores in a clay loam soil under viticulture. Soil and Tillage Research 4:433–444

Patel JK, Read CB (1996). Handbook of the normal distribution. Dekker, New York

Ritter A, Muñoz-Carpena R, Regalado CM, Vanclooster M, Lambot S (2004). Analysis of alternative measurement strategies for the inverse optimization of the hydraulic properties of a volcanic soil. Journal of Hydrology 295:124–139

Ross PJ, Smettem RJ (1993). Describing soil hydraulic properties with sums of simple functions. Soil Sci Soc Am J 57:26–29

Sen A, Srivastava M (1990). Regression Analysis. Theory, Methods and Applications. Chapman & Hall, New York

Serra J (1982). Image analysis and mathematical morphology. Academic Press, London

Serra J (1988). Image analysis and mathematical morphology, vol 2, Theoretical advances. Academic Press, London

Sills ID, Aylmore LAG, Quirk JP (1973). An analysis of pore size in illite-kaolinite mixtures. J Soil Sci 24:480–490

Smettem KRJ, Kirkby C (1990). Measuring the hydraulic properties of a stable aggregated soil. Journal of Hydrology 117:1–13

Van Genuchten MTh (1980). A closed-form equation for predicting the hydraulic conductivity of unsaturated soils. Soil Sci Soc Am J 44:892–898

Van Genuchten MTh, Nielsen DR (1985). On describing and predicting the hydraulic properties of unsaturated soils. Annales Geophysicae 3:615–628

Vogel T, Cislerova M (1988). On the reliability of unsaturated hydraulic conductivity calculated from the moisture retention curve. Transport in Porous Media 3:1–15

Physical properties in European volcanic soils: a synthesis and recent developments

F. Bartoli, C.M. Regalado, A. Basile, P. Buurman and A. Coppola

Introduction

In advanced stages of soil formation on volcanic ash, when more clay is formed, the combination of high surface area and variable charge causes strong soil aggregation, and very large porosity, water retention capacity and shrinkage (e.g. Nanzyo et al. 1993, Poulenard et al. 2002, 2003). Despite previous works, physical properties of Andosols have not been fully explored and explained.

Maeda and Soma (1985), Warkentin et al. (1988), Mizota and van Reeuwijk (1993), Nanzyo et al. (1993), Pinheiro et al. (2001) and Poulenard et al. (2003) pointed out that, besides allophanes, organic colloids also influence bulk density and soil water retention. However, the interpretation by these authors are constituent-based and not physical-based. On another hand, most of the published results on hydraulic properties are related to the water retention at 1500 kPa and sometimes at 33 kPa (see the review Nanzyo et al. 1993). Rare are the published results on the effect on pedogenesis or/and land use the entire retention curve or on hydraulic conductivity as a function of soil saturation (Warkentin and Maeda 1980, Basile and De Mascellis 1999, Poulenard et al. 2003, Fernandez et al. 2004) or on the hydraulic conductivity and solute dispersivity (Katou et al. 1996, Basile and De Mascellis 1999, Fontes et al. 2004). Aggregation in many Andosols (WRB 2001) is also so strong that they fail to disperse completely when dispersion agents are used that are successful in other soils (e.g. Nanzyo et al. 1993, Mizota and van Reeuwijk 1993). Research in the areas of hydraulic properties, solute transport, aggregation and clay dispersion is therefore still required.

Finally, relationships between properties at different scales, such as organo-mineral clay, physico-chemical properties, elementary aggregates and physical macro-properties (water retention, water and solute transport, soil hydrophobicity, aggregate stability, shrinkage etc.) are still unclear. Some expected relationships will be reported in the present synthesis, which is based both on studies by the authors and co-workers in the frame of the COST-622 Action (Bartoli and Burtin, Basile et al., Buurman and

van Doesburg this book section, other published or unpublished works of co-authors of this chapter) and on a detailed analysis of literature.

This chapter is organised as follows. First, micro-aggregation and clay dispersibility of the European reference pedon soil samples are reported. Second, we will highlight the key role played by capillary porosity in both soil water retention and shrinkage for the same soils. Third, irreversible drying effect on aggregate stability, hydraulic properties and solute transport parameters will be presented, followed by preliminary results on pore size distribution of the reference soil samples. Finally, recent results on (i) dielectric behaviour and water mobility, (ii) water and solute transport and (iii) soil hydrophobicity will be reported for European and other Andosols.

Water-stable aggregates: characteristics, disaggregation and clay dispersion

If soil samples are shaken overnight (1–10 grams of well-homogenized soil sample <2 mm or wet bulk soil sample with 50 or 200 ml distilled water) a considerable amount of aggregates is not disrupted. Such aggregates have been characterized by laser-diffraction grain-size analysis (Buurman and van Doesburg this book section) and classical particle size analysis (sequential sieving and sedimentation: Robinson pipette method; Bartoli and Burtin this book section).

All the soil suspensions remained partially flocculated in water, being mainly composed of sandy and silty water-stable elementary soil aggregates and particles (Figures 1 and 2), with often complex size distributions. Aggregation varied as a function of pedon and horizon, with, e.g., a peak centered within the 20 to 100 μm size range for most of the A_h horizons of the reference pedons and a pronounced multimodal aggregate size-distribution, with much larger diameters, for, e.g., the Azores Andosol (EUR05 and 06) topsoils (Figure 1). Such water-stable aggregates are the basic structural units of the fine granular microstructures commonly observed in the non-vitric reference Andosols (Stoops and Gérard, this book).

It was often shown that dissolution of organic matter, allophane, ferrihydrite, and Al-organic matter associations lead to disaggregation and dispersion of finer aggregates and particles (Buurman and van Doesburg this book section). For example, the major size peak of the EUR10 A_h size distribution shifted from 50 μm in the water-shaken samples to 2–18 μm in peroxide- and oxalate-treated suspensions (Figure 3a). In samples such those from the Azores, standard chemical treatments were inadequate and repeated oxalate dissolutions were necessary to dissolve the allophane/

ferrihydrite cements (Buurman and van Doesburg this book section). We obtained differential size distributions by subtracting the water-dispersed size-distribution from the peroxide- or oxalate-treated distributions (e.g. Figure 3b). These differential size distributions allow the identification of size fractions with net losses or gains upon the respective treatment.

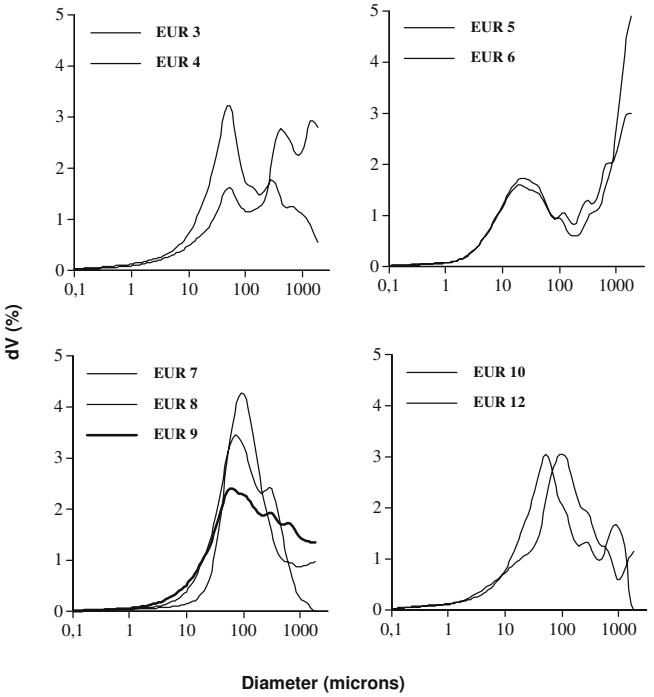

Figure 1. Volumetric aggregate- and particle size distribution (laser diffraction data plots with the diameter X-axis in log scale) of water-shaken topsoils (A_h, mostly A_{h1}) of the reference pedons (data of the Buurman and van Doesburg CD files this book).

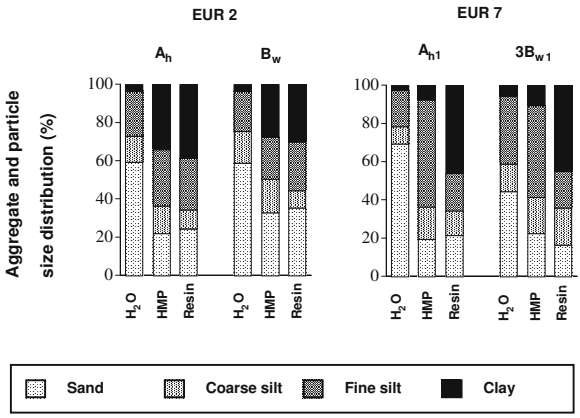

Figure 2. Aggregate and particle size distribution of wet samples of the A_h and B_w horizons of a representative vitric soil (EUR02, Italy) and a non-vitric soil (EUR07, Iceland). Dispersion in water (H_2O) or sodium hexametaphosphate (HMP), or by ultrasonic and Na-resin sequential treatment (Resin) (from Bartoli and Burtin this book section).

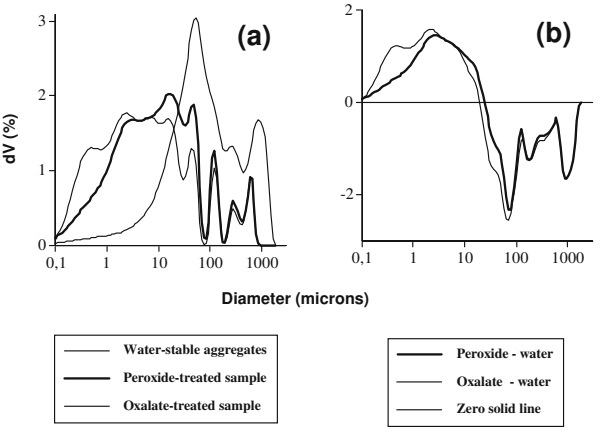

Figure 3. Volumetric aggregate and particle size distribution (laser diffraction data plots with the diameter x-axis in log scale) of the water-stable aggregates of the EUR10 A_h soil sample and their peroxiode- and oxalate-treated soil water suspension counterparts (a) and corresponding differential volumetric aggregate and particle size distribution (b) (from the data of the Buurman and van Doesburg CD files this book). Vertical scale denotes change in the volume % of the size fraction.

Negative values indicate size classes that incurred losses, while positive values indicate size classes that increased because of disaggregation of coarser ones. In case of EUR10 (Figure 3b), the threshold value between losses and gains is 20–25 μm.

Although clay was highly flocculated (only 6 to 16% of total clay was water-dispersible in most samples), it was possible to relate the proportion of organo-mineral clay dispersed by water to both soil organic matter and soil surface charge. The ratio Water-dispersible clay / Na resin clay decreased non-linearly as a function of organic carbon content whereas it decreased linearly with increasing ΔpH (pH-KCl N – pH-H_20) (Bartoli and Burtin this book section).

The Na-resin and Na-hexametaphosphate (HMP) clay contents were very similar for the wet samples of vitric soils, but very different for the wet non-vitric Andosol samples. The latter were much more readily dispersed by the resin treatment than by HMP (e.g. Figure 2). The Na-resin method was specifically adapted for Andosols to obtain most of the organo-mineral clay fraction (Bartoli and Burtin this book section). This relatively new methodology is therefore recommended for characterizing the fine particle-size distribution in non-vitric Andosols, as previously discussed by Bartoli et al. (1991) and Churchman et al. (1999).

A positive but scattered linear relationship ($p<0.001$) was found between the Na-resin clay content (all volcanic soil samples) or the HMP clay content (only the non-vitric Andosol samples) and the andic index $Al_o+½Fe_o$ (Bartoli and Burtin this book section). This suggests that allophane, organo-aluminium associations and ferrihydrite, when dispersed, are part of the clay fraction. The more 'andic' the Andosol sample, the more apparently clayey it is. Most B_w horizons were richer in total 'clay' than the overlying horizons. Therefore, Na-resin clay content could be a useful indicator of weathering, organo-mineral interactions and soil development.

Capillary porosity: a key physical property controlling soil water retention and shrinkage

At the small core scale (core volume of 28.6 cm^3), field volumetric soil moisture or capillary porosity and Na-resin clay content show significant ($p<0.001$) but scattered linear relationships (Bartoli and Burtin this book section). The more clayey the soil, the larger its microporosity, and the more water it retains in its capillary pores. This partially explains why most B_w horizons had higher water contents than the corresponding topsoils.

Actual water content in the field is controlled, in a complex way, by the various climatic, vegetative and pedoclimatic conditions previous to sampling. In most field-moist samples, 45 to 83% of the capillary porosity was filled by water, while in EUR05 and 06 the capillary porosity was filled for 75 to 83%. In the vitric soil samples these values were much lower and only amounted to 45 to 72%. This shows the high capacity of volcanic soils to retain water within their very large capillary porosity. Only a few samples were relatively dry at the time of sampling. For most of the studied soil samples, except the driest ones, the volumetric soil moisture at the time of sampling was similar to the soil moisture at a suction value of 33 kPa as reported by Basile et al. (this book section).

Nanzyo et al. (1993) reported water content values at suction values >1500 kPa (mainly referred to hygroscopic forces, micropores) of 30–35 vol%, water content values at suction values from 1500 to 33 kPa (mainly referred to capillary forces, mesopores) of 25 vol% and water content values at suction values from 33 to 0 kPa (mainly referred to gravitational forces, macropores) of 10–30 vol% in representative Andosol samples. This leads to 33 kPa water content values of nearly 0.55 to 0.6 $cm^3\ cm^{-3}$ which appear to be underestimates when compared to capillary porosity

values of 0.6 to 0.8 cm^3 cm^{-3} determined by capillary rise on wet undisturbed soil cores (Bartoli and Burtin this book section). Basile et al. (this book section) demonstrated that the widely used wilting point (log |h| ≈ 4.2) is less representative of the entire water retention behaviour than higher-saturation values (log |h| ≈ 2 or alternatively ≈ 2.5). It is therefore recommended to estimate capillary porosity on wet undisturbed soil cores either by capillary rise (Bartoli and Burtin this book section) or by a combination of capillary rise and increasing the outside water level up to 1 cm above soil surface (Basile et al. this book section).

We will now focus on the predominance of capillary porosity. Initial capillary porosity represents 87 to 97% of total porosity in most non-vitric wet Andosol samples, with a negligible macroporosity, and 75 to 85% for the vitric soil samples (Figure 4 and Bartoli and Burtin this book section). This is exceptionally high for soils and has notable consequences for physical properties of these volcanic soils. By contrast, macroporosity values (calculated either as difference between calculated total porosity and capillary porosity or from 2D-image analysis on resin-impregnated soil block samples) were extremely low (Figure 4). The observed discrepancies for the Azores Andosol samples (EUR05 and 06) should be attributed to an overestimate of porosity by image analysis (some overlapping with soil water retention porosity, as discussed by Basile et al. this book section) and errors in estimates of total porosity (experimental determination of solid density by helium pycnometry would be required).

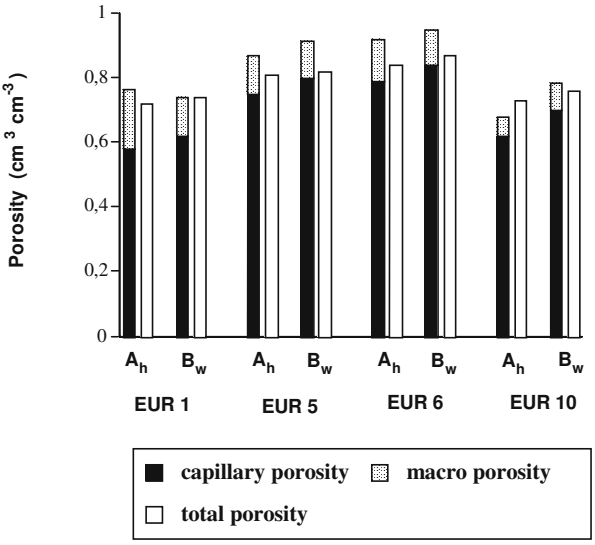

Figure 4. Relationships between the capillary porosity + image analysis macroporosity and calculated total porosity for a range of European volcanic soil samples (2 vitric and 6 Andosol A_h and B_w samples, from Bartoli and Burtin this book section and from Terribile et al. unpublished data related to the Basile et al. Chapter).

Pore size distributions determined by 3D reconstructed macrostructure and on 2D macrostructure were statistically similar (Basile et al. this book section). This was attributed to the well-developed isotropic granular microstructure occurring in most of the non-vitric reference Andosols (Stoops and Gérard this book). Estimates of capillary porosity are essentially independent of core volume (Figure 5). Previously, Sato and Tokunaga (1976) and Miyazaki (1993) recommended 100 cm^3 cylindrical samples with a cross-sectional area of at least 20 cm^2 as Representative Elementary Volume (REV) for undisturbed Andosols. In this study, we showed that sample volumes of 28.6 cm^3 were still sufficient to capture structural heterogeneity of volcanic soils.

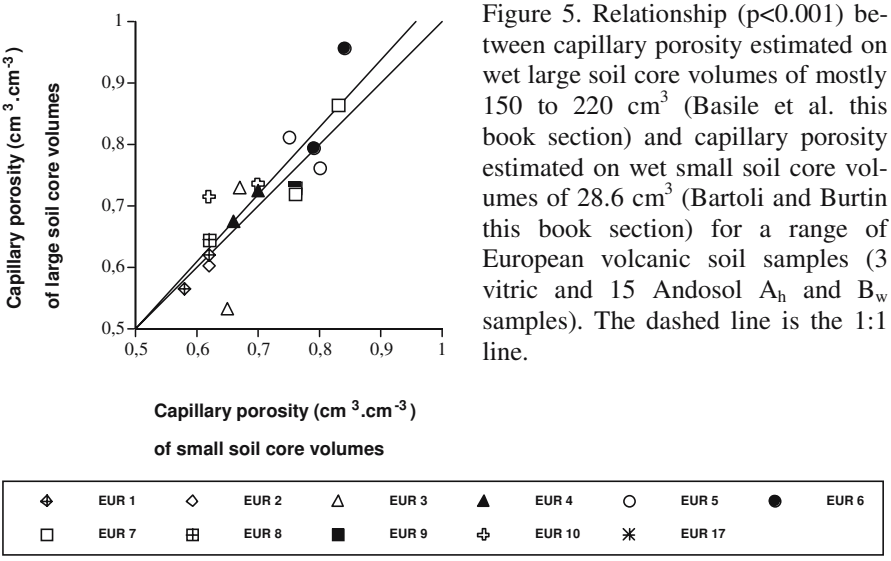

Figure 5. Relationship ($p<0.001$) between capillary porosity estimated on wet large soil core volumes of mostly 150 to 220 cm^3 (Basile et al. this book section) and capillary porosity estimated on wet small soil core volumes of 28.6 cm^3 (Bartoli and Burtin this book section) for a range of European volcanic soil samples (3 vitric and 15 Andosol A_h and B_w samples). The dashed line is the 1:1 line.

Because the dependence of soil properties on scale is a crucial issue in soil physics, more work on REV size and on allowed scaling of soil structure and soil water retention in Andosols is required. Regalado (2005) applied scaling techniques to water retention and hydraulic conductivity in an agricultural Andisol from Tenerife. Far from being homogeneously distributed in the field, hydraulic parameters showed anisotropy as a consequence of agricultural practices that promote soil degradation, induced by tillage and localized irrigation.

Capillary porosity regulates water retention and also all processes where capillary forces are involved, such as is shrinkage of fine-grained soils upon drying. This can be demonstrated as follows.

First, each whole soil water retention curve is characterized by converting it into a single characteristic value called the "Integrated Retention Index", *IRI* (Basile et al. this book section), which is positively correlated with both the andic index (Al_o+½Fe_o) (Basile et al. this book section) and resin clay content (result not shown). These indirect relationships are based on the physical relationship between the "Integrated Retention Index" and capillary porosity (Figure 6).

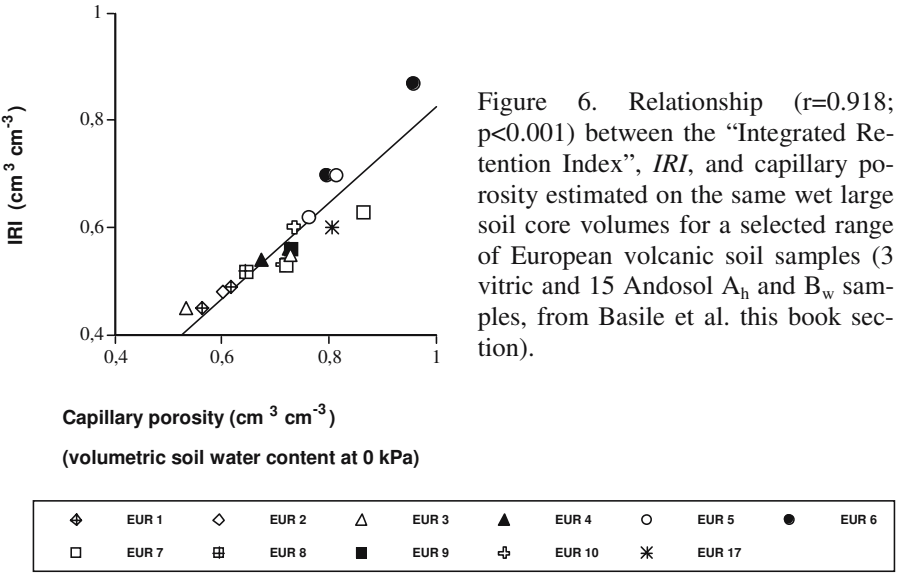

Figure 6. Relationship (r=0.918; p<0.001) between the "Integrated Retention Index", *IRI*, and capillary porosity estimated on the same wet large soil core volumes for a selected range of European volcanic soil samples (3 vitric and 15 Andosol A_h and B_w samples, from Basile et al. this book section).

A correlation between the *IRI* and the water content at each single pressure head value was also calculated by Basile et al. (this book section) for all the analyzed horizons. Two peaks were distinguished: the first (p<0.001), close to saturation, at around 6 cm (log |h| ≈ 0.84) of pressure head and the second (p<0.001) at around 400 cm (log |h| ≈ 2.6) of pressure head. If few points of the retention curve can be measured, it is recommended to choose a point close to saturation.

Second, the main results of the 40°C drying experiment carried out on the reference soils have been reported in detail by Bartoli and Burtin (this book section) and can be summarized as follows. The studied soil samples fall in two categories: those that dried without (or very moderate) shrinkage and those that shrank upon drying. Above Na-resin clay contents of 20–30% or a capillary porosity of 0.60–0.65 cm^3 cm^{-3}, total shrinkage increased as a function of Na-resin clay content or of initial capillary porosity (p<0.001), the latter relationship being physical-based. The maximum

recorded shrinkage of 60–80% is exceptional for soils. The more clayey a volcanic soil, the more microporous it is and the more it shrinks upon drying (Figure 7).

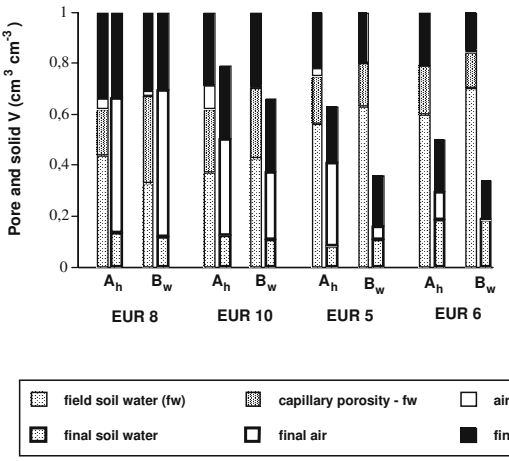

Figure 7. Void and solid volumes after water-filling of capillary porosity (initial state) and at the end of the controlled 40°C drying (final state) for a range of European Andosol A_h and B_w samples. Towards the right the samples show both larger clay content and stronger shrinkage (from Bartoli and Burtin this book section). Capillary porosity – fw = field air-filled capillary porosity.

Similar results were obtained on the same reference soils by changing both the observation scale and the drying method (air-drying of soil blocks for preparing thin soil sections, air under vacuum drying of wet aggregates: Bartoli et al. unpublished results, 105°C oven-drying of the largest undisturbed saturated soil cores: Basile et al. unpublished results). A similar relationship between soil shrinkage (40 to 75%) and initial void ratio was also reported by Poulenard et al. (2002) for a range of Andosols from Central America, Japan and the West Indies.

This emphasizes the exceptional predominance of capillary porosity within the total soil volume, capillary porosity controlling such intense shrinkage. Shrinkage of fine-grained and highly microporous Andosols upon drying is caused by movement of microaggregates as a result of pore-water tension developed by capillary menisci.

Many changes in physical properties are associated with shrinkage, as follows.

Irreversible drying effect on aggregate stability, hydraulic properties and solute transport parameters

For a wide range of reference volcanic soils from Europe, an increase in water-stable aggregates upon drying was reported, being proportional to

volumetric shrinkage (Bartoli and Burtin this book section). The more shrunken the soil is, the more water-stable the >200 μm aggregates are. The exceptional increase of 40–70% in the proportion of water-stable aggregates (of 105°C dried soil) found for the most clayey Andosol samples was attributed to a strong reduction of porosity occurring upon drying, itself related to the very large values of initial capillary porosity. Such irreversible mechanical changes caused by drying have been previously reported for Japanese Andosols (e.g. Kutoba 1971). Similarly, Fontes et al. (2004) reported that shrinkage caused by drying influenced the hydraulic properties of Azores Andosols.

In this study, two soil samples were selected, roughly representing the volcanic soils which dried without (or very moderate) shrinkage and those which shrank, were submitted to oven-drying at 105°C. The main characteristics of these contrasting soils are listed in Table 1. Note that no (or very moderate) volumetric shrinkage occurred during the records of the soil water retention curves (drainage) from the field-wet large soil cores. The field moisture and oven dried soil water retention curves are shown in Figure 8. In this figure, under each soil water retention cumulative curve, the pore size volume distribution (PDF) has also been plotted as a function of the equivalent pore diameter (see Basile et al. this book section, for a larger discussion on its significance). The results are as follows.

Table 1. Main characteristics of the investigated volcanic soils.

					Field moisture			Oven dried		
Soil (Location)	Classification ST, 1999	Horizon	Texture	$Al_o+½Fe_o$	k_s cm min^{-1}	Bulk density g cm^{-3}	Capillary porosity cm^3 cm^{-3}	k_s cm min^{-1}	Bulk density g cm^{-3}	Capillary porosity cm^3 cm^{-3}
Nocera (South IT)	Humic Haplustand	A_p	Loamy	2.05	9.3	1.06	0.62	50.0	1.08	0.42
EUR05 (Azores-PT)	Typic Hapludand	A_h	Silty-loam	6.60	-	0.42	0.79	-	0.75	0.67

A marked reduction in water retention after drying was observed for both undisturbed topsoils (Figure 8), with a decrease of the *IRI* index (eq. 5 in Basile et al. this book section) of nearly 60%. Moreover, the undisturbed topsoil sample from the Italian Andosol was characterized by a nearly constant porosity reduction in the entire pore domain, resulting in a unimodal PDF similar to the original one (the mode pore diameter only shifted from 17 to 26 μm). By contrast, the undisturbed topsoil sample from the Azorian Andosol was characterized by a predominant decrease of porosity in the range of micropore diameters (pores diameter values less than 0.3 μm),

producing a PDF with a completely different shape (Figure 8). The original distribution changed from platikurtic to strongly leptokurtic with a peak slightly shifting towards larger pore diameter values (from 53 to 66 μm).

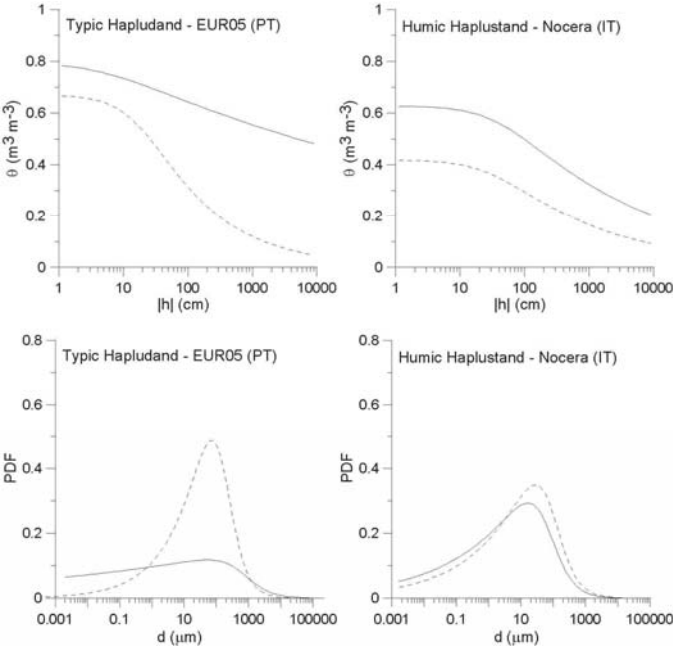

Figure 8. On the top the soil water retention curves (drainage) of the EUR05 (PT) and Nocera (IT) undisturbed Andosol topsoils (see Table 1). On the bottom the respective pore size volume distribution, PDF (see eq. 6 Basile et al. this book section).

For the undisturbed topsoil sample from the Italian Andosol, no volumetric shrinkage occurred upon 105°C drying (bulk density did not changed appreciably during the drying process going from 1.06 to 1.08 g cm^{-3}, Table 1) whereas the capillary porosity value significantly decreased from 0.62 to 0.42 cm^3 cm^{-3} (Table 1). This means that the differences shown in Figure 9 were due to rearrangement of pores due to capillary stresses upon 105°C drying: decrease of capillary porosity (internal shrinkage) and, as a complement, increase of macroporosity. This increase of macroporosity was validated by the significant increase of saturated conductivity from 9.3 to 50.0 cm min^{-1} (Table 1). This has a crucial role in the hydrological cycle, as shown by Basile and Coppola (2004) who performed a solute balance on the selected undisturbed topsoil sample from Nocera (IT), before and after the drying of the top 10 cm of the soil profile. The results showed that the solute flux at the bottom boundary of the soil profile was 20 times higher when the top 10 cm of the soil were oven-dried.

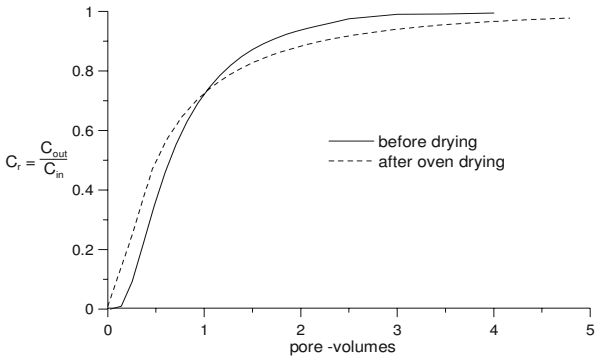

Figure 9. Cl^- breakthrough curves for the Humic Haplustand undisturbed topsoil sample from Nocera, Italy, before (solid line) and after oven drying (dashed line).

By contrast, a pronounced volumetric shrinkage of 56% occurred upon 105°C drying for the undisturbed topsoil sample from the Azorian Andosol, its bulk density increasing from 0.42 to 0.75 g cm^{-3}, with a pronounced PDF change from a complex multiscaled PDF (attributed to an interconnected meso- and micro-pore network) to an unimodal PDF centered at 55 μm pore diameter due to the collapse of the finest pores (Table 1, Figure 8).

Moreover, Figure 9 illustrates the steady-state saturated breakthrough curves of the leaching experiment carried out on undisturbed topsoil samples from the selected Italian Andosol (see Table 1) before and after 105°C oven-drying. The Convective-Dispersive model (van Genuchten and Wierenga 1986) fitting curves are displayed and the results are as follows.

Although a high flow velocity characterized the miscible flow experiment carried out before drying (data not shown here but reported by Basile and De Mascellis 1999), no early appearance of Cl^- in the effluent was detected, thus signifying absence of any preferential paths. The retardation coefficients *R* was relatively low (0.84); this value less than 1 indicates the occurrence of anion exclusion or relatively immobile liquid regions that do not contribute to convective transport (van Genuchten and Wierenga 1986). The chemical and physical exclusions are both possible in volcanic soils. Due to the presence of "allophane-like" clay-size material, the volcanic soils exhibit variable surface charges. The presence of negative charges on some surface particles results in the repulsion of anion from these regions (Bolt 1982). At once due to the swift convective flow, a portion of the highly structured intra fabric unit pores may be partially excluded or considered relatively immobile. The quasi symmetry of the breakthrough curve indicates the anion exclusion as the prevailing phenomena in order to explain the retardation coefficients less than 1.

By contrast, the steady-state saturated breakthrough curve of the undisturbed Italian topsoil sample after oven-drying was characterized by a

more pronounced asymmetry (Figure 9). The corresponding R value becomes ≈1 so that the anion exclusion is no longer recognizable in the dried soil samples. The dispersivity (3.2–9.3 cm) and the average pore-water velocity (0.14–0.77 cm min^{-1}) increased after drying. Such conditions would suggest the activation of some preferential flow paths with an enlarged solute dispersion, and the breakthrough curve can be properly described by a mobile-immobile liquid phase approach (see the subsection Water and Solute Transport).

Soil structure heterogeneity and functionality: a preliminary examination

In addition to the micromorphological approach (Stoops and Gérard this book), an attempt was made to characterize soil structure both directly by image analysis (IA) on resin-impregnated soil blocks and indirectly by water retention curves (Basile et al. this book section). To our knowledge, this is the first time that such a combined soil structure analysis has been done on volcanic soils. The main results are as follows.

Although macroporosity values estimated by image analysis were relatively low (e.g., Figure 5), IA pore size distribution (PoSD) was a good fingerprint of soil structure heterogeneity. Apart from the long-term cultivated Italian vitric soil (EUR01), IA pore size distributions were mostly unimodal, with a pore diameter peak centered at 150–400 μm and a strong tailing to pore diameters up to 1000–2000 μm (Figure 5 of Basile et al. this book section). Such large PoSD should be attributed to the high pore connectivity already observed in micromorphology (Stoops and Gérard this book).

The match of pores size diameters estimated by soil water retention and by image analysis varied strongly (Basile et al. this book section). The numerical comparison of the two estimates produced poor results; this was especially caused by the influence of the pore size classes <500 μm. To solve this problem, calculation of the correlation coefficient was iterated after step-wise elimination of pore size classes, starting from the smallest. The coefficients were stable after the first seven points for all the curves. Low correlations were obtained for soil samples in which the macropores were estimated by the integrated fitting parameter ϕ_1 of the soil water retention curves ($0.08<\phi_1<0.18$), whereas the best correlation between the two methods was found when the pore-size distribution was unimodal (Basile et al. this book section). Such behaviour suggests that (i) the image analysis approach should be a powerful tool for both description and analytical interpretation of such complex soil structures and (ii) with correct

parameterisation, the hydraulic properties could properly describe such pore complexity. However, more work is still required to characterize the multiscaled relationship between soil structure and soil water retention in volcanic soils.

Dielectric behaviour and water mobility

Dielectric properties are related to the mobility of water and thus its implication for water movement. The dielectric behaviour of moist soils, i.e. the polarizability of the soil constituents under an electromagnetic field, is very peculiar in volcanic soils, as described in detail by Regalado et al. (2003). Four possible reasons have been suggested to explain why volcanic soils exhibit such a peculiar dielectric response (Regalado et al. 2003): (i) the permittivity of the solid phase is closer to 15 (typical of metal oxides) than to 5 (quartz), as in mineral soils, (ii) due to the electrical charge and high surface area of the mineral phase, a larger proportion of water, with a dielectric constant close to that of ice, is bound to the particle surfaces, (iii) a low bulk density implies that a large volumetric fraction of free water affects the soil bulk dielectric constant and (iv) at low water contents, rotationally hindered water trapped within allophane spherules may play an important role in the dielectric response of allophanic soils (Regalado 2006). Of these four phenomena, the effect of bulk density, i.e. the ratio of free to bound water plays an important role.

This is shown in Figure 10, where the water content scaled for bulk density gives a better correlation with the dielectric constant than the unscaled values (see Regalado et al. 2003 for soil description and scaling methodology).

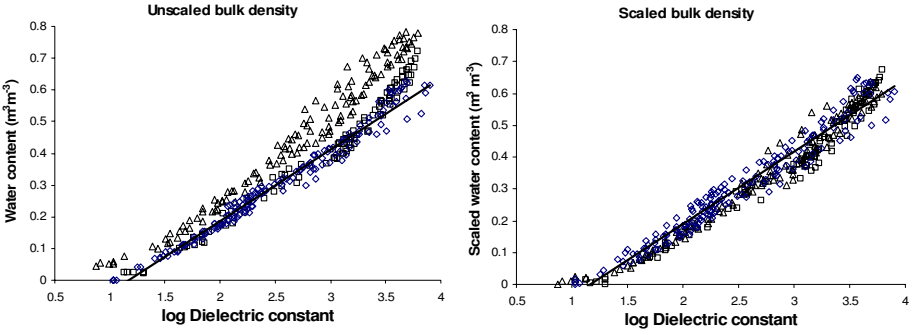

Figure 10. The effect of bulk density on the dielectric behaviour of volcanic soils of the Canary Islands. Different symbols represent different topsoils: □ Barlovento soils, ◊ Pajalillos soils, Δ Aves soils (from Regalado et al. 2003).

To understand this atypical dielectric behaviour, TDR (Time Domain Reflectometry) calibration curves for the soil water content have been previously proposed for tropical volcanic soils (Weitz et al. 1997), and temperate volcanic soils from New Zealand (Tomer et al. 1999), Japan (Miyamoto et al. 2001), and the Canary Islands (Regalado et al. 2003).

This complex dielectric response affects not only the soil water status but also TDR estimates of salinity in volcanic soils. Alternative calibration equations, that encompass both the relative dielectric dominance of the mobile water fraction at high water content typical of volcanic soils, and of the immobile fraction at low water contents have been also proposed for soils from the Canary Islands and New Zealand (Muñoz-Carpena et al. 2004).

Water and solute transport

One of the key peculiar properties of volcanic soils is the successive ash deposition, leading to a complex development of successive soils. Basile et al. (2003) related the high vertical variability of soil water retention curves and hydraulic conductivity values to complex stratification of Italian Andosols (Vesuvio volcanic area). These authors showed that anisotropy of the hydraulic conductivity produced an increase in soil water storage where soil discontinuities are present, while a decrease was observed where slopes had homogeneous soils. Thus, stratification could be one of the key causes of water overloading and catastrophic landslides (Basile et al. 2003).

In the upper A and B_w horizons of Andosols, the stable natural aggregation and high content of variable-charge minerals of volcanic soils may facilitate water and solute transport. Although capillary porosity predominates in Andosols, two different domains of water often appear to be present: a mobile (dynamic) phase and an immobile (stagnant) phase, the latter associated with the less permeable regions of the soil matrix (see, e.g. Miyazaki 1993, Regalado 2004, Basile et al. this book Section). As an example of these concepts, in Figure 11 hydraulic functions and breakthrough curves for an Aquic Haplustand and an Humic Hustivitrand soils (Soil Survey Staff 1999) are shown (data presented by Coppola, Basile and De Mascellis at the COST 622 International Workshop "Volcanic soils: properties, processes and land sue" held at Ponta Delgada, Azores, PT, 3–7 October 2001).

The soils are located in the alluvial plane of Sarno river, South of Italy. The Ustivitrand and the Haplustand soils were selected, among others in

the same area, as representative of soils with unimodal and bimodal pore size distribution, respectively. Soils like the former have a behavior which is more typical of sandy soils, characterized by relatively high Peclet number (P) accompanied by small dispersivities, λ. Such a behaviour has to be related to a narrow pore-size distribution where convection along streamlines dominates the dispersion process. The apparent symmetry of the pertaining breakthrough curve and PDF in Figure 11 confirms the occurrence of a unimodal pore system and would reflect a type of transport consistent with a wholly mobile pore water and a completely miscible solute.

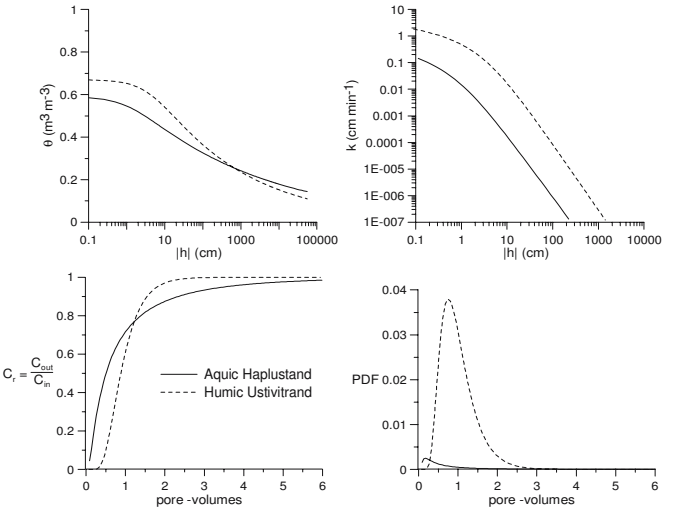

Figure 11. On the top the soil water retention curves (left) and unsaturated hydraulic conductivity (right) of the Aquic Haplustand (solid line) and Humic Ustivitrand (dashed line) soils. On the bottom the breakthrough curves (left) and the PDF (right).

By contrast, soils like the studied Haplustand soil sample are characterized by small Peclet number (P<1) and high α, along with a very high dispersivity (λ). This indicates a transport occurring in a bimodal porous system. Dispersivity is generally considered an intrinsic property of porous media related to the soil particle aggregation and the consequent pore-size distribution. A large dispersivity value generally implies a wide distribution of local velocities, distinctive of a well-structured porous medium, with intra-aggregate and inter-aggregate pore-size classes. In this case, the sequences of larger pores will be dominant in solution transfer and exchange of solutes between the two porosities may be important in transport phenomena. The breakthrough shows tailing and asymmetry, the extent of which may change with saturation of the medium and average pore water velocity. Early appearance of tracer in the leachate and tailing apparently reflect a type of transport which typically occurs when the solute is conducted relatively rapidly through more permeable regions in the soil ma-

trix. The tailing indicates very long time of solute release, suggesting a sort of isolated volumes of water with very slow convection.

We are aware that, due to the complex heterogeneity inherent in soils, looking for a complete and reliable characterization of the water flow-solute transport relationships would call for a larger quantity of available data to be used, in order to achieve results of applicative interest. This, in turn, requires a real improvement in equipment and techniques for measuring transport parameters, accounting for the specificities of the volcanic soil properties. With more data to hand, we believe that this work could in future allow an analytical formulation for predicting the solute transport properties based on the soil water retention characteristics.

Finally, solute transport in volcanic soils, as in other variable-charge soils, is characterized by specific anion sorption independent of the reactivity of the anion (non reactive or weakly reactive such as bromide, chloride and nitrate, or reactive such as phosphate, sulphate and acidic pesticides (e.g. Hyun et al. 2003). Sorption experiments with Br, a non-reactive tracer, were carried out by Ritter et al. (2005) in a layered, agricultural volcanic soil monolith from Tenerife (Canary Islands, Spain). The main conclusions were: (i) under moisture conditions close to saturation, anion movement was governed by the mobile phase, a result reported earlier by Comegna et al. (1999, 2001) in volcanic soils from southern Italy, and (ii) a delayed transport of Br^- in the bottom part of the profile was explained in terms of anion adsorption by variable charge minerals (Fe- and Al-oxihydrates). Such anion retardation was also encountered in the field by Reynolds-Vargas et al. (1994), who reported retardation of ^{15}N-labeled nitrate against a tritium-water tracer in Andosols of a Costa Rican coffee plantation. Similarly, nitrate retardation in New Zealand Andosol columns was reported by Magesan et al. (2003) who used the breakthrough curve approach.

Katou et al. (1996) suggested that if the initial electrolyte concentration of soil solution is low enough, the adsorption of monovalent anions (Cl^- and NO_3^-) upon invasion of a salt solution into dried Andosol aggregates is largely due to the increase in anion exchange capacity of the soil upon increased ionic strength of the solution, while desorption of SO_4^{2-} in exchange for monovalent anions is limited. The capillary invasion theory was successfully applied by Katou et al. (2001) to solute transport in unsaturated Andosols, demonstrating that chloride was retarded against immobile water during capillary invasion of a chloride solution in air-dried soil aggregates from a New Zealandian Andosol. The theory assumes a piston-like displacement of previous soil solution by the invading solution. This validates our own results on the predominance of capillary porosity in volcanic soils (this study). Capillary invasion experiments and theory are

therefore best suited for Andosols and other variable-charge soils where adsorption of weakly reactive ions is largely due to an increase in the exchange capacity as a result of the higher ionic strength of the invading solution. Capillary invasion is also recommended for the overdue study of solute transport in unsaturated Andosols which is crucial for a better understanding of the observed low anion availability to plants cultivated on Andosols.

Further studies are necessary to verify expected interrelationships between amount of variable-charge minerals, capillary porosity, delayed transport of solutes in unsaturated Andosols and plant nutrient availability.

Soil hydrophobicity

A final aspect relevant to water transport is soil water repellency, because of its impact on infiltration and preferential flow. This is a little studied area of solute transport in volcanic soils. Clothier et al. (2000) reported that TDR measurements in a hydrophobic New Zealandian Andosol described a transient behaviour of fingered preferential flow into this soil during the breakdown of hydrophobicity. These authors demonstrated that, despite initial water repellency, the infiltrating bromide solution was able to invade the entire wetted pore space, once the hydrophobicity had dissipated. Therefore, the entire wetted pore space could be considered mobile, although a large dispersivity was needed to predict the smeared profile of solute invasion caused by a multitude of preferential flow processes.

Hydrophobicity, characterised by the time takes for a water drop to penetrate into the soil surface, was recently reported for volcanic soils from Iceland (Regalado et al. unpublished data) and La Gomera, Canary Islands (Regalado and Ritter 2005). It showed a strong dependence on the soil moisture status and organic matter content (Figure 12). Icelandic Histosol samples, with 80% organic matter, were the most water repellent and are, like peats in general, water repellent even when saturated. By contrast, Brown Andosols samples ICE1 to ICE 4 were wettable at saturation. As moisture content diminishes, water repellency increased to a maximum and then decreased again. The same moisture-dependent behaviour was observed in an organo-mineral Andosol from La Gomera, with 42% organic matter (Regalado and Ritter 2005). By contrast, Brown Andosols samples ICE8 to ICE 11 with higher organic matter content than ICE1-4 (31% versus 16%), maintained maximum water repellence at low moisture contents (Figure 12). A similar increase of water repellency upon drying (Molarity Ethanol Droplet values) was reported from Ecuadorian volcanic

ash soils by Poulenard et al. (2004) who further characterized these 30°C-dried soils by capillary rise (calculated advancing water contact-angle values ranging from 78° to 89°) and by characterization of hydrophobic organic matter (elemental organic analysis, IR spectroscopy and GC-MS analysis).

Hydrophobicity in dry topsoil of European Andosols was also indirectly reported by Rodriguez- Rodriguez et al. (2002) who observed *in situ* flotation of water-repellent and water-stable aggregates in the runoff water. Similar observations were made by Poulenard et al. (2001) during controlled erosion of dried Ecuadorian Andosol topsoils the hydrophobicity of which is characterised elsewhere (Poulenard et al. 2004).

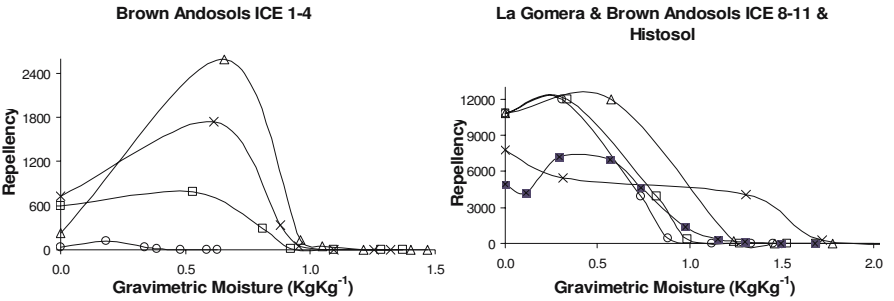

Figure 12. Water dependence of soil repellency in Brown Andosol (□, o, ∆, x) and Histosol (x) samples from Iceland, and La Gomera organo-mineral soil (■). OY axis represents repellency persistency, as the time (s) taken for a water drop to penetrate into the soil surface. Main Icelandic soil characteristics are listed in the accompanying table.

Sample	Location	Soil type	OM (%)
ICE-01	Raudavatn, SV Iceland	Brown Andosol	14.53
ICE-02	Raudavatn, SV Iceland	Brown Andosol	8.66
ICE-03	Raudavatn, SV Iceland	Brown Andosol	19.42
ICE-04	Raudavatn, SV Iceland	Brown Andosol	19.42
ICE-05A	Thverholt, V Iceland	Histosol	85.05
ICE-05B	Thverholt, V Iceland	Histosol	87.82
ICE-08	Sleggjulaek-1, V Iceland	Brown Andosol	29.34
ICE-09	Sleggjulaek-1, V Iceland	Brown Andosol	34.92
ICE-10	Sleggjulaek-2, V Iceland	Brown Andosol	-
ICE-11	Sleggjulaek-2, V Iceland	Brown Andosol	28.64

A question arises about the relationship between organic matter and volcanic soil hydrophobicity. Few studies have been carried out in this area. A clear relation between calculated advancing water contact-angle of dried Andosol samples and their hydrophobic organic matter (long-chain fatty acids and more complex non-polar alkyl components) has been reported by Poulenard et al. (2004) who also demonstrated that, after a period of drying, these hydrophobic organic materials occurred as coatings; their extrac-

tion rendered the soils rather hydrophilic. To our knowledge, such studies have not yet been done on European volcanic soils and few studies have been carried out on soil organic matter of European volcanic soils. Conte et al. (2003) have shown that humic acids extracted from an Italian Andosol (from Vico, soil sample collected very near the reference EUR04 pedon) were less aliphatic and more aromatic than their non-andic soil humic acid counterparts (soil samples from the same Vico volcanic system). On the other hand, Nierop et al. (2005), Nierop and Buurman (this book), and Buurman and Nierop (this book) reported that organic matter of the reference EUR05 and 06 pedons was very poor in lignin, in lipids, and in aliphatics in general, compared to non-andic soils and to the Ecuadorian Andosols studied by Poulenard et al. (2004). The reference EUR05 and 06 pedon samples were also rich in polysaccharides, which should be rather hydrophilic. It is therefore clear that further work is required on interrelationships between organic matter, soil microstructure and soil hydrophobicity at the aggregate scale.

References

Bartoli F, Burtin G, Herbillon A (1991). Disaggregation and clay dispersion of Oxisols: Na resin, a recommended methodology. Geoderma 49:301–317

Bartoli F, Burtin G (2006). Organo-mineral clay and physical properties in COST 622 European volcanic soils. This book section

Basile A, Coppola A (2004). Effects of drying on volcanic soil degradation: Practical implication on hydrological behaviour. In: Oskarsson H, Arnalds O (eds) Volcanic Soil Resources in Europe, COST Action final meeting, RALA Report no 214, 53–54

Basile A, Coppola A, De Mascellis R, Mele G, Terribile F (2006). A comparative analysis of the pore system in volcanic soils by means of soil hydrology and image analysis. This book section

Basile A, De Mascellis R (1999). Change of hydraulic properties and solute transport parameters in volcanic soils after drying. In: Leuven (Be), Feyen & K. Wiyo (eds) Modelling of transport processes in soils. Int. Workshop of EurAgEng's on Soil and Water, pp. 267–275

Basile A, Mele G, Terribile F (2003). Soil hydraulic behavior of a selected benchmark soil involved in the landslide of Sarno 1998. Geoderma, 117 special issue (Volcanic soils; properties and processes as a function of soil genesis and land use, Bartoli F, Buurman P, Delvaux B, Madeira M, eds), pp 331–346

Bolt GH (ed) (1982). Soil chemistry: B. Physico-chemical models. Elsevier Scientific Publishing Co, Amsterdam, The Netherlands

Buurman P, van Doesburg JDJ (2006). Laser-diffraction grain-size analyses of reference profiles. This book section

Churchman GJ, Bartoli F, Burtin G, Rouiller J, Weismann D (1999). Comparison of methods using sodium for the size fractionation of soil. 11th International Clay Conference Proceedings, June 15–21 1997, Ottawa (Canada), pp 331–338

Clothier BE, Vogeler I, Magesan GN (2000). The breakdown of water repellency and solute transport through a hydrophobic soil. Journal of Hydrology 307:112–125

Comegna V, Coppola A, Sommella A (1999). Nonreactive solute transport in variously structured soil materials as determined by laboratory-based time domain reflectometry (TDR). Geoderma 92:167–184

Comegna V, Coppola A, Sommella A (2001). Effectiveness of equilibrium and physical non-equilibrium approaches for interpreting solute transport through undisturbed soil columns. Journal of Contaminant Hydrology 50:121–138

Conte P, Spaccini R, Chiarella M, Piccolo A (2003). Chemical properties of humic substances in soils of an Italian volcanic system. Geoderma, 117 special issue (Volcanic soils; properties and processes as a function of soil genesis and land use, Bartoli F, Buurman P, Delvaux B Madeira M, eds), pp. 243–250

Fernandez C, van Oort F, Lamy I (2004). Physical and chemical study on irreversible changes of water retention properties in an Azores Andisol. In: Oskarsson H, Arnalds O (eds) Volcanic Soil Resources in Europe, COST Action final meeting, RALA Report no 214, 51–52

Fontes JC, Gonçalves MC, Pereira LS (2004). Andosols of Terceira, Azores: measurement and significance of soil hydraulic properties. Catena, 56 special issue (Volcanic soil Resources: occurrence, development and properties, Arnalds O, Stahr K, eds), pp. 145–154

Hyun S, Lee LS, Rao PSC (2003). Significance of anion exchange in pentachlorophenol sorption by variable-charge soils. J Environ Qual 32:966–976

Katou H, Clothier BE, Green SR (1996). Anion transport involving competitive adsorption during transient water flow in an Andisol. Soil Sci Soc Am J 60:1368–1375

Katou H, Uchimura K, Clothier BE (2001). An unsaturated flow method for determining solute adsorption by variable-charge soils. Soil Sci Soc Am J 65:283–290

Kutoba T (1971). Aggregate-formation of allophanic soils: effect of drying on the dispersion of the soils. Soil Sci and Plant Nutr 18:79–87

Maeda T, Soma K (1985). Classification of Andisols in Japan based on physical properties. Int Clay Conf Proc (Schultz LG, van Olphen H, Mumpton FA, eds). The Clay Minerals Society, Denver, pp. 174–178

Magesan GN, Vogeler I, Clothier BE, Green SR, Lee R (2003). Solute movement through an allophanic soil. J Environ Qual 32:2325–2333

Miyamoto T, Kobayashi R, Annaka T, Chikushi J (2001). Applicability of multiple length TDR probes to measure water distributions in an Andisol under different tillage systems in Japan. Soil and Tillage Research 60:91–99

Miyazaki T (1993). Water flow in soils. Marcel Dekker, New York

Mizota C, van Reeuwijk LP (1993). Clay mineralogy and chemistry of soils formed in volcanic material in diverse climatic regions. Soil Monograph, vol 2, ISRIC, Wageningen

Muñoz-Carpena R, Regalado CM, Ritter A, Alvarez-Benedí J, Socorro AR (2004). TDR estimation of electrical conductivity and saline solute concentration in a volcanic soil. Geoderma 124:399–413

Nanzyo M, Shoji S, Dahlgren R (1993). Physical characteristics of volcanic ash soils. In: Shoji S, Nanzio M, Dahlgren R (eds) Volcanic Ash Soils: Genesis, Properties and Utilization. Development in Soil Science, vol 17, Elsevier, Amsterdam, pp 189–201

Nierop KGJ, van Bergen PF, Buurman P, van Lagen B (2005). NaOH and $Na_4P_20_7$ extractable organic matter in two allophanic volcanic ash soils of the Azores Islands – a pyrolysis GC/MS study. Geoderma 127:36–51

Pinheiro J, Madeira M, Monteiro F, Medina J (2001). Caracteristicas e classifiçao dos Andossolos da Ihla do Pico 'Arguipélago dos Açores). Rev Cienc Agrarias 24:48–60

Poulenard J, Bartoli F, Burtin G (2002). Shrinkage and drainage in volcanic soil aggregates: a structural approach combining air under vacuum drying kinetics and mercury porosimetry. Eur J Soil Sci 52:563–574

Poulenard J, Michel JC, Bartoli F, Portal JM, Podwojewski P (2004). Water repellency of volcanic ash soils from Ecuadorian paramo: effect of water content and characteristics of hydrophobic organic matter. Eur J Soil Sci 55:487–496

Poulenard J, Podwojewski P, Herbillon AJ (2003). Characteristics of non-allophanic Andisols with hydric properties from the Ecuadorian paramos. Geoderma, 117 special issue (Volcanic soils; properties and processes as a function of soil genesis and land use, Bartoli F, Buurman P, Delvaux B, Madeira M, eds), pp. 267–281

Poulenard J, Podwojewski P, Janeau JL, Collinet J (2001). Runoff and soil erosion under rainfall simulation of Andisols from the Ecuadorian paramo: effect of tillage and burning. Catena 45:185–207

Regalado CM (2004). A physical interpretation of logarithmic TDR calibration equations of volcanic soils and their solid fraction permittivity based on Lichtenecker's mixing formulae. Geoderma 123:41–50

Regalado CM (2005). On the distribution of scaling hydraulic parameters in a spatially anisotropic banana field. Journal of Hydrology 307:112–125

Regalado CM (2006). A geometrical model based on weighted averages to estimate the permittivity of water adsorbed in porous media: the allophane analogue. Journal of Hydrology (10 p in press)

Regalado CM, Muñoz-Carpena R, Socorro AR, Hernández-Moreno JM (2003). Time Domain Reflectometry models as a tool to understand the dielectric response of volcanic soils. Geoderma, 117 special issue (Volcanic soils; properties and processes as a function of soil genesis and land use, Bartoli F, Buurman P, Delvaux B, Madeira M, eds), pp. 313–330

Regalado CM, Ritter A (2005). Characterizing water dependent soil repellency with minimal parameter requirement. Soil Sci Soc Am J 69:1955–1966

Reynolds-Vargas J, Richter DD, Borneminsza E (1994). Environmental impacts of nitrification and nitrate adsorption in fertilized Andisols in the Valle Central, Costa Rica, using TDR and inverse modeling to characterize solute transport in a layered agricultural volcanic. Soil Sci 157:289–299

Ritter A, Muñoz-Carpena R, Regalado CM, Javaux M, Vanclooster M (2005). Using TDR and inverse modeling to characterize solute transport in a layered agricultural volcanic. Vadose Zone Journal 4:300–309

Rodriguez- Rodriguez A, Guerra JA, Gorrin SP, Arbelo CD, Mora JL (2002). Aggregates stability and water erosion in Andosols of the Canary Islands. Land Degradation and Development 13:515–523

Sato T, Tokunaga K (1976). The fundamental studies on the soil sampling method: II. Analysis of sampled area variation of the distribution of the physical properties of soils found in large area farm land. Trans Jpn Soc Irrig Drain Reclam Eng 63:1–7

Soil Survey Staff (1999). Soil Taxonomy. A Basic System of Soil Classification for Making and Interpreting Soil Surveys, 2nd edn. USDA-NRCS. Agriculture Handbook No 436. Washington

Stoops G, Gérard M (2006). Micromorphology. This book

Tomer MD, Clothier BE, Vogeler I, Green S (1999). A dielectric–water content relationship for sandy volcanic soils in New Zealand. Soil Sci Soc Am J 63:777–781

van Genuchten MTh, Wierenga PJ (1986). Solute dispersion coefficients and retardation factors. In: Klute (ed) Methods of soil analysis, Part I, 2nd edn, Agron Monogr, 9 ASA and SSSA, Madison WI, pp. 1025–1054

Warkentin BP, Maeda T (1980). Physical and mechanical characteristics of Andisols. In: Theng BKG (ed) Soils with variable charge. New Zealand Soc Soil Sci, Soil Bureau, Lower Hutt, pp. 281–299

Warkentin BP, Maeda T, Soma K (1988). Physical characteristics for classification of Andisols. Proc 9th Int Soil Classif Workshop for Soil Management (Kinloch DJ, Shoji S, Beinroth FH, Eswaran H, eds). Support Service, Washington, pp. 97–107

Weitz AM, Grauel WT, Keller M, Veldkamp E (1997). Calibration of time domain reflectometry technique using undisturbed soil samples from humid tropical soils of volcanic origin. Water Resource Research 33: 1241–1249

WRB (World Reference Base for Soil Resources, 2001. Lecture Notes on the Major Soils of the World (Driessen P, Deckers J, Spaargaren O, Nachtergaele F, eds). FAO World Soil Resources Reports 94, Rome

V. Volcanic Soils and Land Use

Ed.: H. Oskarsson

Introduction to Section V. European Volcanic Soils and Land Use

H. Oskarsson

Introduction

Non-sustainable use of soil is a world wide phenomenon stemming from over-population, poverty and improper land use (Oldeman et al. 1991). As a consequence the soil resource is degraded over time, often leading to desertification with dire consequences for the local community and the ecological diversity of the area. In the last two decades there have been a number of global conventions for sustainable development, with the "*UN-Convention to Combat Desertification*" and the *Tutzing proposal for a* "*Convention on Sustainable Use of Soils*" being some of the most relevant for sustainable use of soil (Held et al. 1998, United Nations 1994). Despite these advances, soil degradation is still not adequately addressed at levels from the local to the global (Hurni 2002).

Globally, volcanic soils cover only around 1% of the Earth's terrestrial surface (Takahasi and Shoji 2005). Yet, because they are some of the most densely populated areas of the world, volcanic areas harbour a disproportionably greater portion of the Earth's population. One of the main reasons for this is that soils of volcanic areas are often fertile and therefore extensively used for agricultural purposes. Additionally, many of the volcanic areas are very scenic and hence popular tourist destinations. But, in addition to being fertile soils in scenic environs, volcanic soils are also a fragile resource susceptible to physical disturbance (e.g. Lemenih et al. 2005) and vulnerable to pollution by pesticides and heavy metals (e.g. Suzuki 2000, Latrille et al. 2003, Hou et al. 2005, Zhao et al. 2006). The intense land use pressure often exerted upon these soils has in many instances lead to soil degradation and erosion (e.g. Perret and Dorel 1999, Poulenard et al. 2001) with subsequent loss of valuable agricultural land (e.g. Perret and Dorel 1999, Vaje et al. 2005), reduced potential for tourism, loss of biodiversity, and, in the instances of landslides, property damage and loss of human lives (e.g. Ngecu and Ichang'I 1999).

Land use of European volcanic soils

There exists, to date, no comprehensive synopsis of land use on European volcanic soils. Publications by authors from different regions of Europe (e.g. Rodríguez et al. 1998, Basile et al. 2003, Fontes et al. 2004, Óskarsson et al. 2004) indicate that soil degradation is both widespread and serious in many of the volcanic areas of the continent. The results of a simple questionnaire answered by representatives from each of the countries participating in the COST-622 Action (see chapter one of this book) give a coarse overview of the situation (Table 1). According to the results the main land use of European volcanic soils is agriculture, with forestry also being a prevalent land use in many of the areas.

Table 1. Land use on European volcanic soils and the main types of stresses leading to soil degradation.

Country	Volcanic areas (km^2)	Main soil types	Climate	Population (no./km^2)	Land use on volcanic soils	Land use related stresses
France	12250	Andosols and Cambisols	Humid Continental	50–90	Mostly grasslands grazed by cattle, but also some forests	Tourism, acidification and some erosion
Germany	1850	Andosols and andic Luvisol	Humid Continental	63–218	Forestry and agriculture	Erosion, acidification and quarry opperations
Greece	2700	Regosols, Acrisols, Cambisols and Luvisols	Mediterranean to Sub-Mediterranean	33–988	Phrygana shrublands, agriculture, grasslands, forestry	Erosion, tourism, over-grazing, mining and drought
Hungary	7050	Umbrisols and Phaeozems	Humid Continental	97–108	Forests and conservation areas, agriculture	Tourism and erosion
Iceland	93000	Andosols, Vitrisols, Leptosols and Histosols	Cool Oceanic	0–13	Farming areas and natural areas, some protected	Erosion, over-grazing, reservoirs, tourism in some places
Italy	2050	Andosols; andic Cambisols and Luvisols	Mediterranean	5–5000	Forestry, orchards, agriculture and urban areas	Pollution, erosion, landslides and tourism
Portugal	3100	Vitrands, Hapludands, Placudands and Fulvudands	Oceanic	110–315	Agriculture, forests and areas conserveded for tourism	Landslides and erosion; eutrophication of water bodies
Romania	6400	Andosols and andic Cambisols	Cool Continental	10–50	Forestry and pasture	Mining and quarry opperations, timber harvesting
Slovakia	5150	Cambisols; Leptosols; Andosols; Regosols; Planosols; Luvisols	Mainly termperate and moderately moist, but also warm and dry	5–80	Agriculture and forestry	Water erosion
Spain	7600	Andosols; Aridisols; Vertisols; Alfisols; Ultisols; Inceptisols; Cambisols	Ranges from humid mountain to dry Mediterranean	35–484	Mainly agriculture and forestry, but also tourism and conservation areas	Desertification, tourism, erosion, urbanization and pollution

A noticeable outcome of the survey is the fact that soil erosion is a problem in all of the areas except Romania. This fact is particularly interesting considering both that the volcanic areas of Europe are found in extremely variable climates, ranging from the cool, wet and windy climate of Iceland to the dry and warm Mediterranean climate of Santorini, and that the population density, and hence pressure on the land, varies tremendously, rang-

ing from very low in Iceland to very high in the vicinity of Vesuvius. The fact that soil erosion takes place in almost all of these areas, independent of climate and population pressure, indicates that at least a part of the problem has to do with the properties of the soil itself. And in deed, certain andic properties make volcanic soils more vulnerable to erosion. The lack of cohesion when dry and the low bulk density of Andosols (Maeda et al. 1977) make them prone to wind erosion, particularly in areas where the vegetation has been degraded (Arnalds et al. 2001). Also, the very high water holding capacity of these soils (Maeda et al. 1977) makes them, when occurring in steep terrain, susceptible to collapse leading to landslides (e.g. Basile et al. 2003), especially in areas where forests have been removed (Glade 2003) or the natural vegetation degraded (Arnalds et al. 2001).

In addition to erosion, the survey identifies problems of desertification (Spain), acidification (France, Germany), mining (Germany, Greece, Romania), pressure from heavy tourism (France, Greece, Hungary, Iceland, Italy, Spain), over-grazing (Greece, Iceland) and pollution (Italy, Spain).

The papers

This section of the book is comprised of seven papers on various effects of land use on European volcanic soils.

Three of the papers address general land use issues of volcanic soil areas in island settings, i.e. in the Canary Islands (Hernández-Moreno et al.), in Santorini, Greece (Economou et al.) and on the slopes of Mount Etna, Sicily (Dazzi). The focus of the Canary Islands paper is on soil degradation and restoration measures that take note of traditional agricultural methods. In their paper on Santorini, Economou et al. give a general overview of the main features of the island's soil environment and the present day rapid land use changes where traditional agriculture is being replaced by urban development due to increased tourism. The highly variable agricultural land use on the slopes of Etna is the subject of the paper by Dazzi. This variation in land use is in large part associated with variability in the geomorphic and soil features of the Etna landscape.

Two of the papers in this section address pollution in volcanic soils (Adamo and Zampella; Füleky and Konda). This is very relevant subject because the high organic matter content and the prevalence of Si and Al oxides in volcanic soils make them vulnerable to pollution by pesticides and heavy metals (e.g. Latrille et al. 2003, Zhao et al. 2006). In their paper, Adamo and Zampella give an overview of trace element content in pol-

luted Italian volcanic soils and conclude that the properties of these soils can have strong influence on trace element accumulation, but also, that the strong elemental retention of volcanic soils may also reduce the risk of mobility and transfer of elements. The paper by Füleky and Konda presents the results of a comparative study of atrazine adsorption by volcanic soils from various parts of Europe. The authors conclude that the atrazine adsorption of the studied soils is high and can to a large degree be attributed to the high humus content of the investigated soils.

Eutrophication within the Sete Cidades watershed, S. Miguel Island, Azores, is the subject of the paper by Pinheiro et al. High phosphate retention is characteristic to volcanic soils (Takahasi and Shoji 2005) and hence, farmers commonly use high levels of phosphorus fertilizers on such soils. In steep terrain with abundant precipitation this practice can lead to P saturation and runoff which could lead to eutrophication of the receiving body of water. The results of the Sete Cidades study do indicate that there is a cause for concern regarding eutrophication in agricultural areas on volcanic soils.

Lastly, the paper by Terribile et al. examines the relationship between Andosols and fast mudflow landslides, based on evidence from the Campania region of Italy. As discussed earlier, certain hydrological and morphological properties of Andosols make them susceptible in steep terrain to collapsing and forming fast mudflows. Landslides are thus all too common events in many of the volcanic areas of Europe, for example Iceland (Arnalds et al. 2001), and this is certainly evident within the Campania region of Italy, an area that has seen over 1100 such events in the last 100 years.

The collection of papers in this section of this book highlights the multifaceted problems associated with improper land use on volcanic soils. Numerous properties specific to volcanic soils make them vulnerable to physical and chemical disturbance. The fact that this sensitivity is, to a degree, independent of climate and geographical setting, underscores the importance of conserving this valuable resource as an important part of the overall diversity of European soils.

Acknowledgments

The following persons contributed information on land use on volcanic soils of Europe: Bohdan Jurani, György Füleky, Jorge Pinheiro, Markus Kleber, Sámuel Jakab, Carmelo Dazzi, Fabio Terribile, Tassos Economou, Asimina Skouteri, Jose M. Hernandez-Moreno, Balázs Madarász, Ádám

Kertész, François Bartoli. Their contribution is greatly appreciated. Tables with more detailed information on the land use of volcanic soils within each country can be found on the accompanying CD-Rom.

References

Arnalds O, Thorarinsdottir EF, Metusalemsson S, Jonsson A, Gretarsson E, Arnason A (2001). Soil Erosion in Iceland. Soil Conservation Service and Agricultural Research Institute, Reykjavik, 155 pp. Original edition in Icelandic, 1997

Basile A, Mele G, Terribile F (2003). Soil hydrolic behaviour of a selected benchmark soil involved in the landslide of Sarno 1998. Geoderma 117:331–346

Fontes JC, Pereira LS, Smith RE (2004). Runoff and erosion in volcanic soils of Azores: simulation with OPUS. Catena 56:199–212

Glade T (2003). Landslide occurrence as a response to land use change: a review of evidence from New Zealand. Catena 51(3–4):297–314

Held M, Kummerer K, Odendalh K (1998). Preserving Soils for Life, the Tutzing Project. In: Proposal for a "Convention on Sustainable Use of Soils". Verlag, Munich.

Hou A, Takamatsu T, Koshikawa MK, Hosomi M (2005). Migration of silver, indium, tin, antimony, and bismuth and variations in their chemical fractions on addition to uncontaminated soils. Soil Science 170(8):624–639

Hurni H (2002). Current international actions for furthering the sustainable use of soils. 17th WCSS. Bangkok, Thailand. 14–21 August 2002. Symposium 61 (IUSS Working Group IASUS)

Latrille C, Denaix L, Lamy I (2003). Interaction of copper and zinc with allophane and organic matter in the B horizon of an Andosol. European Journal of Soil Science 54(2):357–364

Lemenih M, Karltun E, Olsson M (2005). Assessing soil chemical and physical responses to deforestation and subsequent cultivation in smallholders farming system in Ethiopia. Agriculture Ecosystems & Environment 105(1–2):373–386

Maeda T, Takenaka H, Warkentin BP (1977). Physical properties of allophane soils. Advanced in Agronomy 29:229–264

Ngecu WM, Ichang'I DW (1999). The environmental impact of landslides on the population living on the eastern footslopes of the Aberdare ranges in Kenya: A case study of Maringa Village landslide. Environmental Geology 38(3): 259–264

Oldeman LR, Hakkeling RTA, Sombroek WG (1991). World Map of the Status of Human-Induced Soil Degradation. International Soil Reference and Information Center – United Nations Environmental Programme, Wageningen, Netherlands

Óskarsson H, Arnalds Ó, Gudmundsson J, Gudbergsson G (2004). Organic carbon in Icelandic Andosols: geographical variation and impact of erosion. Catena 56:225–238

Perret S, Dorel M (1999). Relationship between land use, fertility and Andisol behaviour: examples from volcanic islands. Soil Use and Management 15(3): 144–149

Poulenard J, Podwojewski P, Janeau J, Collinet J (2001). Runoff and soil erosion under rainfall simulation of Andisol from the Ecuadorian *Páramo*: effect of tillage and burning. Catena 45:185–207

Rodríguez A, Jiménez CC, Tejedor M (1998). Soil degradation and desertification in the Canary Islands. In: The soil as a strategic resource: degradation processes and conservation measures. Geoforma Ediciones, pp 13–22

Suzuki S (2000). Leaching of several pesticides in Andosol upland field under natural rain conditions. Journal of Pesticide Science 25(1):1–9

Takahasi T, Shoji S (2005). Distribution and Classification of Volcanic Ash Soils. Global Environmental Research 6(2):83–97

United Nations (1994). Convention on Desertification. Earth Summit. United Nations Conference on Environment and Development. Rio de Janeiro, Brazil 1992

Vaje PI, Singh BR, Lal R (2005). Soil erosion and nutrient losses from a volcanic ash soil in Kilimanjaro region, Tanzania. Journal of Sustainable Agriculture 26(4):95–117

Zhao BZ, Maeda M, Zhang JB, Zhu AN, Ozaki Y (2006). Accumulation and chemical fractionation of heavy metals in Andisols after a different, 6-year fertilization management. Environmental Science and Pollution Research 13(2):90–97

Appendix materials on CD-Rom

Landuse on European volcanic soils.xls

Landslide processes and Andosols: the case study of the Campania region, Italy

F. Terribile, A. Basile, R. De Mascellis,
M. Iamarino, P. Magliulo, S. Pepe and S. Vingiani

Introduction

The aim of this study is to examine the relationships between Andosols and fast mudflow landslides. The results are important both locally and in other volcanic areas of the world where this type of landslide occurs. Mudflow is a very rapid to extremely rapid flow (i.e. velocity 0.05–5 m s^{-1}) of plastic materials having high water content (Cruden and Varnes 1996, Hungr et al. 2001). Fast mudflow landslides are grave dangers to people and infrastructure as they do not have clear warning signs, they have devastating power and they can potentially activate large amounts of materials across extended distances in very short time periods. In the last 100 years there have been more than 1100 natural catastrophic landslide and flooding events in the Campania region in Italy. Landslides, including both debris and mudflows, have caused the greatest amounts of damage, resulting in more than 550 injured or deceased victims over the past 50 years.

The study of these processes in the Campania region is of primary importance for classifying zones of different landslide hazard risk (landslide hazard assessment). Previous work (Terribile et al. 2000ab, Basile et al. 2003) has been conducted in locations struck by the large mudflows of Sarno and Quindici in 1998, that produced 181 victims, serious damage to infrastructure and major modifications of slope morphology. The work demonstrates that the presence of a complex sequence of Andosols, with properties specific to Andosols (i.e. high water retention, tixotropy, etc.), make these fertile forest ecosystems very vulnerable to disturbance. Geomorphological, hydrogeological, land use and anthropic factors are also important. This paper extends the study conducted in Sarno and Quindici to major landslide events in the Campania region.

Materials and methods

The point based and land based integrated analysis carried out in this study focus on the only catastrophic landslides producing fast mudflows (Table 1).

We selected landslides that caused human victims and have suitable technical documentation in the published literature (see below). Landslides occurring before 1841 have not been considered. The landslides of 1910 (Amalfi Coast, Ischia, Vesuvio: 200 victims, Bordiga 1915, CNR-GNDCI 1998) and of 1924 (Amalfi Coast: approx. 100 victims; Bordiga 1924, CNR-GNDCI 1998) were not considered due to the lack of reliable technical documentation.

Table 1. Major features of the investigated catastrophic landslides.

Date	Location	Main land use	Map land unit	Elevation (m)	Aspect	Slope gr.(°)	NDVI	Victims	Damages
20/01/1841 (1)	Monte Pendolo - Gragnano (Napoli)	chestnut woodland	Very deep Hapludand on steep slope of limestone Lattari Mountains	475	N	48	0.65	120 (multiple events)	Economic damages due to destruction of many houses
20/01/1841 (2)	Monte Pendolo - Gragnano (Napoli)	dense woodland, chestnut and olive trees	Very deep Hapludand on steep slope of limestone Lattari Mountains	500	N	45	0.65	120 (multiple events)	Destruction of Molino delle Capre, economic damages due to destruction of many houses
26/10/1954	Basins between Salerno and Minori . Es. Molina - Vietri (Salerno)	chestnut and abandoned agricultural terraces	Very deep Hapludand on steep slope of limestone Lattari Mountains	275	E	40	0.68	321 (multiple events)	Many houses and roads destroyed between Salerno and Minori. 5466 homeless.
17/02/1963	Monte Muto - Gragnano (Napoli)	dense woodland of chestnut and olive trees	Very deep Hapludand on steep slope of limestone Lattari Mountains	370	N	35	0.66	none	Damages to Mandrio street
22/02/1986	Eastern margin of the Campanian Plain - Palma Campania (Napoli)		Very deep Hapludand on steep alluvial fan located at the foothill of limestone Sarno Mountains	225	W	35	0.61	8	The rapid flow has truncated the surface soil and the plants; breaking of agriculture terraces and 1 house
09/01/1997	Pozzano - Castellammare di Stabia (Napoli)	chestnut, woodland	Very deep Hapludand on steep slope of limestone Lattari Mountains	360	NW	40	0.67	4	Road S.S. 145 interruption
10/01/1997	Collina San Pantaleone - Pagani (Napoli)	chestnut, woodland	Very deep (vitric) Haplustand on steep slope of low energy limestone relieves	175	N	35	0.57	1	The rapid flow has truncated the surface soil and it has covered and interrupted the highway Pompei-Salerno
11/01/1997	Monte Pendolo - Gragnano (Napoli)	chestnut, woodland	Very deep Hapludand on steep slope of limestone Lattari Mountains	325	N	43	0.65	none	Economic damages due to destruction of some houses

Date	Location	Main land use	Map land unit	Elevation (m)	Aspect	Slope gr. (°)	NDVI	Victims	Damages
05/05/1998 (1)	Severa Avalle - San Felice a Cancello (Caserta)	chestnut, woodland	Very deep (typic and vitric) Hapludand on moderate slopes of pre-Apennine limestone relieves	325	N	43	0.60	Multiple events with a total of 1 victim	Relevant damages to agriculture production and to an industrial plan
05/05/1998 (2)	Severa Avalle - San Felice a Cancello (Caserta)	chestnut, woodland	Very deep (typic and vitric) Hapludand on moderate sloping pre-Apennine limestone relieves	325	NE	41	0.63	Multiple events with a total of 1 victim	Relevant damage to agriculture production and to an industrial plan
05/05/1998	Siano (Avellino)	chestnut, woodland	Very deep Hapludand on steep sloping alluvial fan at the foothill of limestone Sarno Mountains	475	SE	40	0.67	None	Economic damages due to destrudion of some houses
05/05/1998	Montoro Inf. (Avellino)	chestnut, woodland	Very deep Hapludand on steep sloping alluvial fan at the foothill of limestone Sarno Mountains	750	E	50	0.72	None	Economic damages due to destruction of some houses
05/05/1998	Quindici (Avellino)	chestnut, woodland	Very deep Hapludand on steep sloping alluvial fan at the foothill of limestone Sarno Mountains	800	N	42	0.73	181 (including Sarno and Bracigliano)	Destruction of many houses
05/05/1998	Quindici (Avellino)	chestnut, woodland	Very deep Hapludand on steep sloping alluvial fan at the foothill of limestone Sarno Mountains	900	NE	40	0.73	181 (including Sarno and Bracigliano)	Destruction of many houses
05/05/1998	Sarno (Salerno)	chestnut, woodland	Very deep Hapludand on steep sloping alluvial fan at the foothill of limestone Sarno Mountains	800	SW	47	0.70	181 (including Quindici and Bracigliano)	Destruction of many houses

Table 1 (cont.).

Date	Location	Main land use	Map land unit	Elevation (m)	Aspect	Slope gr. (°)	NDVI	Victims	Damages
05/05/1998	Sarno (Salerno)	chestnut, woodland	Very deep Hapludand on steep sloping alluvial fan at the foothill of limestone Sarno Mountains	800	S	35	0.70	181 (including Quindici and Bracigliano)	Destruction of many houses
06/05/1998	Sarno (Salerno)	chestnut, woodland	Very deep Hapludand on steep sloping alluvial fan at the foothill of limestone Sarno Mountains	800	SW	41	0.71	181 (including Quindici and Bracigliano)	Destruction of 400 hundred houses and of an hospital
05/05/1998	Bracigliano (Salerno)	chestnut, woodland	Very deep Hapludand on steep sloping alluvial fan at the foothill of limestone Sarno Mountains	825	NE	41	0.20	181 (including Quindici and Sarno)	Destruction of many houses
15/12/1999	Ioffredo - Cervinara (Avellino)	chestnut, woodland	Very deep Hapludand on steep sloping alluvial fan at the foothill of limestone Sarno Mountains	825	NE	42	0.70	5	Destruction of many houses
nd/02/1986	Monte Chianello – Cilento (Salerno)	chestnut, woodland	Moderately deep Hapludand on moderate slope of pre-appennine limestone relieves	620	NE	45	0.72	none	Damages to forestry and agriculture
26/12/1993	Solopaca (Benevento)	chestnut, woodland	Moderately deep and shallow Hapludand on moderate slope of Appennine limestone Mountains	800	N	41	0.69	none	Damages to forestry and agriculture

More than 20 soil profiles from 19 highly representative detachment crowns were described and analysed in the field. The upper parts of slopes where detachment occurs are generally extremely steep (more than 50–60°). The location of sampling points is shown in Figure 1. The profiles have been described using the FAO system (1990). Undisturbed soil samples for hydrological analysis were collected from the main horizons with steel cylinders of 100 and 200 cm^3. Bulk soil samples for chemical and hydrological analysis were collected from all soil horizons.

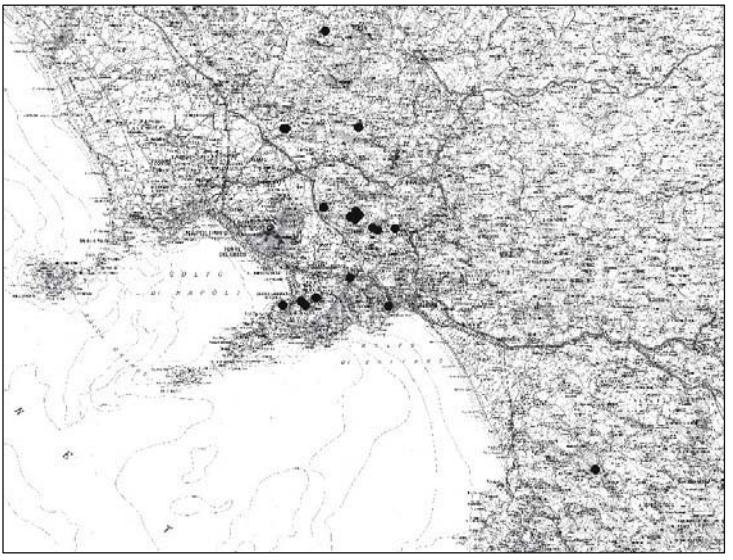

Figure 1. Location of the landslides studied sites (black circles).

After air drying, samples were sieved to less than 2 mm and analysed according to USDA (1996) methods: pH in H_2O, organic matter by the Walkley-Black method, Al, Fe and Si in the amorphous oxides/hydroxides and in the organic matter were selectively extracted with ammonium oxalate (Fe_o, Al_o, Si_o) treatment at pH=3 (Schwertmann 1964) and with sodium pyrophospate (Fe_p, Al_p, Si_p) (Bascomb 1968), respectively, and their content levels were determined by ICP-AES. Values of Al and Fe extracted with ammonium oxalate were used to calculate the andic property index $Al_o+½Fe_o$. Allophane and imogolite quantities were estimated using the Parfitt (1990) method, based on selective extractions. The studied soils were difficult to disperse and, after substantial drying, some of their physical properties change irreversibly (similar to soils studied by Adamo et al. 1996, Basile et al. 1999). All soils were classified using Soil Taxonomy (USDA 1998).

To evaluate the interaction between land and soil features, an evaluation of the andic properties for the whole soils was used. For this, the contents of Al and Fe extracted with ammonium oxalate were weighted based different horizon thickness for each solum. Undisturbed soil samples were slowly saturated from the bottom in the laboratory. The saturated samples were placed in a permeameter and the saturated hydraulic conductivity was measured using the constant head method (Klute and Dirksen 1986). Three tensiometers were installed in the 200 cm^3 sample at a distance from the surface of 2.5, 5.0 and 7.5 cm. The samples were placed on a load cell and, starting from saturation, a 1-dimensional transient upward flow was monitored, automatically recording the weight of the sample and the pressure head at the three depths until air was observed in the circuit of the uppermost tensiometer. The soil sample was then dismantled and placed for 24 h in the oven at 105°C in order to determine the water content from the weight data set.

An iterative method was applied to obtain the water retention curves (Tamari et al. 1993). The unsaturated hydraulic conductivity was derived according to the instantaneous profile methods (Watson 1966) by dividing the water fluxes by the hydraulic gradients between two consecutive compartments. The gradients were calculated from the tensiometer readings; the fluxes were calculated based on changes in water content of each compartment over time, as derived from the tensiometer readings and the water retention curve.

The soil water retention curves $\theta(h)$ of smaller samples (100 cm^3) were determined through use of the tension table (Klute 1986). Ten points of the curve ranging from near saturation to –300 cm of potential were measured. In addition, 3 points at –1, –5 and –10 bars of the water retention curve

were determined through the use of a pressure plate apparatus (Klute 1986).

The water retention experimental data were parameterised according to the unimodal θ(h) relationship proposed by van Genuchten (1980), expressed here in terms of the scaled water content, S_e, as Equation (1) below:

$$S_e = \left[\frac{1}{1+(\alpha|h|)^n} \right]^m \quad (1)$$

with $S_e=(\theta-\theta_r)/(\theta_0-\theta_r)$, and in which α ($cm^{-1}$), n and m are curve-fitting parameters. In particular, α^{-1} corresponds roughly to the so-called air entry pressure value for low ratios of m/n. Meanwhile for high m/n values α^{-1} is roughly equal to the pressure head at the inflection point of the curve (van Genuchten and Nielsen 1985). θ_0 and θ_r respectively represent the saturated water content (at h=0) and the residual water content, and may either be fixed or treated as parameters to be optimized.

Mualem's expression (Mualem 1986), Equation (2), to calculate relative hydraulic conductivity, k_r, is based on the capillary bundle theory (Childs and Collis-George 1950) and is represented as follows:

$$k_r(S_e) = \frac{k(S_e)}{k_0} = S_e^{\tau} \left[\int_0^{S_e} \frac{1}{h(S_e)} dS_e \Big/ \int_0^1 \frac{1}{h(S_e)} dS_e \right]^2 \quad (2)$$

in which k_0 is the hydraulic conductivity measured at θ_0, and τ is a parameter which accounts for the dependence of the tortuosity and the correlation factors on the water content, estimated by Mualem to have an optimum average of ~0.5. Using Mualem's model and assuming *m*=1–1/*n*, van Genuchten (1980) obtained a closed-form analytical solution to equation (2) to predict k_r at specified volumetric water content:

$$k_r(S_e) = \frac{k(S_e)}{k_0} = S_e^{\tau} \left[1 - \left(1 - S_e^{1/m} \right)^m \right]^2 \quad (3)$$

Equation (3) allows hydraulic conductivity to be estimated when k_0 is known through the parameters that appear in equation (1). The estimation is derived by applying a nonlinear least-squares procedure to fit the measured retention data to equation 1.

Vegetation was analysed using a vegetation index model, Normalized Difference Vegetation Index (NDVI, Rouse et al. 1974). To obtain the NDVI, Landsat-TM5 satellite images of June 2000 with a resolution of 28 m were used. A Digital Elevation Model (DEM) was created with a resolu-

tion of 20 m for the analysis of the landscape features and was used to calculate the slope of the detachment area. Land unit type was derived from di Gennaro et al. (2002). Information on landslide length, number of victims and damages were obtained from the literature (Bordiga 1915, 1924, Lazzari 1954, Calcaterra and Guarino 1997, Mele and Del Prete 1999, Calcaterra et al. 2000, Vallario 2001, Esposito et al. 2003).

Results

Land based analysis

The major features of examined mudflows are shown in Table 1. The table presents two types of land features: (i) those detected directly on the site of the landslide detachment crown (main land use, elevation, slope gradient, aspect) and (ii) more general landscape features obtained by pre-existing maps (map land unit). The land based analysis demonstrates that all the sampled Map Land Units are characterized by the presence of Andosols. Sixteen of 20 landslides examined occurred on very deep Hapludands overlying the steep slopes of the carbonatic Campanian relieves. The remaining four were on moderately dipping slopes, hills, and occasionally on shallow soils. Slope, except for one case, is always higher than 35° (maximum 50°) but we did not observe any occurrence of a slope value that was sufficiently specific, or within a narrow enough range, to be predictive a landslide. In all cases NDVI values were high (>0.60), indicating the presence of a high photosynthetic active biomass and, therefore, the presence of productive ecosystems. This is consistent with the presence of chestnut tree forests on Andosols.

The time-based evolution (Table 1) of examined catastrophic landslides suggests a trend of recent landslides occurring at high altitude, while older ones occur at both high and low elevations. Such trends could be related to the human activities moving to higher elevations in recent decades and the opening of small roads for forest and fire access (Terribile et al. 2000ab, Basile et al. 2003, Guadagno et al. 1988). Figure 2

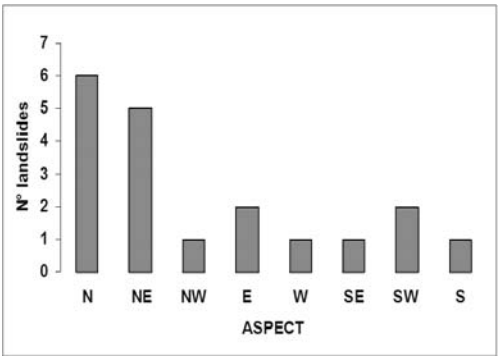

Figure 2. Aspect distribution of the studied mudflows.

shows the relationship between landslides and slope aspect. It is notable that 12 of 19 landslides were located on North-facing slopes, suggesting that there may be a relationship between soils developed on the North-facing carbonatic slopes and mudflow triggering mechanisms. This implication requires careful investigation.

Point based analysis: the soils of the detachment crowns

The morphological and chemical data for 7 selected profiles, representative of the 20 sampled and analysed soils, are presented in Table 2. The soils are all Andosols with a moderate to strong smeariness. All soils are characterized by a marked vertical and lateral morphological variability, with alternation of allophanic, vitric and skeletal coarse horizons, deriving from the deposition of different age volcanic products. Most of the soils are classified as Hapludands and Udivitrands (USDA 1998).

Table 2. Main soil features of the studied soils sampled from the landslide detachment crowns.

Profile	Horizon	Boundary (cm)	Colour (moist)	Coarse fragments (% and size)	pH in H_2O	Organic matter (g/kg)	Al (ox) + 0,5 Fe(ox) (%)	allophane %
Cervinara	A	0 - 15	10YR 2/1		6.6	146.7	4.1	0.7
	Bw1	15 - 40	10YR 3/3	12 (very fine)	6.5	43.8	4.9	13.7
	Bw2	40 - 75	10YR 3/3	12 (very fine)	6.7	35.3	4.7	16.4
	Ab	75 - 85	10YR 3/3	1 (very fine)	6.7	22.2	4.8	17.7
	Bwb1	85 - 105	10YR 3/3	10 (fine)	6.8	18.1	6.0	16.4
	Bwb2	105 - 140	2.5Y 4/3	22 (fine)	6.7	16.6	4.1	24.6
	Tasca Bwb2	105 - 122	2.5Y 3/2	7 (fine)	6.5	12.5	3.8	16.7
	Bwb3	140 - 170	10YR 3/4	3 (fine)	6.9	15.2	4.5	15.3
Monte Pendolo	A	0 - 5	10YR 2/2	1 (very fine)	6.9	119.1	2.3	17.8
	Bw	5 - 30	10YR 3/3	50 (very fine)	7.2	55.6	0.3	7.3
	BC	30 - 60	10YR 3/3	80 (fine. very fine and medium)	7.7	47.3	2.4	0.7
	2Bw	60 - 90+	10YR 3/4	20 (fine and very fine)	7.8	34.2	3.2	8.0
Quindici	A	0 - 10	10YR 3/2	3 (very fine)	6.8	60.3	2.2	
	Bw	10 - 25	10YR 3/3	3 (very fine)	7.3	25.2	3.1	6.3
	Ab	25 - 30	10YR 3/2	3 (very fine)				9.7
	Bwb1	30 - 80	10YR 3/3	3 (very fine)	7.2	26.4	3.1	
	Bwb2	80 - 100	10YR 4/4	3 (fine)	7.4	13.8	1.7	9.2
	Bwb3	100 - 115	10YR 5/4	3 (fine and very fine)	7.5			5.6
	Cb	115 - 140	2.5Y 4/3	3 (fine and very fine)	7.4	8.5	3.2	
	2Bwb4	140 - 185	10YR 4/4	3 (fine and very fine)	7.4	17.4	3.4	11.7
	2Bwb5	185 - 240	10YR 3/4	3 (fine and very fine)	6.8	16.7	2.6	12.0

Profile	Horizon	Boundary (cm)	Colour (moist)	Coarse fragments (% and size)	pH in H_2O	Organic matter (g/kg)	Al (ox) + 0,5 Fe(ox) (%)	allophane %
Sarno	A	0 - 20	10YR 3/1	12 (very fine)	7.3	169.8	5.0	9.4
	Bw	20 - 38	10YR 4/3	10 (very fine)	7.5	18.5	2.5	16.8
	BC	38 - 71	2.5Y 4/2	3 (very fine)		7.2	5.7	8.1
	C	71 - 100	5Y 7/3	80 (fine and very fine)	7.50			21.1
	2Ab/Bwb	100 - 140	10YR 3/4	10 (very fine)		18.1	2.1	
	2Bwb/Cb	140 - 150	2.5Y 4/4					7.1
	2Cb	150 - 200	2.5Y 5/4					
S. Felice C. 1	A	0 -7	10YR 3/2		7.6	48.5	1.9	
	AB	7 - 20	10YR 3/3	5 (fine)	7.6	26.3	1.3	5.7
	Bw	20 - 55	10YR 3/4	90 (very fine)	7.9	7.1	0.5	4.1
	BC1	55 - 65	10YR 3/4	80 (fine)	7.2	11.2	0.5	1.6
	BC2	65 - 82	10YR 3/4	80 (fine)	7.4	6.9	0.3	1.8
	C1	82 - 90	10YR 3/4	80 (fine)	7.3	3.6	0.1	0.7
	C2/2Ab	90 -105	2.5Y 4/4	70 (fine)	7.6	16.7	0.1	0.2
	2Bwb1	105 - 180	10YR 3/6	1 (fine)	8.2	5.5	0.7	0.3
	2Bwb2	180 - 190	10YR 4/6		8.3	3.8	1.0	3.1
	R	190 - 200 +						
S. Felice C. 2	A1	0 - 6	10YR 2/1	1 (very fine)	7.1	105.3	1.2	
	A2	6 - 47	10YR 3/3	5 (very fine)	7.5	38.9	1.4	3.3
	Bw	47 - 60	10YR 4/4		8.0	19.7	1.7	4.1
	R	60 - 70+						5.5
Molina	A	0 - 9	10YR 2/2	20 (very fine)	7.3	99.9	4.5	
	Bw1	9 - 28	10YR 3/3	10 (very fine)	7.4	14.0	5.0	16.0
	Bw2	28 - 48	10YR 3/3	5 (very fine)	7.6	22.2	5.5	19.4
	Bw3	48 - 70	10YR 3/4	1 (fine)	7.8	27.9	3.5	23.5
	R	70 +						12.4

Table 2 (cont.).

Profile	Horizon	Boundary (cm)	Colour (moist)	Coarse fragments (% and size)	pH in H_2O	Organic matter (g/kg)	Al (ox) + 0,5 Fe(ox) (%)	allophane %
Molina 1	A	0 - 9	10YR 2/2	20 (very fine)	7.3	99.9	4.5	
Molina 1	Bw1	9 - 28	10YR 3/3	10 (very fine)	7.4	14.0	5.0	16.0
Molina 1	Bw2	28 - 48	10YR 3/3	5 (very fine)	7.6	22.2	5.5	19.4
Molina 1	Bw3	48 - 70	10YR 3/4	1 (fine)	7.8	27.9	3.5	23.5
Molina 1	R	70 +						12.4
Fle 1	A/Bw	0 - 12	7.5YR 2.5/2	2 (fine)	6.6	79.9	2.1	
Fle 1	Bw/A	12 - 35	2.5YR 3/3	1 (fine)	7.2	24.5	2.6	5.7
Fle 1	Bw1	35 - 50	2.5YR 4/4	5 (fine)	7.0	13.1	2.1	8.5
Fle 1	Bw2	50 - 85	2.5YR 3/3	2 (fine)	7.3	8.1	1.6	7.1
Fle 1	CB	85 - 110	2.5YR 5/4	5 (fine)	7.2	2.7	0.5	5.2
Fle 2	A1	0 - 5	10YR 2/1	2 (fine)	7.2	88.0	0.6	1.5
Fle 2	A2	5 - 15	10YR 2/2	10 (fine)	7.2	36.9	0.6	1.4
Fle 2	Bw1	15 - 40	2YR 4/3	3 (fine)	7.4	18.1	0.6	1.4
Fle 2	Bw2	40 - 70	2YR 4/3	5 (fine)	7.6	12.8	0.6	1.7
Fle 2	Ab	70 - 110	2.5YR 3/3	7 (fine)	7.4	22.5	1.0	1.8

The Cervinara case study

The profile Cervinara, located on a northeast-facing slope, is very deep (approx. 170 cm) and characterised by soil horizons with brownish colours (10YR). The profile demonstrates a recent soil with a thickness of 75 cm (from A to Bw2 horizons) overlying a more ancient soil (from Ab to Bwb3 horizons) directly in contact with limestone bedrock. All horizons have a neutral pH, except for the Bw1 which is weakly acid, with a sandy texture. The amount of organic matter is very high at the surface (146.7 g kg^{-1} in the horizon A) and decreases with depth reaching values of 15.2 g kg^{-1} in the horizon Bwb3. The andic properties, expressed by the index Al_o+½Fe_o, are well developed both in the recent and in the ancient soil (index values range between from 4.6 and to 4.7%). Allophane and imogolite contents are high, varying between 13.7 and 24.6% respectively in the horizons A and Bwb1. All horizons are moist, while Bwb2 and Bwb3 are wet.

The Monte Pendolo case study

The Monte Pendolo profile is located on a North-facing slope and is moderately deep (approx. 90 cm). The profile is characterised by horizons with brownish colours (10YR) and the presence of two overlapping soil types. The pH is neutral in the upper horizons and weakly alkaline in the lower ones; the amount of organic matter is high in the upper horizons (119.1 g kg^{-1}), but lower in the deeper ones (34.2 g kg^{-1}). All horizons have sandy texture. The very pomiceous (80%) horizon BC, separates the more recent soil (horizons A and Bw), characterized by poorly expressed andic properties (Al_o+½Fe_o=1.6%) from the ancient one, characterised by the horizon Bwb and having very well expressed andic soil properties (Al_o+½Fe_o =3.2%). The allophane and imogolite content varies from 7.3 to 10.6%.

The Quindici case study

The Quindici soil, located on a North-facing slope, is a very deep and complex profile in which 3 soils overlap. Texture is loamy sand at the surface and sandy loam at higher depth. The deeper buried soils (horizons Bwb4 and Bwb5) had a finer particle size distribution than the more recent and superficial soils. Organic matter content is moderately high at the surface (60.3 g kg^{-1}) and decreases irregularly with the depth. The andic properties are generally very well developed, with values increasing with the depth (from 2.8 to 3.0%), as well as the allophane and imogolite content, which is higher (11%) in the deepest horizons than at the surface (5–9%). The horizon Cb, while having a yellow-brownish colour and a typical morphology of a weakly weathered horizon, has high allophane and imogolite content (11%) denoting an unexpected marked pedogenesis.

The Sarno case study

The Sarno profile, located on a southwest-facing slope, is very deep (~200 cm) and characterised by soil horizons with brownish colours (10YR) at the surface and brown-yellowish (2.5Y) at depth. A recent soil (between the horizons BC and A) covers a buried soil sequence (from horizon Ab to Bwb). The two soils are separated by a pomiceous horizon. The recent soil has neutral pH, while the buried soil is weakly alkaline. The texture of the both soils is sandy loam. The organic matter content is high at the surface (169.8 g kg^{-1} in horizon A), but decreases quickly with the depth (7.2 g kg^{-1} in horizon BC). In the deeper soil (horizon Ab/Bwb) the measured content of organic matter is 18.1 g kg^{-1}. Andic properties are well developed in the recent soil (Al_o+½Fe_o=4.7%), displaying an amount of allophane and imogolite between 8.1 and 21.1%. Andic soil properties are only moderately developed in the buried soil (2.1%), with values of allophane and imogolite of 7.1%.

The S. Felice a Cancello case study

The S. Felice a Cancello 1 profile (SFC1), located on a North-facing slope, is deep (approx. 200 cm) and characterised by soil horizons with brownish colours (10YR). The profile displays two soil sequences, a recent soil (horizons A, AB, Bw, BC1, BC2, C1, C2) and a buried soil (horizons 2Ab, 2Bwb1, 2Bwb2) directly overlying limestone bedrock. The two soils are

separated by pomiceous layers (horizons C1 and C2). In the recent soil, the pH ranges from neutral to weakly alkaline, while in the buried soil it is moderately alkaline. In the recent soil the texture is sandy and organic matter content is high (48.5 g kg^{-1} in the horizon A) at the surface but decreases with the depth (35.6 g kg^{-1} in horizon C1). The texture of the buried soil is loamy sand and the organic matter content is high for the horizon Ab (16.7 g kg^{-1}) but decreases with the depth (3.84 g kg^{-1} in horizon Bwb2). The andic properties are weakly expressed in both recent and ancient soil (Al_o+½Fe_o index values range from 0.5 to 0.6%), and the allophane and imogolite content is between 5.7 and 0.2%.

The Molina case study

The Molina profile has an eastern facing aspect. It is moderately deep (70 cm) and directly overlies limestone bedrock. It is characterised by soil horizons with brownish colour (10YR). The surface soil pH is neutral, whereas the deeper soil has a weakly alkaline pH. The surface texture is sandy and the deeper soil texture is silty loam. The organic matter content is high at the surface (99.9 g kg^{-1} in horizon A) but decreases irregularly and quickly with increasing depth. The andic properties are strongly expressed (Al_o+½Fe_o=4.6%) and the amount of allophane and imogolite is between 12.4 and 23.5%.

Integrated analysis of the land-soil system

Figures 3 and 4 illustrate relationships between altitude and NDVI and andic properties (weighted for the profile). An increase in elevation correlated with an increase in NDVI ($P<0.01$), but elevation and andic properties did not correlate. Similar correlations are observed with organic matter (data not shown). The results suggest that, in contrast to many volcanic areas where Andosols have been studied (e.g. Canary Islands, Açores, La Reunion, Hawaii), the development of andic properties in Campania are

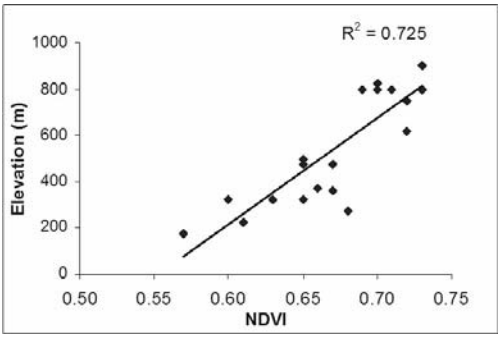

Figure 3. NDVI against elevation distribution of the landslide detachment crowns. $P<0.01$.

not well explained by elevation, but instead are associated with other factors such as aspect, ash spatial distribution, time of pedogenesis and land use.

To examine the role of aspect as a landslide triggering mechanism, we evaluated the andic properties of whole soils. There are small (approx. 1 unit of pH in NaF) but consistent differences in andic properties among the soils developing on south-facing and north-facing slopes (Figure 5).

To directly determine the role of aspect as a triggering mechanism of landslides, we conducted a more detailed examination of the case study of S. Felice a Cancello. This case study is representative of the typical Campanian landscape, characterized by the presence of two different ecosystems, chestnut on the north-facing slopes and pasture or uncultivated lands on the south-facing slopes. The northern slope was affected by landslides in 1998.

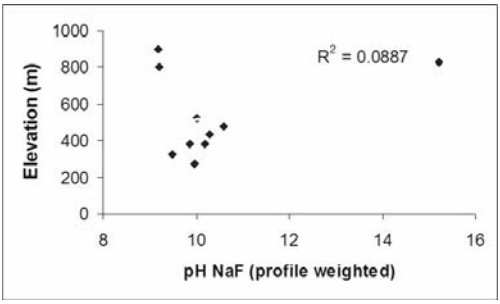

Figure 4. Andic features estimated by pH NaF (weighted for the whole profile), against elevation distribution of the landslide detachment crowns.

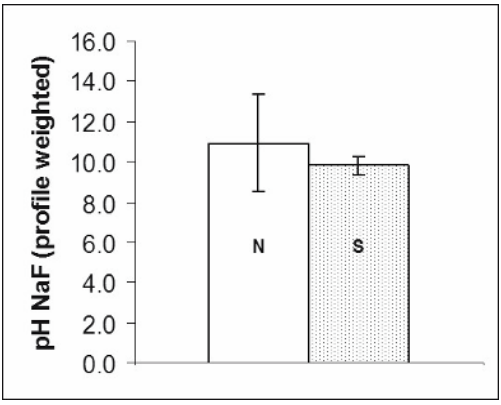

Figure 5. Andic features estimated by pH NaF (weighted for the whole profile), against the aspect of the landslide detachment crowns.

The soil of the southern aspect slope of S. Felice a Cancello (SFC2, Table 2) is moderately deep (approx. 70 cm) and is characterised by horizons with brownish colours (10YR). The organic matter content is very high (105.3 g kg^{-1}) at the surface and decreases with increasing depth. The pH is weakly alkaline at the surface and the texture is sandy, while at greater depths the pH is moderately alkaline and the texture is sandy loam. All horizons are moist except the deepest one (horizon Bw) which is wet. The andic properties are weakly developed (Al_o+½Fe_o=1.5%) and the allophane and imogolite content is between 3.3 and 5.5%. Analysis of the north-facing slope is presented above in the S. Felice a Cancello case study.

Comparison of north- and south-facing soil profiles shows that they have similar morphological features and chemical-physical properties. Specifically, they are similar in colour, field moisture and soil structure consistency (horizons Bwb1 and Bwb2 of the north-facing slope and horizon Bw of the south-facing slope). Soils on the North-facing slope, however, are considerably deeper relative to those on the south-facing slope.

We conducted a soil hydraulic characterization for the profiles SFC1 and SFC2. Figures 6 and 7 show water retention and hydraulic conductivity curves of 3 horizons (AB of surface, Bw and C1) of SFC1 and 2 horizons (A2 and Bw) of SFC2.

The mean value of the saturated water content and the bulk density for each characteristic horizon are shown in Table 3.

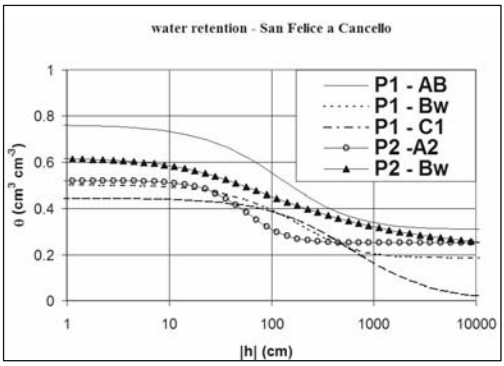

Figure 6. Water retention curves of S. Felice a Cancello P1 (North) and P2 (South) soils.

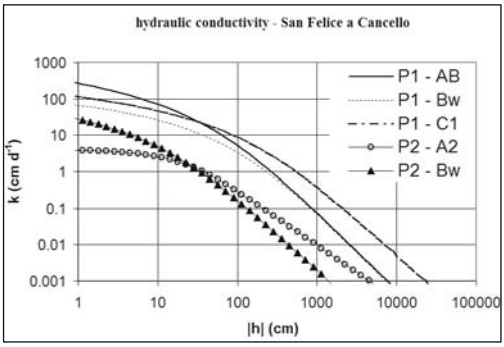

Figure 7. Hydraulic conductivity curves of S. Felice a Cancello P1 (North) and P2 (South) soils.

These analyses suggest the following conclusions:

- the two soils present a complex sequence of horizons (A, AB, Bw, C), characterised by a strong vertical variability of water retention parameters
- all horizons have, on average, high values of saturated water content; these values are very high (0.76 cm^3 cm^{-3} of water) in the surface horizons (for example horizon AB)
- the vertical variability is significant for all water retention values analyzed, from saturation to low water content. In the SFC1 soil, the differences at saturation are elevated (on average 0.25 cm^3 cm^{-3} of water), in particular between horizons AB and both Bw and C1, and greater than in SFC2. In the SFC2 soil, the differences in water retention between the

surface horizon A and the underlying Bw are low (at saturation, approx. 0.08 cm^3 cm^{-3} of water)
- the shape of the water retention curve shows a different distribution of equivalent pores of the horizons in both SFC1 and SFC2
- all horizons of SFC1 profile have hydraulic conductivity values greater than those observed for the SFC2 profile, which is characterized by lower variability
- the saturated hydraulic conductivity (k_0) varies between moderate and high, in the order of 10^1–10^3 cm d^{-1} (with the exception of A2 of SFC2). Greater differences (an order of magnitude) have been found between topsoil horizons A and AB and the subsoil horizons. This behaviour, in the case of SFC1 soil, is related to the well-developed microstructure of the A soil horizons, due to the high biological activity of the soil fauna. The k_0 of the horizon A of SFC1 is much higher than the k_0 of the same horizon (horizon A) in the SFC2. This result is important in the determination of infiltration-outflow dynamics of these soils
- the low bulk density is typical of soils with andic properties (see allophane content in Table 2)

Table 3. Mean values of the saturated water content and the bulk density for characteristic horizons of the S. Felice a Cancello soils.

Profile	SFC1					SFC2		
Horizon	A	AB	Bw	C1/C2	BC2	A1	A2	Bw
Bulk density	0.68	1.1	1.1	0.96	0.9	0.63	0.97	0.91
Θsat	0.793	0.76	0.5	0.51	0.682	0.834	0.64	0.720

The influence of the aspect on the landslide phenomena: hydrological behaviour by means of modelling of the hydrologic processes

Previous studies (Basile et al. 2003) have demonstrated the importance of water balance for evaluating soil susceptibility to landslide triggering mechanisms. A soil water balance simulations approach can be used to evaluate the risk of landslide on the north- and the south-facing slopes. The procedure is described in detail (Basile et al. 2003), but the key aspects are as follows:
- HYDRUS-2D software was used simulate two-dimensional variably-saturated water flow in hill slopes (Simunek et al. 1999). Simulations were performed in a vertical plane X, Z according to the maximum steepness (55°). The saturated-unsaturated two-dimensional water flow

process in soil slopes can be described by the following modified form of Richards' equations:

$$\frac{\partial h}{\partial t} C(h) = \frac{\partial}{\partial x_i}\left[K(\theta)\left(K_{ij}^{A} \frac{\partial h}{\partial x_j} - K_{iz}^{A} \right)\right] - S$$

in which K_{ij}^{A} are components of the dimensionless anisotropy tensor K^A; x_i or x_j (cm), with i and j =1, 2 being the spatial coordinates

- In order to emphasise the difference between the northern and southern aspects of the landslide triggering, the same upper boundary conditions (rain and ET_{ref}) were applied to the soils. Simulations were performed from January to May 1998, using the same climatic data of the catastrophic events of Sarno/Quindici, for a period of 123 days
- An area covered by chestnuts, 2000 m long and a having a slope of 55° was hypothesized without track, road or other pedo-continuity breaks
- The lower boundary condition (free drainage) and initial condition (profile near saturation) were the same for both simulations

Figure 8 illustrates the time evolution of the cumulative water storage in the soil profiles SFC1 and SFC2. At a 70 cm depth, the SFC1 water storage is almost double that of the SFC2. This is determined by higher water retention capacity of the upper horizons. SFC1 soil is deeper than that of SFC2 (200 cm vs. 70 cm), reflecting a 5-fold greater water storage capacity.

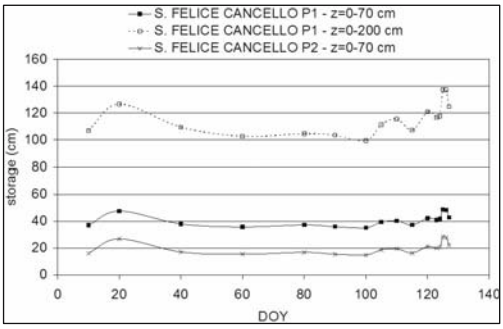

Figure 8. Simulation modelling of the water storage dynamics against a time series. Abbr. DOY: day of the year.

Discussion

The landscape

All investigated landslides occurred on carbonatic relieves characterised by high slope gradient and high fertility ecosystems, as indicated by high NDVI values (Table 1). Landslide detachment crowns occurred at different altitudes and slope gradients across years. This suggests that these two parameters, which are likely to be important mechanisms in landslide trigger-

ing and propagation, play a role in conjunction with other environmental factors, such as soil factors. In the case of S. Felice a Cancello, it appeared that deep soil was an important predisposing factor to landslide triggering processes. Numerical simulations showed a higher potentiality of water accumulation and, therefore, greater weight and pressure on deep layers, particularly in the northern aspect soils.

The soils

The soils represent the product of successive weathering cycles that have taken place on volcanic ash fall and/or pyroclastic flow deposits of Vesuvian and Phlegrean eruptions. Soils are interlayered with pomiceous or scoriaceous horizons. In stable geomorphological conditions, it is possible to recognize each pedogenetic cycle in the soil profile by the presence of a sequence of horizons A, B (solum) and C. In high to moderate gradient slope positions, this sequence has often been altered by erosion and deposition dynamics (colluvium). Such processes refer both to past and present day geomorphologic landscape dynamics and must be considered of primary importance in the analysis of the distribution of these Andosols. These processes also appear to be responsible for the following pedological features present in most of the investigated soil landscapes: (i) absence of horizons A in many buried soils, (ii) vertical discontinuity in the distribution of organic matter, (iii) absence of a reference pedological stratigraphy, (iv) a marked morphological variability frequently observed between different profiles (i.e. 20–30 m apart) in the same detachment crown. Specifically, all the examined soils exhibit common characteristics that are highly relevant for understanding the mechanisms of landslide triggering and propagation.

All soils are classified as Andosols (WRB; Soil Taxonomy; Referential Pedologique) with most classified as Hapludands and Udivitrands (USDA 1998). They are primarily forest soils, rich in easily weatherable minerals and characterized by high chemical, physical and biological fertility and high root density within 80–120 cm depth. This depth of root system seems to satisfy the trophic and water requirements of the woodland under local climatic conditions. Soil thickness ranges from medium to deep (70–110 cm), but it can also be very deep (170–240 cm). The soil morphology is complex due to overlapping of different pedogenetical cycles (buried soils), where the deeper and older soils are often those where the detachment plane of the slide occurred.

A marked vertical morphological variability characterizes the soil profiles. Frequent alternation of allophanic, vitric and skeletal coarse horizons produced contrasting chemical, physical and mechanical properties along the profile. Such marked vertical variability was also measured in the water retention properties, especially at the interface between the weakly weathered horizons C and the other more weathered soil horizons. All the weathered horizons are characterized by high values of saturated water content (0.5–0.75 cm^3 cm^{-3}) and low values of bulk density (0.6–1.1 g cm^{-3}). Thus, they are able to retain high contents of water (as weight) that is equal or higher than their own dry weight. All horizons have good water conductivity, both when saturated and at lower water content. In contrast to water retention this is less affected by vertical variability.

The profiles, generally, have a deep buried soil layer whose properties are different from those of the recent surface soil. Buried soils (especially the deepest), in comparison to the surface soils, are relatively finer and rich in silt, with less coarse sand content and evidence of strong weathering. They are characterized by higher water retention for all water potential levels, lower hydraulic conductivity and lower bulk density. The andic properties, mostly due to short-range clay minerals, are often well developed in all horizons (except in some horizons C), except for S. Felice a Cancello. The measured andic properties in these Campanian soils are relatively high with respect to Italian Andosols, but moderate in comparison to Andosols from tropical environments.

All soil horizons and especially the deepest horizons Bw show marked smeariness properties due to the presence of low ordered clay minerals, which enable the soil to quickly release water after the application of an abrupt mechanical (i.e. pressure) energy. All these features are mechanisms that contribute to the triggering and propagation of landslides. Specifically, soil type along with high soil depth and high water retention properties of Andosols result in a high water storage and consequently a high weight of soil bodies.

High variability of morphological, chemical and physical soil properties causes vertical discontinuities that represent weakness points or weakness planes in the soil cover. Root bodies, which are (mainly) located in the surface soil, do not contribute to strengthening the link between such discontinuities. High soil smeariness of the whole soil, and especially of the deep horizons Bw, represents a high potential and a high danger for soil liquefaction under a mechanical pressure. A very high sensitivity for triggering and propagation of landslides occurs when the following factors are combined: (i) high weight of hydrated soil bodies; (ii) physical planar discontinuities in the soils and (iii) high potential for liquefaction. Given these conditions, careful management techniques are required. However field

observations have demonstrated that this is often not the case. Analysis of the effects of different landscape managements indicates that the actual practice of forest harvesting (mainly chestnut in these areas) results in (i) opening of small roads (for use of farm tractors) that interrupt the continuity of the soil cover (Basile et al. 2003) and (ii) marked erosion of surface horizons, thus exposing the underlying horizons Bw to water erosion. The horizons Bw are characterized by a less developed structure, higher water retention and, in general, an estimated higher vulnerability to erosion. Exposure of horizons Bw creates conditions of great instability to the whole ecosystem.

Conclusions

Most catastrophic mudslides in Campania are related to soils developing upon pyroclastic materials covering carbonatic relieves of the Campanian Apennines. The soil observed in the detachment crowns of the investigated fast mudflow consisted of fertile Andosols (generally Hapludands and Udivitrands) that were very sensitive to anthropic or natural changes. This is due to the unique chemical, physical, morphological and hydrological behaviour of these soils, including (i) high water retention near saturation, (ii) high hydraulic conductivity, (iii) high smeariness of most horizons, and (iv) high vertical and lateral variability of the properties of the soil horizons. Aspect is important in determining soil susceptibility to landslide triggering and landslide susceptibility is related to hydrological properties that induce higher water storage especially in northern aspect soils. It is clear that stability of these soils requires conservation, implemented through appropriate forest planning and management. Improved risk management policies are necessary to preserve soil continuity and to decrease the risk both of surface soil erosion and to human lives and infrastructure.

References

Adamo P, Basile A, Di Meo V, Violante P (1996). Effetti dell'essiccamento sulle proprietà fisiche e chimiche di andisuoli: indagini preliminari. Atti del XIII Convegno Nazionale S.I.C.A., Bologna, pp 27–38

Bascomb CL (1968). Distribution of pyrophosphate-extractable iron and organic carbon in soils of various groups. J Soil Sci 19:251–268

Basile A, De Mascellis R, Terribile F (1999). Il suolo e la protezione degli acquiferi: studio pedologico e idrologico dei suoli della piana del F. Sarno (Campania). Atti del 3° Conv. Naz. Sulla Protezione e Gestione delle Acque

sotterranee per il III Millennio, Parma 13–15 ottobre 1999, Quad di Geol Applicata, suppl 2, Vol 1, pp 1251–1261

Basile A, Mele G, Terribile F (2003). Soil hydraulic behaviour of a selected benchmark soil involved in the landslide of Sarno 1998. Geoderma 117(3–4):331–346

Bordiga O (1915). Il nubifragio del 24 ottobre 1910 nei suoi effetti sulle colture dell'isola d'Ischia e della Costiera Amalfitana e le stime dei danni. Atti del Reale Istituto d'Incoraggiamento di Napoli 66:211–221

Bordiga O (1924). Le frane dell'amalfitano nel 1924. Cause effetti e rimedi. Atti del Reale Istituto d'Incoraggiamento di Napoli 76:167–179

Calcaterra D, Guarino PM (1997). Dinamica morfologica e fenomeni recenti nell'area collinare napoletana (Settore occidentale). Geologia Tecnica e Ambientale 371. IX Congresso O.N.G., Roma 17–20 Aprile 1997, pp 1–15

Calcaterra D, Parise M, Palma B, Palella L (2000). Multiple debris-flow in volcaniclastic materials mantling carbonate slopes. In: Wieczorek GF, Naeser ND (eds.) Debris Flow Hazards Mitigation, mechanics, Predition and Assessment. A.A. Balkema/Rotterdam/Brookfield, pp 99–107

Childs EC, Collis-George N, (1950). The permeability of porous media. Proc R Soc London, Ser A 201:392–405

CNR-GNDCI (1998). Ricerca storica sulle colate di fango in terreni piroclastici della Campania. Università degli studi di Salerno - Unità Operativa 2.38. Responsabile prof. L. Cascini, coautori L. S. Migale e A. Milone. Pubblicazione a cura della Presidenza del Consiglio dei Ministri - Dipartimento della Protezione civile - Ordinanza 2787 del 21 maggio 1998 e successive

Cruden DM, Varnes DJ (1996). Landslide types and Processes. In: Turner AK Shuster RL (eds) Landslides: Investigation and Mitigation. Transportation Research Board Special Report 247, National Research Council, pp 36–75

di Gennaro A, Aronne G, De Mascellis R, Vingiani S, Sarnataro M, Vitelli L, Arpaia G (2002). I sistemi di Terre della Campania. Carta 1:250,000. S.EL.CA. Firenze, 63 pp

Esposito L, Magliocca G, Nappi M (2003). Alcune considerazioni sugli episodi di frana di San Felice a Cancello (CE). Atti AIGA – 1° Convegno Nazionale, pp 369–377

FAO (1990). Guidelines for Soil Profile Description. 3rd edn (rev.). Rome, 70 pp

Guadagno FM, Palmieri M, Siviero V, Vallario A (1988). Alcuni aspetti degli eventi franosi tipo colata in vulcanoclastiti incoerenti dell'area campana. Atti del 74° Convegno della Soc Geol It (Sezione B), pp 259–262

Hungr O, Evans SG, Bovis MJ, Hutchinson JN (2001). A Review of the Classification of Landslides of the Flow Type. Environmental & Engineering Geoscience 7:221–238

Klute A (1986). Water retention: Laboratory methods. In: Klute (ed.) Methods of soil analysis, Part I, 2nd edn, Agron Monogr 9, ASA and SSSA, Madison, pp 635–662

Klute A, Dirksen C (1986). Hydraulic conductivity and diffusivity: Laboratory methods. In: Klute A (ed.) Methods of soil analysis. Part 1. Agron Monogr 9. ASA and SSSA, Madison, WI, pp 687–734

Lazzari A (1954). Aspetti geologici dei fenomeni verificatisi nel Salernitano in conseguenza del nubifragio del 25–26 ottobre 1954. Boll Soc Nat In Napoli 63:131–142

Mele R, Del Prete S (1999). Lo studio della franosità storica come utile strumento per la valutazione della pericolosità da frane. Un esempio nell'area di Gragnano (Campania). Boll Soc Geol It 118:91–111

Mualem Y (1986). Hydraulic conductivity of unsaturated soils: Prediction and formulas. In: Klute A (ed.) Methods of soil analysis, Part 1, Physical and mineralogical methods, 2nd edn. Agronomy 9(2). American Society of Agronomy. Madison, Wisconsin, pp 799–823

Parfitt RL (1990). Allophane in New Zealand – a review. Aust J Soil Res 28:343–360

Rouse JW, Haas RH, Schell JA, Deering DW, Harlan JC (1974). Monitoring the vernal advancement of retrogradation of natural vegetation. Greenbelt, MD NASA/GSFC (type III, Final Report), p 371

Schwertmann U (1964). Differenzierung der Eisenoxide des Bodens durch Extraktion mit Ammoniumoxalat-Lösung. Zeitschrift Pflanzenernähr. Dungung Bodenkunde 105:194–202

Simunek J, Sejna M, van Genuchten MTh (1999). The HYDRUS-2D Software Package for Simulating the Two-Dimensional Movement of Water, Heat, and Multiple Solute in Variably-Saturated Media. Ver. 2.0. U.S. Salinity Laboratory, ARS, USDA, Riverside, CA, USA, p 228

Tamari S, Bruckler L, Halbertsma J, Chadoeuf J (1993). A simple method for determining soil hydraulic properties in the laboratory. Soil Sci Soc Am J 57:642–651

Terribile F, Basile A, De Mascellis R, di Gennaro A, Mele G, Vingiani S (2000a). I suoli delle aree di crisi di Quindici e Sarno: proprietà e comportamenti in relazione ai fenomeni franosi. Quaderni di Geologia Applicata 7-1:59–79

Terribile F, di Gennaro A, Aronne G, Basile A, Buonanno M, Mele G, Vingiani S (2000b). I suoli delle aree di crisi di Quindici e Sarno: aspetti pedogeografici in relazione ai fenomeni franosi. Quaderni di Geologia Applicata 7-1:81–95

USDA (United States Department of Agriculture) (1996). Soil Survey Laboratory Methods Manual. Natural Resources Conservation Service. National Soil Survey Center. Soil Survey Investigations Report No 42. Version 3.0

USDA (United States Department of Agriculture) (1998). Keys to Soil Taxonomy. 8th edn. NRSC, 325 pp

van Genuchten MTh (1980). A closed-form equation for predicting the hydraulic conductivity of unsaturated soils. Soil Sci Soc Am J 44:892–898

van Genuchten MTh, Nielsen DR (1985). On describing and predicting the hydraulic properties of unsaturated soils. Ann Geophis 3:615–628

Watson KK (1966). An instantaneous profile method for determining the hydraulic conductivity of unsaturated porous materials. Water Resour Res 2:709–715

Vallario A (2001). Il dissesto idrogeologico in Campania. CUEN, 295 pp

Effects of land use on soil degradation and restoration in the Canary Islands

J.M. Hernández-Moreno, M. Tejedor and C.C. Jiménez

Introduction

Soil degradation, defined as the loss of the soil's productive capacity, is caused by a series of different processes that lead to changes in the physical, chemical and biological properties of soils. Among processes implicated are water and wind erosion, structural degradation, compaction, sealing, salinisation-sodification, pollution, acidification and loss of organic matter (Lal et al. 1989).

Soil quality loss affects the soil's functions which, as the European Commission's Communication on "Thematic Strategy for Soil Protection" illustrates, are vital for life and include environmental as well as economic, social and cultural aspects (European Commission Communication 2002).

Although many degradation processes may be caused naturally, they can also be triggered, accelerated or slowed down by human actions. Given the seriousness of the processes, attention in many regions tends to focus on the depredatory side of human actions as opposed to the rehabilitation aspects. However, in recent years there has been an increase in studies on traditional farming practices used as soil and water conservation strategies, especially in arid and semiarid regions (Seckler and Tejwani 1983, Gale et al. 1993, FAO 1994, Poesen and Lavee 1997, Li Xiao-Yan et al. 2000, Cerdá 2001, Tesfai 2001).

This chapter examines the physical environment conditions in the Canary Islands that propitiate soil degradation. It also discusses the main processes involved in the degradation and how important properties of the volcanic soils, particularly andic soils, influence these processes. The main management practices used as strategies for soil conservation and rehabilitation in the Islands will also be described.

Soil degradation

Environmental characteristics

The chapter on *Soils of Volcanic Systems in Spain* in this book describes the natural environment of the Canary Islands and underlines the high degree of variability that exists not only between the different islands but even within each island. We can distinguish "low" and "high" islands. In the latter, mountainous islands, altitudes over 1000 m lead to a northern, humid side and a southern, arid one. In the former, the absence of orographic barriers leads to a more homogeneous, arid climate. In this chapter we will refer only to aspects influencing degradation processes and will differentiate between natural and human factors.

Natural factors

The low islands, Fuerteventura and Lanzarote, are among the most arid parts of the European Union, bordering on desert. Their natural characteristics propitiate degradation processes to such an extent that the two islands may be considered as being in a relatively advanced state of desertification. Annual rainfall is seasonal in nature and does not exceed 150 mm, with high inter-annual variability, and there are prolonged droughts and a high evaporation rate. The intensity of the rainfall is variable. The torrential rain associated with south-easterly and south-westerly storms accounts for the bulk of the water. Heavy rain falling in 24-hour periods represents over 50% of the monthly and over 40% of the annual totals, which gives some idea of the torrential nature of the rain (Dávila and Romero 1994). Although intensities of above 10 mm in 24 hours represent less than 35% of the total (Marzol 1988), a study of the maximum recorded intensities and of water collected in harvesting systems (Díaz 2004) shows that these intensities are sufficient to produce runoff, given the conditions on the two islands. In addition to the erosion caused by this type of rainfall, the scarcity of water prevents soil leaching, therefore, the natural soils show a high degree of salinisation and sodification due to sea spray salt (Torres et al. 2005).

Given that these two islands are the lowest in the archipelago, relief does not appear in itself to be a decisive factor in the erosion process. In Fuerteventura, 61% of the land area consists of slopes of less than 10% (Criado 1991). However, the combination of topography, sparse vegetation (mostly scattered shrubland) and the characteristics of the soil surface (presence of a petrocalcic horizon and formation of sealing crusts, among

others) accounts for the widespread erosion. In addition, the very strong and constant winds give rise to wind erosion.

The mountainous islands, while sharing common characteristics with the above islands on their arid sides, are markedly different in the more humid parts. A more detailed study of the environment of these islands can be found in the chapter "Soils of volcanic systems in Spain" in this book. In the western Canary Islands, high and severe erosion has been described only for a small number of parts of Tenerife. Nonetheless, water erosion processes are important on these islands, although they tend to be related primarily to the abrupt relief (37% of Tenerife's land area has slopes of above of 30%).

Human factors

To the above factors we must also add those arising out of human action, including canopy loss, overgrazing, intensive farming, inappropriate farming practices, irrigation with poor quality water, demographic pressure, etc. The needs for timber for fuel, agriculture or construction, and the occupation of land for farming and grazing, are some of the leading causes of the deforestation suffered by Canarian forests, particularly the green forest, up to the mid-20th century. Combined with the steep slopes, deforestation has propitiated soil loss, with corresponding repercussions on condensation catchment and aquifer recharge (Rodríguez et al. 1998).

Although having different vegetation to the others, the low islands have also lost much of their plant cover, with resulting soil destabilisation. Fuerteventura, formerly known as 'Herbania' on account of its meadows, has lost a sizeable part of its vegetation due to tree-felling and overgrazing. It is also the island where the soil has been most adversely affected by livestock, in this case herds of goats whose constant trampling has destroyed the structure of the soil (Torres 2005).

Socio-economic changes have led to a reduction in farmland, particularly that formerly used for traditional and sustainable practices, which have been replaced today by intensive and less environmentally-friendly farming. Intensive single-crop farming has caused serious salinisation and sodification problems in soils. Rodríguez et al. (1998) noted that 57% of irrigated soils in the Canaries are affected by secondary salinisation. Poor quality water, inappropriate irrigation techniques and the indiscriminate use of agrochemicals have been recognized as contributing factors. Such problems were uncommon in the Canaries when flood irrigation was used, even with relatively saline water, given that the soil was washed periodically. The salinisation has been caused by the use of microirrigation

which, although eliminating salts from areas near the plants, does not eliminate them from the rest of the soil. The important chemical degradation of the soil is not the only problem caused, but also the side effects on contamination of the aquifers which are so vital in the Canaries.

By way of summary, the main degradation processes affecting soils in the Canary Islands, reported as percentages of the total archipelago surface, are as follows (Rodríguez et al. 1998): erosion (45%), salinisation-sodification (20%), physical degradation (15%), biological degradation (10%) and, to a lesser extent, acidification (5%) and chemical contamination (5%). Table 1 gives, for each island, the approximate percentages for the most important processes, erosion and salinisation-sodification.

Table 1. Percentage of land area affected by the main degradation processes, by islands.

	% of the total area of each island		
Island	Erosion (>12 t ha^{-1})	Salinization-sodification in general	Salinization-sodification in irrigated soils
Fuerteventura	59.4	54.0	-
Gran Canaria	56.7	12.2	67.0
La Gomera	47.1	9.6	70.2
Tenerife	41.9	8.7	59.0
Lanzarote	30.6	30.2	-
La Palma	8.0	0.2	49.3
El Hierro	5.9	0.1	39.5

Properties of volcanic soils associated with degradation processes

Andic materials confer good physical qualities on soils, especially high water retention and transmission and structural stability. However, these properties can diminish and even be lost, when environmental conditions are modified.

Desiccation caused by deforestation or agronomic practices is a major risk to Andosols and has been recognised as a first step towards soil degradation (Dorel et al. 2000). This is particularly true in semiarid, subtropical islands such as the Canaries. The main consequences of desiccation are a loss of aggregate coherence and irreversible changes to amorphous materials, with a reduction of porosity and surface area. The loss of aggregate coherence is partly due to hydrophobization (Poulenard et al. 2001); the resulting low-density aggregates are prone to wind and water erosion (in-

deed, these soils are known locally as "polvillo", which means fine dust, in reference to the physical state of the soils after a prolonged dry season).

One important effect of drying on amorphous materials is the reduction of water retention capacity (Warkentin and Maeda 1980). The data available from the islands show that soil water retention values relative to the amorphous contents are lower than in zones without a dry season, especially in cultivated soils (Armas-Espinel et al. 2003). Fortunately, the physical properties of andic soils appear to be highly resilient and soils cultivated for many years still retain their low density and high water retention capacity (Armas-Espinel et al. 2005).

Andosols and andic soils are good buffers against changes in soils' chemical conditions resulting from agronomic practices. The insensitivity of their structural stability to sodium (El-Swaify et al. 1969) and their solute binding capacity are among their properties that deserve mention. These properties help counter the physical and chemical degradation of the soil, especially under intensive agricultural use. The groundwaters used for irrigation in the Canary Islands are alkaline (sodium and/or magnesium bicarbonate), as is frequently the case in volcanic regions, and they pose a high risk to the permeability of non-andic soils. However, evidence of the structural stability of andic soils irrigated with high-risk waters has led local experts to adapt irrigation water quality guidelines to Canarian conditions (Plan Hidrológico Insular de Tenerife 1989).

The binding capacity of andic soils also explains their peculiar response to intensive fertilisation. The build-up of potential pollutants such as heavy metals and boron in cultivated soils often leads soil concentration levels to greatly exceed the accepted maximum concentrations but without harmful effects to plants (Arbelo and Hernández-Moreno 1998, Hernández-Moreno et al. 2001).

Soil conservation and rehabilitation practices

A range of site-specific traditional farming practices have evolved in the Canaries, particularly in the most arid parts and on the most arid islands. These practices contribute to soil and water conservation and have been adapted to ensure respect for the environment. These systems permit a certain amount of dry farming without giving rise to soil degradation problems.

These soil management systems have shown their effectiveness over the years and remain today an important component of agriculture on some of the islands. Although still used, they are in decline due to socio-economic

changes. Some of the farms have switched from dry to irrigation farming, using reclaimed and desalinated water. Preliminary results of this new practice point to a short and medium-term risk of degradation due to salinisation and loss of permeability (Hernández-Moreno 2005).

The principles underlying these practices can be summed up as follows: protecting the soil against the impact of rain drops, increasing infiltration capacity and reducing runoff loss, modifying the soil surface by increasing its roughness, breaking up slopes through the use of terraces, and catching and storing runoff. To these one can also add the transportation of soils from elsewhere.

Below, a brief description is given of the main types of practices.

Farming systems based on surface mulching

The inorganic materials used as surface mulch on soils are pyroclastic volcanic products – basaltic in Lanzarote and pumice in Tenerife – and organogenic marine sands (Lanzarote).

The local term 'arenados' is given to the practice of using coverings of basaltic pyroclasts in farming; a practice thought to have originated with the volcanic eruptions in Lanzarote during the period 1730–1736. Some authors (Quintana and de León 2000) have traced the existence of crops grown using this method as far back as 1733.

Natural "arenados" are used in parts of Lanzarote which have a natural presence of tephra, near volcanic cones. Although the covering can be

relatively thick, it tends to be around three metres. The farmers dig a hole approx. 3 m in diameter (the depth depends on the thickness of the ash covering) as far the soil level where planting takes place and a layer of manure is then added on top. In this way the plant is in contact with the soil below and is protected from the wind by the hole. Stone walls made from fragments of the basaltic outcrops are often erected around the hole. The walls are semicircular and face the direction of the prevailing wind. This dry farming technique is very common, although it tends to be used only for vines or figs.

Artificial "arenados" are made – again mainly in Lanzarote – by the farmers in the same way as their natural counterparts, but this time in areas not covered by the volcanic materials. Volcanic tephra is placed over the soil, which may be either natural or brought in from elsewhere, as occurs when the natural soils are too poor for agricultural purposes or are not readily available. The thickness of the layer of ash varies between 5–20 cm, with 10–12 cm being the most common. Before the soil is covered with the tephra, organic material (usually manure) is added mechanically at around 10 cm depth. The average life of the system is approx. 20 years. The most common crops are onions, potatoes, pumpkins, beans and lentils. Since very little fertiliser is used, this type of farming can be considered ecological and the characteristics of the produce, with a lesser influence of agrochemicals, compensate for the relatively low yield. In the past this practice has taken up 6000 ha on Lanzarote although the current figure is just over half that.

Crops grown in the lava "cracks" (Lanzarote). This occurs in parts where the soil was formerly covered by lava outcrops. The cracks in the lava are used by the farmers to access the soil underneath to grow deep-rooted plants (vines and figs). The method is included here as a curious example of a traditional system given the very small land area and production involved.

Crops grown under pumice. This practice is found in the south and southeast of Tenerife, occupying a total area of approx. 3800 ha. In this case, the soil is covered with a 20–60 cm layer of pumice pyroclasts. Vegetables and grapes grow in the soil, while other crops (potatoes) may grow in the pumice layer, which is mixed with the soil to some extent.

Crops grown under sands (locally known as "jable"). With this method the natural soils are covered with the aeolic marine sands that have covered central parts of Lanzarote, more exposed to the action of the trade winds. The thickness of the sand layer varies depending on the area, from 2 m to a few centimetres, becoming thinner further inland. Crops tend to be grown in parts where the sand layer is less than one metre. The main crops grown are sweet potato, melon and water melon. The crops grow both in the ground, using a procedure similar to that described above for the natural 'arenados', or directly in the sand layer.

The influence exerted by surface mulching systems on soil properties has been studied by a number of authors (Tejedor et al. 2002abc, 2003ab, 2004ab, 2005, Jiménez et al. 2004b, Díaz et al. 2005, Neris et al. 2005). All these systems help conserve both soil and water and contribute to the rehabilitation of degraded soils. They differ greatly in terms of effectiveness, however. Compared to the bare soils, all the coverings described above improve soil moisture conservation due to the positive effect on in-

filtration and evaporation. Given their properties and behaviour, however, the coverings of basaltic pyroclasts of all origins are considerably more effective than pumice or aeolic sands. Up to eight times more water has been recorded in soils covered with these pyroclasts compared to bare soils, even in the driest period of the year (Tejedor et al. 2003a). In addition to the nature of the materials, granulometry and the thickness of the covering also play a part. The most effective basaltic coverings are those with grains of fine-medium size, which are considerably better than coarse-grain materials (Tejedor et al. 2002c). A thickness of 10–15 cm is appropriate, conserving moisture much better than a layer of 5 cm. The important modifications caused to the soil moisture conditions lead to a change in the soil moisture regime (Soil Survey Staff 1999), which can even become udic instead of aridic (Tejedor et al. 2002b).

These systems also influence soil temperature by reducing diurnal and seasonal fluctuations, even leading to an 'iso' characteristic (Soil Staff Survey 1999). The improved infiltration (the basic rate is at least doubled) means that erosive processes are reduced considerably. Recent studies (Tejedor et al. 2004b) have shown not only that basaltic mulch is effective in rehabilitating soils degraded by salinisation-sodification but also that the rehabilitation occurs relatively quickly.

Farming system based on runoff harvesting

The farming system for runoff harvesting, known locally as 'gavia', existed at one time on all the islands in the Canaries but is confined today to Fuerteventura, where it is used over 7000 ha, half of which are in permanent use. It belongs to the microcatchment category, given that the runoff catchment area is always some distance away from where the water is accumulated and also in view of the high ratio between the respective area sizes (anywhere between 10:1 and 110:1, Díaz 2004). Cultivation takes place on flat land, perpendicular to the runoff catchment zones (hillsides for the most part). The 'gavias' are surrounded by stone walls approx. 0.5–1.25 m in height. The upper walls have openings to allow water to enter and the walls directly opposite also have openings to drain excess water. The height of the intake and drainage openings needs to be in proportion to the height of the wall itself, with lowerings of 30 cm most commonly used. The width of the openings is also crucial: it is recommended that the drainage opening be at least twice as wide as the intake one. Water reaches the cultivated plots directly or along small gullies. The main crops grown are winter cereals – wheat, barley, oats, corn – along with lentils, chickpeas, beans and, to a lesser extent, saffron and potatoes.

Gavias' are a soil and soil water conservation system which modifies the soil's water conditions so extensively that dry farming becomes possible, with water available to plants in the root zone throughout the winter and spring months (Jiménez et al. 2002). In adjacent soils that receive only rain water crops cannot be planted. The 'gavias' also contribute to aquifer recharge. Moreover, the soil water modifications improve salinity and sodicity, reducing them to levels that do not hinder the development of most crops. The 'gavias', therefore, help rehabilitate soils degraded by these two processes. Soil fertility is also improved due to the uptake of nutrients carried by the runoff (Jiménez et al. 2004a).

The 'gavia' system is designed in such a way that wind and water erosion is reduced to a minimum. To that end, the appropriate proportions must be maintained between the heights and widths of the protection walls and the water entry and exit points. This helps minimise any 'river' effect caused by the water from the catchment areas. The design and proper upkeep of the elements of the system are also crucial.

Terraces

The lack of land, together with the presence of steep slopes on the medium-height and higher islands (and to a lesser extent in Lanzarote and Fuerteventura), have encouraged Canarian farmers to devote painstaking

efforts to building the terraces that have transformed the landscape of the islands. The terraces take different forms (González and Martín 1993) depending on whether the land is levelled or not, which has repercussions for management. Eliminating the slope entirely usually requires, in addition to a retaining wall perpendicular to the slope, soil to be brought in to fill the cultivation area. If the natural slope (where this is lower than the previous case) is kept, the original soil is retained also with no major modifications and a smaller wall can be used. Another type of terracing is that seen on volcanic cones. Here, unlike the previous cases, heavy machinery is required to build the terraces, which are not protected by walls. Moreover, since earth shifting leads to a loss of organic horizons and the tephra becomes exposed, erosive processes will set in inevitably unless vegetation is planted quickly. This is an example of a cultivation practice which accelerates erosive processes.

The size of the terrace depends on the slope. In very steep parts they can be so small that only one plant per terrace is grown. The system is renowned for its soil and soil water conservation effectiveness. Another aspect to take into account is the low level of production: farming in these areas, for the most part at heights of between 300–700 m, is of the subsistence type, geared to a domestic market. The main crops grown are potatoes, cereals, fruit trees, citrus fruits and grapes.

Sorribas

Although the coastal strips of the mountainous islands offer ideal climatic conditions for a range of crops, they also suffer from a series of limiting soil-related factors, including lack of soil, high stoniness, salinity and sodicity. In such cases, it is common to make ‘sorribas’, the name given to cultivation plots where soil is brought in from other areas of the island, usually from the north side between 300–700 m, where soils are more fertile. Prior to adding the imported soil, the ground is levelled, the stones removed and a layer of 30–40 cm of stony material (e.g. basaltic scoria) is placed to facilitate drainage. Once all this is completed a layer of soil between 50–100 cm thick is added. The soils most commonly used for building ‘sorribas’ are Inceptisols, Andisols and Alfisols. The plots are often protected using windbreaks and greenhouses.

‘Sorribas’, found normally at heights of below 300 m, are used for intensive irrigation farming of bananas, which are easily the most important crop grown in the Canaries. The amount of land occupied by bananas has fallen (from 12,747 ha in 1984 to 8563 in 1995), although yield has increased by more than 10%.

The intense nature of the farming and the use of agrochemicals and water which is not always of ideal quality, combined with the emergence of micro irrigation, have all led to extensive changes in the soils in a relatively short time, and particularly to problems of sodification and salinisation (Armas-Espinel et al. 2003). In over 80% of banana groves sodium levels in solution and in the exchange complex exceed those recommended for the crop (Vargas 2001).

Conclusion

The traditional farming systems described in this chapter are a good example of soil and soil water conservation strategies in fragile island regions. The systems are adapted to the environment and have allowed farming without irrigation in very adverse environmental conditions.

They improve the soil moisture conditions, reduce soil salinity and sodicity, buffer temperature variations and extreme temperature values, improve soil fertility, and also minimise degradation. In short, they can be considered sustainable practices.

Despite the plentiful production, the economic profitability of these farming systems under the current conditions cannot compete with that of other sectors, particularly tourism.. In view of their important role, and their significance for the cultural identity of the Canary Islands, these systems should be re-encouraged through measures to increase productivity.

The principles underlying the practices described can easily be transferred to other arid regions of the world, particularly volcanic ones, given that no major investment or sophisticated technology is required. Indeed, some such systems have already been used in other regions (Woldeab et al. 1994).

References

Arbelo C, Hernández-Moreno JM (1998). Boron buffer capacity of andic soils irrigated with urban waste water.16th World Congress of Soil Science Montpellier, Symposium 21, pp 43

Armas-Espinel S, Hernández-Moreno JM, Muñoz-Carpena R, Regalado CM (2003). Physical properties of “sorriba” cultivated volcanic soils from Tenerife in relation to andic diagnostic parameters. Geoderma 117:297–311

Armas-Espinel S, Regalado C, Hernández-Moreno JM (2005). Consecuencias de las prácticas de manejo en la calidad física de suelos altamente agregados de Tenerife. Edafología (in press, ref. RV8304)

Cerdá A (2001). Effects of rock fragment cover on soil infiltration, interrill runoff and erosion. Eur J Soil Sci 52:59–68

Criado C (1991). La evolución del relieve de Fuerteventura. Serv. Public. Excm. Cabildo Insular de Fuerteventura, 318 pp

Dávila P, Romero LE (1994). Precipitaciones máximas en Lanzarote: régimen de intensidades y frecuencias. V Jornadas de Estudios sobre Fuerteventura y Lanzarote. Serv. de Publicaciones de los Cabildos de Fuerteventura y Lanzarote, 2:53–72

Díaz F (2004). Sistemas agrícolas tradicionales de las zonas áridas de las islas Canarias. Tesis Doctoral. Universidad de La Laguna, Tenerife, Spain, 417 pp

Díaz F, Jiménez CC, Tejedor M (2005). Influence of the thickness and grain size of tephra mulch on soil water evaporation. Agricultural Water Management 74(1):47–55

Dorel M, Roger-Strade J, Manichon H, Delvaux B (2000). Porosity and soil water properties of Caribbean volcanic ash soils. Soil Use and Management 16: 133–140

El-Swaify SA, Swindale LD, Uehara G (1969). Salinity tolerance of certain tropical soils and relationships between sodium ion activities and soil physical properties. Research and Development Progress Report, vol. 419. United States Department of the Interior, pp 1–46

European Commission Communication (2002). Towards a Thematic Strategy for Soil Protection. COM (2002) 179 final

FAO (1994). Water harvesting for improved agriculture production. Water Report. Proceedings of the FAO Expert Consultation, Cairo, Egypt, 21–25 November 1993. Food and Agriculture Organization

Gale WJ, Mc Coll RW, Fang X (1993). Sandy fields traditional farming for water conservation in China. J Soil and Water Conserv 48:474–477

González A, Martín C (1993). La agricultura familiar y de mercado interior. In: Geografía de Canarias, vol 1. Gobierno de Canarias, pp 342–356

Hernández-Moreno JM, Espino-Mesa M, Arbelo C (2001). Speciation of Cu and Zn in Andisols and Andic soils: short- and long- term effects of metal loading. COST Action 622 Soil Resources of European Volcanic Systems – International Workshop on Volcanic Soils. Ponta Delgada (San Miguel) Azores, Portugal

Hernández M, Tejedor M, Jiménez CC, Díaz F, Hernández-Moreno JM (2005). Comportamiento de suelos volcánicos frente al riego con aguas depuradas y desalinizadas. Influencia del yeso en la corrección de problemas de boro y sodio. Reunión Internacional sobre avances en riego localizado, 2–5 december 2002. INIA, pp 220–226

Jiménez CC, Tejedor M, Díaz F (2002). Runoff harvesting systems in the Canaries. In: TRMP paper nº 40 "Water harvesting in Mediterranean zones: an impact assessment and economic evaluation", 2:41–48

Jiménez CC, Tejedor M, Díaz F (2004a). The impact of water harvesting on soil properties in the island of Fuerteventura, Spain. Soil Use and Management 20:89–91

Jiménez CC, Tejedor M, Neris J, Mejías G (2004b). Influence of pumice mulch on soil infiltration rate. 13th Int. Soil Conservation organization Conference Abstracts 631, Brisbane, Australia, Julio 2004

Lal R, Hall CF, Miller FP (1989). Soil Degradation: I. basic processes. Land Degradation and Rehabilitation 1:51–69

Li Xiao-Yan, Gong Jiadong, Gao Qianzhao, Wei Xinghu (2000). Rainfall interceptation loss by pebble mulch in the semiarid region of China. J Hydrol 228: 165–173

Marzol Jaén V (1988). La lluvia, un recurso natural para Canarias. Serv. Public. de la Caja General de Ahorros de Canarias 130, 220 pp

Neris J, Rodríguez-Paz M, Jiménez CC, Tejedor M (2005). Influence of management with salic mulch on soil temperatura. International Symposium on Land Degradation and Desertification. Uberlândia, Brasil, 16–22 may 2005

Padrón PA, González MC, Hernández LA, Jiménez CC, Ortega MJ, Rodríguez A, Torres JM, Vargas GE (1991). Erosividad de las lluvias en las Islas Canarias Occidentales. Libro de Comunicaciones XVIII Reunión Nacional de Suelos, pp 459–470

Plan Hidrológico Insular de Tenerife (1989). Calificación hidroquímica de las aguas de Tenerife. Tomo II. Gobierno de Canarias, Cabildo Insular de Tenerife

Poesen J, Lavee H (1997). How efficient were ancient rainwater harvesting systems in the Negev desert, Israel? Bull. Séanc. Acad. Royale Sciences d'Outremer 43:405–419

Poulenard J, Podwojewski P, Janeau JL, Collinet J (2001). Effects of tillage and burning on hydrodynamic properties of volcanic ash soil in Ecuadorian páramos. Catena 45:185–207

Quintana Andrés P, de León Hernández J (2000). Los resabios del volcán: los lanzaroteños desplazados a Fuerteventura entre 1730–36. In: IX Jornadas de Estudios sobre Fuerteventura y Lanzarote. Tomo I Historia, Prehistoria, pp 227–247

Rodríguez, A, Jiménez CC, Tejedor M (1998). Soil degradation and desertification in the Canary Islands. In: The soil as a strategic resource: degradation processes and conservation measures. Geoforma Ediciones, pp 13–22

Seckler DW, Tejwani KG (1983). Effect of sand and gravel mulching on moisture conservation for tree saplings. J Tree Sci 2(1–2):20–23

Soil Survey Staff (1999). Soil Taxonomy. 2nd edn. NRCS-USDA. Agric- Hand. 436, U.S.Gov.Print.Office, Washington, DC

Tesfai M (2001). Soil and water management in spate irrigation systems in Eritrea. Tropical Resources Managements Paper 36. Wageningen, The Netherlands

Tejedor M, Jiménez CC, Díaz F (2002a). Traditional agricultural practices in the Canaries as soil and water conservation techniques. In: TRMP paper nº 40 "Water harvesting in Mediterranean zones: an impact assessment and economic evaluation" 1:3–11

Tejedor M, Jiménez CC, Díaz F (2002b). Soil moisture regime changes in tephra-mulched soils: implications for Soil Taxonomy. Soil Sci Soc Am J 66(1): 202–206

Tejedor M, Jiménez CC, Díaz F (2002c). Volcanic mulching: a soil and water conservation strategy. Int. Symp. on Sustainable Use and Management of Soils in Arid and Semiarid regions vol I, Cartagena, Murcia, pp 221–232

Tejedor M, Jiménez CC, Díaz F (2003a). Volcanic materials as mulches for water conservation. Geoderma 117(3–4):283–295

Tejedor M, Jiménez CC, Díaz F (2003b). Use of volcanic mulch to rehabilitate saline-sodic soils. Soil Sci Soc Am J 67:1856–1861

Tejedor M, Jiménez CC, Díaz F (2004a). Dry farming with soils under natural tephra cover in Lanzarote, Spain. Soil Use and Management 20:360–362

Tejedor M, Jiménez CC, Díaz F (2004b). Use of volcanic mulch for saline-sodic rehabilitation: short and long term experiences in Canary Islands. Volcanic Soil Resources in Europe COST Action 622 Final Meeting, Iceland Rala Report 214, p 127

Tejedor M, Jiménez CC, Díaz F, Rodríguez CM (2005). Effectiveness of sand mulch in soil and water conservation in an arid region, Lanzarote, Canary Islands, Spain. J Soil and Water Conserv 60(1):63–67

Torres JM, Rodríguez A, Tejedor M (2005). Los Suelos. In: Patrimonio Natural de la isla de Fuerteventura. Cabildo de Fuerteventura, pp 59–80

Vargas GE (2001). Salinización inducida en los suelos agrícolas de Canarias: caracterización y prognosis. Tesis Doctoral, Universidad de La Laguna, Tenerife, Spain, 457 pp

Warkentin BP, Maeda T (1980). Physical and mechanical characteristics of Andisols. In: Theng BKG (ed.) Soils with Variable Charge. New Zealand Society of Soil Science, Soil Bureau, Lower Hutt, pp 281–299

Woldeab A, Assefa A, Yematawork A, Abera S, van Straaten P, Chesworth W (1994). Report on the Results of the Ethiopia-Canada Agrogeology Project-Rock-Mulch. (IDRC-Project 88-1032), 76 pp

Appendix materials on CD-Rom

artificial_arenados.jpg
natural_arenados.jpg
gavias.jpg
jable.jpg

Trace elements in polluted Italian volcanic soils

P. Adamo and M. Zampella

Introduction

Trace element content and speciation in soil essentially depend on soil parent material, on weathering processes, biocycling, and additional inputs via atmospheric wet and dry deposition due to natural sources, as well as on anthropogenic sources (i.e. agricultural, industrial, urban activities) (Alloway 1995). Soil pollution by trace elements is of critical importance because the soil can become decontaminated slowly and partially, and pollutants tend to accumulate in it (Kabata-Pendias 2001). Soil properties, according to the variability in organic and inorganic soil constituents, may have a strong influence on progressive trace element accumulation (Alloway 1995). Volcanic soils, and in particular andosols, which are known for their abundance of neoformed amorphous aluminosilicates and organo-mineral compounds, have a high binding capacity for trace metals (Tanneberg et al. 2001). They can retain metals by specific adsorption on hydrous oxide and oxyhydroxide surfaces and by organic complexation (Denaix et al. 1999), and some elements may be so strongly bound that they become unavailable to plants (Tanneberg et al. 2001).

Characterization of soil trace metal contamination is commonly based on the determination of total contents. However, the elements are present in soil in various forms and these can strongly affect their behaviour in terms of biological availability, potential toxicity and mobility within the profile (Ure and Davidson 2002). Therefore, in order to understand soil contamination and to assess the potential effects of soils polluted by trace metals, the following are required: identification of the geochemical phases in which the metals are bound, evaluation of metal retention and bioavailability, and the assessment of the effect of heavy metal contamination on plants, soil fauna, soil bacterial diversity and biological and biochemical soil properties.

Recent and past intense volcanic activity generated volcanic soils in many different regions of Italy, including: Sicily with in east the active Etna volcano and in north and south the Aeolian and Pelagie Islands; Campania with the Somma-Vesuvius, the volcanic complex of Phlegrean Fields, the Roccamonfina volcano, and the Ischia Island; Lazio with the

Ernici Mounts, the Albani Hills, the Tolfa, Sabatini, Volsini and Cimini Mountains and the Ponza Island; Tuscany with the Amiata Mount; Basilicata with the Vulture Mount; Sardinia with the Ferru Mount (Figure 1) (Pasquarè and Vezzoli 1991). A considerable number of studies were performed on soils from these areas, mostly focusing on soil genesis and classification, with special emphasis to the influence of parent material and climate on clay mineral formation (De Gennaro et al. 1973, Violante et al. 1979, 1983, Bidini et al. 1984, Quantin et al. 1985, 1988, Lulli et al. 1989, Lorenzoni et al. 1995, Vacca et al. 2003, García-Rodeja et al. 2004), on chemical properties of humic substances (Conte et al. 2003) and on soil hydraulic behaviour (Terribile et al. 2000, Basile et al. 2003). However, there is a scarcity of data on trace elements for volcanic soils and it is only recently that few papers have contributed to enlarge this field of research, providing in some cases evidence of soil contamination (Buondonno et al. 1998, Palumbo et al. 2000, Adamo et al. 2000, 2001, 2002, 2003, 2005, Tarzia et al. 2002, Martínez Cortizas et al. 2003).

Figure 1. Italian volcanic areas and location of the study sites discussed in the text.

The total contents and distribution among geochemical forms of trace elements, namely As, Cd, Co, Cr, Cu, Ni, Pb, Zn and Hg, in polluted Italian volcanic soils will be discussed in the present chapter, with reference to

environmental studies carried out on agricultural and industrial volcanic lands of southern Italy. In particular, the two case studies of the Solofrana river valley and of the dismantled ILVA industrial site will be described and discussed in detail. We shall then consider briefly some other examples of trace metal pollution with reference to urban and remote areas. The location of the main study sites discussed in the text is shown in Figure 1.

Agricultural volcanic soils: the case study of the Solofrana River Valley

The Solofrana river valley constitutes the intramountain inland portion of the Sarno plain, located in the Campania Region (southern Italy) between the volcanic complex of Somma-Vesuvius (NW), the Sarno Mountains (NE), the limestone Lattari Mountains (S) and the Tyrrhenian coast (W). It covers an area of approx. 3000 ha of cultivated soils originated by pyroclastic material from Somma-Vesuvius colluviated to the valley (Terribile and Di Gennaro 1996). Field horticulture, orchards and greenhouse horticulture and floriculture are the main productions of the very intensive Solofrana valley agriculture. Land use on the southern slope generally consists in terraces with coexisting horticulture, fruit trees and vineyards, while chestnuts are widely present on the north-facing slopes. The intensive agriculture and the numerous industrial activities occurring in this territory have produced a widespread degradation of the local natural resources. In particular, numerous tanning plants (~160) operating in the upper Solofrana valley, caused in the past a Cr-enrichment of the Solofrana river waters by their Cr-rich effluents (Basile et al. 1985). Recently, a decline of Cr content in river waters was observed (Adamo et al. 2001), while the river sediments (De Vivo et al. 2003) and the soils of the valley still contain Cr at concentrations above natural background (Adamo et al. 2003, 2005) (Table 1). The high metal retention properties of the volcanic soils of the valley might have played a key role in maintaining the element in soil for a long time. Besides the use of the polluted river waters for irrigation (prohibited since 1990), repeated flooding events, which, due to weakness of the river embankments, occur after intense rainfall events, have been playing a key role, both in the past and at present time, in the progressive Cr enrichment of the valley soils. According to a survey carried out in the valley by Local Administration, in 1998 about 400 ha were flooded (Consorzio di Bonifica Integrale dell'Agro Sarnese Nocerino 1996).

Table 1. Range or mean levels of trace elements total content of selected Italian volcanic soils.

Soil	As mg kg^{-1}	Cd mg kg^{-1}	Co mg kg^{-1}	Cr mg kg^{-1}	Cu mg kg^{-1}	Ni mg kg^{-1}	Pb mg kg^{-1}	Zn mg kg^{-1}	Hg µg kg^{-1}	References
Solofrana valley agricultural soils (Campania Region)										
Surface horizon overflowed soils	nd	nd	nd	100–378	114–151	57–65	nd	139–157	nd	Adamo et al. 2006
Surface horizon irrigated soils	nd	nd	nd	137–219	77–565	56–84	21–98	99–135	nd	Adamo et al. 2003
Subsurface horizon overflowed and/or irrigated soils	nd	nd	nd	62–335	70–239	60–80	23–58	72–109	nd	Adamo et al. 2003
Surface horizon no overflowed or irrigated soil	nd	nd	nd	21–45	110–229	41–55	63*	82–142	nd	Adamo et al. 2003, 2006
Solofrana river sediments	nd	nd	nd	12–1118	50–182	14–68	41–166	85–342	nd	Adamo et al. 2006, Albanese et al. 2006
ex-ILVA industrial soils (Campania Region)										
Surface horizon	nd	nd	11	73–368	97–377	69–125	36–366	143–679	nd	Adamo et al. 2002, Arienzo et al. 2004
Subsurface horizons	nd	nd	13–45	50–416	18–207	68–166	6–448	72–281	nd	Adamo et al. 2002
soil	8.3–117	bdl–2.7	2.1–23	0.5–18	5.8–135	1.0–26	13–775	32–2442	5–545	Tarzia et al. 2002
slags	0.1–4.5	0.1–0.4	0.7–3.7	5.1–48	4.0–26	1.4–8.4	13–260	54–786	212–2154	Tarzia et al. 2002
scums	10–57	0.1–2.9	3.2–12	2.6–105	14–207	3.2–19.5	26–442	61–1846	10–3347	Tarzia et al. 2002
landfill materials	3.3–164	0.1–5.0	2.3–33	0.8–292	7.4–346	1.5–101	20–935	45–2526	12–1375	Tarzia et al. 2002
Urban and remote areas										
Naples city urban soils	nd	nd	nd	1.7–73	6.2–286	nd	4–3420	30–2550	nd	Imperato et al. 2003
Campania Region urban sites	nd	1.11	nd	39.87	46.7	nd	188.5	nd	nd	Maisto et al. 2004
Campania Region remote sites	nd	1.54	nd	60.59	36.7	nd	100.1	nd	nd	Maisto et al. 2004
Gauro Volcano soils	19–30	nd	nd	nd	15–219	bdl–12	87–122	86–116	111–381	Martínez Cortizas et al. 2003
Vico Volcano soils	15–23	nd	nd	nd	17–39	16–33	46–104	66–109	58–198	Martínez Cortizas et al. 2003
Etna Volcano soils	nd	0.13–0.28	nd	23–28	112–130	18–35	8–9	105–123	nd	Palumbo et al. 2000

nd = Not determined.
bdl = Below detection limit.

In many cases, Solofrana valley soils were found to contain also Cu in amounts exceeding the Italian Ministry of Environment regulatory levels (Cu:120, Cr:150 mg kg^{-1}) (Adamo et al. 2003, 2005) (Table 1). However, Cu contamination never seemed to be associated with polluted sediment deposition by flooding, but appeared to depend more on past widespread agricultural practices of Cu-rich pesticides and fertilizers utilization. The Solofrana river sediments, particularly rich in Cr (542 mg kg^{-1}), had always a relatively low Cu total content (97 mg kg^{-1}) (Adamo et al. 2005) (Table 1). Copper total content was above regulatory levels also in the surface horizon of soils never irrigated with contaminated waters or affected by flooding. Copper concentration in the flooded soil surface horizons tended to decrease with the repetition of the flooding events, presumably as a consequence of the 'dilution' effect due to low Cu sediment deposition.

Results from physical fractionation procedures and selective chemical extractions revealed that concentrations of metal contaminants in silt and clay fractions were preferentially associated with short-range-order weathering materials and organo-mineral complexes (Adamo et al. 2003). Both Cr and Cu in polluted soils were mainly associated with the organic fraction, whereas other trace elements and Fe, which never exceeded the regulatory limits, were mostly found in the residual fraction (Adamo et al. 2003, 2005) (Table 2). The amounts of Cr and Cu associated with the organic fraction increased where the extent of soil contamination by these metals increased, suggesting high formation constants of organic-Cr and organic-Cu complexes (Donisa et al. 1999, McGrath 1995). However, the interpretation of speciation data should also take into account some methodological aspects, regarding the possibility of underestimation of trace elements bound to allophane and overestimation of metals associated with organic matter (Adamo et al. 2005). The amounts of metal elements extracted by ammonium oxalate followed a remarkably similar trend in the respective amounts removed by the three steps of BCR sequential extraction procedure, indicating that ammonium oxalate was able to remove most of the non-residual metal forms at the same time (Adamo et al. 2003). In volcanic soils, where the content of amorphous materials is significant, the ammonium oxalate might represent a simple effective reagent to extract heavy metals bound to these low crystalline phases, providing an indication of the actual and potential mobility of contaminants in soil.

Table 2. Range or mean levels (% of the total) of trace elements in geochemical forms determined by EU-BCR sequential extraction for selected Italian volcanic soils. HOAc= Acetic acid extractable forms (soluble, exchangeable, carbonate), RED= Reducible forms (Mn and Fe easily reducible oxides and hydroxides), OXI= Oxidizable forms (organic and sulphides), RES= Residual forms (primary and secondary silicate minerals).

		Solofrana valley agricultural soils (Campania Region)					ex-ILVA industrial soils (Campania Region)		Urban and remote areas		
										Etna Volcano soils	
	Forms	Surface horizon overflowed soils	Surface horizon irrigated soils	Subsurface horizon overflowed and/or irrigated soils	Surface horizon no overflowed or irrigated soil	Solofrana river sediments	Surface horizon	Subsurface horizons	Naples city urban soils	Surface horizon	Subsurface horizons
Cu	HOAc	3–4	2–3	2	4	3	5	0–10	1–9	6	8
	RED	23–31	2–14	1	24	12	5	8–64	1–4	3	5
	OXI	25–35	57–60	39	48	27	19	2–50	28–88	18	5
	RES	40–41	24–39	58	24	48	71	0–89	8–42	72	83
Cr	HOAc	1	2	2	1	2	0	0	1–12	0	0
	RED	6–9	1	1	4	12	0	0	1–7	0	0
	OXI	41–67	28–76	21	5	72	0	0	42–90	0	0
	RES	23–51	21–69	76	90	14	100	100	6–43	100	100
Ni	HOAc	1	0–1	0	0	1	0	0	nd	0	0
	RED	1–2	0–11	0	1	2	0	0	nd	0	5
	OXI	4–6	1–5	0	6	6	12	1–12	nd	2	2
	RES	92	84–98	100	93	91	88	88–99	nd	98	93
Pb	HOAc	nd	18–34	11	nd	nd	0	0	0–8	0	0
	RED	nd	5–12	4	nd	nd	0	0	0–7	0	0
	OXI	nd	17–34	15	nd	nd	17	5–100	14–23	nd	nd
	RES	nd	27–53	70	nd	nd	83	0–95	67–82	100	100
Zn	HOAc	6–9	2–14	1	12	6	35	4–30	6–40	5	2
	RED	23–33	6–42	8	24	34	35	4–29	8–35	4	4
	OXI	7–9	13–32	10	10	8	7	3–22	1–10	3	2
	RES	51–61	30–60	81	54	52	23	32–87	24–80	88	91

nd = Not determined.

DTPA extractable Cr and Cu amounts were always higher in polluted soils, compared with non-polluted soils (Table 3). However, the amounts of available trace elements were always very low, when compared with their respective total contents (Adamo et al. 2003, 2005). Despite this observation, an assessment of metal bioavailability in plants showed significant Cu accumulation in dwarf beans and lettuce, and evidenced high POD activity in the roots, indication of oxidative stress induced by metals. On the contrary, Cr accumulation in vegetables was very low and no negative effects were found (Adamo et al. 2003). In the soils subjected to repeated flooding events, total microbial biomass C, fungal mycelium and enzyme activity (FDA hydrolase, dehydrogenase, β-glucosidase, urease, arylsulphatase, acid phosphatase) did not appear to be significantly affected by trace metal pollution, whilst the amount of organic carbon was the most important factor influencing the growth of the microbial community and the soil enzymatic activity (D'Ascoli et al. 2006). Data from this study showed that organic matter can counterbalance the negative effects of trace metals in contaminated soils. In fact, expressing biological-biochemical parameters per unit of total organic C, soil Cu contamination appeared the most important factor affecting microbial biomass, fungal mycelium and several enzyme activities.

On the other hand, a negative effect of the high Cr content of the Solofrana valley soils was observed for bacterial diversity, with a loss of sensitive species. Nevertheless, the change in bacterial diversity did not cause visible changes in soil activity, probably because of the redundancy of functions within species of soil microbial community (D'Ascoli et al. 2006).

Plagioclases, quartz, halloysite/kaolinite, illite, vermiculite, smectite, allophane and both crystalline and amorphous Fe minerals occurred in both Solofrana valley soils and river sediments (Adamo et al. 2003, 2006). Among identified clay minerals, particular attention was paid by the Authors to the expandable layer silicates which, in contaminated sediments and soils, may act as effective sinks of Cr (Bartlett and Kimble 1976, Dubbin et al. 1994). The potential interaction between smectites and organic matter, with the formation of organo-clays, could have improved the soil adsorbing capacity for inorganic contaminants.

Application of optical microscopy (OM) on thin sections of undisturbed flooded soil samples revealed soil physical incorporation of the river sediments and alteration of the sediment aggregates to silt and clay size, as well as occurrence in the surface and subsurface horizons of coatings along elongated pores (Adamo et al. 2003, 2006). The clayey aggregates, analysed by scanning microscope equipped with electron microprobe (SEM/WDS), exhibited enrichment in Cr and Cu (Adamo et al. 2006). Therefore, although the occurrence of soluble and exchangeable metals in

the soils was extremely limited, and the relatively insoluble and less mobile Cr (III) form predominated in the more soluble and less strongly adsorbed to soil particles Cr (VI) (Adamo et al. 2003), the possibility of a risk, due to metal migration as solid suspension down the soil profile through the pore network associated with the soil water flow, was considered.

Table 3. Ranges or mean levels of trace elements available amounts (mg kg^{-1}) in selected Italian volcanic soils as determined by different methods (in parenthesis values are expressed as percent of total soil trace element content).

	Cd	Co	Cr	Cu	Ni	Pb	Zn	Extractant
Solofrana valley agricultural soils (Campania Region)								
Surface horizon overflowed soils	nd	nd	nd	19–25 (16–17)	nd	nd	nd	DTPA
Surface horizon irrigated soils	nd	nd	0.002–0.17 (0.001–0.05)	14.7–114 (15–20)	0.12–0.71 (0.19–1.3)	1.38–4.4 (0.29–8.1)	3.70–137 (3.3–13)	DTPA
Subsurface horizon overflowed and/or irrigated soils	nd	nd	0.08 (0.04)	12.7 (5.3)	0.13 (0.20)	2.2 (6.7)	7.71 (8.4)	DTPA
Surface horizon no overflowed or irrigated soil	nd	nd	bdl	22–44 (19–20)	0.08 (0.20)	6.3 (1.0)	4.9 (6.0)	DTPA
Solofrana river sediments	nd	nd	nd	14.5 (15)	nd	nd	nd	DTPA
Urban and remote areas								
Naples city urban soils	nd	nd	nd	16–88	nd	45–325	66–434	EDTA
Campania Region urban sites	0.08 (7.40)	nd	0.03 (0.07)	5.7 (12.27)	nd	16.6 (8.78)	nd	EDTA/DTPA
Campania Region remote sites	0.16 (10.48)	nd	0.02 (0.04)	2.3 (7.75)	nd	9.3 (9.26)	nd	EDTA/DTPA

nd = Not determined.
bdl = Below detection limit.

Industrial volcanic soils: the case study of the siderurgical ILVA dismantled site

The siderurgical ILVA plant, formerly the second largest integrated steelworks in Italy and actually under a government remediation project, covers an area of approx. 300 ha in the polygenic volcanic complex of Phlegrean Fields (Campania Region, southern Italy). This is a large 13 km wide caldera on the outskirts of Naples city, containing numerous phreatic tuff rings and pyroclastic cones. The steel plant operated from 1910 and, after reaching a peak of steel production of $2x10^6$ millions of tons at the end of 1960, was closed in 1991 and dismantled since 1998.

Industrial activity dramatically affected the whole surface of the ILVA plant area, including even the sites not directly affected by specific production activities (Buondonno et al. 1998, Adamo et al. 2002). Modifications resulted in the disturbance or burial of pre-existing volcanic natural soils. The dominant soil profile morphology was determined by the occurrence and arrangement of the materials used in the industrial cycle (carbonates, Fe minerals, Fe pellets, coke, slags), variously mixed with earthy materials. Soil surface horizons were characterized by notable compactness and high variability of colour and mottling, indicating heterogeneity of the sediments at varying extents. Occurrence of sedimentary environments and processes of translocation of fine sediments down the profile was suggested by observation at various depths of layers with a platy structure with fine lamination and of clay and silt coatings. The deepest volcanic horizons were generally formed of volcanic ash and pumice layers, apparently not disturbed by the presence of industrial materials (Adamo et al. 2002). The adoption of the *foundric* subgroup of the Xerorthents was proposed to overcome difficulties which emerged in soil classification with the current U.S. taxonomy requirements (Buondonno et al. 1998).

In many of the analysed soil samples taken from both surface and subsurface layers of representative profiles and at various depths from selected drill-cores, total contents of Cd, Cu, Co, Pb, Zn, Ni and As exceeded the maximum permissible concentrations (Cd:2, Cu:120, Co:20, Cr:150, Pb:100, Zn:150, Ni:120 and As:20 mg kg^{-1}) established by the Italian Ministry of Environment (1999) for soils of public, private and residential green areas. Only for some elements (Cu, Ni and Zn) total contents also exceeded regulatory levels for soils of industrial and commercial sites (Cd:15, Cu:600, Co:250, Cr:800, Pb:1000, Zn:1500, Ni:500 and As:50 mg kg^{-1}) (Adamo et al. 2002, Tarzia et al. 2002) (Table 1). In general, the data did not indicate a clear distribution of values with depths, although some trace elements were shown to be enriched in the upper cores (e.g. Pb up to

a maximum of 900 mg kg^{-1}, Zn up to 2530 mg kg^{-1}, As up to 160 mg kg^{-1}) where by-products of steel production were more widespread and abundant compared to earthy material (Tarzia et al. 2002).

Tarzia et al. (2002) distinguished sources of anthropogenic pollution owing to industrial activity from the natural (geogenic) component, connected with the Phlegrean Fields volcanic activity (i.e. epithermal fluids), by comparing trace metal concentrations and Pb isotopic composition of metallurgical slags (by-product of cast-iron production), scums (by-product of steel production), landfill materials (consisting mainly of volcanic sand, volcanic ash and industrial by-products) and soil (consisting mainly of volcanic ash, pumice and sub-aerial scoriae). Chemically, scums, slags and filling showed enrichment in some trace elements (e.g. Cr, Pb, Mn, Hg) with respect to soils (Table 1). Bivariate plots of elements, such as Cd, Cr, Cu, Mn, Ni, As, Pb and Zn, which could potentially have both a metallurgical and a natural origin, clearly showed the convergence of data towards "natural values" (values, which prevalently characterize the soils). This strongly suggested the existence of a mixing trend between a natural (related to lithology and epithermal fluid) and an anthropogenic component, connected with the local industry. Elemental concentrations and isotopic data showed both the existence of contamination from anthropogenic activity (industrial) and a strong natural metal component related to hydrothermal activity occurring in the Phlegrean Fields plain. This caused enrichment of As, Mn and other elements that are mobile under hydrothermal conditions. Furthermore, isotopic analyses suggested the mixing of potentially different sources of Pb in soils, scums, slags and filling materials.

In the horizons of a soil profile representative of the area around the steel plant where raw materials were usually stocked, Cu, Co, Cr, Pb, Zn and Ni were predominantly associated with residual mineral components, presumably of oxide and silicate species, and with poorly ordered iron and manganese oxides (Table 2). Copper, Co, Pb and Zn were also present to a moderate extent in the organic matter (Table 2). Only Zn was associated in significant amounts with soluble, exchangeable and carbonate-bound fraction, indicating this metal more bioavailable than the other examined metals (Adamo et al. 2000, 2002) (Table 2). An association of the elements with both amorphous (Cu, Co, Zn) and crystalline iron oxides (Cu, Cr, Pb, Zn, Ni), as well as with non-Fe oxides and clay minerals (Cu, Co, Cr, Pb, Zn, Ni) was shown in the soil clay-size fraction (<2μm) (Adamo et al. 2002). Magnetite, hematite and goethite, the most important iron-containing components of the ores used for the production of iron and steel (Cornell and Schwertmann 1996), were all found in the surface soil sand fraction (2–0.02 mm). Only goethite, along with kaolinite, illite and clay

minerals at 1.4 nm, was detected in the clay fraction (<2μm). Taking into account that trace metals in iron oxides commonly exhibit high chemical stability due to strong occlusion mechanisms (Schwertmann 1964), and assuming that in the EU-BCR residual and reducible fractions metals were mainly present in an iron oxide form, it was suggested that only limited metal remobilization through leaching could take place in the soil under consideration. However, similarly with what observed in the Solofrana valley overflowed soils, the occurrence in the deeper pyroclastic horizons of illuvial Fe-rich clay coatings, characterised by strong Cu, Co, Cr and Zn enrichment, suggested a risk of metal migration along the profile in association with fine particles (Adamo et al. 2002).

In the former ILVA industrial site, the natural contribution of hydrothermal fluids to soil pollution, in addition to the limited bioavailability of metal pollutants from industrial materials, indicated that the most common soil remediation approaches in this area would be of little use (Basile Gianni et al. 2001, Tarzia et al. 2002). On this basis, Arienzo et al. (2003) carried out a study in greenhouse to determine the possibility of using *Lolium perenne* L. to replant the ILVA area devoted to raw materials stocking. *L. perenne* grew, without showing any visible symptoms of metal toxicity or nutrient deficiency. In contaminated soils, the plant content of Cu (12.6–19.3 mg kg^{-1}), Pb (0.67–0.98 mg kg^{-1}) and Zn (88–99 mg kg^{-1}) was higher than that of plants grown on non-contaminated soil (Cu 10.1, Pb<0.2, Zn 79 mg kg^{-1}), but still in the range of physiologically acceptable levels. The distribution of Cu, Pb and Zn in soil was slightly affected by *L. perenne* growth with changes only regarding the organic-bound Cu and Zn pool, with reduction up to 24%. Results indicated that an acceptable healthy vegetative cover could be achieved on the contaminated soils of the former industrial ILVA site, by the replanting test proposed by the Authors, and that metals would remain stable over the study period with slight variation of the more available metal forms.

Miscellaneous studies from urban and remote volcanic areas

In the past few years, the trace element content and availability of volcanic soils from different urban and remote areas of Italy have been presented in a number of studies, considering also other types of soils. In some cases, trace elements were not the main aspect of the study and results were reported only partially in the papers.

Spatial and temporal distribution of Cu, Cr, Pb and Zn, in surface and sub-surface soils from the Naples city urban area, was investigated by Imperato et al. (2003). Naples (Campania Region, southern Italy) is a big and very densely populated city. The soils are derived from volcanic parent materials from the nearby major volcanic systems, the Phlegrean Fields and Somma-Vesuvio Mount. The study concentrated on the urban core area, including the western and eastern districts of the city, where, respectively, the motorway and the old oil refineries along with combustible deposits are located. A total of 173 surface soil samples were collected in gardens, parks, roadside fields and industrial sites. In 36 of the selected sites soil samples at 10, 20 and 30 cm of depth were also collected. At twelve sites, Cu, Pb and Zn levels in soil were compared with those from a 1974 sampling (Basile et al. 1974). Many surface soils from the urban area, as well as from the eastern industrial district, contained levels of Cu (6.2–286 mg kg^{-1}), Pb (4–3420 mg kg^{-1}) and Zn (30–2550 mg kg^{-1}) that largely exceeded the limits established by the Italian Ministry of Environment (120, 100 and 150 mg kg^{-1} for Cu, Pb and Zn, respectively) (Table 1). Chromium values (1.7–73 mg kg^{-1}) were never above regulatory limits (120 mg kg^{-1}) (Table 1). The percentages of soil samples contaminated by Cu, Pb and Zn were respectively 15%, 76% and 53%. Speciation by BCR sequential extraction showed that Cu and Cr existed in soil mainly in organic forms (68%), which can become available after organic matter mineralization, whereas Pb occurred essentially as residual mineral phases of low availability (77%) (Table 2). The considerable presence of Zn in the soluble, exchangeable and carbonate bound fraction (23%) suggested high potential bioavailability and leachability of the element through the soil (Table 2). Concentrations of Cu, Pb and Zn had greatly increased since the 1974 sampling, with higher accumulation in soils from roadside fields. The topsoil enrichment clearly revealed an anthropogenic origin of the pollution. The distribution of trace element soil content in the city of Naples indicated that the industries together with the traffic were mainly responsible for metal pollution. Automobile emissions were probably the major source of the elevated Pb content of Naples urban soils. Highest Pb concentrations were detected in soil samples collected from the border of the city motorway and from streets in areas with high traffic flows. It is probable that automobile exhausts were also a source of Zn and Cu. The industrial activity in the east area might have contributed to most Zn accumulation in soil over the past 20 years. Tyre and line abrasion processes in the rail and tram-ways might be also responsible for the soil Cu pollution (Imperato et al. 2003).

Fifteen urban and suburban as well as rural sites of the Campania Region were investigated by Maisto et al. (2004) in order to study the Cd, Cu,

Cr and Pb pattern of translocation from soil to plant. Some of the sampled soils, as those collected in the Naples urban area, originated from pyroclastic materials from Somma-Vesuvius (di Gennaro 2002). The concentration of trace elements was measured in soil and in *Quercus ilex* L. leaves, in order to evaluate the effect of translocation and/or direct air-to-leaf and to evaluate the suitability of *Q. ilex* leaves as pollution monitors. Soil trace element total and available contents (DTPA and EDTA extractable metals, expressed as percentage of the total content) were reported as means of the rural and of the urban sites (Tables 1 and 3). Soil trace element content reflected a mixture of past and recent inputs, whereas leaf contents reflected the element inputs for a known exposure time and were affected significantly by air concentration (Maisto et al. 2004).

In still active volcanic areas, high concentrations of trace elements in geothermal groundwaters contribute to continuous trace metal enrichment in soil (Tarzia et al. 2002). Lima et al. (2003) performed minor and trace element investigations on groundwater of Ischia Island (Campania Region), formed entirely of Quaternary volcanic rocks, with mainly volcanic soils, and still characterised by seismicity, widespread fumaroles and thermal springs. Concentrations of some elements, such as As, Be, Cu, Fe, Mn, Sb and Tl in Ischia groundwaters were often higher than limits fixed by Italian law for waters (Italian Ministry of Environment 1999). Therefore, in addition to anthropogenic sources, environment contribution may play an important role in determining the high concentration of trace elements in the island (Lima et al. 2003), as well as in the ex-ILVA industrial site (Tarzia et al. 2002).

Two young Andosols from a rural area near to Etna volcano (Sicily Region) were analysed, along with other various soil types from sedimentary substrates, in order to compare trace element distribution under different geological and pedological conditions (Palumbo et al. 2000). The trace element content of the parent material influenced the content of soils to a variable extent, that was maximum in the young Andisols. Modifications induced by pedogenesis (soil formation) in the Andisols was less evident than in the other soils: trace element composition strongly reflected that of interbedded pyroclastic material. Neogenic halloysite, imogolite and allophane were minor constituents, while primary mineral phases, such as plagioclases, feldspars, pyroxenes, magnetite, ferrihydrite, along with volcanic glass, predominated. Trace element total content range in Andosols was 0.09–0.28 mg kg^{-1} for Cd, 11–74 mg kg^{-1} for Cr, 75–201 mg kg^{-1} for Cu, 11–40 mg kg^{-1} for Ni, 2–11 mg kg^{-1} for Pb and 99–179 mg kg^{-1} for Zn (Table 1). All the elements were predominantly found in the mineral lattice structures by BCR sequential extractions (Table 2). A comparison of sequential extraction data in Andisols for horizons A and C showed no evi-

dence for significant differences in metal partitioning pattern. Nevertheless, a pedogenic redistribution of Cu was suggested by remarkable amounts of the element bound to organic matter in the A horizon. Although Cu was more concentrated in pyroxenes than in volcanic glass, the latter was believed to be the major source of the element, due to the high proportion and susceptibility of weathering of glass particles (Palumbo et al. 2000).

Trace element contents in soils are of great interest not only for environmental studies, but also for pedogenetic interpretation since they provide a good way to decipher the relevance of the main factors affecting soil evolution (Laruelle and Stoops 1967, Fujikawa et al. 2000, Martínez Cortizas et al. 2003). Martínez Cortizas et al. (2003) investigated the vertical distribution of 21 elements (macro, micro and trace elements) in four COST 622 reference profiles of Italian volcanic soils located near to Gauro volcano (Campania Region) and Vico volcano (Lazio Region). Little enrichment/depletion of most of the analysed elements indicated a low degree of weathering and a great similarity to parent material, showing a profound effect of the different volcanic parent materials on the resulting soils. In relative terms, the degree of soil evolution and the depletion of the more mobile elements seemed to increase with increasing rainfall and soil age. Discontinuities in the soil profile due to the accretion of new volcanic material were detectable from the geochemical composition of the horizons. Some metallic elements as Hg, Pb, Cu and Zn showed enrichment in the organic-rich horizons (O and A), with wide ranges (Hg:26.3–1.0, Pb:2.3–1.0, Cu:29.1–1.0, Zn:2.3–0.8 mg kg^{-1}) (Table 1). The consistent intensity of enrichment suggested that, besides biorecycling and weathering processes, human activity (soil management, fertilizing, and atmospheric pollution) might have been a significant source of trace elements (Martínez Cortizas et al. 2003). Chemical analyses (contents of major and trace elements) were performed on the four Italian COST 622 soil reference profiles, located near to Gauro and Vico volcanoes, also by Buurman et al. (2004). Cluster analysis of lithogenic elements ratios and grain-size analyses were found to be good indicators of sedimentary stratification as identified by field description.

Concluding remarks

Trace element contamination in the environment is of major concern because of their toxicity and threat to human life and the environment. Volcanic soils are known to be naturally enriched in trace elements. Neverthe-

less, this does not pose a hazard to the environment according with the low mobility and availability of the trace elements of geochemical origin. Studies carried out on Italian volcanic soils have highlighted several phenomena of trace element pollution from different anthropogenic sources, such as industrial activities and wastes, agricultural practices and automobile emissions. The properties of volcanic soils, according to the nature and variability in organic and inorganic soil constituents, may have had a strong influence on progressive trace elements accumulation. In the same way the strong trace element retention of these soils seems to reduce risks of mobility and transfer of elements in water and plants.

The contents of trace elements in a soil depend mainly on the nature of the rocks from which it was derived and on weathering processes to which the soil-forming materials were subjected, and they are also considerably influenced by the vegetation and anthropogenic activities. Metal toxicity depends on chemical association in soils. For this reason, determining the chemical form of a metal in soils is important to evaluate its mobility and bioavailability. Biocycling processes in the organic rich surface horizons likely results in the formation of trace elements (mainly Cu and Cr) organic complexes which are very stable and in the slow mobility of elements in the volcanic soil profile. Effective adsorption of cation trace elements on organo-clays might contribute to volcanic soil sorption capacity.

So far, there has been relatively little effort to determine the adsorptive capacity for trace element ions of variable charge to mineral surfaces and organo-mineral complexes, which are widely present in andosols. Such studies are essential since these phases certainly play an important role in metallic cation trapping, transport and circulation in soils and aquifers of volcanic areas. The combined application of direct and indirect speciation analytical techniques and the close collaboration among biologists, chemists and mineralogists are fundamental requisites for future progress on the knowledge of the behaviour and reactions of trace elements with separate soil components, on the evaluation of metal retention and bioavailability, and on the assessment of the effect of trace elements contamination on plants, on soil micro and mesofauna, on soil bacterial diversity and on biological and biochemical soil properties.

References

Adamo P, Arienzo M, Bianco MR, Terribile F, Violante P (2002). Heavy metal contamination of the soils used for stocking raw materials in the former ILVA iron-steel industrial plant of Bagnoli (southern Italy). The Science of Total Environment 295:17–34

Adamo P, Arienzo M, Bianco MR, Terribile F, Violante P (2000). Distribution and mobility of heavy metals in the soils of the dismantled urban industrial site of ILVA (Bagnoli-Napoli), Italy. In: First International Conference on Soils of Urban, Industrial, Traffic and Mining Areas. Proceedings, vol III. The Soil Quality and Problems: what shall we do? University of Essen, Germany, July 12–18, 2000, pp 849–856

Adamo P, Arienzo M, Bianco MR, Violante P (2001). Impact of land use and urban runoff on the contamination of the Sarno river basin in Southwestern Italy. Water, Air and Soil Pollution 131:36–45

Adamo P, Denaix L, Terribile F, Zampella M (2003). Characterization of heavy metals in contaminated volcanic soils of the Solofrana river valley (southern Italy). Geoderma 117:347–366

Adamo P, Zampella M, Gianfreda L, Renella G, Rutigliano FA, Terribile F (2006). Impact of river overflowing on trace element contamination of volcanic soils in south Italy: Part I. Trace element speciation in relation to soil properties. Environmental Pollution (on line - doi:10.1016/j.envpol.2005.11.017)

Albanese S, De Vivo B, Cicchella D. Lima A (2006) Background and baseline concentration values of toxic elements in stream sediments of Campania Region (Italy). Journal of Geochemical Exploration (In press)

Alloway BJ (1995). The origin of heavy metals in soils. In: Alloway BJ (ed.) Heavy metals in soils. Blackie Academic and Professional, London, UK, pp 38–57

Arienzo M, Adamo P, Cozzolino V (2003). The potential of Lolium perenne for revegetation of contaminated soil from a metallurgical site. The Science of Total Environment 319:13–25

Bartlett RJ, Kimble JM (1976). Behaviour of chromium in soils: I. Trivalent forms. J Envir Qual 5:379–383

Basile Gianni P, D'Ambrosio A, De Vivo B, Kipar A, Musumeci L, Milano V, Rolle E (2001). Risultati delle attività di monitoraggio per il risanamento dei siti ex industriali dell'area di Bagnoli. Siti Contaminati 1:14–22

Basile A, Mele G, Terribile F (2003). Soil hydraulic behaviour of a selected benchmark soil involved in the landslide of Sarno 1998. Geoderma 117:331–346

Basile G, Palmieri F, Violante P (1974). Inquinamento da zinco, rame e piombo nel suolo dell'area urbana ed industriale di Napoli. Annali della Facoltà di Scienze Agrarie dell'Università di Napoli, Vol VIII, 3–12. A.G. Della Torre, Portici

Basile G, Palmieri F, Violante P (1985). Il fiume Sarno: valutazione delle variazioni dell'inquinamento. Università degli studi di Napoli Federico II. Istituto di Chimica Agraria. Convegno Nazionale. Inquinamento idrico e conservazione dell'Ecosistema. Vico Equense 22–23 February, pp 258–293

Bidini D, Dabin B, Lorenzoni P, Lulli L, Quantin P, Raglione M (1984). The soils of Vico, an extinct volcano to the north of Rome, an example of the most typical Italian pedogenesis on volcanic materials. Comun Congr Int Suelos

Volcanicos, Dep Edaf, Univ La Laguna, Tenerife (Islas Canarias). Ser Inf 13:334–340

Buondonno C, Ermice A, Buondonno A, Murolo M, Pugliano ML (1998). Human-influenced soils from an iron steel works in Naples, Italy. Soil Sci Soc Am J 62:694–700

Buurman P, García Rodeja E, Martínez Cortiza A, van Doesburg JDJ (2004). Stratification of parent material in European volcanic and related soils studied by laser-diffraction grain-sizing and chemical analysis. Catena 56:127–144

Consorzio di Bonifica Integrale dell'Agro Sarnese Nocerino (1996). Carta delle aree esondate dell'Agro Sarnese Nocerino. Conference on "Situazioni e prospettive del Consorzio di Bonifica Integrale e ruoli di contribuenza extragricola". Nocera Inferiore, 15 luglio 1996

Conte P, Spaccini R, Chiarella M, Piccolo A (2003). Chemical properties of humic substances in soils of an Italian volcanic system. Geoderma 117:243–250

Cornell RM, Schwertmann U (1996). The iron oxides. Structure, properties, reactions, occurrence and uses. Federal Republic of Germany. VCH, Weinheim, pp 463–482

D'Ascoli R, Rao MA, Adamo P, Renella G, Landi L, Rutigliano FA, Terribile F, Gianfreda L (2006). Impact of river overflowing on trace element contamination of volcanic soils in south Italy: Part II. Soil biological and biochemical properties in relation to trace element speciation. Environmental Pollution (on line - doi:10.1016/j.envpol.2005.11.017)

De Gennaro M, Franco E, Stanzione D (1973). L'halloysite come prodotto di alterazione nelle vulcaniti campane e laziali. Memorie Geomineralogiche sull'Italia centro-meridionale n. 9, Atti della Accademia di Scienze Fisiche e Matematiche della Società Nazionale di Scienze, Lettere ed Arti in Napoli, serie 3[a], vol VIII, n 2:13–35

De Vivo B, Lima A, Albanese S, Cicchella D (2003). Atlante di geochimica ambientale della Regione Campania. Dipartimento di Geofisica e Vulcanologia, Università di Napoli Federico II

Denaix L, Lamy I, Bottero JY (1999), Structure and affinity towards Cd2+, Cu2+, Pb2+ of synthetic colloidal amorphous aluminosilicates and their precursors. Colloids and Surfaces, A: Physicochemical and Engineering Aspects 158: 315–325

di Gennaro A (2002). I sistemi di terre della Campania. Risorsa e Regione Campania, Naples, Italy

Donisa C, Steinnes E, Mocanu R, Rusu C (1999). Organo-metallic complexes with major and minor elements in some andic soils from the North-Western Carpathians (Romania). In: Wenzel WW, Adriano DC, Alloway B, Doner HE, Keller C, Lepp NW, Mench M, Naidu R, Pierzynski GM (eds) Proceeding of extended abstracts. 5th International Conference on the biogeochemistry of trace elements. July 11–15, 1999, Vienna, Austria. Vol I, pp 386–387

Dubbin WE, Goh TB (1994). Sorptive capacity of montmorillonite for hydroxy-Cr polymers and the mode of Cr complexation. Clay Minerals 30:175–185

Fujikawa Y, Fuki M, Kudo A (2000). Vertical distribution of trace elements in natural soil horizons from Japan: Part I. Effect of soil types. Water, Air and Soil Pollution 124:1–21

García-Rodeja E, Nóova JC, Pontevedra X, Martínez Cortizas A, Buurman P (2004). Aluminium fractionation of European volcanic soils by selective dissolution techniques. Catena 56:155–183

Imperato M, Adamo P, Naimo D, Arienzo M, Stanzione D, Violante P (2003). Spatial distribution of heavy metals in urban soils of Naples city (Italy). Environmental Pollution 124:247–256

Italian Ministry of Environment (1999). Regolamento recante criteri, procedure e modalità per la messa in sicurezza, la bonifica e il ripristino ambientale dei siti inquinati, ai sensi dell'articolo 17 del decreto legislativo 5/2/1997, n. 22, e successive modificazioni e integrazioni. Gazzetta Ufficiale della Repubblica Italiana 471, pp 67

Kabata-Pendias A (2001). Trace elements in soils and plants. CRC Press, Boca Raton, FL

Laruelle J, Stoops G (1967). Minor elements in Galapagos soils. Pedologie 17:232–258

Lima A, Cicchella D, Di Francia S (2003). Natural contribution of harmful elements in thermal groundwaters of Ischia Island (southern Italy). Environmental Geology 43:930–940

Lorenzoni P, Mirabella A, Bidini D, Lulli L (1995). Soil genesis on trachytic and leucitic lavas of Cimini volcanic complex (Latium, Italy). Geoderma 68:79–99

Lulli L, Bidini D, Quantin P (1989). A climo and litho soil-sequence on the vico volcano (Italy). Cat ORSTOM Ser Pédol 24:49–60

Maisto G, Alfani A, Baldantoni D, De Marco A, Virzo De Santo A (2004). Trace metals in soil and *Quercus ilex* L. leaves at anthropic and remote sites of the Campania Region of Italy. Geoderma 122:269–279

Martínez Cortizas A, García-Rodeja Gayoso E, Nóova Muñoz JC, Pontevedra Pombal X, Buurman P, Terribile F (2003). Distribution of some selected major and trace elements in four Italian soils developed from the deposits of the Gauro and Vico volcanoes. Geoderma 117:215–224

McGrath SP (1995). Chromium and nickel. In: Alloway BJ (ed.) Heavy metals in soils. Blackie Academic and Professional, London, UK, pp 152–178

Palumbo B, Angelone M, Bellanca A, Dazzi C, Hauser S, Neri R, Wilson J (2000). Influence of inheritance and pedogenesis on heavy metal distribution in soils of Sicily, Italy. Geoderma 95:247–266

Pasquaré G, Vezzoli L (1991). Atlante Tematico d'Italia – l'Ambiente e l'Uomo. Tavola 8: Dinamica endogena I. Touring Club Italiano – Consiglio Nazionale delle Ricerche

Quantin P, Dabin B, Bouleau A, Lulli L, Bidini D (1985). Characteristics and genesis of two Andosols in central Italy. In: Fernandez Caldas E, Yaalon DH, (ed.) Volcanic soils. CATENA Suppl 7. Braunschweig. Catena Verlag, Desdedt, Germany, pp 107–117

Quantin P, Gautheyoru J, Lorenzoni P (1988). Halloysite formation through in situ weathering of volcanic glass from trachytic pumices,Vico's volcano, Italy. Clay Minerals 23:423–437

Schwertmann S (1964). The differentiation of iron oxide in soils by a photochemical extraction with acid ammonium oxalate. Z. Pflanzenernächr. Dueng. Bodenkund 105:194–201

Soil Survey Staff (1998). Keys to soil Taxonomy. United States Department of Agriculture Natural Resources Conservation Service (USDA), Washington, pp 22–23

Tanneberg H, Jahn R, Meijer EL, Kleber M (2001). Sorption (kinetic and capacity) and desorption of trace elements in volcanic soils of Italy and the Azores. In: COST Action 622, Soil Resources of European Volcanic Systems. Volcanic Soils: Properties, Processes and Land Use. International Workshop, Abstracts. 3–7, October 2001. Ponta Delgada (S. Miguel), Azores, Portugal, pp 58–59

Tarzia M, Be Vivo B, Somma R, Ayuso RA, McGill RAR, Parrish RR (2002). Anthropogenic vs. natural pollution: an environmental study of an industrial site under remediation (Naples, Italy). Geochemistry: Exploration, Environment, Analysis 2:45–56

Terribile F, Basile A, de Mascellis R, di Gennaro A, Mele G, Vingiani S (2000). I suoli delle aree crisi di Quindici e Sarno: proprietà comportamanti in relazione ai fenomeni franosi del 1998. Quaderni di Geologia Applicata 7(1):59–77

Terribile F, Di Gennaro A (1996). Rapporto conclusivo U.O.T. Convenzione Regione Campania. Carta dei suoli (1:50,000) dell'Agro Nocerino Sarnese

Ure A, Davidson CM (2002). Chemical Speciation in the Environment. Blackwell, Oxford

Vacca A, Adamo P, Pigna M, Violante P (2003). Genesis of Tephra-derived soils from the Roccamonfina volcano, south central Italy. Soil Sci Soc Am J 67:198–207

Violante P, Tait JM (1979). Identification of imogolite in some volcanic soils from Italy. Clay Minerals 14:155–158

Violante P, Wilson MJ (1983). Mineralogy of some Italian Andosols with special reference to the origin of the clay fraction. Geoderma 29:157–174

Pesticide sorption of European volcanic soils

Gy. Füleky and L.N. Konda

Introduction

Dissolved pesticides, or those adsorbed to eroding soil particles, can result in contamination of surface water resources. This is of particular concern in relation to persistent pesticides on highly erodible soils. Pesticides, which are strongly adsorbed to soil, are not carried downward through the soil profile with percolating water. However, strongly adsorbed pesticides can be carried with eroded soil particles by surface runoff (Konda 2002). The pesticides may subsequently desorb from soil particles and become surface water contaminants as well (Celis and Koskinen 1999, Konda and Pásztor 2001, Piccolo 1994). The adsorption rate is affected by the properties of the pesticide and the soil characteristics as well. With respect to mineral components, the content and nature of organic matter in soil plays a key role in the performance of applied pesticides (Dawis 1993, Kozak et al. 1994, Ramos et al. 2000). Soil organic matter has a polydisperse nature with polyelectrolytic character, surface activity properties and various chemically-reactive functional groups, hydrophilic and hydrophobic sites, which qualify these substances as privileged in the interaction with organic pesticides (Maqueda et al. 1993, Piccolo 1994, Sanchez-Camazano et al. 2000, Torrents et al. 1997). Nevertheless, in arid zones and regions with low soil organic matter content and long period of dryness, the mineral surface is the main active sites in adsorbing pesticides (Hermosin and Cornejo 1994, Pusino et al. 1992). The pH is another factor, which has significant influence on adsorption-desorption processes of pesticides in soils, in particular for polar substances. During the process of protonation-deprotonation, chemicals become either uncharged or negatively/positively charged. Pesticides containing carboxylic acid (COOH) groups or hydroxyl groups (OH) exhibit certain dissociation constants (pK_a). The pK_a associated with the carboxylic acid is commonly less than 5 (e.g. phenoxyacetic acid), whereas the OH group, if present, most likely exhibits a pK_a of 9 or higher (Evangelou 1998). Basic pesticides such as s-triazines may become cationic through protonation depending on their basicity and the pH of the system that also governs the degree of ionization of acidic groups of the humic substances. Maximum adsorption of s-

triazines in organic soils occurs at pH levels close to the dissociation constant of the herbicide as an indication of ion exchange (Senesi 1992, Senesi and Testini 1983).

The four parameters that have been used most frequently for prediction of the mobility of chemicals in soil environment are the octanol/water partition coefficient (P_{ow}), the water solubility of the compound, the adsorption coefficient normalized by organic carbon content of soil (K_{oc}) and the soil dissipation half-life (Brouwer et al. 1994, Konda 2002). The equilibrium sorption of chemicals is commonly described by adsorption isotherms. The most frequently suggested type is the Freundlich equation; however, even the Langmuir and the multisite Langmuir isotherm can sometimes be applied (Ho and Mckay 1999, Willis et al. 1970). These commonly used equations have the advantage of linearization giving the adsorption parameters by the plot.

Triazine herbicides have been widely applied for crop protection during the past four decades. Among them, atrazine (2-chloro-4-ethylamino-6-isopropilamino-s-triazine) is one of the most effective and inexpensive herbicides in the world and is the most commonly used in USA and probably also in the other part of the world. Nevertheless its application has been banned in some countries, e.g., Germany and Italy. Atrazine represents a moderately persistent compound with relatively low water solubility and soil adsorption character. The water solubility, dissociation coefficient and logarithm of the octanol/water partition coefficient for atrazine are 33 mg dm^{-3}, 2.75 and 2.88 respectively (Konda et al. 2002a).

Based on our previous experiments, and data available in the international scientific literature, it is assumed that atrazine represents a good test compound for investigating soil-pesticide interactions in andic type soils with high organic matter content (Konda et al. 2002abc). To achieve the scientific objectives of this study selected COST-622 volcanic soils along with some German and Romanian volcanic soil types, all together 48 samples, were investigated.

The properties of the soils used are described elsewhere in this book.

Sorption experiments

Adsorption was studied experimentally in soils by means of laboratory experiments: reactions of the soil with a solution of known composition at fixed temperature for a prescribed period of time and chemical analysis of the soil solution to determine its composition.

To estimate the sorption capacity of 48 different soil samples, adsorption experiments were carried out at single concentration level (15 mg dm^{-3} atrazine) using the batch equilibrium technique. To establish the sorption isotherms, equilibrium studies were repeated at predetermined concentration ranges (0.5–15.0 mg dm^{-3}) using four selected representative soil samples. The soil samples were air-dried, homogenised and passed through a 2.0 mm sieve. Stock standard solution of atrazine was prepared by dissolving the required amount in acetonitrile and then stored under refrigeration. Pesticide dilutions were prepared in 0.01 M calcium chloride to maintain constant ionic strength. Each sample consisted of 2 g of soil mixed with 20 cm^3 of the pesticide solution in 50 cm^3 polypropylene centrifuge tube sealed with screw caps. The tubes were agitated on a rotary shaker for 16 hours at 20°C to achieve equilibrium. Blank sample was prepared without soil in the same way to confirm that no significant degradation of the atrazine or sorption on the tube wall occurred during equilibration time. Supernatant was separated from soil by sedimentation. Ten cm^3 aliquots of liquid phase were centrifuged at 8000 rpm for 20 min. Samples were passed through disposable membrane filters and equilibrium concentrations were determined in supernatants. The amount of pesticide adsorbed by the soil was calculated from the difference between the initial and equilibrium pesticide concentrations in the liquid phase. The adsorption equilibration process was made in duplicate.

Pesticide analysis

The atrazin concentration in the equilibrated liquid phase was quantified using High Performance Liquid Chromatograph (Waters, Milford, MA, USA) equipped with Photo Diode Array (PDA) detector. Symmetry C_{18} column (150×2.1 mm i.d., 5 µm particle size, Waters, Milford, MA, USA) preceded by a guard column (BST C18, 20x4 mm, Budapest, Hungary) was used as stationary phase. Samples were eluted and analyzed using 10:20:70 (v/v/v) tetrahydrofurane-methanol – 0.1% (m/v) citrate buffer (pH 5.8) mobile phase. The analyte was quantitatively determined at 220 nm wavelength. Calibration curve for atrazine was linear up to 10 mg dm^{-3} with regression coefficients of 0.999. Detection limit was 0.2 µg dm^{-3} as determined according to the American Society of Testing and Materials ASTM D4210 standard. Reproducibility was lower than 2.5% (RSD).

Result and discussion

The result of the preliminary sorption experiment for all soil samples at 15 mg dm^{-3} initial pesticide concentration are presented in Table 1.

Table 1. Adsorbed amount of atrazine from the 15 mg dm^{-3} solution on 48 volcanic soil samples.

Soil no.	A_{Ads} mg kg^{-1}	Soil no.	A_{Ads} mg kg^{-1}
15 Ah2	3.84	13 Ah	33.67
2 C1	7.21	9 BC	36.70
3 2Bw2	8.38	Ro 8Bs	37.00
5 2Bw/2C1	9.45	5 Ah	44.96
12 2Ahb	10.68	18 Ah1	45.54
13 AC	10.77	16 A/B	45.79
4 Bw2	10.95	8 Ah2	48.27
14 A	12.06	Ro 7Ao	50.77
1 BC	13.25	17 Ah2	51.27
8 2Bw	14.32	Windsborn A/Bu	55.98
12 Bw	15.00	20 Ah1	61.66
11 2Bw6	16.58	19 Ah2	63.62
Ro 7ABw	17.05	4 Ah1	63.65
6 2Bw2	17.06	20 Ah2	64.30
15 Ah1	17.67	6 Ah	70.60
3 AB	18.39	9 Ah	71.79
10 Bw	18.66	Windsborn Ah1	77.51
18 Ah2	22.90	Ro 1AB	84.13
Ro 8Bw2	23.88	2 Oi	88.30
17 2Bw	24.22	19 Ah1	88.55
16 Bw	25.81	7 2Ah2	88.58
Ro 8Bw1	26.75	7 3Bw2	92.07
10 Ah	29.03	Ro 1Au	104.61
Windsborn Ah2	31.82	Ro 8Au	117.69

Ro= Romanian soil.

The soil samples adsorbed 3.8–118 mg kg^{-1} atrazine, which corresponds to 2.5%–78% of the added pesticide quantity. These data show a wide range of sorption ability, and hence it was assumed that this wide range could be used to find the soil properties which determine the different sorption capacity of the tested volcanic soils. For this reason a special sorption experiment was carried out on the following four soil samples 6Ah, 6 2Bw2, 7Ah1, 7 3Bw2 at 10 increasing atrazine concentration level.

The highest atrazine dose was the same as in the previous one-concentration experiment. Fitting the one term Langmuir isotherm

$$A_{ads} = \frac{A_{\max} kc}{1 + kc}$$

to the measured data (c represents the equilibrium concentration in the liquid phase) the sorption maximum (A_{max}) and the equilibrium constant (k) were calculated. The calculated A_{max} values were 398, 234, 488 and 333 mg kg^{-1} atrazine and the equilibrium constant values were 0.027597, 0.006552, 0.03153 and 0.05606, respectively. Illustrating the Langmuir adsorption isotherms, 4 linear-like curves with different slopes are shown in Figure 1. Shape of isotherms represents a quasi-constant distribution of atrazine between the solid and liquid phase of the system, and it is concluded that the adsorption maximum (A_{max}) is far from the upper limit of the used concentration interval.

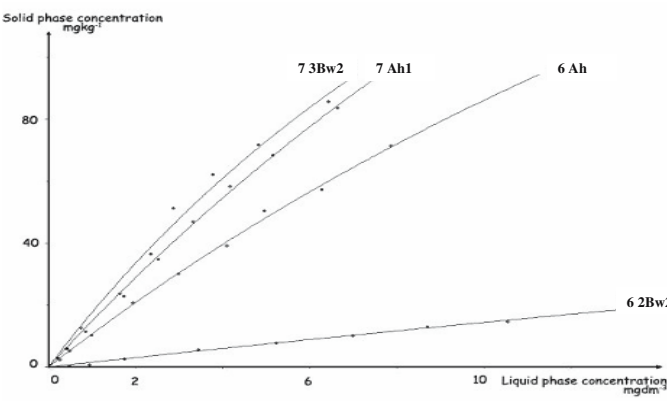

Figure 1. Langmuir adsorption isotherms of atrazine for the selected representative EUR volcanic soils.

The saturation part of the isotherm is difficult to produce under laboratory condition, since the preparation of more concentrated atrazine solutions is impossible because of the limited water solubility of the compound. The adsorbed amount of atrazine at the highest initial solution concentration is about 80 mg kg^{-1} for 6Ah, 7Ah1 and 7 3Bw2 soil samples and 19 mg kg^{-1} in case of 6 2Bw2 horizon. These data are considerably lower than the calculated A_{max} values.

Which soil properties are responsible for the differences in atrazine sorption among the different soils? For answering this question the amount of atrazine adsorbed from the 15 mg dm^{-3} solution was correlated with 16 characteristic soil properties, which can be found in other chapter of the book. The linear correlation coefficient values are in Table 2.

The pH of the volcanic soils used in this experiment varied between pH 3.8 and 9.0. Statistical analysis of the data acknowledged weak negative correlation between atrazine sorption and pH (R^2=0.3320). Nevertheless it represents a very determined effect of pH at low (pH 4) and high values (pH 8.5–9.0) as well. At low pH the adsorbed atrazine amount exceeded 100 mg kg^{-1}, but it was below the 10 mg kg^{-1} in case of high pH value (Figure 2). Positive correlation was found (R^2=0.3847) between CEC and the atrazine amount adsorbed. The most significant correlation (R^2=0.7682) exists between the organic matter content of the soil samples and adsorbed amount of atrazine, indicating that higher humus content of the soil leads to more pronounced adsorption. Significant correlation could be established between the total N content of soil and adsorbed atrazine (R^2=0.6314) as a consequence of inner correlation of humus content and N content originated from humus (Figure 3–4).

Table 2. Linear correlation between adsorbed atrazine and some characteristic properties of volcanic soil (n=48).

Soil properties	R^2
Al_o, %	0.0044
Al_d, %	0.0074
Fe_d, %	0.0112
Mg_{exch}, cmol kg^{-1}	0.0181
Base saturation, %	0.0262
Allophane, %	0.0279
Summa bases, cmol kg^{-1}	0.0297
Ca_{exch}, cmol kg^{-1}	0.0534
Clay, %	0.0567
Al_p, %	0.1234
Fe_o, %	0.1292
Fe_p, %	0.1846
pH_{H2O}	0.3320
CEC_{NH4OAc}, cmol kg^{-1}	0.3847
N_{tot}, %	0.6314
Organic matter, %	0.7682

The negative and positive correlations of atrazine sorption with pH and CEC show that the atrazine molecule is able to adsorb both onto positively and negatively charged soil surfaces. The atrazine molecule is able to change its binding ability to the negative and positive charges on the solid surface depending on the pH. The significant positive correlation with the humus content of soil demonstrates the role of humus matter in binding the organic molecules with different bonding forms. The adsorption processes and the nature of the binding forces and the type of mechanisms existing in atrazine-soil interaction have been presented in several studies (Senesi and Chen 1989, Senesi and Testini 1983, Senesi et al. 1987). Occurrence of ionic bonds between protonated secondary amino-group of s-triazine and carboxylate anion, and possibly phenolate group of the humic acid, as well as H-bonds between C=O groups of humic substance and secondary amino-group of s-triazine, are acknowledged. Formation of covalent binding of amino groups of the s-triazines to carbonyl and quinone groups of

the humic acids and ligand exchange mechanism in the humic substance-cation-water bridge enrichment are confirmed as well (Senesi 1992).

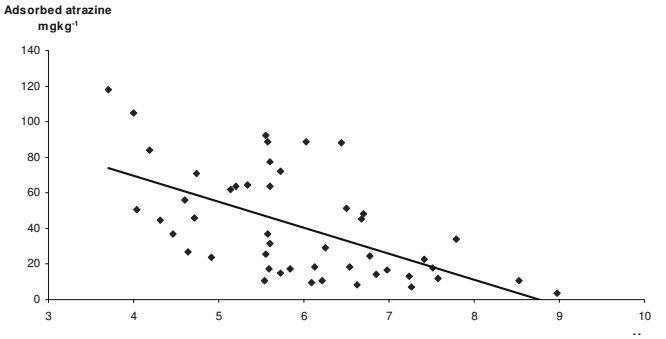

Figure 2. Relationship between soil pH and adsorbed amount of atrazine.

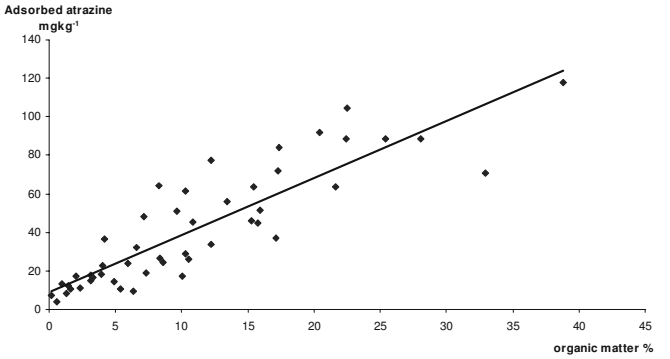

Figure 3. Relationship between soil organic matter content and adsorbed amount of atrazine.

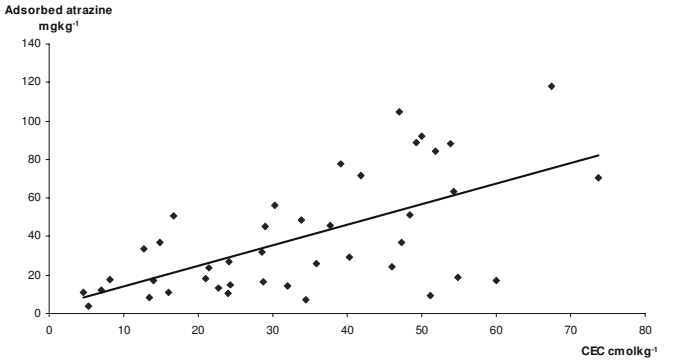

Figure 4. Relationship between cation exchange capacity (CEC) of soil and adsorbed amount of atrazine.

Based on the results obtained, the adsorption capacities of volcanic soils investigated are considered much higher than those of an average European agricultural soil; e.g., 17 mg kg^{-1} adsorbed amount of atrazine was measured on Hungarian Luvisol using the same experimental arrangement and analytical technique (Konda et al. 2002c). It can be concluded that the high extent of atrazine adsorption of volcanic soils could be explained by such characteristic andic property as the high soil humus content. However, the soil pH and CEC likewise have notably importance in this regard. The shape of the sorption isotherms and the calculated adsorption parameters (A_{max}) allow for the prediction of enhanced accumulation of atrazine onto soil particles in the volcanic soil-pesticide system.

Acknowledgement

The technical support of the Department for Soil Science and Agricultural Chemistry of Szent Istvan University and the Institute for Veterinary Medicinal Products is gratefully acknowledged.

References

Brouwer WWM, Boesten JJTI, Linders JBHJ, Van Der Linden AMA (1994). The behaviour of pesticides in soil: Dutch guidelines for laboratory studies and their evaluation. Pesticide-Outlook 5(5):23–28

Celis R, Koskinen WC (1999). An isotopic exchange method for the characterization of the irreversible pesticide sorption-desorption in soil. J Agric Food Chem 47(2):782–790

Dawis JW (1993). Physico-chemical factors influencing ethylenamine sorption to soil. Environ Toxicol Chem 12:27–32

Evangelou VP (1998). Environmental Soil and Water Chemistry: Principles and Applications. Chapter 4. Wiley

Hermosin MC, Cornejo J (1994). It is possible to use in some cases a K_{clay} coefficient to define soil adsorption capacity? In: Copin A et al. (eds) Proc 5th Int. Workshop Environ. Behavior Pest. Regulatory Aspects. Brussels, pp 206–207

Ho YS, Mckay G (1999). Pseudo-second model for sorption processes. Process Biochemistry 34:451–465

Konda LN (2002). Runoff. In: David Pimentel (ed) Encyclopedia of Pest Management. Cornell University, Marcel Dekker Inc, New York

Konda LN, Czinkota I, Füleky Gy, Morovjan Gy (2002a). Modelling of Single- and Multi-Step Adsorption Isotherms of Organic Pesticides on Soil. J Agric Food Chem 50:7326–7331

Konda LN, Füleky Gy, Morovjan Gy (2002b). Sorption Behaviour of Acetochlor, Atrazine, Carbendazim, Imidacloprid and Isoproturon on Hungarian Agricultural Soil. Chemosphere 48(5):545–552

Konda LN, Füleky Gy, Morovjan Gy (2002c). Subcritical Water Extraction to Evaluate Desorption Behavior of Organic Pesticides on Soil. J Agric Food Chem 50:2338–2343

Konda LN, Pásztor Zs (2001). Environmental Distribution of Acetochlor, Atrazine, Chlorpyrifos and Propisochlor under Field Conditions. J Agric Food Chem 49:3859–3863

Kozak J, Valla M, Vacek O (1994). Evaluation of the influence of soil characteristics on the herbicide sorption by means of the correspondence analysis. In: Senesi N, Miano TH (eds) Humic Substances in the Global Environment and Implications on Human Health. Elsevier, Amsterdam, pp 1141–1148

Maqueda C, Morillo E, Martin F, Undabeytia T (1993). Interaction of pesticides with the soluble fraction of natural and artificial humic substances. J Environ Sci Health B28:655–670

Piccolo A (1994). Interaction between organic pollutants and humic substances in the environment. In: Senesi N, Miano TH (eds) Humic Substances in the Global Environment and Implications on Human Health. Elsevier, Amsterdam, pp 961–980

Pusino A, Liu W, Gessa C (1992). Influence of organic matter and its clay complexes on metolachlor adsorption on soil. Pest Sci 36:283–286

Ramos L, Sojo LE, Brinkman UATh (2000). Study of the fast competitive adsorption of pesticides in soils by simultaneous filtration and solid-phase extraction with subsequent GC-MS. Environ Sci Technol 34(6):1049–1055

Sanchez-Camazano M, Sanchez-Martin MJ, Delgado-Pascal (2000). Adsorption and mobility of linuron in soils as influenced by soil properties, organic amendments, and surfactants. J Agric Food Chem 48(7):3018–3026

Senesi N (1992). Binding mechanisms of pesticides to soil humic substances. The Science of the total Environment 123/124:63–76

Senesi N, Chen Y (1989). Interactions of Toxic Organic Chemicals with Humic Substances. In: Gestl Z, Chen U, Mingelgrin, Yaron B (eds) Toxic Organic Chemicals in Porous Media. Springel-Verlag, Berlin, pp 37–90

Senesi N, Testini C (1983). Physico-chemical investigations of interaction mechanisms between s-triazine herbicides and soil humic acids. Geoderma 28:129–146

Senesi N, Testini C, Miano TM (1987). Interaction mechanisms between humic acids of different origin and nature and electron donor herbicides: a comparative IR and ESR study. Org Geochem 11:25–30

Torrents A, Jayasundera S, Schmidt WJ (1997). Influence of the Polarity of Organic Matter on the Sorption of Acetamide Pesticides. J Agric Food Chem 45:3320–3325

Willis BG, Woodruff WH, Frysinger JR, Margerum DW, Pardue HL (1970). Simultaneous kinetic determination of mixtures by on-line regression analysis. Anal Chem 42:1350–1355

Eutrophication in the Azores Islands

J. Pinheiro, L. Matos, V. Simões and J. Madruga

Introduction

Phosphorus, well known as an essential nutrient for plant and animal growth, has been recognized as one of the major elements affecting surface waters by leading to eutrophication.

The eutrophication of fresh waters affects its quality for most of human uses (drinking, fisheries or recreation), because of the excessive growth of algae and aquatic weeds and the subsequent anoxia phenomena caused by their decomposition. Also, periodic blooms of cyanobacteria in drinking waters may pose serious health hazard to livestock and humans.

Nonpoint source pollution, especially from fertilizer and manure applications in agricultural lands, has in many parts of the world been identified as the major source of nutrients responsible for accelerating the rate of eutrophication.

Over the last two decades the intensification of pasture production and cattle grazing in the Azores archipelago have brought excess nutrient loads to the soils and as a consequence several lakes are currently under eutrophic conditions. The lake has been reported as being under a meso-eutrophic condition (22–29 mg P L^{-1}) (INOVA 1999).

The Lagoa das Sete Cidades – a typical picture postcard of the S. Miguel Island – is a volcanic caldera which forms a large watershed approximately circular in shape, with an average diameter of 5 km and delimited by a ridge of almost vertical slopes, with a maximum height of 500 m. Two interconnecting lakes occupy a central position in the watershed. In this chapter, we take Sete Cidades as a case example for the Azores, presenting some results discussed in the context of the global issue of eutrophication.

General characteristics of the Sete Cidades watershed

Climate and Hydrology

The Azorean climate, strongly influenced by the surrounding ocean mass and by physiographic factors can be generally characterized by its amenity

and low thermal amplitude, high air humidity, persistent wind regime and regular and abundant rainfall distribution.

Within the general characteristics of S. Miguel Island, the local climatic conditions of the Sete Cidades watershed are furthermore determined both by the geomorphology of the caldera, which has the form of a bowl, deeply depressed in its central part with steep walls, and by the thermal regulation effect of the hydric mass of the lakes.

The average annual precipitation is above 2000 mm. The average monthly rain distribution for Sete Cidades is shown in Figure 1. The average annual temperature is 15°C and the thermal amplitude is of 5°C (Bettencourt 1977, Azevedo 1996).

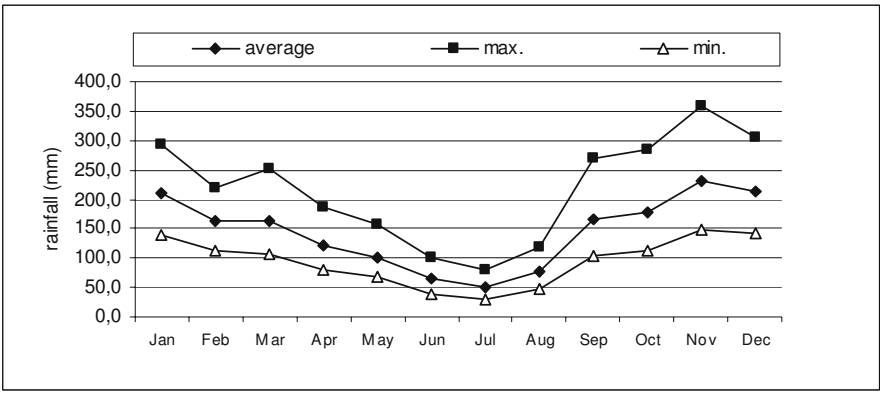

Figure 1. Average monthly precipitation of the Sete Cidades watershed. (Adapted from Universidade dos Açores 1998).

The Sete Cidades watershed has an overall area of 1908 ha and of that the lakes constitute 25%.

There are no permanent streams in this watershed and the general hydrographical network is poorly defined, but the eastern sector has a higher drainage density associated with steeper slopes. The main hydrological features are shown in Figure 2. Runoff is either of a diffusing pattern or converging to generally shallow torrential streams. Two of these streams – Grota do Inferno and Vala das Sete Cidades – are of particular importance and length as they transport and discharge the runoff from two main pasture areas, which, when combined, account for 72% of the total watershed grazing land.

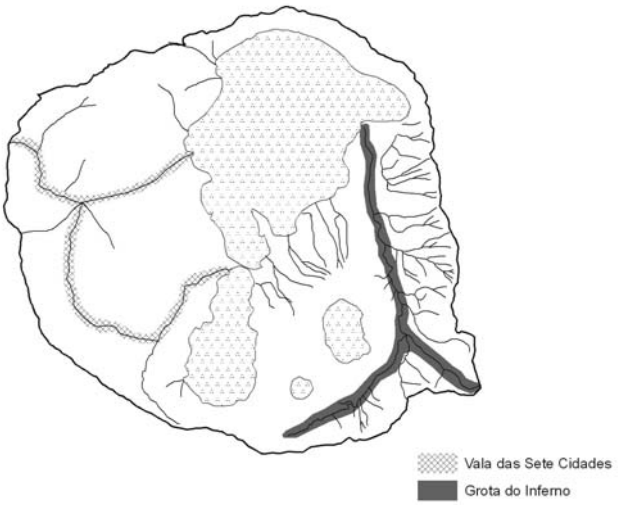

Figure 2. Main hydrological features of the Sete Cidades watershed.

Soils and Land Use

Soils of the Sete Cidades watershed originate from young ryolitic pyroclastic materials (pumice ash and cinders). These materials form deposits several meters deep comprised of layers of different textures, in incipient to weak weathering stages. Having poorly expressed andic properties these soils are classified as Vitrandic Udipsamments and Typic Udivitrands (Soil Survey Staff 1999). The organic matter content of the top horizons varies between 6.7 and 14.9% and decreases drastically in the underlying horizons to values not higher then 2.9%. Soil pH varies at the surface between 4.6 and 5.9 and increases up to 6.8 in the underlying horizons (Universidade dos Açores 1998).

The deep deposits of unconsolidated fragmentary materials that form most of the watershed substrate, bring a significant instability condition to the soils, especially on the steep slopes of the caldera as well as in its eastern internal sector. Under these conditions, agricultural mechanical interventions (ploughing, cultivation, etc.) tend to induce a high risk of severe erosion loss, especially when the vegetative cover of the soil is suppressed for pasture renovation. Sediments that have accumulated over the years at the discharge areas of the major torrential streams are evidence of past erosion losses.

The general land use of the Sete Cidades watershed is depicted in Figure 3. In general the land use is well adjusted to the physiographic characteristics of the terrain. Forest is the main land use type (46% of the total watershed area) covering the steeper slopes of the caldera, *Criptomeria japonica*

being the dominant species. Pastures occupy about 26% of the total area, in gentle to moderate slopes. The urban structure of the existing village is modest in its size (1.3% of the area – 880 resident inhabitants) and the infrastructures are adequately adjusted to the environmental susceptibility of the watershed (Universidade dos Açores 1998).

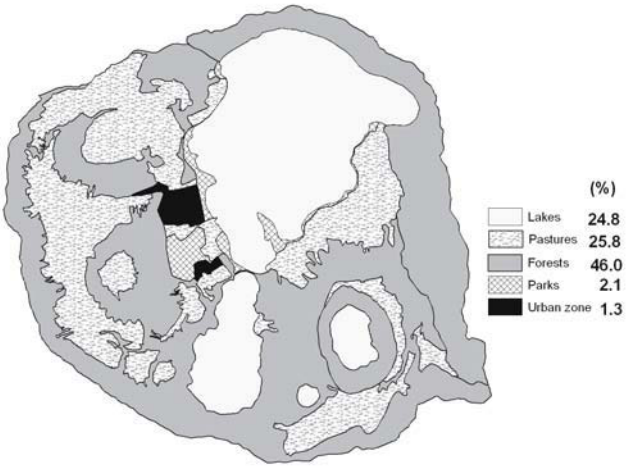

Figure 3. Land use map of the Sete Cidades watershed.

Estimation of phosphorus in soils and risk of losses

Soil testing

Pasture-based grazing of dairy cattle is the dominant agricultural system within the Sete Cidades watershed. Rotational grazing takes place all year around in the lower lands and high fertilizer and stocking rates (2.2 cows per hectare) are being used to increase productivity. At the highest pasture lands (about 35% of the total pasture area) the period of grazing lasts about 8 months per year.

The average application rate of phosphorus to pastures is 135 kg P_2O_5 ha^{-1} yr^{-1}, as estimated from an enquiry conducted to the farmers in 1997 (Universidade dos Açores 1998). For nitrogen fertilizers the estimated average amount is 750 kg N ha^{-1} yr^{-1}.

As the native P fertility of these soils is low, fertilizer applications by farmers is high and has increased over the years. Figure 4 shows the results of a systematic soil P survey (Olsen soil test) conducted over the entire pasture area of the watershed in 1998 (Universidade dos Açores 1998). As, for this analytical method, values above 25 ppm indicate a very low probability of pasture response to P fertilizer, and hence, the re-

sults of the soil survey identify an obvious excess of P load in these soils, dramatically above the agronomic sufficiency limits. The geographical perspective of the P Olsen distribution levels in the pasture fields is shown in Figure 5.

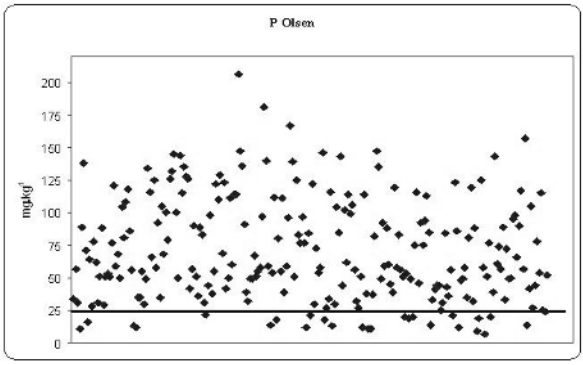

Figure 4. Results of a systematic soil P survey (Olsen soil test) conducted over the entire pasture area of the watershed in 1998. The line in the graph signals the agricultural optimum value (25 ppm) for the Olsen soil test.

Figure 5. Geographical perspective of the P Olsen status of pasture fields of the Sete Cidades watershed.

From this exploratory approach it can be inferred that the continued application of phosphorus fertilizer in excess of the crop removal in Sete Cidades pasture lands, exasperated by the excreta of the grazing animals, has resulted in a significant build-up of available P in the soil. Consequently, this has increased the risk of P-enriched runoff leading to P enrichment of the lakes and eutrophication.

Based on the above referred value of the efficiency limit for the P Olsen soil test, an estimate of the "excess" of available P in the overall pasture area of the watershed was determined (Table 1). This, perhaps simplistic, estimation has at least the virtue of pointing out the obvious

excess condition of the soil P load and the urgent need to reorient the P fertilizer strategy within the watershed if the more obvious cause for the eutrophication process is to be limited.

Table 1. "Total" and "excess" amounts of "available" P based on Olsen soil test results for the entire pasture area within the Sete Cidades watershed.

	"Total"	"Excess"
Kg P_2O_5 / 320 ha	66500	47600
Kg P_2O_5 / ha	208	149

Degree of P saturation (DPS)

The phosphorus sorption capacity (PSC) of a soil, conceptually, expresses the maximum sorption of P in a given soil condition (evaluated by the sum of Al and Fe extracted by acid ammonium oxalate) as proposed by Beek (1979). This relation has been used to predict P release from soil to solution by estimating the degree of P saturation (DPS) in the soil:

$$DPS = (\text{sorbed P}/PSC) \times 100$$

(P extracted by acid ammonium oxalate).

DPS (van der Zee and van Riemsdijk 1986, 1988, van der Zee et al. 1988, Breeuwsma and Silva 1992) estimates how close the soil is to saturation, allowing for comparison of soils with varying P sorption capacities (Börling et al. 2004). DPS can thus be useful as an estimate of P sources in risk assessment systems (Maguire et al. 2001), probably in a more consistent manner then simply using soil test P figures. In fact, research in the Netherlands and Belgium, and more recently in the U.S., has shown that chemical measures of DPS in a soil can accurately predict the amount of soluble phosphorus, desorbable phosphorus and phosphorus lost in runoff under field conditions (Sims 2000). For non-calcareous soils in the Netherlands, DPS values above 25% are considered to be high enough to be of environmental concern (Breeuwsma et al. 1995).

Figures 6 and 7 show the DPS values calculated for the whole soil sample set of Sete Cidades and its geographical distribution over the pasture fields of the watershed. According to these, a significant proportion of the pasture fields is still at or above the critical limit of P desorption and transport (DPS>25%). However, when comparing these data with those of soil testing (Figures 4 and 5) there is an obvious decrease in the number of samples/parcels above the respective threshold value, suggesting an attenuation effect of the sorptive properties of the soil in the risk of P dissolution and transport in runoff.

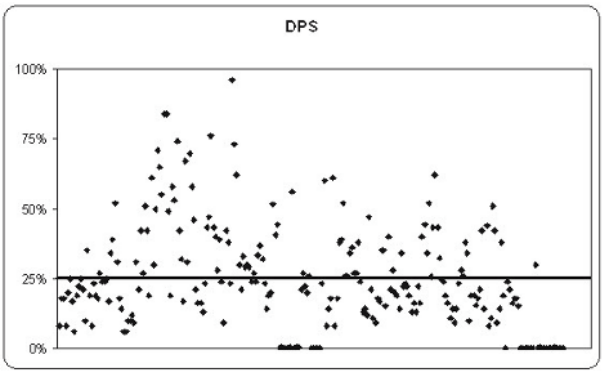

Figure 6. Degree of P saturation (DPS) calculated for pasture fields of the Sete Cidades watershed. The line in the graph signals the ISP value (25%) above which the risk of soil P loss becomes high.

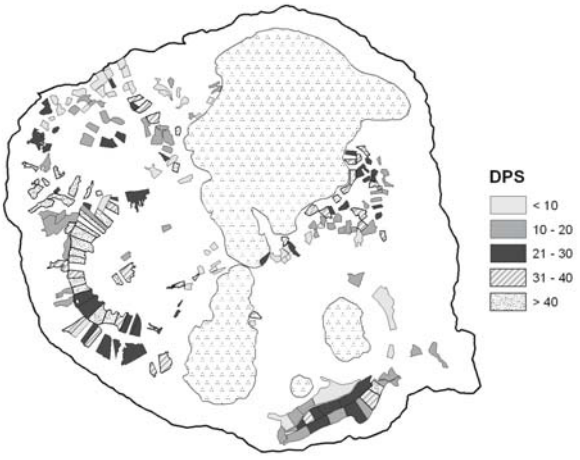

Figure 7. Geographical perspective of the degree of P saturation (DPS) calculated for pasture fields of the Sete Cidades watershed.

A highly significant correlation was observed between the P Olsen and DPS data (r=0.74) for Sete Cidades. High pedological uniformity has been observed within the watershed in previous studies (Universidade dos Açores 1998) and this suggest that, for Sete Cidades a simple and quick analytical procedure as the Olsen P soil test may be taken as a reliable environmental diagnostic tool, comparable to the much more elaborated DPS determination.

P Index

It may prove too simplistic to use upper limits, either for soil P test or DPS, as a sole environmental criterion for P management.

In risk assessment for P losses, both transport mechanisms and P source may need to be considered (Gburek et al. 2000). The P source component

can be inferred from P soil status or by potential P release from soil to solution. Additional site-specific factors that regulate soil P transport, such as soil erosion, cultural practices, slope and drainage characteristics of a particular field, have to be taken into consideration as well.

The Phosphorus Index, first developed by Lemunyon and Gilbert (1993), is a rating system that integrates the most significant factors controlling soil's potential for phosphorus loss by surface runoff. The Index is thus an additional tool for assessing P transport risk and often gives a better estimate for the risk of a given area then just P source estimates alone. In fact, soils that are considered to be at an agronomical "optimum" in phosphorus may be of a greater environmental risk if situated on a steep slope and experiencing erosion compared to soils that are P "excessive" and located in a flat topography (Sims 2000). Therefore, it has been suggested that for adjacent fields with similar test P levels or DPS but different runoff and erosion susceptibilities, different P management recommendations should apply (Sharpley et al. 2003). The P Index is thus designed to identify "critical areas" of P export potential (i.e. sites with high P loads and susceptible to runoff or erosion) on a field-by-field basis within the watershed.

Site vulnerability to P loss in surface runoff is assessed by selecting rating values for the relevant source and transport factors. In the absence of calibrated data of these factors for the Sete Cidades conditions, we applied the P indexing approach to two main pasture areas of the watershed using the Pennsylvania's index version from July 2001 (Sharpley et al. 2003). The output of this preliminary exercise is presented in Figure 8, indicating a high risk of P loss from almost all considered fields.

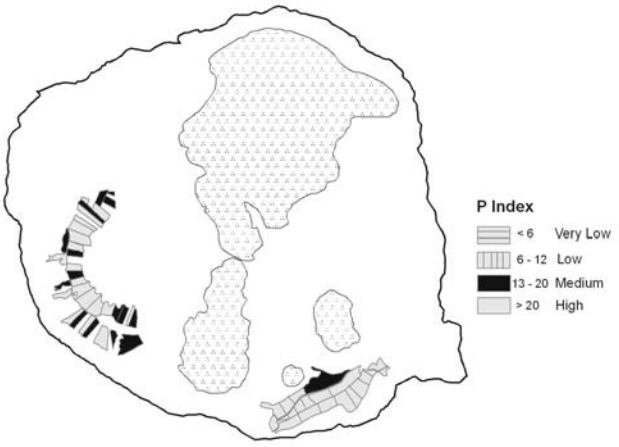

Figure 8. Perspective of the P Index concept application to two pasture areas of the Sete Cidades watershed.

Final remarks and future trends

The efficiency of ecological phosphorus management is dependent upon the ability to accurately predict the potential for phosphorus transport across the landscape and to superficial waters. However, risk assessment of P transport from diffuse P sources becomes a complex task due to the high variability, in space and time, of the source and transport factors that interactively command P movement in runoff. Variables such as climate (rainfall quantity/intensity), land use, topographic features (slope and distance to the water mass), as well as the concentration, bioavailability and saturation degree of phosphorus in soils, are some of the more obvious factors contributing to complexity of the task.

The practice of soil monitoring and the establishment of a threshold limit for P in agricultural soils appear to be simple but significant steps towards ecological sustainability under conditions where the eutrophication risk is high. However, P soil tests are considered reliable agronomic tools for diagnostic of soil fertility and fertilizer recommendations, but, their use for assessing environmental risk of phosphorus to water quality is not as well accepted, being frequently argued in the literature (Pote et al. 1999, Sharpley et al. 2002). Nevertheless, Sims (2000) points out that a number of advances have made P soil analysis more reliable for environmental purposes. Certain aspects of P soil tests such as the depth of soil sample, the measurement of the amount of soluble P in the soil (either by extraction with water or a dilute salt solution) and the quantification of potentially desorbable P by reaction of the soil with a "sink" that can absorb P in solution (ion exchange membrane or iron-oxide-coated filter paper strips) are taken as examples of such improvements.

It seams thus plausible that soil testing programs can become important in the development of the environmentally oriented best management practices (BMP) to be applied within the Sete Cidades watershed, as well as in other situations under risk of eutrophication. Incorporation of P soil tests to risk assessment plans and other environmentally oriented tools such as DPS and the P Index, when supplemented by advisory programs to the farm community, could possibly become an adequate and realistic strategy to be implemented in the near future.

References

Azevedo EB (1996). Modelação do Clima Insular à Escala Local. Modelo CIELO aplicado à Ilha Terceira. Tese de Doutoramento pela Universidade dos Açores na especialidade das Ciências do Ambiente, pp 247

Bettencourt ML (1977). O clima dos Açores como recurso natural na aplicação especialmente em Agricultura e indústria de Turismo. INMG, Lisboa

Beek J (1979). Phosphate retention by soil in relation to waste disposal. Doctoral thesis, Agricultural University, Wageningen

Börling K, Otabbong E, Barbaris E (2004). Soil variables for predicting phosphorus release in Swedish noncacareous soils. J Environ Qual 33:99–106

Breeuwsma A, Silva S (1992). Phosphorus fertilization and environmental effects in The Netherlands and the Po region (Italy). Report 57, Agricultural Research Department, The Winand Staring Center, Wageningen

Breeuwsma A, Reijerink JGA, Schoumans OF (1995). Impact of manure on accumulation and leaching of phosphate in areas of intensive livestock farming. In: Steele K (ed.) Animal Waste and the Land-Water Interface. Lewis Publishers, Boca Raton, Florida, pp 239–251

Gburek WJ, Sharpley AN, Folmar GJ (2000). Critical areas of phosphorus export from agricultural watersheds. In: Sharpley AN (ed.) Agriculture and Phosphorus Management: The Chesapeake Bay. Lewis Publishers, Boca Raton, Florida, pp 83–104

INOVA (1999). Análise das Águas das Lagoas da Região Autónoma dos Açores. Relatório final. Instituto de Inovação Tecnológica dos Açores, Ponta Delgada

Lemunyon JL, Gilbert RG (1993). Concept and need for a phosphorus assessment tool. J Prod Agr 6:483–486

Maguire RO, Foy RH, Bailey JS, Sims JT (2001). Estimation of the phosphorus sorption capacity of acidic soils in Ireland. Eur J Soil Sci 52:479–487

Pote DH, Daniel TC, Nicols DJ, Moore PA, Jr Miller DM, Edwards DR (1999). Seasonal and soil-drying effects on runoff phosphorus relationships to soil phosphorus. Soil Sci Soc Am J 63:1006–1012

Sharpley AN, Kleinman PJA, McDowell RW, Gitau M, Bryant RB (2002). Modeling phosphorus transport in agricultural watersheds: Processes and possibilities. J Soil Water Conserv 57:425–439

Sharpley AN, Daniel T, Sims T, Lemunyon J, Stevens R, Parry R (2003). Agricultural Phosphorus and Eutrophication. 2nd edn. ARS-149. United States Department of Agriculture, Government Printing Office, Washington DC

Sims JT (2000). The role of soil testing in environmental risk assessment for phosphorus. In: Sharpley AN (ed.) Agriculture and Phosphorus Management: The Chesapeake Bay. Lewis Publishers, Boca Raton, Florida, pp 57–81

Soil Survey Staff (1999). Soil Taxonomy: A Basic System of Soil Classification for Making and Interpreting Soil Surveys. 2nd edn. USDA Handbook No 436, United States Department of Agriculture, Government Printing Office, Washington DC

Universidade dos Açores (1998). 1.ª Fase dos Planos de Ordenamento das Bacias Hidrográficas das Lagoas das Furnas e Sete Cidades. Universidade dos Açores, Ponta Delgada

van der Zee SEATM, van Riemsdijk WH (1986). Transport of phosphate in a heterogeneous field. Transport in Porous Media 1:339–359

van der Zee SEATM, van Riemsdijk WH (1988). Model for long-term phosphate reactions in soil. J Environ Qual 17:35–41

van der Zee SEATM, Nederlof MM, van Riemsdijk WH, de Hann FAM (1988). Spatial variability of phosphate adsorption parameters. J Environ Qual 17: 682–688

Appendix materials on CD-Rom

Eutrophication in the Azores Islands_Figure 2_colour
Eutrophication in the Azores Islands_Figure 3_colour
Eutrophication in the Azores Islands_Figure 5_colour
Eutrophication in the Azores Islands_Figure 7_colour
Eutrophication in the Azores Islands_Figure 8_colour

Soils and Land Use of Santorini, Greece

A. Economou, A. Skouteri and P. Michopoulos

Introduction

The island of Thira is called Santorini but in the past the name Santorini had been given to the volcanic cluster (Figure 1) of the southwest Aegean Islands of Thira (75.8 km^2), Thirasia (9.3 km^2), Aspronisi (0.1 km^2), Palea Kameni (0.5 km^2) and Nea Kameni (3.4 km^2). Thira is located in the northern part of the Cyclades, between 36º19'45" and 36º29'00" latitude and between 25º19'10" and 25º29'15" longitude (Georgoulias and Moustakas 2002).

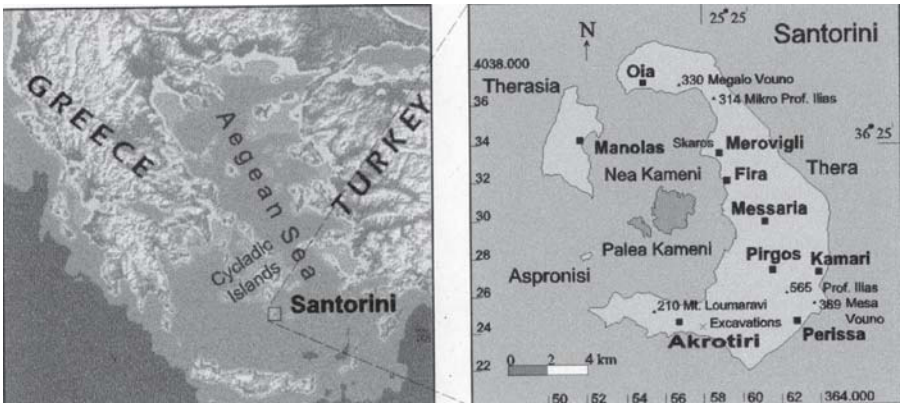

Figure 1. Location of Santorini (Thira) Island.

In a tremendous volcanic explosion approx. 3600 years ago, an island named Strogili collapsed, creating the present day caldera (8 km × 10 km size and 300–400 m deep). Thira, Thirasia and Aspronisi are the fragments of the Strogili Island that remained above the sea surface after the collapse of the volcano's cone, while the rest of the island disappeared under seawater (Druitt et al. 1989, Vougioukalakis 1995). Apart from a small non-volcanic basement in southeastern Thira, these islands are composed of volcanic rocks derived from hundreds of eruptions during the last 3.5 million years. Palea Kameni (Old Burnt Island) is less than 2000 years old,

while Nea Kameni (New Burnt Island) began to form only 425 years ago and its youngest lavas are less than 50 years old.

The highest elevations on Thira are Profitis Elias Mount (565 m) in the southeast and Mikros Profitis Elias (314 m) and Megalo Vouno (330 m) in the north.

Soils of Thira's Island are basically derived from volcanic material (pumice, volcanic ash and other pyroclastic materials) under very dry and warm climate and have been intensively cultivated at least for the last few hundred years. Sustainable land use of these volcanic soils is very important because of risks of erosion, loss of fertility, deterioration of water quality, as well as loss of prime agricultural land to housing. These problems require rational land use planning and management decisions. In fulfilling these needs, the land resource survey of Greece provides the proper ecological information (Nakos 1983) like landforms (geology and physiography), soil depth, erosion and slope gradient classes, land regions, degree of human influence on natural vegetation and slope aspect (Greek Ministry of Agriculture 1996).

Materials and methods

The land resource survey of Thira Island was carried out and completed in 1996 using aerial-photographs taken in 1988, together with orthophotomaps, geological and topo-maps. Mapping was done at the association level (1:50,000) and the map units described by the kind and state of natural vegetation (human influence), landforms and classes of soil depth, gully erosion, slope and aspect. Physiography, geology and natural vegetation zones (climatic zones) were also taken into account and incorporated in the survey (Nakos 1983). The information was collected (extracted) from the published soil (land) map of the whole cluster of islands.

Soil chemical and physical information was derived from various other studies (Stoyiannis 1971, Misopolinos et al. 1994, Georgoulias 2001, Georgoulias and Moustakas 2002) together with soil chemical analysis data of the soil samples collected during the preparation of the COST Action 622 meeting held in Santorini, 24–28 April 2001 (Pateras and Economou 2001).

Land use data of the national statistical service of Greece (1971, 1981, 1991) were utilized along with the information of the land resource survey.

Results

Lithology and physiography

The soil parent materials found on Thira Island according to the land resource survey are: Tertiary deposits (volcanic tuffs and lavas, 83.5%), peridotites (8.1%), limestones (7.4%) and schists (1%). The Tertiary deposits consist mainly of several pumice series, dacitic pumice tuffs and lavas. Peridotites (quaternary volcanic rocks) consist of extrusive dacitic to latiandecitic volcanic rocks, upper, middle and lower lavas (quartz latiandesitic) and corresponding pyroclastics which are found mainly in caldera walls below Mikros Profitis Elias Mount and in northern Thira (cape Ayios Nikolaos). Crystalline limestones (upper Triassic) are found in the southeast part of the island (Profitis Elias Mount). Schists, consisting of semimetamorphic phyllites to calcareous phyllites and other layers, are found in the caldera walls around the Athenios port.

The main physiographic units are: the lower slopes (61.6%), the rounded summits (24%), escarpments and cliffs (8.1% – caldera walls) and steep summits (1.7% – Profitis Elias Mount).

Soils, slope gradient and erosion

The soils of Thira were developed under a Mediterranean type of climate which is semi-arid with mean annual rainfall <400 mm and mean air temperature 17°C (absolute maximum 39.9°C and absolute minimum –4.8°C). The potential annual evapotranspiration is 1100 mm and the mean annual relative humidity 68% (Stoyiannis 1971). The soils of the volcanic ash and pumice parent material are slightly acid to alkaline (pH 5.8–8.6) with a low clay content consisting of illite and vermiculite. They have a low CEC (<12 $cmol_c\,kg^{-1}$) and a very low to low organic matter content (<4.7%), especially the cultivated soils (Missopolinos et al. 1994, Pateras and Economou 2001, Georgoulias 2001).

Most of the volcanic soils have been under cultivation but in recent years a great portion of them has been used for housing and tourism and are therefore lost for agricultural activities, due to these socio-economic changes. Until recently, the main agricultural crop has been grapes from which the famous Santorinean wine is produced. Natural vegetation is very scarce.

According to WRB (ISSS, ISRIC & FAO 1994), the soils of Santorini are classified as Tephric Regosols because they do not fulfill the requirements of Andosols. Georgoulias and Moustakas (2002) classified three soil

profiles of Santorini according to Soil Taxonomy as Entisols (Vitrandic Xeropsaments) but Missopolinos et at. (1994) argued that the soils examined are Andisols developed under xeric moisture conditions.

Most (72%) of the soils of the island are deep (>30 cm), 14% are shallow (5–30 cm) and finally 14% of the land is bare rocks, mainly those of limestone and the caldera walls (Ministry of Agriculture 1996).

The dominant (86%) slope gradient is moderate (<40%) and the steep slopes (>70%) occur on 14% of the land.

A large portion of the soils (38%) suffer from moderate gully erosion, while most of the volcanic soils suffer seriously from surface erosion caused by prevailing strong winds.

Land use and land use change

According to the land resource survey of Greece (Greek Ministry of Agriculture 1996, Nakos 1983) 74% of the island of Thira consists of agricultural land, 13% is covered by phrygana (*Atriplex halimus*, *Phagnalon rupestrae*, *Thymelaea hirsuta,* etc.), 8% is devoid of vegetation and only 5% is covered by shrubs of low canopy closure (<40%).

Data from the National Statistical Service of Greece, (NSSG 1971, 1981, 1991) states that the main land use of the island is agriculture, which between 1971 and 1991, decreased by 17%. Annual crops, vineyards and orchards decreased by 73%, 7% and 63%, respectively, between 1971 and 1991. In contrast, the area of the settled and abandoned agricultural lands increased in the decades of 1960's, 1970's and 1980's (Figures 2 and 3). The urban area increased by 38% due to changes of socio-economic conditions of the population, mainly because of increased tourism and summer housing on the island.

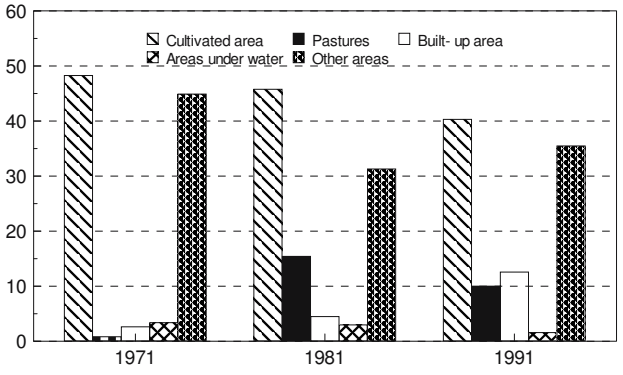

Figure 2. Land use in Thira Island in the decades of 1960's, 1971's and 1980's. (Source: National Statistical Service of Greece 1971, 1981, 1991).

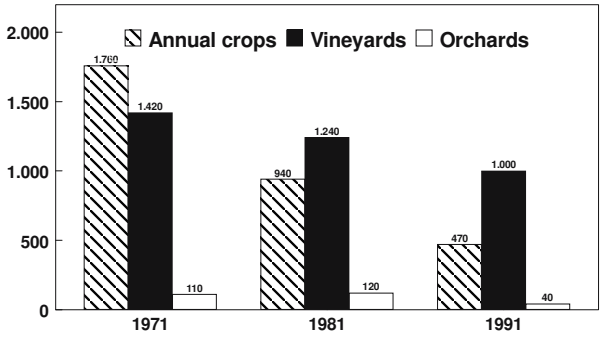

Figure 3. Distribution of agricultural land (ha) on Thira by crop categories in the decades of 1970's, 1980's and 1990's. (Source: National Statistical Service of Greece 1971, 1981, 1991).

Conclusions

The Santorini Islands represent a fragile volcanic area with poorly developed soils due to dry climatic conditions. The soils are vitric in character and many are influenced by accelerated erosion. However, these soils have in the past supported thriving agriculture, including the production of famous vines. Currently agriculture is being replaced by other land uses due to rapid socio-economic changes.

References

Druitt TH, Mellors RA, Pylet DM, Sparks RSJ (1989). Explosive volcanism on Santorini, Greece. Geol Mag 126(2):95–126

Georgoulias F (2001). Investigation of the physical and mineralogical properties of Thiras' island soils. Post graduate study. Agricultural University of Athens, 111 pp

Georgoulias F, Moustakas N (2002). Soils Developed on Volcanic Materials in Thira island do they Classify as Andisols? Proceedings of the 9th Panhellenic Congress of the Soil Science Association, pp 559–568

Greek Ministry of Agriculture (1996). Soil Map of Greece (scale 1:50,000), Nisos Thira

IGME (1980). Geological Map of Greece (scale 1:50,000), Thira island

Missopolinos N, Syllaios N, Prodromou K (1994). Physiographic and soil mapping of Santorini island (In Greek). Edited by the laboratories of Soil Science and Remote Sensing of the School of Agronomy, Aristotle University of Thessaloniki, 110 pp

Nakos G (1983). The Land Resource Survey of Greece. J Envir Management 17:153–169

National Statistical Service of Greece (1971, 1981, 1991). Agricultural Statistics of Greece

National Statistical Service of Greece (1971, 1981, 1991). Distribution of the country's area by basic categories of land use

Pateras D, Economou A (2001). Soil profiles of Santorini island. Internal report for the Cost Action 622 meeting, Santorini (24–28 April, 2001), 12 pp

Stoyiannis G (1971). Soil and agriculture examination of the island of Thera. Athens, Greece (In Greek). Internal edition of the Institute of Chemistry and Agriculture, Athens, Greece, 63 pp

Vougioukalakis G (1995). Santorini "the volcano". Palea and Nea Kameni. The volcanic activity in historic time, 78 pp

WRB (World Reference Base) 1994. World Reference Base for Soil Resources. (ISSS, ISRIC, FAO). Edited by OC Spaargaren. Wageningen/Rome, 161 pp

Environmental features and land use of Etna (Sicily – Italy)

C. Dazzi

Introduction

The history of Etna, Europe's highest active volcano, whose name derives from the Phoenician word "*athana*" meaning "*furnace*", roams through myth, marvel and science.

Etna's oldest myth was narrated by Ovid in '*The Metamorphoses'*. He describes how Tifeo, the monster born from Earth who was joined with Hell, was imprisoned by Zeus beneath Sicily with his feet tied to Cape Lilibeo (W), his left arm to Cape Pachino (S-E) and his right arm to Cape Peloro (N-E); his head remaining below the volcano. When the monster roared and writhed he created earthquakes and eruptions.

In Greek and Latin mythology, Etna was the home of the god Volcano. Homer also placed the dwelling of Polyphemus there, the giant with only one eye who was blinded by Ulysses. As civilisation evolved, the myths linked to Etna became complicated and confused, with pagan beliefs sometimes overlapping those of Christianity.

The fires of Etna are seen in their twofold aspect as the origins of Good and Evil: they can produce fertile soil to grow crops but they can also be a source of destruction and thereby an instrument to expiate sin. Even today people carry the image of the Madonna towards a lava flow to deter the forces of evil.

The spirit of enquiry was a motivating force in the 17th and even more the 18th centuries which inspired many travellers to make expeditions to the Etna area. Maupassant, Lawrence, Brydone, Houel, von Borch, Münter, Bartels, Maeterlinck, Gonçalve de Nervo, Peyrefitte, Schneegans and Goethe are some of the more famous travellers who were encouraged by the romantic age to visit Etna and left exotic and impressive descriptions of the volcano.

With regard to scientific studies, the first work that provided systematic descriptions of the places and eruptions of Etna was that of Sartorious von Waltershausen (1880) which is particularly praiseworthy when considering the difficulties of exploration and the limited knowledge of those times. Later there were many authorities of different disciplines who studied Etna and the mountain continues to be the subject of scientific enquires today.

Main environmental features of Etna

Etna lies near the eastern coast of Sicily, Italy (37.743°N, 15.004°E) (Figure 1). Its main environmental features are linked to its position as an isolated mountain in the middle of the Mediterranean sea, and to its shape and size (Figure 2).

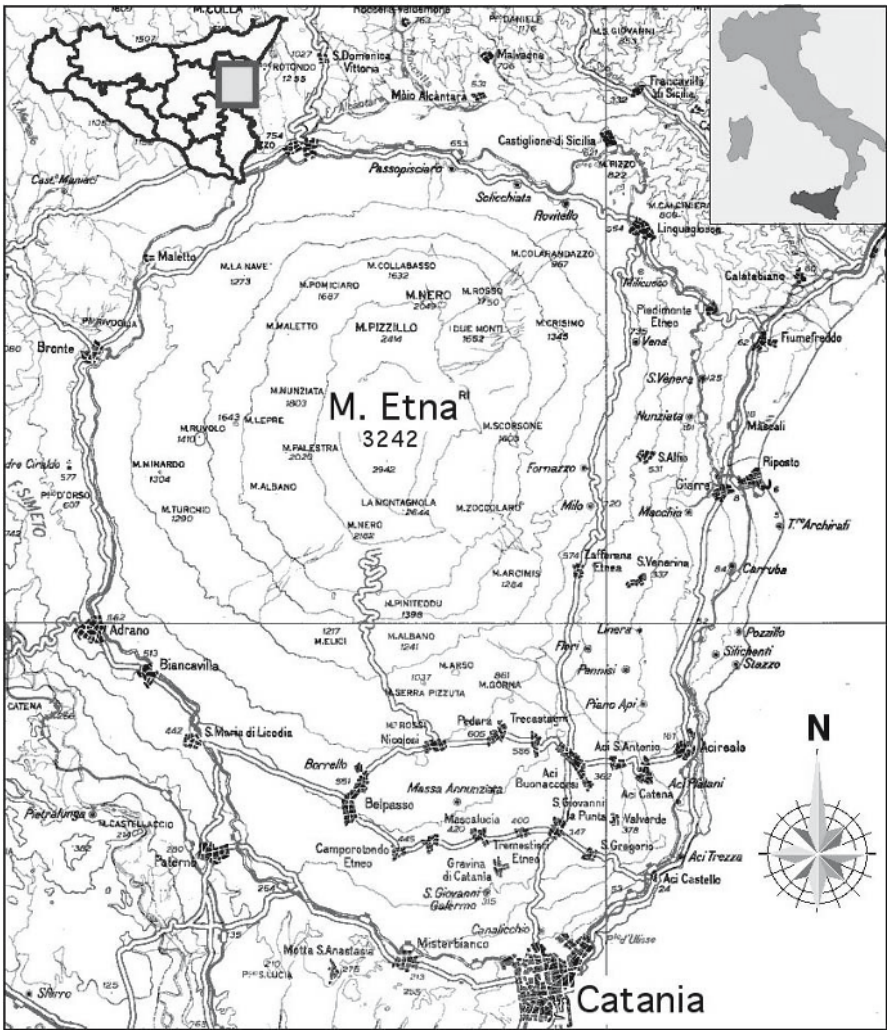

Figure 1. Schematic map of the Etna area.

Figure 2. Panoramic view of Etna from the West side.

Geology

The oval-shaped base of Etna measures 1,600 km^2. The main axis is approx. 60 km and the lesser axis is approx. 40 km. Its volume is around 500 km^3. Due to its activity, which has continued uninterruptedly since erupting from the sea approx. 550,000 years BP, Etna is certainly one of the important volcanoes of the world and one of the most active, both in the sense of production and frequency of eruption. There are frequent periods of intermittent to persistent activity in the summit area and major eruptions from new vents on its sides every one to twenty years (Behncke 2004).

It is a complex strato-volcano, formed of lava flows alternating with pyroclastic materials, emitted over various eruptive areas which over the centuries have built up the existing volcano that lies on a base of Pleistocene clays (Parello et al. 2001).

Although the volcano is 3242 m high, the vulcanites have an actual thickness of about 2000 m as the sedimentary base on which it stands reaches a height of 1300 m. As a result the estimated volume of the volcano does not exceed 350 km^3 (Tanguy et al. 1997).

Etna is schematically characterised by (Behncke 2004):

- A pre-Etnean sedimentary base
- Volcanic products older than Holocene
- Holocene but prehistoric lava flows
- Lavas erupted between the period of early history until 1600
- Lavas erupted between 1600 and the present

Climate

The climate of the Etna area has characteristic features and is affected not only by the height and exposure of its slopes but also by being an isolated mountain in the middle of the Mediterranean sea. The altitude causes a gradual transfer from the sub-tropical conditions of the base area to a moderate warmth in the middle and moderately cold and cold towards the higher regions (Chester et al. 1985, Raimondi et al. 1999). Poli Marchese (2000) defines a thermomediterranean climate for the base area, a mesomediterranean climate for the middle area and an oroxerothermic climate at the highest altitude. The rainfall and temperature distribution are clearly influenced by altitude, slope direction and dominant winds, with cloud mass approaching mainly from the east. As a result, maximum rainfall occurs on east facing slopes at an altitude of 700–900 m a.s.l., caused both by aspect and proximity to the sea which acts by reducing the temperatures caused by rising damp air currents meeting cooler layers of the atmosphere. In addition, a notable and abrupt increase in rainfall occurs from south to north and from west to east.

Average rainfall data register a minimum of 600–700 mm for low altitudes and a maximum 1300–1500 mm at 600–700 m a.s.l., with an average of approx. 800 mm for the whole Etna area. These figures diminish with altitude since rainfall is largely replaced by abundant snowfall over extended periods of the year and from other sources which are difficult to assess but have considerable input (the so called hidden rainfall such as the dew or the mist). On the western and northern slopes snow is more widespread and lasts longer, due to greater frequency of snow precipitation. Thermal figures show a similar range, with lower registration at higher altitudes and on western slopes. Uniformity of thermometric conditions in these areas is apparent in spite of wide variation in annual figures and the variable influence of climatic factors on absolute temperature values (Ferrara 1975).

The pedoclimate shows an udometric regime ranging, according to altitude, from xeric to udic and a thermometric regime ranging from thermic to mesic to frigid (Raimondi et al. 1999).

Hydrology

The high permeability and irregularity of the lava, prevents the formation of any hydrographic network and erosion phenomena. There are very few small streams, which are mainly present at lower altitudes, and are undeveloped both in length and depth. Generally such streams are only active for a short period of the year following heavy rainfall. They can be found where the substrata show a low permeability or where the morphology allows water to escape between the vulcanites and the sedimentary substratum. Ogniben (1966) considers that of the total precipitation, surface water represents 5%, evapotraspiration approx. 20% and effective infiltration 75%.

Geomorphology

On a geo-morphological base, Etna can be divided schematically into three belts:

1. Base belt: from sea level to approx. 900 m
2. Wooded belt: from 900 to approx. 2000 m
3. Desert belt: from 2000 m to the summit

On the lower slopes of the south-western flank the morphological features show alluvial terraces, with marine terraces on the south-east. These may be interrupted by sub-vertical escarpments which reach 200 m in height and several kilometres in length (Aureli 1973). On the same slopes the so called 'Chiancone' appears in the area between Riposto, Pozzillo and Santa Venerina. This is a detritic-alluvial deposit characterised by a sublevel morphology that inclines towards the coast with an average slope of 5%. Above 900 m, in the wooded belt, the slopes become steeper with frequent and abrupt variations though there are also areas with gentle slopes and regular contours. The landscape is also strongly influence by lava flows which have produced morphologies with irregular and rough surfaces.

Another unusual morphological element is represented by the huge depression known as 'Valle del Bove' whose origin is partly linked to the collapse of various calderas. There are many ephemeral cones formed by the accumulation of pyroclastic materials in this area and all round the perimeter of the volcano. The distribution of such cones, together with their associated eruptive fractures, does not have a radial symmetry but appears to be linked to regional tectonic structures. In the desert belt the slopes are very steep and culminate in the main craters. The presence of recent lava flows confers a wild and striking aspect to the landscape.

Soils

The wide variation of soil types that characterise Etna is due to variability in parent material, age, various morphologies, climatic features and, lastly, to exposure and winds which carry and deposit the abundant ash and lapilli. The relatively few soil surveys made so far describe soils mainly with vitric features (Certini et al. 2001, Lo Papa et al. 2003). Vitrandic Udorthents and Typic Vitrixerand can both be found on pyroclastic cones; they are also found on the volcano slopes together with Lithic Haploxerands, Typic Udivitrand and Vitric Hapludands. In a very few instances Humic Haploxerands can be found under woodlands and where the morphology is less steep.

Unpublished data from soils sampled along the southern flank of Etna at elevations between 800 and 1900 m a.s.l., and at several peripheral vents or in areas with a thick tephra substrate, show that recent tephra (e.g. 1669) have an almost unaltered composition, irrespective of the analysed horizon depth (Cristofolini pers. com.). In other cases like in the Salto del Cane area (Busà et al. 1998), distinct soil horizons with particular textural characteristics may be related to the processes from which the deposits originated. The major element contents of each horizon are controlled both by their original composition and the intensity of weathering processes, which are not strictly related to the profile depth but to the age of the horizon as well. Levels dating back to less than a few thousand years, those at the top, are definitely less altered than those which are older and deeper, which in turn vary according to how they were exposed on the surface and to the climatic conditions prevailing at the time. In each of these horizons the finer grained fragments (<2 mm) are more altered than the coarse ones which preserve a better record of the original composition. There is strong evidence that weathering leads to selective leaching of Si, Na and K and to a passive enrichment of rather immobile elements like Al, Fe and Ti (Busà et al. 1998).

Land use of Etna

The considerable anthropic presence apparent in the Etna area has, over time, significantly modified the original vegetation, reducing forest cover and providing good quality crop cultivation, mainly in the lowland areas.

The simplest and best way to describe the characteristics of Etna land use is to divide the volcano into vegetation belts on an altitudinal basis. These correspond roughly to the morpho-climatic belts as follows (Figure 3):

1. Base to approx. 900 m: crop belt with various fruit orchards

2. From 900 m to approx. 1500 m: woodland belt where forest vegetation prevails
3. From 1500 m to 1800/2200 m: mountain belt dominated by vegetation of high Mediterranean mountains up to the vegetation limit which ranges from 1800 to 2200 m a.s.l., depending on exposure and morpho-climatic conditions

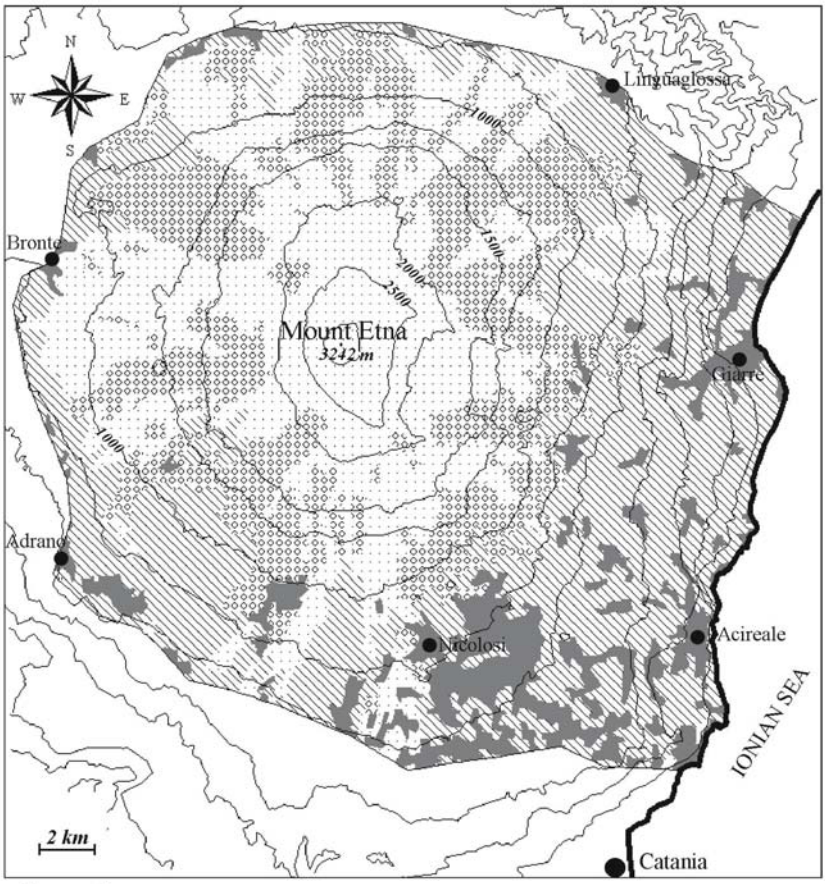

Figure 3. Schematic map of the land use of the Etna area (mod. from Corine land cover 2000).

Land use of crop belt

As has happened in many other volcanic areas of the world, man has energetically colonized the more gradual slopes of Etna, particularly after WW II. The volcanic lowlands have been strongly influenced by this human presence and this belt displays particular characteristics caused not only by the physical features of the landscape but also by the history of Etna.

Vines (*Vitis vinifera*) and olive (*Olea europea*) were the first widespread cultivation introduced by man and date back to Greek colonization while apple (*Malus communis*), pear (*Pirus communis*) and chestnut (*Castanea sativa*) were introduced by the Romans. During their domination the Arabs subsequently introduced sugar cane (*Saccharum officinarum*), cotton (*Gossypium hirsutum*), pistachio (*Pistacia vera*) and citrus (*Citrus* spp.) and extended the growing of the olive, mulberry (*Morus nigra*), carob (*Ceratonia siliqua*) and fig (*Ficus carica*).

Although a few hundred hectares are used for arable land, it is above all the cultivation of fruit trees that occupies a large area and characterises the landscape of the Etna crop belt. The most widespread species, grown either as a single crop or in mixed cultivation, are citrus, olive, vines, pistachio, apple, pear, cherry and hazel (Messina et al. 2004). The prickly pear and less widespread fruit trees are of some importance in the fruit yields of Etna but, as with Maletto strawberries and local market garden production, the trade is limited to local markets.

Citrus trees occupy an area of approx. 20,000 ha, in which the lemon (*Citrus limon*), clementine (*Citrus reticulata*) and orange (*Citrus sinensis*) are particularly important. The lemon, for obvious climatic reasons, dominates the coastal landscape up to about 200 m. Beyond this and up to 400 m the lemon is replaced by the clementine.

The olive has been cultivated on the slopes of Etna since ancient times. It is present on the slopes of Etna where it replaces the citrus at about 200–300 m; sometimes it survives up to about 1000 m. Single-crop olive groves characterise the landscape of Paternò, Adrano, Belpasso, Biancavilla and Bronte. On other slopes the olive is grown as part of mixed cultivation or as a windbreak in the citrus orchards.

Vines strongly characterise the agricultural landscape of the southern, eastern and western slopes of Etna. This is not due so much to their extent, approximately 5000 ha in total, but to the remarkable effects on the landscape made necessary by the requirements of their cultivation. Particularly on the eastern and northern slopes, terraces have been constructed over time which represent masterpieces of land adaptation. Land structuring of this nature requires the use of traditional techniques of cultivation, such as the head pruning system and the use of the hoe. Only where there is a fa-

vourable morphology the grapes are grown with the trellis system and the use of machinery is possible.

The cultivar Nerello Mascalese, deriving its name from the town of Mascali, and the cultivar Carricante are the most widespread vine stocks. Besides these two varieties, the cultivars Insolia and Cataratto are well known while others are of more recent date. An interesting aspect of Etnean grape production is the occasional use of wood litter mulch to increase the amount of organic soil matter. The areas where vines are most widely grown are Randazzo and Castiglione di Sicilia. Here wine is produced where the influence of the soil on the grapes is unmistakable.

Pistachio was introduced to Sicily by the Arabs in the 9th century and represents a significant feature of Etnean cultivation. Particularly on the western slopes of the volcano the agricultural economy largely depends on the cultivation of these trees, over an area of approx. 3500 ha, at a height of between 400 and 700 m.

The apple is one of the most representative fruit trees of the Etna landscape (Figure 4), particularly due to its adaptability to colder climates. It is widespread in the belt between 600 and 900 m and, depending on the degree of slope, can grow at 1100 m. To the south-west apples are grown at Pedara, Nicolosi, Ragalna, Biancavilla and Adrano, and on the western slopes at Zafferana, Milo and Sant'Alfio.

Figure 4. Terracing with apple and pear trees in the Biancavilla area (northern slopes of Etna).

The pear tree is not only one of the most important and representative features of Etnean fruit cultivation but is also notable for its widespread diffusion on the landscape due to the habit of the farmers to graft the tree on spontaneous wild peer. Together with traditional methods of cultivation, innovative systems are now in place regarding the varieties and agronomic techniques in use.

Cherries (*Cerasus avium*) are of important economic significance to the Etna area. They are particularly grown in the hilly areas of the east coast, between 200 and 1000 m. The best-known area for cherry cultivation is around Giarre, Mascali, Aci S. Antonio, Trecastagni, Pedara, Viagrande and Zafferana. A particular aspect of cherry cultivation on Etna is the remarkable range of varieties grown, illustrative of their ancient origin and the need for different tree types to grow together to overcome the phenomenon of incompatibility, to adapt to different climatic conditions and the necessity of co-ordinating the times of maturity and demand for their produce.

The extent to which hazelnut (*Corylus avellana*) is grown on Etna is linked to the tree's climatic requirements. As it needs cold temperatures it is planted on the northern slopes, from the area of Sanfilippo to Linguaglossa. Occasionally it reaches 1000 m and always grows on sandy soils formed from pyroclastites. The particular features of the tree include its shrubby habit determined by a large number of suckers that emerge from the base of the trunk, the presence of male and female flowers on the same tree, and the male flowers flowering before the female.

After its introduction to Sicily in the 16th century, prickly pear (*Opuntia ficus-indica*) quickly naturalised in the Etna area, becoming one of the symbolic plants of Sicily. Originally it was used to border plots of land together with lava stone walls. Today, as well as the production of fruit, prickly pear is used as a fodder crop for cattle, medicine (decoctions of the flower have a diuretic effect) and for ornament. The increased demand for exotic fruits has caused a remarkable boost to its cultivation and a complete re-thinking of the necessary techniques.

The range of lesser fruit trees of Etna includes numerous species not considered to be of very widespread or economic importance but are often of remarkable historical and agronomic interest. Some represent indicators of climatic conditions which are more or less comparable to sub-tropical such as the loquat (*Eriobotrya japonica*), the avocado (*Persea gratissima*), the feijoa (*Feijoa sellowiana*) and the pecan (*Pecan illinoensis*) which are present only in the warmer, irrigated coastal belt. Other species that occur sporadically up to 1000 m include the pomegranate (*Punica granatum*), apricot (*Prunus armeniaca*), fig (*Ficus carica*), peach (*Persica vulgaris*), almond (*Amygdalus communis*) and quince (*Pirus cydonia*).

On the wide terraces that slope towards the south-west and in areas close to town centres, particularly of Adrano, Belpasso and Biancavilla, are intensely cultivated vegetable species. These include fennel, lettuce, spinach, broccoli, cauliflower, pepper, tomato and aubergine.

Land use of wooded belt

This belt lies mainly between 900 and 1500 m and the vegetation is characterised by important forest growth (Figure 5): the Laricio pine, Etna birch, beech and poplar predominate. The chestnut (*Castanea sativa*) is widespread: it is of primary importance to the economy of the Etna area and is therefore one of the most common forest trees. It grows on the south-eastern slopes, particularly in the areas of Tarderia, Milia and Zafferana. The trees are frequently grown as coppice and undergo alternate cutting according to the local need for timber while the artificial stands are permitted to grow to their full height and also produce fruit.

Figure 5. The forested areas of Etna are frequently threaten by lava flows. In this photo the remains of a forest stand with trembling poplar (*Populus tremula*), Laricio pine (*Pinus nigra*) and birch trees (*Betula aetnensis*) with the characteristic pale bark.

There are less extensive woods of trembling poplar (*Populus tremula*) on all the slopes of Etna above the height of 900 m and on concave morphologies which indicate good water content in the soil. Sometimes the poplar forms dense unmixed stands within other forests as in the chestnut wood in the Tardaria area or the beech woods of Mt. Minardo.

The beech *(Fagus sylvatica*) is well represented on all slopes of the volcano (particularly those of Mt. Maletto and Piano Provenzana), except on the southern slope where only the small beech wood of Mt. Vetore stands. Beech extends close to the higher limits of the forest belt but, can also be found up to 2000 m or down to 800 m as in some deep and damp valleys of the eastern slopes. Even though the beech does not represent such important wood cover on Etna as in other mountainous areas of Sicily where it has an important role in the composition of the island's timber heritage, it is of remarkable scientific interest as it reaches its southern limits on Etna. These beech woods can be considered as a residue of the post-glacial period and the few areas where it is still found testify to the former presence of forests decimated over time by eruptions and the activities of man.

On the western and eastern slopes the landscape of the wooded belt is characterised by extensive woods of birch trees (*Betula aetnensis*) with a characteristic pale bark. These woods are fairly open and have a pioneering role in colonizing soil often consisting of accumulated loose and permeable volcanic sands. Their pioneer character is not, however, linked to soil conditions but to the climate (intensity of rainfall, humidity, snow). On Etna's north-eastern slopes the birch has a very limited distribution and gives a particular beauty and fascination to the landscape.

The wooded belt also contains pine woods with Laricio pine (*Pinus nigra* ssp. *calabrica*). The Laricio pine is a species that performs a pioneer role by colonizing successfully on the rockiest landscape and lava flows. It is a coniferous tree of significance that is used for reforestation and its timber was widely used in the past as fuel and for building. Together with natural forests it also provides extensive artificial pine woods, thereby affecting the appearance of the area's vegetation.

The Etna broom (*Genista aetnensis*) has a notable presence in the wooded areas (Figure 6); in the late spring it blooms vividly and profusely. It is distributed widely on all the slopes of Etna and can grow at 1700–1800 m, in particular colonizing open sunny areas with inadequate or poor soil.

Figure 6. The Etna broom (*Genista aetnensis*) very often colonizes the open and sunny areas with inadequate or poor soils.

Land use of the mountain belt

Thorny cushion (*Astragaletum*) vegetation of compact formation is characteristic of the mountain belt (Figure 7). At these altitudes it has various forms, the most important being the Spino Santo (*Astragalus siculus*), a dominant feature of this environment where spiny xerophytes prevail. The barberry (*Berberis aetnensis*) and juniper (*Juniperus hemisphaerica*) grow in the same habitat. The flowers of the Etna pansy (*Viola aetnensis*) and the characteristic cushions of the saponaria (*Saponaria sicula*) are frequently found with the Spino Santo. The vegetation is remarkably depleted above the habitat of *Astragalus siculus*, higher than 2400 m and up to approx. 2800 m. Only *Rumex aetnensis* and *Anthemis aetnensis* still grow, constituting extreme examples of high-altitude vegetation on the volcano (Poli Marchese 2000). Above 2900 m any form of macroscopic vegetation can no longer be found and only the volcanic desert remains.

Figure 7. The "Spino Santo" (*Astragalus siculus*), characterized the barren areas of the Etna mountain belt.

Conclusions

Etna is an environment of great naturalistic importance: it is a complex strato-volcano, formed of lava flows alternating with pyroclastic materials, emitted over various eruptive areas which have, over centuries, built up the actual volcano. The gentle slopes towards the base of Pleistocene clays, form most of the eastern third of Sicily. On the lower slopes of the south-western flank the morphological features show alluvial terraces, while there are marine terraces on the south-eastern flank that may be interrupted by sub-vertical escarpments. Above 1000 m altitude, lava flows greatly influence the landscape producing morphologies with irregular, rough surfaces. A peculiar morphological feature are the numerous ephemeral cones that are the result of the accumulation of the pyroclastic ejected. Above 2000 m the very steep slopes reach the main craters and the landscape looks like a blackened moonscape.

But, Etna is also an area of considerable interest because of its agricultural activity. On its landscape agriculture displays many different biologi-

cal and agronomic features, which have been determined not only by historical and economic-social causes but also by the peculiar features of the physical landscape, the geo-morphological characteristics, climatic conditions and soil features. These last, in particular show a wide range of variability due to the parent material, age, different morphologies, climatic features and last, but not least, to exposure and to winds which carry and deposit ash and lapilli which may be abundant.

The influence of man, established since the remote past on the slopes of Etna, is certainly the most important elements in shaping the environment. Its ancient presence on the volcano and its activities have effected radical transformations to the natural landscape of Etna: the wooden areas were reduced while the cultivated areas were increased (Poli 2000). The lowlands of the volcano have been most influenced by these transformations due not only to urbanization but also to the cultivation of high-income crops, typical of the Mediterranean area.

The main characteristic of agriculture of Etna is not only the abundance of the varieties, particularly of apple and pear, but also the aspects linked to the growing of old cultivars that cannot be find in others Sicilian areas and that allow to preserve a very important genetic heritage.

Between 1000 and 1500 m, in the forest area prevail the pine-wood with Laricio pine, the birch-wood with Etna birch, the beech-wood and the poplar-wood with trembling poplar. Also the chestnut-wood is diffused and depending on the local situations represents a wooden tree used mostly for timber production, and sometimes for the fruit yields. In the mountain belt (>1500 m) the thorny xerophytes prevail.

But, as happens in others volcanic areas of the world, all the vegetation and particularly the crops, are exposed to danger due to ash emission that can injured the crops mainly when the ash emission take place during the harvest period. In 2002, in consequence of a three months eruption citrus fruits, vegetables and grapes were injured. It was the adherence of the ash to the fruit's skin or to the leaves of the vegetables responsible for such damages. Grapes needed to be washed individually before consumption to avoid ingestion of fine ash while the mechanical processing of the citrus fruit was stopped because the abrasive nature of the ash would have damaged the machinery. Moreover the oranges for the juice production could not be used because of the cleaning of the fruit skin was a difficult task from an economical point of view. The same happen for the vegetables (mostly leafy crops), over both the immediate area around Etna, i.e. the province of Catania and in the neighbouring province of Siracura (South of Catania) were a lost of 80% of vegetable was estimated.

References

Aureli A (1973). Idrogeologia del fianco occidentale etneo. Proceedings 2nd Inter. Symposium on Groundwaters. Palermo, pp 425–487

Behncke B (2004). Italy's Volcanoes: the Cradle of Volcanology. http://boris.vulcanoetna.com [verified on November 29, 2004]

Busà T, Cirrincione R, Cristofolini R, Pezzino A (1998). Caratterizzazione petrologico-tessiturale di una successione piroclastica in prossimità di Monte Salto del Cane (versante meridionale dell'Etna): implicazioni sui processi di alterazione e di pedogenesi. Miner Petrogr Acta Vol XLI, pp 61–78

Certini G, Fernandez Sanjurjo MJ, Corti G, Ugolini FC (2001). The contrasting effect of broom and pine on pedogenesis processes in volcanic soils (Mt. Etna, Italy). Geoderma 102:239–254

Chester DK, Duncan AM, Guest JE, Kilburn CRJ (1985). Mount Etna: the anatomy of a volcano. Chapman and Hall, London, pp 404

Corine (2000). Land Cover 2000. In: http://image2000.jrc.it/ [verified November 19, 2005]

Ferrara V (1975). Idrogeologia del versante orientale dell'Etna. Proceedings 3rd Inter. Symposium on Groundwaters. Palermo, pp 91–134

Lo Papa G, Palermo V, Parisi S, Laudicina V, Tusa D, Scalenghe R (2003). Caratteristiche di una sequenza di suoli forestali nel versante nord-occidentale dell'Etna. Boll Soc It Scienza Suolo 52(1–2):513–522

Messina A, Pavone P, Viglianisi F (2004). L'agricoltura nel massiccio etneo. http://www.dipbot.unict.it/ctnatura/agro/agro05.html [verified on May 28, 2004]

Ogniben L (1966). Lineamenti idrogeologici dell'Etna. Rivista Mineraria Siciliana n° 100–102, pp 151–174

Parello F, D'Alessandro W, Aiuppa A, Federico C (2001). Cartografia geochimica degli acquiferi etnei. CNR – GNDCI. Pubb N° 2190, p 103

Poli Marchese E (2000). Carta della Vegetazione dell'Etna: note illustrative. Selca, Firenze

Raimondi S, Lupo M, Tusa D (1999). Il clima ed il pedoclima dei suoli vulcanici dell'Etna. Sicilia Foreste, n° 23/24:2–7, Palermo

Sartorious von Waltershausen W (1880). Der Aetna. Lipsia, 371 pp

Tangyi JC, Condomines M, Kieffer G (1997). Evolution of the Mount Etna magma: constraints on the present feeding system and eruptive mechanism. J Vol Geotherm Res 75:221–250

Appendix materials on CD-Rom

view_of_etna.jpg
terracing.jpg
lava_and_forest.jpg
etna_broom.jpg
spino_santo.jpg